

**Shoreline Response to  
Relative Sea Level Change:  
Culbin Sands, Northeast Scotland**

Thesis submitted for the degree of Doctor of Philosophy

by

Darren P.M. Comber

September 1993

Department of Geography & Topographic Science  
University of Glasgow  
Glasgow G12 8QQ

ProQuest Number: 13818516

All rights reserved

INFORMATION TO ALL USERS

The quality of this reproduction is dependent upon the quality of the copy submitted.

In the unlikely event that the author did not send a complete manuscript and there are missing pages, these will be noted. Also, if material had to be removed, a note will indicate the deletion.



ProQuest 13818516

Published by ProQuest LLC (2018). Copyright of the Dissertation is held by the Author.

All rights reserved.

This work is protected against unauthorized copying under Title 17, United States Code  
Microform Edition © ProQuest LLC.

ProQuest LLC.  
789 East Eisenhower Parkway  
P.O. Box 1346  
Ann Arbor, MI 48106 – 1346

thesis  
9495  
copy 1  
Vol 1

GLASGOW  
UNIVERSITY  
LIBRARY

*I wonder if the ground has anything to say? I wonder if the ground is  
listening to what is said?*

Young Chief, Cayuse Indian (1855)

## ABSTRACT

The aims of this research are to establish shoreline responses to relative sea level change in the Moray Firth. Using both the sea level history and contemporary coastal sediment budgets, a "palaeosediment budget" is presented, which is used to assess the response of the shoreline to changing conditions of relative sea level and sediment supply during the Holocene.

The area around Culbin and Burghead Bay in NE Scotland comprises a series of relict shoreline and associated unconsolidated deposits which have formed since the last glacial maximum *ca.* 18 000 years ago. The Culbin foreland is composed of a suite of shingle storm beach ridges abandoned at up to 3 km inland. The storm ridges were deposited under falling relative sea level after the peak of the Holocene sea level maximum *ca.* 6500 BP as a staircase of features between 11 and 3 m OD, and are backed landwards by fine grained sediments which have been deposited in their lee. Using modern analogues from The Bar, a barrier beach 3 km downdrift, these are successfully used in conjunction with more standard dated indicators in the reconstruction of relative sea level trends for the area. Detailed morphological investigation of the shingle ridges demonstrates relationships between crest spacing and the regularity of sediment supply, which demonstrate rapid changes in ridge altitude to be directly related to sediment supply, and indirectly related to relative sea level change,

An allied study of contemporary processes operating along the Culbin foreshore and at The Bar was also undertaken. Wave data from commercial sources was supplemented by data from a directional wave recorder constructed specifically for the project. Modal wave height and period in the Culbin area are low, at only 1 m and 4 s respectively. The wave recorder demonstrates the under-representation of low (< 0.5 m) waves in commercial records and the presence of converging wave trains. The incidence of swell from the NE sector creates a dominant westerly longshore current, responsible for the strong sediment sorting and drift-aligned landform assemblage at the coast. Tidal currents were found to be very weak in the Culbin area, and are not an important sediment transport mechanism.

The primary mode of contemporary foreshore sedimentation has altered radically from a shingle to a sand dominated environment, with shingle now only actively deposited at the proximal end of The Bar. Quantification of the sedimentary inputs and outputs to the Culbin area allowed two sediment budgets to be calculated, one for the sandy Culbin foreshore, and a second shingle budget for The Bar. These

both indicate that longshore transport remains the dominant mode of transport, with up to  $3.3 \times 10^4 \text{ m}^3 \text{ a}^{-1}$  of sand transported along the Culbin foreshore, and  $0.1 \times 10^4 \text{ m}^3 \text{ a}^{-1}$  of shingle along the proximal flank of The Bar.

The calculation of a palaeosediment budget aimed to produce a first order quantification of the volumetric development of Culbin during the Holocene period. Adopting a similar methodology as the contemporary sediment budget, the inputs and outputs of sediment to the coastal zone during the Holocene were quantified, although at an order-of-magnitude scale. The supply of shingle from the neighbouring River Findhorn was insufficient to account for the development of Culbin alone, and an additional updrift supply of shingle from the Spey helps to explain the genesis of a composite landform the size of Culbin. A three stage developmental model is proposed, which attempts to explain the variable nature of sediment supply to Culbin under different relative sea levels at Culbin throughout the Holocene. This is based upon the identification of an operational water depth of 6 m around the northern flank of the present Covesea-Burghead area, defining a critical depth below which shingle is no longer actively transported in the nearshore zone. Phase 1 relates to the period 9500-7200 BP, when operational depths were below 6 m, allowing the free passage of shingle from the River Spey to augment the supply from the River Findhorn reaching Culbin. Phase 2 occurs between 7200 and 4300 BP, when operational depths exceeded 6 m and the supply of shingle from the Spey to Culbin was halted. Phase 3 is dated post-4300 BP, when the Spey link was re-established, but shingle supplies were beginning to fail from both rivers.

From this, a developmental model is described, which attempts to explain the evolution of the Culbin area under conditions of varying relative sea level and sediment supply.

Having considered the past and present evolution of Culbin, an assessment of the future development of the area is made in the light of potentially rising relative sea level as eustatic sea level begins to match the rate of isostatic rebound in the Moray Firth.

## ACKNOWLEDGEMENTS

This study was carried out while I was in receipt of a Natural Environment Research Council studentship no. GT4/89/AAPS/61. The cost of 13 radiocarbon dates was met by NERC Scientific Services, allocation 485/1291. A grant awarded by the Bill Bishop Memorial Trust towards fieldwork expenses during 1991 is also gratefully acknowledged.

The completion of this thesis would not have been possible without the guidance, encouragement and friendship of my supervisor, Dr Jim Hansom, whose faith in this thesis has on more than one occasion saved it from the bin. Thanks are due to Dr David Thomas, who stepped into the breach and kept the research on track during my formative year, and to Dr David Evans, who has provided some "quite remarkable" insights into all things Canadian, and kept small Scottish events firmly in their context.

The former Forestry Commission Moray Office kindly allowed access into Culbin Forest, without which this study could not have taken place. Fieldwork formed the basis of this thesis, and without the aid of field assistants would have been impossible to complete. The following are to be commended for their bravery in the face of adverse weather: Helen Barham, Richard Burn, Peter Chung, "St." Felicity Fahy, Amanda Hastings, Dave Kelly, Jim McCormick, Sean McDonald, Alastair McPherson and Leo Murray. Special mention goes to Steve "ranging pole" Godby (fieldworker to the gentry) for two years of summer holidays at Culbin, for being consistently last to the bar and for loitering with intent outside the Co-Op in Forres in the name of real research.

The kindness of the people of Forres and Nairn made the work all the more enjoyable, particularly Jim and Winnie Falconer at Snab of Moy Farm, who generously provided a space for the caravan over the two years of fieldwork and cheerfully put up with the comings and goings associated with catching tides at odd hours of the day and night. Isobel Ferguson of Brodie Mains provided sanctuary when the weather became too much, and her home baking was much appreciated. Helpful comments and stimulating conversations were provided by Sinclair Ross, whose enthusiasm and energy were an inspiration throughout the duration of the thesis. The help of Tony Cowey of the Royal Findhorn Yacht Club in rescuing the current meter is also gratefully acknowledged.

Technical support was provided by both the University of Sheffield and the University of Glasgow, and thanks are due to Paul Benton and Chris Turner (Sheffield) for the construction of the wave recorder, and Peter Chung (Glasgow) for building just about everything else. NERC RVS at Barry kindly loaned the RCM-4 and translated the data. Thanks too to Brenda Scott at the University of Ulster (Coleraine) for the crash course in using the wave refraction package WAVENRG, and for showing me what real shingle looks like.

Final mention goes to "King" Sean "yooz creep" McDonald, whose friendship over the past two years has led to monumental acts of ignorance, both at home and abroad, but without whom this tome would still be in pieces.

# CONTENTS

LIST OF FIGURES.....	iv
LIST OF PLATES.....	viii
LIST OF TABLES.....	ix
<b>CHAPTER 1 INTRODUCTION.....</b>	<b>1</b>
1.1 AIMS OF RESEARCH.....	3
1.2 EXPERIMENTAL DESIGN AND PROCEDURE.....	4
<b>CHAPTER 2 LITERATURE REVIEW.....</b>	<b>7</b>
2.1 INTRODUCTION.....	7
2.2 RELATIVE SEA LEVEL HISTORIES: MEASUREMENT AND SCOTTISH CASE STUDIES.....	7
2.2.1 Indicators of RSL change.....	8
2.3 RELATIVE SEA LEVEL HISTORIES.....	11
2.3.1 Global sea levels.....	11
2.3.2 Scottish sea level histories.....	13
2.4 CONTEMPORARY COASTAL PROCESSES.....	19
2.4.1 Tides and tidal currents.....	19
2.4.2 Waves and wave theory.....	20
2.4.3 Shallow Water Wave Transformations.....	21
2.4.4 Wave Recording.....	23
2.4.5 Beach sediment budgets.....	24
2.4.6 Shingle Beaches:- processes and landforms.....	27
2.4.7 Present and future trends in global sea level.....	36
2.5 FLUVIAL SEDIMENT INPUTS TO THE COASTAL ZONE.....	41
2.5.1 Fluvial bedload equations.....	41
2.5.2 Sedimentation studies in enclosed basins.....	42
2.5.3 Palaeodischarge methods.....	43
2.6 CULBIN AND THE MORAY FIRTH.....	45
2.6.1 Geomorphological setting.....	45
2.6.2 Regional Geomorphology of the Moray Firth.....	46
2.6.3 Geology of the Moray Firth.....	47
2.6.4 Glacial History of the Moray Firth.....	49
2.6.5 Relative sea level history of the Moray Firth.....	52
2.6.6 Reiteration of aims.....	54
<b>CHAPTER 3 METHODS.....</b>	<b>56</b>
3.1 INVESTIGATION OF HOLOCENE ENVIRONMENTS AT CULBIN AND SURROUNDING AREAS.....	56
3.1.1 Shingle ridge location and altitudes.....	56
3.1.2 Sedimentology of the shingle ridges.....	58
3.1.3 Stratigraphy.....	59
3.2 CONTEMPORARY COASTAL PROCESSES AND LANDFORMS.....	62
3.2.1 Contemporary coastal processes.....	62
3.2.2 Wave refraction modelling.....	69
3.2.3 Contemporary Coastal Landforms and Foreshore sediments.....	75
3.2.4 Modelling the beach sediment budget.....	78
3.2.5 Beach sediment budget via beach profile and spit extension methods.....	80
3.3 LINKAGES BETWEEN HOLOCENE AND CONTEMPORARY PROCESSES.....	84
3.3.1 Introduction.....	84

3.3.3 Volumetric calculations of shingle at Culbin.....	85
3.3.4 Volumetric delivery of shingle to Culbin during the Holocene .....	88
3.3.5 Losses to the system .....	91
<b>CHAPTER 4 RESULTS.....</b>	<b>93</b>
<b>4.1 INVESTIGATION OF HOLOCENE ENVIRONMENTS OF CULBIN AND BURGHEAD BAY .....</b>	<b>93</b>
4.1.1 Geomorphology of Culbin .....	93
4.1.2 Stratigraphy of the Culbin foreland .....	101
4.1.3 Geomorphology of Burghead Bay.....	107
4.1.4 Relative sea level history of the Culbin area.....	121
<b>4.2 CONTEMPORARY COASTAL PROCESSES AND LANDFORMS.....</b>	<b>133</b>
4.2.1 Contemporary coastal processes .....	133
4.2.2 Contemporary coastal landforms at Culbin: Introduction .....	152
4.2.3 Sand sediment budget: Culbin foreshore.....	167
4.2.4 Inputs.....	168
4.2.5 Outputs .....	170
4.2.6 Shingle sediment budget: The Bar.....	175
4.2.7 Inputs .....	176
4.2.8 Outputs .....	178
<b>4.3 LINKAGES BETWEEN HOLOCENE AND CONTEMPORARY PROCESSES .....</b>	<b>183</b>
4.3.1 Inputs .....	183
4.3.2 Outputs .....	186
4.3.3 Calculation of the palaeosédiment budget .....	189
<b>CHAPTER 5 DISCUSSION.....</b>	<b>194</b>
<b>5.1 THE HOLOCENE DEVELOPMENT OF CULBIN AND BURGHEAD BAY .....</b>	<b>194</b>
5.1.1 Relative sea level history of the Culbin area.....	194
5.1.2 The use of shingle storm ridges in the reconstruction of RSL at Culbin.....	208
5.1.3 A model of RSL and sediment supply at Culbin .....	213
5.1.4 Shoreline response to RSL change .....	214
<b>5.2 CONTEMPORARY COASTAL PROCESSES AND LANDFORMS AT CULBIN .....</b>	<b>226</b>
5.2.1 Contemporary coastal processes .....	226
5.2.2 Contemporary coastal sediments and landforms.....	240
5.2.3 Sand sediment budget: Culbin foreshore.....	260
<b>5.3 LINKAGES BETWEEN HOLOCENE AND CONTEMPORARY PROCESSES .....</b>	<b>271</b>
5.3.1 Synthesis of Holocene and contemporary coastal studies: the application of the coastal sediment budget at Culbin.....	272
5.3.2 Shoreline response to RSL change at Culbin and Burghead Bay .....	282
<b>CHAPTER 6 ESTIMATION OF ERRORS.....</b>	<b>297</b>
6.1 SURVEYING ERRORS .....	297
6.2 ERRORS IN THE MAGNITUDE OF STRATIGRAPHIC BOUNDARIES .....	297
6.3 SEDIMENT BUDGET CALCULATION .....	298
6.3.1 Surveyed sediment budget .....	298
6.3.2 Inputs to the modelled beach sediment budget .....	299
6.4 PALAEOSEDIMENT BUDGET CALCULATIONS .....	301
6.4.1 Depth of shingle movement .....	301
6.4.2 Areal mapping accuracy .....	302
6.4.3 River terrace reconstruction .....	302
6.5 General Critique.....	303
<b>CHAPTER 7 CONCLUSIONS.....</b>	<b>304</b>
7.1 GENERAL CONCLUSIONS .....	304
7.2 SUMMARY OF FINDINGS .....	304
7.2.1 Holocene sea level studies .....	304
7.2.2 Contemporary coastal studies .....	306

7.2.3 Linkages between Holocene and contemporary processes .....	307
7.3 CRITIQUE.....	309
7.3.1 Holocene sea level studies .....	309
7.3.2 Contemporary coastal studies .....	311
7.3.3 Linkages between Holocene and contemporary processes .....	312
7.4 SCOPE FOR FUTURE RESEARCH .....	313
7.4.1 Sea level studies .....	313
7.4.2 Shingle ridge studies .....	313
7.4.3 Sediment budget .....	314
7.4.4 Wave recorder .....	314
7.4.5 Palaeosediment budget .....	315
7.5 Conclusion .....	316
<b>REFERENCES.....</b>	<b>317</b>
<b>GLOSSARY.....</b>	<b>340</b>
<b>APPENDICES</b>	

## LIST OF FIGURES

Figure 1.1 General location map

Figure 1.1a Site location map

Figure 2.1 Eustatic sea level curves: a) Fairbridge, 1961. b) Shepard, 1963. c) Jelgersma 1961 (from Jelgersma, 1966). d) Mörner, 1971

Figure 2.2 Eustatic sea level curve (source: Fairbanks, 1989)

Figure 2.3 Isobase map of the Main Postglacial Shoreline (MPG) in Scotland (source; Price, 1983)

Figure 2.4 Relative sea level trends in the Beaully Firth (source: Haggart, 1983)

Figure 2.5 Resolution of an incident wave into shore-normal and shore-parallel components

Figure 2.6 Location of relict shingle storm ridges at Culbin

Figure 2.7 Regional divisions of the Moray Firth (source: Smith, 1986)

Figure 2.8 Quaternary basins in the Moray Firth (source: Chesher & Lawson, 1983)

Figure 3.1 1:10 000 scale geomorphological map of Culbin (in folder at rear)

Figure 3.2 Location of transects A and B, Culbin

Figure 3.3 Location of transects C and D, Culbin

Figure 3.4 Location of clast sampling sites, Culbin

Figure 3.5 Division of the major sedimentological units at Culbin (source: Gauld, 1981)

Figure 3.6 Location of ponds at Snab of Moy

Figure 3.7 Elements of the beach sediment budget

Figure 3.8 Method of deployment of the current meter, Culbin June-July 1991

Figure 3.9 Principle of directional wave recording

Figure 3.10 Simultaneous plots of wave height and windspeed (data from Beatrice Alpha)

Figure 3.11 Location of beach profiling stations and sediment sampling locations

Figure 3.12 Plan of submarine profile locations

Figure 3.13 Diagrammatic cross-section through Buckie Loch spit

Figure 3.14 Subdivision of Culbin shingle ridges into confidence levels for volumetric calculation

Figure 3.15 Hypothetical cross-section through a shingle storm ridge

Figure 3.16 Map of the lower Strathspey river terraces (source: Peacock *et al.*, 1968)

Figure 3.17 The "wedge" method for estimating the volume of sediment in a river terrace sequence

Figure 4.1 Location of relict shingle storm ridges at Culbin

Figure 4.2 Section measured across Transect A

Figure 4.3 Plot of mean wavelength against mean crest altitude

Figure 4.4 Plot of standard deviation of wavelength against standard deviation of crest altitude

Figure 4.5 Location of sediment sampling sites LAG 1-3

Figure 4.6 Stratigraphic log from LAG 1

Figure 4.7 Stratigraphic log from LAG 2  
Figure 4.8 Stratigraphic log from LAG 3  
Figure 4.9 Stratigraphic log from Pond 1  
Figure 4.10 Stratigraphic log from Pond 3  
Figure 4.10a Location of raised cliffline around the inner Moray Firth (source: Hansom, 1988)  
Figure 4.11 Raised shingle ridges in Burghead Bay (source: Steers, 1937)  
Figure 4.12 Location of boreholes and transects at RAF Kinloss  
Figure 4.13 RAF Kinloss central transect: stratigraphy  
Figure 4.14 RAF Kinloss east and west transects: stratigraphy  
Figure 4.15 Cliff section diagram: Burghead Bay 1991  
Figure 4.16 Clast sampling locations in Burghead Bay  
Figure 4.17 Plan of the Bessie Burn site  
Figure 4.18 Bessie Burn stratigraphic log  
Figure 4.19 Bessie Burn stratigraphic log  
Figure 4.20 Relative sea level indicators from Culbin and Burghead Bay (uncorrected altitudes)  
Figure 4.21 Relative sea level trends in the Dornoch Firth (source: Hansom & Leafe, 1990)  
Figure 4.22 Relative sea level indicators from the Culbin area (corrected altitudes)  
Figure 4.23 Composite shingle ridge transect A and B  
Figure 4.24 Paired ridge crest mean altitudinal trends  
Figure 4.25 Three ridge mean altitudinal trends  
Figure 4.26 Transect A plotted against control transect C  
Figure 4.27 Transect A plotted against control transect D  
Figure 4.28 Declining altitude across the composite shingle ridge transect  
Figure 4.29 Transects across the central, east and west shingle ridge populations  
Figure 4.30 Composite plot of sea level indicators from the Moray Firth  
Figure 4.31 Exponentially declining RSL demonstrated by the Culbin sea level indicators  
Figure 4.32 Tidal current direction frequency as a percentage of the total record  
Figure 4.33 Tidal current speed as a percentage of the total record  
Figure 4.34 Tidal current direction: June 6/7 and 14/15 1991  
Figure 4.35 Tidal current speed: June 6/7 and 14/15 1991  
Figure 4.36 Tidal current velocity: June 6/7 and 14/15 1991  
Figure 4.37 Total tidal current velocity: June 1991  
Figure 4.38 Frequency histogram of tidal current velocity: June 1991  
Figure 4.39 Tidal current velocity residuals  
Figure 4.40 Windspeed frequency at RAF Kinloss during 1990 and 1991  
Figure 4.41 Windrose from RAF Kinloss 1990-91  
Figure 4.42 Beatrice Alpha: seasonal wave periods  
Figure 4.43 Beatrice Alpha: annual wave period  
Figure 4.44 Beatrice Alpha: seasonal wave heights

- Figure 4.45 Beatrice Alpha: annual wave heights
- Figure 4.46 Calibration curve used for the pressure transducer
- Figure 4.47 Raw data from the wave recorder
- Figure 4.48 Frequency histogram of wave heights: wave recorder
- Figure 4.49 Rose diagram of wave directions: wave recorder
- Figure 4.50 Plot of incident wave direction and height: wave recorder
- Figure 4.51 Sample plot of orthogonal output from WAVENRG
- Figure 4.52 Foreshore sediments at Culbin: summary statistics
- Figure 4.53 Sweep zone plots from the Culbin foreshore
- Figure 4.54 Beach volumes recorded at Culbin
- Figure 4.55 Offshore profiles recorded at Culbin
- Figure 4.56 Beach profiles recorded on The Bar
- Figure 4.57 Mean dune heights backing the Culbin foreshore
- Figure 4.58 Dune cliff recession rates at Culbin 1990-92
- Figure 4.58a Residual POZ: cells B1 and B2
- Figure 4.59 Diagrammatic representation of the sand sediment budget
- Figure 4.60 River terraces of lower Strathspey (source: Peacock *et al.*, 1968)
- Figure 4.61 Elements of the palaeosediment budget
- 
- Figure 5.1 Isobase map of the Main Postglacial Shoreline (MPG) in Scotland (source; Price, 1983)
- Figure 5.2 Composite plot of sea level indicators from the Moray Firth
- Figure 5.3 The approximate location of the Scottish coastline with sea level reduced by *ca.* 100 m (source: Price, 1983)
- Figure 5.4 Lateglacial shorelines in the Loch Loy area (source: Firth, 1989a)
- Figure 5.5 Subsurface extent of peat below RAF Kinloss derived from borehole information
- Figure 5.6 The extent of the Moniak alluvial fan in the Beaully Firth (source: Haggart, 1987)
- Figure 5.7 Scottish isostatic rebound curve showing the negligible impact of a modelled Loch Lomond Readvance (source: Lambeck, 1991a)
- Figure 5.8 Relative sea level indicators from the Culbin area (corrected altitudes)
- Figure 5.8a Submarine section offshore from Burghead
- Figure 5.8b Submarine section offshore from Lossiemouth
- Figure 5.9 Three phase model of Late Quaternary relative sea level and sediment supply to Culbin
- Figure 5.10 Reproduction of the Anderson map of 1749 (source: Ross, 1992)
- Figure 5.11 Stratigraphy of the Nairn Basin (source: Chesher & Lawson, 1983)
- Figure 5.12 Tidal streams in the Moray Firth
- Figure 5.13 Wind data from RAF Kinloss a) 10 years data (modified from Ross, 1992) b) data from 1990-91
- Figure 5.14 Winds at RAF Kinloss (source: Ritchie *et al.*, 1978)
- Figure 5.15 Wave parameters recorded at Kinnairds Head (source: Thorne & Gleason, 1986)

Figure 5.16 Beatrice Alpha: annual wave heights

Figure 5.17 Beatrice alpha: annual wave period

Figure 5.18 The Pont map of 1590

Figure 5.19 The May map of 1758

Figure 5.20 Time series plot of the location of the distal end of the forerunners of The Bar (source: Ross, 1992)

Figure 5.21 Offshore sediments in the Moray Firth (source: Chesher & Lawson, 1983)

Figure 5.22 The Covesea Ridge and the flooded Spynie channel (source: Ogilvie, 1923)

Figure 5.23 Elements of the palaeosediment budget

Figure 5.24 Stages in the development of Culbin and Burghead Bay (source: Ross, 1992)

## LIST OF PLATES

Plate 1 Buckie Loch spit and the Culbin foreland viewed east towards the Findhorn estuary.

Plate 2 Relict shingle storm ridge forming part of set D.

Plate 3 Aerial photographic montage of Culbin and Burghead Bay in 1989.

Plate 4 Deployment of the wave recorder, June 1991 (original in colour)

Plate 5 Organic induration, possibly representing a poorly developed palaeosol within the upper layers of a relict shingle storm ridge, Culbin.

Plate 6 Aerial view westwards along Buckie Loch spit and onto The Bar.

Plate 7 Dune cliffing and derelict groyne on the eastern Culbin foreshore (cell B2).

Plate 8 Low, yellow dunes at Shellyhead.

Plate 9 Shingle recurve on the landward side of The Bar.

Plate 10 Shingle point bars in the River Findhorn.

## LIST OF TABLES

- Table 2.1 Indicative ranges of contemporary landforms (source: Firth & Haggart, 1989)
- Table 2.2 Elements of the beach sediment budget (modified from Komar, 1976)
- Table 2.3 Estimates of rates of global sea level rise (source: Pirazzoli, 1990)
- Table 2.4 Anticipated rise in relative sea level for four sites around the British coast (source: Pugh, 1990)
- Table 2.5 Relative proportions of the major coastal environments in the Moray Firth (source: Smith, 1986)
- Table 4.1 Culbin shingle ridge altitudes: means and standard deviations
- Table 4.2 Mean 'b' axis and roundness parameters: Culbin shingle ridges
- Table 4.3 Mean 'b' axis lengths from the seaward inland shingle ridges at Culbin
- Table 4.4 Mean 'b' axis lengths of clasts measured along the western flank of the Bar (source: Hastings, 1991)
- Table 4.5 Sedimentary characteristics of the basal fine sand unit: estuarine sites LAG 1-3, Culbin
- Table 4.6 Burghead Bay raised shingle deposits: vector magnitudes
- Table 4.7 Ages and classifications of radiocarbon dated samples from Culbin and Burghead Bay
- Table 4.8 Maximum age range associated with the drop in altitude recorded in the Culbin shingle ridge sequence, central and east transects
- Table 4.9 Tidal range at Nairn and Burghead (source: Admiralty, 1992)
- Table 4.10 Tidal current speeds and associated maximum sediment diameters for suspension: Culbin offshore zone
- Table 4.11 Summary data from the Culbin wave recorder
- Table 4.12 Proportion of waves from each major direction at Culbin, by season (source: BMT, 1986)
- Table 4.13 Proportion of wave generating winds by season recorded at RAF Kinloss during 1990
- Table 4.14 Wave parameters generated from onshore winds at Culbin
- Table 4.15 Summary wave and wind frequency data at Culbin
- Table 4.16 Wind generated breaking wave heights corrected for refraction
- Table 4.17  $P_L$  values derived from wind waves
- Table 4.18 Wave data for input into the wave refraction program WAVENRG (source: BMT, 1986)
- Table 4.19 Resultant longshore power values by season using the wave refraction program WAVENRG
- Table 4.20 Sediment analysis results: Culbin foreshore
- Table 4.21 Analysis of wave orthogonal landfall data
- Table 4.22 Input of sediment to the foreshore from dune cliff recession: Culbin foreshore

- Table 4.23 Aerial and volumetric extension rates measured at Buckie Loch spit 1870-1989
- Table 4.24 Effective wave days recorded at Culbin and subsequent conversion factor for  $Q_L$
- Table 4.25 Summary of  $P_L$  and  $Q_L$  calculations by season: Culbin foreshore
- Table 4.26 Summary of the inputs and outputs to the modelled sand beach sediment budget: Culbin foreshore
- Table 4.27 Difference between observed and modelled volumetric changes: Culbin foreshore
- Table 4.28 Aerial and volumetric extension rates at The Bar 1870-1989
- Table 4.29 Summary of the inputs and outputs to the shingle sediment budget: The Bar
- Table 4.30 Percentage of shingle present in boreholes sunk in lower Strathspey
- Table 4.31 Volumetric calculations of shingle exposures at sites between Speymouth and Culbin
- Table 4.32 Shingle volumes in the Culbin foreland
- Table 4.33 Summary of the inputs and outputs to the palaeosediment budget
- 
- Table 5.1 10 year return wave parameters calculated for the middle Moray Firth (source: Conoco Ltd)
- Table 5.2 Distances and errors measured from the May map of 1758
- Table 5.3 Difference between observed and modelled volumetric beach changes: Culbin foreshore
- Table 5.4 Summary of the inputs and outputs to the shingle sediment budget
- 
- Table 6.1 Possible error factors in the measurement of stratigraphic boundaries (source: Shennan, 1982)
- Table 6.2 Potential errors resulting from the surveyed sediment budget

Plate 1

Buckie Loch spit and the Culbin foreland viewed east towards the Findhorn estuary. Dune covered recurves are clearly visible along the length of the spit, whose extension has encouraged sandflat and saltmarsh development in its lee (bottom foreground). A series of semi-continuous offshore bar features can be seen extending along the length of the foreshore.



## CHAPTER 1 INTRODUCTION

The two principal factors affecting the position of the shoreline are sea level (Leatherman, 1989) and sediment supply. Since the decay of the last British ice sheet around 13 000 years ago the position of the shoreline around Britain has altered dramatically due to the complex interplay between the relative levels of land and sea on both a regional and global scale (Tooley, 1982).

The position of the British coastline has been largely inherited from the direct and indirect effects of the various glacial-interglacial cycles experienced over the Quaternary Period. Of particular importance in British coastal evolution since the last glacial maximum has been the supply of sediment to the coastal zone. Downwasting glaciers released immense volumes of sediment to the coastal zone which were subsequently reworked by marine processes to form many of the beaches found today in Britain.

These once-plentiful sediment sources have now begun to fail as offshore sources have been used up or drowned *in situ*, and inland sources have become stabilized by vegetation cover. Accompanying this general change in sediment regime has been the effect on global sea levels of the so-called "Greenhouse Effect". Estimates regarding the possible effects of rising sea levels caused by increased atmospheric CO<sub>2</sub> and its effect on global temperatures are widespread and varied. While many "predictions" have been made somewhat prematurely on the basis of poor input data and models still in their infancy, there is little doubt that over the next century relative sea levels will rise around much of the British coast.

The effect of failing sediment supply combined with rising relative sea level has done much to focus attention on what has become known as the coastal "erosion crisis". Bird (1985) estimated that 90% of the world's sandy shorelines are eroding at 0.5-1.0 m a<sup>-1</sup>. The need for effective planning at this stage in order for society to accommodate future changes at the coast requires the development of models of coastal response. Models presently available were formulated for use primarily on the eastern seaboard of the USA (eg Dean & Maurmeyer, 1983; Pilkey & Davis, 1987; Swain 1989). Given the different environmental controls operating on the British and North American coasts, the application of such models outside the boundary conditions under which they were originally devised may not provide accurate determination of the conditions at various locations around the British coast.

For example, in NE Scotland, the coast has undergone a different evolutionary history from that elsewhere in Britain. Proximity to the former Scottish ice centre (based approximately on Rannoch Moor) has meant that the effects of isostatic uplift have been more pronounced over the Holocene in NE Scotland than elsewhere in Britain. Examination of Late Quaternary sea level records from around the Scottish coast reveals that the processes of both relative sea level (RSL) rise and fall have occurred before, and the effects of such events are frequently preserved in the sedimentary record. Thus to understand the likely effects of the *present* rise in relative sea level it might be profitable to examine the preserved effects of *former* changes in relative sea level.

In addition, the *supply* of sediment to the coast over the Holocene has also varied. Shoreline evolution owes its existence to the interaction between the supply of sediment and RSL change (Swift, 1975; Carter, 1988). Quantification of the *contemporary* coastal sedimentary regime provides a baseline against which *former* sedimentary systems may be measured, aiding the interpretation of spatially similar coastal units at different stages within a chronological development continuum.

Thus, the explanation of the detailed nature of the shoreline response to RSL change in Scotland lies in the interplay between isostatic elements and sediment supply during the Holocene. This hypothesis forms the focus of the research reported here.

The remainder of this chapter states the hypotheses to be tested, and is followed both by an overview of the experimental design and an outline of the thesis structure.

## **1.1 AIMS OF RESEARCH**

The aim of this research is to investigate the Holocene and contemporary development of a coastal site in NE Scotland in terms of its shoreline response to changing RSL under differing sedimentary domains, and to formulate a model to explain the observed changes at the site using previous responses recorded in the sedimentary record as boundary controls.

In order to achieve these aims the work was divided into two sub-areas, each of which provide stand-alone data on specific aspects of the coastal environment, but which link together at a later stage in order to achieve the overall aim of the project. These general research aims are:

- i) the establishment of the sea level history for a previously unrecorded site in NE Scotland;
- ii) examination and assessment of contemporary coastal processes and landforms, and the calculation of a sediment budget for the field site;
- iii) an attempt to link aims i) & ii) through the medium of a "palaeosediment budget" in order to assess former responses of the shoreline to changes in RSL and sediment supply.

The research was not specifically aimed at the production of a sea level history for its own sake, this having been achieved for the inner Moray and Dornoch Firths in earlier studies. Rather, by attempting to combine the approaches of the Quaternary sciences with those of contemporary coastal studies, it was hoped that a better understanding of the dual role of RSL change and the supply of sediment in coastal development would lead to a better appreciation of the genesis of the present coast. This in turn should aid the prediction of future coastal development.

The field site chosen for this investigation was Culbin Sands and Forest, a Site of Special Scientific Interest (SSSI) on the southern coast of the Moray Firth in NE Scotland (Figure 1.1 & 1.1a (insert)). This site is particularly suitable for study, with a highly dynamic coastal zone backed by an exceptionally well-preserved suite of Holocene raised marine landforms. These include an extensive suite of shingle storm ridges, now abandoned at up to 3 km inland, which provide an unusual insight into the detailed response of a coarse, clastic beach environment to changing RSL in Scotland. Of particular importance at this

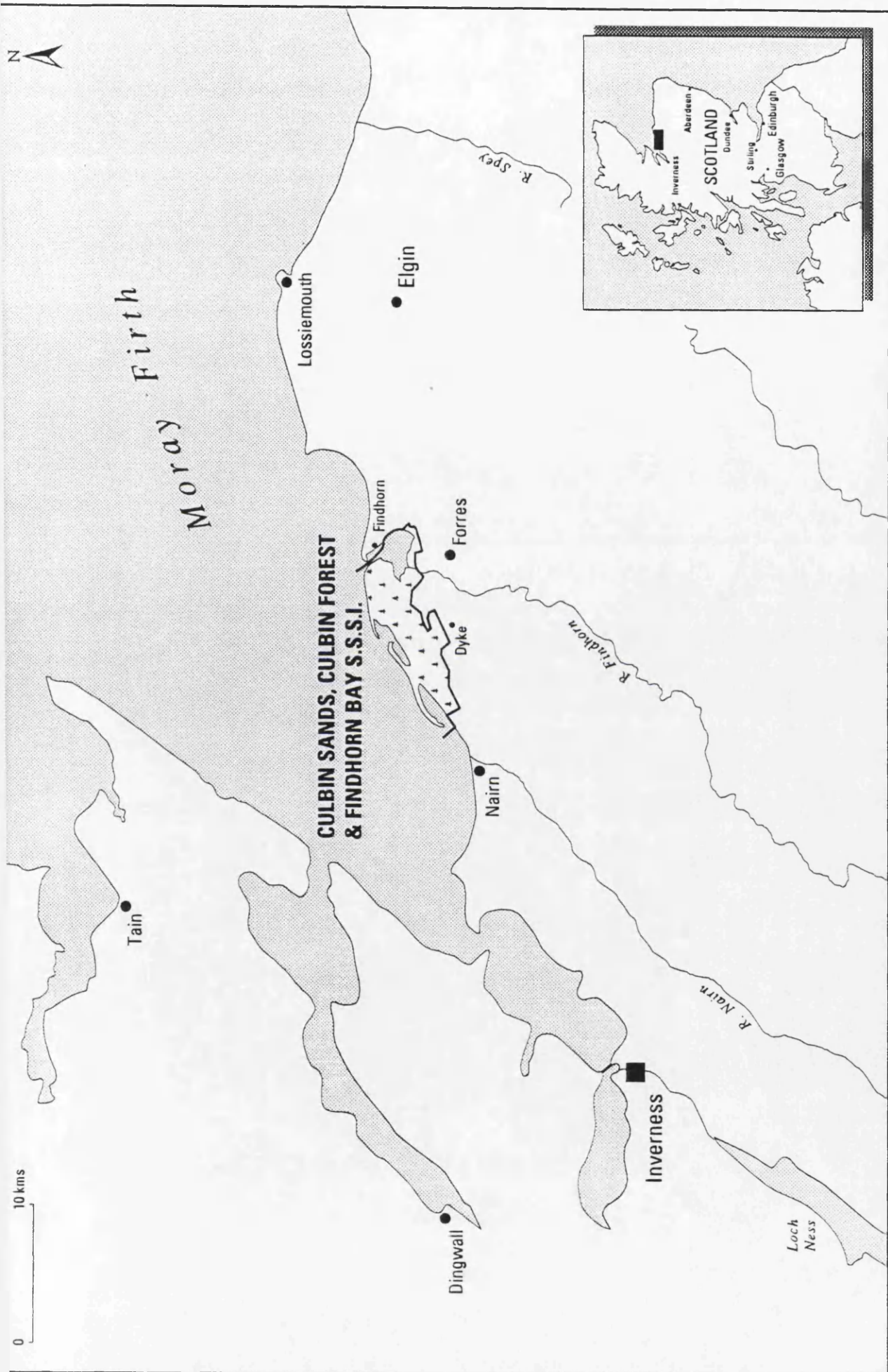


Figure 1.1 Location Map

site is the presence of The Bar, a semi-detached offshore structure displaying a series of active and recently abandoned shingle ridges. This provides an ideal modern analogue for comparison with the relict features further inland.

## **1.2 EXPERIMENTAL DESIGN AND PROCEDURE**

The study was designed to achieve three main aims. Firstly, the description and measurement of the raised coastal features in the Culbin area was designed to produce a sea level history for the area. Secondly, the description and measurement of the present coastal features in the Culbin area was designed in order to produce a sediment budget for the contemporary littoral environment by quantifying the rates of sediment transport operating in the present littoral zone. Thirdly, a comparison between contemporary sedimentation rates and the gross scale sedimentation, which has been continuous at Culbin throughout the Holocene period, was aimed at establishing the nature of former responses of the shoreline to RSL changes and fluctuations in sediment supply.

Investigation of the raised marine features in both Culbin and Burghead Bay involved field survey and description of the deposits, followed by determination of their altitudinal relationships. This information was used to compile a developmental history and sea level curve for the Culbin Forest/Burghead Bay area over the Holocene period. The development of Culbin Forest has been influenced by the changes in RSL which have been recorded in the sedimentary and landform record over the last 10 000 years, and so to fully appreciate the nature of the development sequence, RSL changes in this sector of the Moray Firth required investigation.

Production of a RSL curve involved the use of "traditional" sea level indicator deposits (stratigraphic analysis, dating of organic material etc.) in order to produce control points for a sea level curve showing trends in RSL over the Holocene period in the study area. Next, detailed mapping and levelling of the series of raised shingle storm ridges located between HWST and an abandoned Holocene cliffline at *ca.* 9 m OD was required. Given the number, quality and position of the shingle ridges, a test was designed to assess the potential use of multiple shingle ridges as potential RSL trend indicators. Deposits were levelled into a network of OS benchmarks in order to provide internally consistent results, and to allow comparison with existing reports in Scottish sea level literature as outlined under IGCP project 274.

The processes operating on the contemporary beach were investigated in order to quantify the input, throughput and output of sediment in the beach system. Measurements were made of:-

- i) beach profiles and their variation over a two year period;
- ii) rates of coastal recession over the same two year period;
- iii) waves and currents at the field site;
- iv) rates of distal extension (both planimetric and volumetric) of the drift-aligned landforms of this section of the coast.

Measurement of beach variables was undertaken in order to calculate the annual sediment transport along this section of the coast. The monitoring of beach profiles allowed direct evaluation of the amount of sediment exchange along the coast between fixed periods of time. Profiles were measured at seven locations, reflecting differences in semi-permanent beach morphology noted during early reconnaissance visits to the site during 1989. The measurement of wave and tidal current conditions, both in the field and from secondary sources was undertaken in order to describe the wave climate and energy regime of this part of the Firth. The wave data was used as input to a computer generated wave refraction simulation program designed to provide a potential annual beach sediment budget, to be compared with the actual sediment regime as measured from beach profile changes. The calculation of distal extension of drift-aligned features on the coast was used:

- i) as a final control over the sediment budget;
- ii) to provide information concerning recent historical changes experienced along this stretch of coast;
- iii) as a comparison between a sand and a shingle dominated drift-aligned landform.

Quantification of the volumes of sediment involved in the sequential development of the Culbin foreland was based on the estimation of the volumes contained in the shingle ridge sequence together with an estimate of the volumes of sediment removed from the series of river terraces found in the lower reaches of the Rivers Findhorn and Spey, the two major rivers in the area. Results from this exercise provided an order-of-magnitude estimate of the

volumes of sediment involved in the production of a large coastal foreland such as Culbin, and demonstrates the importance of processes acting under different RSLs to those of the present in understanding the coastal landforms found today along the southern Moray Firth.

The experimental design outlined above feeds through the remainder of the thesis, with the three primary aims of the research forming independent lines of enquiry, but contributing to an eventual understanding of the evolution of the coastal geomorphology of Culbin as it is seen today.

Chapter 2 will present a review of selected literature relevant to the topics of both Holocene and contemporary coastal processes and landforms, highlighting inadequacies and gaps in existing knowledge. Chapter 3 will introduce the methods employed in addressing the aims, with the results of these investigations presented in Chapter 4. Chapter 5 is used to discuss the results, both on a site scale and in the light of available literature, and to assess the degree of success in meeting the initial aims of the thesis. Chapter 6 provides a series of calculations of the errors introduced into the various stages of the calculations in the results, and briefly discusses their potential impact on the remainder of the investigation. A summary and concluding remarks are presented in Chapter 7.

## CHAPTER 2. LITERATURE REVIEW

### 2.1 INTRODUCTION

This chapter aims to review the pertinent literature relating to Holocene sea level fluctuations and subsequent landform evolution, contemporary coastal processes and landform evolution, and the possible linkages between these two aspects of coastal geomorphology. This both sets the scene and highlights any inadequacies in these fields which may be addressed by this research.

### 2.2 RELATIVE SEA LEVEL HISTORIES: MEASUREMENT AND SCOTTISH CASE STUDIES

One of the main aims of this thesis is to understand the nature of sediment supply and transport in the coastal zone of the southern Moray Firth. The sequence of RSL changes which occurred during the Holocene provided a set of background conditions which, arguably, represented the most important controlling factor over the supply of sediment to the coastal zone. This has proved particularly true in the development of the Culbin foreland. It is therefore important that the general nature of RSL change in Scotland, and in the Moray Firth in particular, is understood.

Prior to reviewing the available literature concerning RSL changes in Scotland, it is important to understand the nature of the evidence used to construct RSL histories. Early work on the methodical reconstruction of RSL histories was heavily based on palynological work, for example Godwin & Clifford's (1938) work on the English Fenlands. This methodology was supplemented during the 1960s and 70s by the geomorphological approach taken by Sissons & co-workers, working initially in the Forth Valley in Scotland (eg Sissons, 1962; 1969; Sissons *et al.*, 1966; Brooks, 1972). The geomorphological approach to assessing RSL changes advocated by Sissons contrasted sharply with the combined microfossil and radiocarbon analysis methods employed by Tooley in his benchmark studies on the RSL history of northwest England (Tooley, 1974, 1978, 1980, 1982, 1985 a,b). Sea level studies in the Moray Firth have been divided between the microfossil/C14 methodology (eg Haggart, 1983, 1986, 1987) and a geomorphologically based approach (eg Firth, 1984, 1989a; Firth & Haggart, 1989). The use, reliability and confidence placed on these various forms of evidence to reconstruct RSL histories will be critically reviewed.

### 2.2.1 Indicators of RSL change

The reconstruction of a sea level curve requires careful definition of the deposits used in the reconstruction. Long a source of debate, both the interpretation of intercalated clastic/biogenic deposits (most typically used as sea level indicators) and the inferences built from these interpretations have been subject to change as understanding increases.

One of the areas of disagreement has been over the terms "transgression" and "regression". The simplest definition of "transgression" is when the sea covers the land, and "regression" when the sea retreats (Tooley, 1982). These were the initial definitions used by Curray (1964), who implied no process associated with the event. Confusion arose due to the propensity to associate a lithostratigraphic unit with an implicit process, generally a change in RSL (Tooley, 1982). For example Köster (1971) discussed the idea of a "Baltic shoreline transgression", an impossible event since a shoreline cannot transgress. Jardine (1975) also erroneously defined transgression and regression as movements of the sea relative to the level of the land, irrespective of the cause.

When the lithostratigraphic unit under scrutiny is a sea level indicator, then it is tempting to associate changes in the sedimentology of the deposit with a change in RSL. For example, Tooley (1974) attempted to relate each of the fluctuations in his sea level curve for NW England to a minor sea level fluctuation, an error which was later redressed by Tooley (1982). Other examples of such interpretations include the curve produced by Sissons & Brooks (1971). Both Kidson (1982) and Haggart (1986) refer to the difficulty in attempting to relate lithological and/or vegetational changes to changes in RSL, since a combination of factors other than RSL changes can have an impact on the sedimentary record, particularly changes to the nature and the *rate* of sediment supply (Curray, 1964).

To avoid such problems, Shennan (1983) advocated the use of terminology such as increasing or decreasing marine influence to describe the contacts and reversals in coastal sedimentary sequences. Tooley (1982) described transgressive and regressive overlaps as sedimentary sequences displaying increasing and decreasing marine characteristics respectively. Haggart (1986) furthered this with the use of the *dominant tendency* in sea level, based on the interpretation of the deposit alone.

The possibility of such trends appearing at odds with the actual RSL trend was raised due to the fact that a sufficient supply of sediment could apparently offset a rise in RSL, creating a regressional sequence under such conditions (Kidson & Heyworth, 1976; Haggart, 1986; Pilkey & Davis, 1987; Leatherman, 1991). Unfortunately all of these definitions were designed specifically around the interpretation of intercalated clastic/organic sequences via microfossil analysis, and are clearly susceptible to misinterpretation, despite the assurances of Haggart (1986) that when all the data is considered together the dominant sea level tendency will become apparent.

Problems also exist with both the interpretation of deposits and the accuracy with which deposits are inferred to relate to a given sea level. Kidson (1982) pointed out that established sea level indicators frequently bore only a crude relationship to the sea level at which they formed. Quinlan & Beaumont (1981) recognized that a typical error envelope around a sea level curve is often much greater than the fluctuations the curve attempts to display. This is a particularly pertinent point when comparing the intricate sea level curves from Britain with the often much simpler curves from North American sites (usefully summarized in Pirazzoli, 1990). Kidson (1982) and Jardine (1982) reviewed the range of possible errors in relating sea level indicators to "sea level". Kidson (1982) regarded the representation of sea level information as a point on a graph as unrealistic, and was the first to advocate that the presentation of sea level fluctuations as a single curve was implying an accuracy impossible to attain given the nature of the deposits. Firth & Haggart (1989) proposed the use of the *indicative range* of altitudes within which a sea level indicator would be expected to have formed, based on contemporary analogues. These have been used to express the possible error range inherent in the sample prior to the addition of measurement error, and are shown in Table 2.1 (overleaf).

Landform	Indicative range (m)
Saltmarshes	0.30
Mudflats	0.35
Sand beaches	0.40
Shingle ridges	0.80

Table 2.1 Indicative ranges of contemporary landforms (source: Firth & Haggart, 1989)

The discussion so far has centred on the use of "traditional" sea level indicators such as intercalated clastic/organic sedimentary sequences. The use of other indicators (shells, driftwood, bones) has not been as widely accepted in British sea level studies as elsewhere (Andrews, 1970; England, 1983; Evans, 1989, 1990; Dyke *et al.*, 1991), due in part to a dearth of such material in the field plus a reluctance to use such material, in spite of potentially higher accuracy (Bradley, 1985). Such conservatism has also extended to the use of non-traditional forms of sea level indicator; in particular the shingle storm ridge. Steers (in discussion, Lewis & Balchin, 1940) described shingle ridges as "fickle structures", whose altitude bore little consistent relationship to the sea level which formed them. Firth & Haggart (1989) stated that shingle ridges in the inner Moray Firth bear little consistent relationship to other ridges around them, relating instead to the intensity of the process which emplaced them. However, the authors admitted that their study site actually contained no contemporary shingle ridges for detailed analysis to be carried out upon, and relied upon Gray's (1983) estimates of the ranges of shingle ridge structures, which provided an indicative range of 0.80 m (Table 1).

Despite such doubts, various reports suggest that shingle ridge structures can provide a useful framework of RSL changes. Lewis & Balchin (1940) were amongst the first to suggest that while absolute dates could not be obtained, suites of shingle ridges might be used with caution to reconstruct sequences of RSL events. They suggested that a change in the absolute height of a sufficient number of shingle ridge crests related to a change in RSL. This view was supported by Lake & Shepard-Thorn (1984) and Long & Fox (1988) in studies of Dungeness on the English south coast, where dating was undertaken using

historical maps of the coastline. A direct correlation was found between shingle ridge crest altitude and both the low RSL during the Roman period and the period of high RSL during the thirteenth century. Other studies employing shingle ridges as sea level indicators include Mitchell & Stephens (1974) (in Carter, 1983), and Stephens & McCabe (1977).

Whilst the use of individual shingle ridge structures as sea level indicators would not be advocated, provided sufficient numbers of ridges are present then trends in their crest altitude may be used to suggest trends in RSL, particularly if supported by absolute dating from nearby sites.

## **2.3 RELATIVE SEA LEVEL HISTORIES**

In order to understand the regional sea level history of the Moray Firth, it is important to place local events into a wider chronological framework. The aim of this section is to describe the sequence of events which have occurred on a global scale since the last (Devensian) glacial maximum, before discussing the shoreline response to these events in Scotland, and the Moray Firth in particular.

### **2.3.1 Global sea levels**

There is little doubt from the available literature that global sea levels have risen over at least the last 12 000 years. Global sea level changes are primarily a function of the build-up and decay of land ice (Clark *et al.*, 1978; Hansom, 1988), and subsequent impacts on the hydrosphere. Causative mechanisms are differentiated between *eustatic* and *isostatic* effects. Eustatic sea level changes represent changes in the shape and level of the global oceans, which exist in dynamic equilibrium with the gravitational field of the earth (Mörner, 1976; Dawson, 1992). Isostatic mechanisms represent changes in sea level caused by changes in the surface level of the land or the sea bed, either due to the effects of ice loading/unloading (Clark *et al.*, 1978) or due to tectonic activity, and as such are localized in their detailed response (Mörner, 1976; Pethick, 1984; Dyke *et al.*, 1991).

Such events have been responsible for changes in sea level of between 100 and 150 m over the Late Quaternary (Devoy, 1987; Pirazzoli, 1991). The close correlation between large-scale global sea level fluctuations and glacial/interglacial cycles becomes increasingly indistinct with age. Shackleton & Opdyke (1976) record between 17 and 20 glacial/interglacial cycles during the late Pleistocene. Only the last four glacial events can be recognized with

certainty in Britain, and only the effects since the last glacial maximum are of direct relevance to this study.

Attempts to construct a single, universally acceptable global sea level curve representing purely eustatic changes consumed much effort on the part of researchers during the 1960s since the production of an initial curve by Fairbridge (1961) (Figure 2.1). Curves claiming to show "global" sea level trends were also produced by Jelgersma (1966), Shepard (1963) and Mörner (1971) (Figure 2.1). While the form of all of these curves was largely similar, and the trends they displayed generally accepted, the *nature* of the fluctuations which they displayed proved to be extremely contentious. Fairbridge's (1961) curve utilized data from many sources, including tectonically unstable areas, and so the fluctuating nature of the curve could not be relied upon as an accurate representation of eustatic sea level trends. Additionally, Fairbridge's (1961) curve suggested that global sea levels had attained altitudes of up to 3 m above those of the present during the Holocene sea level maximum *ca.* 6000 BP. This was in sharp contrast to the smooth curve produced by Shepard (1963), which suggested that global sea levels during the Holocene had not exceeded those of the present. Jelgersma (1966) produced a curve of remarkable similarity to that of Shepard (1963), but was criticized on the grounds of its derivation from sites in the Netherlands, where net subsidence has occurred over the Holocene. The effect of subsidence was considered to be sufficient to mask any fluctuations, should they be present, and thus this curve was also discounted as a valid eustatic curve. Mörner (1971) produced what was perhaps the closest approximation to a true eustatic curve, being derived from southern Sweden, where the impacts of isostatic rebound were known in detail and could be closely controlled (Figure 2).

After the production of Mörner's (1971) curve, it was soon realized that the assumptions behind the entire concept of a single, universally acceptable sea level curve were fundamentally flawed. Developments in geophysics (Peltier & Andrews, 1976; Farrel & Clark, 1978; Clark *et al.*, 1978) produced a fuller appreciation of the actual mechanisms associated with changes in the relative proportions of ice and water on the surface of the earth, and demonstrated that eustatic changes occurred both discretely, and in conjunction with isostatic adjustments of the lithosphere.

As a result, the concept of a single, universally accepted eustatic sea level curve was finally abandoned (Mörner, 1976; Bowen, 1978; Kidson, 1982; Devoy,

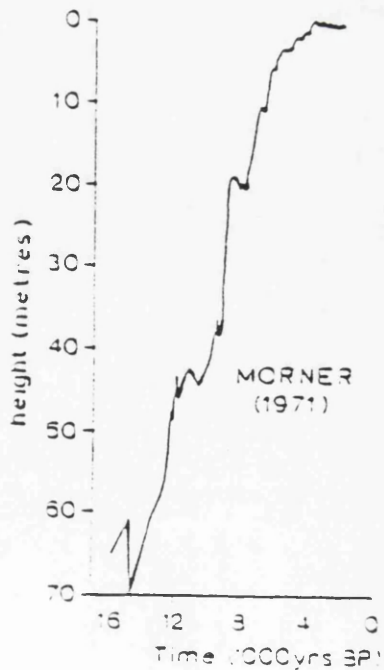
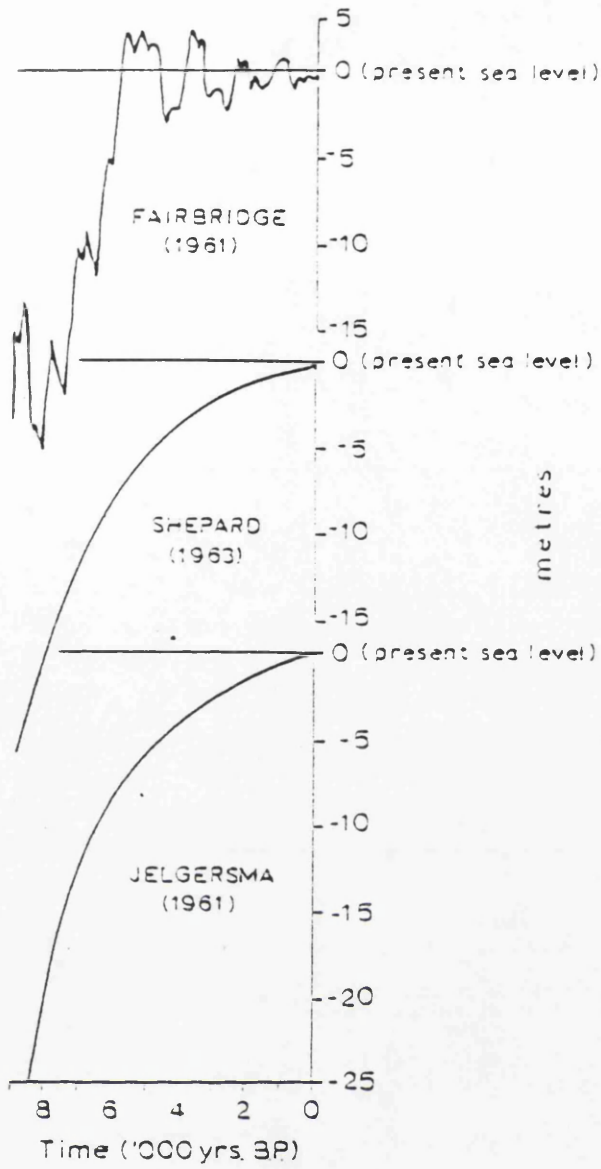


Figure 2.1 Eustatic sea level curves: a) Fairbridge, 1961. b) Shepard, 1963. c) Jelgersma 1961 (from Jelgersma, 1966). d) Mörner, 1971.

1987). The interplay of eustatic, isostatic and tectonic factors was finally accepted as producing untenable background conditions from which to attempt to derive a eustatic signal. From this acceptance came the concept of *relative* sea level changes, recorded on a local scale, and representing the movements of both land and sea level in relation to each other. This proved to be probably the most fundamental change in the study of former sea level changes, accepting that the effects of isostasy, eustasy and tectonic effects could not be realistically separated. Indeed, in terms of the geomorphological reconstruction of the sea level events recorded at a site, this approach is clearly more useful as it defines the total record of change, albeit locally, which can then be incorporated into a wider regional framework. The locally derived differences in the RSL histories of the sites can then be highlighted. Pethick (1984) summed up this final stage in the development of a strategy for the study of sea level changes:

"For us, as geomorphologists, relative sea levels are not a second best, but are an absolute requirement."

Despite the use of relative sea level studies as the accepted means of describing sea level events, the concept of a eustatic rise in sea level remains. Fairbanks (1989) produced a eustatic curve from corals in the tectonically stable Caribbean area (Figure 2.2). This shows that a rise in sea level of *ca.* 121 m has occurred since the last glacial maximum. Comparison between this curve and the oxygen isotope record for the North Atlantic suggested that the periods of fastest sea level rise were *ca.* 12 000 and 9500 BP. Much slower rates were recorded during the Younger Dryas, presumably as a result of the regrowth of ice sheets during this short period of climatic deterioration.

### **2.3.2 Scottish sea level histories**

Having described the trends in global sea levels over the Late Quaternary, attention can now be focussed on the interaction between global and local factors, and their implications for coastal development in Scotland.

Deglaciation led to a rapid fall in RSL around the Scottish coast after *ca.* 13 000 BP, and with continued isostatic rebound led to the abandonment of Lateglacial shorelines around the Scottish coast. Due to the relatively small size of the Scottish ice sheet, Lateglacial shorelines in Scotland are not found above *ca.* 40 m OD on the west coast (Dawson, 1992), with altitudes along the Moray Firth recorded by Firth (1984) at only *ca.* 25 m due to its distance from the centre of the former ice sheet. This fall in regional eustatic sea level continued to *ca.* -45

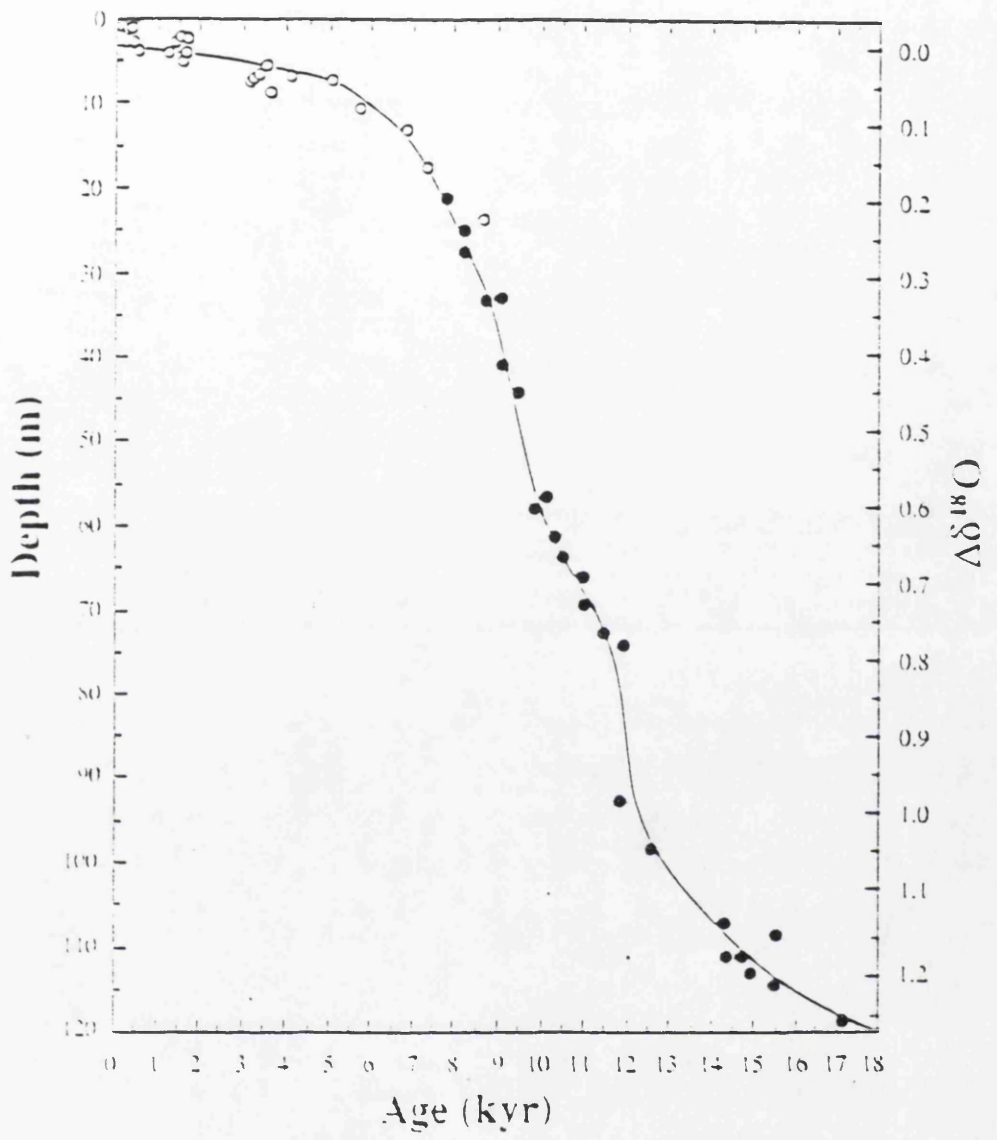


Figure 2.2 Eustatic sea level curve (source: Fairbanks, 1989)

m during the Younger Dryas (Mörner, 1971), forming shorelines now located at ca. 10-11 m ASL on the west coast of Scotland. Their proximity to the former ice centre suggests that approximately 55 m of glacio-isostatic uplift has occurred since the Younger Dryas (Dawson, 1992). This fall in RSL was reversed by a rapid rise in eustatic sea levels, caused by the decay of the Laurentide and Fennoscandian ice sheets (Fairbanks, 1989), which outpaced glacio-isostatic uplift in Scotland and caused a rise in RSL (the "Holocene Transgression") of up to ca. 9 m in the inner Moray Firth (Haggart, 1983). Once decay of these ice sheets was complete their effect on the eustatic signal effectively ended, but glacio-isostatic uplift in Scotland continued, heralding the onset of a period of falling RSL through until the present. Figure 2.3 shows the altitude of the Main Postglacial Shoreline (MPG), plotted as an isobase map to display the declining altitudes with distance east along the southern Moray Firth.

### **2.3.2.1 Firth of Forth**

The work of Sissons in the Forth valley during the 1960s heralded the beginning of rigorous levelling and dating of Late Devensian/Holocene marine deposits in Scotland. This work formed an informal "model" of RSL changes which dominated Scottish sea level studies until the 1980s. Sissons *et al.* (1966) provides a good summary of early studies in the Firth of Forth.

The oldest (steepest tilting) shorelines in the area were thought to have formed during the retreat of the Late Devensian ice margin. This was proposed from evidence of merging of outwash material into the upper raised shoreline sequence, and demonstrated the encroachment of the sea into the Forth area. This downwasting was followed by a readvance (the Perth Readvance, now discredited), which was dated from geomorphological evidence only as occurring not later than 12 000 BP, and which led to the formation of the Main Perth Raised Shoreline. A falling RSL was suggested to have followed the formation of the Main Perth, producing a fall in the altitude of raised shoreline features at altitudes below the Main Perth in the vicinity of Stirling. Sissons (1969) explained the presence of a buried gravel layer in the Forth as a product of a period of general erosion followed by this same low sea stand. Again the event was undated by absolute methods, but was placed as between 13 000 and 10 300 BP. This theory reappeared in Sissons' later work in the Beaully Firth (Sissons, 1981). A rise in RSL was thought to have occurred following this low stand to ca 6 m OD to form the Main Buried Shoreline (Sissons *et al.*, 1966) at ca. 9500 BP. A second falling period of RSL formed the Low Buried Shoreline at

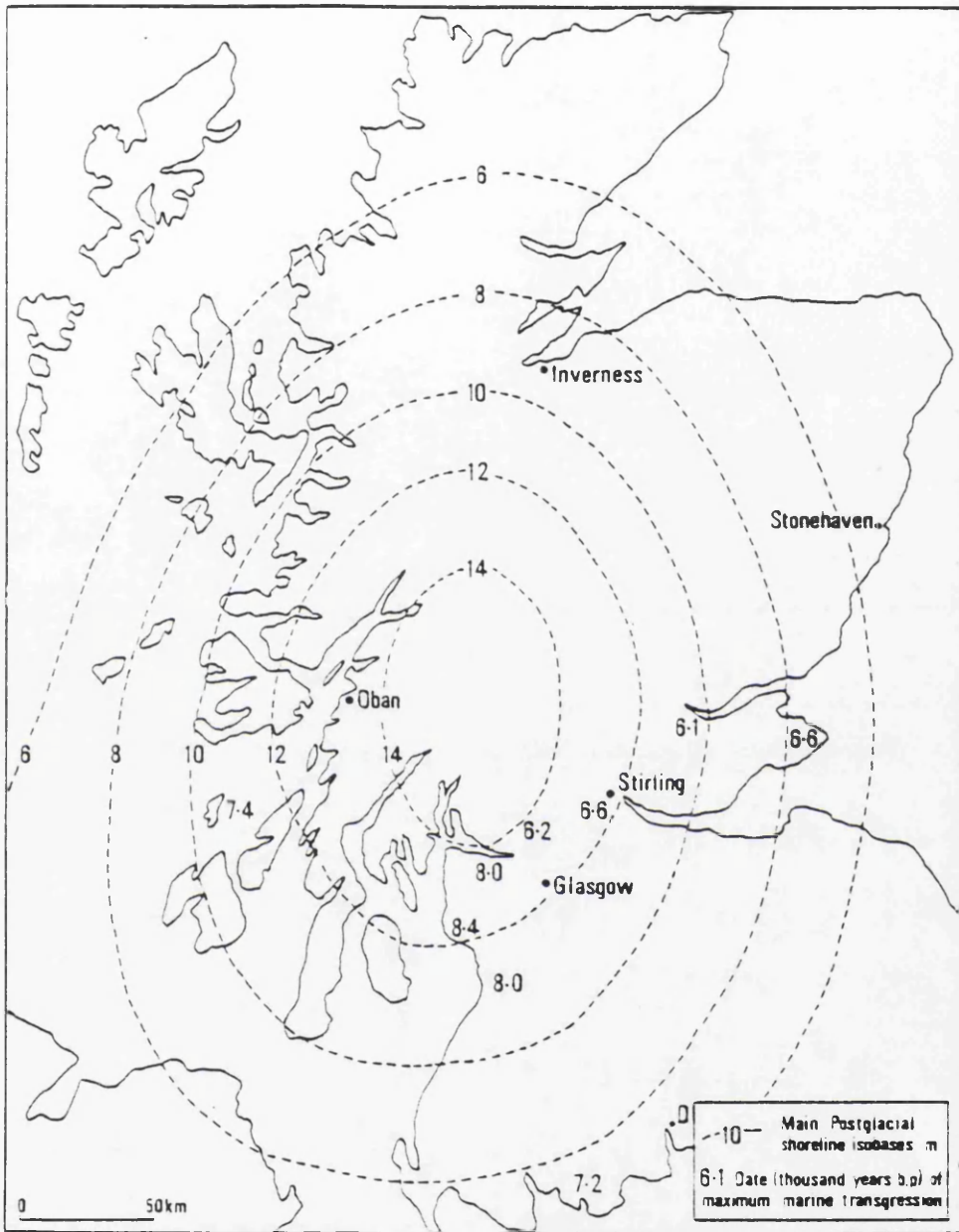


Figure 2.3 Isobase map of the Main Postglacial Shoreline (MPG) in Scotland (source; Price, 1983)

ca. 5.1 m OD, and which was abandoned by 8500 BP. RSL continued to fall before rising again during the rise to the Holocene sea level maximum (Sissons *et al.*, 1966; Chisholm, 1971), to form the MPG, (located between 16.3 and 6.6 m OD), before falling to approximately the present level.

### **2.3.2.2 Earn-Tay**

Using Sissons' work as a baseline, Smith *et al.* (1969) traced the Main Perth Raised Shoreline from the Forth valley along the Fife coast and into the Earn-Tay area. They recognized a slight difference in gradient along the feature ( $0.07 \text{ m km}^{-1}$ ) between the two areas, and interpreted this as demonstrating regional variation in uplift conditions, sediment supply, degree of exposure and estuarine configuration. The greater proximity of the Firth of Tay to the minor axis of the elliptical dome of uplift (centred approximately on Rannoch Moor) was believed to be responsible for the steeper gradient of the Main Perth in the Firth of Tay.

The sequence of deposits which had originally been interpreted as evidence of the Perth Re-advance event were suggested by Paterson (1974) to relate to an older ice sheet in the Perth vicinity, while Frances *et al.* (1970) thought that the sequence could also be deposited at the head of an advancing marine delta. Cullingford (1977) proposed that with the addition to his own field data there was insufficient evidence to support the concept of a Perth Re-advance, and the event was dropped from general useage thereafter.

Further work in the Earn-Tay system concentrated on the later Postglacial situation. Cullingford *et al.* (1980) dated the Main Postglacial Shoreline (9.8-10.2 m OD) to between 5900-7200 BP, broadly in agreement with Sissons *et al.* (1966) in the Firth of Forth. The sequence of sea level events in the Earn-Tay system began with a fall in RSL during the Late- or early Postglacial, with a series of stillstands or minor rises in RSL producing a staircase of estuarine deposits descending in both age and altitude. A later rise in RSL buried these shorelines and their surface peat deposits with estuarine clays (carse clays), providing good dating control on the burial event. A bottom peat date from the Glencarse site (transgression onset) produced a date of  $6679 \pm 440$  BP, and a top peat date (regression onset) of  $6083 \pm 40$  BP. An unexplained fall in RSL occurred between ca. 8500-7700 BP, possibly reflecting a similar fall in the Firth of Forth between ca. 8690-8270 BP.

Morrison *et al.* (1981) dated the culmination of the Holocene sea level maximum to between  $6679 \pm 40$  and  $6160 \pm 35$  BP at Glencarse in the inner Firth, whilst at St.

Michaels Wood in the outer Firth the culmination was found between  $7180\pm70$  and  $5890\pm95$  BP. These dates broadly correlated with those of Smith *et al.* (1985), who dated a rapid rise in RSL to the Holocene sea level maximum onset at ca. 7600 BP in the same area, culminating between  $6240\pm80$  and  $6030\pm80$  BP.

### **2.3.2.3 Montrose Basin**

Smith *et al.* (1980), working in the Montrose area found the same major trends as found in the Earn-Tay system. A pink silty clay, interpreted as a Late Devensian unit, was overlain by marine deposits and capped by peats which provided a date of  $7340\pm75$  BP. This peat growth continued with a minor interruption until ca.  $6930\pm60$  BP, when the deposition of the grey silty carse clays occurred during the Holocene sea level maximum, culminating at ca.  $6704\pm55$  BP.

In the Philorth valley, Smith *et al.* (1982) found a minimum date for the culmination of the Holocene sea level maximum of  $6095\pm75$  BP, with peat growth established on the resultant surface by  $5700\pm90$  BP. However this period of peat formation was halted by a possible second marine incursion suggested by the presence of a brown silty clay emplaced over peat, providing a minimum age of  $4760\pm60$  BP. The lack of any simultaneous event at any sites along the east coast suggests that the event may have been localized, although the authors maintained the inference of a true sea level event from the deposit.

### **2.3.2.4 Ythan Valley**

In the Ythan valley Smith *et al.* (1983) suggested the same general RSL sequence as above emerging from the north-east coast, with peat developed over an early Holocene gravel layer. These peats were buried by carse deposits which formed the highest Holocene deposit in the area. Again the carse clays were correlated with the Main Postglacial Shoreline (MPG) further south, both via altitude, degree of tilt and areal extent. The onset of the carse accumulation was dated to ca.  $6189\pm95$  BP, and ended at a maximum of  $4000\pm80$  BP.

### **2.3.2.5 Moray Firth**

The detailed relative sea level history of the Moray Firth will be addressed in section 2.6.5, and is outlined briefly here for comparative purposes.

Patterns in the trend of RSL movements in the Moray Firth are similar to those described for the remainder of the Scottish east coast sites described previously.

Falling RSL during the Lateglacial slowed to a low stand at the onset of the Loch Lomond Stadial (Synge, 1977; Haggart, 1987), but a postulated rise in RSL under renewed crustal depression was thought to have deposited a gravel layer across much of the coastal lowlands of the inner Firth (Sissons, 1981b). This unit is found at altitudes of up to 10 m OD at Barnyards in the Beaully Firth (Haggart, 1986, 1987).

A fall in RSL is suggested after this time based upon the interpretation of marine/brackish deposits at ca. 6.5 m OD capped with peat dated  $9610 \pm 130$  BP by Haggart (1986) (Figure 2.4). This falling RSL was thought to be complete by ca. 8700 BP, prior to the onset of the rise to the Holocene sea level maximum. A transgressive overlap in the Beaully Firth was interpreted by Haggart (1986) as evidence of RSL rising once more by ca. 8800 BP. The culmination of the rise was dated ca. 6500 BP, leading to the formation of the MPG at ca. 9 m OD in the Beaully Firth (Firth & Haggart, 1989), and at 6.8 m OD in the Dornoch Firth (Hansom & Leafe, 1990).

After the peak of the Holocene sea level maximum, falling RSL through to present is reflected in a series of raised Holocene shoreline features between 9 and 0 m OD along the southern Moray Firth coast (Firth & Haggart, 1989).

### **2.3.2.6 Summary**

To summarize the sea level history of the east coast of Scotland, a Postglacial low sea stand envisaged for the period prior to  $8344 \pm 143$  BP (Morrison *et al.*, 1981), was followed by a widespread transgressive event (rising to the Holocene sea level maximum) between this date and  $6095 \pm 75$  BP (Smith *et al.*, 1982). RSL then fell, with a possible series of minor stillstands until the present (Smith *et al.*, 1982).

A notable feature of the marine deposits of the Scottish east coast deposits has been the identification of a micaceous silty sand found within the transgressive carse clay deposits. Dates from peats found within the carse clays around the micaceous sand layer have provided dates of;

$7140 \pm 120$  BP (Smith *et al.*, 1980)

Between  $7050 \pm 100$  &  $7555 \pm 110$  BP (Morrison *et al.*, 1981)

$6850 \pm 40$  BP (Smith *et al.*, 1983)

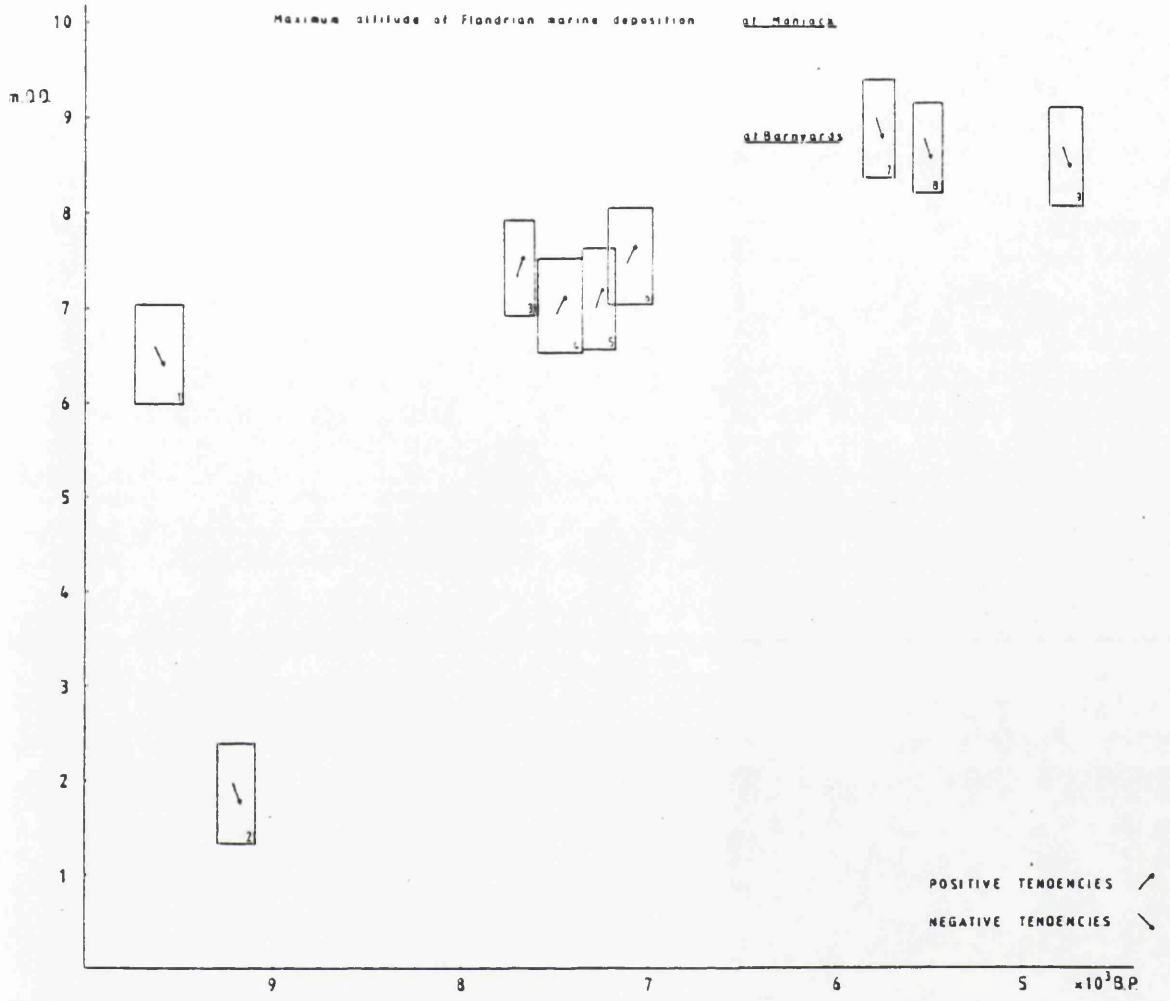


Figure 2.4 Relative sea level trends in the Beaulieu Firth (source: Haggart, 1983)

After 7080±85 BP (Dawson *et al.*, 1990)

This deposit has been interpreted as representing a high magnitude, low frequency event by Dawson *et al.*, (1988). They suggested that the layer may have been deposited by a tsunami event, possibly a result of one of a series of large submarine landslides known to have occurred off Norway (the Storegga Slides). The lack of sorting and presence of tythropelagic (deepwater) diatoms in the deposit would appear to provide support for this mode of formation. One of these events, the second Storegga Slide, has been dated as occurring *ca.* 7000 BP, which broadly correlates with the dates from the Scottish east coast.

From this review of the RSL histories of various sites around the coast of NE Scotland, it is clear that while a generally accepted series of sea level events has been established, local differences occur in the coastal response to these imposed changes. Driven primarily by the availability of sediment, these differences make the establishment of a RSL history essential for a detailed study of the genesis of Culbin.

## 2.4 CONTEMPORARY COASTAL PROCESSES

### 2.4.1 Tides and tidal currents

The Moray Firth experiences semi-diurnal tides, with high water occurring approximately every 12.5 hours. The flood tide flows southwards along the Caithness coast having entered the North Sea from the open Atlantic via the Pentland Firth. The tidal wave travels through the North Sea, is reflected from the northern European coast and travels northwards again as the ebb tide. The entire journey takes three tidal periods (Pethick, 1984).

Examination of the North Sea tidal wave in the Moray Firth (Lee & Ramster, 1981) shows that the flood tide flows south down the coast of Caithness and Wester Ross, and then eastwards along the southern coast of the Moray Firth. Current reversal on the ebb tide produces westwards flow into the Moray Firth and northwards deflection towards Caithness. However, Dooley (1971) recognized that along the southern coast of the outer Moray Firth an easterly flowing current exists for up to 9 hours out of the 12 hour tidal cycle. Early work (Craig, 1959; Payne, 1963) also recognized this element of the tidal pattern of the southern Moray Firth, and attributed it to an eddy-like circulation pattern existing in the Firth, an idea which was not totally unsupported by Reid & McManus (1987). In the offshore zone at Culbin, Craig (1959) demonstrated a "usual" net bottom water movement trending south from the Easter Ross coast, displaying a marked east-west divide in the vicinity of Culbin, with currents flowing both into the inner Firth and eastwards towards Spey Bay, a feature also recorded by Reid (1988).

The height of the tide determines the level at which coastal processes operate on the beach profile. Komar (1976) describes micro-scale changes in topography occurring on the beach profile due to the detailed migration of the location of the breaker zone.

Tidal streams produce a measureable tractive force, which has implications for sediment transport at and near the sea bed. Such relationships are described by the Hjulstrom curve and its derivatives (Leeder, 1982; Briggs & Smithson, 1985). Tidal currents are prone to reversal near the foreshore, but further offshore are rotatory (King, 1972), with the swing in direction from flood to ebb taking a longer period. The difference between the vectors of tidal transport in either direction over a single tidal cycle defines the *residual tidal current* (King, 1972). This in

turn defines the net movement of water and sediment in suspension, and is therefore an important element in sediment transport studies. Sediment transport is a cube function of tidal current velocity, and thus a small residual current may be responsible for considerable net sediment transport (Belderson *et al.*, 1978; Leeder, 1982). Leeder (1982) also points out that increased turbidity intensity during decelerating tidal flow may lead to increased sediment transport than during increasing tidal flow.

Techniques for measuring tidal currents are summarized in Pethick (1984) and Hemsley *et al.* (1991).

#### **2.4.2 Waves and wave theory**

Waves comprise the most important energy source to the foreshore, and are mainly responsible for sediment transport and landform development in the littoral zone. The term "wave" covers features with periodicities ranging over more than 8 orders-of-magnitude, from water ripples (capillary waves) to oceanic-scale tidal waves (Leeder, 1982). Of primary concern to this report are features of up to  $10^1$  seconds.

Most of the energy arriving at the shoreline is contained in wind-generated progressive waves (UN, 1982). The distinction is made between locally generated wind waves (sea waves) and waves generated in the open ocean and which have travelled to the point of measurement (swell waves). Sea waves are typically irregular in wavelength and frequency, whilst swell waves are smoother in appearance and display more regular wavelength and frequency (UN, 1982).

The rigorous physical investigation of waves involves the assumption that the sea surface is approximated by waves of different shapes. Two of the earliest wave forms proposed were the Airy wave (sinusoidal) and the Stokes wave (a form of solitary wave) (Komar, 1976; Leeder, 1982). These two wave forms were sufficient for explaining deep water wave propagation, but were insufficient to describe subsequent shallow water transformations, and so two further forms were developed; the cnoidal wave and the solitary wave (Komar, 1976). Of these the solitary wave form has been generally adopted as the most realistic form for use in shallow water wave transformation calculations.

### 2.4.3 Shallow Water Wave Transformations

As a wave approaches the coast it undergoes transformations in both magnitude and direction, although its period remains constant. The wave decreases in velocity and wavelength, with a subsequent increase in height (law of conservation of energy), and if travelling at an angle oblique to the coastline it will refract. The increase in height is due primarily to the effect of shoaling but is also related to the degree of refraction experienced. Corrections for these effects are outlined by CERC (1984).

Wave refraction occurs when a wave train approaches the coast at an oblique angle and has been described as "...the most important process on the continental shelf...resulting in the observed non-uniform wave energy distribution over the shelf and along the nearshore zone." (Goldsmith, 1976). Refraction occurs as the direction of travel of a wave train changes so that individual crests bend to parallel the sea bed contours in order to maintain stage equal to wave phase velocity (Komar, 1976; Pethick, 1984). This process is outlined in Figure 6. The amount of refraction which occurs is governed by Snell's Law of optical refraction:-

$$\begin{aligned}\sin\alpha_1 &= C_1 = L_1 \\ \sin\alpha_2 &= C_2 = L_2\end{aligned}\tag{1}$$

where  $\alpha$  = angle between the wave crest and the shoreline

C = wave velocity (celerity)

L = wavelength

The law of conservation of energy between orthogonals (rays drawn at right angles to the wave crests) means that when plotted, a diagram showing convergence of orthogonals suggests focussing of wave energy, while divergence of orthogonals results in the spreading of wave energy (Komar, 1976).

Wave refraction modelling involves the "generation" of wave crests in deep water, plotting their route across the sea bed and finally analyzing the resultant wave parameters at the shoreline once the various shoaling transformations have taken place. This procedure was originally carried out graphically (eg Johnson *et al.*, 1948), but is now usually generated by computer. The output from these exercises was formerly qualitative, with identification of potential areas of

erosion and deposition estimated from the convergence or divergence of orthogonals (Fico, 1978). However, modern computer generated wave refraction models have made the quantitative analysis of refraction plots possible, making the method a much-used tool in the study of longshore sediment movement (eg Davidson-Arnott & Amin, 1974; Goldsmith, 1976; Carr *et al.*, 1982; Mason, 1985, Mason & Hansom, 1986).

The importance of waves approaching the coast at an oblique angle can be understood if the transfer of wave energy at the coast is resolved into its perpendicular components, as demonstrated in Figure 2.5. Oblique wave attack results in the creation of a shore-parallel current in the vector direction  $E_L$ , the magnitude of which being defined primarily by the angle between the wave crest and the shoreline ( $\alpha$ ). This *longshore wave energy flux* ( $P_L$ ) was defined by Komar (1976) as:

$$P_L = ECn \sin\alpha \cos\alpha \quad (2)$$

where  $E$  = wave energy (J)

$Cn$  = wave phase velocity ( $m\ s^{-1}$ ) ( $n = 1$  in shallow water)

$\alpha$  = angle between wave crest and shoreline ( $^\circ$ )

$P_L$  effectively defines the flux parallel to the shoreline of momentum directed towards the shoreline ( $ECn$ ). Komar & Inman (1970) found no dependence between this function and the slope of the subject beach in their study, and so this equation has become the standard for longshore power calculations.

Once calculated, this equation must be transformed to account for a longshore sediment transport rate. Komar & Inman (1970) defined a relationship between  $P_L$  and a longshore sediment transport rate ( $S_L$ ), which when converted to SI units became:

$$S_L = 0.77 P_L \quad (3)$$

When applying these formulae it must be considered that they do not account for long term sediment transport, which is more correctly defined as the sum of all wave effects over a given time period (Leeder, 1982). Along a given stretch of coastline the incident wave spectrum will consist of a series of different wave conditions operating for variable periods, with the interplay at the shore of both locally generated sea waves plus swell waves (Pethick, 1984; CERC, 1984). The

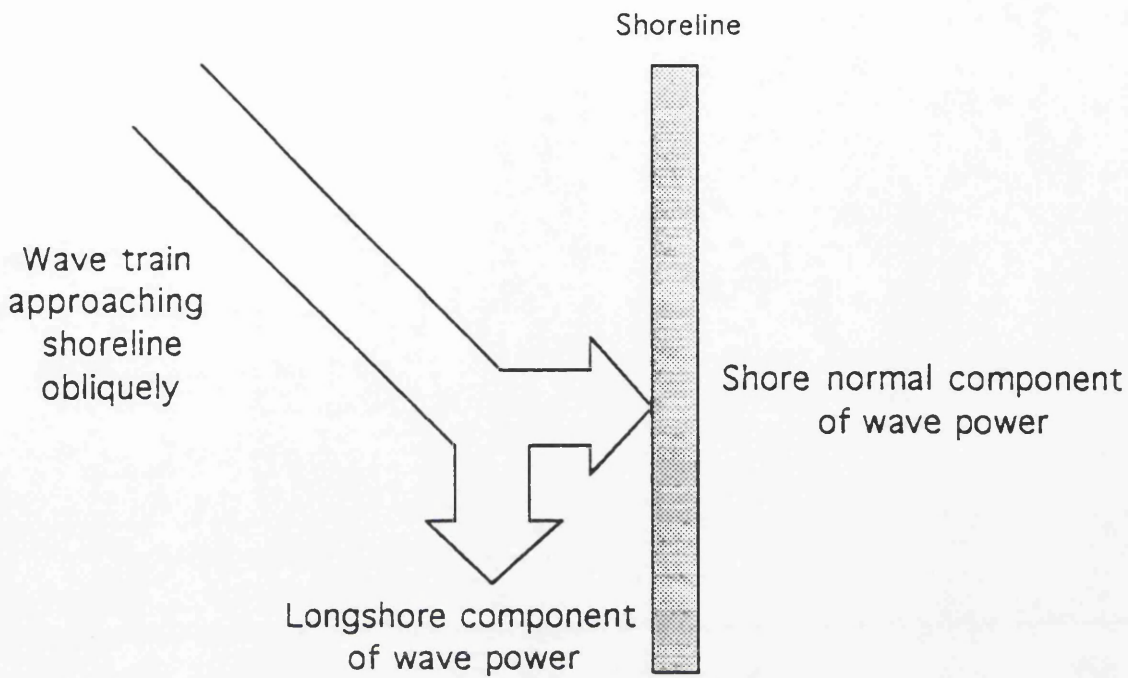


Figure 2.5 Resolution of an incident wave into shore-normal and shore-parallel components

long term sediment transport value obtained from studies such as these must account for the entire wave spectrum encountered at a site.

At this juncture two points should be stressed. Firstly, these equations produce *potential* values of longshore sediment transport, and as such when used in practice should be calibrated against field measurements. Secondly, they refer only to the transport of *sand*, and as such are not reliable indicators of the potential transport of shingle under similar boundary conditions.

#### **2.4.4 Wave Recording**

The equations described above have been shown to be extremely sensitive to input wave height and direction. It was thus essential that an accurate record of the wave spectrum at the field site was obtained if the calculation of sediment transport by waves was to be as accurate as possible.

Wave recording in the field has been attempted in a variety of ways. The parameters which are of most importance in coastal studies are wave height, wavelength and direction of travel. Measurement has been undertaken ranging from the simplest visual estimates (eg Balsillie & Carter, 1984), a variety of electronic devices such as sparkers, wave wires and pressure transducers (outlined in Hardisty, 1988, 1990) through to remotely sensed methods involving high frequency radar (eg Wyatt, 1990). The main problem with wave data is that it is difficult to obtain a long, unbroken record due to the frequently harsh operating environment, which is not conducive to the longevity of sensitive electronic measuring devices (Hemsley *et al.*, 1991).

The single most difficult parameter to measure accurately has been wave direction. Wind direction is often substituted as a surrogate variable for wave approach, and simultaneous logs of windspeed and wave height show a positive relationship (eg MAREX, 1975). These demonstrate that hindcasting wave parameters from available meteorological data can be a useful method if no other data is available (eg Davidson-Arnott & Pollard, 1980). Hindcasting techniques fall into two categories; a simple method for producing a single wave height/period (the Sverdrup-Munk-Bretschneider method) and a complex but more realistic wave spectrum model. Both of these are outlined in Komar (1976) and CERC (1984). The lack of directional wave recording appears to be a serious deficiency in available coastal literature. As noted above, equations predicting longshore sediment transport to the input wave approach angle are extremely sensitive to the value of the input angle of incident wave approach,

and the lack of detailed attempts to measure such a critical parameter under field conditions is a problem towards which more effort should be directed.

Fully directional wave recording has only recently become a practical proposition due to the availability of equipment capable of logging at the high frequencies required for the differentiation of individual wave crests. Hardisty (1988, 1990) outlined methods for the construction of low cost, directional wave recorders, but these are designed only for relatively short deployments. Longer term deployments of wave recorders tend to rely on more expensive systems such as waverider buoys.

#### **2.4.5 Beach sediment budgets**

Waves, and to a limited extent tides, form the primary energy sources at the coast. Expenditure of energy results in the entrainment and/or transport of sediments, and thus these elements represent the main driving forces behind the beach sediment budget.

The concept of the beach sediment budget has been used with varying degrees of success to identify individual components of the coastal sedimentary system. Once highlighted, this information can then be used to tackle specific problems associated with either sedimentary depletion or accretion at the site scale. Thus the method is potentially of great value in the field of applied coastal geomorphology, where knowledge of even such basic precepts as whether the sediment budget for an area is either positive or negative is vital if the medium-long term development of the beach is to be understood in the future.

The sediment budget depends on the principle of the conservation of mass of sediment in the littoral zone. Specifically the method requires the careful definition of an operating unit, or coastal compartment;

"...a unit within which it is theoretically possible to compute sediment gains and losses and so arrive at a quantitative budget statement." (Clayton, 1980).

Within this unit the rate of change of the volume of sediment within the compartment depends on the rate of input of sediment in relation to the rate of output (Komar, 1976). A net deficit of sediment resulting from losses to the compartment outweighing the gains produces a decline in the volume of sediment on the beach, and vice versa.

The sediment budget thus attempts to quantify all of the inputs and outputs to the coastal compartment. Table 2.2 lists all of the possible inputs and outputs of sediment which may affect a coastal compartment, or cell. Not all of these factors will affect any one cell or site, and the applicable factors for each site must be identified.

Inputs	Outputs	Balance
Longshore in	Longshore out	Beach erosion/deposition
Onshore	Offshore	
Aeolian in	Aeolian out	
Beach nourishment	Beach mining	
Cliff erosion	Solution and abrasion	
Fluvial	Loss to submarine canyons	
Hydrogenous	Infill of inlets	
Biogenous		

Table 2.2 Elements of the beach sediment budget (modified from Komar, 1976).

The sediment budget is however somewhat more difficult to construct than its simple nature suggests (Carter, 1988), although if applied correctly the method is potentially very powerful as a predictive tool in coastal erosion problems (Allen, 1981; UN, 1982).

The sedimentary cell requires careful definition and ideally should be *morphodynamically* defined in order to provide meaningful conclusions for the sediment budget. In a simple scenario the boundaries may be defined by marked breaks in foreshore continuity such as a headland-bay-headland situation. Frequently though the cell boundaries are not geomorphologically defined and require the assumption that the boundaries of the cell allow unhindered convective transport (throughflow) (Carter, 1988). This can cause problems in the

quantification of a sediment budget, and caution should be taken in the definition of cell boundaries.

A significant difference exists between the *potential* and the *actual* sediment budget (Carter, 1988). The potential sediment budget is usually calculated from a modelled wave refraction series run at a site, which provides a value for potential total longshore transport of sediment. This takes no account of on-site factors, and simply provides an upper transport limit as defined by input waves and currents (Carter, 1988). The actual sediment budget may be lower than the potential value, for example if the actual availability of sediment is lower than that predicted (eg Allen, 1981; Mason & Hansom, 1988). Such values are used as a useful calibration of the modelled values, and tend to be derived from beach profile data taken ideally over periods greater than one year (eg Walton, 1977; Walton & Polpura, 1977). Examples of the application of beach sediment budgets have been reported from the Great Lakes (Davidson-Arnott & Amin, 1974; Davidson-Arnott & Pollard, 1980), eastern USA (Allen, 1981; Bruun, 1984), East Anglia (Vincent, 1979) and Holderness, UK (Mason, 1985; Mason & Hansom, 1988).

The main problem with the estimation of a beach sediment budget stems from the often unknown value of the on-offshore component of sediment transport (Carter, 1988). Clayton (1980) considered that while this component of sediment transport is important, if rates of longshore transport are high, then these will probably dominate the sediment budget. On-offshore transport is frequently used as the 'balancing' item in calculated beach sediment budgets, as in reality inputs rarely equal outputs. This use is accepted as valid in the face of the difficulties inherent in attempting to quantify the shore-normal element of sediment transport (Komar, 1976; Carter, 1988). Numerical attempts have been made to quantify the on-offshore element of beach sediment transport (Hardisty, 1984; Hardisty *et al.*, 1984). The equations produced by Hardisty require detailed measurement of post-breaking conditions on the foreshore in order to calculate swash and backwash velocity. While potentially useful, these equations require an enormous amount of field effort and equipment for relatively short data runs, provide only potential rates of transport, and are assumed to break down under a predominantly longshore-driven system, precluding their use in this study.

Provided that the sediment budget is calculated over a sufficiently long timespan, preferably greater than a year (Clayton, 1980), and ideally up to ten years, then the method can provide realistic and useful predictions regarding volumetric

beach changes. The art of the beach sediment budget is the evaluation of the inputs and outputs so that the outcome of these predictions matches field based measurements of gross scale changes in beach volumes (Komar, 1976).

So far the primary energy inputs to the foreshore have been described. The impact of these processes on coastal sediments can be quantified using the beach sediment budget. However, quantification of the response of the foreshore to incident variables forms only one aspect of coastal development. In order to appreciate more fully the range of landforms which are found at the coast, a more detailed investigation of their formative processes and distinctive morphology is required.

#### **2.4.6 Shingle Beaches:- processes and landforms**

In order to understand the nature of the depositional processes responsible for the emplacement of the Culbin shingle ridge sequence throughout the Holocene, it is necessary to examine available literature concerning the more specific aspects of coarse, clastic beach formation. Due to the differences in the depositional process environment of shingle beaches, a body of literature concerning this aspect of contemporary coastal geomorphology has developed parallel to the literature primarily concerning sand beaches.

A division exists within the literature concerning shingle dynamics in the coastal zone. Early studies tended to concentrate on the resultant landforms (eg. Lewis, 1932, Lewis & Balchin, 1940), and in particular on the larger examples of shingle based landforms (eg. Dungeness, Orfordness). Later work concerned itself with the processes and detailed sedimentology of shingle movement in the coastal zone (eg Bluck, 1969; Orford, 1975). Only within the last decade has any attempt been made to combine studies of both sedimentology and landform evolution in order to understand the process-reponse dynamics of shingle based landforms, and with reference to past and present responses to changes in relative sea level.

##### **2.4.6.1 Shingle beaches:- processes**

The formation of shingle storm ridges was critically assessed by Orford (1977). Early theories on the formation of shingle storm ridges stressed the importance of "destructive" waves, which, upon breaking, would throw shingle forwards (King, 1972), whilst simultaneous beach face saturation would enhance gravity-aided backwash. This would lead to the deposition of a coarse upper beach deposit,

while the accompanying backwash would remove the finer beach fraction offshore. Orford (1977) argued that while such processes can be observed on shingle beaches, their scale of operation would be too small to account for the emplacement of a shingle storm ridge at the top of the beach profile. He proposed a mechanism for storm ridge modification based upon the incidence of spilling breakers coincident with storm surges at the tidal maxima. Such conditions would be most likely to produce the required hydrodynamic environment necessary to produce an asymmetric, onshore force through which the upper storm ridge crest could be modified.

Longshore shingle sorting has been investigated by Carr (1969) on Chesil Beach. The extreme degree of longshore sorting on Chesil Beach has long been a source of debate (Coode, 1853; Prestwich, 1875). Chesil presently receives very little fresh shingle (King, 1972), and represents an essentially relict deposit (Carr & Blackley, 1972, 1974) which continues to be affected by contemporary processes. With little new shingle being added to the beach, shingle sorting is closely related to the amount of wave energy received. The east end of the beach is exposed to the majority of high energy wave activity from the Atlantic, and consequently displays the highest mean clast size, with a reduction in clast size with distance west as increasing shelter from incident swell produces lower energy conditions. Underwater studies by Neate (1967) finally disproved the unlikely suggestion that grading of shingle below LWST along Chesil Bank was opposite to that found along the foreshore. The relationship between wave energy and shingle mobility was also recorded by Kidson (1963). Tracer experiments suggested possible preferential transport of larger material alongshore (Carr, 1969). Further tracer studies recorded extremely high short term rates of shingle transport along Chesil Beach, reaching a maximum of 343 m day<sup>-1</sup> (Carr, 1971). However this rate was not sustained, and after 165 days the tracers were only 3952 m from their origin, suggesting burial of shingle was effective in temporarily immobilizing it. Additionally, changes in the angle of wave incidence on the beach caused temporary reversals in the direction of longshore sediment movement, again reducing the net transport rate alongshore (Carr, 1971). The longshore effects of clast shape recognized by Dobkins & Folk (1970) were recognized in the short term, with evidence of a relationship between clast 'c' axis length and distance travelled. However, in the longer term this relationship decayed due to the variable angle of wave incidence experienced on Chesil Beach (Carr, 1971).

Studies of shingle mobility at Orfordness (Suffolk, England) by Kidson *et al.* (1958) were undertaken using clasts from the natural beach population coated with radioactive barium 140. The spit at North Weir Point has extended south from Orfordness by approximately 16 km (Carr, 1965), deflecting the course of the River Alde and creating a complex series of elongate shingle ridges. Despite a net southerly extensional trend, under winds from the southern sectors all of the tagged clasts were recorded as moving north along the spit, with a maximum migration of 2.2 km in four weeks, and a mean of 0.6 km. However, once waves were generated from a northern sector, shingle movement was abruptly reversed. A net southerly migration was recorded even under the incidence of low (0.6 m) waves, leading to the rapid migration and eventual loss of shingle from the tip of the spit. Similar effects were recorded on the mixed sand and shingle spit at Blakeney (Norfolk, England) by Hardy (1964), where the suggestion of a "drift parting" leading to the separation of fine and coarse shingle was thought to be caused by the influence of waves from different sectors. Hardy (1964) considered Blakeney spit to be an essentially relict feature, (as at Chesil), with little or no fresh shingle being introduced. A strong size gradient was recorded along the spit, with a reduction in clast size with distance west. However, the lack of significant erosion along the length of the spit suggested that while transport of shingle clearly occurred in either direction under different wave approach, little loss at either end was experienced.

Carter & Orford (1984) discuss the importance of the proportion of sand to shingle in the beachface in terms of the possibility of transition from reflective to dissipative beachface conditions. They suggest that low volumes of interstitial sand in a predominantly shingle beach face will allow continued percolation and throughflow of back-beach water and swash, maintaining a high storm ridge and preventing comb-down. However, when infilling of inter-clast spaces reaches matrix capacity, excess sand will become available for the production of a low-angled, dissipative sand beach fronting the shingle storm ridge, possibly leading to increased mobility of the shingle on the upper beachface through decreased swash percolation. Once sand becomes dominant, the increased mobility of shingle may produce "overpassing" of sand by the coarser shingle (Carr, 1971) due to its larger mass and hence propensity to remain in the surf zone (Evans, 1939). Zenkovitch (1967) suggested that in situations where sediment supply is low, this may lead to downdrift coarsening of sediment.

The submarine mobility of shingle was investigated by Steers & Smith (1956) at Scolt Head Island (Norfolk, England). Using radioactive tracers, albeit of a

slightly lower specific gravity than the host population, they recorded movement of shingle at ca. 8 m depth of water under wave conditions of only 0.6-1.0 m, and current speeds of  $1 \text{ m s}^{-1}$ . Kidson *et al.* (1958) attempted to bracket this depth in order to delimit a critical depth below which shingle was found to be immobile. Work at North Weir Point (Orfordness) found no movement at a maximum depth of 9m, despite windspeeds of up to  $10 \text{ m s}^{-1}$  creating relatively high energy conditions at the time of tracing. Neate (1967) recorded a "dead" shingle zone at ca. 10 m depth offshore from Chesil Bank, above which shingle was clearly fresh and mobile, but within which the shingle was weed and barnacle encrusted. In contrast, King (1972) recorded mobile shingle at depths of 57 m between the Isle of Wight and Hurst Castle spit on the English south coast, due to exceptionally high tidal currents in this area (up to  $2.3 \text{ m s}^{-1}$ ) rather than wave generated bottom currents, as in the earlier studies.

These submarine studies demonstrate a generally consistent picture of shingle becoming immobile below a critical depth of ca. 9 m, unless exceptional conditions occur, such as high magnitude storm events (Neate, 1967) or strong tidal currents prevail (King, 1972).

#### **2.4.6.2 Shingle beaches:- geomorphology**

The geomorphology of shingle ridge systems has been summarized from the study of both large multiple ridge sequences, individual shingle ridges and some common details from shingle barrier systems.

Shingle beaches in Britain as a whole owe their existence primarily to the onshore forcing of sediment of all grades during rising RSL leading to the Holocene sea level maximum. Rising RSL "bulldozed" sediment deposited on the exposed inner continental shelf floor onshore (Kidson, 1977; Pethick, 1984), creating a potentially vast store of mixed grade sediment in the nearshore zone from which beaches could form in close relation to the incident energy conditions to which they were exposed. This has led to the construction of shingle beaches in areas unlikely to support such structures today, such as Chesil Beach (Dorset)(Carr & Blackley, 1972, 1974). Thus with a failing supply of sediment to the coast, shingle structures in Britain are frequently out of sedimentary equilibrium with their contemporary environment, and their continued existence is due in part to their dynamic nature. Such a concept is not confined to British shingle environments, and Shaw & Forbes (1990) suggest a similar genesis for the landforms of north east Newfoundland.

Altitudes of shingle beaches are typically significantly higher than contemporaneous sand beaches, relating primarily to formation and modification under storm wave activity (Orford, 1977). The highest recorded altitude of a shingle beach in Britain is at Chesil Beach, where the ridge crest attains 13.1 m above HWM at its eastern extremity (King, 1972). Similarly, gradients of shingle beaches are also higher than their sand counterparts, relating to the size of the constituent material. Shepard (1963) reported beach face slopes of up to 25° on cobble (i.e. coarse shingle) beaches, approaching the critical angle of repose (32°) at which loose sediment can be sustained (Komar, 1976). The degree of sorting is critical in the establishment of the beach face gradient. McClean & Kirk (1969) recognized a levelling in the mean beach face gradient with increasing grain size due to the presence of interstitial sand on mixed sand and shingle beaches in New Zealand.

Recurving of shingle ridges at their distal ends has been reported from most major shingle landforms. Early work (eg Steers, 1926) frequently invoked tidal eddying as the formative process leading to recurving. However, it was also Steers (1926) who suggested that recurving could occur due to the influence of waves approaching the distal end of the landform from directions other than the "dominant" (i.e. net formative) sector. Thus while the supply of sediment to the distal end continues, the foreshore rapidly swivels to face the incident wave crests (Lewis, 1938), creating recurves related to the incidence of more occasional waves. Refraction of waves from the dominant sector also enhances the supply of sediment around the tip of the distal portion, (King, 1972), although refracted waves may contribute little to the actual construction of a storm ridge.

The largest shingle ridge sequence in the country is found at Dungeness on the south coast of England. The feature covers 259 km<sup>2</sup> (Cunliffe, 1980), and displays a series of fronting shingle ridges enclosing the extensive low-lying marshlands of Romney Marsh and Denge Marsh (Green, 1968). The ridges were divided into five discrete populations (or 'beaches'), separated by areas of alluvial fill (Green & McGregor, 1986; Long & Fox, 1988). These beaches have also been delimited on the basis of ridge/trough altitude, amplitude and orientation (Long & Fox, 1988).

Levelled transects across the ridge sequence at Dungeness (Lewis & Balchin, 1940; Long & Fox, 1988) revealed much information concerning the altitude, orientation and density of ridges. Ridge density varies between 32-62 ridges km<sup>-1</sup> (Lewis & Balchin, 1940), although estimates of numbers vary in

detail (Eddison, 1983; Green & McGregor, 1986). Widths of the ridges is between 16-28 m, with ridge flank gradients recorded between 2 & 8° (Green & McGregor, 1986). The anastomosing nature of the Dungeness ridges is a feature of note, particularly at the distal ends (Lewis & Balchin, 1940; Green & McGregor, 1986). "Parasitic" ridges are also common, represented in the field as bifurcation structures fragmenting the continuity of the main ridge crest. Coupled with inter-ridge recurve features, the presence of parasitic ridges makes the tracing of an individual ridge crest extremely difficult. The altitude of the ridge crests was reported by Lewis & Balchin (1940) as bearing little relationship to the adjacent trough altitude. However, Long & Fox (1988) reported a correlation coefficient of 0.88 between these two variables, suggesting a stronger relationship than originally thought. Altitudes of the ridges was seen to vary along their length slightly, with a more significant fall at the "bend" of the foreland (Lewis & Balchin, 1940), possibly as a response to decreased wave energy at this point.

Carr (1965) also reported variations in altitude of only 3-4" (5-7 cm) over a mile (1.61 km) along straight sections of the spit at North Weir Point (Orfordness), although variations increased on the recurved sections. This feature differed from Dungeness in that it had formed as a spit across the mouth of the River Alde, extending south for approximately 16 km. Development of the spit through wave activity varying from north-northeasterly through to south-southwest has led to the formation of a series of recurves at the distal end, although under sustained wave attack from the southern sectors, the distal recurves have been completely destroyed. Despite extensive removal of recurves being recorded on three occasions between 1955 and 1965, the rate of reformation actually exceeded the long term mean annual extension rate of the spit (*ca.* 33 m a<sup>-1</sup>), although extension on an annual basis was described as erratic. Similarly, Steers (1926) reported that the spit attained its greatest length in 1897, but storms during that year removed approximately 1 mile (1.6 km) of the distal end, forcing this shingle onshore to form the irregular shingle formation of Shingle Street, now attached to the mainland. Landward translation of the spit was not recorded at North Weir Point due to the presence of high current velocities and depth of water in the River Alde. Development of the ridges was seen as extensional, but with the addition of younger ridges to the seaward face of older ridges, merging with them at both the distal and proximal ends. This was considered problematic, in that while it would be simple to differentiate two sequential ridges formed at different times in a central section of the spit, at either of the end sections apparently continuous ridges could represent features formed at widely different times (Carr, 1965).

### **2.4.6.3 Shingle beaches:- sedimentology**

Much of the work on shingle dynamics is based directly upon the principles of clast size, sorting and shape developed since the 1940s (eg Krumbein, 1941). Whilst many general observations had been assumed in relation to shingle shape and size, particularly the increase in sphericity of clasts upon transfer from a fluvial to a coastal environment, it was readily apparent that many of these assumptions have only a limited basis in field studies. Sneed & Folk (1958) suggested that "...particle size has a greater effect on sphericity than 200 miles of fluvial transport.". Their study in the Colorado River showed a tendency for clast sphericity to rise with increasing size and then fall again beyond a critical limit. The sphericity/distance debate was further complicated by the influence of lithology of the source bedrock, which dominated the results of these early studies (Sneed & Folk, 1958; Sames, 1966). An ideal control situation was investigated by Dobkins & Folk (1970) on Tahiti Nui, where a single bedrock lithology (basalt) made lithological discrimination unnecessary. Clast roundness was seen to increase from river to beach, whilst sphericity fell due to the tendency for beach material to slide whilst in transit on the beach face. Roundness of beach material was seen to correlate with wave height once emplaced, although the "...surgeon-like.." precision with which beach clasts are selected for rounding is questionable in its applicability to the varied wave climate experienced on any British beach. Bluck (1969) suggested that clast roundness also tended to increase with increasing size before reaching a critical size and falling again. As might be expected, abrasion was also found to be most effective in this mid-range clast size, suggesting a possible link, whilst splitting and crushing processes tended to simply increase with increasing size (Bluck, 1969). Russell (1968) recognized a concentration of grain sizes in the range 1-6mm (Bluck's [1969] lower clast size range) in beach material, a size class which he noted was frequently underrepresented in fluvial sediment samples. This size class was not preferentially susceptible to abrasive processes, (Bluck, 1969), was not mechanically unstable (Russell, 1968), and its concentration in beach sediments was attributed to preferential transport under fluvial flow regimes.

Sedimentological studies of shingle beaches has been mainly confined to the beach surface due to the difficulty in penetrating a coarse, disaggregated deposit. Bluck (1969) and Orford (1975) both described a series of downbeach shingle facies based upon shape characteristics. The shape selection process was based upon suspension and pivotability characteristics of individual clasts. Discs were found to be susceptible to wave/swash turbulent flow, and were

moved preferentially upbeach, whilst spheres and rollers tended to move under gravity flow, and were thus found at the bottom of the beach. The sorting process also occurred in a longshore manner, related to incident wave energy (Carr, 1971; Orford, 1975). Longshore sorting was similarly noted on shingle ridges at Orfordness (Carr, 1965).

Observations of the cross-sectional characteristics of shingle beaches were made by Hey (1967) during excavations in the Dungeness shingle complex during construction of the nearby CEGB plant. The ridges were described as essentially structureless, with only a general subsurface dip of 8-10° to seaward. The ridges contained much interstitial sand, a factor recognized by Carter & Orford (1984) as evidence of low transportability of the surrounding shingle mass leading to eventual stabilization, as occurred at this site (Hey, 1967). Increasing interstitial sand content was thought to lead to reduction in the permeability of the beach face, leading to eventual decreasing angles of the beach face and transition from a reflective to dissipative state (Guza & Inman, 1975; Short, 1991). This was followed by eventual stabilization of the beach. (Carter & Orford, 1984).

#### **2.4.6.4 Shingle beaches:- response to RSL change**

Studies of the trends in shingle ridge altitudes at Dungeness on the English south coast has validated large multiple shingle ridge sequences as reasonably reliable indicators of RSL change (Lewis & Balchin, 1940). Sufficient numbers of ridges are essential in such studies in order to offset the inherent degree of randomness of shingle ridge altitudes due to their relationship with high energy marine events (Carter, 1983).

Such a study has been undertaken on the shingle plain at Dungeness in southern England. The general details regarding the geomorphology of Dungeness were outlined above. Whilst the variation in local storm ridge relief (crest to trough) was recorded as reaching up to 3 m, the variation in ridge crest altitude was recorded as "usually small" (Green & McGregor, 1986). This contrasts strongly with the more usual idea that the process of storm ridge deposition creates landforms bearing little resemblance to the original sea level at which they were formed (Steers, 1937). Correlating the five ridge populations of Dungeness (Long & Fox, 1988) with the development history based upon both documentary sources (Ward, 1931; Cunliffe, 1980) and absolute dating techniques show the development of Dungeness to display a trend of relative sea level changes recorded over the historical period as follows:

- i) RSL stood some 1.7-2.0 m lower than present during the Roman period (ca 200 A.D.);
- ii) RSL stood ca. 0.3 m lower than at present around the eighth century AD;
- iii) thirteenth century RSL was approximately the same as at present, which represented a high stand relative to relative sea level before and after this period;
- iv) rising RSL at ca. 0.3 m century<sup>-1</sup> since the fifteenth century AD.

(after Lewis & Balchin, 1940)

Observations of detailed responses of shingle beaches to changes in RSL have been dominated by studies from shingle barriers rather than fixed beaches (Carter & Orford, 1984; Forbes *et al.*, 1991; Orford *et al.*, 1991). These studies have also concentrated on recessional scenarios, with detailed measurements of landform retreat under rising relative sea level. Studies on Story Head barrier in Nova Scotia, Canada, demonstrate shingle barrier migration through rollover processes, in particular overwashing, with the transport of sediment over the crest of the beach through storm wave activity (Orford *et al.*, 1991). However, these studies were made on a system where longshore transport of shingle was minimal, representing a considerably different scenario to those where the primary mode of formation is through longshore extension.

Carter & Orford (1984) and Forman *et al.* (1987) noted that landward migration of shingle barriers will occur even under stable RSL situations simply due to the nature of the sedimentation process, i.e. crest lowering and storm overwash of clasts, with a lack of a seawards compensatory mechanism to return overwashed clasts to the foreshore. This occurs despite relative stability in the short term, partly as a result of the inability of coarse, clastic material to become entrained except under high energy conditions, and partly through their strongly reflective shoreface morphology (Short, 1979). Few studies consider the detailed response of shingle beaches to changing RSL under a scenario of strong longshore transport or under falling RSL. In such a situation the overwash processes reported by Carter & Orford (1984) would still occur, but their relative importance would diminish as distal extension dominates the developmental process. Forman *et al.*, (1987), using evidence from dated RSL events in Spitsbergen, suggested that the rate of RSL decline might be reflected in storm ridge

morphology. A slow rate of RSL fall would increase the time available for ridge construction prior to its abandonment, and would produce wide ridges. Conversely, a rapid fall in RSL would produce only minor shingle strandlines. However, their argument only considered the effects of RSL change on storm ridge morphology, failing to recognize the possible impact of changing rates of sediment supply to the foreshore during formation. The impact of detailed sediment supply on the stability shingle beaches is discussed by Carter & Orford (1988). Barriers forming between the submerged drumlins in Clew Bay (Ireland) are shown to be sensitive to the continued supply of sediment from updrift. Limited sediment supplies from essentially small point sources leads to a system of active barrier formation and destruction over the medium term, representing a small scale model of larger barrier development elsewhere in the world.

Lake & Shepard-Thorn (1987) produced a model of the accumulation of multiple shingle ridges at Dungeness, although this took little account of changes in RSL. Jennings & Smyth (1990) produced a model of possible shingle beach development based on rising RSL and changing sedimentary inputs over time for the south coast of England.

#### **2.4.7 Present and future trends in global sea level**

##### **2.4.7.1 Contributing factors**

Having reviewed literature concerning former changes in RSL, the present and future aspects of sea level change must be considered if the contemporary coastal situation at Culbin is to be understood.

Modern studies of global warming have identified a variety of gases which display "greenhouse" properties, including carbon dioxide (CO<sub>2</sub>), methane (CH<sub>4</sub>), nitrous oxide (N<sub>2</sub>O) and chlorofluorocarbons (CFCs) (Hoffman *et al.*, 1986; Gornitz & Lebedeff, 1987; Viles, 1989; Warrick & Barrow, 1991). The most widely quoted figures have emerged from studies of the concentration of atmospheric CO<sub>2</sub>, particularly using concentrations measured from air bubbles trapped in Antarctic ice. These studies suggest that a 40% increase in CO<sub>2</sub> between the last glacial maximum and the pre-industrial period (*ca.* 1850 AD) has been matched between 1850 and 1985 AD (Pirazzoli, 1990). Monitoring of atmospheric CO<sub>2</sub> began formally in 1957, and results show an increase in atmospheric CO<sub>2</sub> from 315 parts per million (ppm) to 340 ppm between 1958 and 1980 (Titus, 1987).

An increase in the concentrations of radiatively active "greenhouse" gases is generally considered to lead to an increase in global air temperatures (DOE, 1991), which will cause a rise in global sea levels. Two principal mechanisms would be involved in such a process:

- i) thermal expansion of the upper ocean layers;
- ii) melting of non-polar land based ice.

(Gornitz *et al.*, 1982; Jelgersma, 1990; Pugh, 1990)

Whilst this would appear to be a straightforward scenario, the quality of the data and the relationships inferred from it must both be treated with caution. Gornitz *et al.* (1982) suggested a high correlation between recorded global sea level changes and global air temperature trends. Pirazzoli (1990), however, demonstrated that the similar increase in atmospheric CO<sub>2</sub> recorded over both the glacial maximum-pre-industrial and the pre-industrial-present periods was not matched by a similar rise in global sea level. Since the last full glacial period, global sea levels have risen in the order of 10<sup>2</sup> m, whilst since the pre-industrial period a rise of the order of 10<sup>-1</sup> m may have occurred. Barnett (1990) stated that the link between global warming and rising global sea levels was "...while suggestive, ...hardly convincing...". He noted a disparity between the global air temperature curve, which shows a general rise until 1940 and then a fall. This effect is not mirrored by the global sea level curve or the ocean temperature curve, which both show a linear increase, although with a downward trend since around 1960.

Fairbridge & Jelgersma (1990) suggested that there was agreement between CO<sub>2</sub> concentrations and mean global temperature trends, but proof of a link between cause and effect was still absent. They also made the point that during recovery from the period of cooling experienced between the thirteenth and mid-nineteenth centuries (the "Little Ice Age") the rate of global air temperature rise might be expected to be greater than is currently experienced.

#### **2.4.7.2 The nature of the data used in global sea level estimates**

Considerable effort has been expended in attempting to produce a figure which represents a global mean trend in sea level. The simplest and most widely used method has been to take a mean value from tide gauges around the world, filter for unreliable sites, correct the data for regional concentrations and adjust for

tectonic effects (Fairbridge & Jelgersma, 1990). Unfortunately this method is subject to a variety of potential errors, stemming from two principal factors:

- i) the concept of a global sea level;
- ii) measurements using tide gauges.

In describing the trends in global sea level it has been formerly accepted that sea level can be used as a reliable reference datum (ESA, 1991). However, it is now recognized that "sea level" is neither level nor still (Carter, 1988). The ocean surface, if representing a motionless uniform water body on a rotating earth would reflect the earth's gravity field, forming an equipotential surface termed the geoid. Models of the geoid surface show significant surface relief (ESA, 1991) reflecting the effects of structure, density, rheology and rotation on the earth's gravitational field (Mörner, 1976). The geoid surface is not stationary over time, and displays both horizontal and vertical changes under the combined influence of waves, currents and salinity variations (Mörner, 1976; Carter, 1988).

Whilst global warming might provide a partial explanation for the observed trends in global relative sea level, it represents only one of a number of variables which may be invoked as possible causes of eustatic sea level change. Secular deformation of the geoid due to differential lithological loading, variations in regional water balance and changes in the shape of ocean basins all provide further complications in the determination of the geoid surface (Carter, 1988), whilst the effects of subsidence, polar wandering, length of day and glacial retreat further affect the sea level signal at a variety of spatial and temporal scales (Barnett, 1990).

The use of tide gauges in determining long term trends in eustatic sea level is also problematic. A major drawback of this method is the geographic distribution of tide gauges, which tend to be located at the periphery of the global oceans (Barnett, 1990) as a single line of stations along a single shore (Natural Research Council [NRC], 1990) with no effective common baseline (ESA, 1991). Additionally, tide gauges tend to be located in harbours and other human-influenced locations. The global distribution of tide gauges is poor both geographically and tectonically, tending to compound regional errors (Emery & Aubrey, 1985; NRC, 1990; Pirazzoli, 1990 ). The interplay between the eustatic element of sea level change and tectonic effects creates an additional set of problems in the provision of a sea level record. Vertical trends recorded by the tide gauge represent the sum of actual changes in eustatic sea level plus the

trend in the land surface to which the tide gauge is attached (NRC, 1990). Additionally the effect of "earth tides", which may attain magnitudes of up to 50 cm per day will also be included in the tide gauge record (NRC, 1990). Further potential problems are reviewed by Barnett (1990).

The nature of the evidence presented demonstrates that due to the complexity of the geoid and its relationship with oceanic and terrestrial variables, the concept of a uniform eustatic change cannot be globally valid (Mörner, 1976). However, within this complex framework attempts are still made to calculate global sea level changes. Despite the variety of environmental controls on the data, the range of estimates of a global mean trend in sea level remains remarkably limited. Table 2.3 presents a summary of the estimates of global sea level generated since the initial estimates of Gutenberg (1941).

This suggests that a best estimate of  $1-1.5 \text{ mm a}^{-1}$  reflects the rate of rise in global sea level (Pirazzoli, 1990). However this trend must be considered as an average of means, since Pirazzoli (1990) noted that 28.5% of tide gauge records of "sufficient length" (undefined) from various sites around the world recorded a stable or falling sea level signal, whilst NRC (1990) considered the proportion to be nearly 50%. From his records, Pirazzoli (1990) observed that only 13% of the records actually fell into the  $1-1.5 \text{ mm a}^{-1}$  rise class, highlighting the problem of assigning a single figure to a phenomenon described as "global".

#### **2.4.7.3 Future trends in global sea level**

Whether the linkage between cause and effect is accepted or rejected, the evidence proposed suggests that over the past century global mean air temperature has increased by  $0.4-0.5^{\circ}\text{C}$ ., while global sea levels have risen by 10-20 cm (Jelgersma, 1980; Salinas *et al.*, 1986; Pugh, 1990). Tide gauge records worldwide suggest that, in the Northern Hemisphere at least, tectonically stable coasts are experiencing a rising relative sea level of between  $1-2 \text{ mm a}^{-1}$ .

Changes in global sea levels over the next century will be fuelled by four main factors:

- i) thermal expansion of upper ocean layers;
- ii) decay of non-polar land based ice;
- iii) decay of the Greenland ice sheet;

iv) decay of the Antarctic ice sheet.

The maximum sea level scenario would occur if all of the ice presently on the earth were to melt. This would cause a rise in global sea levels of ca 88m (Mercer, 1978; Pugh, 1990). However this is an unrealistic situation as a variety of climatically and tectonically controlled feedback mechanisms would counter such an effect at a range of scales. A long time lag between event and impact might also be expected (Pugh, 1990).

The Intergovernmental Panel on Climate Change (IPCC) "Business-as-Usual" scenarios are described by Warrick & Barrow (1991). The estimates appear within an error envelope designed to account for climatic uncertainties, but broadly suggest that global RSL will rise by  $20\pm 10$ cm by 2030, increasing to  $30\pm 15$ cm by 2050.

The estimates of global sea level changes presented so far have been of a global and thus by definition generalized nature. The detailed response of particular areas of the world's coastline to such changes will also depend upon local tectonic factors, which will modify the observed response significantly. Predictions made by Pugh (1990) for four sites around the British coast suggest that in areas still responding isostatically to the removal of Late Devensian glacier ice, the regional response to a "global" phenomenon may differ significantly. Table 2.4 below outlines the four sites used in these predictions.

	Anticipated rise by 2027 (m)	Anticipated rise by 2087 (m)
Newlyn	0.14	0.63
Aberdeen	0.09	0.51
Sheerness	0.16	0.69
North Shields	0.16	0.71

Table 2.4 Anticipated rise in RSL for four sites around the British coast (source: Pugh, 1990)

The anticipated rise in RSL is lowest in Aberdeen, where isostatic uplift is still occurring, while at Sheerness the combination of subsidence and crustal depression in the southern North Sea enhances the magnitude of RSL rise.

In summary it appears likely that in the northern hemisphere at least, the last century has seen a eustatic sea level rise of around 1-2 mm a<sup>-1</sup>, although the limited database from which this inference is drawn means that this is by no means a certainty. From GCMs it would appear that with increasing concentrations of atmospheric CO<sub>2</sub>, the rate of eustatic sea level rise is set to increase. In terms of the potential impact of RSL rise on the Scottish coast, it is the *rate of change* which is of primary importance in assessing likely outcomes and responses to changing RSL at a particular location.

## **2.5 FLUVIAL SEDIMENT INPUTS TO THE COASTAL ZONE**

One of the primary aims of this thesis is to produce a volumetric assessment of the Holocene landform development of Culbin, using a method which allows quantification of the individual sedimentary inputs to the coastal zone in a form of "palaeosediment budget". Since fluvial inputs into the coastal zone are responsible for large quantities of sediment entering the sediment budget, a critical area of investigation is an assessment of the amounts of sediment formerly contributed to the coast. In many areas, glacial activity has been responsible for an enhanced sediment supply to the coast; an effect which has lingered well into the present Holocene interglacial period.

Quantification of sediment supply to the coastal zone over the Holocene is a field which, due to the potential magnitude of the errors involved in calculation (up to 400% - Renwick, pers. comm.), has received relatively little attention. Analysis of former sediment supply to the coastal zone has been studied via three main methods:

- i) fluvial bedload equations;
- ii) sedimentation studies in enclosed basins;
- iii) palaeodischarge methods.

### **2.5.1 Fluvial bedload equations**

When calculating contemporary fluvial sediment supplies to the coastal zone, a major source of error arises from the quantification of bedload transport (Newson

& Leeks, 1985; Richards & McCaig, 1985; Ferguson, 1987). Studies of the physics of bedload transport are still in their relative infancy. Various bedload prediction equations have been produced and tested, with significant differences in the predicted entrainment volumes produced. Nakato (1990) estimated up to a 100-fold difference between formulae predictions, whilst Gomez & Church (1989) found that a test of 12 equations covered an 8 order-of-magnitude range in predicted bedload transport. Additionally, predictions made from equations provide only a maximum transport value and assume an unlimited sediment supply (Knighton, 1984), possibly leading to overestimates of the bedload fraction. This problem was highlighted by McManus (1986), who noted bed armouring producing no bedload movement at flows up to 20 cumecs in the Forth and Tay estuaries, with transport across the whole stream only occurring at very high flows. Similar effects were reported by Reid *et al.* (1985).

Contemporary coastal studies have tended to either ignore the contribution of bedload entirely (eg Marcus & Kearney, 1991), or accept a best estimate based upon total load. Reid & McManus (1987) took a value of 10% of the suspended and solutional load in the rivers of the Moray Firth as an estimate of bedload transport, based on Parker *et al.*'s (1964) consideration of this value as a general best estimate for bedload transport in temperate latitudes. However, Al-Ansari & McManus (1979) measured a lower value of only 3-5% of suspended/solution load in the River Earn in eastern Scotland, suggesting that Parker *et al.*'s value may be an overestimate.

### **2.5.2 Sedimentation studies in enclosed basins**

Upland loch infill studies provide a more direct estimate of sediment supply, but conversion of the accumulation rate in the loch to a basin-wide estimate of mean erosion is an area fraught with overgeneralization, particularly when the original data source was from a single sediment core (Edwards & Rowntree, 1980). However some significant results have been recorded. O'Sullivan (1976), working in Loch Pityoulish in upper Strathspey noted a low rate of sediment accumulation until *ca.* 4300 BP, when the accumulation rate increased sharply. Edwards & Rowntree (1980) found a similar trend in Braerrodach Loch in Deeside, with a slowly increasing accumulation rate which increased markedly after *ca.* 5000 BP, coinciding with the introduction of widespread forest clearance for agriculture during the early Bronze Age.

The trend thus far described is obviously very generalized. The coarse sampling network imposed by the need for samples of sufficient size for C14 dating,

coupled with the use of only a single core will tend to mask actual and possibly more detailed trends, as suggested for example by phases of terrace incision (Robertson-Rintoul, 1986), and localized sediment source inputs with vegetational histories differing from the trend described above (eg. Brazier *et al.*, 1988).

### **2.5.3 Palaeodischarge methods**

Palaeodischarge methods involve the determination of former river discharge from sedimentary characteristics of abandoned river channels (Dury, 1976; Briggs, 1977). However, the inaccuracies of the method (up to a possible 100% error - Church *et al.*, 1990) prompted Briggs (1977) to note that "...we cannot gain any great precision in extending these studies to past environments.", and considered the values produced to be no more than order-of-magnitude estimates.

Sediment supply to the coastal zone from inland sources has been a crucial factor in the development of the Culbin shingle system. Massive volumes of unconsolidated sand and gravel were produced with the retreat of Late Devensian ice *ca.* 13 000 BP (Maizels & Aitken, 1991), both as ice contact material and outwash. Such material forms thick deposits in the upper and middle reaches of the Findhorn (Fairburn, 1967; Auton, 1990) and the Spey (Young, 1978; Maizels, 1987). Transport of this material to the coastal lowlands has been facilitated in the past by higher fluvial discharges (Young, 1978; Maizels, 1987), which has led to the formation of extensive river terrace sequences in the lower reaches of the Moray Firth rivers. Whilst many of the upland terraces have traditionally been thought of as outwash terraces (Young, 1978; Sissons, 1981a), evidence from Glen Feshie in upper Strathspey suggests that periods of terrace incision have occurred throughout the Holocene period (Robertson-Rintoul, 1986).

Studies of terrace incision in upland catchments clearly remain in their infancy, and extension of such studies to a basin scale in order to attempt to quantify the potential inputs to the coastal zone remains untested in Britain, although preliminary studies from the US (Ashley & Renwick, 1983; Renwick & Ashley, 1984; Marcus & Kearney, 1991) have successfully quantified fine sedimentary inputs to the coast. Calculation of coarse sedimentary inputs to the coast such as those required in this study have not been attempted. A model of palaeohydrological changes in the rivers of NE Scotland has been produced by Maizels & Aitken (1991). From a study of seven rivers and their terrace

sequences, they recognized an early phase of valley aggradation during the Lateglacial cold phase (ca. 14 500-13 000 BP), while surfaces remained unvegetated and sediment delivery to the fluvial system was high. At this time discharges were up to 1.7 orders-of-magnitude greater than at present. Between 13 000 and 11 000 BP climatic amelioration led to widespread vegetation growth on the newly deglaciated surfaces, and a period of valley incision. This cycle was then repeated during the Loch Lomond Stadial climatic deterioration and the Holocene amelioration (Maizels & Aitken, 1991).

Chapter 3 will review the method eventually adopted in order to calculate the amount of sediment input to the Culbin system throughout the Holocene.

## **2.6 CULBIN AND THE MORAY FIRTH**

### **2.6.1 Geomorphological setting**

Culbin Sands and Forest (from hereon referred to simply as Culbin) provides an excellent field site for the study of both Holocene and contemporary coastal changes, and as such provides a good platform to attempt a linkage between them. The site is 12 km in length, covering approximately 28 km<sup>2</sup> (Ross, 1992), and extending up to 3.5 km inland, tapering towards the town of Nairn in the west. Within this area, a series of relict shingle storm ridges form a discontinuously exposed arc ca. 4.5 km in length. These raised shingle storm beach ridges are located between ca. 4 and 11 m OD, extending approximately 3 km inland from the coast, and stretching from Burghead Bay in the east as far as The Bar in the west (Figure 2.6). Landwards of this sequence fine grained sediments have accumulated, and organic layers found at various positions within these sediments allow a sea level history of the site to be constructed. Numerous studies concerning changes in RSL have been undertaken in the area, particularly in the inner Moray Firth and Dornoch Firth, which allow a regional sea level framework to be constructed against which to test any data obtained from Culbin and the surrounding area. Additionally, the particularly complete raised shingle ridge sequence at the site allows testing of the hypothesis that shingle ridges, if represented in sufficient numbers, can provide a record of RSL changes.

The preservation of the Holocene landforms at Culbin has been aided by the physical remoteness of the site plus a cover of blown sand which formerly constituted the largest area of open sand dune in Britain (Forestry Commission, 1988; Ross, 1992). The sands have been stabilized by the planting of conifers between 1922-1954, which has aided the preservation of landforms by channelling visitors along established tracks and rides (Comber & Hansom, 1993), although serve to partly obscure the features for the purposes of identification and mapping (Plate 2).

The contemporary coastal system at Culbin Forest is highly dynamic, providing scope for process measurements over the timescale allowed for this project. The wave climate of the middle Firth is of limited energy, allowing the installation of a wave recorder built specifically for the project without the need for heavy installation equipment. The limited number of inputs to the coastal system at

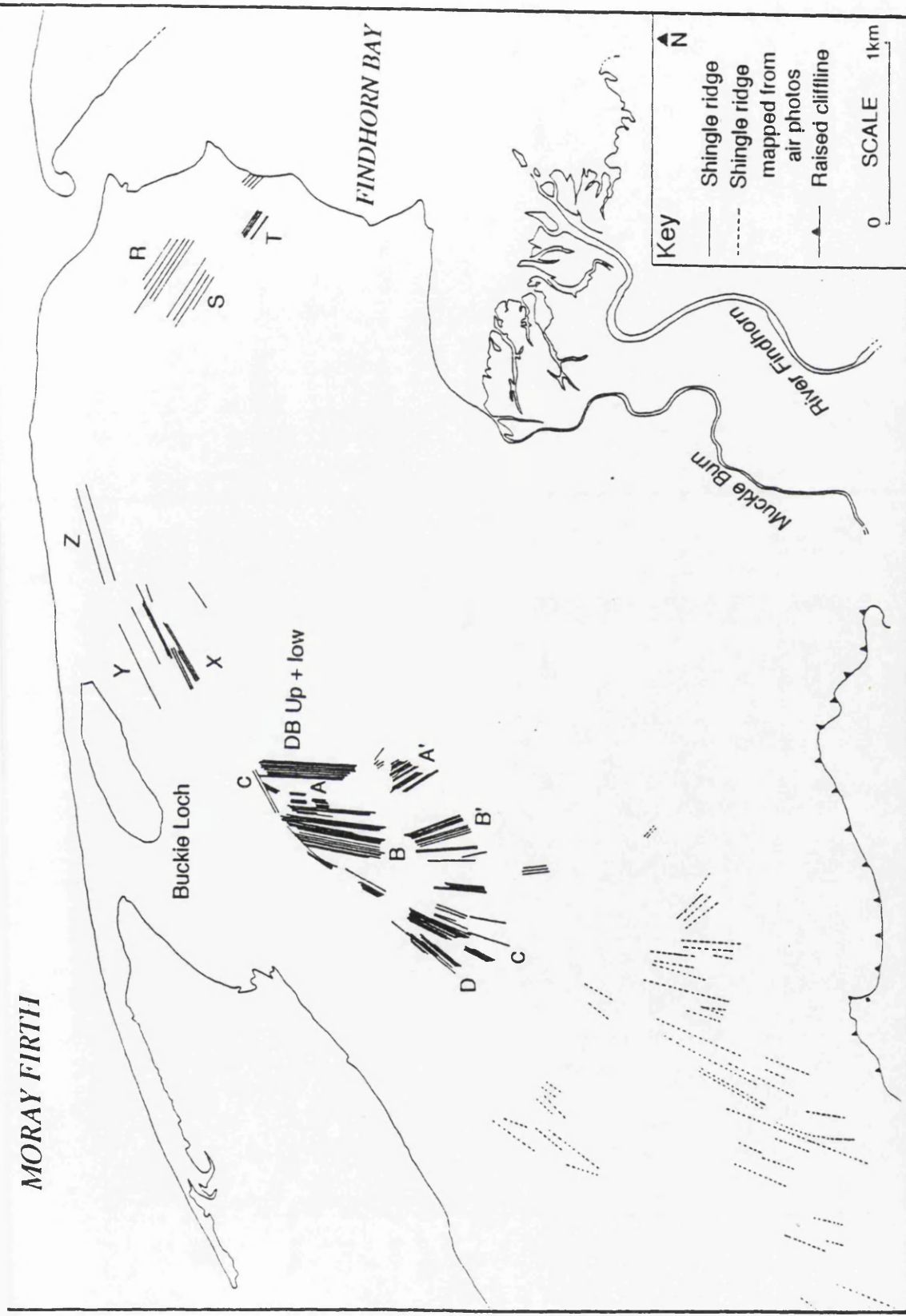


Figure 2.6 Location of relict shingle storm ridges at Culbin

Culbin meant that the quantification of a sediment budget for this stretch of coastline was a realistic target.

### 2.6.2 Regional Geomorphology of the Moray Firth

The coastline of the Moray Firth forms a triangular inlet of the North Sea with a NE-SW trending axis, and contains a total coastline length of 650 km as measured at high water mark (Smith, 1986). The entrance to the Firth is controlled by the NE-SW orientation of the Caithness/Easter Ross coast and the E-W orientation of the Moray/Buchan coast. The proportion of each of the major coastal types has been measured by Smith (1986) (Table 2.5).

Coastal Environment	Relative Area (%)
Cliff-girthed	43
Low, sandy	9
Shore platform	11
Intertidal flats	37

Table 2.5 Relative proportions of the major coastal environments in the Moray Firth (source: Smith, 1986)

Smith (1986) subdivided the Moray Firth into three sections (outer, middle and inner), as shown in Figure 2.7. Along the outer firth east of Spey Bay the coastline is predominantly rocky, with a relatively high incident wave energy. Wave energy decreases towards the inner firth with increasing shelter, producing extensive areas of intertidal flats. The intermediate wave energy environment of the middle firth combined with the generally low topography and an abundance of sediment has produced a series of extensive sand and shingle forelands, including those at Culbin, Speymouth, Burghead Bay and Whiteness Head. These forelands are frequently anchored to a bedrock tie, the most important of these in the Culbin area being formed by the bedrock ridge between Burghead and Lossiemouth. The predominant wave approach directions within the firth are from the N/NE. Refraction of incident waves into shallow water creates shore parallel currents producing net transport of both fluvial and nearshore sediment westwards into the firth. The evolution of coastal landforms of Culbin has been

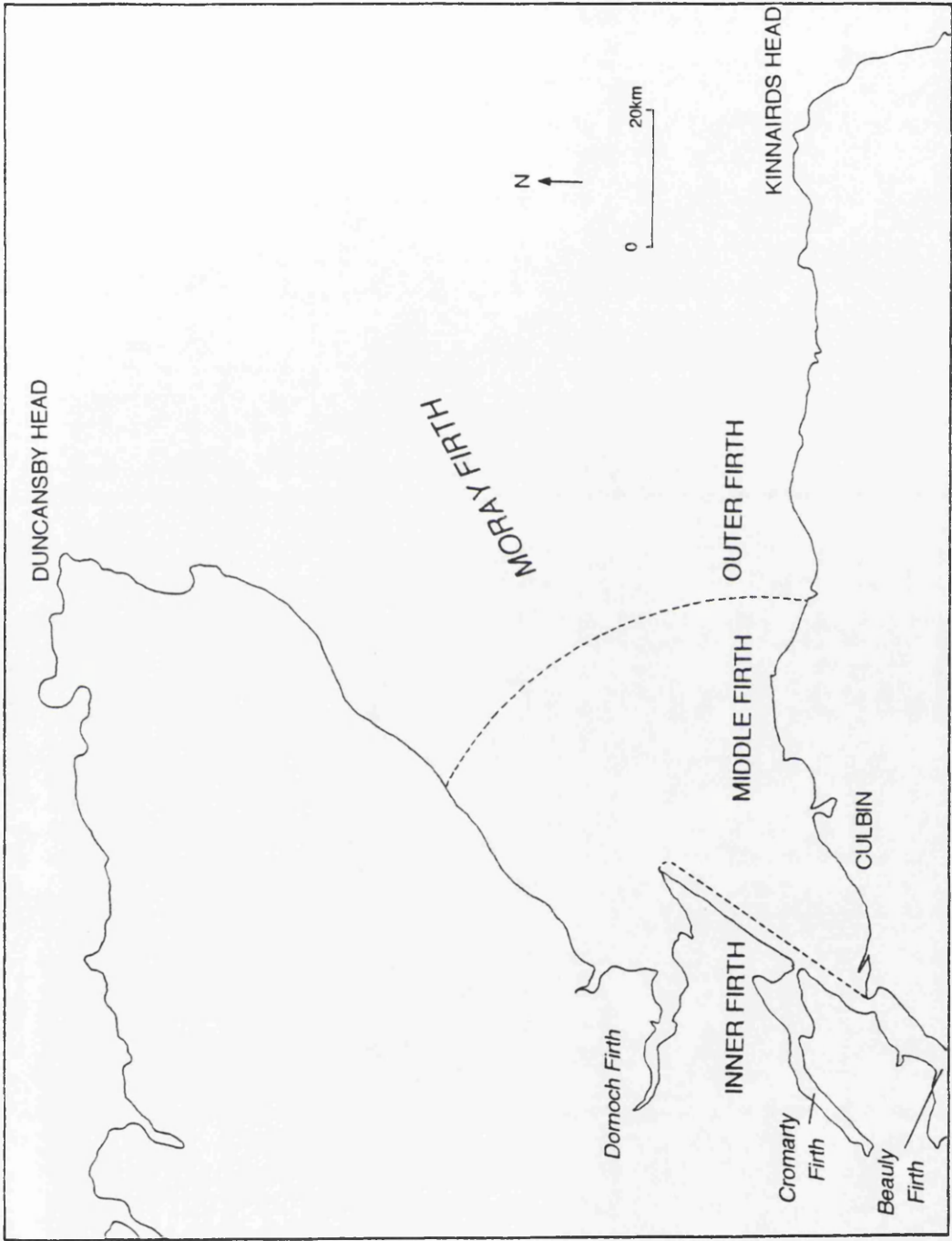


Figure 2.7 Regional divisions of the Moray Firth (source: Smith, 1986)

intimately linked to this westwards drift of sediment from the major rivers of the Spey and Findhorn and from an extensive nearshore zone veneered with glacial sediments.

### **2.6.3 Geology of the Moray Firth**

The solid geology of the Moray Firth has provided a basement upon which more recent events have operated (Smith, 1986). Additionally, the geology of the area has strongly influenced the nature and amounts of material made available to the coastal zone. Thus while providing an effectively passive surface, the geology of the area has contributed directly to the coastal development of the Culbin area through the interaction with the large scale processes which have acted upon it.

The axis of the main Moray Firth basin trends NE-SW, forming a major inlet of the North Sea. The area is an effective extension of the Buchan/Witchground Graben, which is in turn the westerly arm of the main North Sea graben system (Barr, 1985), initiated during the late Jurassic/early Cretaceous (Andrews *et al.*, 1990). Structurally the Firth is bounded to the north and south by major east-west trending faults (the Wick and Banff faults respectively), and to the west by the Great Glen fault and the Helmsdale Fault, the former representing the major fault in this area. Limited evidence suggests that the Great Glen Fault may still be intermittently active. Davison (1902) reported on the effects of the Inverness earthquake of September 1901, and also recognized a series of earlier shocks in 1816, 1888 and 1890, all of which were attributed to fault line activity along the Great Glen.

The present position of the Firth coincides with the former position of an Orcadian ORS basin (Chesher & Lawson, 1983), representing a large Mesozoic basin in terms of solid geology, with a broadly conformable succession from Devonian to Cretaceous dipping uniformly towards the centre (Chesher & Lawson, 1983). The Moray Firth thus represents a net depositional zone which has been accumulating sediment almost continuously since the Devonian to the present, with up to 16 km of sedimentary units found in the deepest sections of the basin (Andrews *et al.*, 1990).

Both the onshore and offshore geology of the Moray Firth consists of a basement of Dalradian and Moinian metasediments, folded and metamorphosed during the Caledonian orogeny, and possibly earlier in the case of the Moinian series (Andrews *et al.*, 1990). Onshore the Dalradian series in the east of the Moray Firth give way towards the west to the Moinian rocks of the Inverness area, with

granitic intrusives appearing at a number of localities. Along the southern coast of the Moray Firth from the Dornoch/Tarbet Ness area to Buckie the basement is unconformably overlain by sandstones and shales of the Devonian (upper ORS). The ORS units along this stretch of the coast attain a maximum thickness of ca. 1200 m of red, pink or yellow current bedded fluvial sandstones with intercalated shale units (Chesher & Lawson, 1983). Locally important outcrops of Permo-Triassic and Jurassic rocks are found on the coastal margin in the Burghead-Lossiemouth area, while younger Cretaceous rocks are only found onshore as glacial erratics.

Offshore the Mesozoic sedimentary cover becomes much thicker, particularly towards the centre of the Firth. From the southern coast northwards a unconformable series of sedimentary units from the coastal ORS through to the Cretaceous are found dipping uniformly towards the centre of the basin. The most widespread unit within the bounds of the outer Firth is the lower Cretaceous, found across the entire central section of the Firth.

Beyond the entrance to the Moray Firth the lower Cretaceous passes conformably upwards through the limited outcrop of the upper Cretaceous and into the extensive Tertiary beds of the northern North Sea (Andrews *et al.*, 1990).

Quaternary deposits exist across the entire Firth except for an area SE of Brora, north of Fraserburgh and east of Wick (Chesher & Lawson, 1983). Thicknesses of up to 70 m are found within the Firth (Chesher & Lawson, 1983), increasing to a maximum of 400 m in the Witch Ground Basin in the northern North Sea ca. 100km off the outer Firth (Andrews *et al.*, 1990).

Within the Moray Firth Chesher & Lawson (1983) subdivided the Quaternary deposits about latitude 58°N into northern and southern units, based upon thickness. The northern units ("northern drift") are poorly defined, generally thinner deposits with varied accumulation sequences. The southern units were found to be much thicker, and have been further subdivided into a series of five elongate basins aligned approximately E-W; locally they contain over 40 m of unconsolidated deposits. Their location is shown in Figure 2.8, and stratigraphic details are found in Chesher & Lawson (1983). Andrews *et al.* (1990) found little correlation between the deposits found in these basins, although a generalized sequence was suggested. This comprised a basal diamict containing shell material dated as mid-Weichselian (Devensian) or younger, overlain by "glaciomarine" sequences, and overlain in turn by a second diamict. A date from the top of this upper diamict of 12 398±100 BP suggests a similar

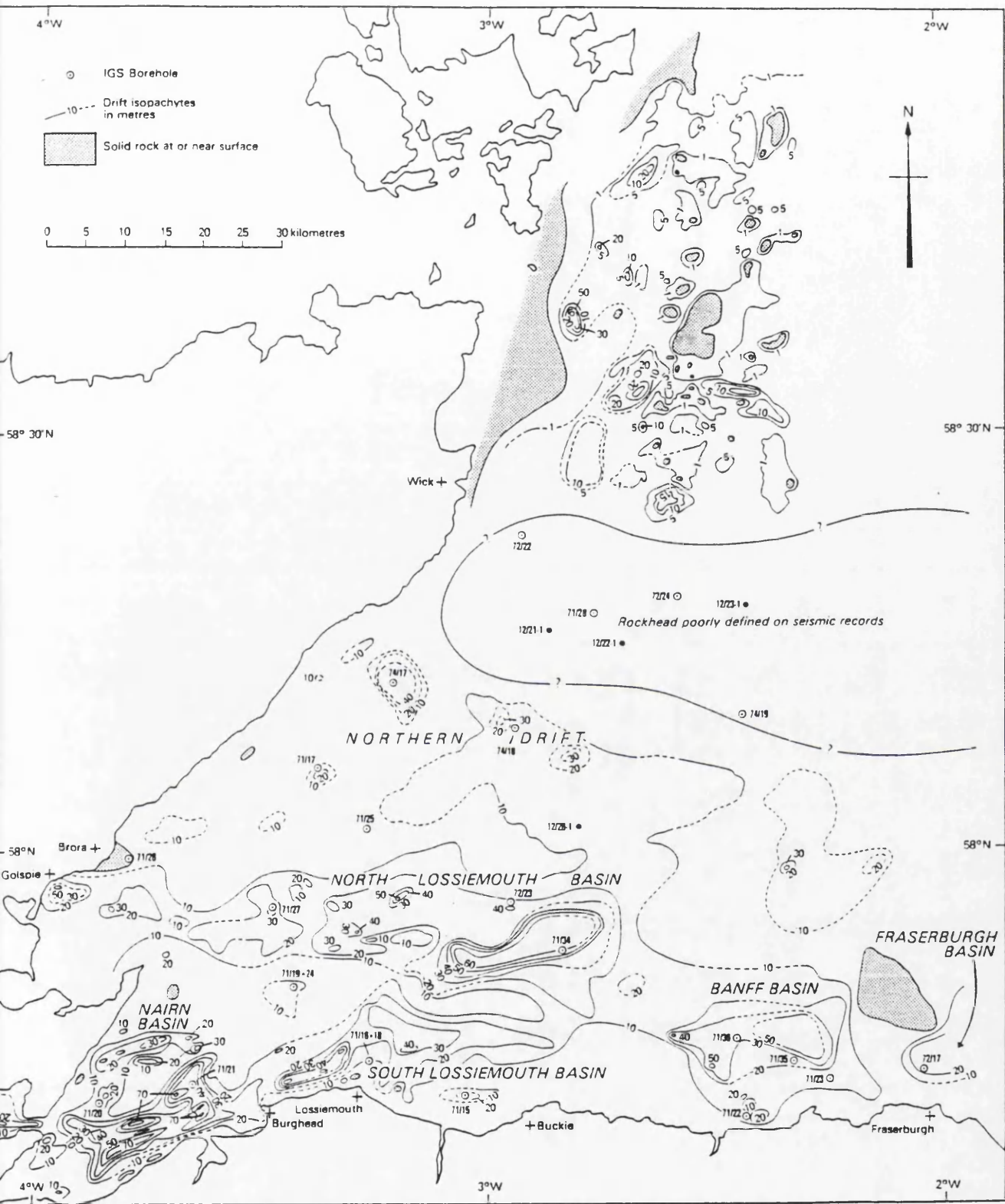


Figure 2.8 Quaternary basins in the Moray Firth (source: Chesher & Lawson, 1983)

accumulation sequence to that found offshore from Buchan and Caithness, indicating that two separate ice streams crossed the area during the Late Devensian glaciation (Hall & Whittington, 1989).

#### **2.6.4 Glacial History of the Moray Firth**

The impact of glaciation on the coastal genesis of the Moray Firth has been profound. In terms of the development of "soft" (i.e. depositional) coastal environments, glaciation controls;

- i) the form and spatial location of the sediment;
- ii) the amount of sediment available for entry into the coastal zone;
- iii) the vertical range across which this sediment is subsequently deposited;

The form and location of the sediment are controlled directly through the erosion and subsequent deposition/reworking of glacial sediments, while the vertical range of its distribution is controlled indirectly by glaciation through the impact of both eustatic (global) and isostatic (local) sea levels.

The Moray Firth has been glaciated on more than one occasion, although material evidence for events pre-dating *ca.* 13 000 BP is scarce (Merritt, 1990a). Reworking and trimming of the glacial features in the Eastern Highlands of Scotland during the last glaciation, while locally significant, has made few major alterations to the upland landscape, but have been fundamental to the coastal evolution of the Moray Firth (Smith, 1968). The evidence for glaciation during the Late Devensian is extensive around the Moray Firth, and an understanding of the movement and extent of ice during the last glacial period is important in interpreting its coastal evolution.

Fragmented evidence exists at sites around the Moray Firth to demonstrate the occurrence of glacial activity prior to the Late Devensian. Two of the most important sites in the inner Moray Firth are located at Dalcharn and Allt Odhar, located SE of Inverness. At Allt Odhar, a peat containing a pollen assemblage interpreted as interglacial is found above a gravel/till sequence and below a second gravel/till unit. Radiocarbon dating of the peat produced a non-finite age (>62.3 ka). Uranium series disequilibrium dating suggested an age of *ca.* 124 000 BP, correlating with oxygen isotope stage 5e (Ipswichian interglacial) (Heijnis, 1990). The Dalcharn site provides material interpreted to be even older,

with a compressed peat displaying a pollen assemblage of interglacial affinity, overlying a basal till. However, the organic unit is overlain by two separate (lodgement) tills, and using the "count from the top" method, the lower till may have been deposited during the Anglian glacial period (Merritt & Auton, 1990).

These two sites provide evidence to suggest that glaciation has occurred in the Moray Firth on at least two occasions prior to the Late Devensian. Evidence from the last glacial event to affect the Moray Firth suggests that the impacts of glaciation on coastal development are of the most fundamental nature. If this is true, then it is clear that the depositional coastal landform assemblage of the Moray Firth must have undergone almost total renewal at semi-periodic intervals throughout the Pleistocene.

Ice forming the Late Devensian Moray Firth glacier advanced east from the Great Glen along the present location of the southern Moray Firth, (Smith, 1968; Firth, 1984), gouging a deep trough from Kessock (Smith 1968) along the southern Moray Firth as far east as the Fraserburgh Basin (Chesher & Lawson, 1983). This glacier formed one of a series of ice tongues extending east from the main Scottish ice-shed, which extended south from the NW Highlands, through Rannoch Moor and into the SW Highlands. This in turn represented only one of a number of ice centres in a polycentric series of ice domes envisaged at the maximum of the Late Devensian glaciation (Sutherland, 1984).

The extent of the Moray Firth glacier has been the subject of wide debate. Smith (1968) proposed a Late Devensian glacial limit, represented in the vicinity of Elgin on the southern Moray Firth by a large moraine at Llanbryde village. To the east of this moraine, periglacially altered tills and deep oxidation layers fitted with the traditional idea of a "moraineless Buchan", unglaciated during the Late Devensian (Synge, 1956). A similarly large moraine near Brora on the north side of the Firth was thought to be the outer glacial limit in this area. The two were tentatively linked to produce an outer ice limit for the Moray Firth glacier (Smith, 1968). However, once the glaciation of Buchan was accepted (Clapperton & Sugden, 1975), Sutherland (1984) was free to propose a Moray Firth glacier extending to the Buchan coast, while later workers (Hall & Whittington, 1989; Andrews *et al.*, 1990) suggested that the glacial limit was even more extensive. A maximum ice front position beyond the outer limits of the Firth was suggested, with a floating ice shelf extending east beyond this. However, Boulton *et al.*, (1977) envisaged the Scottish Late Devensian ice sheet as confluent with Scandinavian ice, theoretically producing full ice cover across the entire North

Sea and Moray Firth. Cameron *et al.* (1987) used submarine evidence provided by large, infilled valleys in the northern North Sea to demonstrate that the Late Devensian British ice sheet extended up to 100 km offshore. The lack of loading structures within channel infill sediments of the central North Sea between the Norwegian trench and a position approximately 100 km off the Scottish coast was seen as evidence of open water conditions. If this was the case, then there was no link between the Scandinavian and British ice sheets at the peak of the Late Devensian, as postulated by Boulton *et al.*, (1977). The subsequent infill of the channels was interpreted as glaciomarine rainout material at the margins of the former ice sheets, with marine sediments deposited in the deep water channel in between (Cameron *et al.*, 1987), as described by Kempema *et al.* (1989).

Interaction between the Moray Firth glacier and land based ice has been proposed from limited evidence around the Moray Firth. Peacock *et al.* (1968) described a sequence of three tills from Rothes in Strathspey, whose erratic content suggested that ice flows from the NW and SW were dominant at different phases during the Late Devensian. A similar sequence was described from the Caithness coast by Hall & Whittington (1989).

Decay of the Moray Firth ice released vast amounts of sediment onto the present inner continental shelf (Harris & Peacock, 1969). A rapid rise in the altitude of the marine limit along the southern coast of the Moray Firth was thought to represent a response to the active westward decay of ice along the Firth rather than stagnation and decay *in situ* (Smith, 1968; Sutherland, 1984). Firth (1989a) suggested that Late Devensian shorelines in the Kingsteps/Cothill area (east of Nairn) were contemporaneous with locally stagnant glacier ice lying south of the present coastline, while the Moray Firth was at this time ice free. Backwasting of the ice margin was accompanied by marine inundation of the newly deglaciated surfaces. Evidence from the Cromarty Firth (Peacock, 1974; Peacock *et al.*, 1980) suggested that the Cromarty Firth was still ice covered at 13 500 BP on the basis of the apparent absence of Errol beds, normally indicative of high arctic marine conditions.

Early theories suggested that the decay of the Moray Firth ice was interrupted twice, producing evidence for a stillstand at Alturlie, and a readvance at Ardersier (Smith, 1977; Synge & Smith, 1980). However, Merritt (1990b) suggested that the Alturlie deposits represent a glaciomarine deltaic sequence, with the topset units located at ca. 20 m OD altered through marine modification during

formation. The deposits display no evidence of downwasting *in situ*, as might be expected if the feature formed during a stillstand. The concept of an Ardersier 'readvance' has also been placed in doubt. Smith (1977, 1986), Synge (1977) and Synge & Smith (1980) suggested that folded, faulted and thrust sand and silt units found in section at Ardersier represent evidence for a readvance of the Moray Firth glacier. However, Firth (1989a) and Merritt & Auton (1990) proposed that the deposits represent *in situ* glaciomarine sediments, that the silts and clays of the Ardersier Silt unit were deposited subaqueously, and that the folding represented simple de-watering structures.

From this brief overview, it can be seen that the Moray Firth has been glaciated on more than one occasion. However in terms of the impacts on the coastal development history of the Firth, the effects of the last (Late Devensian) glaciation were the most significant. Glaciation effectively reset the coastal "clock" in the Moray Firth, removing the majority of any pre-existing elements of the "soft" coastal landform assemblage. Deposition of glacial and glaciomarine sediments at the former ice/ocean interface would have provided material from which a rejuvenated coastal landscape could have been constructed. Evidence for glacial events pre-dating the Late Devensian suggests that "purging" of the depositional coastal landscape due to glacial activity has occurred on at least three occasions, with the development of the depositional coastal landscape following a broadly cyclic pattern occurring exactly out-of-phase with periods of glacial activity.

### **2.6.5 Relative sea level history of the Moray Firth**

Downwasting of Moray Firth ice ca. 13 000 BP allowed marine flooding of newly deglaciated areas (Firth, 1989a). Rapid isostatic recovery of the land surface during this period outstripped the rate of eustatic sea level rise, producing a fall in RSL during the immediate postglacial. RSL was thought to be low by the onset of the Loch Lomond Stadial (Synge, 1977; Haggart, 1987). Truncation of Late Devensian silts by a widely distributed gravel layer in the inner Moray and Beaully Firths has been interpreted as indicative of a rise in RSL during the Loch Lomond Stadial (Sissons, 1981b; Haggart, 1986, 1987). The formation of such a coarse deposit was thought to relate to the severe climatic deterioration experienced during the Loch Lomond Stadial (Sissons, 1981b). The deposit attains a maximum altitude of 10 m OD at Barnyards in the Beaully Firth (Haggart, 1986, 1987), and has been cited as evidence of possible crustal redepression

under the Stadial ice mass. However, this point remains controversial, and will be readdressed in a later section.

Deposition of the gravel layer was followed by emplacement of a series of silty clays, the upper units of which contain a marine/brackish diatom assemblage (Haggart, 1986, 1987). Above this marine sequence a peat layer at ca. 6.5 m OD is interpreted by Haggart (1986) as indicative of a regressive contact. A date from this peat of  $9610 \pm 130$  BP close to the landward limit of the upper silty clay suggested a fall in RSL at this time prior to the onset of the rise in RSL to the Holocene sea level maximum. The seaward boundary of the upper marine silty clay was also dated from an overlying peat deposit at  $9200 \pm 100$  BP. Thus from a high stand envisaged during the Loch Lomond Stadial (Younger Dryas), Haggart (1987) suggests a fall in RSL prior to the onset of the rise to the main Holocene sea level maximum (Figure 2.4).

By ca. 8750 BP the fall was complete, and was reflected in the field by a variety of features. Smith (1966) recorded a series of incised gullies cut to a base level below that of the MPG between Cromarty and Jemimaville on the Black Isle. These gullies cut through a high set of raised beach sediments but display no low level delta sequences, suggesting grading to a lower base level than at present and removal by marine activity. Further evidence for a low sea stand at this period comes from a series of extensive intertidal peat deposits found below HWST around the Moray Firth (Wallace, 1896; Steers, 1937; Godwin, 1943; Haggart, 1983). No evidence has yet been found in the stratigraphic record of the end of this period of falling RSL, although Firth & Haggart (1989) record RSL as still falling ca. 9200 BP on the strength of a regressive contact in the Beaully Firth dated  $9200 \pm 100$  BP. Peacock *et al* (1980) reported a possible low stand at ca. -6m OD from borehole C2 in the Cromarty Firth at  $8748 \pm 100$  BP. Hansom & Leafe (1990) also report a possible low stand of similar age at -6 m OD in the Dornoch Firth.

This period of falling RSL was reversed by a major rise in eustatic sea level (to the Holocene sea level maximum) (Fairbanks, 1989, & Figure 2.2) caused by the final collapse of the Laurentide and Fennoscandian ice sheets (Donner, 1969 [1974]; Dyke & Prest, 1987; Dyke *et al.*, 1991; England, 1992). Haggart (1986) suggested that RSL was rising by ca. 8800 BP on the strength of a dated transgressive overlap in the Beaully Firth. Firth & Haggart (1989) noted that RSL was rising in the inner Moray Firth at ca. 7700 BP, and dated the culmination of this rise to ca. 6400 BP. The peak of the Holocene sea level maximum was

marked in the Beaully, inner Moray and Dornoch Firths by the formation of the MPG. In the inner Moray and Beaully Firths the MPG is manifest as a well formed raised shoreline feature found at ca. 9 m OD. In the outer Dornoch Firth, however, the MPG is represented by a sand beach located at 6.8 m OD, and dated ca. 6445 BP (Hansom & Leafe, 1990). On exposed coasts this feature appears as a coarse clastic beach deposit, while in more sheltered localities it manifests itself as a fine grained estuarine deposit (the top of the "carse clay" deposits).

Following the Holocene sea level maximum, RSL displayed a falling trend through until the present (Firth & Haggart, 1989), Isostatic recovery, although slowing, continued while the sea level signal emplaced by the decaying Laurentide and Fennoscandian ice sheets ended. A series of raised shoreline features have been identified around the inner Moray Firth at successively lower altitudes below the MPG, suggesting minor stillstand events within the overall scenario of falling RSL to the present level (Firth, 1984; Firth & Haggart, 1989).

#### **2.6.6 Reiteration of aims**

Having reviewed the available literature, it is clear that a number of points regarding both specific elements of both Holocene and contemporary coastal evolution require clarification. The construction of a sea level curve for the Culbin area has not been previously attempted, and will form a significant extension to the body of literature concerned with RSL changes in the relatively sheltered Beaully Firth. The use of multiple shingle storm ridges as indicators of formative sea level at Culbin will address the proposal that such features bear little relationship to RSL at the time of formation (Steers, in Lewis & Balchin, 1940). It is clear from the literature that very little work has been attempted in the field of modelling Holocene coastal development based on the quantification of sedimentary inputs to a system through a sediment budget approach.

In the light of these shortcomings, the aims of this thesis are to:

- i) establish a sea level history and developmental history of a previously unrecorded site in the Moray Firth, using both traditional sea level indicators and the multiple shingle ridge sequence of Culbin;
- ii) examine contemporary coastal processes and forms, and to calculate a sediment budget for Culbin,

iii) attempt to link aims i) and ii) through the medium of a palaeosediment budget, in order to assess changes in the coastal sedimentary domain at Culbin throughout the Holocene.

## CHAPTER 3 METHODS

The aim of this section is to outline the methods used in this investigation. The chapter format will be as follows:

- 3.1 Investigation of Holocene environments at Culbin and surrounding areas;
- 3.2 Contemporary coastal landforms and foreshore sediments;
- 3.3 Linkages between Holocene and contemporary processes.

### 3.1 INVESTIGATION OF HOLOCENE ENVIRONMENTS AT CULBIN AND SURROUNDING AREAS

The development of Culbin has been intimately linked to changes in RSL during the Late- and Postglacial periods, both on the site itself and in the surrounding areas of Burghead Bay and the Findhorn estuary. In order to reconstruct the sea level history and sediment supply regime of the area, an accurate inventory of all Holocene landforms at Culbin is required, and thus the first stage in this investigation was to produce a detailed geomorphological map of the site. Due to almost total forest cover since the 1950s (Edlin, 1976, Ross, 1992), the earliest aerial photographs of the area (RAF, 1946) were obtained in order to produce an initial location map of raised marine features. Of particular interest at this stage were the positions of the extensive sequence of raised shingle ridges identified during a field reconnaissance trip during November 1989. These can clearly be seen on the aerial photograph montage (Plate 3.1, insert) This information was cross-checked against the geomorphological survey undertaken by Steers (1937). Once a map had been produced, the details were transferred to an O.S. base map at a scale of approximately 1:17 000 for ease of relating geomorphological features to landmarks, tracks etc, an essential part of the exercise given the problems of navigation under full forest cover (Plate 2).

#### 3.1.1 Shingle ridge location and altitudes

Using the geomorphological map as a guide to locating the more obvious areas of surficial shingle, the exposures were mapped in detail, noting the number of ridges, alignment, length of exposure and ridge spacing. Problems at this stage included post-1946 dune activity obscuring previously mapped exposures and opening new areas of shingle. Mapping at this stage could not be expected to

## Plate 2

Relict shingle storm ridge forming part of set D. The characteristic surface vegetation of lichens, heather and stunted Scots pine allowed rapid identification of shingle ridges simpler in the field, even below a cover of dune sand. This view highlights the difficult terrain through which surveyed traverses were made.



locate all exposures of shingle, and subsequent site visits revealed more subtle surficial expressions of shallow subsurface shingle through atypical vegetation assemblages and impoverished tree growth. In particular the presence of mixed lichen/heather cover on the forest floor frequently signified the presence of shingle close to the surface. Shallow boring with a gravel auger quickly identified the presence of shingle under thin or patchy sand sheets, eventually allowing the majority (ca. 70%) of the shingle ridges to be mapped. Alignment of shingle ridges were converted to grid north, and a final location map produced at a scale of 1:10 000. This map also included the major dune forms, located mainly in the eastern section of Culbin Forest, and is presented in Figure 3.1.

Once the location of the shingle ridges had been established, detailed altitudinal information concerning the ridge sequence was obtained. Measurement of only the ridge crest altitudes was undertaken:

- i) as the inter-ridge troughs were mostly buried beneath a thick (>1.0 m) cover of aeolian sand, their depths were difficult to ascertain;
- ii) work by Long & Fox (1988) on Dungeness revealed a direct relationship between ridge crest and trough altitude, suggesting that little extra information would be gained by gathering trough altitude in addition to crest altitude at Culbin.

Determination of the altitude of the shingle ridges was undertaken using tachaeometry during summer 1991. The strategy adopted was to level across selected transects, and then to extend the levelling network to incorporate as shingle ridges as possible. Surveying was undertaken using a Wild T1 theodolite and either a Wild T1000 Distomat or Citation CI 410 EDM. Due to the presence of only one remaining OS benchmark in the Forest (located at NH 987624, altitude 29.59 m OD), a network of temporary benchmarks (TBMs) was established by levelling from both this point and a benchmark in Findhorn village (NJ 038646, altitude 4.37 m OD). All initial traverses measured while establishing the TBM network were circular, closing on OS benchmarks. All traverses after this were closed onto TBMs. Mean closing errors did not exceed 0.01 m per station (Chapter 6).

Initial surveying comprised two transects across the "fan" section of the central shingle ridge exposure (NH 992627-NH 988628, and NH 998631-NH 995634). These were made perpendicular to the orientation of the shingle ridges, and thus were not straight due to ridge spreading with distance from the east (Figure

3.2). The need for two separate traverses was due to the adjoining section being obscured by a large dune, and the ends of the traverses were made as close together as was possible.

Once this data had been analyzed it was apparent that the ridges were a potentially useful source of data regarding RSL trends despite an abundance of criticism regarding their use (eg Steers, in Lewis & Balchin, 1940). Levelling of as many of the exposed areas of shingle ridges as possible was next undertaken in order to both identify trends in altitude both within and between the groups, and also to facilitate the linking of separate groups by altitude. However, before embarking on this task some simple controls were undertaken in order to ensure that the trends identified were in fact real and not apparent, and that significant longshore changes in altitude were not likely to disrupt interpretation of trends (Lewis & Balchin, 1940). In order to check the reliability of these trends, two parallel transects were made ca. 100 m north and south of transect A (Figure 3.3), in order to test whether the ridge crest altitudes identified in transect A were constant, or whether they varied in an alongshore manner. In order to produce a modern analogue for testing against the relict ridges, a further control set was levelled using the contemporary shingle ridges located at the western end of The Bar (west of NH 935611). Levelling along the crest of three relict ridges plus the contemporary storm ridge provided information regarding trends in ridge altitudes and their relationship with the incident angle of wave approach.

This initial work provided a comprehensive set of data concerning the location, altitudes and spatial relationships of both the relict shingle ridge populations in Culbin and the contemporary shingle system on The Bar.

### **3.1.2 Sedimentology of the shingle ridges**

A sampling strategy was designed to determine whether sorting characteristics shown by the inland, relict shingle ridges were the same as those actively forming on The Bar at present. Sampling sites were selected on the Culbin shingle ridges based on available exposures, and as such were not evenly spaced. An attempt was made to collect a sample from each of the major shingle ridge units, and 11 sites were sampled in total (Figure 3.4). As the majority of the Culbin shingle ridges were obscured by a variable layer of sand over the ridge crest, and a thick fill in the intervening swales, only the ridge crest could be located with any certainty. Free-standing storm ridges frequently display highly stratified shore-normal size grading (Bluck, 1969; Orford, 1975). As no control

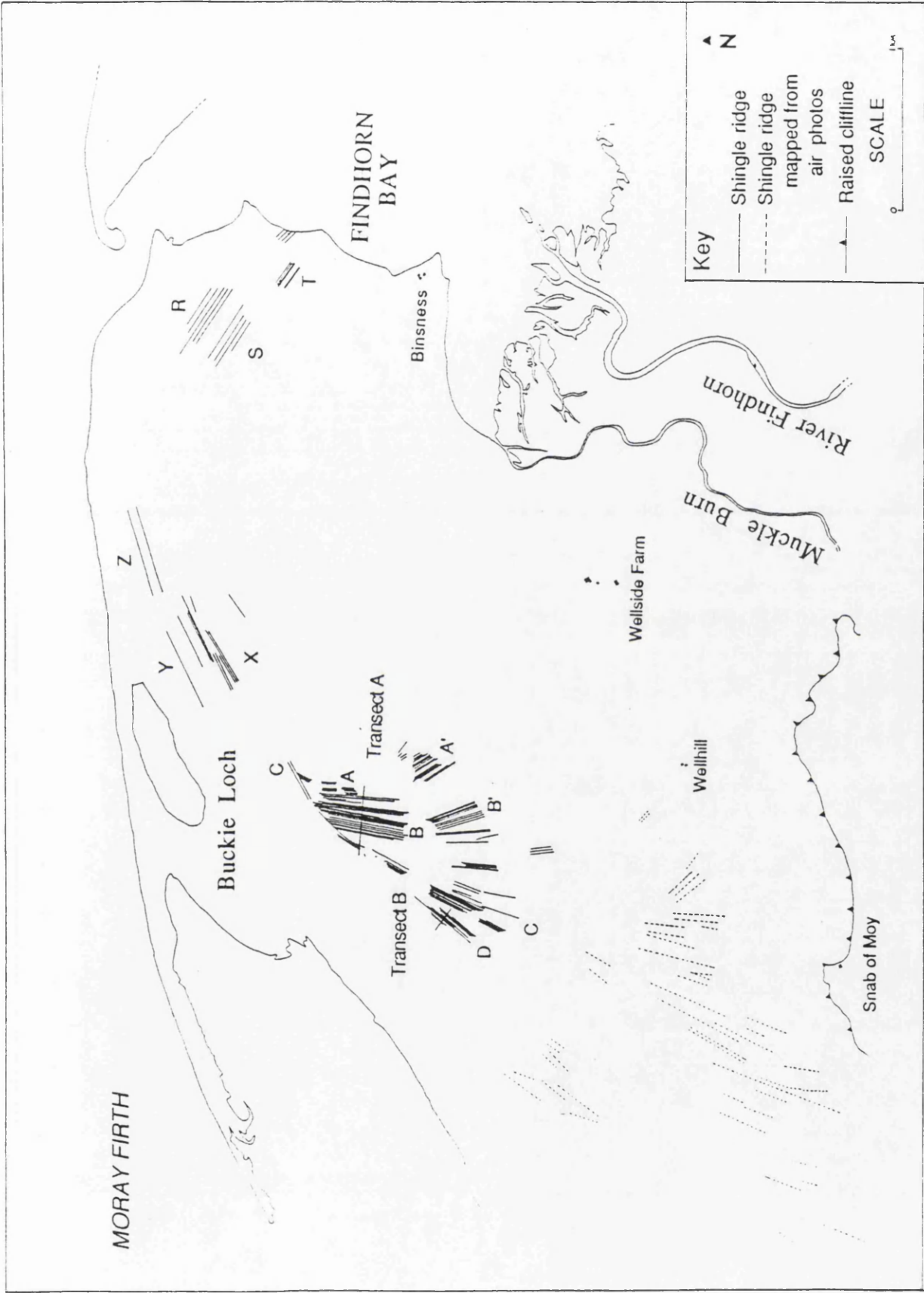


Figure 3.2 Location of transects A and B, Culbin

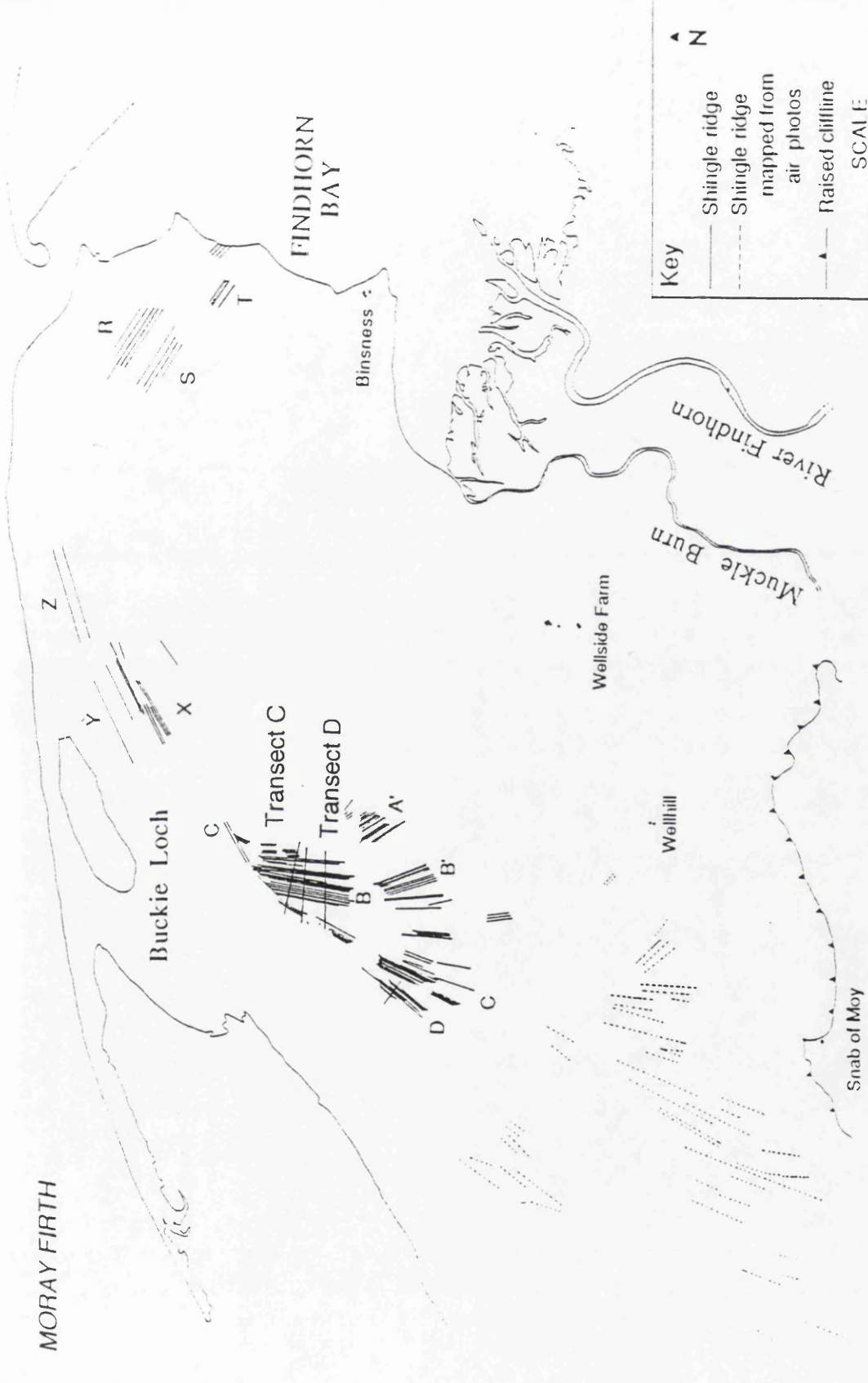


Figure 3.3 Location of transects C and D, Culbin

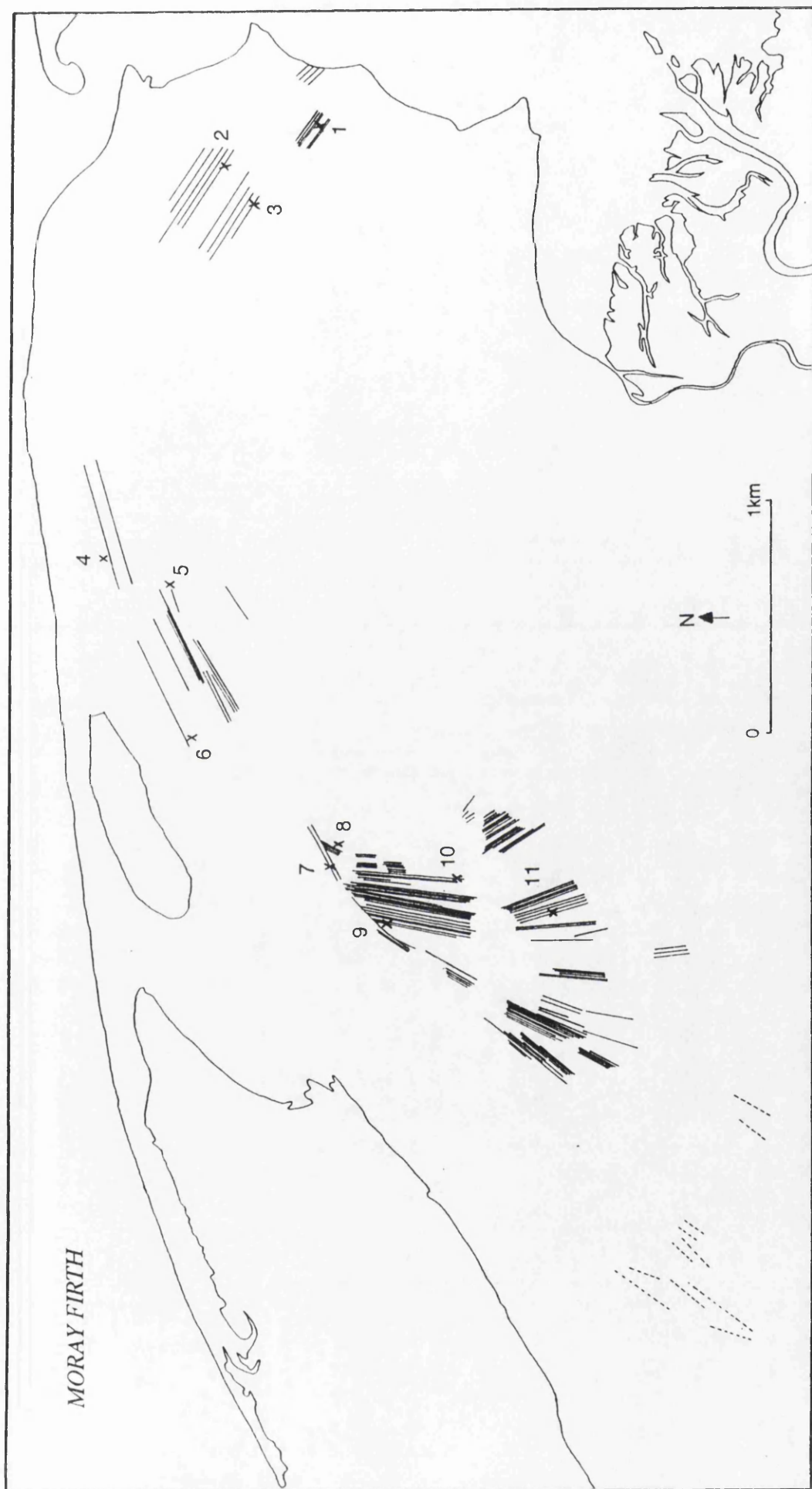


Figure 3.4 Location of clast sampling sites, Culbin

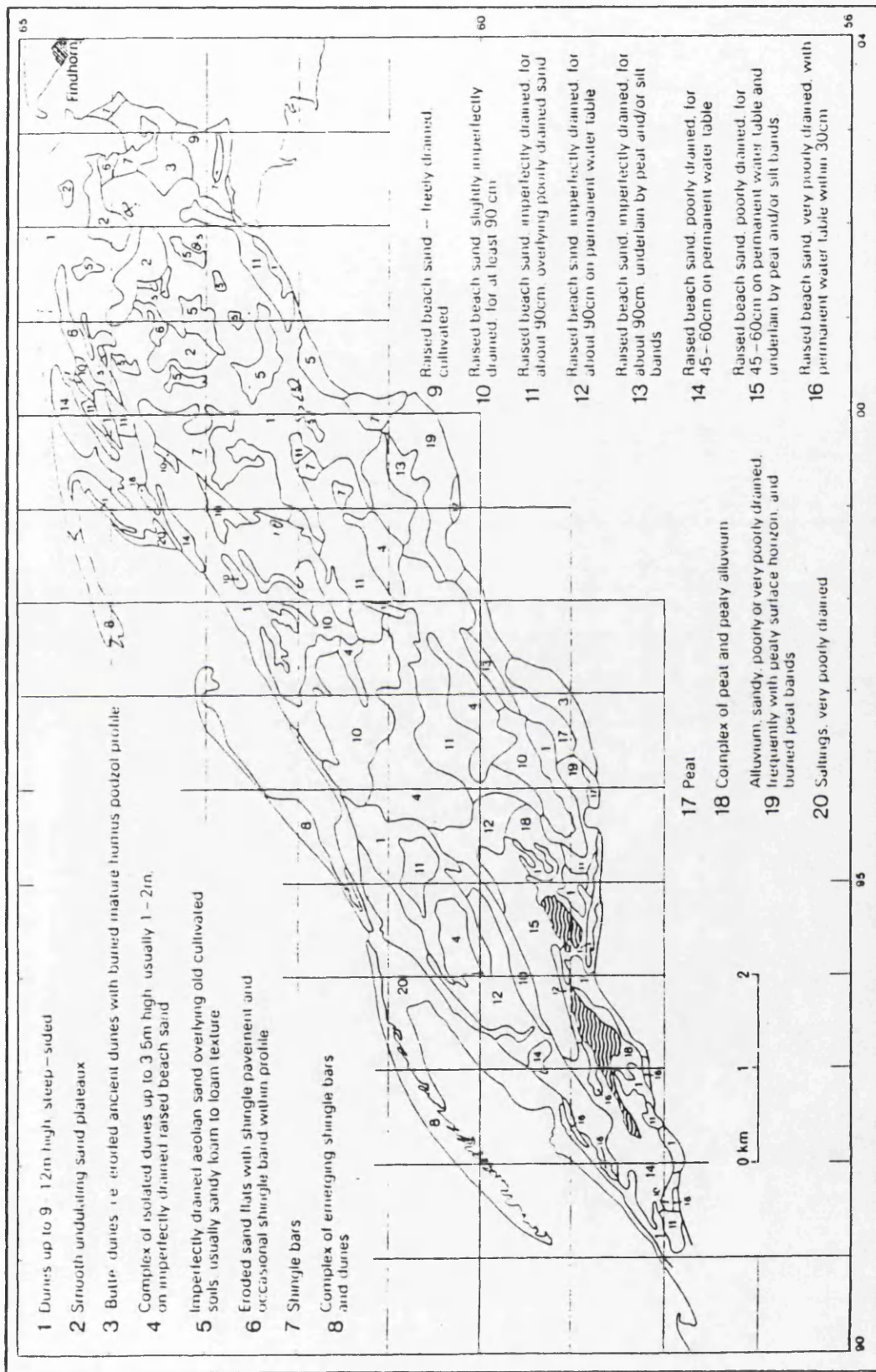


Figure 3.5 Division of the major sedimentological units at Culbin (source: Gauld, 1981)

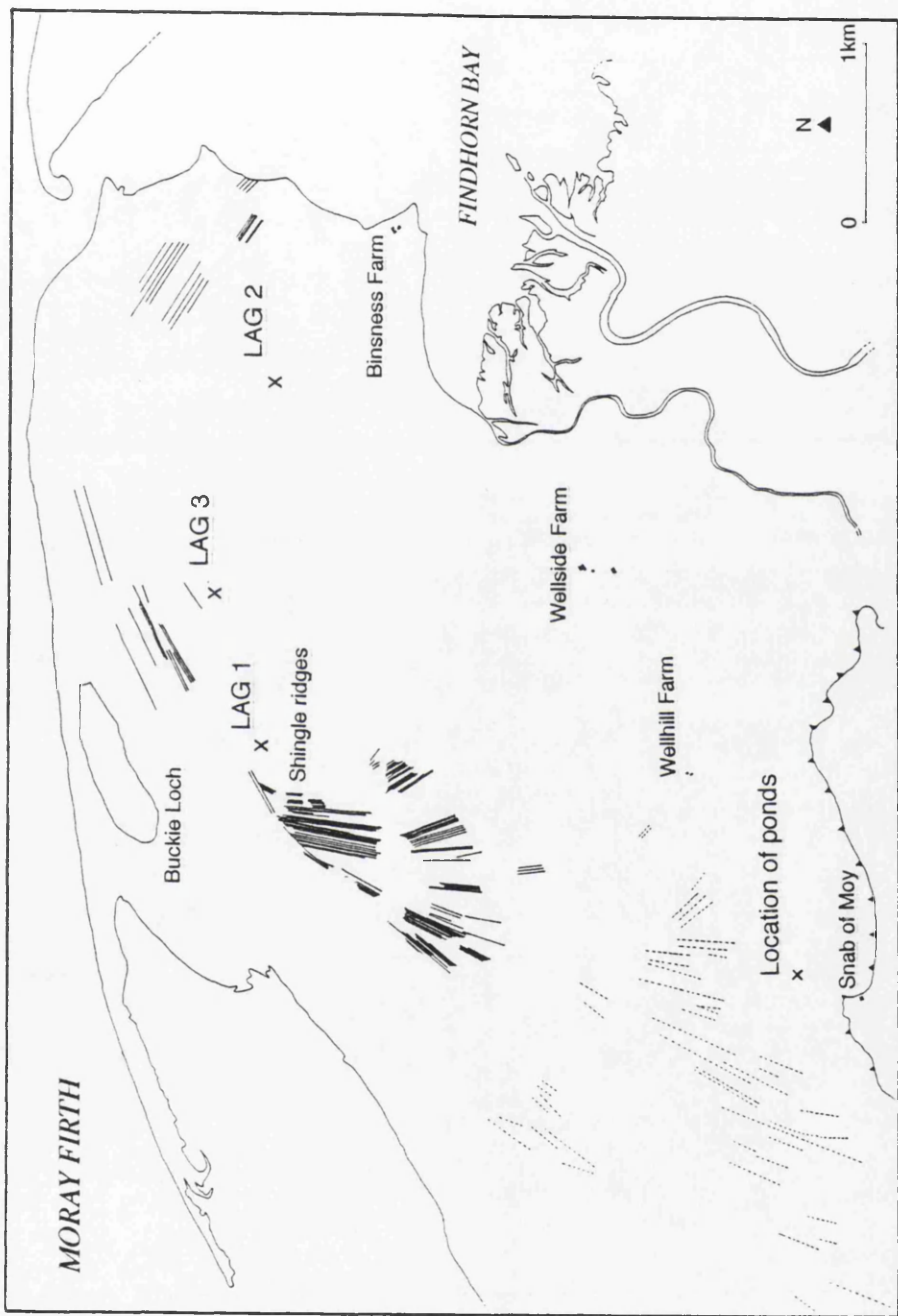


Figure 3.6 Location of ponds at Snab of Moy

was available over samples which may have been taken from zones of higher mean clast size, sampling from each of the ridges was made from the seaward side of the ridge crest, representing the only definite reference point on all individual ridges (Goudie, 1990). On The Bar, seven stations at 350 m intervals were selected for clast analysis. The length of the three principal axes was recorded for fifty randomly selected clasts at each station. This sampling strategy was denser than that on the Culbin ridge suite in order to account for the rapidly increasing mean clast length with distance west, which is of sufficient magnitude to be observed visually.

### **3.1.3 Stratigraphy**

Stratigraphic details within Culbin Forest itself are difficult to obtain due to the thickness of shingle infill and subsequent blown sand cover, which reaches 30 m at Lady Culbin (NJ 013640). Commercial subsurface investigations have tended to ignore the Culbin foreland, and thus the subsurface details obtained have concentrated on commercial borehole records available from adjacent sites in Burghead Bay lowlands in the vicinity of RAF Kinloss. Some limited hand augering was undertaken in the area landward of the shingle belt in the areas identified by Gauld (1981) as containing fine-grained sediments. These are displayed in Figure 3.5. The results from these investigations were augmented with trial pits where discrete samples were required for laboratory analysis.

A limited amount of subsurface data was available from a series of three freshwater ponds found in the vicinity of Snab of Moy farm (NH 987607). The ponds were found below the level of the surrounding terrace surface, and initial coring with a Russian peat corer revealed a sequence of intercalated fine-grained sediments and thin peat layers at depths down to 2.60 m OD. Further investigation of these deposits was essential due to their position between the end of the shingle fan and the abandoned cliffline. The position of these ponds is shown in Figure 3.6. Ponds 1 & 2 were small enough to access using waders, but the size and depth of pond 3 coupled with an unstable pond bed meant that access to the centre of the pond could only be made by boat. Samples were retained for analysis in the laboratory and submitted for radiocarbon dating. Samples were removed from the chamber of the Russian corer intact, and stored in a plastic half-tube wrapped in aluminium foil. Once back in the lab, the samples were stored in a refrigerator at 4°C until required for analysis and dating.

Subsurface data was also obtained from the area around the head of Findhorn Bay and RAF Kinloss. Investigation of these areas was undertaken using borehole logs produced both by Grampian Regional Council and the MOD. This information was supplemented with hand coring and field section descriptions when available. Cores were taken using a Russian peat corer, removing successive 0.5 m increments. All sedimentary logs were levelled in to OS benchmarks where possible, and TBMs where not. Sediment samples were collected for laboratory analysis where appropriate. These were bagged in the field and returned to the laboratory where they were dried, weighed and sieved using a standard methodology (Buller & McManus, 1973).

The borehole information from RAF Kinloss was supplemented by fieldwork, since coastal erosion in Burghead Bay has exposed a cliff of raised foreshore deposits, up to 4 m in height and 5.5 km in length. The majority of the exposure comprises interbedded sand and shingle. A central 660 m exposure contained information considered particularly significant in the reconstruction of the RSL history of the site. This section is described in detail as a series of 18 individual logs, with details of relationships between the individual units in the intervening areas providing a composite log of the entire 660 m exposure. Altitudes of the various sedimentary units were determined from levelling, using an abney level and ranging pole for single user operation. In addition to the composite log produced describing the deposits in a shore-parallel manner, a similar log was produced describing the deposits exposed perpendicular to the coast in Burghead Bay. A section 275 m long incised by the Bessie Burn meets the beach perpendicularly at NJ 097654. Sampling at 5 locations along the section, combined with levelled spot height information at strategic points in between, produced an accurate description of the location and altitude of the deposits exposed in the stream section. The information from these two composite logs was then used in conjunction with the borehole information from RAF Kinloss to identify relationships between individual sedimentary units in Burghead Bay.

A problem noted early in the project was that a sea level curve for this part of the Moray Firth had not yet been produced. As Culbin Forest lies on the same Postglacial isobase as the Dornoch Firth, the use of a "surrogate curve" from this area was deemed acceptable as a first approximation of a RSL history for the area. However, one of the hypotheses under test suggested that shingle ridge altitudes, in sufficient numbers, might provide some insight into the trends in RSL which formed them. To test this hypothesis more fully it was necessary to produce a relative sea level curve for the Culbin area. Dateable sea level

indicators were found to be lacking in the sterile shingle sequences of Culbin Forest, and so the search for suitable material extended as far east as Burghead Bay, and as far inland as Kintessack (Figure 3.1). While peat formed the majority of samples taken, both shell material and palaeosols were also submitted for radiocarbon assay. Samples of peat were taken using either a Russian peat corer (core samples), or a clean spade (monolith samples from sections). Core samples were removed with a clean knife, wrapped in aluminium foil and stored in plastic half-tubes. Samples removed from sections were in blocks of at least 30 cm x 30 cm, allowing samples to be taken from the centre of the block to minimize contamination risk. All samples were stored in refrigerators at 4°C until required for assay. Samples were then halved, retaining a section of the sample in case of loss or laboratory error. Thirteen samples were submitted for assay to the NERC radiocarbon laboratory, East Kilbride.

The possibility of sample contamination through hard water effects was minimal, primarily due to a lack of carbonate material in the surrounding environment. The solid geology of the area is dominated by Devonian sandstones, with a characteristically low carbonate content. Similarly the shingle derived from the surrounding country rocks contains no carbonate rocks from which "old carbon" could occur. The sample ages obtained are not corrected for either plateau effects (Bradley, 1985; Stuiver *et al.*, 1991), or calendar years (eg Tushingham & Peltier, 1993), and as such remain directly comparable with the remainder of radiocarbon dates obtained from the Moray Firth area (eg Firth & Haggart, 1989).

## 3.2 CONTEMPORARY COASTAL PROCESSES AND LANDFORMS

### 3.2.1 Contemporary coastal processes

Examination of the nature of the processes driving, and the landforms resulting from Holocene coastal evolution in the Moray Firth allows a better understanding of the operation of the present sedimentary environment of Culbin and Burghead Bay. Conversely, a detailed understanding of contemporary coastal processes will aid the final interpretation of Holocene sediments and landforms. It is therefore important to understand the full range of processes operating on the contemporary Culbin foreshore, both to aid the interpretation of relict coastal features, and also to interpret the most recent phase of the Holocene evolution of the Culbin coastline.

Investigation of the processes currently active along the Culbin foreshore was made via the medium of the sediment budget. The elements of the sediment budget are outlined in Figure 3.7.

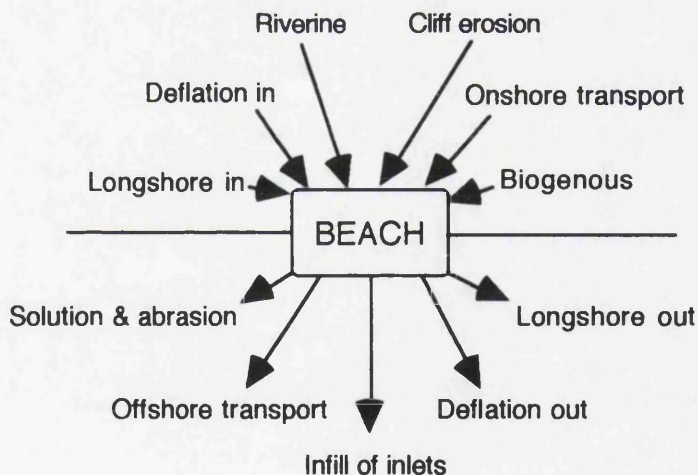


Figure 3.7 Elements of the beach sediment budget

The original concept, (Davies ,1974), sought to compartmentalize the beach through a systems approach, identifying and quantifying inputs and outputs to the beach system by applying the principle of the conservation of mass to beach

sediments (Komar, 1976). The beach sediment budget is one of the most widely used forms of assessing the sedimentary status of beaches, and as such the methodology employed here was considered useful in providing results in a comparable format to those produced elsewhere (eg Mason, 1985). The remainder of this section describes the methods employed in quantifying the processes which drive the beach sediment budget operating along the Culbin foreshore.

### **3.2.1.1 Environmental controls: Introduction**

Prior to describing the elements of the beach sediment budget in detail it is necessary to outline the energy inputs to the beach which drive the sediment system on the Culbin foreshore. The energy regime in the Moray Firth has been categorized as low (Reid, 1988), with the primary energy source derived from waves. Tidal currents provide only a secondary role in sediment transport, particularly in the inner Firth (Lee & Ramster, 1981), which is characterized by low tidal current velocities (maximum of  $0.5 \text{ m s}^{-1}$ ).

Considerable effort was made to obtain a representative sample of the wave spectrum incident along the Culbin foreshore, using a variety of data sources. Additionally measurement of tidal currents was undertaken in order to assess the importance of this process in nearshore sediment transport in comparison with published data collected further offshore. The methods employed in measuring waves and tidal currents will be described in detail before describing the elements of the beach sediment budget and the methods used in its evaluation.

### **3.2.1.2 Tidal currents and current meter measurements**

Sediment entrainment through the medium of tidal currents was considered of secondary importance given the nature of the existing data in the Moray Firth (Dooley, 1971; Lee & Ramster, 1981; Reid & McManus, 1987). However investigation of the exact magnitude of tidally-induced currents in the offshore zone bordering Culbin was undertaken during June 1991. Measurement was undertaken in order to ascertain the following:

- i) whether currents were sufficiently strong to entrain sediment, or simply to transport previously suspended sediment;

ii) whether any residual currents existed, and if so to assess their relative sedimentological importance in transporting material in the nearshore zone.

Measurements of tidal currents were made using an Aanderaa Instruments RCM-4 recording current meter, loaned from NERC RVS, Barry. This instrument recorded current direction and speed at 10 minute intervals, logging onto an internal 6 track magnetic tape.

The current meter was positioned 1.2 km offshore (at NJ 005660) from the bothies at Shellyhead. The location of the instrument was selected so that:

i) the instrument was in a sufficient depth of water for recording under all tidal conditions;

ii) the influence of tidal forcing of river water from the River Findhorn against the coast would be minimized.

The location of the instrument was fixed using triangulation from a boat moored directly above. Deployment of the instrument was between 05/06/91 and 29/07/91, but mechanical failure of the instrument on 22/06/91 produced only 33% of the expected data. However, the record was sufficiently long (18 days) for useful data analysis to be derived, spanning a neap-spring-neap tidal cycle.

Immediately prior to deployment the instrument clock was turned on, ensuring the exact time and date were recorded simultaneously. The method of deployment of the instrument is shown in Figure 3.8. The instrument was placed in 6 m of water at low tide. With a tidal range of ca. 4 m, this gave a maximum water depth of 10m, with the body of the instrument suspended 1.5 m above the sea bed.

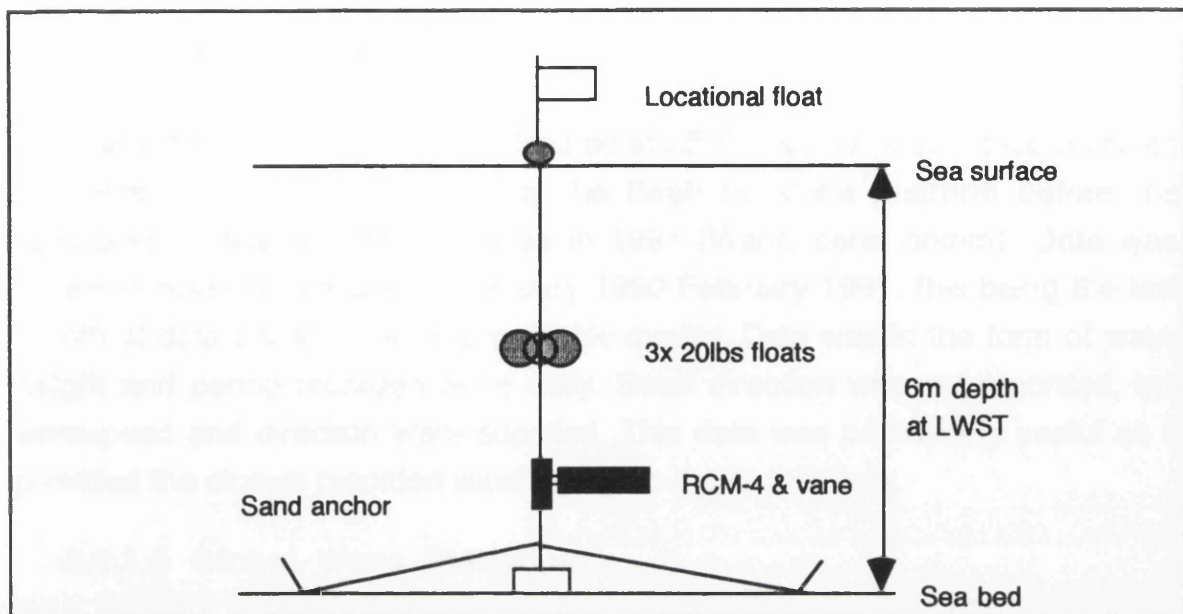


Figure 3.8 Method of deployment of the current meter, Culbin June-July 1991

### 3.2.1.3 Waves and wave recording

Quantification of the nearshore wave climate is the single most important factor in understanding how the nearshore system operates. The wave refraction models outlined in Chapter 1 are extremely sensitive to input parameters, and so it is vital to provide high quality wave data as input. A range of sources were utilized in order to obtain as full a record of waves as possible. Use of different data sources allowed cross-checking, providing maximum accuracy in the production of a relevant wave climate at Culbin. Wave data was obtained from the following sources:

- i) the Beatrice Alpha oil platform in the outer Moray Firth (via Met. Office records);
- ii) Global Wave Statistics: North Sea (filtered for waves entering the Moray Firth);
- iii) Conoco Ltd (extreme wave values only);
- iv) independent wave measurement using a directional wave recorder constructed specifically for this project.

#### **3.2.1.4 Beatrice Alpha**

The Beatrice Alpha oil platform is located at 058°N 003°W. Met. Office archives produced the last records kept by the Beatrice Alpha platform before the recording of sea conditions ceased in 1991 (Want, pers. comm). Data was obtained covering the period February 1990-February 1991, this being the last month of data collected of an acceptable quality. Data was in the form of wave height and period recorded twice daily. Swell direction was not recorded, but windspeed and direction were supplied. This data was particularly useful as it provided the closest recorded wave record to the Culbin area.

#### **3.2.1.5 Global Wave Statistics**

Data from Global Wave Statistics (BMT, 1986) proved extremely useful in assessing both the duration and height of swell encountered in area 11 of the North Sea. Data from Global Wave Statistics is in the form of frequency tables, showing significant wave height ( $H_s$ ) and the zero crossing period ( $T_z$ ) for the eight wave approach directions. Due to the coastal alignment of the Moray Firth it was necessary to filter out waves from all but the north, north-east and eastern sectors. Within these categories it was assumed that data from the north and east sectors covered the incident range 337.5°-022.5° and 067.5°-112.5° respectively. Due to the sheltering effect afforded by the Moray Firth the frequencies of occurrence from the north and east was halved, as including the full frequency would produce an overestimate of waves from these sectors.

Wave climate seasons as defined in Global Wave Statistics are staggered from standard calendar seasons by one month. The winter wave season thus runs from December to February, and the summer season from June to August. As the data from Global Wave Statistics became the standard wave data set used throughout this analysis, this seasonal convention has been used for the remainder of the thesis.

#### **3.2.1.6 Conoco Ltd**

Of more limited use was the summary data provided by Conoco Ltd. Data was collected originally during the deployment of the "Hutton" waverider buoy in order to predict extreme waves in the Moray Firth. The buoy was located at 057°42'N 003°41'W. Data was provided in the form of extreme wave height and the probability of its return period. This data provided a control on the upper

extreme wave conditions recorded at Beatrice Alpha, but was of limited use in the production of the wave climate of the Moray Firth.

### **3.2.1.7 Wave Recorder**

Additional to the secondary data sources outlined, a wave recorder was constructed as an initial step in obtaining an independent record of on-site wave conditions at Culbin. The rig was designed with the following criteria in mind:

- i) sufficient sensitivity to log wave height and period of the lowest waves encountered at the site;
- ii) recording from two channels simultaneously in order to resolve the angle between the breaking wave crest and the shoreline;
- iii) lightweight design for installation without diving assistance;
- iv) independent power and logging since no mains supply was available for PC logging.

Siting the rig required careful planning, and the eventual location was at NH 999648 (adjacent to a beach profiling station, see section 3.2.3). Design criterion iii) above determined the position of the rig at the lowest point possible on the subaerial beach profile and installation was made on a low spring tide. The site indicated was chosen on the basis of:

- i) lack of nearshore bar activity which would lead to problems with effective water depth changes affecting the recorded pressure changes. Additionally the physical burial of the rig would produce gaps in the data record;
- ii) the narrowest section of beach reducing the amount of cable required between the rig and the data logger;
- iii) stable back-beach dune environment for location of the data logger.

The design for the rig was based on that of Hardisty (1988). The elements of the rig were essentially that of two standard pressure-transducers mounted on a shore-parallel rig (Plate 4). Changes in the pressure recorded by the transducer relates to the varying water depths as waves pass overhead. The logger employed had the capacity for high frequency logging (3 Hz) in order to differentiate the passage of individual wave crests on both logging channels.

The rig was constructed as two separate oil-damped pods, each enclosing a pressure transducer. The pods were mounted on "Dexion" pyramid frames 1.4m high which were weighted using sandbags, part-buried in the beach surface and lashed to a series of 0.5 m high disused salmon leader posts (Plate 4). The link between the rig and the data logger was provided by 120 m of 5 core armoured cable buried to a depth of 1 m in the beach. The data logger employed was a Delta T devices "Delta Logger", located in a weatherproof box within the dune system backing the beach.

Data from each transducer was logged on a single channel simultaneously, with each channel triggered by an event timer at 24 hour intervals. Due to constraints on memory space logging periods lasted for 60 seconds every 24 hours, logging at a rate of 3 Hz. Such a logging rate was designed to provide an 18 day record before downloading was required, provided the pods were submerged at all times. A simple computer programme was written to test the efficiency of this logging design. This simulated the passage of two sine waves running slightly out of phase, with wave periods selected to represent wave conditions found on the beach. Total record lengths of 60 seconds were found to be sufficient to identify the independent characteristics of each wave. Thus this method was seen as sufficient to record the relevant wave details whilst accepting the design constraints.

Field measurement of the angle between the wave crest and the shoreline has been rarely attempted. Hardisty (1988) produced the only known attempt to deploy a shore-based directional wave recorder. The theory behind directional wave recording was outlined in Hardisty (1990), and is summarized as follows (refer to Figure 3.9):

i) mean wave velocity (celerity) in shallow water was calculated from

$$c = \sqrt{gh} \quad (3)$$

ii) phase difference ( $T_1 - T_2$ ) between transducer 1 and 2 is obtained from the logging record;

iii) distance travelled ( $D$ ) is calculated from

$$D = cT \quad (4)$$

Plate 4

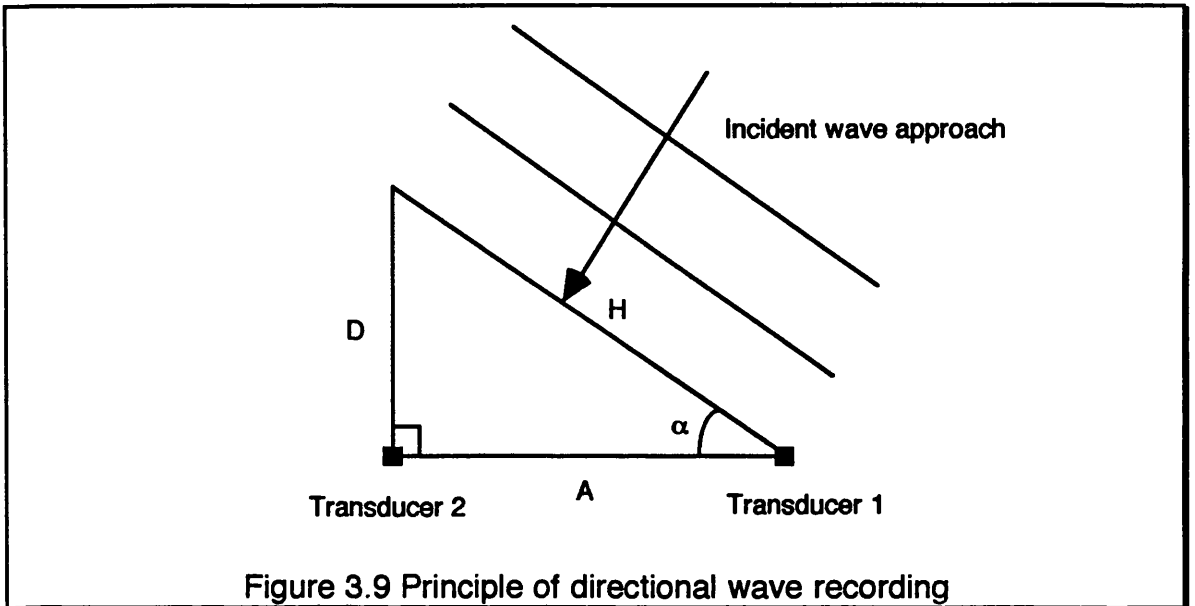
Deployment of the wave recorder, June 1991. The pods are mounted on dexion frames, and are located 7 m apart.

(Original in colour)



iv) incident angle is finally calculated from

$$\sin \alpha H = D \quad (5)$$



Details of wave height, period and direction were recorded for all waves during each data run.

Problems with vandalism and logger failure meant that only a single 18 day run was recorded, out of which the pods were only submerged for 9 days. However the quality of the data produced was such that its inclusion was felt useful in both validating the technique and demonstrating the complex nature of the wave spectrum encountered at Culbin.

### 3.2.2 Wave refraction modelling

Wave refraction modelling was undertaken using two techniques. Simulation of swell wave incidence on the Culbin foreshore was undertaken using the computer generated program WAVENRG (May, 1974). The data obtained from this routine was supplemented to include the effects of wind wave activity using a graphical technique for wave refraction. This latter technique will be described first.

#### 3.2.2.1 Graphical wave refraction modelling of wind waves

In shallow water, wave velocity (celerity) depends upon the depth of water in which a wave is travelling. As velocity decreases with falling water depth, a wave

approaching a shoreline obliquely will find the landward end of its crest in shallower water (and thus will be travelling more slowly) than the seaward end. This variation in velocity along the wave crest causes the wave to "bend" in an attempt to parallel nearshore bathymetry (CERC, 1984). Sea wave refraction follows the principal of Snell's Law for optical refraction (Chapter 2, equation 1). Wave refraction is important for the following reasons:

- i) combined with shoaling, wave refraction determines the wave height at breaking. This is one of the most important variables in the prediction of sediment transport on the beach, second only to incident wave angle;
- ii) refraction produces convergence and divergence in wave energy alongshore, affecting the distribution of sediment and sedimentary processes (Munk & Traylor, 1947).

(after CERC, 1984)

When undertaking wave refraction modelling the following assumptions regarding the nature and behavior of incident waves have to be made:

- i) wave energy between orthogonals is constant;
- ii) wave advance is perpendicular to the wave crest (ie normal to orthogonals);
- iii) specific wave velocity is dependent only on water depth at the point of measurement;
- iv) bathymetric changes are gradual;
- v) incident waves have a constant period, they are long crested, of small amplitude and are derived from a monochromatic source;
- vi) effects of currents, winds and reflected energy from the beach are negligible.

(after CERC, 1984)

Wind wave refraction simulation was undertaken using the graphical method outlined by CERC (1984). The initial stage in this process involved the generation of a series of waves for input into the model.

Locally generated wind waves represent a significant factor in the wave spectrum encountered on the Culbin foreshore. Total swell wave incidence from the North Sea "window" accounts for between 15.46% and 24.12% of the annual wave spectrum. For a significant proportion of the remainder of the year wind waves provided the primary energy input to the beach. In order to include these in the calculation of a sediment budget the frequency of wave generating winds had to be assessed. Wind data was obtained from RAF Kinloss, 6 km east of Culbin and close enough to provide reliable and accurate data. Of interest to this study were the records of winds from the sector 240°-330°, which produce onshore winds at Culbin. These winds represented 51.9% of the annual wind record at RAF Kinloss during 1990.

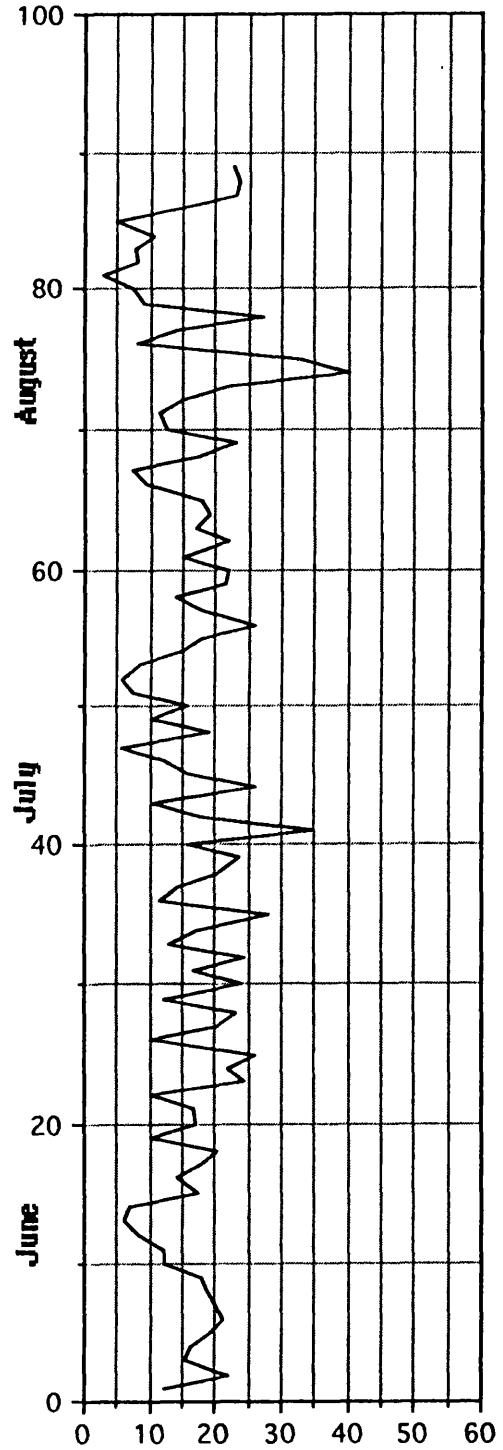
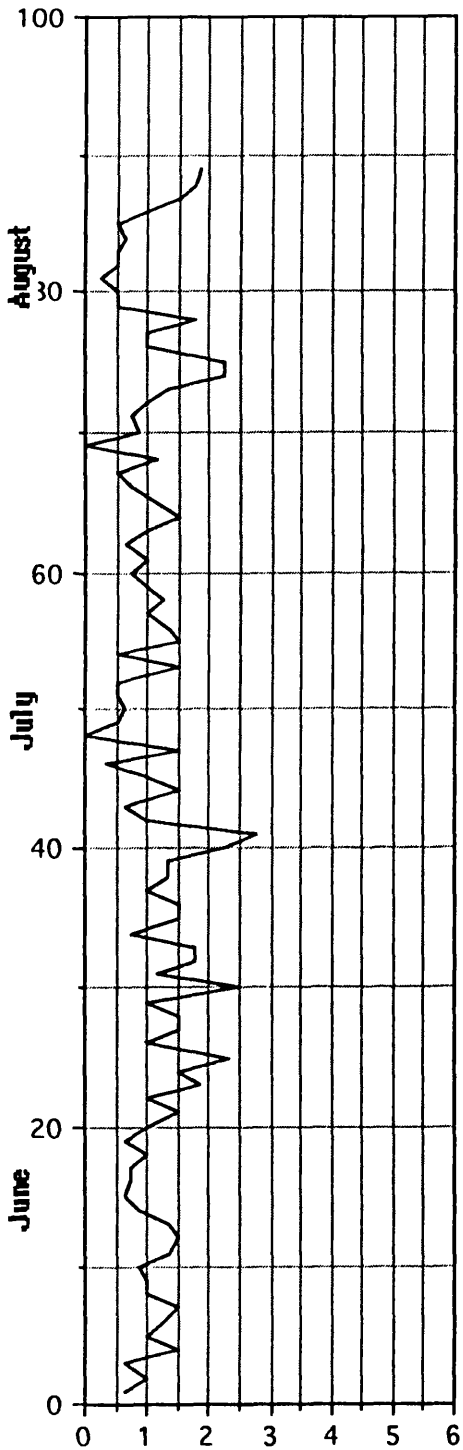
Winds from the sector 010°-080° were assumed to be coincident with incident swell from the same direction due to the strong correlation noted between wind and wave direction from the Beatrice Alpha data (Figure 3.10). However, winds blowing from this sector only accounted for 12.9% of the total wind record, and are less common than those from other sectors. Thus a slight increase in wave height above that predicted due to an accompanying wind might be expected, and the values presented will be slight underestimations of the true sediment movement potential. Winds blowing offshore were discounted in the present study, and it was assumed that offshore winds produced calm conditions.

Having generated an additional set of waves through hindcasting, these values had to be converted to a longshore current. To do this, the total wind hours recorded during 1990 at RAF Kinloss were split into monthly segments, and for each month the wind speeds and directions were grouped. The most common windspeed group for each sector was identified and noted. 5.5-10.5 m s<sup>-1</sup> was the single most common grouping throughout the year, and a group mean velocity of 8 m s<sup>-1</sup> was taken as the most representative velocity given no other data. The wind wave sector 240°-000° was split into 30° sectors, and from these directions the maximum fetch distance across the Firth to Culbin was measured. As the waves were so obviously fetch limited the duration over which the winds blew was irrelevant in this case. Once the fetch had been measured, the mean velocity and fetch were converted to an equivalent wave height and period using a conversion table (Komar, 1976, fig 4.5, p85).

The initial stage in the graphical wave refraction exercise once the waves had been generated involved the construction of a contoured bathymetric chart of the offshore zone using Admiralty chart 233 (Dunrobin Point to Buckie). The next

Wave height - Beatrice 'A'  
Summer 1990

Windspeed - Beatrice 'A'  
Summer 1990



Wave height (m)

Windspeed (k)

Figure 3.10 Simultaneous plots of wave height and windspeed (data from Beatrice Alpha)

stage was to convert the contours to units of equivalent deep water wavelength ( $L_0$ ). To do this the deep water wavelength was calculated from the equation:-

$$L_0 = 5.12 T^2 \quad (6)$$

where  $T$  = wave period (s)

The contours were recalculated by dividing the original contour values by  $L_0$ , and plotting the resulting values on the bathymetric chart. Next the distance of wave advance was plotted on the chart using a ready constructed template (outlined in King, 1972). This described the amount of wave advance in terms of wavelength, expressed as:-

$$n = \frac{0.036 s}{T^2} \quad (7)$$

where  $s$  = map scale

$T$  = wave period (s)

$n$  = number of wave lengths  
advanced

The mid-line of the template was then aligned with the appropriate contour value, and the position of the wave crest at this point marked on the chart. The waves were initiated in "deep" water ( $d/L_0 \geq 0.5$ ) and were assumed to have undergone no refraction prior to entering the study area. Once the wave reached the shoreline it was assumed to have broken, and the refraction exercise ended. The resultant angle between the crest and the shoreline was then measured using a protractor, and the values recorded.

Once the refraction plots had been completed and the angle between crest and shoreline measured, the resultant data required further analysis in order to convert it to a potential longshore sediment transport value. The initial stage involved calculating the changes in wave characteristics as they approached the shoreline. As waves enter shallow water their height increases through shoaling, and the amount of increase is also modified by the degree of refraction which has occurred (Komar, 1976). In order to produce accurate predictions these two factors require quantification. Both Komar (1976) and CERC (1984) suggested possible methods for quantifying these elements. The procedure outlined by CERC (1984) was used in this study due to its fully quantitative nature.

The initial stage of this process involves the calculation of the refracted deep water wave height from the equation

$$H'_o = \frac{b_o^{1/2}}{b} \quad (8)$$

where  $b_o$  = distance between orthogonals in deep water.

$b$  = distance between orthogonals in shallow water.

$$H'_o = \frac{H_o b_o^{1/2}}{b} \quad (9)$$

This equation was then used to calculate the deepwater wave steepness term

$$\frac{H'_o}{gT^2} \quad (10)$$

where  $g = 9.81 \text{ m s}^{-2}$

$T$  = wave period (s)

which was read from graph 2.72 (CERC, 1984) to find the value of the term

$$\frac{H_b}{H'_o} \quad (11)$$

Finally the refracted breaker height  $H_b$  was defined by

$$H_b = \frac{H_b}{H_o} H'_o \quad (12)$$

The refracted breaker heights were then used along with the refracted incident angles to calculate values of potential longshore sediment transport.

### **3.2.2.2 Wave refraction using the computer simulation programme WAVENRG.**

The graphical wave refraction procedure described above is now generally carried out by computer. The programme used in this study was a derivative of the WAVENRG model devised by May (1974). The programme was run on a VAX mainframe system at the University of Coleraine. Input data to the programme consists of a digitized version of the Moray Firth coastline, details of the bathymetry of the area and information concerning wave height, period and angle of approach from "deep" water ( $\geq L/4$ ). Once completed, the user specifies

the combination of wave height, period and angle of approach required, and the co-ordinates of the start position of the waves in deep water. Deep water was required for a starting position as waves were assumed to have been generated in the open ocean (or the North Sea in this case), and as such were assumed to have straight crests with no refraction having occurred prior to entering the study area. Deep water was defined for the purpose of this study as >25 m. As the maximum wave height run on the model was only 2 m, this depth more than satisfied the criteria of no wave-sea bed interference prior to "entering" the model zone.

The initial stage in the programme required the input of a digitized coastline and bathymetric map. This data was again provided from Admiralty chart 233, and a chart was produced covering the whole of the Moray Firth from Spey Bay in the east to the Dornoch Firth in the north west.

Secondly a selection of wave heights, periods and directions were selected for inputting into the model. These were selected on the basis of those used in the first (graphical) wave refraction exercise in order to produce comparable results. Three wave heights (0.5, 1 & 2 m), and three wave periods (6, 8 & 10 s) were selected, based on data derived from Beatrice Alpha. Directions of wave approach are severely limited by the physiography of the Moray Firth, which acts as an energy 'window', allowing entry to waves from a selected sector only. Consequently only incident directions between  $010^{\circ}$  &  $080^{\circ}$  were input, in  $10^{\circ}$  intervals, these representing the only significant directions from which swell waves are likely to occur on the Culbin foreshore. Northerly waves ( $000^{\circ}$ ) were discounted due to the limiting form of the Moray Firth in this sector. Easterly waves ( $090^{\circ}$ ) were not included as experimental orthogonal plots using the refraction program tended to miss Culbin completely.

Once the boundary conditions had been input, the refraction programme was run. Data output was in the form of graphics plots of wave orthogonals, showing the path of wave crests from their 'source' in deep water to their end point at a computed break point. Upon 'breaking', the programme calculated a series of parameters for each orthogonal, including  $P_L$ , which were used in the calculation of the longshore sediment transport regime.

### **3.2.3 Contemporary Coastal Landforms and Foreshore sediments**

#### **3.2.3.1 Beach Profiles**

The collection of beach profile data at regular intervals was undertaken in order to describe the detailed morphology of the foreshore, and to allow the calculation of actual volumetric changes in the beach over a two year recording period. This method thus acted as a control over the calculation of a *potential* sediment budget based on wave refraction modelling. These methods were finally combined to provide a more accurate assessment of sediment transfers within the beach system.

In order to assess changes in beach elevation and volume over the period of study, beach profiles were collected at selected sites along the Culbin foreshore. Choice of position of each profiling position was made during initial fieldwork during February 1990 on the basis of locating the profile in the centre of geomorphologically distinct sections of the beach (Figures 3.1 & 3.11). Seven locations were chosen to represent the range of beach profiles found on the Culbin foreshore, resulting in unevenly spaced profiling stations. Each station was marked using a white painted stake inserted in the dunes at the back of the beach, with a second stake placed further landwards in case of loss or damage to the seaward stake. In order to present the beach profiles in terms of an absolute altitude (relative to OD Newlyn), both the stakes and other convenient intermediate points were levelled to an OS benchmark in Findhorn village. The traverse was extended across Findhorn Bay, along the beach as far west as station 7, then returned to Shellyhead bothies, incorporating all profile points along the way. The traverse was then closed back onto this benchmark via the northern track through the forest in order to incorporate several raised shingle deposits *en route*, before closing again across Findhorn Bay. The closing error on this traverse was 0.227 m.

Beach profiles were measured using the stakes incorporated in this network as TBMs. Profiles were measured using the theodolite/EDM system used throughout the project. The measuring station was installed astride the TBM stake where possible, and measurements of angular distance and declination were measured to each break of slope on the beach. This method was considered more accurate than measuring to fixed positions along each profile (eg. Bowman, 1981), which tends to result in an underestimate of beach volume. Where the theodolite/EDM could not be installed astride the stake (for example when the location peg was located on the high, cliffed dunes at the east end of

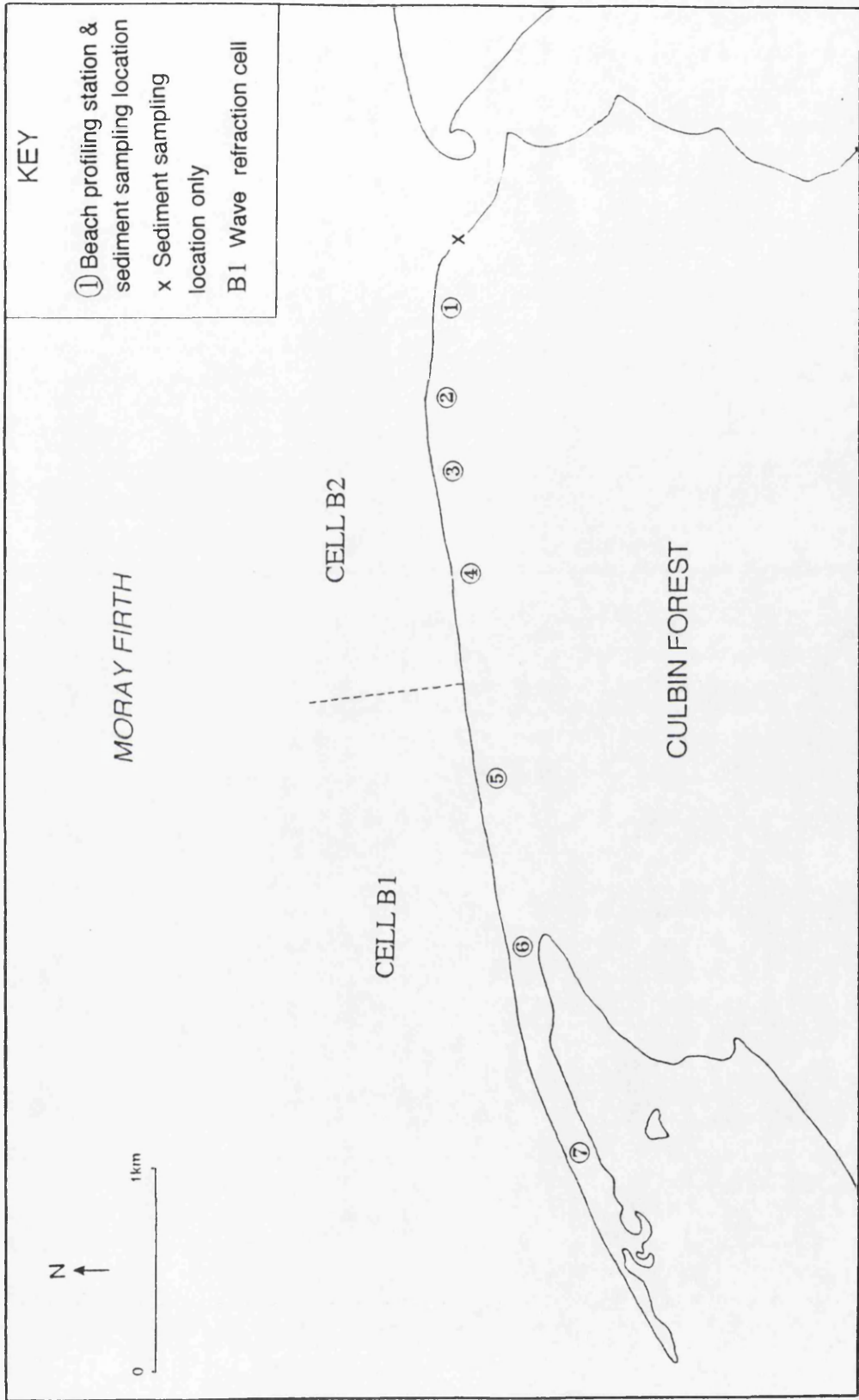


Figure 3.11 Location of beach profiling stations and sediment sampling locations

the beach), the profile was potentially subject to an altitudinal discrepancy. To solve this, the start position of the profile was levelled in on each occasion to a series of groynes found on the beach, which had been previously incorporated into the altitudinal control network outlined above. Profiles measured during the initial field visit were made perpendicular to the beach, and a note made of the bearing taken during the traverse at each site. All subsequent profiles were taken along these bearings, allowing a valid comparison of collated profile data.

Beach profile data was collected on spring tides to allow maximum foreshore exposure at low water. Due to logistical restrictions the initial sampling strategy was to collect data every two months. However, after February 1991 it was possible to sample at monthly intervals. A total of 14 profiles were collected from each station based on this sampling strategy.

### **3.2.3.2 Extension of Beach Profiles into the Offshore Zone**

Beach profile data was supplemented by extending the profiles into the offshore zone using echo sounding. The profiles were measured only once to provide an overview of the offshore profile at each profiling station. This was used to locate the position of offshore bar locations, but did not form part of the sediment budget calculations.

All of the surveys were conducted on 01/06/1992 on a spring tide, and were measured as close to high tide as was possible in order to minimize drift due to tidal currents. This allowed the landward end of the offshore profile to overlap with seaward end of the shore based profile at each station, simplifying the linkage process between the two. Measurement of submarine profiles was undertaken using a boat-mounted echo sounder (FuSo 180m). This produced a hard copy of each profile in the form of a paper trace. These were later converted to a series of distance/depth co-ordinates for plotting in the same manner as standard sub-aerial beach profiles.

At each profiling station the boat proceeded approximately 800 m offshore, along the bearing of the shore-based beach profile measurements. Two buoys were deployed along this bearing in order to keep the offshore profile in line with the beach profile. At each deployment the position of the buoy was fixed by triangulation, as was the seaward end point of the offshore profile. Figure 3.12 shows the plan of the profiles made. The error introduced from drift due to tidal currents was minimal. The boat was driven landwards at a slow but constant speed, sighting on the buoys, with the echo sounder transducer fixed to a boom

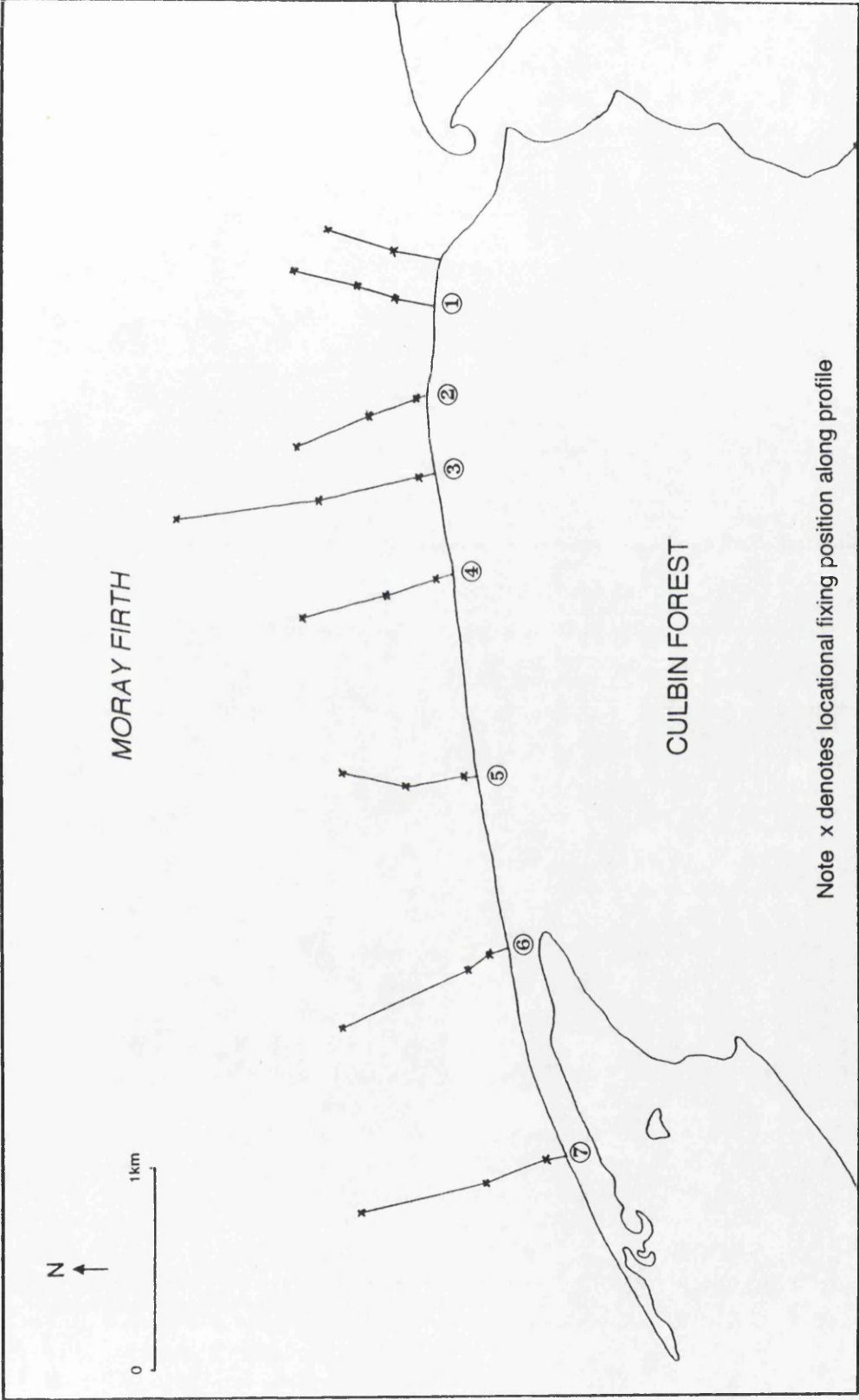


Figure 3.12 Plan of submarine profile locations

attached to the side of the craft at a distance sufficient to avoid bubble interference from the hull. As each buoy was reached the trace on the echo sounder was marked, providing a positional fix on the trace from which to calculate the horizontal scale during analysis. Each traverse was taken inshore as far as the surf zone.

### **3.2.3.3 Sediment samples**

Regular sediment sampling from the foreshore was not a procedure followed in this study since the information provided from a single synoptic view of the status of the beach would provide a satisfactory check on the direction and continuity of the nature of the beach sediment in the littoral compartment (Clayton, 1980).

The location of the sediment sampling stations is shown in Figure 3.11. Sediment samples were collected from each of the regular beach profiling stations 1-7 (section 3.2.3), plus one sample from the foreshore at the mouth of the Findhorn and one from the foreshore within the confines of Findhorn Bay. Additionally, one sediment sample was taken from the contemporary dunes at Shellyhead for comparative purposes.

Samples were collected from the foreshore over the period of a single low tide. They were collected from a position approximately midway down each profile. By sampling at this position the sample would not be biased towards the coarser size fraction as might be expected if samples were collected at either high or low water positions, due to extended exposure to wave action at the tidal stand. The samples were taken from the upper 1 cm layer of the foreshore in order to reflect the sediment movements of only the last tide, ensuring that the samples were comparable (as far as is possible) in terms of wave exposure. Approximately 300 g of sediment were collected at each site, providing sufficient sediment to allow for sample splitting and laboratory errors at a later stage.

Once collected the samples were returned to the laboratory for analysis. The samples were washed, dried and split according to the methods outlined by Buller & McManus (1973). Each sample was sieved at 0.25  $\phi$  intervals and the resultant data plotted up as cumulative percentage curves. These are displayed in Appendix 1. Once plotted, the median and mean grain sizes could be extracted from the graphs. These values were obtained using the formulae given by Leeder (1982).

$$\text{Median grain size} = \phi 50 \quad (13)$$

$$\text{Mean grain size } (\mu_z) = \frac{(\phi 16 + \phi 50 + \phi 84)}{3} \quad (14)$$

The sorting and skewness characteristics of the sediments were also calculated using formulae provided by Leeder (1982).

$$\text{Sorting } (s) = \frac{\phi 84 - \phi 16}{4} + \frac{\phi 95 - \phi 5}{6.6} \quad (15)$$

$$\text{Skewness } (sk_j) = \frac{\phi 16 + \phi 84 - 2\phi 50}{2(\phi 84 - \phi 16)} + \frac{\phi 5 + \phi 95 - 2\phi 50}{2(\phi 95 - \phi 5)} \quad (16)$$

### 3.2.4 Modelling the beach sediment budget

Zenkovitch (1967) and Kirk (1980) recognized that a foreshore composed of both sand and shingle will be more dynamically complex than a foreshore displaying a unimodal sediment distribution, with separate displacement characteristics experienced by sand and shingle. Due to the varied nature of the foreshore sediments at Culbin, two beach sediment budgets were produced. A sand budget was calculated for the Culbin foreshore and Buckie Loch spit, while a separate shingle budget was calculated for the distal section of The Bar. As the two sediment grades are transported at different rates in the nearshore zone, then a single sediment budget would not reflect the transport and volumetric accumulation of these sediments. The beach sediment budget for the Culbin foreshore and Buckie Loch spit is considerably more elaborate than that for The Bar, demonstrating the greater number of variables and a greater understanding of the nature of sand transport. The shingle budget method is relatively simple, based primarily on aerial photography and field data, reflecting the poorly understood theoretical dynamics of the transport of coarse, clastic material in the nearshore zone.

#### 3.2.4.1 Sand budget: Culbin foreshore and Buckie Loch spit

The production of a sand sediment budget for the Culbin foreshore and Buckie Loch used two independent methods. Firstly wave refraction modelling provided a theoretical beach sediment budget based upon computed wave interaction with the foreshore. The second method produced the outcome of a sediment budget based on field measurements made at fixed beach profiling stations, with

a control provided by spit extension rates determined via air photo and historical map interpretation. The two methods in combination provided the most accurate method of producing a beach sediment budget for the Culbin foreshore.

From initial air photo interpretation it was considered that longshore sediment transport constituted one of the most important processes acting along the Culbin foreshore, and indeed along the whole of the middle firth. Extensive westward spit development could be seen, for example at Whiteness Head (NH 805588), The Bar (NH 911591), west of Buckie Loch (NH 972638), Lossiemouth (NJ 240700) and Speymouth (NJ 335655). Any attempt at calculating a sediment budget must therefore account for such longshore transport, and consequently considerable effort was taken in attempting to quantify this process.

#### **3.2.4.2 Graphical refraction of wind waves**

Sediment transport at the coast is initiated by the energy flux incident upon the coast being directed in both an onshore and an alongshore direction. The refraction of wave crests as they approach the coast creates a division of energy contained within the wave train, with the resultant vectors of wave energy directed onshore and alongshore in fractions proportional to the angle of wave approach. The longshore component of the onshore energy flux is of particular interest to this study. This element can be quantified using equation 2 (Chapter 2):

$$P_L = EC_n \sin \alpha \cos \alpha \quad (2)$$

The accepted method of wave representation in marine studies is the breakdown of wave parameters into significant wave heights occurring for 70% ( $H_{s70}$ ) and 30% ( $H_{s30}$ ) of the total wave record. Values of  $H_{s70}$  will henceforth be referred to as low energy conditions, and  $H_{s30}$  as high energy conditions. Given the three wave height and periodicity parameters selected from the data from Beatrice Alpha, high energy conditions are defined as waves with combinations of 2 m height and 10 s periodicity, with all other waves defined as low energy.

#### **3.2.4.3 The seasonal calculation of $P_L$ for input into the beach sediment budget**

Having now converted all of the available wind wave data into a  $P_L$  term, it was next necessary to produce a single figure which would represent the value of

$P_L$  for each season. The same equation was used for both the graphical production of wind generated waves and swell generated by the wave refraction program WAVENRG. In order to do this the method employed by Mason (1985) was used, which relates  $P_L$  to frequencies of occurrence of waves from different directions. Thus for example the calculation for spring would appear as:-

$$\begin{aligned}
 P_L = & \quad 6.41\%(70\% P_{Lhs70N} + 30\%P_{Lhs30N}) \\
 & \quad + \\
 & \quad 11.71\%(70\% P_{Lhs70NE} + 30\%P_{Lhs30NE}) \\
 & \quad + \\
 & \quad 6.0\%(70\%P_{Lhs70E} + 30\%P_{Lhs30E}) \\
 & \quad - \\
 & \quad 31.1\%(P_{L240}) \\
 & \quad - \\
 & \quad 10.3\%(P_{L270}) \\
 & \quad - \\
 & \quad 2.6\%(P_{L300}) \\
 & \quad - \\
 & \quad 1.4\%(P_{L330})
 \end{aligned}
 \left. \begin{array}{l} \\ \\ \\ \\ \\ \\ \\ \\ \\ \\ \\ \end{array} \right\} \begin{array}{l} \text{SWELL} \\ \\ \\ \\ \text{WINDS} \end{array} \quad (17)$$

This equation produced seasonal values of  $P_L$ , the longshore component of wave energy. However these required conversion to the factor  $Q_L$ , a longshore sediment transport term. Conversion to an equivalent sediment transport term will be summarized after the description of the calculation of the actual beach sediment budget from beach profiles and spit extension rates.

### 3.2.5 Beach sediment budget via beach profile and spit extension methods

#### 3.2.5.1 Method 1: beach profiles

Modelled rates of longshore sediment transport were used in conjunction with measurements of the volumes of sediment entering and being removed from the beach, in order to produce a *potential* sediment budget for the Culbin foreshore. However, the outcome of an *actual* sediment budget was produced for the Culbin foreshore using measurements of volumetric beach profile changes over a 12 month period.

Beach profile data over the period 03/91-02/92 was selected for measurement for the following reasons:

- i) it coincided with a "wave year" Spring-Winter period using the same parameters as BMT (1986);

ii) profiling frequency had increased prior to this period to monthly sampling, reducing the potential for high magnitude events to go unnoticed.

Using the data collected over the entire two year sampling period, a mean volume was calculated for each cell represented by a beach profile. This produced seven cells, with the representative beach profile located mid-way along each cell. The mean cell volumes were then compared with the *monthly* cell volumes calculated from the beach profiles, to produce a series of *residual* cell volumes for each month. These residuals contained both positive and negative values, indicating the volumetric state of the beach relative to the mean state during each sampling event. Having selected the period 03/91-02/92 as the target year for the calculation of the budget, the residual volumes measured in each cell on these two dates were summed, with cells 1-4 equivalent to cell B2 from the wave refraction exercise (section 3.2.2.2), and cells 5-7 equivalent to cell B1. The difference between the volumes recorded in each cell on these two dates represents the outcome of the *actual* beach sediment budget measured across the 12 month period, and so can be used to assess the success of the budget calculation.

### **3.2.5.2 Method 2: spit extension rates**

Mean annual accretion rates were measured from Buckie Loch spit on the western extremity of the Culbin foreshore (NH 992646). The aim of the exercise was to produce a volumetric assessment of beach volume increase with spit extension rather than a simple planimetric calculation, in order to provide data as a control over the calculation of the potential sediment budget from the wave refraction exercise (section 3.2.2.2). Measurement of the planimetric extension of the spit was undertaken using air photographs where available, and maps where not. Despite difficulties inherent in the use of air photographs as indicators of spit extension above HWST, the relative simplicity of coastal spits fed purely by longshore sediment transport makes this method more reliable than studies involving spits at river mouths (eg Buchan & Ritchie, 1979). Once these measurements had been made, they had to be converted into volumetric equivalents, for which a series of assumptions had to be made regarding the cross-sectional morphology of the spit.

The spit is presently some 2 km long, trending ENE-WSW. Its evolution has been recorded on both maps and air photos. The earliest survey of the area was carried out on 1870, and the most modern aerial coverage flown in 1989,

representing a span of 119 years. The cross-sectional area of the spit is shown diagrammatically in Figure 3.13. As noted earlier, the beach profiles collected in cell 7 were considered representative of the form of the beach profile along the length of the spit. In order to produce a volumetric calculation based upon the rate of spit extension, an estimate of the mean volume of sediment represented by cell profile 7 was required. Examination of all 14 profiles measured during the beach profiling programme suggested that within the sweep zone, the majority of profiles fell within very definite altitudinal limits, with only two extreme examples outside this zone.

In order to create a profile which best represented the data spread, the two most extreme profiles (23/02/91 [above the central group] and 06/12/90 [below the central group]) were rejected, leaving 85.7% of the original data set intact. Using this remaining data a second sweep zone diagram was plotted. From this plot the maximum and minimum beach elevations were measured at 10 m intervals along the profile. The median and hence the mean elevations were determined from the maximum and minimum altitudes at the upper and lower boundaries of the sweep zone, representing a mean beach profile for cell 7. The cross-sectional area of this profile was found to be 467.8 m<sup>2</sup>.

In order to calculate the cross sectional area of the remainder of the spit, some assumptions had to be made regarding the morphology of the landward edge of the feature (Figure 3.13). The dune cap found on the surface of the spit was disregarded in the calculation of the cross sectional area as aeolian transport was not considered a significant factor in the long term development of the spit. This was particularly the case since the long-term sediment transport pathway along this sector of the southern Moray Firth is westwards (NERC, 1991), whereas the predominant winds are southwesterly, effectively transporting sediment eastwards against the prevailing longshore sediment transport direction. Calculation of the cross-sectional area of the remainder of the spit was based on the assumption that the backing inner marsh surface presented the absolute base level for the development of both dunes (which could not form below it) and saltmarsh (which could not form above it). The gradient between the centre of the spit and this point was thus taken to represent the gradient at which the landward edge of the spit sloped. The distance to which the underlying shingle extends below the marsh surface remains unknown at this point, but production of a cross-sectional area below the assumed base level of -3.269 m OD was not required.

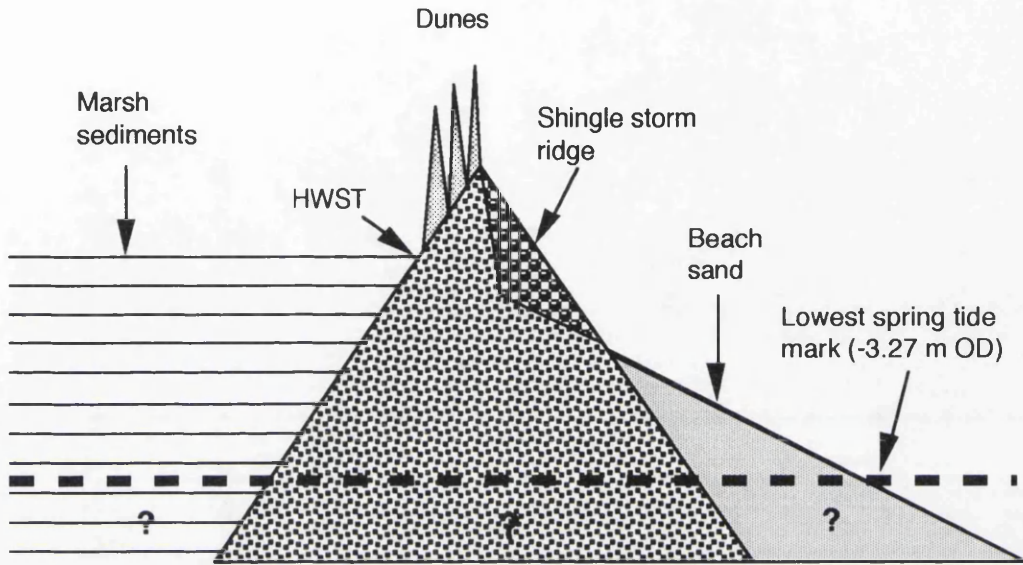


Figure 3.13 Diagrammatic cross section through Buckie Loch Spit (information below -3.27 m OD is inferred diagrammatically only).

### **3.2.5.3 Shingle sediment budget on The Bar**

A similar series of calculations were made using the distal extension rates measured on The Bar between 1878 and 1989. As the western flank of The Bar is comprised primarily of shingle, then this data was used in the calculation of a separate shingle sediment budget. This was of use both for comparative purposes with the sand budget calculated from the Culbin foreshore, and also for comparison with the palaeosediment budget, also concerned primarily with shingle.

Calculation of the cross-sectional area of The Bar was simpler than that of Buckie Loch spit. From beach profile measurements at station B3, the maximum depth of the shingle storm ridge on The Bar was found to be 3.87 m, below which the shingle was overlain by sand, but remained present below this sand surface to at least LWST (-1.4 m OD). This produced a minimum total thickness of shingle on The Bar of at least 5.27 m. Using the beach profile, the cross-sectional area was calculated to be 47.19 m<sup>2</sup>. In a similar manner to the calculation made on Buckie Loch spit, the total cross-sectional area of the extensional portion of The Bar was required for conversion to a volumetric extension rate. However, unlike Buckie Loch spit, the landward side of the contemporary ridge on the Bar was obscured by a further set of relict shingle ridges. Calculation of the back-ridge cross-sectional area could thus not be made in a similar way to that at Buckie Loch spit, and so for the purposes of calculation it was assumed that the shingle ridge was laterally symmetrical about its crest. This produced a cross-sectional area for the operational shingle ridge on The Bar of 94.38 m<sup>2</sup>.

### **3.3 LINKAGES BETWEEN HOLOCENE AND CONTEMPORARY PROCESSES**

#### **3.3.1 Introduction**

Providing a link between the processes presently active on the Culbin foreshore and those which were formerly in operation over the Holocene period is a central aim of this research. As no comprehensive body of literature exists concerning this aspect of the work, the methodology employed drew on sources from both coastal studies and upland sediment removal calculations. The overall aim was to produce an order-of-magnitude estimate of the "palaeosediment budget" of the Culbin coast for comparison with the contemporary sediment budget. This in turn can be used to assess the implications of changes in sediment supply to the coast throughout the fluctuating sea levels of the Holocene, and so understand the nature of the shoreline response. Due to the low resolution of the data involved and the lengthy period of operation, the results obtained are not intended to be used at anything other than an order-of-magnitude scale.

The basis of this series of calculations was to attempt to compare the volumes of sediment deposited in the shingle sequences of Culbin with the amount of sediment delivered. A second aim was to establish a first order chronological framework for the sedimentation rate using a sea level curve based on the altitude and location of the shingle ridge sequence at Culbin.

#### **3.3.2 Location of shingle landforms**

Quantification of the amount of shingle deposited in the Culbin system depends on the identification of the spatial limits of the shingle in the field. Identification of the longshore limit of the Culbin shingle was therefore undertaken, employing the existing modern analogue of the present Culbin foreshore and The Bar.

A theoretical mixed sand and shingle system as presently represented by the Culbin beach and The Bar contains a rapidly migrating shingle "head" and an associated sand "tail". If the "head" of the system can be identified, then this represents the longshore limit of shingle migration. From map evidence and geomorphological survey it could be seen that The Bar represents the most westerly point of shingle accumulation. West of the present distal end of The Bar, the River Nairn enters the Moray Firth, contributing a smaller, though locally

significant sediment load to the coast and contributing to the continuing distal extension of Whiteness Head.

Once the shingle sequence in Culbin Forest had been mapped and levelled , the areal extent of the Culbin shingle needed to be established. The method adopted was to rank the confidence levels to which the shingle ridge exposures were mapped using the following convention:

- i) confidence level 1:- shingle ridges mapped in the field. Details of crest altitude, spacing and length of exposure known in detail;
- ii) confidence level 2:- shingle ridges mapped from secondary sources, eg. air photographs or historical maps (eg Steers, 1937);
- iii) confidence level 3:- shingle ridges inferred as zones lying between ridges mapped at confidence levels 1 or 2.

By using these criteria the level of confidence assigned to each series of calculations was assessed. The location of each of these areas is shown in Figure 3.14. Using all three levels provides the most complete estimate of the areal existence of shingle, but also introduces the highest potential degree of error. Level three measurements were based on a working knowledge of the position of shingle ridges in the field and the likely relationship between those ridges subareally exposed and thus available for measurement, and those obscured, typically by sand dunes. Mapping the shingle ridges proceeded using these criteria.

### **3.3.3 Volumetric calculations of shingle at Culbin**

Having mapped the areal extent of shingle ridges across the Culbin foreland, it was necessary to convert this series of values into a volume in order to provide an estimate of the volume of shingle deposited in the Culbin shingle system. In order to produce such a volume the depth of shingle present was required. Unfortunately no boreholes have been sunk on the site, there being little commercial value in doing so. Thus assumptions had to be made regarding the potential thickness of the shingle body.

Theoretical studies have tended to avoid the problem of maximum transport depth for all grades of sediment, and the calculation of a pinchout, or operating depth, remains one of the most fundamental unknowns in coastal research.

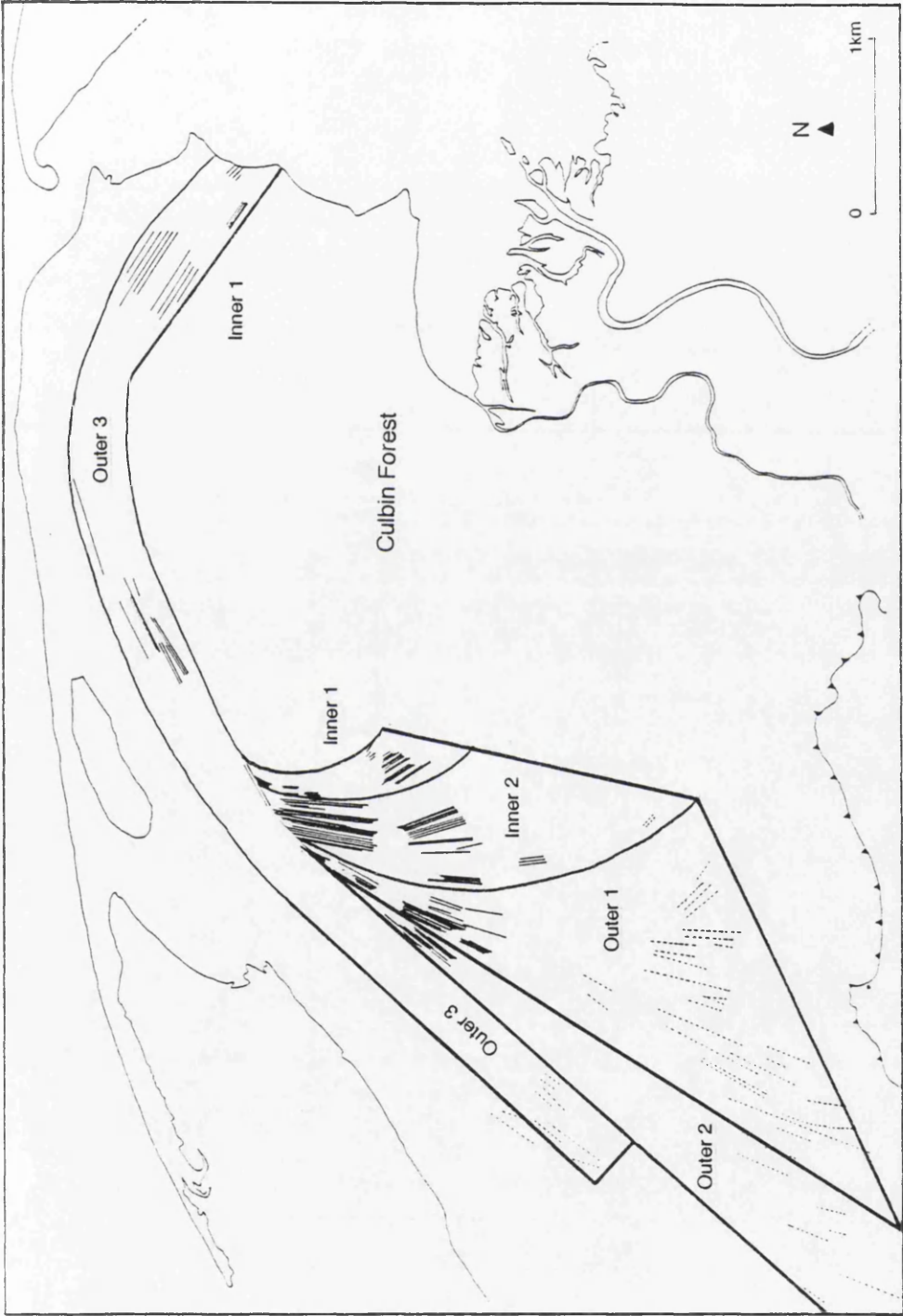


Figure 3.14 Subdivision of Culbin shingle ridges into confidence levels for volumetric calculation

Three lines of evidence were employed to establish the upper and lower limits of calculation:

i) field measurements (Steers & Smith, 1956; Kidson *et al.*, 1958; Neate, 1967) have shown that shingle is immobile below depths of ca. 9 m. depth under waves of 0.91 m. Reviewing the evidence, Hansom (1992) considered 9 m to be a realistic maximum mobility depth for shingle, although substantial quantities of material only become mobile at lesser depths around ca. 6 m;

ii) borehole evidence from Burghead Bay demonstrates the thickest body of shingle present to be 6 m thick. The location of the borehole along the seaward margin of RAF Kinloss suggests that it penetrated a shingle ridge. Assuming a maximum subaerial portion of the ridge similar in size to The Bar presently (3.10 m OD), then this provides a *minimum* depth of 2.9 m for shingle mobility;

iii) using The Bar as a modern analogue, the processes of storm ridge development has implications for calculating an operational depth for shingle. The maximum storm ridge crest height was at 3.87 m OD, while observations at LWST recorded shingle below a thin veneer of sand. In order for deposition at the crest of the storm ridge, shingle must have been mobile at least across the vertical range of the profile represented in the diagram, a minimum of 5.27 m.

In the light of this evidence, coupled with the poorly understood dynamics of shingle in the nearshore zone, it was assumed that shingle would be mobile across a total vertical subaqueous range of at least 6 m.

Having established that 6 m represents a realistic maximum depth for shingle movement, the profile shape of the ridge sequence had to be defined in a way which could be represented in a simple mathematical statement. Further assumptions were required in order to achieve a realistic simplification:

- i) the upper surface of the shingle ridge series is semicircular in form;
- ii) the wavelength of the ridge crests equals half the distance between successive shingle ridges;
- iii) the sediment body at depth is represented by a parallelogram;

The working model of a cross-section through the shingle ridges thus approximates the form shown in Figure 3.15.

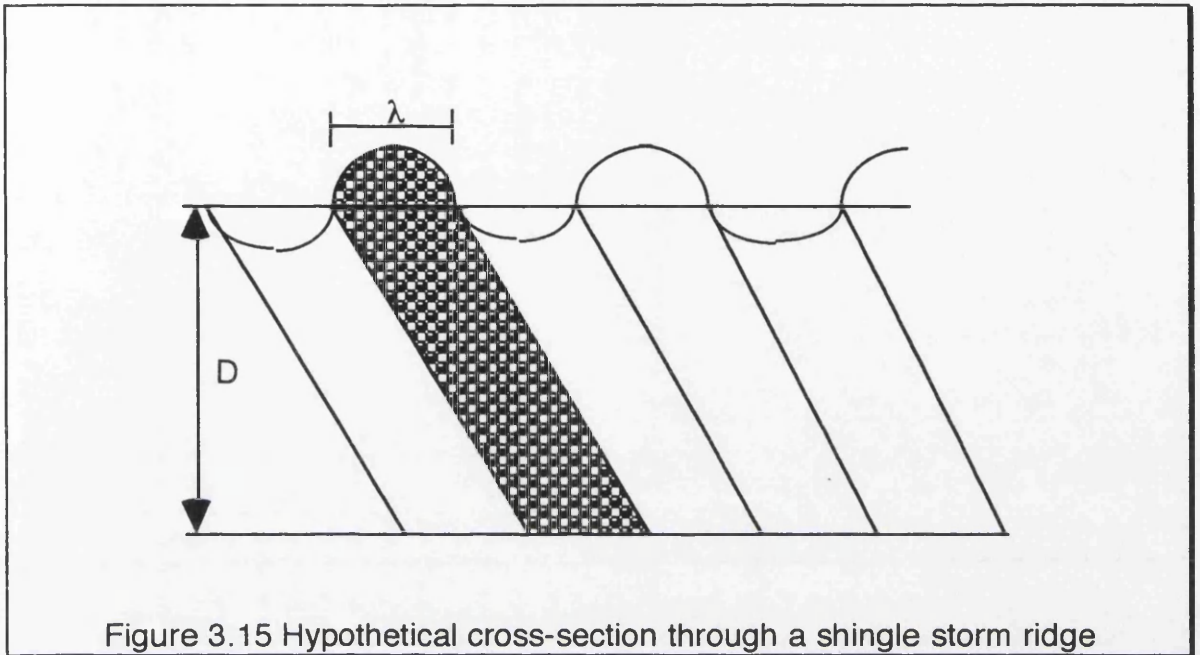


Figure 3.15 Hypothetical cross-section through a shingle storm ridge

The cross sectional area of a shingle ridge based on the assumed form in Figure 3.15 is:

$$\frac{\{\pi[0.5\lambda]^2\} + (\lambda \cdot D)}{2} \quad (18)$$

where  $\pi = 3.14$

$\lambda$  = crest-crest distance

D = operating shingle depth (6 m)

To calculate the associated volume, the cross sectional area was multiplied by the length of exposure as mapped at the range of confidence intervals noted previously, beginning with confidence level 1. The series of calculations required were made using the statistical package MINITAB.

A problem was experienced when attempting the calculation of intervening shingle ridges at confidence level 3. If the two ends of a shingle zone were exposed but the central portion was obscured, for example by a dune, then the exact relationship between the shingle ridges at either end could not be established with confidence. Shingle ridges tend to bifurcate and rejoin on a

secondary scale (Green & McGregor, 1986), making the linking of individual ridges on each side of the obstacle difficult. Additionally, the tendency for the ridges to fan out towards their distal ends meant that an additional volume of shingle needed to be added to the final calculation in order to avoid underestimating the total volume present.

In order to solve this problem it was necessary to study the geometry of shingle ridge morphology. As the fan of ridges widened it had to be assumed that no more ridges appeared in the intervening swales, and that the swale thus appeared as a flat shingle spread. Examples of these flat spreads were found to be relatively common amongst the shingle ridge sequences exposed in Culbin forest (eg in the shingle fan between sets B and C) and also on The Bar, thus such an assumption has some validity. Secondly the depth of shingle in the *swales* was taken to be 6 m, representing the operational depth for shingle as noted above. This value was selected as representative of the thickness of shingle affected by MSL rather than the thickness represented by pinchout depth plus ridge height ( $\lambda/2$ ), since the height of any one ridge crest relates to the nature and intensity of the particular storm event which produced it at a particular mean sea level. Thus the size variability of the shingle ridges found astride the underlying shingle body are effectively irrelevant to the calculation of the residual shingle volume, being added on to the underlying shingle block at the final stage of the volumetric calculation.

The calculation of the volume of shingle represented by these shingle swales was thus made by the multiplication of a detailed volume obtained from level 1 calculations plus a volume obtained as the residual swath width (total swath minus swath width mapped at confidence level 1), multiplied by the product of length of exposure and operating depth. The results of these calculations were broken down into their constituent confidence intervals, and are presented in chapter 4.

### **3.3.4 Volumetric delivery of shingle to Culbin during the Holocene**

The primary sources of sediment to the coastal zone during the Holocene have been derived indirectly from mainly glacifluvial sources, either as fluvial load delivered to the coast from upland sources, or as material forced onshore during the rise in RSL to the Holocene sea level maximum. One of the primary aims of this thesis is to attempt to calculate the amount of sediment delivered to the coastal zone over the Holocene period. This section describes the methodology

employed in calculating palaeosediment supply in order to account for the inputs to a sediment budget describing the Holocene development of Culbin.

#### **3.3.4.1 River Terrace Reconstruction**

The method employed to calculate the amount of sediment introduced to the Culbin system from rivers utilized the reconstruction of fluvial terrace sequences in the lower reaches of the Rivers Spey and Findhorn, a method not identified elsewhere in the available literature (Renwick, pers. comm.). The lower valley terrace surfaces of these two large river valleys are intimately related to RSL, with downcutting having taken place during periods of RSL fall over the Lateglacial period (Maizels & Aitken, 1991). The upper terrace surface of lower Strathspey was described by Peacock *et al.*, (1968) and Sutherland (1984) as displaying kettles and evidence of *in situ* ice stagnation, and as such provided a useful chronological marker in the absence of absolute dates. The method used operated on the principle that if a particular terrace fragment can be dated, then an estimate of the amount of sediment removed since terrace construction can be calculated. It is clear that this method can produce only the broadest of estimates of sediment delivery to the coast. The major potential source of error in this method was from the relationships between the volume of sediment removed from the upper catchment of both rivers over the period since the Lateglacial, and subsequent redeposition in lower terraces. Since sediment throughput at this time cannot be estimated, it was assumed that sediment removed from the upper catchment was redeposited in the lower terrace sequence prior to reworking via channel incision under falling RSL during the late Holocene. The extensive nature of the upper Spey terraces has been described (Young, 1978; Maizels, 1986), although in a non-sequential manner. The middle Findhorn terraces have attracted little attention beyond summary description (Auton, 1990; McEwan & Werrity, 1993).

No absolute dates were available for either the Spey or the Findhorn terraces, the only stratigraphic marker available being the identification of the Lateglacial terrace surface in lower Strathspey by Peacock *et al.*, (1968). In the absence of any other forms of stratigraphic guides, the Lateglacial surface from the Spey was used as a starting point for the method, with refinements made as the exercise progressed.

In order to calibrate the method, initial calculations were made using data from the Spey. These were based on a detailed map of the extensive terrace fragments found in lower Strathspey (Peacock *et al.*, 1968). The southern limit of

the terraces was traced to Haugh of Orton (NJ 314539) and Collie farm (NJ 312516) where the valley width falls to ca. 750 m. The calculation did not extend beyond this point, although terraces continue to border the river for a considerable distance upstream (Maizels, 1987). This gorge is judged to be the effective limit of dateable terrace fragments, and thus volumes of material available to the coast. As such, it will represent an underestimation of the amount of sediment in the calculations. This point will be addressed in a later section.

The map of lower Strathspey (Figure 3.16, from Peacock *et al.*, 1968) shows the location of the Lateglacial terrace, which provides the only chronological marker on the entire lower Spey system. All subsequent major terrace positions are marked, but no dates are available with which to date these. Thus the calculation provides a bulk figure for the introduction of sediment from the terraces into the coastal system since the Lateglacial. The calculations divided the Spey terraces into 5 periods of incision over 3 long profile sections. Each terrace surface was reconstructed as a cross-sectional area at each of the three long profile positions, and then multiplied by the long profile length to provide a volume for each section. Finally, the 3 sections were added, producing a final sum of the total sediment removed from the lower Spey terrace sequence (Appendix 2).

In the absence of any detailed analysis of the relative proportions of sand and gravel present in the terraces an alternative value representing the proportion of gravel in the terraces was required. Borehole data from the contemporary floodplain was obtained from Grampian Regional Council in connection with a water abstraction scheme from the Spey upstream from Fochabers. The boreholes did not pass through the raised terraces on the valley side, but in the absence of other data this was accepted as a good approximation. Three boreholes reached rockhead, and the proportion of gravel present in each of the boreholes was calculated from the thickness of the beds penetrated. The mean proportion of gravel from the three boreholes was thus obtained. This value was then multiplied by the total volume calculated to have been removed from lower Strathspey since the Lateglacial, providing a first order approximation of the volume of gravel delivered to the coastal zone from lower Strathspey over this period.

In order to quantify the amount of sediment delivered to the entire Culbin shingle system the quantity of sediment from both the Rivers Spey and the Findhorn was required. As no accurate map of the Findhorn terraces has been produced, a first

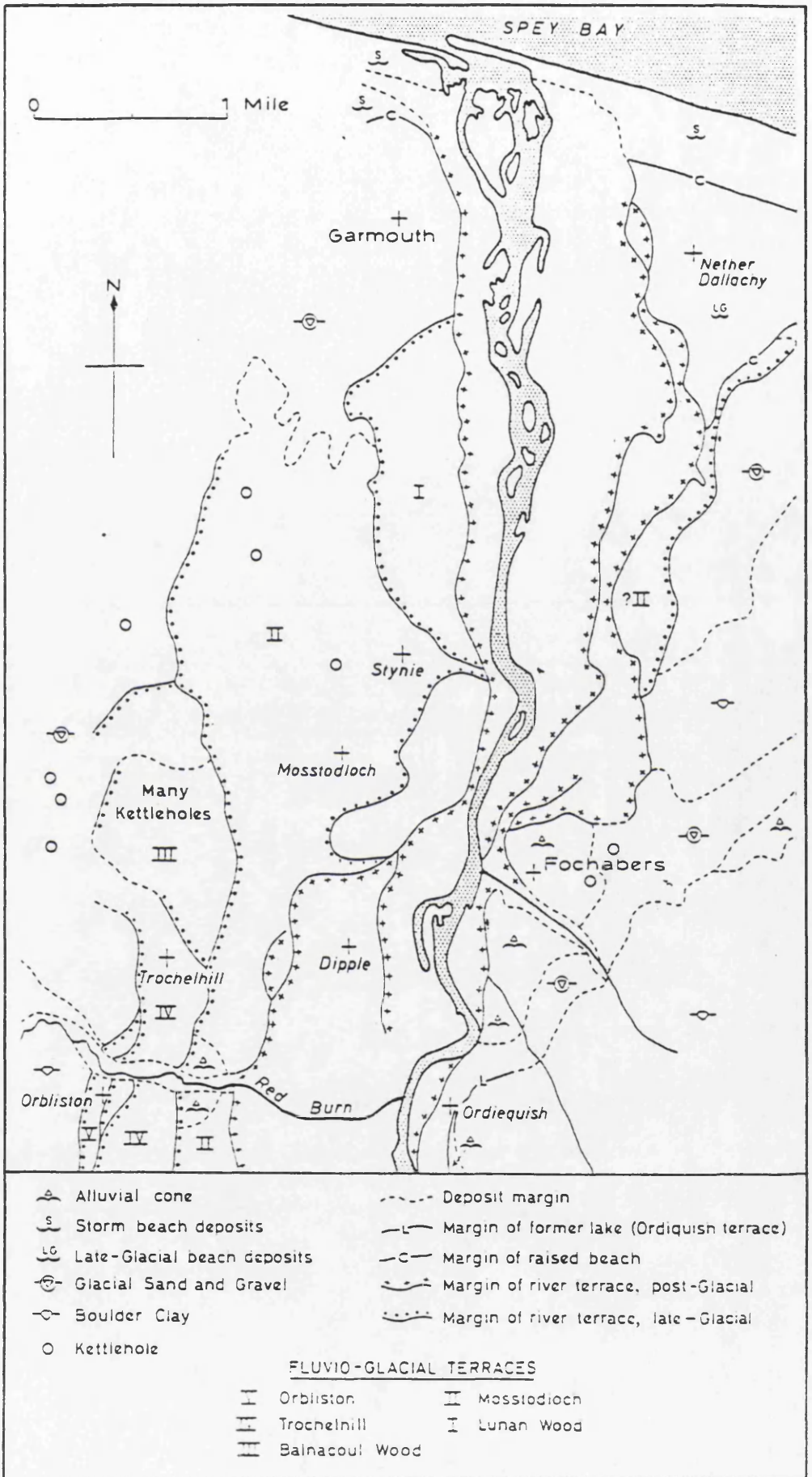


Figure 3.16 Map of the lower Strathspey river terraces (source: Peacock *et al.*, 1968)

order approximation of the amount of sediment delivered was the best result possible at this stage. To produce such an estimate it was decided to use a theoretical "wedge" of sediment based on the depth and width of the lower Findhorn valley up to the point of constriction (Struie Gorge) where the lower river terraces pinch out (Figure 3.17). In this respect, the Findhorn calculation exactly matches that made for the Spey. In order to calibrate the error likely to exist in this gross scale calculation the same exercise was carried out in lower Strathspey, and the results compared with the volume removed as calculated from the reconstruction of the terrace sequence. Thus an error term could be calculated for the Spey, which represents the degree to which the Spey "wedge" underestimates the actual amount of sediment removed as calculated from the terrace reconstruction. This exercise was then repeated for the Findhorn, using the same criteria as used in the Spey to produce a volume of sediment representing the amount removed from the lower Findhorn valley since the Lateglacial. The minimum error margin is defined by the equivalent calculation from the Spey. The sum of the volumes calculated from the bulk figure from the Findhorn and the Spey provides a first approximation of the amount of sediment delivered to the coast due to downcutting through the terrace sequences.

Again it must be stressed that the result of such calculations must only be seen as order-of-magnitude estimates at best, and overconfidence in the accuracy of the figures produced should be avoided.

### **3.3.5 Losses to the system**

#### **3.3.5.1 Offshore**

It has been highlighted that sediment was introduced to the coastal zone from both fluvial and offshore sources. Having described the methodology employed thus far, it would appear that the offshore sources of sediment have not been accounted for in this calculation. However, as the reconstruction of the fluvial terrace surfaces extends back to the Lateglacial surface, then the majority of the sediment supplied to the inner continental shelf by rivers would have been already emplaced during the downwasting period of the Moray Firth ice and immediately preceding this event, while supraglacial surfaces remained unvegetated. This time period was therefore incorporated within the timescale of the terrace reconstruction, and thus the potential offshore deposits have effectively already been counted within the calculation prior to their deposition on the nearshore shelf floor.

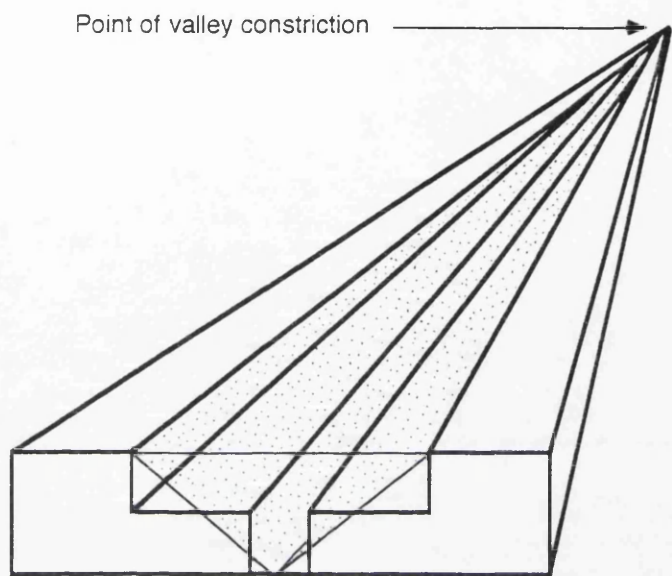


Figure 3.17 The "wedge" method for estimating the volume of sediment in a river terrace sequence

### 3.3.5.2 Sinks *en route*

Having calculated the volume of sediment provided to the coastal system from the two major rivers in the area the volume of shingle lost *en route* from the Spey to Culbin was required. To do this, a similar technique was employed as was used in the quantification of the amount of shingle in the Culbin system. These measurements were only of relevance to the inputs to the coastal zone from the Spey, as it was assumed that all of the sediment derived from the Findhorn would, prior to the development of Findhorn Bay, have been available to the nearshore zone for storm ridge construction at Culbin.

The first loss to the Spey system was from the construction of a large submarine delta at the mouth of the river. The apex of the fan is approximately 8.2 km offshore and shingle at the landward base 10.9 km wide, producing a surface area of 44.69 km<sup>2</sup>. A borehole sunk at the outer extremity of the fan (BGS borehole 71/15, Andrews *et al*, 1990) revealed two distinct shingle units within the fan at this distance offshore. The upper shingle unit was 3 m thick, and was separated from a lower unit 2 m thick by 16 m of gravelly sand. As no borehole information was available further landwards on the fan, it was assumed that these two units maintained their stratigraphic continuity landwards as far as the river mouth for the purposes of calculating the volume of shingle in the fan.

Further losses to the volume of shingle available to the nearshore zone were accounted for by three areas of major shingle storm ridge accumulation located between the mouth of the Spey and the Culbin system. These are found between Kingston (NJ 336656) and Lossie Forest (NJ 255679), Caysbriggs (NJ 249669) and Lossiemouth (NJ 235700), and in Burghead Bay (main area between NJ 096653 and NJ 035647). The two ridge sequences in Spey Bay were measured at confidence level 3, while those in Burghead Bay were mapped from Steers (1937) at confidence level 2. The surficial areas of the ridges were transferred to a base map at a scale of 1:50 000, and the surficial exposure measured. Assuming an operational depth of 6 m as used in the Culbin calculations, the volume of shingle in these areas was calculated simply as a block of shingle, multiplying the surface area of the features by the operating depth. This volume was then subtracted from the residual Spey volume, leaving a potential amount of shingle available for transport west into Burghead Bay.

## CHAPTER 4 RESULTS

This chapter presents the results of the research whose aims and methodology were described in Chapters 2 and 3. The chapter begins with a description and analysis of coastal landforms and nearshore sedimentation in the Culbin area throughout the Holocene. This is followed by a description of the contemporary coastal landforms and processes at Culbin, forming the background to two beach sediment budgets: a sand budget for the Culbin foreland and a shingle budget for the distal flank of The Bar. Finally, using both the methodology from the contemporary sediment budget, and the data from the Holocene sedimentary record, a "palaeosediment budget" is presented, demonstrating the nature of foreshore development at Culbin at different stages of RSL throughout the Holocene.

### 4.1 INVESTIGATION OF HOLOCENE ENVIRONMENTS OF CULBIN AND BURGHEAD BAY

The aim of this section is to describe and report on the Holocene development of Culbin. The scope will then be extended to include Burghead Bay, before fitting the development sequence into a regional context to include the whole of the southern Moray Firth from Spey Bay to Nairn. Finally a synthesis of RSL trends will be presented to demonstrate relative sea level changes in this section of the Moray Firth over the Holocene period.

#### 4.1.1 Geomorphology of Culbin

The Culbin area consists of a series of raised foreshore deposits forming the Culbin foreland, backed by an extensive raised cliffline at ca. 9 m OD. The cliff is 5-7 m high, and is cut into Late Devensian glacial, glacialfluvial and foreshore deposits. It can be traced around much of the coastline of the inner Moray Firth, and forms a continuous feature in the Culbin area, extending east at least as far as Buckie. Fronting this raised cliffline in the Culbin area is a sub-horizontal sandy terrace 300 m wide underlain by shingle, blanketed by a thin, but variable, cover of aeolian sand. This terrace forms a boundary zone between the raised cliffline and the surficial exposure of raised shingle beach deposits in Culbin. Since the emplacement of the raised shingle deposits, an extensive dune system has developed on the exposed foreland surface. The major dune elements are identified on Figure 3.1. The geomorphology of the dunes at Culbin can be divided into an eastern section and a western section. The eastern

section displays a complex series of composite and solitary dune forms, with evidence of blowout activity displayed by the crests of the dune forms both at the coastal edge and further inland (Figure 3.1). There is a clear preferential alignment of the blowout features towards the northeast in this section of Culbin. The highest dunes in the forest are found in the eastern section, with both Lady Culbin (NJ 013640) and the unmarked dune at NH 986624 reaching 30 m in height.

The western section of Culbin consists of a low, undulating sandy surface at ca. 5-7 m OD with few prominent dune features. However, the outstanding parabolic Maviston dunes (NH 949604 & NH 955608) are amongst the largest of their type in Europe (Forestry Commission, 1988), and form an important, though atypical, element of the landform assemblage of the western section of Culbin Forest.

#### **4.1.1.1 Shingle Ridges: location and altitudes**

Culbin has long been recognized as containing an exceptionally well preserved suite of raised shingle storm ridges, related to higher RSLs than are currently experienced in the Moray Firth (Ogilvie, 1923; Steers, 1937; Ritchie *et al.*, 1978; Gauld, 1981; Ross, 1992). However, detailed analysis of the spatial and altitudinal relationships between the ridges has not been studied in detail, with the majority of work based upon the pioneering geomorphological study by Ogilvie (1923). One of the aims of this research was to investigate the detailed morphological relationships between the shingle ridges of the Culbin foreland, in order to establish a developmental history in relation to RSL changes in the Moray Firth, using both the shingle ridges and a more standard series of sea level indicators (peats, shells etc.) as a baseline.

The shingle ridges identified in the field follow a broadly arcuate form across 5 km of discontinuous exposure (Figures 3.1 & 4.1). The eastern set of ridges (R,S,T) lie at 290°, and are approximately parallel. The central set (X,Y,Z) represent the apex of the system trending to 250°, and if traced further to the south west eventually lead into the shingle "fan" area (Figure 4.1, A,B,C,D). The fan consists of a large group of shingle ridges with orientations fanning out from 240° to 130°, with possible extensions to the south-west suggested by aerial photography (Plate 3, feature 1 & Figure 4.1).

The most landward set of ridges are set A and A' (Figure 4.1), and the orientation of these sets (180° to 150°) suggests that they are linked. Levelling the ridge crests revealed the mean altitude of these ridges to be 8.51 m OD.

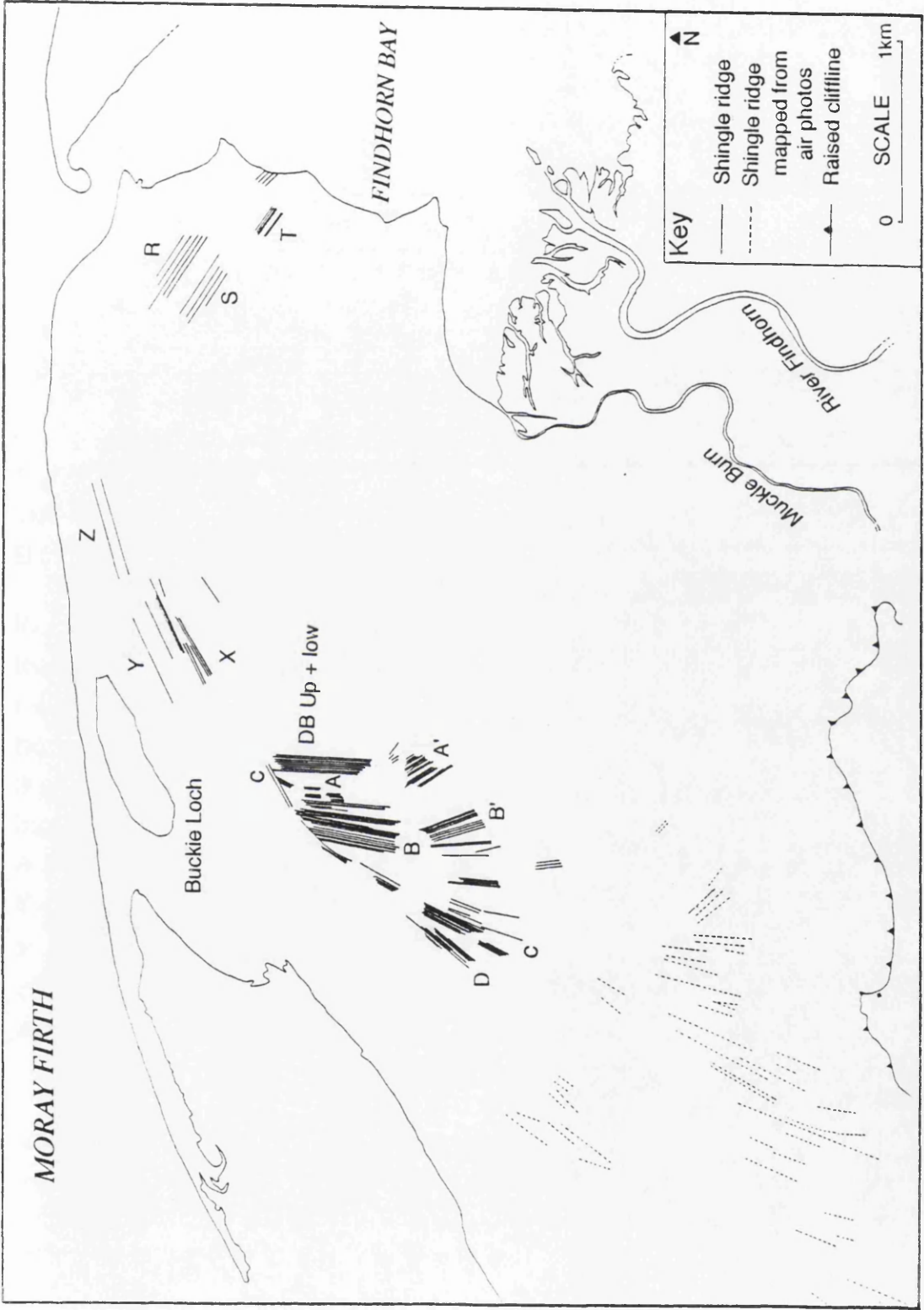


Figure 4.1 Location of relict shingle storm ridges at Culbin

The ridges can be traversed continuously in the field from east to west across the fan area, with no dune interference to hinder interpretation. Between sets A, B and C marked breaks in altitude occur. These coincide with low, flat shingle spreads tapering towards the north east. Trial pits dug into intervening hollows in these spreads were unable to penetrate a thick (>1.5 m) cover of aeolian sand prior to reaching the water table, but the presence on either side of the area of prominent shingle ridges at declining altitudes towards the centre of the area suggests that the intervening areas are also underlain by shingle. Similar features, unobscured by aeolian sand, can be identified on The Bar, supporting the view that their relict counterparts are also shingle based. The apices of these breaks display a laterally erosional contact, with truncation of the landward sets by those immediately seawards. Between sets A-A' and B-B' a change in orientation of 15° occurs, coupled with a rise in mean altitude from 8.81 m to 9.36 m OD.

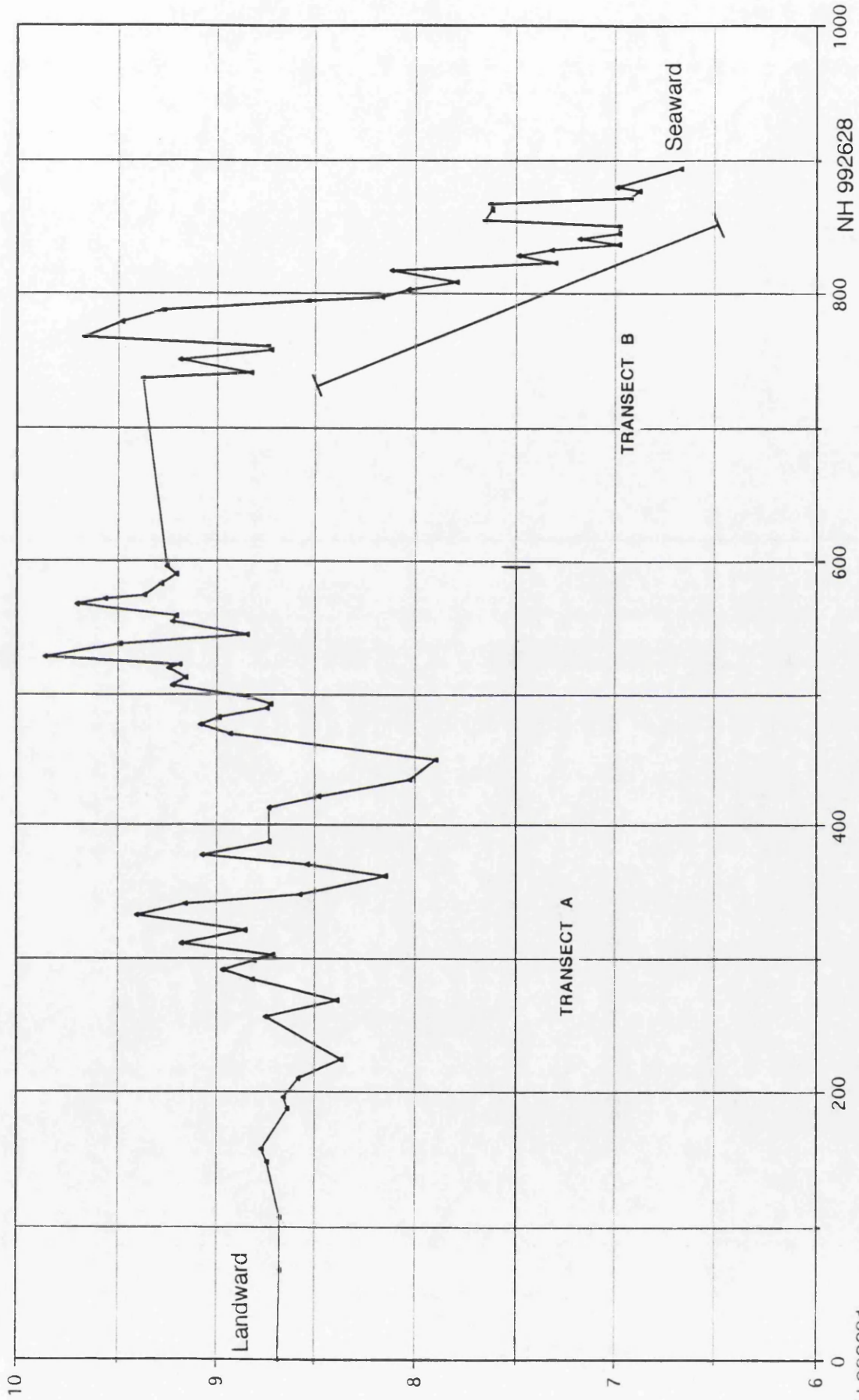
B-B' represents the most extensive set of continuous ridges exposed in Culbin. They form the central set of ridges in the shingle "fan". A change in orientation of 10° divides set B-B' (200°-160°) from set C (210°). Altitude also changes from set B (mean = 9.36 m OD) to set C (mean = 9.16 m OD).

In order to highlight the altitudinal relationships, transects were levelled across the crests of the shingle ridge sets. Transect A (Figure 4.2) shows the altitudinal relationship between sets B and C, and the size of the dividing shingle slack between them at this point. Transect B was made separately from transect A as the NW end of A was obscured by a large dune, and was designed specifically to incorporate set D. The mean altitude of set B is 9.36 m OD and set C 9.16 m OD. A Mann-Whitney U test revealed no statistical difference between the altitudes of these two ridge populations ( $n_1=8$ ,  $n_2=11$ ,  $\alpha_2=5\%$  & Appendix 3). Set D appears to be sub-parallel to set C, although the ridges gradually spread out towards the south west, and display a marked decline in altitude seawards. The mean altitude of set D is 7.44 m OD.

Transect B (Figure 4.2) displays a general decline in altitude of the ridge sequence seawards. Using the altitudes of the first and last five ridges in the sequence, a second Mann-Whitney U test revealed a statistically significant difference between the altitudes of the top and bottom shingle ridges of this set. ( $n_1=10$ ,  $n_2=10$ ,  $\alpha_2=5\%$  & Appendix 4)

Sets X, Y and Z occurs to the northeast of the fan area. Sets Y and Z are lower in altitude than set X, and are separated by a drop in altitude of ca. 3 m. Set X has a

Altitude (mOD)



NH 998631

Figure 4.2 Section measured across Transect A + B

Distance (m)

mean altitude of 9.80m OD (n=5), whilst sets Y and Z are located at a mean altitude of 5.28 m OD (n=3) and 5.60 m OD (n=3) respectively.

Sets R,S and T lie in the eastern section of the forest. Sets S and T are divided from set R by a marked drop in altitude resembling the sequence demonstrated by sets X, Y and Z. Set R has a mean altitude of 6.01 m OD, and is separated from set S by a drop in altitude of *ca.* 4 m. The mean altitude of set S is 10.32 m OD, and while set T was not surveyed in detail, the ridges are at approximately the same altitude as those of set S.

The shingle ridge groups described represent the exposure of shingle found in the field. The intervals between the ridge groups were not deliberately chosen, representing breaks in surficial exposure imposed by the deposition of dune sand. The groupings above are retained throughout this chapter for convenience and ease of relationship to actual field exposures.

The shingle ridge groups were analyzed in detail in terms of their altitudes and "wavelength" (crest-crest distance). The wavelength of the shingle ridge groups is thought to relate to the regularity of sediment supply to the ridge, with a regular supply forming lower ridges and a more regular wavelength, while sporadic sediment supply would contribute to higher, less evenly spaced ridge crests. Thus the wavelength measurements are considered as a surrogate variable for the regularity of sediment supply to the coast during formation. While the amplitude of the crests would have been of interest, the depth of the intervening troughs is a function of the distance between the crests and the gradient of the flanks, itself a function of the angle of repose of the constituent shingle. The absence of this data is thus not seen as detrimental to the study. Long & Fox (1988) demonstrated that trends in the altitude of the troughs was related to trends in crest altitude, and was of little value in determining relationships between either individual or groups of ridges. In addition to the relict shingle ridges in Culbin, a traverse was made across the contemporary set of shingle ridges deposited over the recent historical period on The Bar. Measurements were made of the altitude and wavelength of these shingle ridges in order to compare them with their relict equivalents in Culbin. Details of the recorded values of both mean and standard deviation of altitude and wavelength are shown in Table 4.1.

The highest mean altitude, 9.36 m OD, is shown by set B, in the central section of the shingle fan, closely followed by the adjacent set C at 9.16 m OD. The lowest altitude was, as expected, obtained from the contemporary shingle ridges on The

Bar, at 3.17 m OD. Inland, the lowest relict shingle ridge altitude was measured at set R (6.01 m OD), with the lowest individual ridge altitude (3.58 m OD) recorded from the most northerly of the ridges in this group. The highest altitudinal SD is shown by groups Y & Z, although it is apparent that this set crossed a marked break in altitude, as noted in groups R, S & T, and thus this value should be treated with caution. The next highest SD was recorded from set S (1.38), while the lowest value of altitudinal SD is shown by the DB lower set (0.14), followed by set A' (0.21).

Wavelength analysis displayed different trends from the altitudinal analysis. The highest mean wavelength was recorded from set Y/Z (41.22 m), although it is suspected that several of the constituent shingle ridges had been obscured by dune sand along this transect, thus increasing the apparent inter-crest distances. The next highest value of wavelength is from set R at 34.31 m, also demonstrating very wide ridge spacing. The lowest value is shown by set D, markedly lower than the remainder of the shingle ridge groups at 5.32 m. This set also displays the lowest standard deviation of wavelength at 1.80. The highest standard deviation of wavelength is again displayed by sets Y/Z (24.55), followed by the DB lower set (17.44).

In relation to the contemporary shingle ridges measured on The Bar, the standard deviation of altitude recorded on the relict shingle ridges at Culbin was generally higher, while the standard deviation of wavelength recorded on The Bar ridges falls well within the range of values recorded from the inland ridges (Table 4.1).

In order to investigate the relationships between the inter-ridge morphology further, mean wavelength was plotted against mean crest altitude (Figure 4.3). As a crude approximation at this stage, if ridge crest altitude is substituted for time, then the plot shows little apparent relationship between the variables, suggesting that there was no trend in shingle ridge crest spacing over time. Plotting the standard deviation of wavelength against standard deviation of altitude (Figure 4.4) did, however, suggest that a relationship might exist between these variables, with linear regression displaying a reasonable fit on the data ( $R^2=0.57$ ), implying a weak but positive correlation between wavelength and altitude of the shingle ridge group crests in Culbin Forest.

Figure 4.3

**Culbin shingle ridges:**  
**mean wavelength vs. mean altitude**

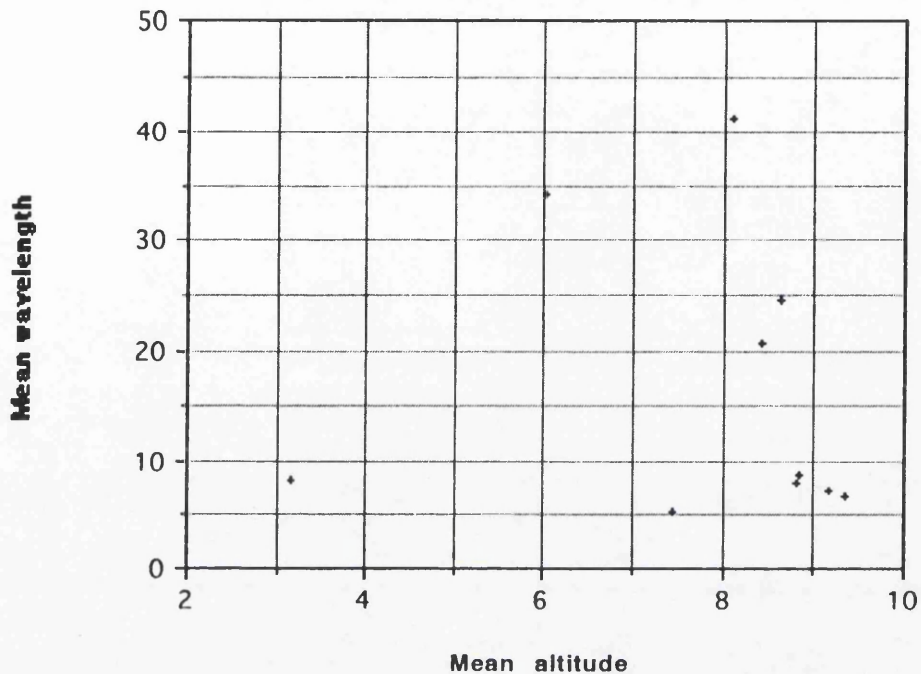
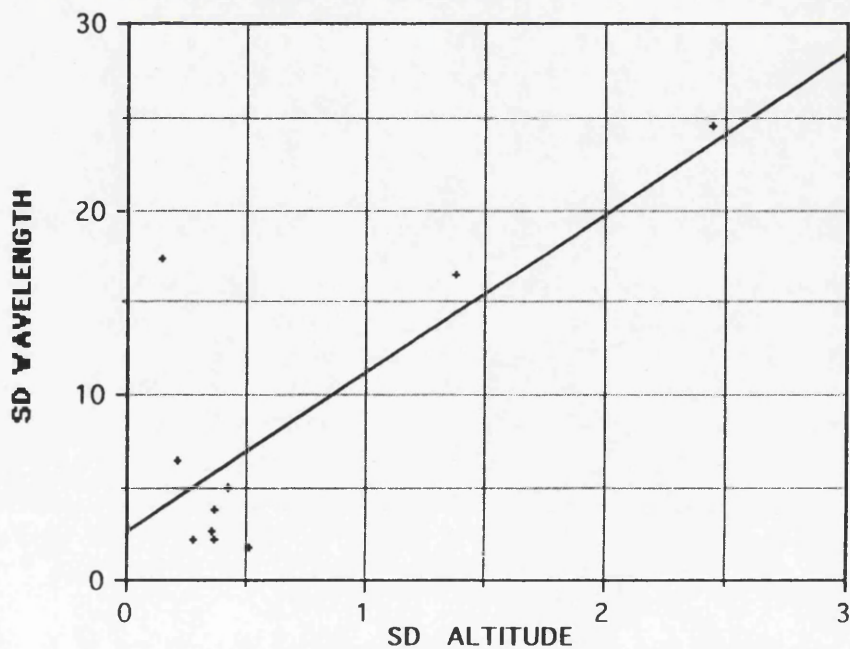


Figure 4.4

**Culbin shingle ridges: standard deviation of wavelength vs.**  
**standard deviation of altitude**



$y = 2.6600 + 8.5863x \quad R^2 = 0.571$

#### 4.1.1.2 Sedimentology of the relict shingle ridges at Culbin

As The Bar was considered to be an important modern analogue with which to compare the geomorphology of the relict shingle ridges at Culbin, an investigation was made into the longshore sorting characteristics of both areas to determine whether processes operating presently on The Bar are reflected in the sedimentology of the relict shingle ridges.

Site	Ridge group	Mean 'b' axis (mm)	Mean roundness
1	T	36.8	0.72
2	R	31.7	0.71
3	S	39.8	0.72
4	Z	32.0	0.72
5	X	32.3	0.68
6	Y	35.5	0.70
7	C	46.9	0.62
8	A	38.9	0.66
9	B	42.3	0.68
10	A'	25.6	0.68
11	B'	32.3	0.74

Table 4.2 Mean 'b' axis and roundness parameters: Culbin shingle ridges

Preliminary fieldwork on the outer shore of the western, shingle dominated flank of The Bar suggested that clast mean 'b' axis length increased with distance west (downdrift). This was supported by two earlier studies on the sedimentology of The Bar (Hall, 1987; Hastings, 1991). In order to test the hypothesis that similar sorting characteristics were shown by the inland, relict shingle ridges as

those actively forming on The Bar at present, the sampling strategy designed in Chapter 3 was implemented, and the results shown in Table 4.2.

Mean 'b' axis lengths and roundness parameters from the 11 sites sampled suggest that there is no apparent E-W trend in roundness around the shingle exposure, although an increase in the clast sizes can be observed along the seaward sets of ridges towards the west (Table 4.2).

Sites 1 and 3 (sets S and T ) display a higher mean 'b' axis length than site 2 (set R), although from the altitudinal analysis are found to be located ca. 2 m above site 2, with a marked break in altitudinal trend between them. A similar altitudinal pattern can be observed between the high level site 5 (set X) and the lower sites 4 and 6 (sets Y and Z) in the central exposure southeast of Buckie Loch, but the clast size relationship at this location is apparently reversed, with a higher mean clast 'b' axis length recorded from the lower altitude ridges at site 6. Between sites 1, 2, 3 and 4, 5, 6 (sets R, S, T and X, Y and Z) there is little variation in the mean 'b' axis lengths, which in all cases falls between 32 and 40 mm.

Samples from site 7 (set C) show an increase in 'b' axis length to 46.9 mm, and site 9 (set D) show a lower, but still relatively high value of 42.3 mm. This contrasts sharply with clast sizes from ridges at sites 8, 10 and 11 in the recurve sequence of the ridges in the fan, which are much smaller. The lowest mean 'b' axis measurement of 25.6 mm was made at site 10 (set A), while sites 8 and 11 contain slightly larger clasts, but which are still smaller than those from the seawards ridge sets C and D.

The problem of positively identifying spatially continuous ridges around the full length of exposure confounded any efforts to quantitatively examine the trends in mean clast 'b' axis length. This problem is reduced if only the most seaward sets of ridges are compared, as these display an element of westwards coarsening from initial inspection of the data. Table 4.3 below shows the mean 'b' axis lengths from these ridges alone.

On initial inspection these sites display an apparent coarsening trend towards the west. While initially convincing, referral to the plots of shingle ridge altitude identify the two westernmost sites (7 and 9) as not necessarily related to sites 6, 4 and 2 since they are located on much higher ridges. It is reasonable to assume that shingle ridges are present seawards of sites 7 and 9 at lower altitudes, as

displayed by the staircase sequence identified at set D (transect B, Figure 4.2), but have been obscured by blown sand.

Site	Mean 'b' axis length (mm)
2	31.7
4	32.0
6	35.5
7	46.9
9	42.3

Table 4.3 Mean 'b' axis lengths from the seaward inland shingle ridges at Culbin

An overview of the general trend in clast mean 'b' axis length was obtained, however, through a comparison of the most easterly and westerly clast populations (sites 2 and 6 respectively). A Mann-Whitney U test (Appendix 5) revealed that the mean clast size at site 6 was significantly greater than that at site 2 ( $n_1=50$ ,  $n_2=50$ ,  $\alpha_1=5\%$ ). This supported the visual inspection of the data, strengthening the contention that the relict shingle storm ridges in Culbin Forest display a downdrift coarsening trend.

#### 4.1.1.3 Clast size analysis on the western flank of The Bar

The western flank of The Bar is dominated by shingle storm ridge deposition. Measurements were made of the characteristics of the clast population as outlined in chapter 3. Clast mean 'b' axis lengths are displayed in Table 4.4.

Station 6 was located at the extreme distal end of The Bar at a location where the storm ridge began to both recurve and become dominated by sand. Excluding this sample from the analysis on the basis of its atypical site characteristics, a coarsening trend can be identified from station 1 (east) to station 5 (west). A Mann-Whitney U test between the clast populations at stations 1 and 5 (Appendix 6) revealed that the clasts recorded at station 5 were statistically larger than those at station 1 ( $n_1=50$ ,  $n_2=50$ ,  $\alpha_1=5\%$ ).

Site	Mean 'b' axis length
1	21.4
2	24.9
3	26.1
4	24.5
5	27.2
6	21.1

Table 4.4 Mean 'b' axis lengths of clasts measured along the western flank of The Bar (source: Hastings, 1991)

#### 4.1.2 Stratigraphy of the Culbin foreland

Stratigraphic investigations at Culbin were limited due to the presence of shingle units at the surface, whose thickness confounded efforts to penetrate them. Boreholes have not been sunk on the Culbin foreland, and so subsurface investigations were limited to areas of fine grained sediments which could be penetrated with hand operated equipment. Three principal areas selected for investigation were areas of former estuarine sedimentation, pond sediments at Snab of Moy, and sediments at the foot of the abandoned cliffline.

##### 4.1.2.1 Estuarine sediments

The presence of the extensive relict storm ridge suites of Culbin suggests that relatively high energy conditions have been a feature of the Culbin foreshore throughout the Holocene. However, landwards of the shingle ridge sequence Gauld (1981) identified a number of sites where fine grained sediments had accumulated (Figure 3.5). Stratigraphic investigation was undertaken to determine the nature of these sediments and to interpret their environment of deposition in relation to the Culbin shingle ridge suite.

Sites containing sequences of fine grained sediments were identified in the field through their surface vegetation assemblage, with grasses and occasional reeds signifying a less freely draining substrate than sand. Additionally, these sites

were typically found in low depressions between dunes, the combination of these two factors making them relatively simple to locate.

Investigation of these sites revealed a general sedimentary sequence of a thin cap of aeolian sand overlying a sand or silt unit of variable thickness, with a basal layer of coarse sand or occasionally a clast-supported shingle unit, below which penetration with hand operated equipment was not possible. Sample pits or cores were sunk at three locations (Figure 4.5, LAG 1-3). The limited amount of information obtained from these sites precluded full investigation of their location, sedimentology and relationships with other sites.

#### **4.1.2.2 Site LAG 1 (NJ 002638)**

This site in the eastern section of the forest formed the largest area of fine grained sediments found. The site consists of a sub-horizontal elliptical depression within the surrounding dune surface at 7.40 m OD, 244 m in length and 133 m wide at the widest point. The northwestern edge of the basin is enclosed by a shingle ridge, while the remainder of the basin is flanked by dunes. Higher ground north of the site at NJ 002639, beyond the immediate dunefield is also underlain by shingle ridges (set X, Figure 4.1).

A trial pit was dug in the southwestern corner of the basin, and the stratigraphy is shown in Figure 4.6. This reveals two distinct units of brown silt reaching a maximum depth of 0.57 m (6.83 m OD) overlying a shingle basement. The silts were capped by 0.12 m of aeolian sand, and were easily exposed.

#### **4.1.2.3 Site LAG 2 (NJ 021635)**

This site represents an area of former ploughed land within the former Culbin agricultural estate. Rigs and furrows are still clearly visible, trending north-south and creating local relief of up to 0.40 m. A pit had already been opened in this area for field parties; this was cleaned up and used for the site description. The pit was not extended beyond its present depth, and the basal unit was located by coring *ca.* 0.30 m below the floor of the pit.

The stratigraphic log recorded from this pit is shown in Figure 4.7, and was dug into a rig feature. This meant that the upper layers of the pit had been artificially emplaced for agricultural purposes, having been removed from the adjacent furrow and piled to form the rig whose surface is located at 6.56 m OD. The depth of disturbance could not be accurately determined, but a pit dug into an adjacent furrow revealed a minimum depth of disturbance of 0.17 m, and suggests that the

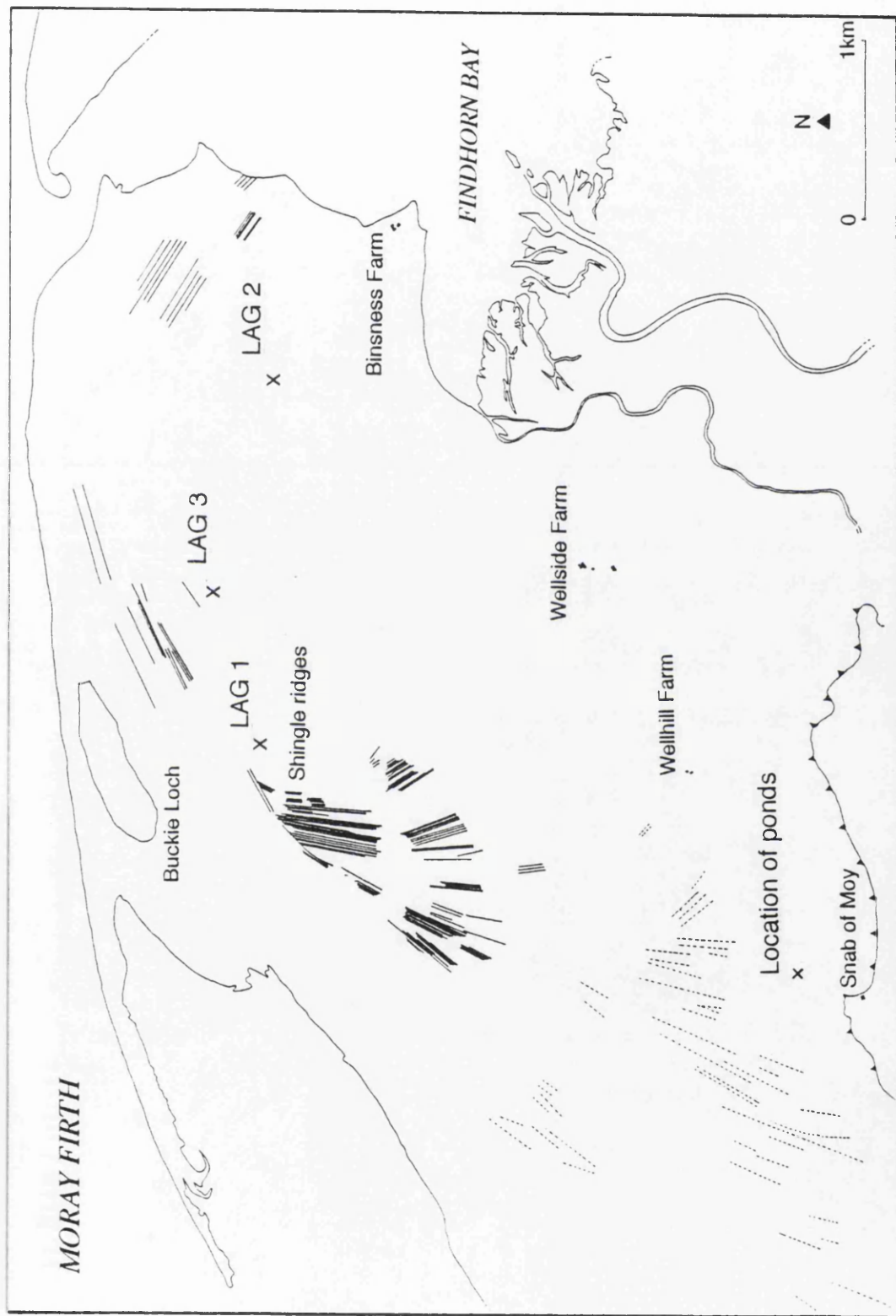


Figure 4.5 Location of sediment sampling sites LAG 1-3

Figure 4.6 Stratigraphic log from LAG 1

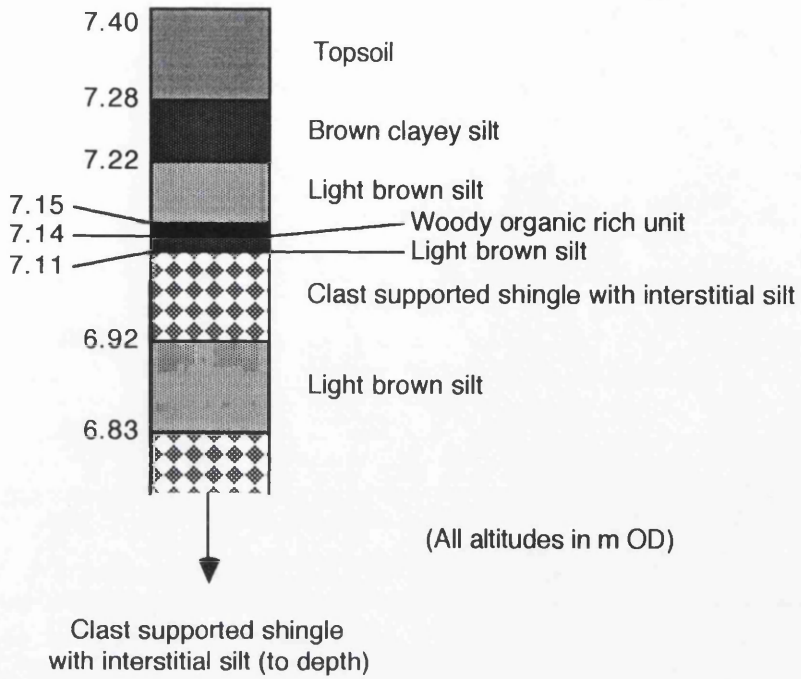
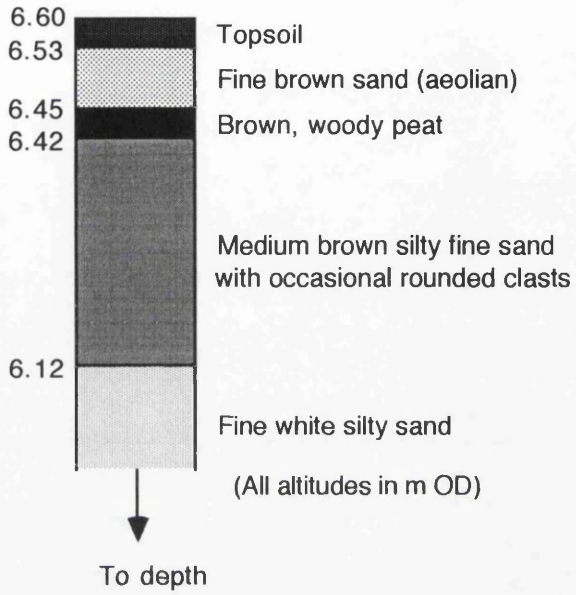


Figure 4.7 Stratigraphic log from LAG 2



upper sand and organic layers shown in Figure 4.7 are artificial. The basal white sand, however, is considered to be in its original position, and as such provides a minimum depth value of 6.12 m OD.

#### 4.1.2.4 Site LAG 3 (NJ 009639)

This site is found in a depression between surrounding dunes, and slightly further inland than site Lag 1. A pit dug through 0.26 m of aeolian sand revealed approximately 1.5 m of silts and fine sands, although the base of the lowest sand unit was not reached. A basal shingle layer was eventually reached at 3.04 m below the surface. The sedimentary sequence revealed in this pit is shown in Figure 4.8. An upper brown silt 0.18 m thick and separated from a fine sand by a thin organic layer. This was again too thin to be sampled accurately. This appeared as an indurated sand layer possessing an undulating contact with the underlying fine sand, which displayed a definite dip towards the south. The underlying fine sand was 0.03 m thick, displaying iron staining and providing a marked boundary with the underlying unit. This lower unit is a fine white sand with limited iron staining, found to extend as far as the shingle basement at this site, representing a total thickness of 3.04 m.

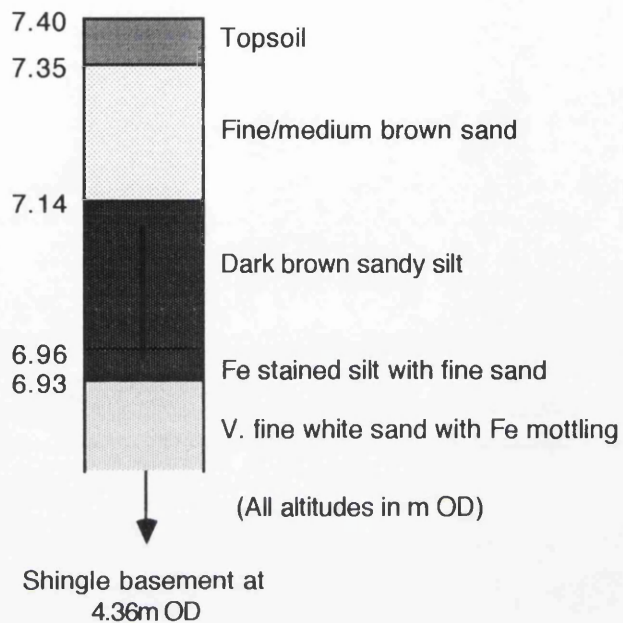
The visual similarity between the basal units of the deposits found in the estuarine sequences was striking. In order to test whether the similarity was real or apparent, samples of this deposit were collected for sieving. Once sieved, the median, mean, sorting and skewness were calculated for each sample. The results are displayed in Table 4.5.

	Median	Mean	Sorting	Skewness
Site LAG 1	3.3	3.40	0.61	0.10
Site LAG 2	2.8	2.85	0.27	0.32
Site LAG 3	2.4	2.48	0.65	0.42

Table 4.5 Sediment characteristics of the basal fine sand unit:- estuarine sites LAG 1-3, Culbin Forest

All of the samples are positively skewed, demonstrating the fine nature of the basal units at each site. The strongest skewness is found at site LAG 3, while site LAG 2 is less skewed (although still strongly so), and LAG 1 is classified as near

Figure 4.8 Stratigraphic log from LAG 3



symmetrical. Median grain sizes ranged between 3.3 & 2.4  $\phi$  (fine-v-fine sand [Wentworth scale]), with an expected inverse relationship displayed between skewness and median/mean grain size. The degree of sorting of the deposits is moderate at sites 1 & 3, and very well sorted at site 2.

#### 4.1.2.5 Snab of Moy pond sites

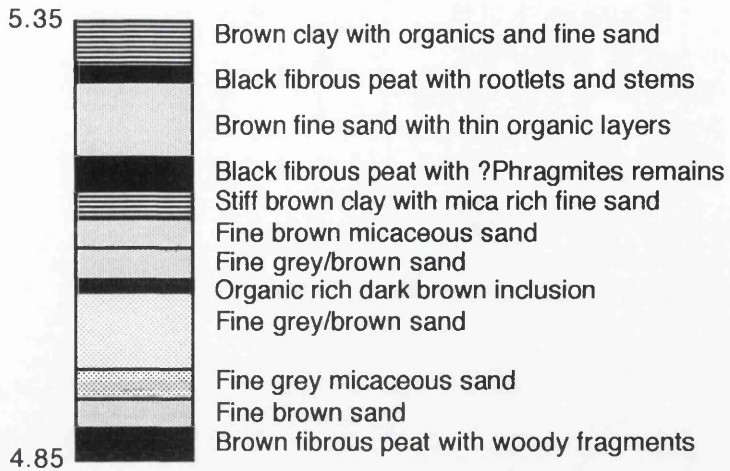
Sequences of fine grained sediments were also identified on the Culbin foreland further landwards of those sampled as the 'estuarine' sequence. A series of three ponds are located north of the bluff at Snab of Moy farm below the level of the surrounding sub-horizontal terrace surface (NH 987607-NH 988607) (Figure 3.6). Preliminary coring using a Russian corer revealed a general sequence of fine sands and silts containing two prominent peat layers. Figures 4.9 and 4.10 display the stratigraphic details of the sections of the cores which were of particular interest.

The core from pond 1 (Figure 4.9) reveals a basal peat at 4.85 m OD, below which depth the corer was unable to penetrate. Above the basal peat are 0.29 m of fine brown and grey sand layers, with a thin brown organic rich inclusion found at 5.03 m OD. Above the upper sand units is a thin layer of stiff brown clay with some fine sand and mica flakes, which underlie a second (middle) peat unit at 5.16 m OD. This peat unit contains two sub-units, a lower brown fibrous peat with plant macrofossils (unidentified) and an upper unit of black fibrous peat with *Phragmites* ? stems present. The combined thickness of the two peat units was 0.04 m. Overlying the middle peat unit is another layer of fine brown sand, merging into contemporary organic gyttja at 5.35 m OD. A date of  $3330 \pm 60$  BP (SRR 4684) was obtained from the basal peat unit.

Sampling from pond 2 was unsuccessful, the deposits being generally much thinner. Additionally, the presence of dumped material (including a car body) suggested that the potential for anthropogenic disturbance was high on this site. Samples from pond 2 were thus rejected.

The deposits in pond 3 show a simpler succession than that of pond 1 (Figure 4.10). The most notable difference between the deposits from the two ponds is that the base of pond 3 is located at a much greater depth than pond 1. The sequence begins as in pond 1 with a basal peat layer 0.05 m thick, but the base of this peat is found in pond 3 at 2.60 m OD, approximately 2 m deeper than in pond 1. This peat contains a parting of fine grey sand with a limited organic content, and continues again above the sand for a further 0.06 m. Above the

Figure 4.9 Stratigraphic log from Snab of Moy Pond 1



(All altitudes in m OD)

Figure 4.10 Stratigraphic log from Snab of Moy Pond 3



(All altitudes in m OD)

basal peat layer is 0.18 m of medium-fine grey micaceous sand, before a black fibrous peat layer is encountered at 2.88 m OD. This peat layer possibly forms the correlative of the middle peat in pond 1, and was encountered in all of the cores made in pond 3. Above the middle peat is a further layer of medium grey sand with thin organic rich layers, before encountering gyttja at the bed of the pond. The size of pond 3 made further investigation of the subsurface deposits essential in order to establish whether the sedimentary sequence encountered in the preliminary cores was applicable across the width of the pond. A total of nine cores were sunk in pond 3 with the aid of a boat, all of which demonstrated the same sequence displayed in Figures 4.9 and 4.10. The basal sand and shingle layer was found to shallow towards the SW however, and the basal peat was found to thicken towards the west.

A sample of the basal peat from pond 3 produced a date of  $3600\pm 45$  BP (SRR-4685). A sample of the middle peat from pond 3 yielded a date of  $3935\pm 55$  BP (SRR 4688). The dates thus show an inversion in pond 3, suggesting either an error or contamination either in the collection or dating process, or that the peats are allochthonous. Whether the peats are in situ or not, the data from the ponds suggests a minimum age for peat development no earlier than ca. 3900 BP, and no later than ca. 3300 BP.

#### **4.1.2.6 Sediments at the base of the raised cliffline**

In the vicinity of Snab of Moy farm a relict shingle storm ridge is located in an exposure created by a drainage ditch at the foot of the raised cliffline at NH 989603. The depth of the shingle could not be determined by hand coring, but was at least 0.3 m thick, providing a minimum altitude of 8.60 m OD. The shingle was clast supported and indurated by fine light brown sand, which was also found as a thin discrete deposit overlying the shingle. On top of the sand layer was 0.60 m of black, well compacted peat with a basal contact at 8.90 m OD. This had been buried further landwards by colluvial deposits on the raised cliff face. A radiocarbon date from this peat yielded a date of  $4335\pm 45$  BP (SRR-4683).

The peat can be traced northwards across the field at the foot of the abandoned cliffline. It extends at ground level as far as the Belmack Burn, where it is found in the stream bank dipping sharply north beneath the cover of blown? sand at the surface of the sub-horizontal terrace feature. Peat can be traced at the ground surface intermittently along the base of the raised cliffline as far west as Cothill (NH 953587), although surficial exposure means that the stratigraphic

relationships with the peats at Snab of Moy and these peats can not be established.

A pit was dug into the surficial peat in the field at NH 989603, 40 m north of the foot of the cliff. The peat at this locality is 0.70 m thick and outcrops at the ground surface. The base of the peat is located at 7.88 m OD. Below the peat is a sand bed 0.20 m thick with a high organic content, including whole branches identified as *Betula* spp. No evidence was found of a continuation of the shingle ridge from the foot of the cliff, this unit having been replaced by sand. This mixed sand unit displays an undulating, graded contact with an underlying bed of featureless medium brown sand at least 0.30 m thick. Two radiocarbon dates were obtained from this peat unit. The first was from the basal contact of the peat, which provided a date of  $4450 \pm 45$  BP (SRR-4686). The second date was from a large branch of *Betula* removed from the peat-sand contact, which yielded a date of  $4570 \pm 45$  BP (SRR-4687). Taken together, the dates indicate that peat began to develop on top of the shingle ridge at the base of the cliff no earlier than ca. 4600 BP.

#### **4.1.2.7 Summary**

The Culbin foreland is composed of a series of raised shoreline deposits of varying lithology, located between an abandoned cliffline and the contemporary coast at altitudes ranging between 11 and 3 m OD. The arcuate suite of shingle storm ridges dominated the northern section of Culbin, attaining a maximum altitude of ca. 11 m OD. These deposits are largely sterile, with only occasional indurations which were found to contain <1% organic matter (Plate 5). To the south, a series of fine-grained sediments have been deposited at up to 7.40 m OD. Limited evidence suggests that these deposits are underlain by shingle. Deposits in the vicinity of the abandoned cliffline reveal a sandy terrace, again underlain by shingle and also backed by a shingle unit banked against the foot of the cliff. A series of ponds at the base of the cliff were cored, and were found to contain intercalated peats and fine sand or silt units.

Radiocarbon dates obtained from peat associated with the deposits at the base of the cliffline produced dates between  $4570 \pm 45$  BP and  $3330 \pm 60$  BP, indicating a relatively young onset of peat development in association with these sediments.

Plate 5

Organic induration, possibly representing a poorly developed palaeosol within the upper layers of a relict shingle storm ridge, Culbin. The ridge is covered by 0.70 m of dune sand.



### **4.1.3 Geomorphology of Burghead Bay**

The Holocene development of Culbin cannot be fully understood without reference to the areas adjacent to it, and particularly updrift of it. These have developed in parallel to Culbin and thus have affected the supply of sediment downdrift. The establishment of a development sequence requires examination of the entire assemblage of landforms from Burghead Bay in the east as far west as The Bar in order to appreciate the operation of this section of the southern Moray Firth coast as a complete geomorphological unit.

Burghead Bay contains a variety of landforms which have been used in this study as evidence of changes in RSL over the late Devensian and Flandrian periods. As some of this evidence is not available in Culbin, the additional data collected proved extremely useful in providing an overview of the landforms and sedimentary history of this section of the southern Moray Firth. The importance of Burghead Bay relates to:

- i) its geomorphology;
- ii) its stratigraphic content in terms of identifying elements of the development sequence of this section of the Moray Firth;
- iii) its suite of dateable material.

Burghead Bay forms an arcuate embayment 10 km long between the towns of Burghead in the east and Findhorn in the west (Figure 1.1a). The western extremity is bounded by Findhorn Bay, while the eastern limit is marked by an outcrop of Devonian sandstone south of Burghead town.

The Bay is cut into raised sand and shingle foreshore deposits reaching up to 8 m OD, forming a cliff backing the contemporary beach (Figure 4.10a). These deposits were mapped by Steers (1937) (Figure 4.11), and show a series of shingle storm ridges trending ESE-WNW. A narrow neck of surficial shingle is indicated in the vicinity of Bessie Burn (NJ 097653), widening gradually towards the west as the ridges begin to recurve around the village of Findhorn. A second set of strongly recurving ridges are indicated further inland in the vicinity of Muirhead (NJ 086630). The map suggests that erosion has sectioned the ridges marked D at their proximal ends.

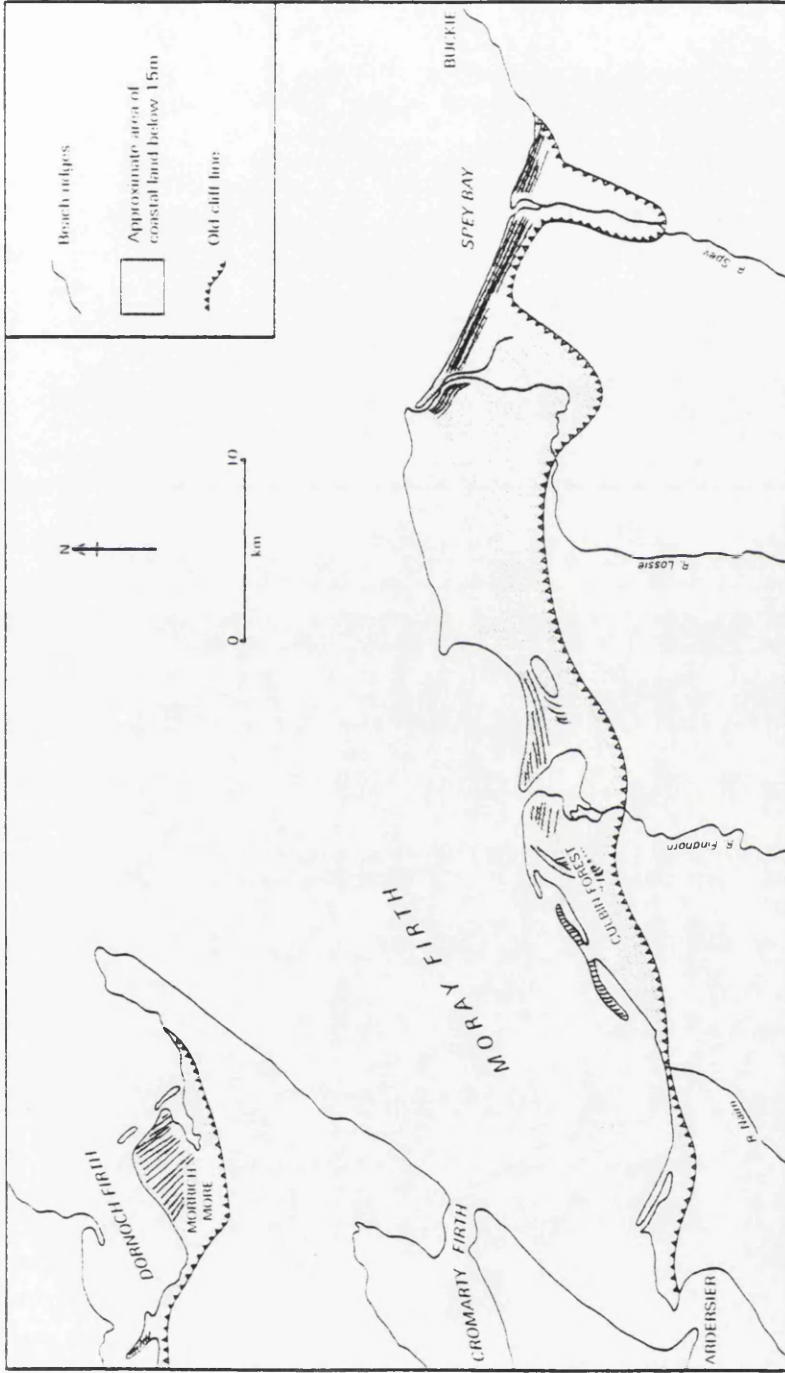


Figure 4.10a Location of raised cliffline around the inner Moray Firth (source: Hansom, 1988)

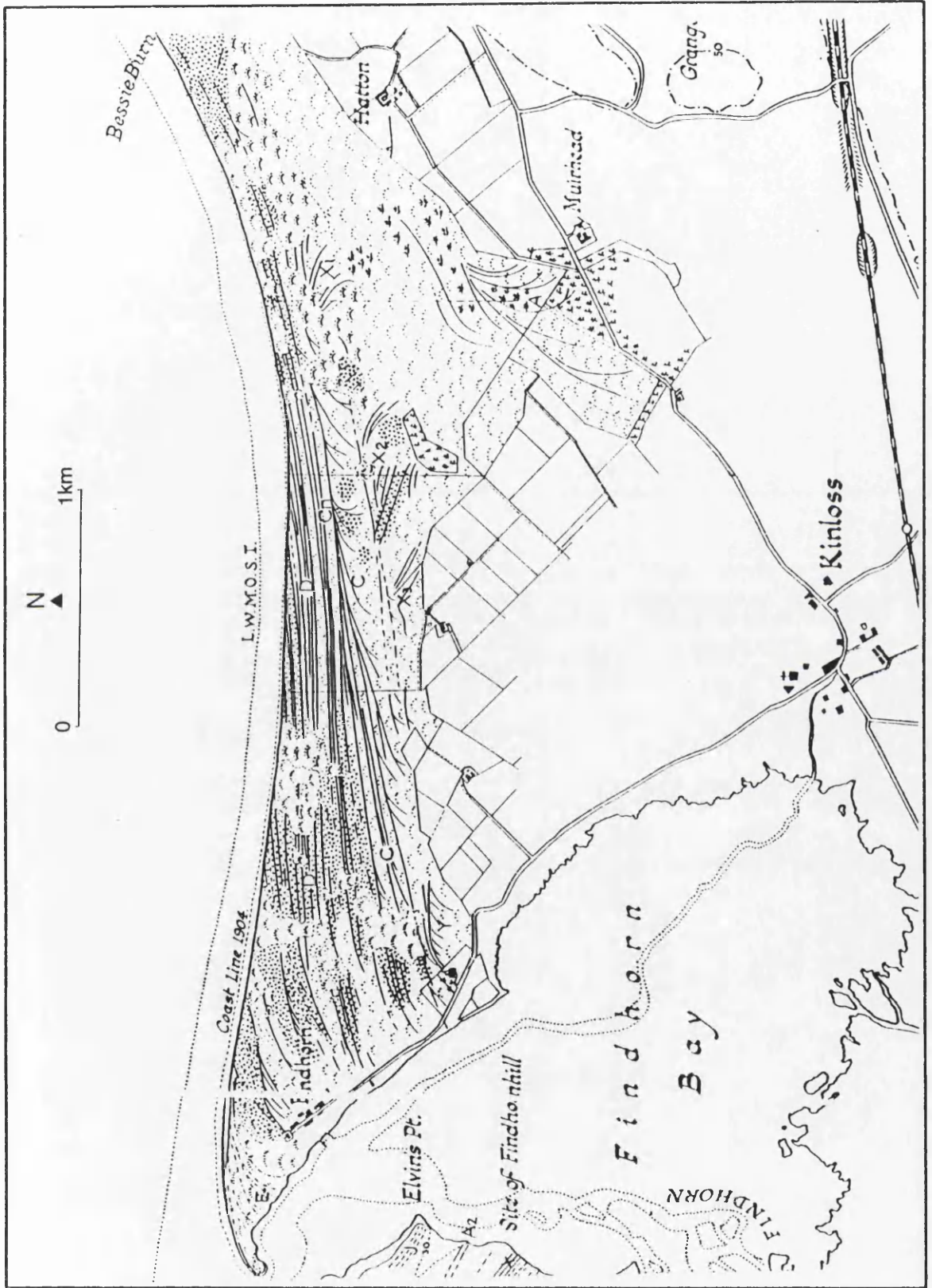


Figure 4.11 Raised shingle ridges in Burghead Bay (source: Steers, 1937)

These sand and shingle deposits form a low surface sloping gently seawards from a landward boundary marked by the same raised cliffline feature noted landwards of Culbin Forest. The raised cliffline feature is not so prominent on the east side of Findhorn Bay, and a large section is obscured by the town of Forres. The most notable exposure occurs where the cliffline is crossed by the B9011 at NJ 057607. The base of the feature remains at ca. 7 m, as observed in the Culbin area.

#### **4.1.3.2 Stratigraphy of Burghead Bay**

The deposits fronting the raised cliffline east of Culbin can be classified into two zones; the Findhorn Bay and the Burghead Bay deposits.

#### **4.1.3.3 Findhorn Bay Deposits**

The area at the head of Findhorn Bay forms a low lying tract of land below 5 m OD, extending from Claypark to the south of Culbin (NJ 001609) in a belt approximately 1.5 km wide around to Milton of Grange farm (NJ 046603) south of Findhorn Bay. The area is traversed by the River Findhorn, Muckle Burn and the Burn of Mosset, while the smaller Kinloss Burn crosses the area to the east.

A stream section in the Findhorn Bay deposits (NJ 050609) reveals blown sand at ca. 4 m OD overlying a bed of black, clayey peat 0.30 m thick which appears to thin landwards. A local farmer reported that deep ploughing revealed a peat in the fields immediately south of the stream section, suggesting that the peat unit continues landwards. The peat rests on a stiff blue-grey clay and an undulating, sharp contact exists between the two units at 1.24 m OD. Penetration with a Russian peat corer revealed coarse, sandy partings within the clay layer.

A sample of the peat at the lower contact with the underlying clay was submitted for radiocarbon assay, and provided a date of 9305±45 BP (SRR 4689).

#### **4.1.3.4 Burghead Bay Deposits**

The area to the east of Findhorn Bay lies considerably further seawards than the Findhorn lowlands, forming a low, gently seaward sloping surface approximately 2.5 km wide from the raised cliffline to the coastal edge. The area above present HWST is composed broadly of interbedded sand and shingle deposits capped by locally bedded sand.

#### **4.1.3.5 Subsurface investigations on the Burghead Bay lowlands**

Borehole data was particularly abundant in this area, the majority of which was compiled by the MOD during the various stages of construction of RAF Kinloss. Additionally, various boreholes were sunk on behalf of Grampian Regional Council during groundwater explorations undertaken in the area in 1986. A single borehole was also sunk privately by the nearby Findhorn Foundation. Selected borehole logs are used to demonstrate the relationships between beds over a wider area. Figure 4.12 shows the distribution of the boreholes described in this investigation.

Depth to rockhead varies across the site suggesting an undulating bedrock surface upon which the subsequent infill of Holocene sediments has taken place. The depth of Holocene sediments decreases towards the NE, draping over the periphery of the outcrop of Devonian sandstone comprising the Covesea "ridge". Rockhead in this area is found at between 0.0 & -0.7 m OD (BH2 & 1 respectively), with a cover of between 9.75 & 11 m of aeolian sand, interbedded sands and silts and "boulder clay", the latter diamict probably representing till at the base of these boreholes. Further west, rockhead is located at -26.9 m OD at KBH 6, and -25.35 m OD at KBH 35, in the centre of the present airfield at RAF Kinloss. On the eastern edge of Findhorn Bay rockhead is reached at -30.20 m OD at KBH 26, and -23.7 m OD in the Findhorn Foundation borehole at NJ 049640. While this data suggests that depth to rockhead is reasonably constant, some deeper boreholes encounter sand and gravel at depths of up to -34.4 m OD (KBH 16). The proximity of these deeper boreholes to those with known rockhead depth limits suggests that the bedrock surface may contain significant hollows which have infilled with younger Holocene sediment. The basal sequences of the Holocene infill in KBH 6, 26 & 35 are angular/subangular gravels with coarse interstitial sand rather than the diamict recorded in boreholes 1 & 2. The basal layer identified in an independent borehole from the Findhorn Foundation at NJ 049640, however, is a stiff sandy clay containing rock fragments, pebbles and "rock flour". It is not known how "rock flour" was defined, or how it differs from clay, but the description of the deposit defines it as a diamicton. Additionally, a thick layer of clay was reported in borehole KBH 25 between -32.2 m and -6.55 m OD, described as a firm, silty clay with silt lenses overlying a fine sand bed. This is the only substantial thickness of clay reported at a depth close to rockhead in any of the remaining

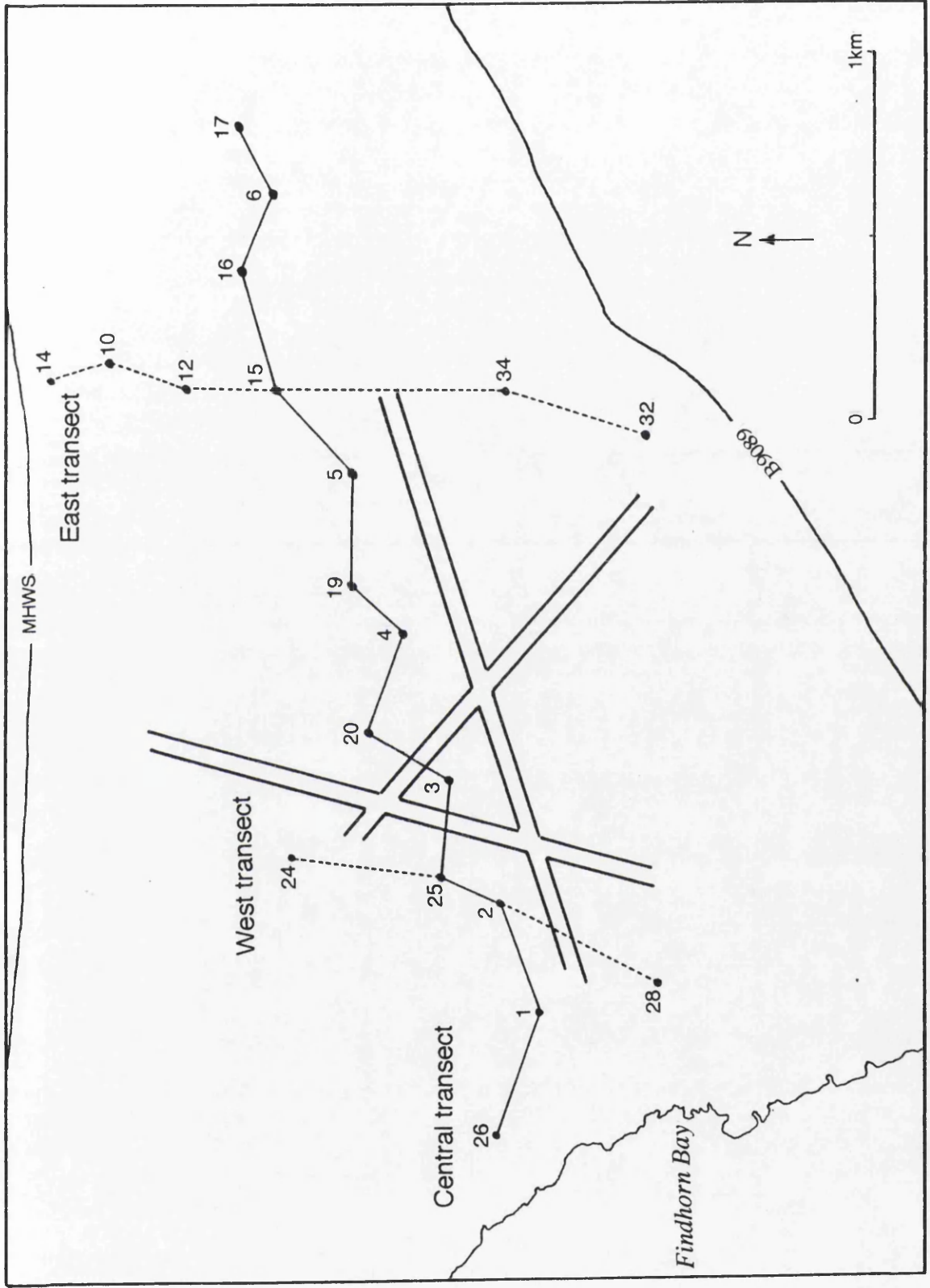


Figure 4.12 Location of boreholes and transects at RAF Kinloss

boreholes. While accepting the limitations placed on interpretation from drilling crew reports, it appears unlikely that this clay represents till.

The deposits underlying RAF Kinloss have been reproduced as a series of transects crossing the airfield at different locations in order to provide maximum areal coverage of the site (Figure 4.12). Two transects cross the airfield from north to south, at NJ 078645-NJ 077627 (east transect) and NJ 064638-NJ 059627 (west transect), and one transect (central) crosses the area from east to west (NJ 055632-NJ 086639). The borehole data has been transferred to these transects, which are shown in Figures 4.13 and 4.14.

#### **4.1.3.6 Central Transect**

Figure 4.13 shows the central transect, made from west to east across the airfield. Basal sediments in the central section of the transect are dominated by a locally thickened bed of silty clay. The base of this clay is located in KBH 25 at -32.3 m OD and KBH 26 at -30.2 m OD (rockhead). The clay is continuous across the central area of the airfield, and demonstrates an almost level upper surface at ca. -7 m OD. Above the clay is a bed of sand which is found across the entire central section of the airfield, although towards both the east (KBH 1, 2) and west (KBH 16, 6) this sand becomes increasingly gravelly. The top surface of this sand/gravel unit displays local relief of up to 2 m, with a marked local thickening in the centre of the transect at KBH 19. This locality contains a series of interbedded sands and silts, with a basal brown, fibrous peat unit at -3.2 m OD, a sequence not repeated elsewhere on the transect. Capping these deposits is a second, more extensive peat unit found in the nine westernmost boreholes of the transect. The base of the peat lies between 0.3 m OD and -3.3 m OD and is described as a brown, spongy peat. The unit is approximately 1m thick across the transect, and appears across a total of 1750 m of the transect. Overlying this peat is an extensive sand unit which appears in all of the boreholes. Locally the bed is gravelly (eg. KBH 3, 5). This unit attains a maximum thickness of 6.0 m in the central section of the airfield, and thins considerably towards the east, reaching only 1.0 m thick in KBH 6. The sequence is capped by a thin layer of topsoil.

#### **4.1.3.7 East transect**

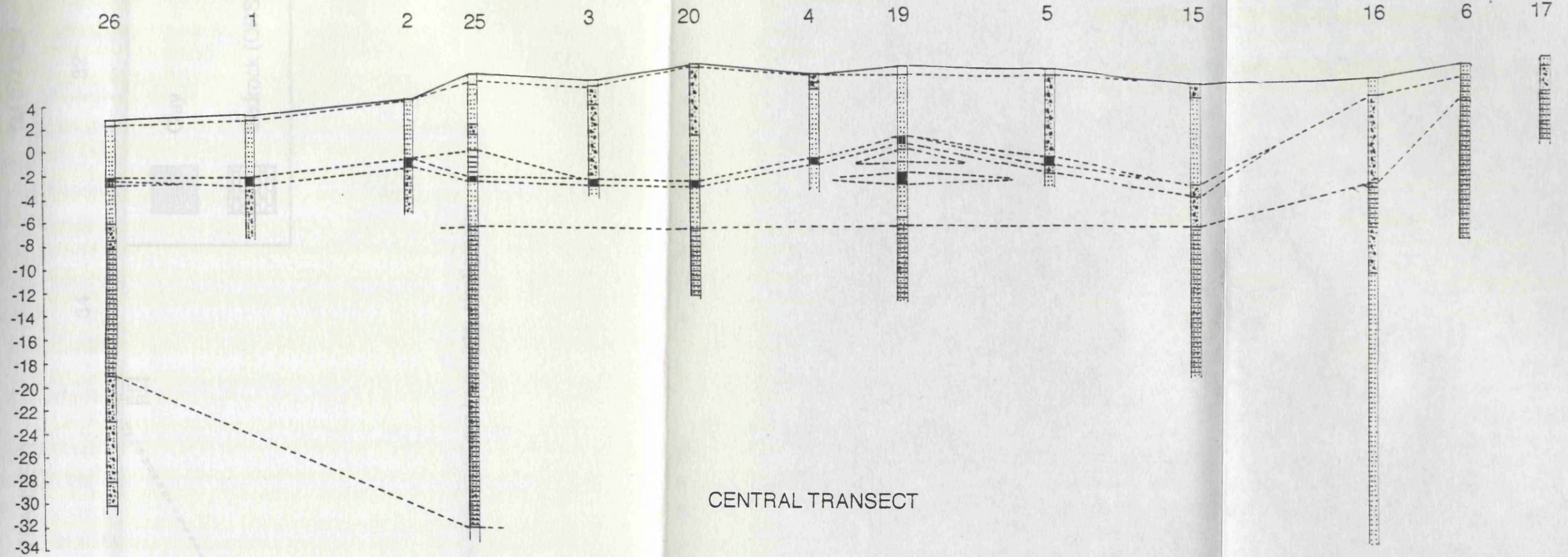
The boreholes comprising the east transect (NJ 078645-NJ 077627) are shown in Figure 4.14. The deposits at the seaward edge are dominated by coarse sands and gravels, while further inland the deposits tend to become finer. KBH

NJ 055 632

NJ 086 639

W

E



CENTRAL TRANSECT

**KEY**

-  Peat
-  Sand
-  Sand & shingle
-  Silt
-  Clay
-  Bedrock (ORS)

Figure 4.13 RAF Kinloss central transect: stratigraphy

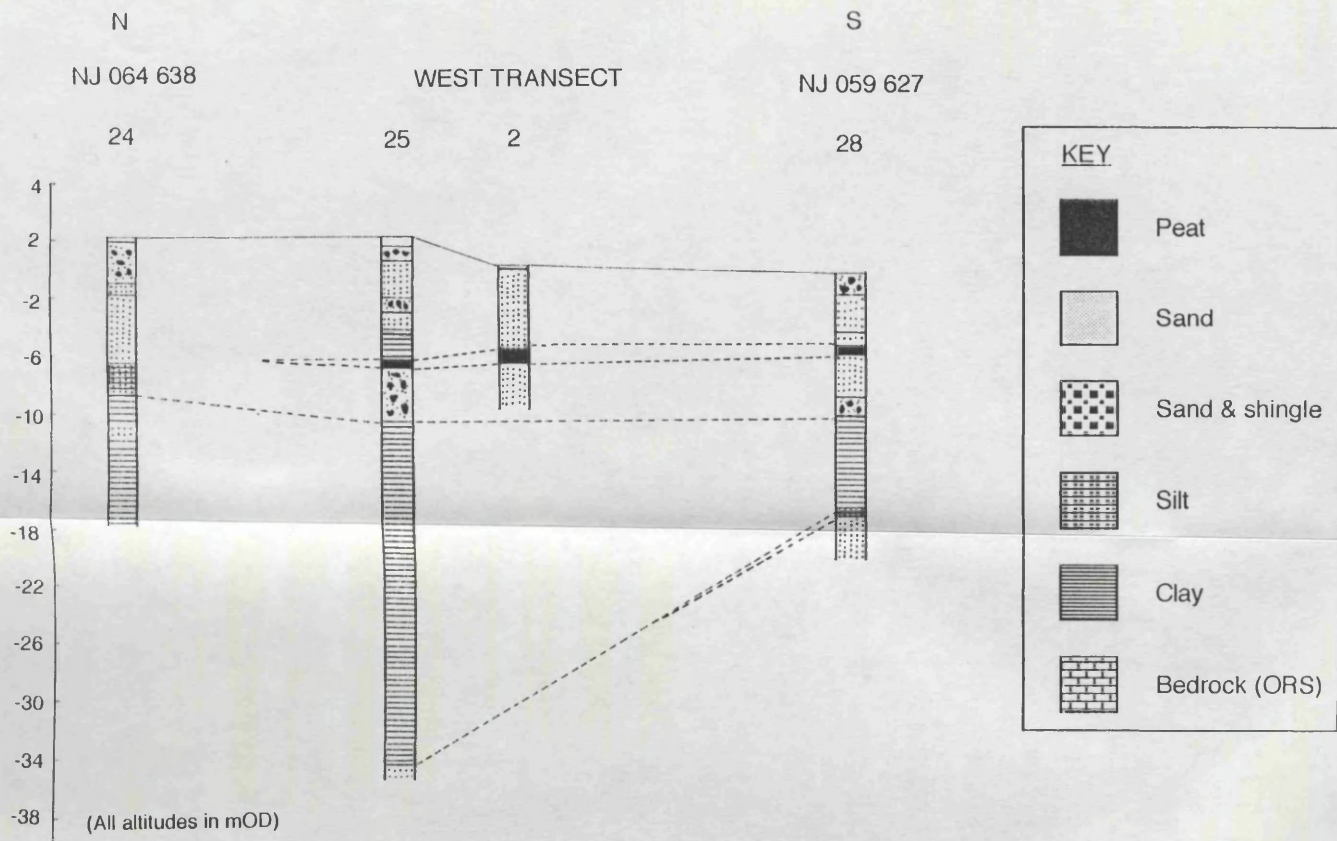
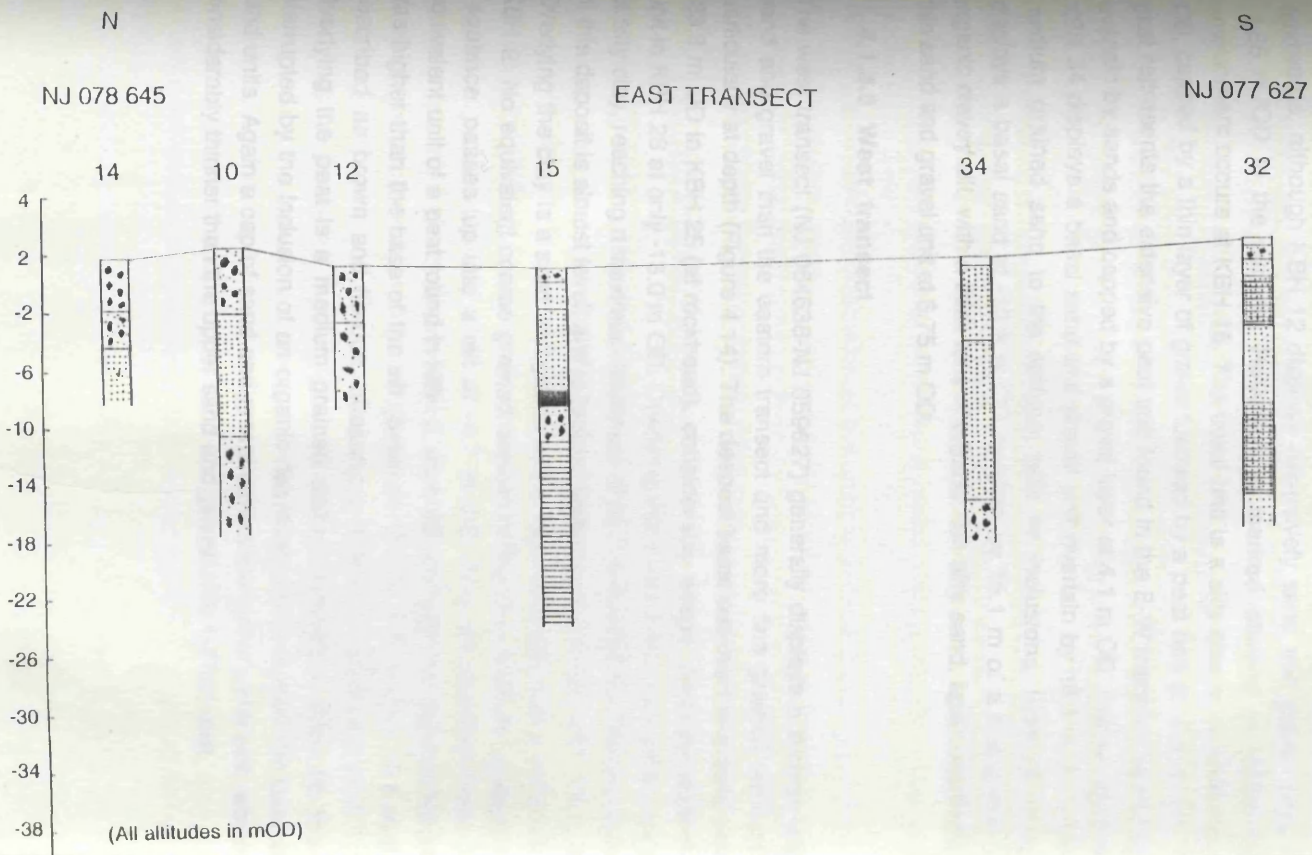


Figure 4.14 RAF Kinloss east and west transects: stratigraphy

10 displays a basal sand unit at -4.2 m OD, overlain by sand and gravel up to 5.8 m OD. KBH 10 displays a similar sequence, with a basal sand and gravel bed at -13.4 m OD. The proportion of gravel in the deposits generally decreases landwards, although KBH 12 displays exclusively sand and gravel units from -4.65 m OD to the surface. However, a marked change in sedimentary environment occurs at KBH 15. The basal unit is a silty clay to at least -19.9 m OD, capped by a thin layer of gravel followed by a peat bed at -4.4 m OD. This peat represents the extensive peat unit found in the E-W transect, and is again overlain by sands and capped by a gravel layer at 4.1 m OD. Further landwards KBH 34 displays a basal sand and gravel unit overlain by 16.5 m of a dense, medium grained sand to the surface, with no inclusions. KBH 32 however displays a basal sand at -13.3 m OD overlain by 15.1 m of a fine grey/brown organic clayey silt, with a thick lens of organic rich silty sand, again capped by a thin sand and gravel unit at 6.75 m OD.

#### **4.1.3.8 West transect**

The west transect (NJ 064638-NJ 059627) generally displays a thinner cap of sand and gravel than the eastern transect and more fine grained sediments, particularly at depth (Figure 4.14). The deepest basal sediment is a sand unit at -33.3 m OD in KBH 25 (at rockhead), considerably deeper than the equivalent unit in KBH 28 at only -13.0 m OD. Overlying this basal sand is an extensive unit of silty clay, reaching a maximum thickness of 25.7 m in KBH 25. The top surface of this deposit is almost level, and is located between -6.5 m OD and -7.8 m OD. Overlying the clay is a sand and gravel unit in KBH 25 & 28, and a sand unit in KBH 2. No equivalent coarse grained deposit is found in KBH 24; instead the sequence passes up into a silt at -4.7 m OD. This silt possibly forms the equivalent unit of a peat found in KBH 2, 25 & 28, although the base of the peat was higher than the base of the silt (between -2.7 & -1.4 m OD). The peat is described as brown and fibrous, attaining a maximum thickness of 0.7 m. Overlying the peat is a medium grained sand, although in KBH 25 this is interrupted by the inclusion of an organic-rich clayey silt between the peat and sand units. Again a cap of sand and gravel covers the upper sand unit, which is considerably thinner than the upper sand and gravel units further east.

#### 4.1.3.9 Summary

In summary, the central transect displays a thick, sub-horizontal silt unit capped by an extensive peat unit and overlain in turn by a variable thickness of sand and shingle. The western transect shows an increased proportion of clay in the lower units, again with the extensive peat unit appearing in the more landward boreholes, and once more capped by sand and shingle, with an increasing amount of shingle to seaward. The eastern transect is more variable, with shingle extending to greater depths, particularly in the boreholes seaward of the central transect intersection. The boreholes display increasing proportions of sand landwards, although locally silt units are significant. The peat unit appears to thin towards the east, appearing in only one borehole on the eastern transect.

The Burghead Bay deposits represent a useful insight into the stratigraphic relationships between the various relict deposits in the absence of similar information at Culbin. Penetration of the shingle units at Culbin was not within the scope of this research, and as such Burghead Bay provides a useful analogue for understanding the sedimentary environment in this area prior to the emplacement of the extensive shingle ridge suite.

#### 4.1.3.10 The intertidal peat unit in Burghead Bay

Outcropping on the foreshore in Burghead Bay is a bed of peat, exposed only at low water. This unit has attracted much attention in literature on the area (Chapter 1), although no formal analysis of the peat has been undertaken. The peat was sampled at a point 90 m west of the Roseisle car park access point (NJ106664), in an exposure 250 m long. A pit dug through the peat bed reveals 0.23 m of dark brown/black compact, *Phragmites* rich peat which also contains roots and twig fragments, including *Betula* spp. The base of the peat is located at -1.75 m OD. The top surface has been eroded by marine activity, and was heavily pitted. Below the undulating but distinct peat contact is a bed of coarse brown sand 0.17 m thick containing dispersed organic material. Below 0.19 m OD the sand becomes finer, extending to depth and containing small fragments of shell. A sample of peat at the basal contact with the underlying sand was submitted for radiocarbon assay, and produced a date of 9105±45 BP (SRR 4677).

#### **4.1.3.11 Raised foreshore deposits in Burghead Bay: Cliff section study**

Marine erosion has sectioned the raised shoreline deposits along the central section of Burghead Bay from the beach access route at Roseisle car park (NJ 110665) as far east as Findhorn, where the deposits become obscured by blown sand and the emplacement of a rock revetment. These deposits provide a cross-sectional view of the raised foreshore deposits in Burghead Bay which is unavailable at Culbin, and provides information concerning the stratigraphic relationships between the individual sedimentary units. Northeast of the car park the curvature of the bay leads to cliffing of the aeolian sands seawards of the raised shoreline deposits. Between the car park entrance and NJ 093651, however, the sediments are revealed in section and are presented in Figure 4.15. The section described does not cover the full length of exposure. The eastern part of the section between the car park entrance and NJ 098653 contains only sub-horizontally bedded sand and shingle, and provides little additional stratigraphic information beyond that obtained from the section further west. For this reason it is excluded from Figure 4.15.

The description of the deposits in the section will commence at the eastern end and extend sequentially westwards by reference to vertical logs. The exposures are described as they were logged in the field, with descriptions of the intervening sedimentary relationships providing a stratigraphic section diagram covering the entire 660 m of exposure. Observations below 2.27 m OD were obscured by the presence of a contemporary shingle storm ridge banked against the foot of the cliff.

Log A commences at NJ 098653 where 2.40 m of sub-horizontal sand and shingle beds at up to 4.45 m OD are capped by 0.60 m of fine grained, cross bedded sand interpreted as an aeolian deposit. The individual beds are up to 0.40 m thick, and contain shingle with a mean 'b' axis length of 26 mm.

The interbedded sand and shingle deposits are continuous for 50 m to log A1. At this point the interbedded sand and shingle layers dip westwards below the level of the contemporary shingle storm ridge at 2.79 m OD. The ground surface at this point appeared to be heavily modified. Overlying the sand and shingle beds in the centre of the section is a fine white sand layer, which in turn underlies a thin peat bed with an apparent westerly dip. The base of this peat is located at 3.88 m OD. Tracing the section 80 m west to log A2, the peat bed is seen to gradually

# Burghhead Bay Cliff Section 1991

(View to SSE)

GR NI 096 653

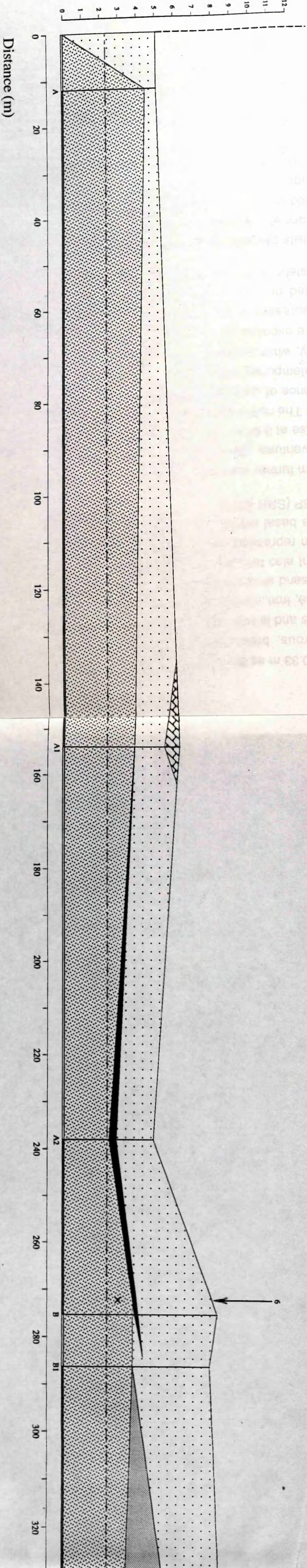
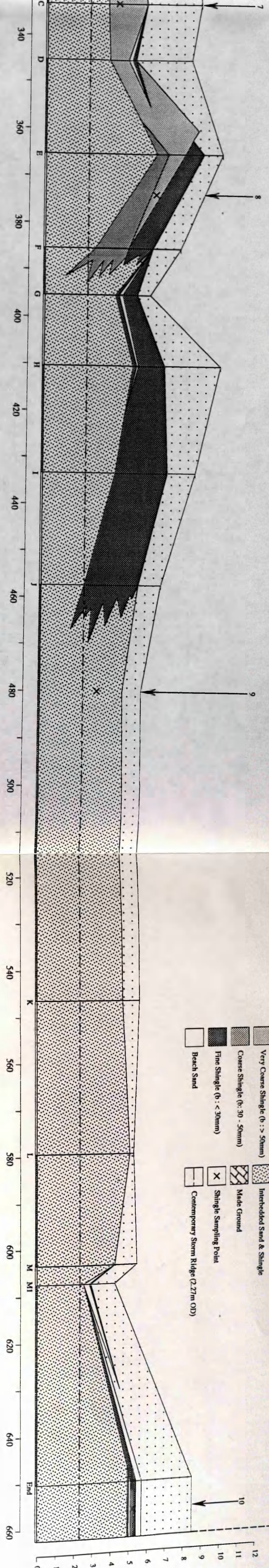


Figure 4.15



GR. NJ 093 651

- |  |                                 |  |                                     |
|--|---------------------------------|--|-------------------------------------|
|  | Peat                            |  | Aeolian Sand                        |
|  | Very Coarse Shingle (b: > 50mm) |  | Interbedded Sand & Shingle          |
|  | Coarse Shingle (b: 30 - 50mm)   |  | Made Ground                         |
|  | Fine Shingle (b: < 30mm)        |  | Shingle Sampling Point              |
|  | Beach Sand                      |  | Contemporary Storm Ridge (2.27m OD) |

thicken to 0.33 m as the basal contact falls to a low point at 2.44 m OD. The peat is stiff, fibrous, brown/black in colour, containing macrofossil fragments of *Phragmites* and is increasingly compact towards the base. Below the peat is 0.1 m of coarse, iron stained sand with partings of brown silt, which in turn overlies fine white sand similar in texture to that observed at log A1. The ground surface at this point also falls to 4.77 m OD, including 2 m of aeolian sand, suggesting this section represents an infilled topographic low. A radiocarbon date from the peat at the basal contact with the underlying coarse sand produced a date of 3140±45 BP (SRR 4679).

Log B 40 m further west shows the peat bed rising and thinning westwards with altitude, eventually grading to a fine, grey/brown structureless sand 0.11 m thick with its base at 3.84 m OD, overlain by a locally thickened cover of aeolian sand at 4.26 m. The rise in altitude of the base of the peat bed is accompanied by the reappearance of underlying interbedded sand and shingle from below the level of the contemporary storm ridge. At log B1, 20 m west of B, the peat tapers out completely, while a minimum thickness of 1.75 m of the interbedded sands and shingle are exposed up to an altitude of 3.69 m OD. The preceding three logs clearly represent a cross section through a former topographic low, still represented on the contemporary ground surface by a marked depression approximately 140 m wide between two large dunes.

The deposits beyond log B1 show a transitional zone to a completely different sedimentary environment. At a point 40 m west of B1 the top surface of the interbedded sands and shingle drops slightly to 2.27 m OD, and are capped by a solid wedge of crudely bedded, clast-supported shingle 2.10 m thick with an apparent westerly dip. The top surface of the shingle is capped by 2.96 m of aeolian sand. The shingle wedge forms a very apparent apex at 5.37 m OD, and is interpreted as a raised shingle storm ridge viewed in cross section. The top surface of the shingle ridge interdigitates with sand deposits over approximately 10 m of exposure, although the lower section of shingle remains as a solid, clast-supported mass with interstitial sand but no discrete sand partings. A sharp rise in the surface of the shingle accompanies the transition to log E. The top surface of the shingle ridge from log D declines in altitude and gradually becomes disseminated by increasingly frequent sand partings until it is indistinguishable from the underlying interbedded sand and shingle beds. On the surface of the former ridge, however, a second body of clast-supported shingle 1.40 m thick is located at 4.80 m OD. This layer increases in thickness to a maximum of 2.00 m with the crest at 8.53 m OD. At a point 5 m west of this crest a third ridge abuts

the eastern flank of the second ridge. Again both units display crude bedding within the shingle body, with individual units identified at up to 0.90 m thick. Only one minor sand parting is found throughout the entire shingle mass, and although only 0.05 m thick represents a continuous unit rather than a simple sand lens commonly found within the shingle bands.

At a point 20 m west of log F a fall in the level of the ground surface to 7.34 m OD is accompanied by a fall in the surface of the westerly shingle ridge structure to 4.51 m OD. Below the top surface at least 3.13 m of unbroken shingle can be observed. Log G 10 m further west shows a slight rise in the altitude of the shingle surface to 4.98 m OD, while the shingle at depth again begins to become interspersed with sand partings, dividing eventually into individual shingle stringers indistinguishable from the interbedded sand and shingle units at ca. 4.70-4.18 m OD.

Log H 20 m west of G shows a gentle rise in the top surface of the solid shingle unit to 6.46 m OD. The deposits continue for a further 25 m (log I), with a slight rise in the surface altitude of the upper shingle unit to 6.73 m OD, before beginning to become interspersed with frequent sand partings, producing a unit of interbedded sand and shingle 2.79 m thick. West of this site the ground surface drops to 5.7 m OD forming a wide, low inter-dune area. The deposits in the section mirror this drop, displaying a simple stratigraphic sequence of interbedded sand and shingle up to 5.17 m OD at log J. This sequence extends for 165 m west of log I, with only a slight fall in the altitude of the top surface of the interbedded sand and shingle to 4.56 m OD (log K) and a rise to 4.95 m OD (log L).

At a point 25 m west of L the aeolian sand cover thickens rapidly to 1.35 m (log M). Below this the top surface of the interbedded sand and shingle sequence is located at 3.55 m OD. The top surface of this sequence dips westwards, with the upper shingle bed thickening in this direction. Log M1 5 m west of M is located in a second topographic low. Log M1 reveals a second peat bed, differentiated into an upper unit 0.20 m thick composed of loose, brown fibrous peat and a lower dense, silty black peat with occasional fine grey sand lenses 0.30 m thick. The base of the lower peat layer is located at 2.51 m OD. The peat rests on a bed of very fine, white structureless sand, extending to depth below the level of the contemporary shingle storm ridge. The contact between the peat and the underlying sand is undulating but distinct, resembling the relationship observed at log A2. A sample of the peat at the basal contact was submitted for

radiocarbon assay, and produced a date of 2900±45 BP (SRR 4681). A large slump obscured the section between M1 and M, and it was assumed that the peat would have appeared as a thin layer dipping westwards in a similar manner to log A2. Overlying the peat is aeolian sand 1.3 m thick, which only partially infills the topographic low, retaining a dune slack in the contemporary dune surface.

Across a distance of 44 m the peat bed rises in altitude towards the west, gradually tapering out completely. This rise in altitude is mirrored by the reappearance of the interbedded sands and shingle from below the level of the contemporary storm ridge up to ca. 2.90 m OD. Overlying these units is a thick series of sub-horizontally bedded sands with occasional pebbles, which also increases in thickness towards the west, reaching a maximum altitude of 5.10 m OD. These sands contain two thin bands which were particularly rich in shell debris, concentrated in stringers abutting individual clasts. Capping these sands is a layer of shingle which appears from below the peat layer as it finally tapered out, and which formed an erosional contact, again dipping eastwards. At 44 m from log M1 the shingle layer becomes horizontal, overlying the sands beneath it rather than abutting them, and becoming interdigitated with a series of thin sand beds. This forms a continuous bed of interbedded sands and shingle 0.55 m thick overlying the shell bearing sands. This sequence is finally capped by 1.45 m of aeolian sand, and forms the end of the section. Beyond this point the raised foreshore deposits continued west with little change. The shell bearing sand becomes interdigitated with shingle units of varied thickness west of NJ 093651, and observations between this point and Findhorn village demonstrated a general stratigraphy of sub-horizontal interbedded sand and shingle overlain by aeolian sand. No other structures of note beyond this were observed throughout the data collection period, although undercutting of the cliff plus tourist activity had obscured a considerable area of the section through slumping. It is considered unlikely that any structures of the type measured further east were present in this zone of the section.

#### **4.1.3.12 Clast fabric analysis**

The series of shingle units exposed in the cliff along Burghead Bay were of particular interest, representing sections through relict foreshore shingle accumulations. Initial examination of the orientation of the long (a) axis of individual clasts suggested that the principal vector of a high frequency of individual clasts was not orientated normal to the present shoreline. The

frequency of observation of clasts with 'a' axis orientation at a marked angle to the present shoreline suggested that these units may have been deposited on a beach with a different orientation to the present beach in Burghead Bay. The sectioning of the deposits in Burghead Bay meant that, with care, clasts could be measured in their original positions. This provided an insight into foreshore deposition which could not be obtained from the unsectioned Culbin shingle ridge structures.

In order to test whether there was a real change in the azimuth of the dominant vector, or whether the observed orientations were simply a function of the curvature of the section, 'a' axis orientation of fifty clasts was measured at ten stations along the section. The interval between the stations was not even, and represented available exposures of shingle in the section. Sampling locations are shown in Figure 4.16.

The fabric diagrams derived from the measurements along Burghead Bay are shown in Appendix 7. Of the ten sites sampled, three possessed dominant vectors displaying a landward trend (sites 1, 9 & 10), whilst the remaining seven displayed the more expected seaward trend. Six of these seven sites displayed a dominant vector in the northwestern sector ( $295^{\circ}$ - $345^{\circ}$ ), with only station 2 displaying a dominant trend of  $255^{\circ}$  (southwesterly). However, while beach clasts will tend to show principal (a) axis alignment parallel to the direction of incident wave energy, the dip of the 'a' axis can easily be landward rather than seaward particularly if the clasts have been deposited in a topographic low or over a beach ridge crest on the foreshore surface as was frequently observed on the contemporary foreshore. Adding  $180^{\circ}$  to the dominant vector displayed by the rose diagrams for sites 1, 9 & 10, the vectors appear in the southwestern sector along with site 2, although with a significantly more southerly aspect. This satisfies the possibility of deposition either landwards or seawards of a berm crest on the foreshore, while still representing the principal direction of incident wave energy.

Fabric strength was calculated in order to determine whether the deposits displayed a sufficiently strong vector magnitude to infer the former alignment of the foreshore upon which the clasts were deposited. The method of calculation of the resultant vector magnitude is shown in Appendix 8. The results of the analysis are displayed as a percentage figure, with a value of 100% representing all observations aligned along the same azimuth. Vector magnitudes calculated from the ten sampling sites are shown in Table 4.6.

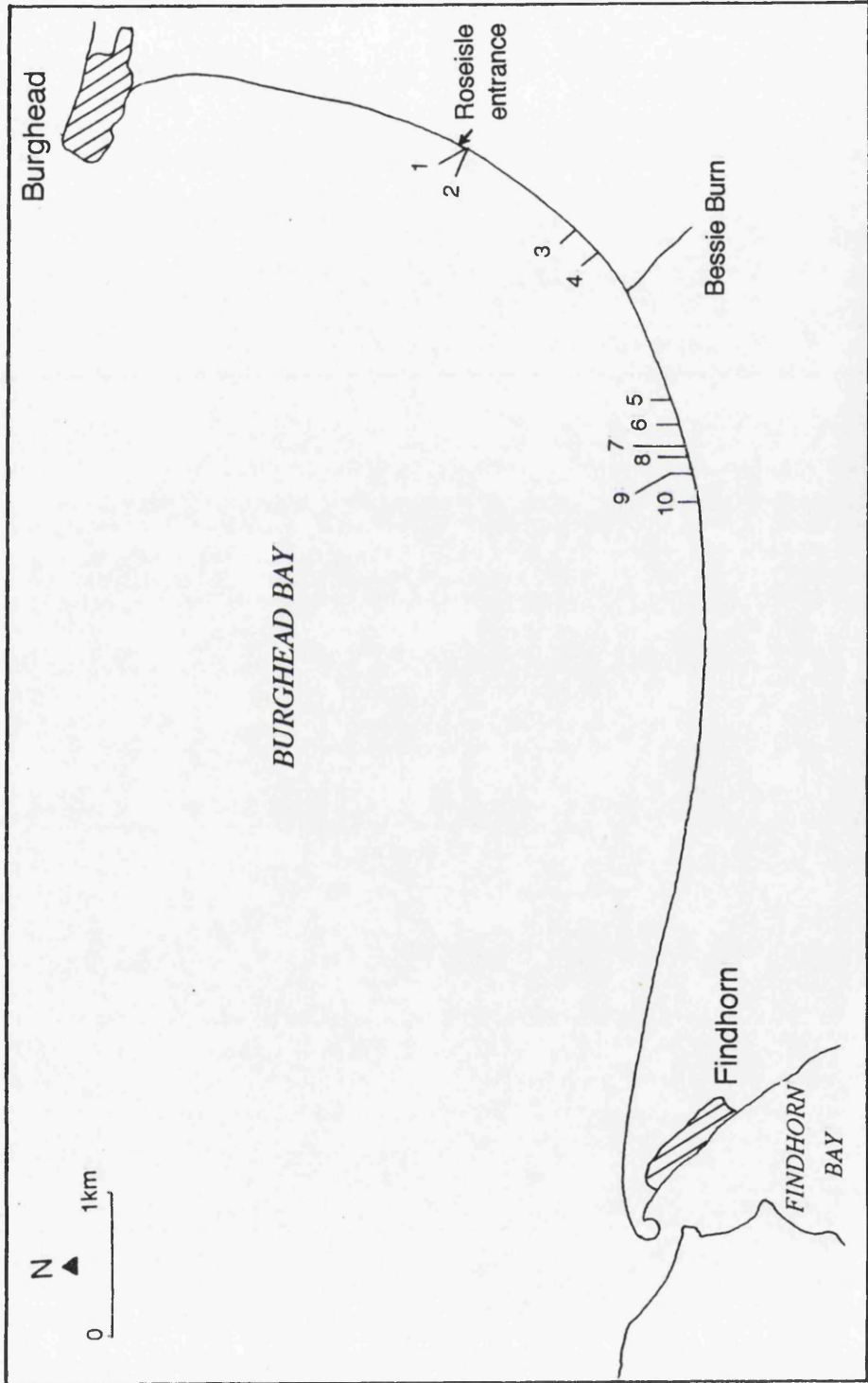


Figure 4.16 Clast sampling locations in Burghead Bay

Site	Vector magnitude (L) (%)	Site	Vector magnitude (L) (%)
1	39.8	6	53.9
2	39.5	7	73.7
3	67.5	8	56.0
4	70.3	9	78.6
5	62.6	10	45.2

Table 4.6 Burghead Bay raised shingle deposits: vector magnitudes

The strength of the fabrics displayed is generally intermediate. Only sites 3 and 9 display a strong cluster of orientations around the dominant vector, and all of the fabrics are bimodal with the exception of site 1, which displays a very weak fabric.

A tangent drawn along the section length in Burghead Bay produces an angle of  $050^\circ$ , suggesting a present shore-normal vector of  $310^\circ$ . This value lies well within the envelope of values produced from sites 3-8, suggesting that the orientation of the clasts within this section of the cliff may have been produced on a beach lying sub-parallel to the tangent described along the contemporary beach.

While the relict beach deposits appear to mirror the alignment of the tangent of the present beach, the deposits display little variation in the dominant vector along the length of exposure. The deposits on the contemporary beach, however, would be expected to display a gradual change in vector alignment around the Bay. In the south the clasts will display a northerly aspect to the dominant vector, which would be replaced with a more westerly aspect with distance north. This suggested that the relict beach deposits represent a formerly straight section of beach which extended at a tangent to the present coastline towards the southern lowlands south of the Burghead promontary. The curvature of the present beach appears to be a recent or historical aspect of coastal change in Burghead Bay (Chapter 5). This theory is supported by a map of the

raised shingle ridges in Burghead Bay (Steers, 1937), which also follow this straighter trend (Figure 4.11).

#### **4.1.3.13 Raised foreshore deposits of Burghead Bay: Bessie Burn section**

While the deposits logged in the cliff section revealed the alongshore variation in sedimentary environments in Burghead Bay, in order to fully understand the relationships between the individual sedimentary units present, a section running normal to the present coastline was required. The small incision formed by Bessie Burn provided an ideal stream section in which to study such relationships. Bessie Burn meets the beach at NJ 097653, and provides a section 271m long. A plan view of the section is shown in Figure 4.17, and consists of two coast-parallel relict shingle storm ridges 171 m apart enclosing a suite of fine-grained sediments in the intervening ridge slack. Inland from the landward of the two shingle ridges the sediments in the stream section are composed entirely of aeolian sand. Additionally, shingle is found at a much shallower depth in this area, with less opportunity for the subsequent deposition of fine grained sediments. Attempts to remove the upper sections of the sand cover with a gravel corer reached the water table at approximately 1 m depth, below which no further details could be recorded.

The section was again reconstructed as a section diagram, this being considered the most accurate method of recording in the light of the data collected from the fronting coastal section along Burghead Bay. The section began at the landward shingle ridge, which was at 31 m wide in section. The crest of the ridge has been flattened slightly by the passage of an access track, and is located at 3.68 m OD. The shingle ridge is overlapped on the seaward side by aeolian sand, which provides continuous cover for 100 m where it reaches a maximum thickness of 1.80 m. Below the sand at this point is a black, clayey peat unit. The peat is 0.10 m thick and contains *Phragmites* stems. At a point 26 m further seawards the peat thickens considerably, and the stratigraphic relationships are displayed in Figure 4.18. The peat is divided into two units, a lower, thicker bed of black, clayey peat 0.90 m thick containing both *Phragmites* and remains of whole branches. The base of the lower peat is located at 1.67 m OD, overlying a layer of stiff, blue-grey clay with a low silt content. A sample of the peat at the basal contact was submitted for radiocarbon assay, and produced a date of 3170±40 BP (SRR 4678).

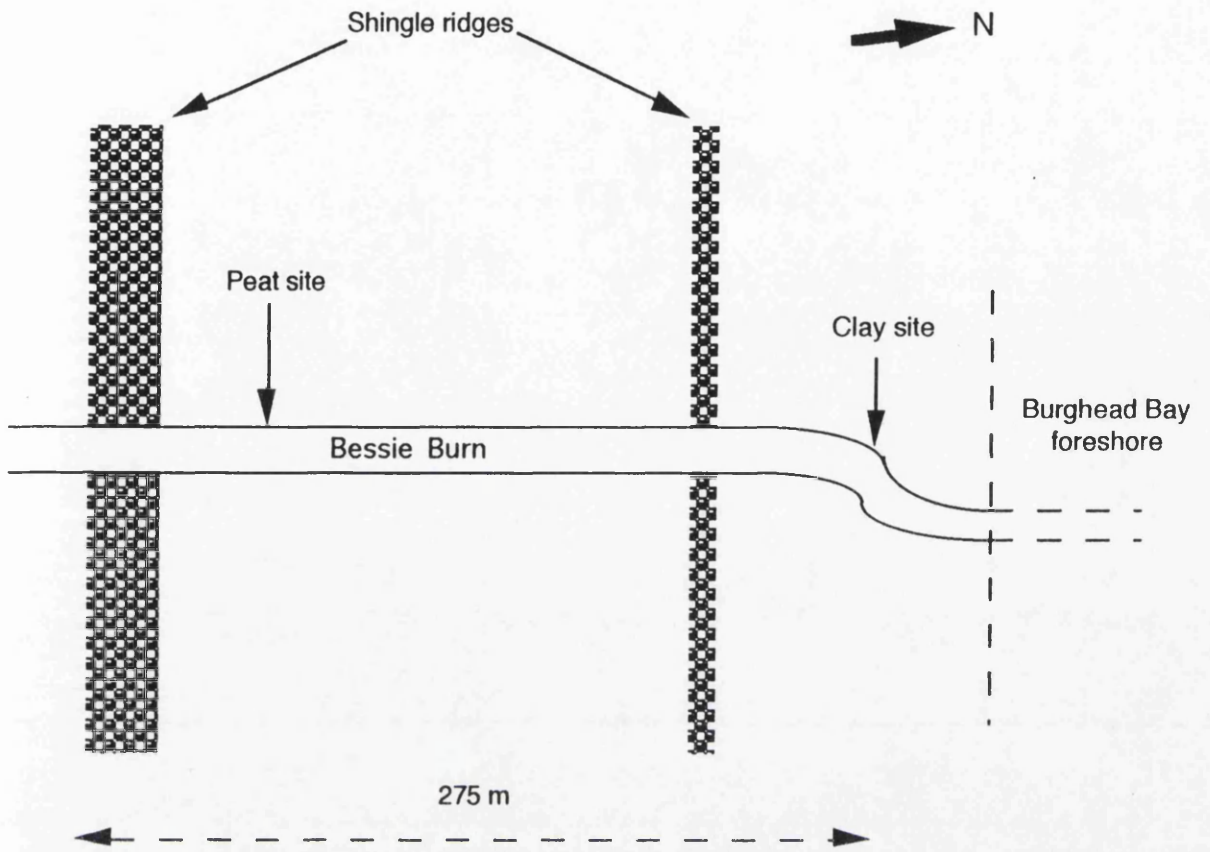
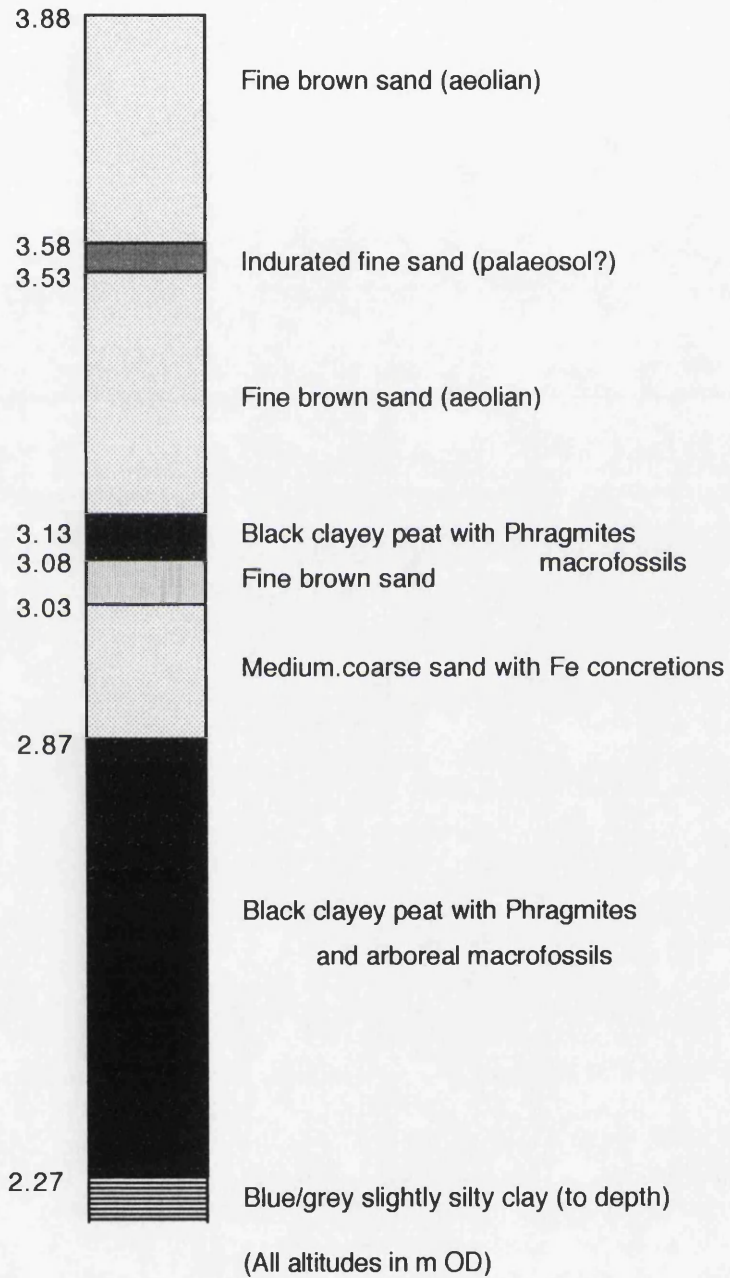


Figure 4.17 Plan of the Bessie Burn site

Figure 4.18 Stratigraphic log from Bessie Burn



Overlying the peat is a medium/coarse sand 0.16 m thick displaying heavy iron staining and iron-rich solid nodules. At the top of this unit is a thin (0.05 m) layer of fine brown sand, which in turn underlies a second, thinner peat. The base of this bed is at 3.08 m OD, and is composed of a black, clayey peat similar to the lower peat. This unit is only 0.07 m thick, and is covered by 0.75 m of aeolian sand.

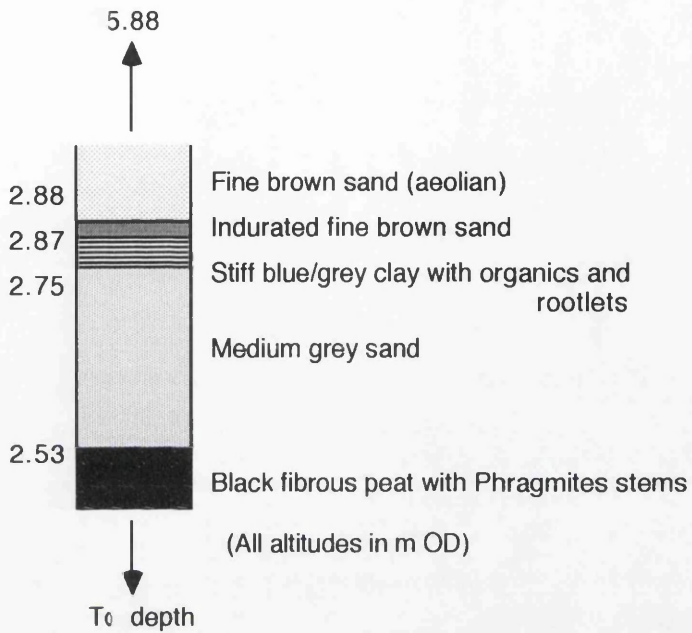
Seawards of this site the upper peat tapers out completely, and by 29 m from the site the clay content of the lower peat increases until the bed resembles an organic-rich dark brown clay with rootlets present. At a point 16 m further seawards, the fine-grained deposits are replaced by a second relict shingle ridge. This ridge is much narrower than the first, with a maximum width of only 4 m. The crest has also been flattened slightly by the construction of a track, and reaches 3.07 m OD. The landward edge of the ridge forms an abrupt ramp of shingle against which the clay layer overlaps slightly, suggested by a slight rise in altitude at the base of the clay to 2.87 m OD.

Seawards of this shingle ridge the deposits become increasingly sandy, with occasional stringers of shingle with 'b' axis lengths up to 0.05 m. These units probably represent the interbedded sands and shingle noted in the fronting cliff section in this area. However, a change in the sedimentary characteristics occurs 69 m seawards of the second shingle ridge at the point where the Burn meets the beach. Figure 4.19 demonstrates the relationships observed at this site. A black, clayey basal peat layer at least 0.60 m thick outcrops at the stream surface, again resembling the peat units located between the shingle ridges. The base of the peat is located at 2.21 m OD. Overlying the peat bed, 0.22 m of grey-brown sand grades up into a stiff blue-grey clay with a low organic content and some rootlet penetration. The base of the clay is at 2.75 m OD. The clay is capped in turn by 2.5 m of aeolian sand with a thin layer of organic rich medium-grained sand at the base overlying the clay. Seawards of this sequence the section was obscured by aeolian sand deposits, which prevented interpretation of the relationship between this area of fine-grained deposits and the fronting raised beach deposits.

#### **4.1.3.14 Summary**

The exposure created by the sweep of Burghead Bay sectioned two shingle storm ridges, two peat-filled hollows and a series of intercalated sand and shingle deposits. This allowed an investigation into the internal structure of the shingle ridges, and also the relationship between the shingle ridges and the

Figure 4.19 Stratigraphic log from Bessie Burn



associated sand deposits. Radiocarbon dates from the peat hollows provided a minimum date for the emplacement of the ridges adjacent to them, demonstrating the onset of peat formation between 3140±45 BP and 2900±45 BP. The section incised by Bessie Burn traversed two shingle ridges, with a peat unit formed in the swale between them. This produced a date of 3170±40 BP. In combination with the two dates above, these dates bracket the onset of peat formation, and hence provide a minimum age of the surrounding shingle ridges, to ca. 3170-2900 BP.

Sectioning of raised shoreline deposits along Burghead Bay allowed a detailed examination of the stratigraphic relationships between the deposits. In the absence of similar exposures at Culbin, this proves useful in understanding the spatial relationships between the deposits, both in a shore-parallel and a shore-normal fashion. The sectioning of the shingle ridges in Burghead bay also provide a useful insight into the internal structure of these features which is not possible at Culbin.

#### **4.1.4 Relative sea level history of the Culbin area**

Having collected datable material in association with a variety of former foreshore and marine deposits, it was possible to examine the altitude/age relationships between these sea level indicators, and then to extend the comparison to other dated indicators from the Beaully and Dornoch Firths. This allowed a picture of regional RSL trends to be constructed, bearing in mind constraints on comparisons of altitude based on differential isostatic response and with distance along the southern Firth.

The reconstruction of a RSL history for Culbin was achieved through the use of datable material, primarily peat, recovered from a range of altitudes between ca. -2 m and 9 m OD. Peat samples represent minimum ages for the abandonment of their related landforms since there may be a lag prior to colonization. As such, the dates are calibrated with dated sea level events from the inner Moray and Dornoch Firths in order to establish a common regional sea level history for the middle/inner Moray Firth. Finally, the established series of sea level trends in conjunction with a modern analogue study from The Bar are used to calibrate a series of sea level events interpreted from the inland shingle ridge suite at Culbin.

Samples of datable material were collected from various locations in Culbin and Burghead Bay. A total of 13 samples were submitted for radiocarbon assay (Table 4.7). Further details including sample locations are shown in Appendix 10.

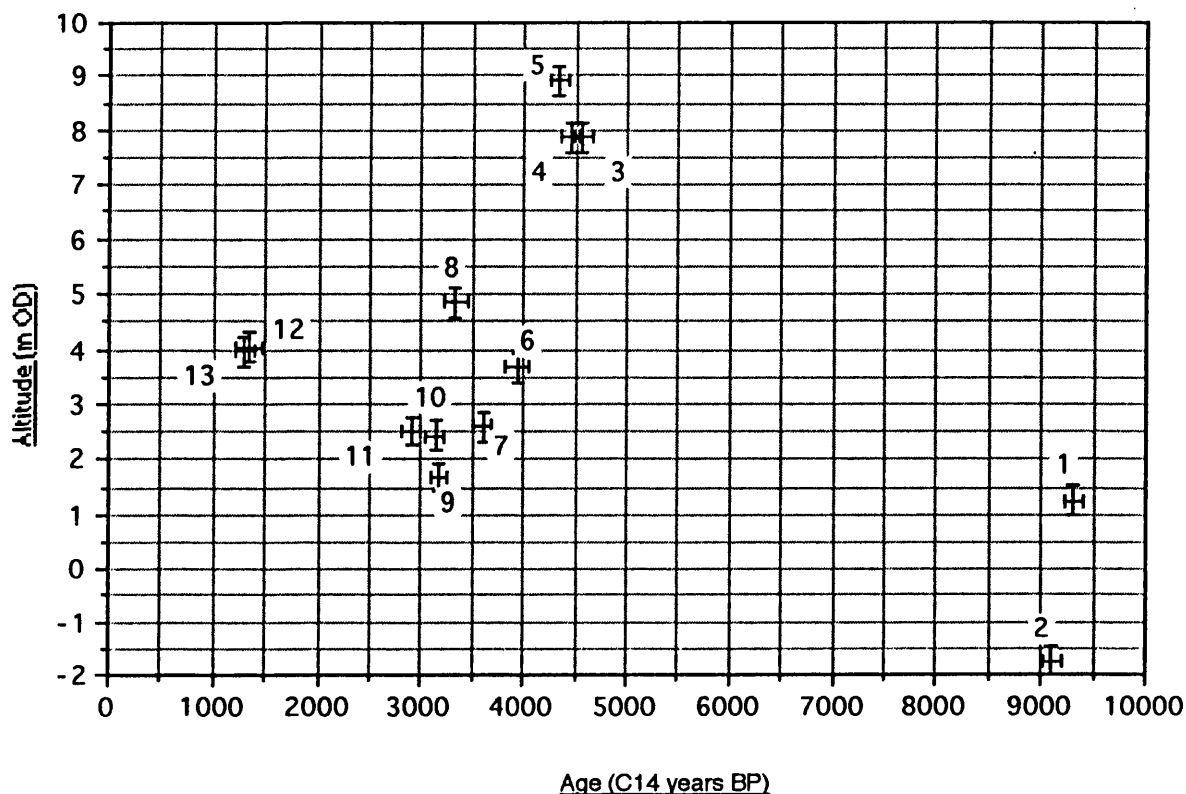
Peat samples SRR-4680 and SRR-4682 were obtained from positions within shingle ridge sequences in Burghead Bay, and SRR-4683 was collected overlying a shingle ridge at the base of the raised cliffline at Snab of Moy farm adjacent to Culbin Forest. These samples were collected in order to provide a test of the accuracy of applying a shingle ridge correction factor to dated shingle RSL indicators based upon the altitude of the ridge crest (section 4.1.4.1).

The samples were plotted on time/altitude axes as shown in Figure 4.20. This shows the samples plotted with error bars at 2 standard deviations about the mean along the age axis, and the individual altitudinal error factor. This plot shows the data in its raw form, excluding the correction factors which may be applied due to the altitude of the samples obtained from shingle ridges in Burghead Bay.

Plotting sea level indicators has proved a contentious issue over the past decade, but has finally become a reasonably standardised procedure in Britain. The approach used in this chapter is that employed by Kidson (1982), who advocated the use of error bars denoting the age of each individual sample to within 2-3 standard deviations about the mean, and error bars indicating the degree of uncertainty in the altitude of the sample. As such, the plot of sea level indicators from the Moray lowlands is not a curve in the accepted sense, the use of a single line implying an unattainable accuracy. Sea level indicators of the type collected in this study can only be crude indicators of the level of the sea at the time of formation, and thus the plot in Figure 4.20 represents the maximum possible errors. If a coherent picture can be drawn from such a source, then the exercise has been successful.

The trends displayed by the sea level indicators from the Culbin area broadly follow the trends in the curve from the Dornoch Firth (Figure 4.21), as was expected given their similar position on the 7 m Postglacial isobase (Price, 1983). The two low altitude peat dates, if *in situ*, display a time transgressive regressive contact. The landward peat (at 1.24 m OD) provides a date of  $9305 \pm 45$  BP, while seawards of this the intertidal peat from Burghead Bay at -1.75m OD is dated to  $9105 \pm 45$  BP. The stratigraphic evidence from beneath RAF Kinloss is sufficiently strong to suggest that these samples were part of a continuous single unit extending from the lowlands at the head of Findhorn Bay

## Sea level indicators from Culbin and Burghead Bay (uncorrected altitudes)



Sample number codes correspond to the following key:

- |                       |                        |
|-----------------------|------------------------|
| 1. 9305±45 (SRR 4689) | 8. 3330±60 (SRR 4684)  |
| 2. 9105±45 (SRR 4677) | 9. 3170±40 (SRR 4678)  |
| 3. 4570±45 (SRR 4687) | 10. 3140±45 (SRR 4679) |
| 4. 4450±45 (SRR 4686) | 11. 2900±45 (SRR 4681) |
| 5. 4335±45 (SRR 4683) | 12. 1340±65 (SRR 4682) |
| 6. 3935±55 (SRR 4688) | 13. 1300±45 (SRR 4680) |
| 7. 3600±45 (SRR 4685) |                        |

Figure 4.20

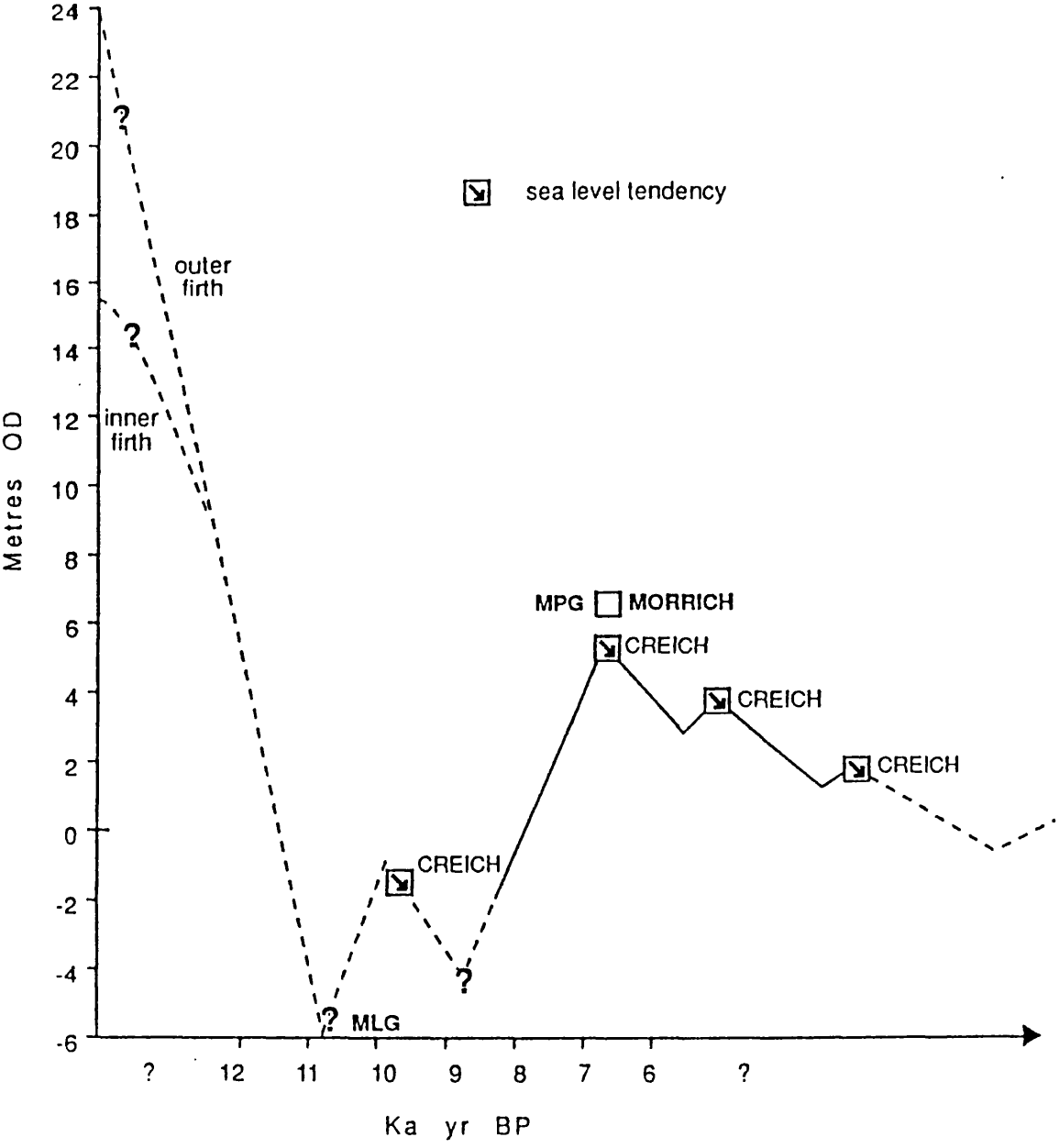


Figure 4.21 Relative sea level trends in the Dornoch Firth (source: Hansom & Leafe, 1990)

out into Burghead Bay. However, the vertical range which separates these two samples is not sufficient to differentiate between them.

The next youngest dated indicators are from the raised cliffline at Snab of Moy farm, a significant distance inland. The peat dates obtained provide only minimum ages for the abandonment of the shingle ridge and the fronting deposits at the foot of the cliff, and are likely to be too young to be taken as representative sea level indicators. This is apparent from the sea level diagram in Figure 4.20. Samples SRR 4684 & 4688 collected from the ponds at Snab of Moy similarly display dates suggesting minimum ages for the development of the ponds as back-beach depressions formed in the lee of the shingle ridge complex.

The basal peat unit from pond 3 at Snab of Moy (SRR 4685) appears to fit the trend of the RSL movements indicated in the Dornoch Firth, with a date of  $3600\pm 45$  from an altitude of 2.58 m OD overlying shingle, which from air photographs can be seen to form part of the fan section of the Culbin shingle ridges. However, the reversal in dates provided by the middle peat (SRR 4688) of  $3935\pm 55$  at 3.67 m OD suggests either that one of the samples is in error, or that the samples are allochthonous. The young date from this peat at such a distance inland also suggests that the date represents a minimum age, and may be only indirectly related to RSL movements in the area.

Samples SRR 4679 and 4681 were collected from positions between shingle ridges in Burghead Bay. Their relationship with the surrounding ridges was, however, carefully scrutinized, and examination of the composite log section reveals that the two sites do not appear to have been influenced by the proximity of the ridges. The two sites provided dates of  $3140\pm 45$  and  $2900\pm 45$  respectively from altitudes of 2.43 m OD and 2.51 m OD. Their appearance in the field suggests that they represent infilled lochans or stream beds, whose beds graded to a RSL slightly higher than that of present.

SRR 4678 was also obtained from a position between two shingle ridges at 1.67 m OD. The date of  $3170\pm 40$  BP is again broadly in line with a falling RSL trend after the peak of the Holocene sea level maximum, and the position of the sample adjacent to two shingle ridges appears not to have affected the altitude/age relationship of the sample to any great degree.

#### **4.1.4.1 Correction factors applied for shingle ridge altitude**

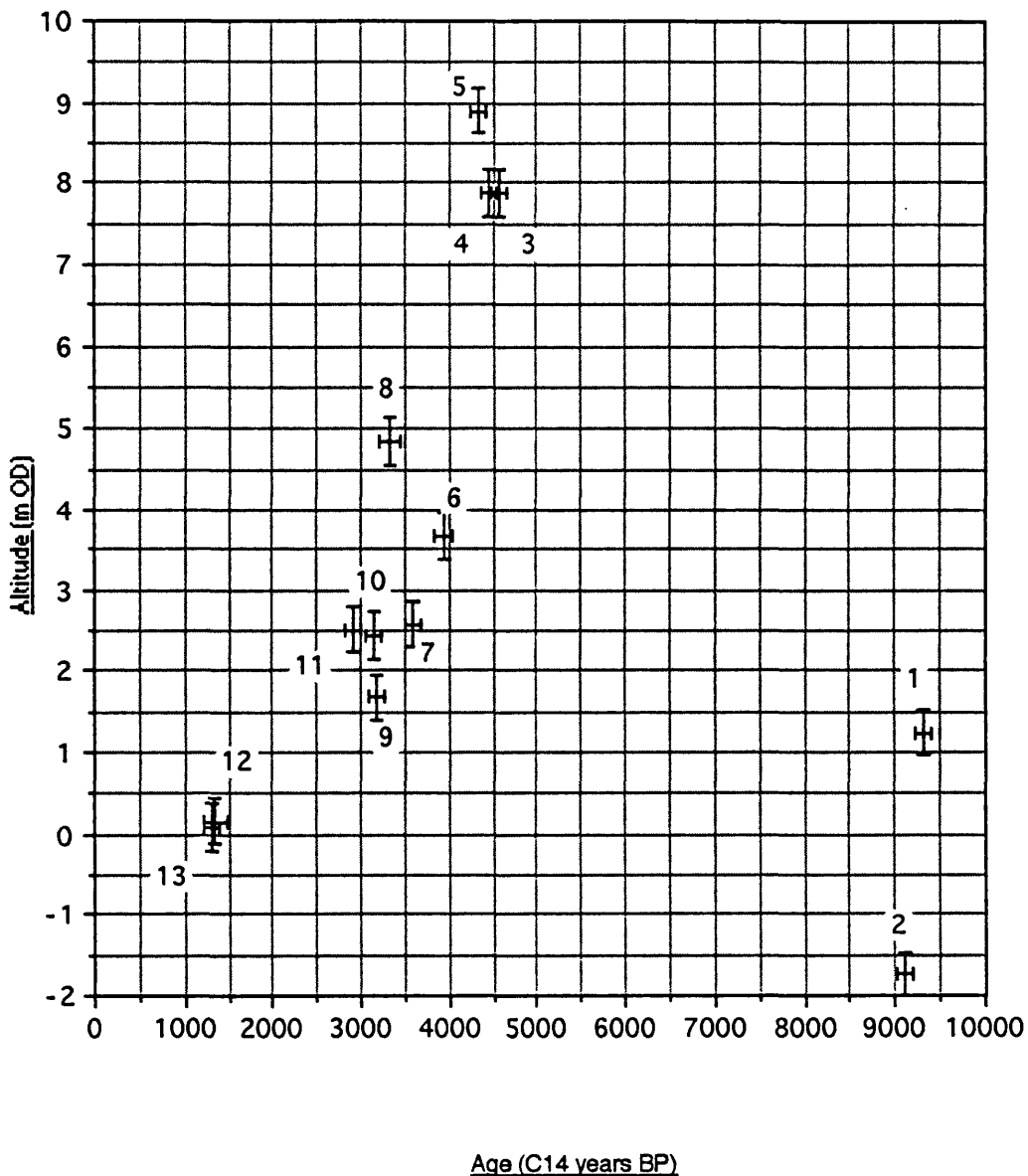
The use of correction factors to reduce the altitude of sea level indicators to a common datum has been reported from earlier studies (Sollid *et al.*, 1973; Møller, 1990). Correction factors were applied to samples obtained from positions on or between shingle ridges in Burghead Bay. The correction factor was calculated to be 3.17 m OD, the mean height of the contemporary shingle ridges found on The Bar at present. In order to correct the altitudes of the adjacent ridges, this value was subtracted from all ridge altitudes. The corrected sea level indicator trend is shown in Figure 4.22. Sample SRR 4683 still appears to be at a higher altitude than would be expected from its age, adding further weight to the argument that the date represents a minimum age of the sample, as would be expected from a peat date. The application of this correction factor to samples SRR 4680 & 4682, collected from locations within shingle ridges in Burghead Bay, provided more satisfactory results (Figure 4.22). The samples fall close to a possible best fit correlation line applied to the data on the falling limb of the curve. Sample SRR 4678 was the only other sample associated directly with a shingle ridge. The altitude of this sample was considerably lower than its age suggested. However, the sample was located in an inter-ridge trough, and so its altitude is unlikely to relate to the altitude of the surrounding shingle ridge crests which were being tested in this analysis as possible sea level indicators. As such, the low altitude of this peat was not unexpected considering its location, and the inclusion of this sample in the testing of the applicability of shingle ridge correction factors was discounted.

Only two of the possible three dated samples obtained from locations within the shingle ridge system were found to be appropriate for testing the shingle ridge correction factor. These two samples were obtained from within shingle ridges in Burghead Bay, and in order to test their applicability further, the correction factor was then applied to the shingle ridge system at Culbin itself.

#### **4.1.4.2 Application of the sea level curve to the shingle ridges at Culbin**

The aim of this section is to establish whether the observed trends in the altitude of the shingle ridge sequence match trends in the sea level history of this section of the Moray Firth.

**Figure 4.22 Sea level indicators from Culbin and Burghead Bay (corrected altitudes)**



Sample number codes correspond to the following key:

- |                       |                        |
|-----------------------|------------------------|
| 1. 9305±45 (SRR 4689) | 8. 3330±60 (SRR 4684)  |
| 2. 9105±45 (SRR 4677) | 9. 3170±40 (SRR 4678)  |
| 3. 4570±45 (SRR 4687) | 10. 3140±45 (SRR 4679) |
| 4. 4450±45 (SRR 4686) | 11. 2900±45 (SRR 4681) |
| 5. 4335±45 (SRR 4683) | 12. 1340±65 (SRR 4682) |
| 6. 3935±55 (SRR 4688) | 13. 1300±45 (SRR 4680) |
| 7. 3600±45 (SRR 4685) |                        |

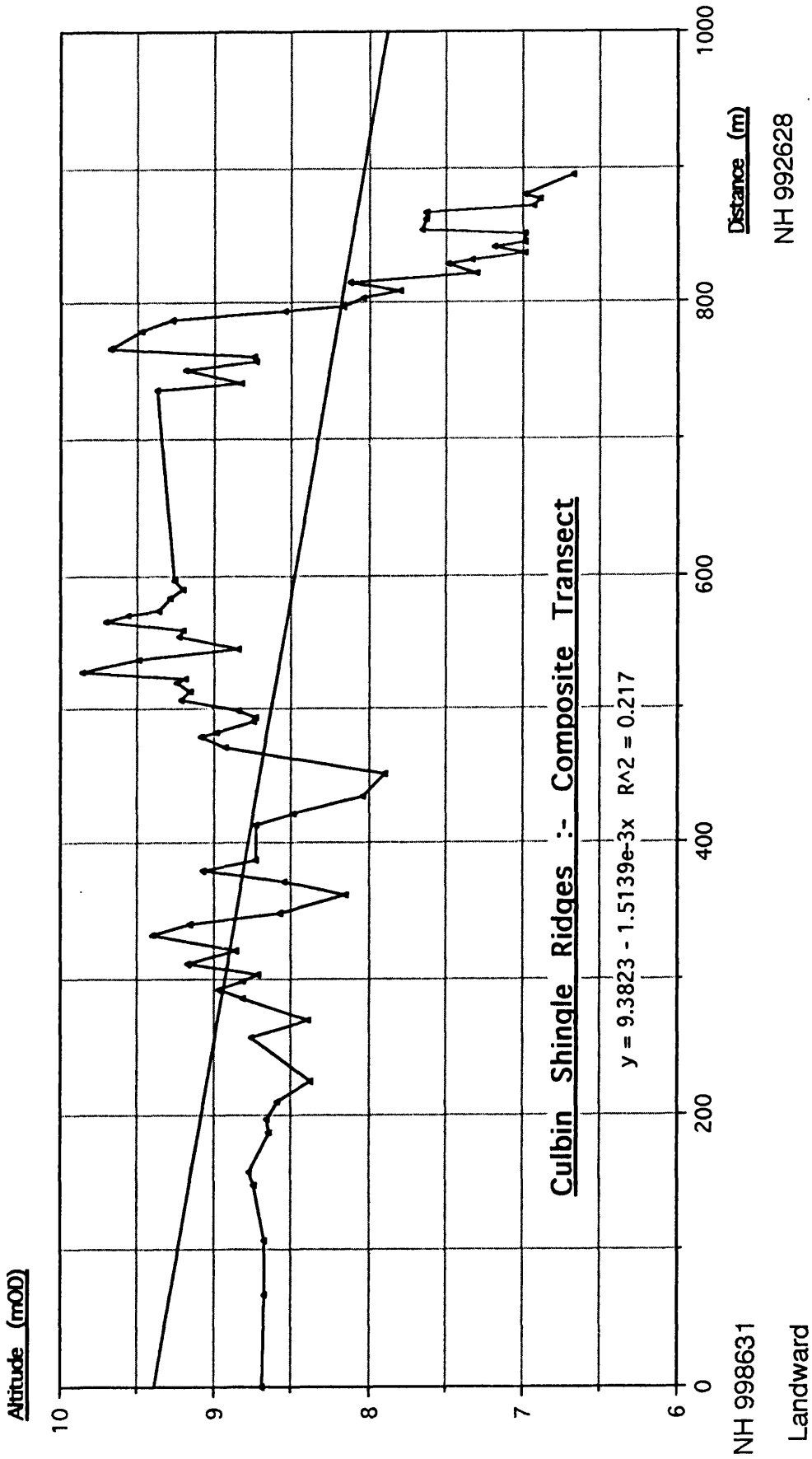
Having established a tentative relationship between the corrected altitude of the shingle ridge crests in Burghead Bay and an approximate RSL trend, a method was then used to test the correction factor on the more extensive shingle ridge system at Culbin. Altitudes of the raised shingle ridges found at Culbin are in the range 3.58-10.45 m OD at the eastern set of ridges (R, S, T), 5.15-9.86 m OD in the western set (A, B, C, D) and 4.68-10.99 m OD in the central set (X, Y, Z) .

The altitudinal relationships between both the individual shingle ridges and their composite units are important. To understand these more fully, a series of distance/altitude plots were constructed. These plots used the groupings of shingle ridges located in the field, and thus are equal in neither number nor spatial coverage. The first stage in such a task involves the identification of observed trends in the altitudes of the shingle ridges measured in Culbin.

From initial survey work it became apparent that the altitude of the shingle ridges is maintained seawards for a considerable distance before falling at a noticeable gradient in a staircase-like sequence of ridges. By fitting the sequences of ridges surveyed in transects A and B together, a composite transect was produced which represents the maximum surficial exposure of shingle ridges. The distance between the end of transect A and the start of transect B is 430 m. The composite transect produced is shown in Figure 4.23.

The total altitudinal trend displayed by the ridges shows a simple regression line fitted to all points (Figure 4.23). While the fit of the curve was not expected to be good ( $R^2 = 0.217$ ), the regression displays a falling trend seawards across the entire suite of ridges. This is no doubt aided by the distinct drop in altitude at the seaward end of the transect due to the inclusion of set D. While this relationship is of significance, it is not representative of the entire transect. Indeed, if set D is removed from the transect, the remaining groups of ridges show an altitudinal reversal, with a rising trend to seaward. The transect is thus subdivided into the original seven surveyed groups of ridges in order to determine whether any trends in altitude might be apparent at a smaller scale.

Once subdivided into these seven groups, each set of shingle ridges was plotted individually as a distance/altitude diagram, and a regression line fitted to the data. Once these regressions had been fitted, the end points were measured from the individual plots and replotted on the appropriate section of the composite log, providing an overview of the trends of subgroups within the overall composite framework.



NH 998631

Landward

Distance (m)

NH 992628

Seaward

Figure 4.23

The variable nature of the altitude of individual shingle ridge crests meant that it was necessary to provide a check on the regression trends identified by the plots of individual crest altitudes. Shingle ridge crest altitudes were grouped into subsets of two and three ridges, with the mean of each set taken and plotted against mean distance along the transect. If, as has been suggested, the altitude of individual shingle ridges is highly variable, then by using the mean value from a subset of ridge crests, then some of the variation ought to have been removed, or at least smoothed. Comparing the final result with the plots from the individual ridge crest altitudes highlights the possible limitations of using individual ridge crests as sea level indicators.

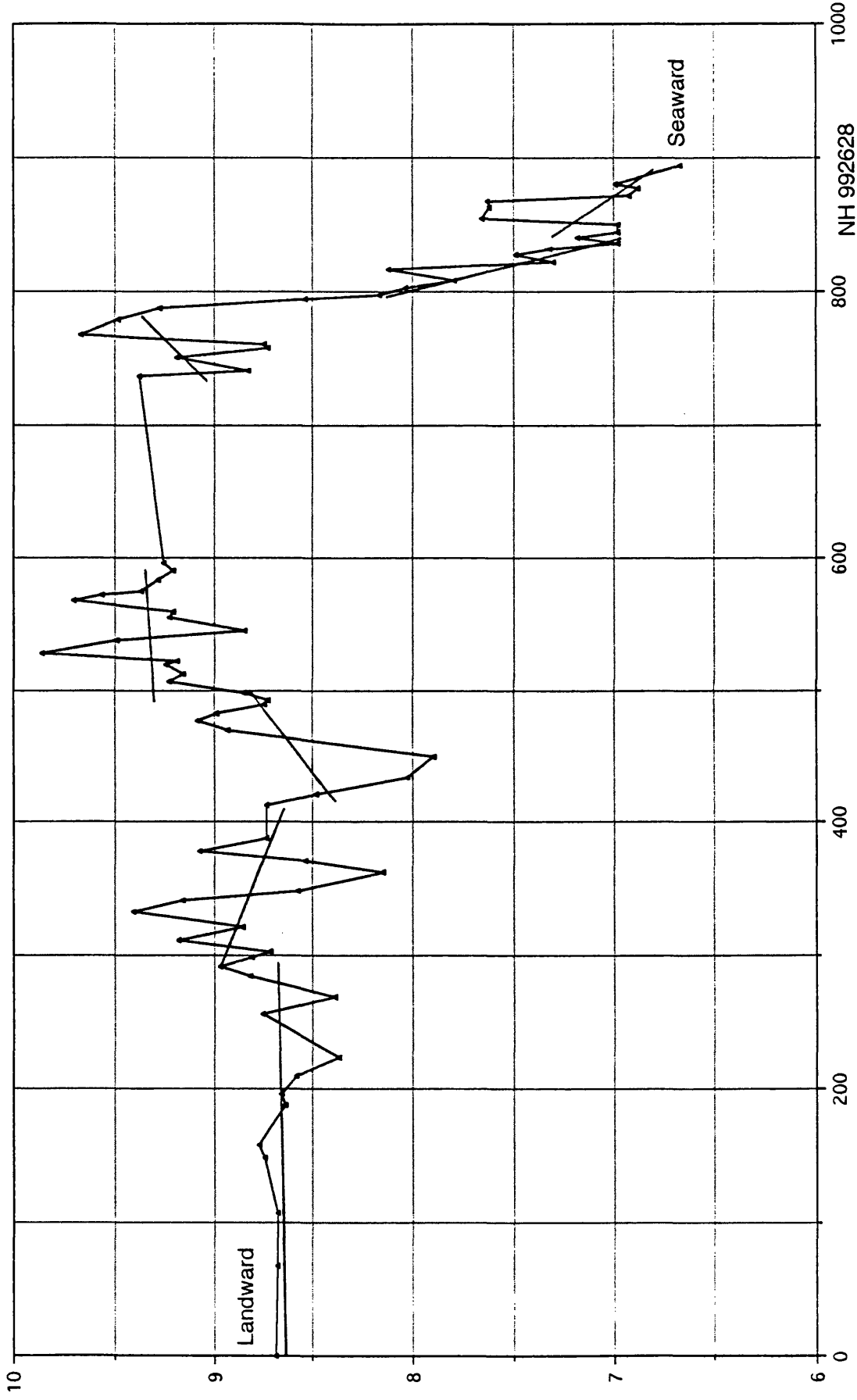
Regression lines were fitted to the plots of the two and three ridge subsets, and the end points of the regression lines once more transferred to a composite traverse plot. The results of this exercise are shown in Figures 4.24 and 4.25. The major point arising from inspection of these diagrams is that there is little difference between the regression trends in plots of one, two or three ridge mean crest altitudes. In only one group is there a suggestion of a reversal in the trend shown by the plot of single crest altitude rather than two or three ridge mean altitude against distance, this being in set C. The plot of single crest altitude against distance in set C demonstrates a rising trend, whilst two and three ridge mean altitude plots suggest a falling trend.

Long & Fox (1988) observed a drop in shingle ridge crest altitude with increasing curvature at Dungeness, although along the straight sections of the ridge series little altitudinal variation was observed (Lewis & Balchin, 1932). The composite transect produced at Culbin was noted from Figure 3.2 to cross a curved section of ridges. In order to provide a control over the altitudinal data produced from the Culbin ridges, two parallel transects were made to the east and west of transect A. The position of the control traverses is shown in Figure 3.3, and the results shown in Figures 4.26 and 4.27.

Transect C was made 70 m west of transect A (Figure 3.3), and the altitudinal relationships between the ridges in transect C and A are shown in Figure 4.26. The data shows a clear decline in altitude between transect A to transect C, whilst retaining the clear patterns of individual ridge relationships. The altitude of the highest ridge on transect C is 9.45 m OD compared to 9.86 m OD on transect A.

Figure 4.27 shows transect A plotted against transect D, which was located 50 m east of A. As transect D was located closer to the apex of the fan at this point, the

Altitude (mOD)

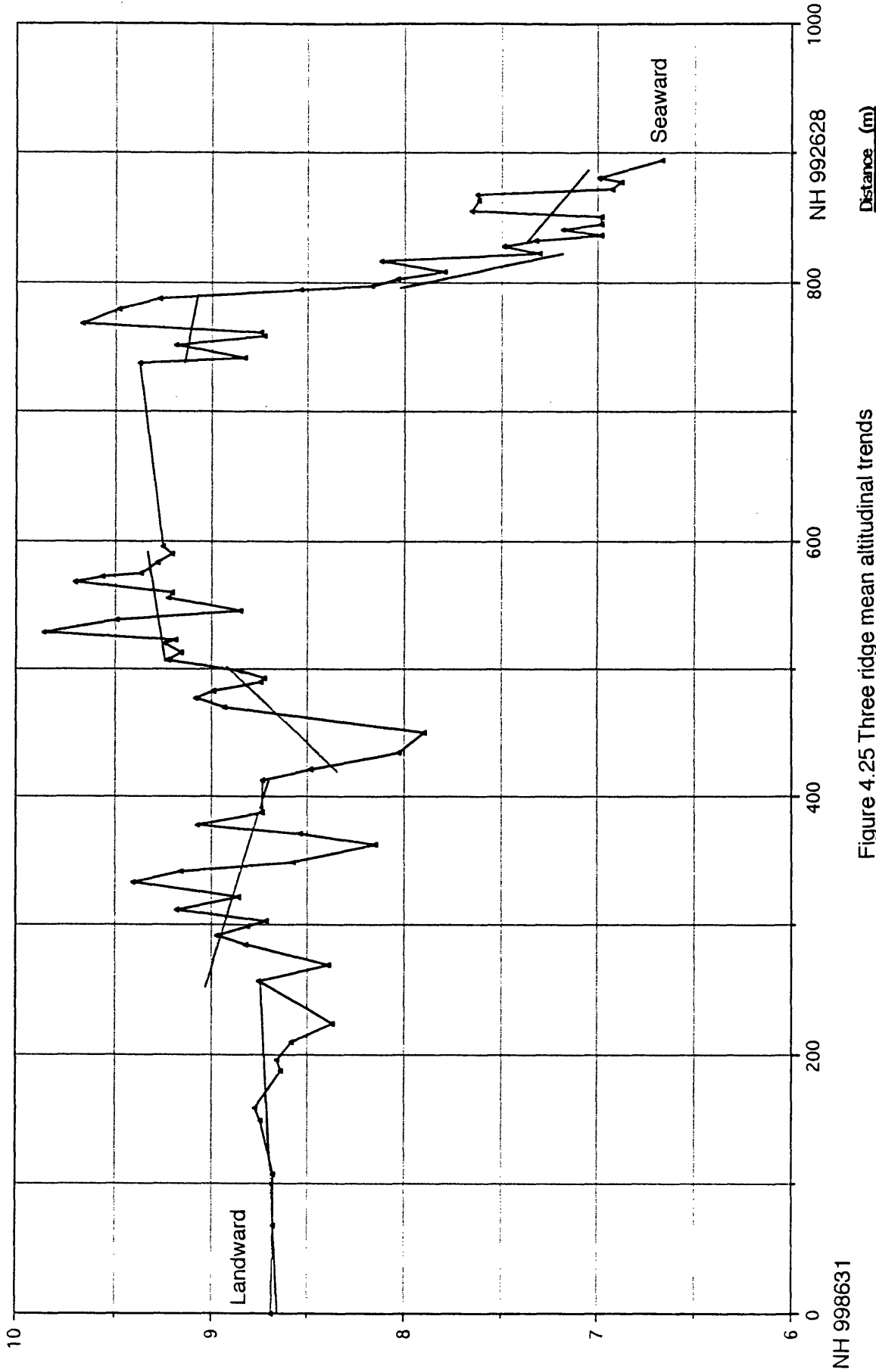


NH 998631

Figure 4.24 Paired ridge crest mean altitudinal trends

Distance (m)

Altitude (mOD)



NH 998631

Figure 4.25 Three ridge mean altitudinal trends

Control traverse C plotted against  
traverse A

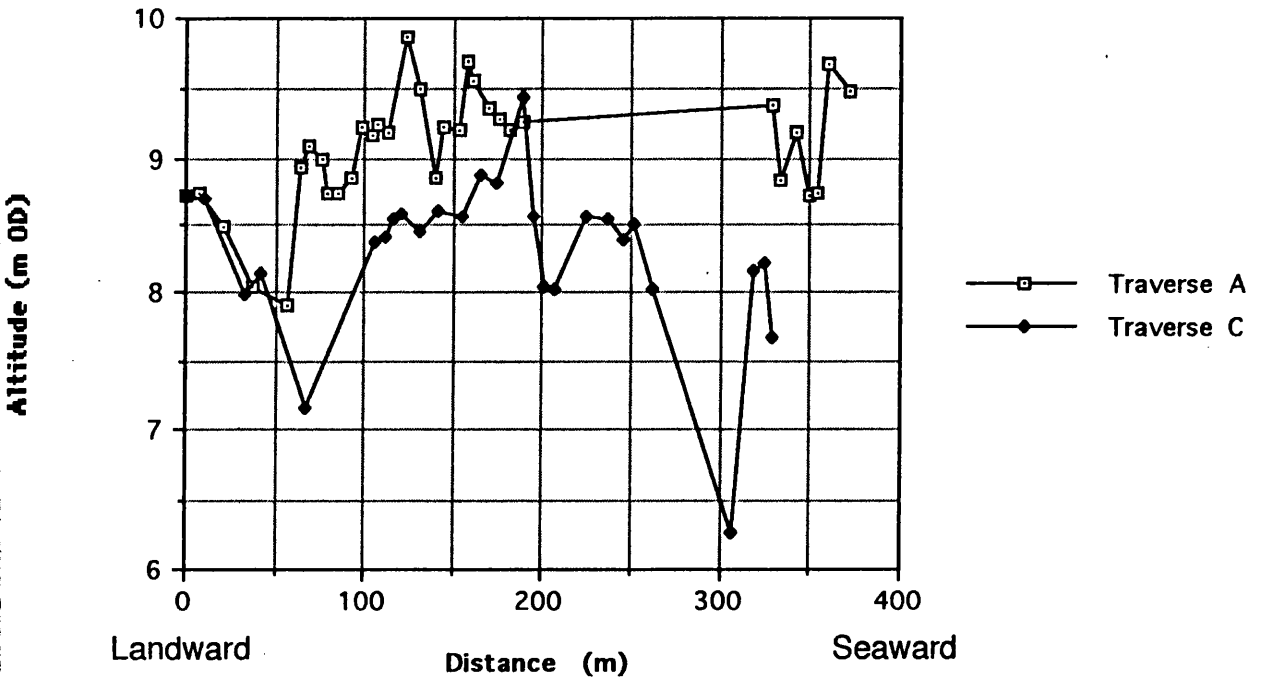


Figure 4.26

Control traverse D plotted against  
traverse A

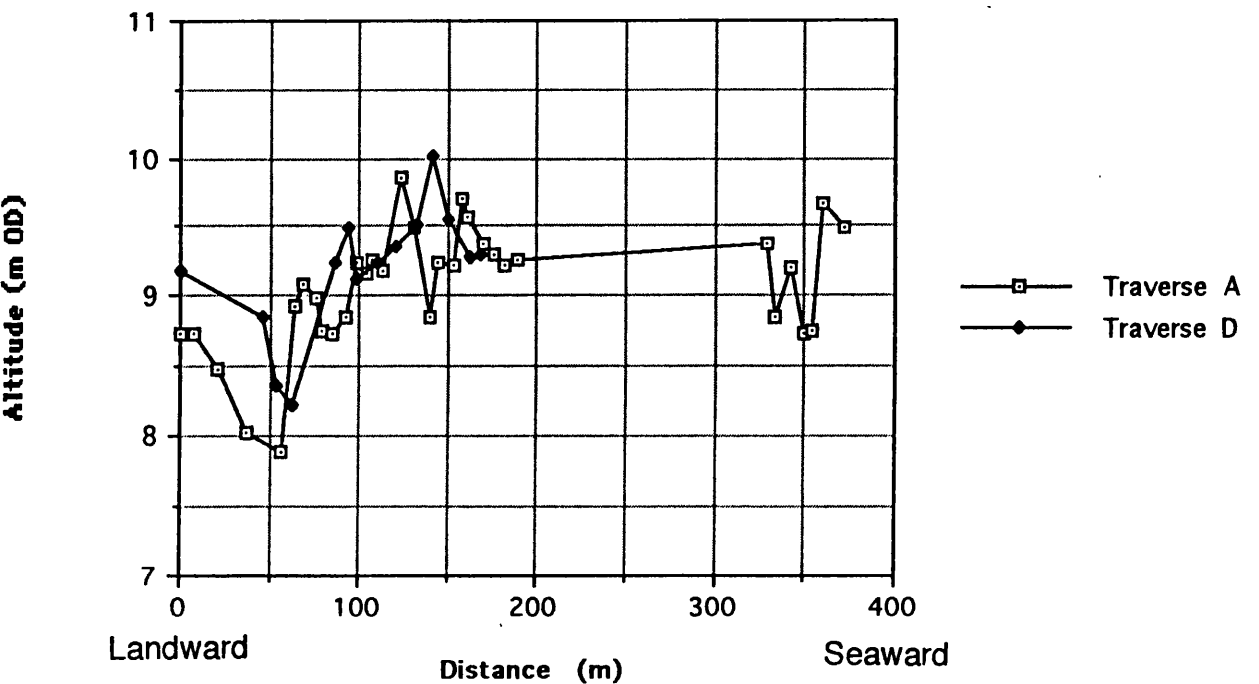


Figure 4.27

total transect length was shorter than transect A. It is clear from transect D that the gross pattern of shingle ridges is broadly the same as at A, with the high ridge in the centre of the transect at 10.01 m OD on transect D and at 9.86 m OD on transect A. Similarly the low ridge series at ca. 60m along each transect can be identified, the lowest ridge on transect D recorded at 8.22 m OD and on transect A at 7.89 m OD. Due to the non-coincidence of shingle ridge numbers, quantitative comparisons between the two ridge sets is not possible. It appears, however, that the altitude of the ridges along transect D are slightly higher than those on transect A.

It is clear from the data provided by these parallel transects that while the individual shingle ridge forms retain their *relative* relationships with each other internally, the altitude of the ridges tends to decline across the shingle fan towards the SW, i.e. downdrift. Based on the altitudinal relationships established between the two shingle ridges which were positively identified as linked at the three transect positions, gradients along the ridge crest were calculated. The high ridge displays a falling gradient of 4.6 m km<sup>-1</sup>, while the lower ridge displays a steeper gradient of 8.6 m km<sup>-1</sup> (Figure 4.28).

The decline in altitude appears to coincide with increasing curvature of the fan ridges in an increasingly southerly direction. In order to test whether this relationship occurs under present day conditions, traverses were made along the length of three distinct relict shingle ridges on The Bar. Additional control was provided by a longer traverse made along the length of the contemporary storm ridge on The Bar. The three ridges selected were at the eastern end of the exposed shingle ridge sequence on The Bar, with their eastern ends at ca. NH 926607. The eastern ends of these ridges had been truncated as the proximal end of the contemporary ridge began to re-align itself to the orientation of the erosional bight in the central zone of The Bar, eroding the eastward ends of the ridges immediately to landward. All three of the sampled ridges displayed a gentle southwards curve, which increased relatively abruptly with distance and ended in a recurve of variable radius and completeness. In contrast, the contemporary ridge crest was only slightly curved for the majority of the 1800 m length measured, but with a marked change in angle approximately mid-way along its length (at NH 916600).

Surveying along the length of two of the relict ridges on The Bar demonstrates that two of the crests remain level for a minimum distance of 310 m, before a drop in altitude of up to 1.5 m is recorded relative to the starting position. The

Falling altitude with increasing curvature:  
shingle fan, Culbin forest.

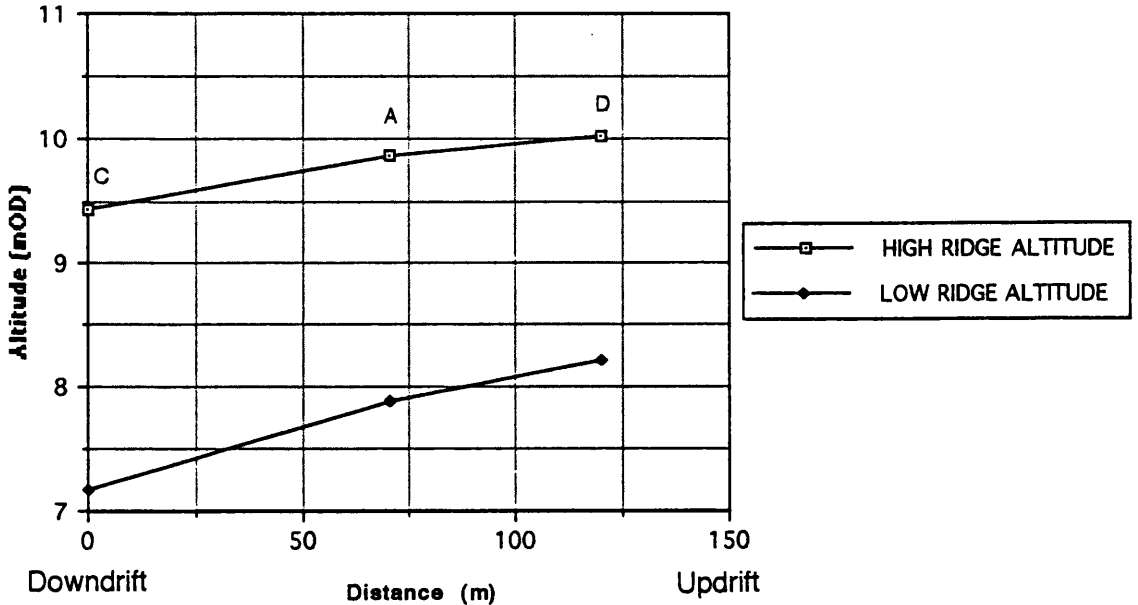


Figure 4.28

third ridge displays a rise in altitude with increasing curvature, to a maximum of 1.1 m above the starting position. Simultaneous control is maintained on the alignment of the shingle ridge crests, and it is found that once the crest azimuth falls below *ca.* 045° then the altitude of the ridge no longer remained constant. The crest of the contemporary shingle ridge, while not disproving this hypothesis, displays a maximum vertical discrepancy along its length of 0.87 m, and actually displays a net rise in altitude over the surveyed length from 3.14 m OD at the eastern end (NH 926607) to 3.27 m OD at the western end (NH 915598).

It is thus established that the altitudes of the shingle ridges tend to remain at a constant altitude within a given error band (0.87 m), provided a critical azimuth angle is not exceeded, and that the relationships between the individual ridges remain constant. However, once the azimuth of the shingle ridge crest exceeds a critical angle, in this case 045°, then altitude begins to decline. This effectively discounts the shingle ridges used in the fan traverses from an analysis of RSL trends encountered at Culbin, leaving two remaining sets of shingle ridges (the eastern [R, S, T] and central [X, Y, Z] sets) for analysis. Of these, the central set (Figure 4.29) most closely matched the azimuth of the shingle ridges found on The Bar.

An altitude/distance plot of the shingle ridges in the central set of shingle ridge crest altitudes (Figure 4.29) shows that there is little difference between plotting best fit lines onto individual ridge crest altitude or the paired or three-ridge mean crest altitude. Owing to the lower number of ridges in the central suite ( $n=8$ ), individual ridge crests only were plotted. The transect produced is also shown in Figure 4.29. Interference by overlying sand meant that some shingle ridges were probably excluded from the traverse, but the general trend of a high set of ridges falling abruptly to a lower plateau can be seen. A similar trend is observed on the eastern transect (Figure 4.29).

The declining limb of the RSL diagram of the Moray Firth post-dating the Holocene sea level maximum (Figure 4.22) displays an curvilinear form. Andrews (1987), Shennan (1989a) and Dawson (1992) suggested that the form of RSL trends at this time would be exponential or smoothly falling, reflecting a gradual decline in the rate of isostatic uplift as the state of residual rebound was approached. Using the composite Moray Firth sea level curve (Figure 4.30), an exponential function was fitted to the data for the falling limb of the Holocene sea level maximum only, as this represented the RSL trend occurring during which these deposits were emplaced. The fitted curve is shown in Figure 4.31. It is

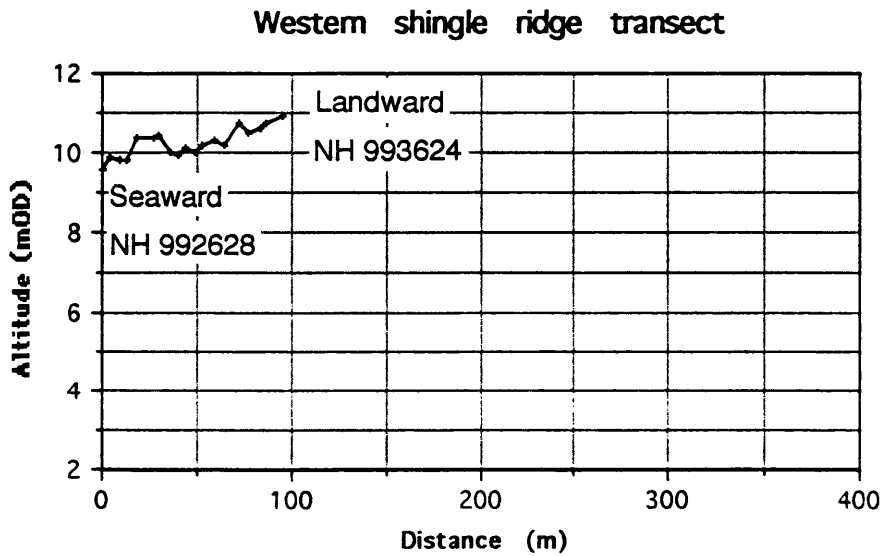
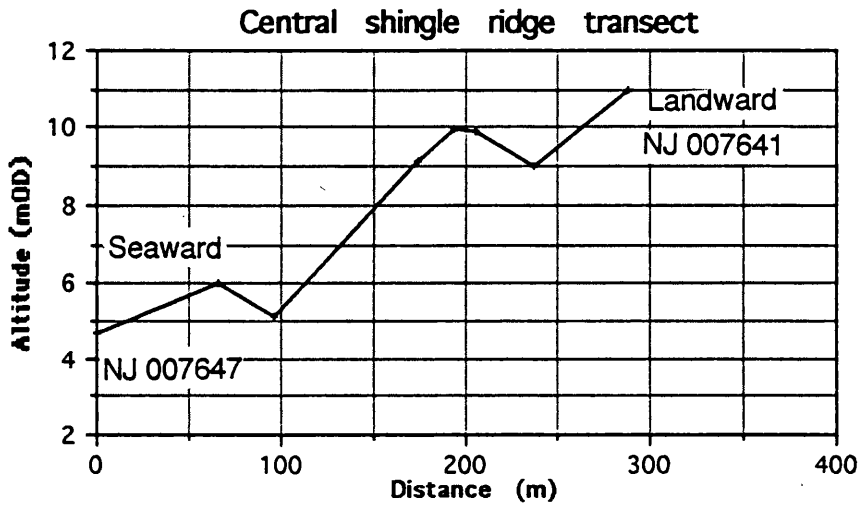
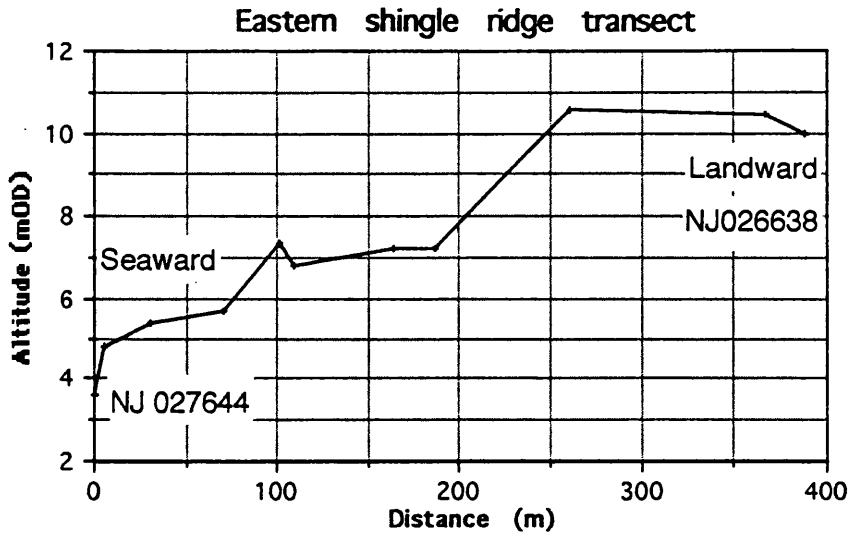
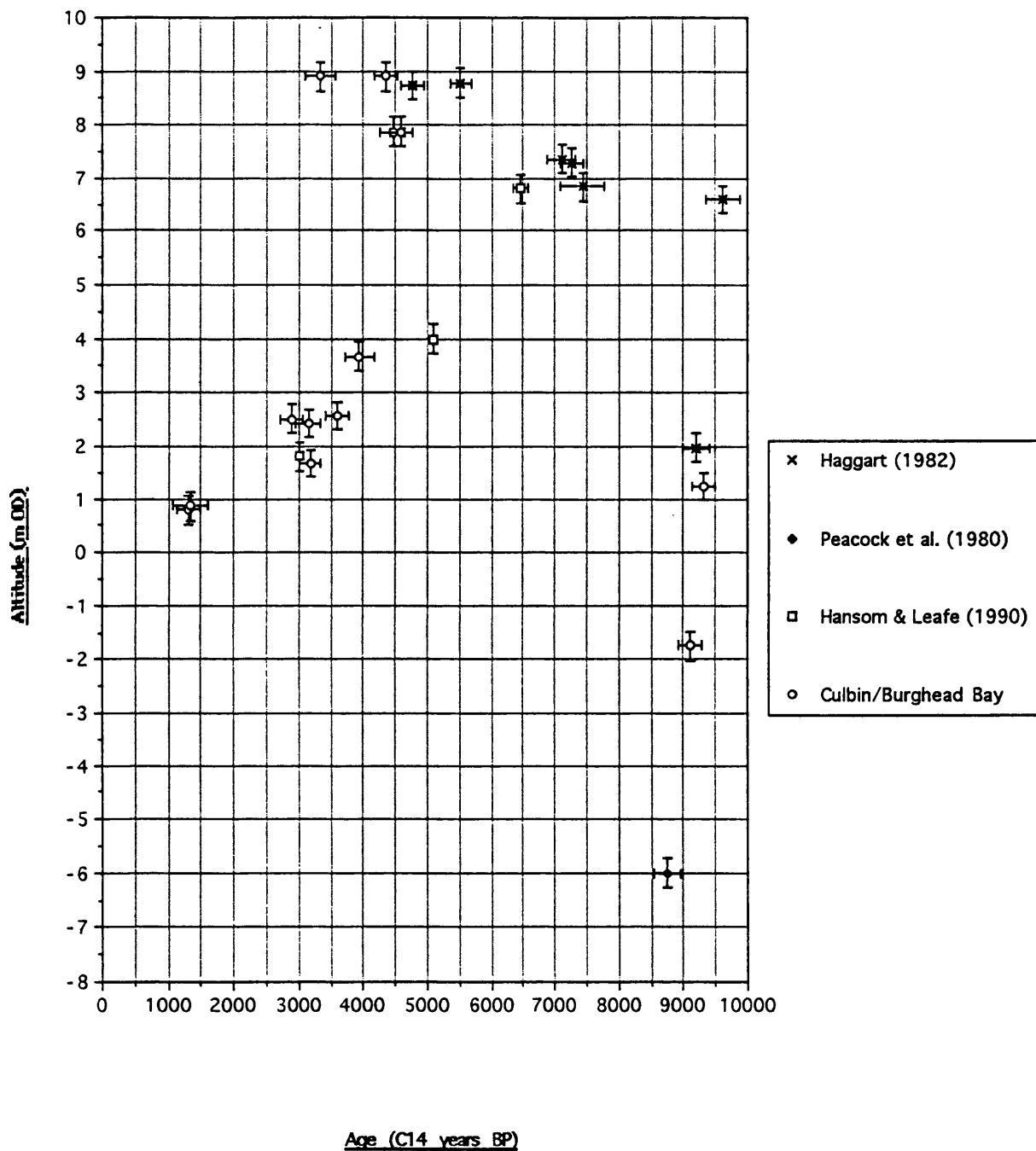


Figure 4.29

Figure 4.30

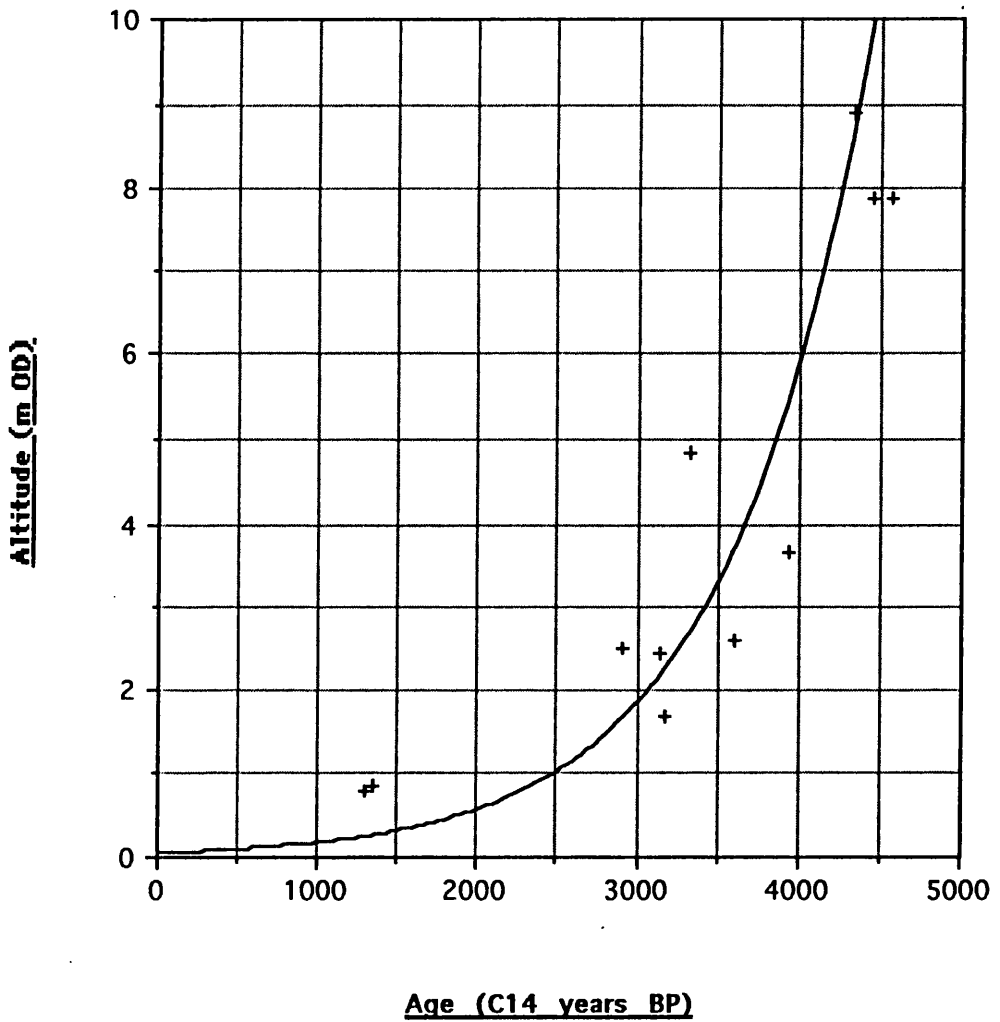
Composite sea level curve from the Moray Firth



Vertical error bars  $\pm 0.265$  m (Shennan, 1982)

Horizontal error bars  $\pm 2$  standard deviations

**Figure 4.31. Exponentially declining RSL demonstrated by Culbin sea level indicators**



important to note that earlier than *ca.* 4500 BP the form of the curve will begin to flatten, reflecting continued influence of the eustatic signal still being emplaced over the Scottish isostatic rebound element on the curve. As this would have interfered with the derivation of the isostatic signal, ages in excess of *ca.* 4500 BP were not included in this analysis.

This procedure established a best fit curve which adequately describes the sea level indicators emplaced after the Holocene sea level maximum. The next stage involved fitting this curve to the shingle ridge crest altitudes. In order to do this, the correction factor obtained from the contemporary shingle storm ridges on The Bar (3.17 m) was subtracted from the altitudes of each of the shingle ridge crests recorded along the eastern and central transects (Figure 4.29). This data was then used in the following section in the investigation of the abrupt altitudinal decline recorded on the transects.

#### **4.1.4.3 Abrupt altitudinal drops in shingle ridge altitudes**

As recorded earlier, a marked drop in altitude at the seaward end was measured in all three of the major shingle units exposed in Culbin. Figure 4.29 shows plots of the three transects. While the altitudinal break is very apparent on the central and eastern transects, the western transect (crossing ridge series D) is not so clearly defined. This may be explained as a function of the position of the transects across the shingle exposure, together with burial of the lower ridges of the western transect below a deep cover of sand. As such, the number of ridges on the western transect is much greater than that of the central and eastern transects, despite the shorter length. The generally falling trend noted across these ridges does not extend to a sufficiently low altitude prior to burial by blown sand to encompass the abrupt break in altitude recorded on the other two transects.

In the central series a fall of 4 m was observed between ridge crests located at 5.15 and 9.15 m OD. Similarly on the eastern transect a fall of 3.31 m was recorded between ridge crests at 7.40 and 4.09 m OD. Such an abrupt break in the ridge sequence may represent a definite event in the developmental history of the foreland due to its magnitude and presence on two of the major ridge sequences of the forest. Use was made of the sea level curve constructed for the Culbin area to place an approximate date on this event. Applying the shingle ridge correction factor to the ridge crests on either side of the altitudinal break reduced their absolute altitudes, as shown in Table 4.8. Next, by using the maximum error factor of  $\pm 0.87$  m calculated from the contemporary, active

shingle ridge on The Bar, the date range indicated by the ridge altitudes was calculated.

Transect	Ridge crest altitude (mOD)	Corrected ridge crest altitude (mOD)	Age (C14 years BP)	Error term (m) ( $\pm$ )	Error range (C14 years BP)
Central (top)	9.15	5.98	4150	0.87	4300-3900
Central (bottom)	5.15	1.98	2550	0.87	3150-1800
Eastern (top)	10.57	7.40	4450	0.87	4600-4250
Eastern (bottom)	7.26	4.09	3600	0.87	3900-3250

Table 4.8 Maximum age range associated with the drop in altitude recorded in the Culbin shingle ridge sequence, central and eastern ridge transects.

Due to the width of the error bands emplaced on the crest altitudes, the central ridge transect produced no conclusive date band within which the event responsible for the abrupt drop in altitude could be bracketed. Use of the maximum and minimum error bands (i.e. maximum altitude plus the error term, and minimum altitude minus the error term) produces a date with a range between 4150 and 2550 years respectively. However, the additional data provided from the eastern transect gives a closer dated interval of between 4450 and 3600 years BP for the approximate timing of an event which led to abrupt drops in shingle ridge altitudes.

#### 4.1.4.4 Holocene Environments at Culbin and Burghead Bay: Summary

i) A RSL history has been constructed for the Culbin area. This indicates a falling RSL between  $9305 \pm 45$  and  $9105 \pm 45$  BP, apparently fitting the trend for the Beaully and Dornoch Firths. Rising RSL to the Holocene sea level maximum deposited shingle storm ridges at ca. 11 m OD, representing the MPG in the Culbin area. RSL has fallen continuously since this period, depositing the extensive Culbin shingle ridge suite and allied storm ridges in Burghead Bay.

ii) The use of a shingle ridge correction factor based on modern analogue studies from The Bar, and supported by dated material from within shingle ridges in Burghead Bay supports the contention that shingle ridges, if adequately controlled, can be used as indicators of RSL.

iii) The dated shingle ridge relationships were used to date the abrupt drop in shingle ridge altitude noted in the Culbin ridges. This was dated to a minimum of between *ca.* 4300 and 3550 BP. With no significant sea level events occurring at this time, it is inferred that this drop relates to interference with sediment supply from updrift.

iv) The crest-crest spacing of the shingle ridges has been used as a surrogate variable for the regularity of sediment supply to the ridges. A higher standard deviation of spacing is suggested to demonstrate a more sporadic supply of sediment, and vice versa.

v) The sedimentology of the shingle ridges displays coarsening from east to west. Such an effect is also found on The Bar at present, demonstrating that similar processes of longshore sediment transport were operating up to 6500 BP as are operating currently.

## 4.2 CONTEMPORARY COASTAL PROCESSES AND LANDFORMS

### 4.2.1 Contemporary coastal processes

As noted in Chapter 2, the primary environmental driving forces behind sediment movements in the Moray Firth are waves, with a more minor role played by tidal currents. As the immediate source of energy driving the wave field is derived from winds, a description of the winds measured at RAF Kinloss over the two year monitoring period of the thesis is included. This is followed by a description of the wave climate in the middle Firth, using data from both the Beatrice Alpha platform and the wave recorder constructed for this project. The results of the current meter deployment offshore from Culbin Forest during summer 1991 are presented. Wave refraction modelling to generate a longshore current precedes beach profile analysis and an assessment of erosional inputs into the beach. A beach sediment budget for both sand and shingle is then presented.

#### 4.2.1.1 Tides

The restricted tidal range in the Moray Firth is primarily controlled by an amphidromic point off the Norwegian coast. The tidal range remains relatively constant along the outer coast from Burghead to Nairn on the Culbin sector of the southern Moray Firth. Spring tidal range at Nairn is 3.6 m, falling to 1.7 m on neaps (Table 4.9).

	Spring tidal range (m OD)	Neap tidal range (m OD)
Nairn	+2.2- -1.4	+1.2- -0.5
Burghead	+2.1- -1.2	+1.2- -0.4

Table 4.9 Tidal range at Nairn and Burghead (source: Admiralty, 1992)

Whilst these values represent predicted tidal heights, values may vary considerably depending on barometric pressure at the peak high or low tide. A 10 mb drop in atmospheric pressure is capable of producing a 0.1 m elevation of the sea surface (Hansom, 1988; BMT, 1990). Such storm surge conditions result in forced elevation of the sea surface when coupled with wave set-up and enhanced water levels associated with onshore gales during cyclonic activity.

On-site observations at Culbin suggest that the coincidence of a northeasterly gale and high spring tides can elevate water levels considerably along the coast, producing locally significant erosion along the southern Moray Firth.

#### **4.2.1.2 Tidal currents in the offshore zone: June 1991**

As a result of restricted tidal range, currents in the Moray Firth are generally weak, and as such provide a secondary energy input to the coastal sediment budget (Reid, 1988). However, it is essential to attempt to quantify the effects of tidal currents on sediment movement at Culbin, and thus a current meter was deployed. While measurements were made *ca.* 1200 m offshore, similar conditions were also assumed to be operating further inshore, affecting sediments on the foreshore.

Tidal currents were recorded between June 5th-22nd 1991 in the offshore zone at Culbin. The recording period spanned a neap-spring-neap tidal cycle, providing a record of tidal current speed and direction for 18 days. Prior to analyzing the results, some preparation was required in order to present the results in a comprehensible form. Data which would be of use to the project included the direction of tidal currents and their maximum, minimum and modal speeds. Additionally, tidal current *velocity* (the shore parallel vector of speed) was calculated in order to determine the influence of tidal currents in a longshore context. Residual current flow, defined as the net difference between the duration/speed of each tidal cycle was calculated in order to determine the net potential for sediment distribution over discrete tidal cycles, and finally the immersed sediment transport weight was calculated using the values of tidal current velocity recorded.

The data from the current meter was recorded in a coded format onto an internal 6 channel magnetic tape. Decoding of the data was undertaken by NERC RVS, and the decoded data dumped onto disk. Further manipulation was required in order to reproduce the data in engineering units. This was undertaken using a data transfer program (Aanderaa Insts. P3059) supplied with the current meter, which transformed the data into a readable format upon which data analysis could be performed.

Figure 4.32 shows the plot of current direction frequency as a percentage of the total recording period. The data is strongly bimodal, with the peaks of the plot coinciding with the directions of tidal streams along the coast. As the exact time of the deployment was recorded and the state of the tide at this time was known

RCM4 - June 1991 - Tidal current frequency (%)

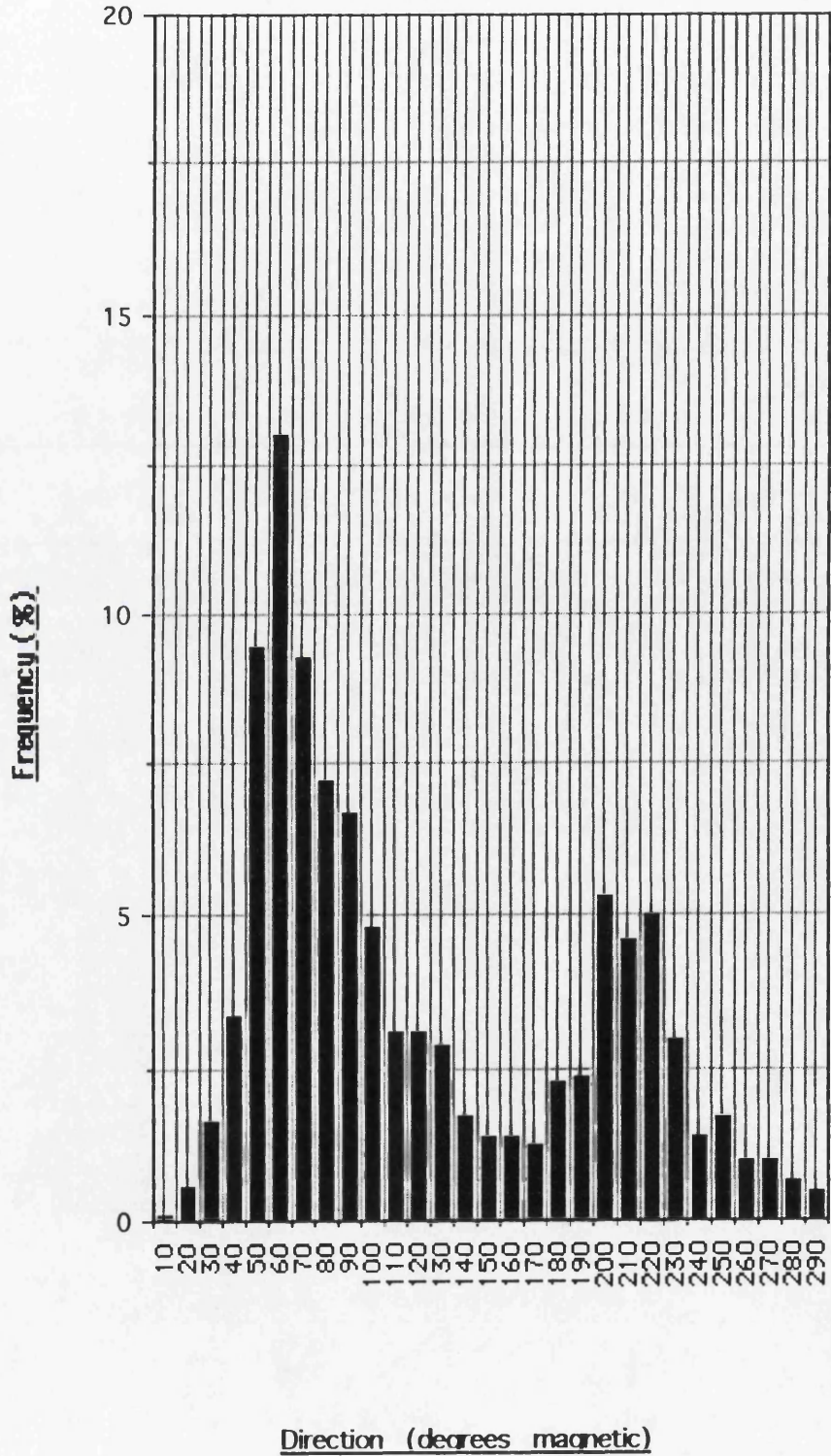


Figure 4.32

from tidal predictions, then from the direction of currents at time zero the direction of flood and ebb tides were determined throughout the remainder of the deployment. The ebb tide in the offshore zone at Culbin flows towards the east, and the flood tide towards the west. Modal peaks in the plot occur at 60° and 200°, reflecting the direction of the semidiurnal tidal streams (Figure 4.32). For the purposes of analysis the dominant directions of each tidal stream were defined as lying within a 30° sector, due to the inherently slow response rate of a vane-type current meter such as the RCM-4 (Hemsley *et al.*, 1991). The ebb tide thus registers as a current in the sector 50°-70°, and the flood tide in the sector 200°-220°. The greatest frequency of observations were recorded on the ebb tide (31.7% of all observations), with only 14.9% of observations on the flood tide. If the tidal sectors are extended to include readings in a further 10° band on each side of the modal peak, then the ebb tide frequencies increase to 42.2% and the flood tide frequencies to 20.2%, accounting for a total of 62.4% of total readings. This implies that weak or slack tides contribute 37.6% of the total record. The lack of readings in the northerly sector (300°-000°) demonstrates a net on/alongshore trend in the tidal current record.

The speed of the tidal streams are shown in Figure 4.33 as a percentage of the total recording period. The data is strongly positively skewed, suggesting generally low current speeds recorded over the whole period. The modal peak is located at 5 cm s<sup>-1</sup>, with a spread of speeds between 1 cm s<sup>-1</sup> and a maximum of 28 cm s<sup>-1</sup>. 43.3% of the speeds recorded were below 5 cm s<sup>-1</sup>, and 83.5% were below 10 cm s<sup>-1</sup>.

Data from the current meter was recorded as current speed. If the current speeds are resolved into their east-west vector of velocity, then the amount of sediment movement in a longshore direction relative to the Culbin coast can be calculated. This is because the orientation of the Culbin coastline lies at 260°-080°. Resolution of tidal currents into an east-west component was achieved by using the formula:-

$$v = s \sin O \quad (19)$$

where  $v$  = current velocity (cm s<sup>-1</sup>) (shore-parallel vector of speed)

$s$  = current speed (cm s<sup>-1</sup>)

$O$  = tidal stream orientation (relative to north)

RCM4 - June 1991 - % frequency of recorded tidal current speed

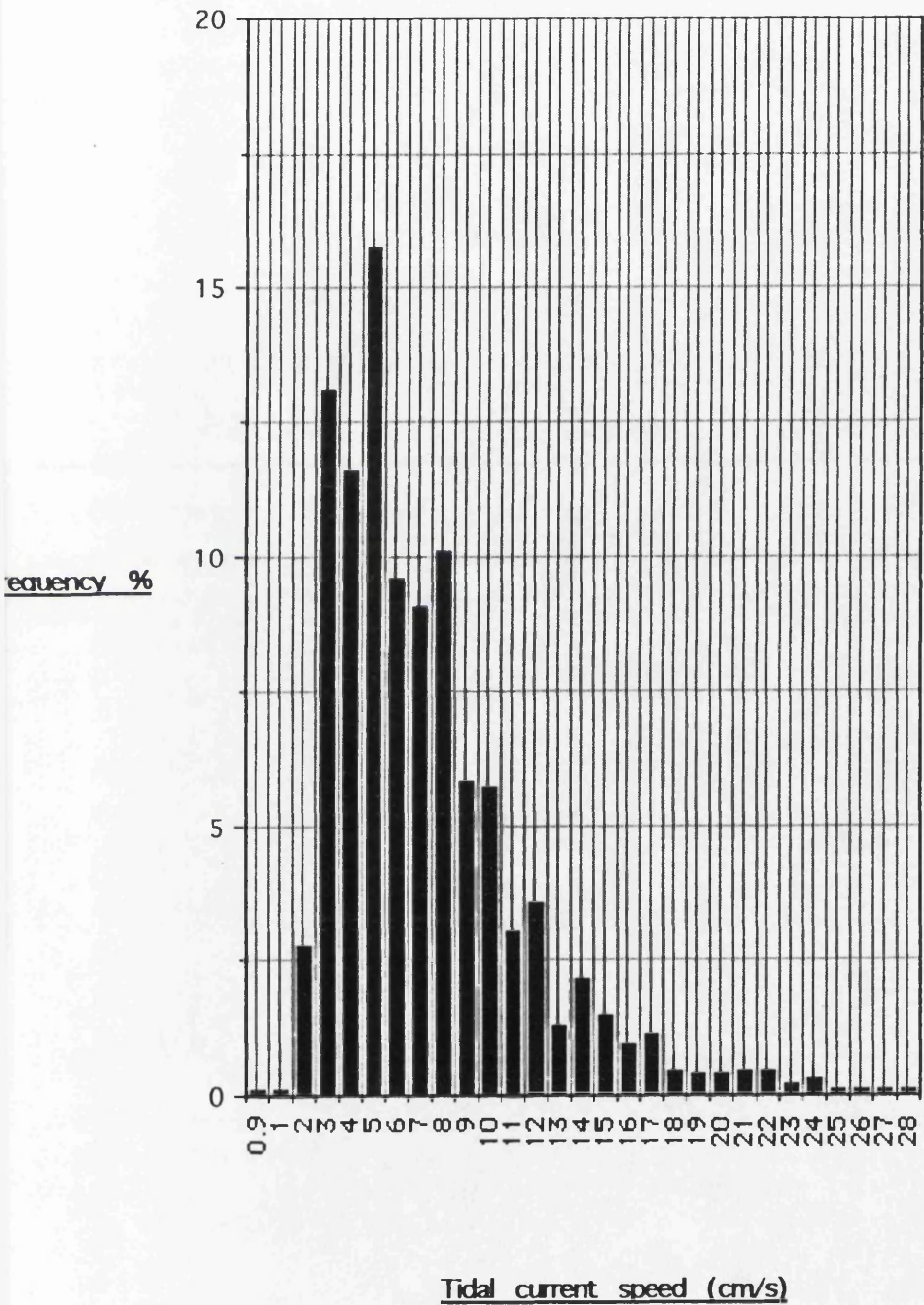


Figure 4.33

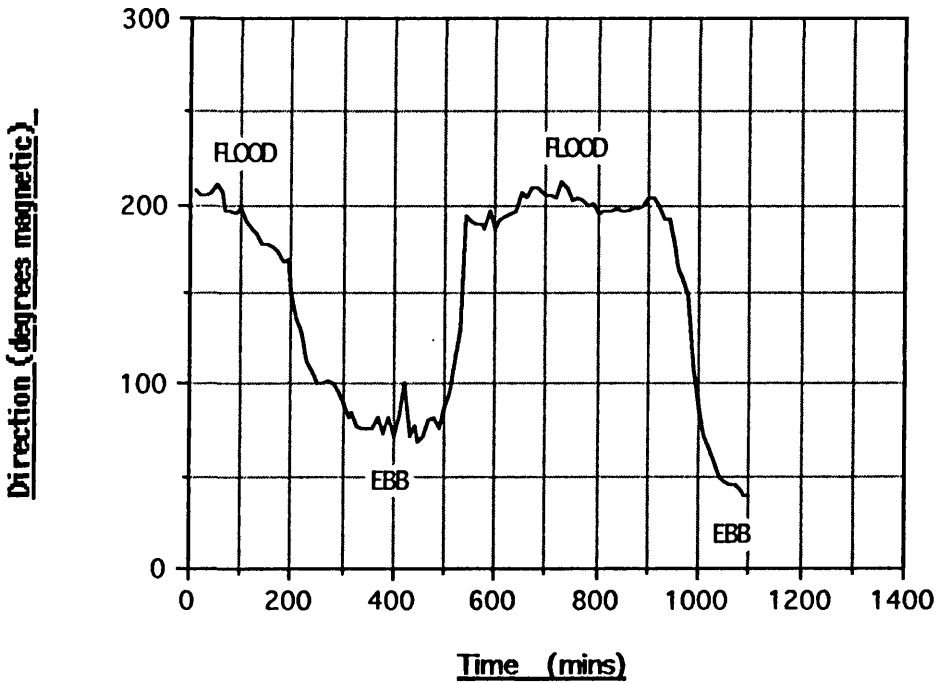
Examination of the values of current velocity obtained from this transformation reveal little change in the dominant tidal velocities from the original tidal speeds, suggesting that the maximum tidal influence on sediment transport operates in an almost shore-parallel fashion.

In order to illustrate the more detailed aspects of the tidal current regime in the area, data from two single days at the spring and neap tide maxima were selected, and analyzed in detail in order to demonstrate the differences experienced under the extremes of tidal variation in the middle Moray Firth.

The two days selected were June 6/7th and June 14/15th 1991, which were taken on the neap and spring tide maxima respectively. The data from each cycle is presented in Figures 4.34 - 4.36 as the direction, speed and velocity of tidal currents recorded during the logging period respectively. Directional data from both data sets clearly demonstrates the influence of tidal stage, with a current reversal accompanying the change of the tide. The record taken on the spring tide (Figure 4.34) shows a much stronger directional contrast than on the neap tide, with an extremely abrupt directional reversal accompanying the onset of the flood tide, but a gradual swing in direction marking the change from flood to ebb tide. The neap tide by contrast shows a longer response time during the change of the tide in both directions, but with a better defined ebb tidal vector.

Tidal speed records for both spring and neap tides shows peak current speeds attained during mid-tide as might be expected (Figure 4.35). Maximum tidal current speeds are higher on the spring tide than the neap, attaining  $12 \text{ cm s}^{-1}$  on the neap tide and  $17 \text{ cm s}^{-1}$  on the spring tide. Minimum tidal current speeds are attained during slack tides, falling to a minimum of  $2 \text{ cm s}^{-1}$  on the neap tide and  $3 \text{ cm s}^{-1}$  on the spring tide (Figure 4.35). Although these speeds are low, tidal currents throughout the total record were always flowing and never fell to zero. The plot of tidal speed on the spring tide is more clearly defined than on the neap tide, with marked peaks accompanying the periods of mid-tide and troughs at slack tide, as opposed to the less well defined and generally more noisy signal obtained on the neap. Perhaps the most noteworthy feature of these plots is the apparent reversal in the stage at which tidal current speed reaches a maximum. On the neap tide tidal speeds reach their highest values on the flood tide, while on the spring tide the maxima are recorded on the ebb tide. However, this apparent anomaly was resolved by plotting tidal current *velocity* against tidal stage, as shown in Figure 4.36. The plots show a much clearer relationship with

Direction of tidal currents - 6/7 June 1991



Direction of tidal currents - 14/15 June 1991

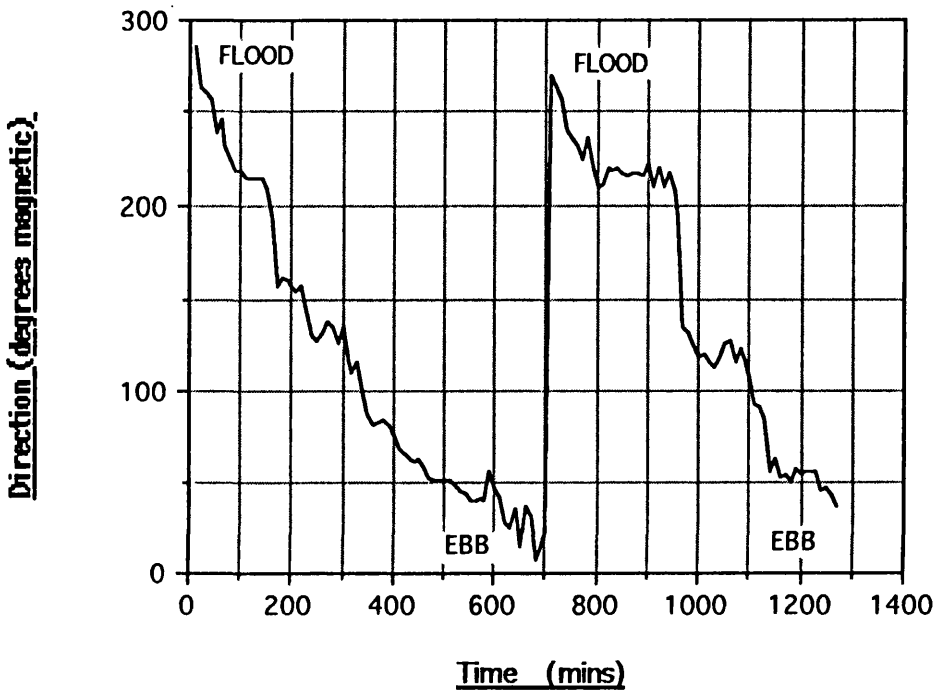
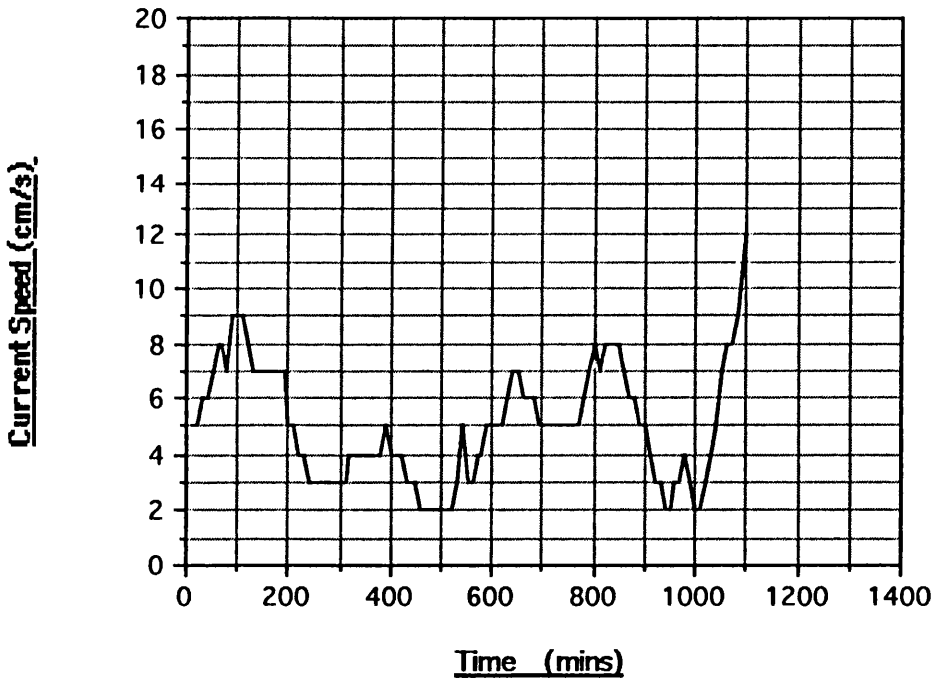


Figure 4.34

Tidal current speed - 6/7 June 1991



Tidal current speed - 14/15 June 1991

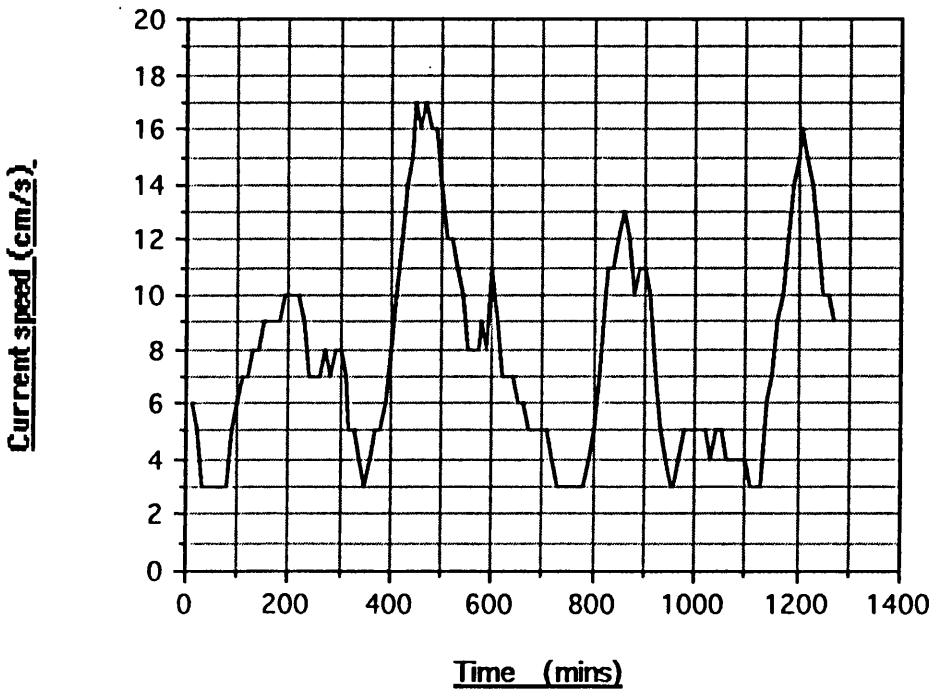
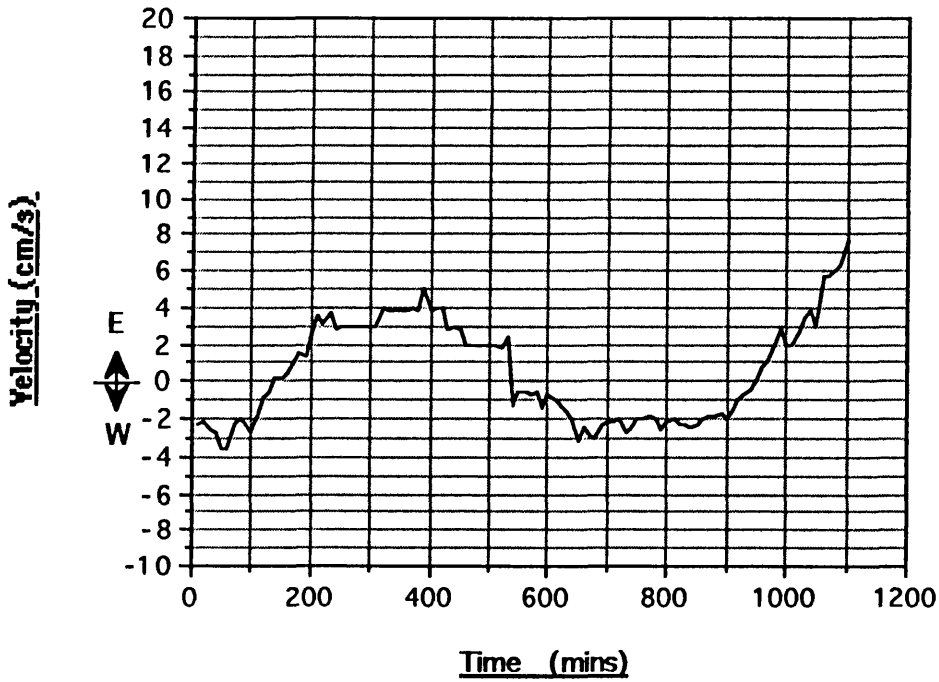


Figure 4.35

Tidal current velocity - 6/7 June 1991



Tidal current velocity - 14/15 June 1991

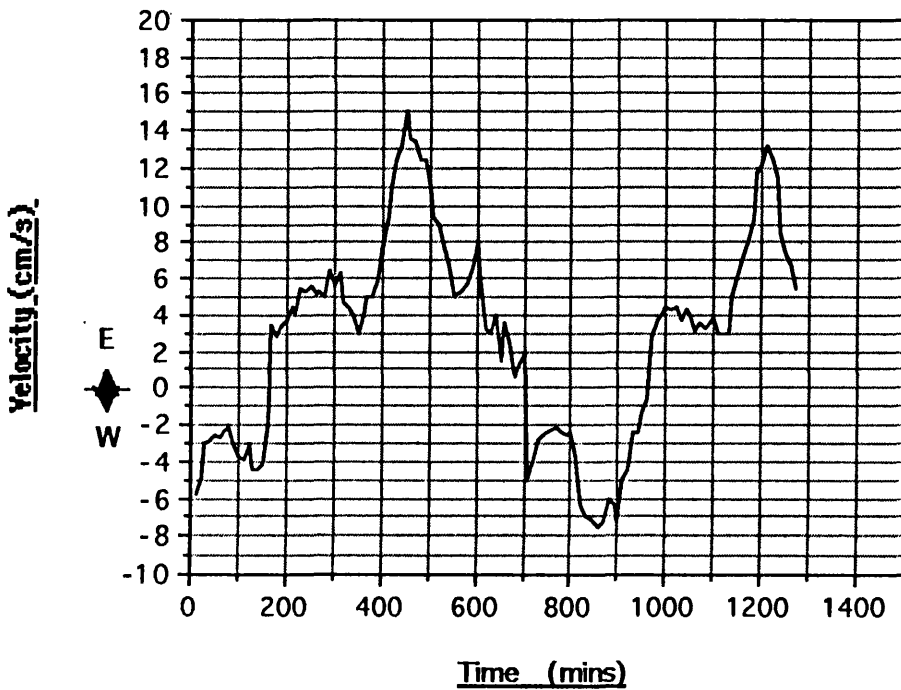


Figure 4.36 Tidal current velocity: June 6/7 and 14/15 1991

tidal stage than the plots of current speed, reflecting tidal current speed in its shore-normal vector.

Plots for both spring and neap tide show a peak velocity attained on the ebb tide, although the velocity maximum is only  $5 \text{ cm s}^{-1}$  on the neap tide as opposed to  $15 \text{ cm s}^{-1}$  on the spring, a considerable difference. This difference is highlighted in the plot of tidal velocity recorded over the entire recording period (Figure 4.37). This shows the dominance of tidal currents flowing towards the east (ebb currents), shown on the plot as positive values, with an increase in velocity overall from the start of the trace (neap tide) through to the spring tide indicated on the trace. Peak velocities for the entire recording period reached  $28 \text{ cm s}^{-1}$  on the ebb tide, and  $10 \text{ cm s}^{-1}$  on the flood tide. A frequency histogram of tidal current velocities is shown in Figure 4.38. The plot is again bimodal, reflecting the dominant current velocities recorded on the flood and ebb tides. The dominant modal class is  $4\text{-}5 \text{ cm s}^{-1}$ , which was the modal velocity recorded on the ebb tide, and which accounts for 22.8% of all readings. A secondary peak occurs at  $-2 \text{ cm s}^{-1}$ , which was the modal velocity attained on the flood tide. The data set is markedly asymmetrical, with the frequency of ebb tide readings dominating over the flood tide. 26.3% of velocity readings fell in the  $0\text{-} -10 \text{ cm s}^{-1}$  class (flood tide velocity), while 66.9% of readings fell in the  $0\text{-} +10 \text{ cm s}^{-1}$  class (ebb tide velocity).

Sediment entrainment is controlled by tidal current *speed*, reflecting the maximum force applied to sediment on the sea bed. The amount of sediment which is subsequently transported in a longshore direction is controlled by current *velocity*, and the relative distance travelled after one tidal cycle is defined by the *residual current velocity* (King, 1972).

Table 4.10 shows the maximum current speeds attained on each tidal cycle during the recording period and the largest grade of material which could be potentially entrained, using the Hjulstrom critical entrainment velocity curve (in Briggs & Smithson, 1985). On only five separate occasions was the current speed of sufficient magnitude to entrain sediment, assuming a minimum critical entrainment velocity of  $20 \text{ cm s}^{-1}$ . These periods all occurred on ebb tides.

From the preceding data two main points are clear:

- i) tidal current velocities at Culbin are very low;
- ii) ebb tide dominance produces a net *easterly* transport of sediment.

RCM4 - June 5-22 1991 - Total velocity

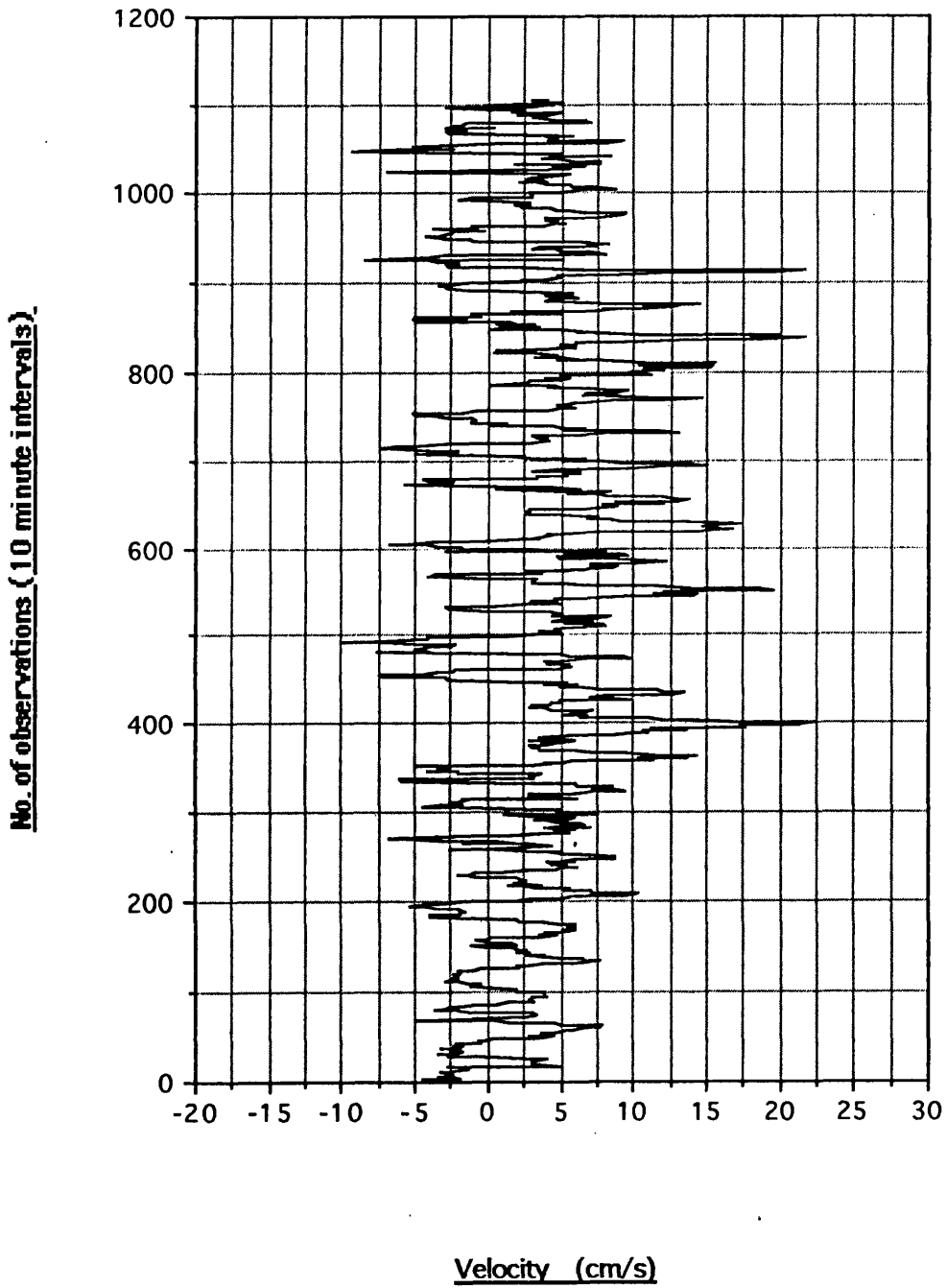


Figure 4.37 Total tidal current velocity: June 1991

RCM4 - June 1991 - Tidal current velocity frequency

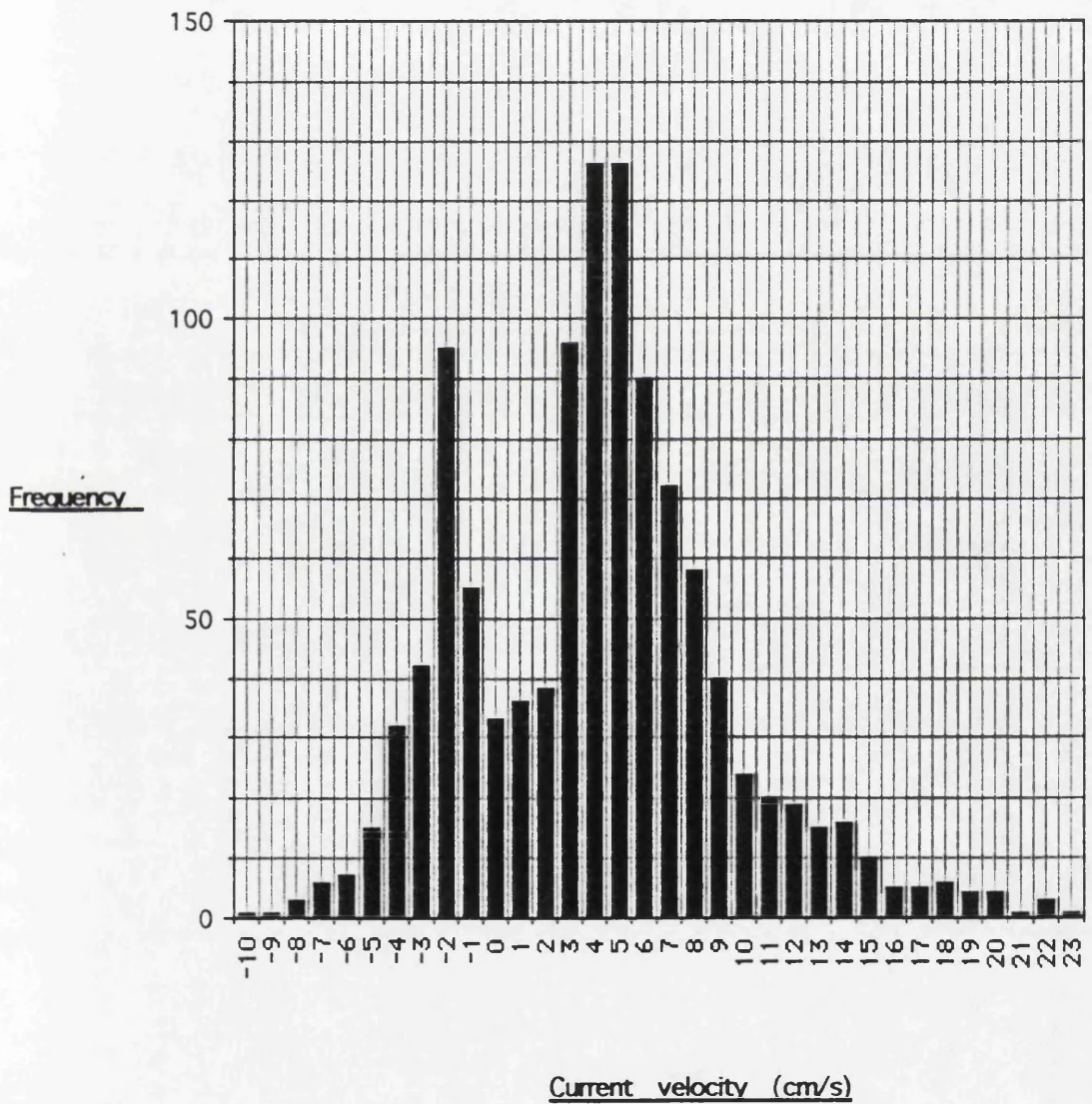


Figure 4.38 Frequency histogram of tidal current velocity: June 1991

From the recorded current speeds, it can be seen that sediment entrainment will be dominated by the ebb tide. However, net transport of previously entrained sediment, either under tidal or wave generated currents, is controlled by the magnitude of the residual tidal current. This residual current is measured as the differential transport of a hypothetical sediment particle occurring due to the difference between the duration and velocity of each tidal stream.

Figure 4.39 shows the magnitude of the residual currents recorded at Culbin. The greatest residual velocity recorded was  $10 \text{ cm s}^{-1}$ , and the lowest  $0.4 \text{ cm s}^{-1}$ , all flowing eastwards. Again no periods of zero flow were recorded, suggesting the process to be continuous, albeit of a low magnitude. The residuals show a rising trend in velocity from the neap tide towards the spring, followed by a fall after the peak of the spring tide at the 20th tidal cycle.

From the speeds recorded, the maximum size of material which could be entrained is 0.8 mm (Briggs & Smithson, 1985). Sea bed sediments in the vicinity of the current meter site are predominantly sand, with muddy facies (silts and clays) recorded further offshore (Chesher & Lawson, 1983). Details of the grade of sand were not revealed, and the available data is insufficient to determine whether the sands are fine grained and in transit through the action of tidal currents, or a coarser lag deposit reflecting winnowing of the finer sand fraction.

Only selected tidal cycles showed current speeds of sufficient magnitude to entrain sediment. These are indicated on Table 4.10. Within these cycles speeds were high enough to entrain sediment for only a limited period during mid-tide. Over the whole recording period (24 750 minutes.) only 500 minutes, or 2% of recorded velocities were high enough to entrain sediment assuming a minimum critical entrainment velocity of  $20 \text{ cm s}^{-1}$ . As the recording period itself (27 tidal cycles) represented only 1.93% of the annual tidal record, then extrapolation suggested that, on an annual basis, tidal speeds capable of entraining sediment would occur for:

$$2\% \times 1.93\% = 0.04\%$$

of the year, or 3.50 hours.

Experimental calculations of the immersed sediment transport potentially occurring in the Culbin offshore zone as a result of this entrainment period produced a potential volume of  $5.0 \times 10^8 \text{ m}^3 \text{ a}^{-1}$  in an easterly direction. The

RCM4 June 1991 - Residual tidal velocity

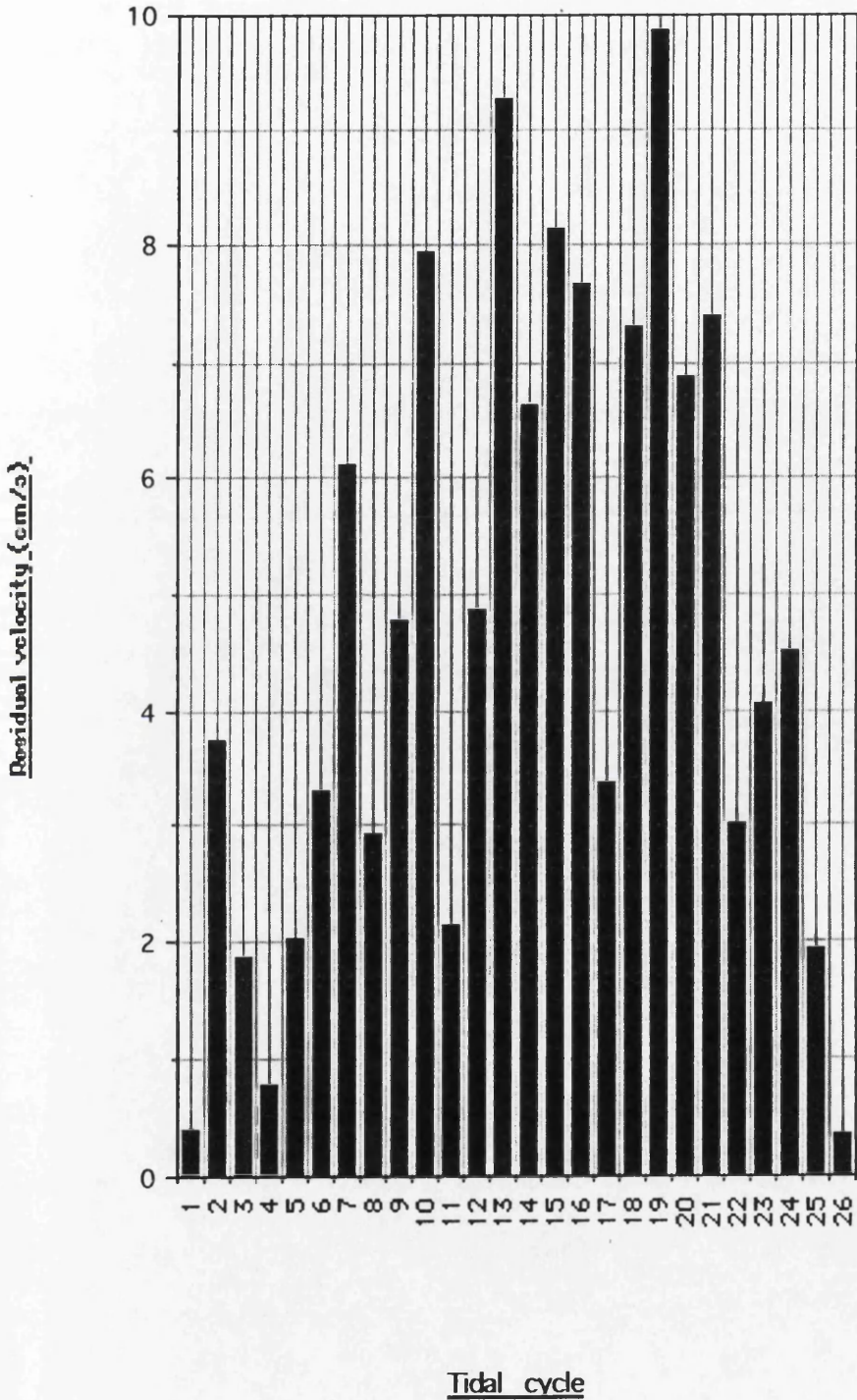


Figure 4.39 Tidal current velocity residuals

magnitude of this calculated amount may have been due to the assumption of an infinite depth of sediment in the offshore zone to allow continuity of the equation (Komar, 1976), a condition which does not exist at Culbin due to the thin, patchy nature of the sediments on the sea bed (Chesher & Lawson, 1983). On the grounds of geomorphological evidence, plus the long term trend in sediment movement in the Moray Firth (NERC, 1991), the results from this calculation were not considered realistic. Additionally, if the diameter of the sand grains in the offshore zone are assumed to be a similar size to those on the foreshore at the closest sampling station to the current meter (station 5), then the mean particle diameter is 1.70 mm. Entrainment of particles of this size would require a current speed of 50 cm s<sup>-1</sup>. Given that the sediments further offshore zone are reported as silts and clays, then the current speed required to entrain these would be higher still. As a result, the results from these calculations are not included in the beach sediment budget. The implications of these results are discussed in Chapter 5.

#### **4.2.1.3 Summary**

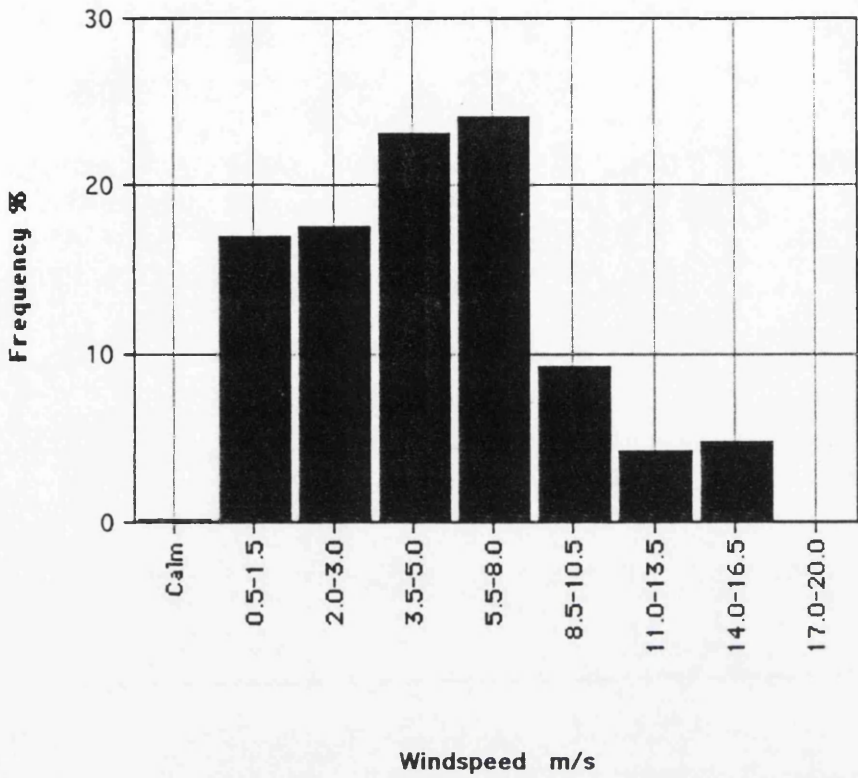
Tidal current speeds in the offshore zone at Culbin are low, attaining a maximum of 0.28 m s<sup>-1</sup>. The ebb tide is dominant in terms of both speed and duration. Current speeds only achieve sufficient magnitude to entrain sediment on the ebb. Calculation of residual currents also demonstrated an ebb-dominated potential net sediment transport. Calculation of an immersed sediment transport volume produced a value unreconcilable with long term sediment movement trends (NERC, 1991), previous studies (Reid, 1988) and geomorphological evidence. Tidal sediment transport was thus omitted from the sediment budget.

#### **4.2.1.4 Winds**

Wind data spanning 1990 and 1991 were obtained from RAF Kinloss on the eastern side of Findhorn Bay, approximately 6 km east of Culbin. The raw data was received in the form of hourly records of windspeed and direction, grouped into variable sized classes and summed for each month. The raw speed data were recorded in knots, which were converted to units of metres per second (m s<sup>-1</sup>) prior to collation.

The total windspeed frequencies were added, and expressed as a percentage of the total observations during each year. Histograms of windspeed frequency at RAF Kinloss for 1990 and 1991 are presented in Figure 4.40.

Windspeed frequency: RAF Kinloss 1990



Windspeed frequency: RAF Kinloss 1991

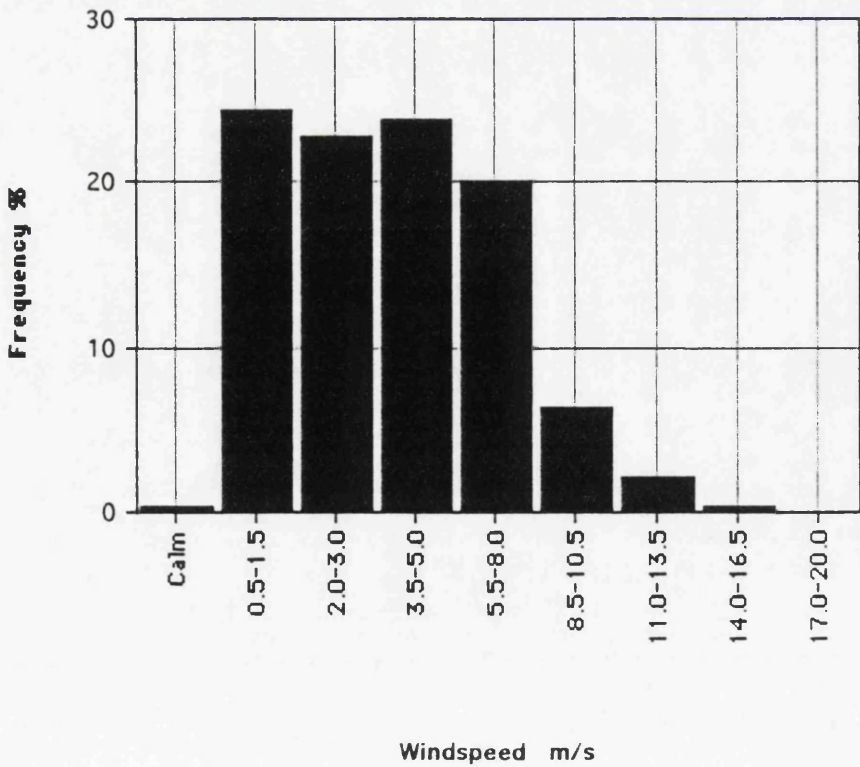


Figure 4.40 Windspeed frequency at RAF Kinloss during 1990 and 1991

Windspeeds were generally low over the two years, with 81.6% and 91.1% of all observations below  $8.0 \text{ m s}^{-1}$  during 1990 and 1991 respectively, and no speeds exceeding  $16.5 \text{ m s}^{-1}$ . 1990 saw a slightly higher frequency of winds in the mid-range classes of  $3.5\text{-}8.0 \text{ m s}^{-1}$ , while during 1991 the modal class appeared at  $0.5\text{-}1.5 \text{ m s}^{-1}$ . During 1990 18.42% of winds were greater than  $8.0 \text{ m s}^{-1}$ , while in 1991 this number fell to 8.92%. A comparison of the data suggests that windspeeds were slightly lower overall during 1991 than 1990, with a lower frequency of stronger winds ( $>8.0 \text{ m s}^{-1}$ ) recorded.

Wind direction data were also analyzed over the period 1990-91. Windspeeds in excess of  $11 \text{ m s}^{-1}$  were plotted as a wind rose, presented in Figure 4.41.  $11 \text{ m s}^{-1}$  was chosen in order to compare the data from the two year study period with a ten year record of winds of the same velocity recorded at RAF Kinloss by Ross (1992).

Figure 4.41 shows the clear dominance of winds from the southwestern sector, with winds from  $235^\circ$  accounting for 43% of all observations during 1990-91. Of note are the secondary arms of the rose, which also appear in the southwestern sector, and the very low frequency (24.4%) of onshore winds in relation to those from the southwest. The data suggest that offshore winds are dominant at Culbin, with 24.4% of winds blowing offshore. The dominant wind direction is similar to that recorded by Ross (1992), who noted a dominant wind direction of  $250^\circ$ , although this accounted for 16.4% of all observations, as opposed to the 43% noted during 1991-92. However, if a similar  $30^\circ$  sector through which the 1991-92 data were analyzed is considered, then the 10 year frequency of winds from the southwesterly sector rises to 41%, only slightly lower than those recorded during 1991-92.

#### **4.2.1.5 Waves**

The natural wave climate incident upon a stretch of coastline is extremely varied in terms of the range of wave heights and periods experienced. When undertaking wave refraction modelling it is necessary to simplify the range of incident waves in order to minimize calculations, while avoiding oversimplification and producing an unrealistic final value for longshore transport. In order to provide the most accurate range of wave parameters for input into the wave refraction program, wave records from three main sources were investigated: a 12 month record from the Beatrice Alpha oil platform; waves recorded directly with a wave recorder; and secondary data from Global Wave Statistics (BMT, 1986).

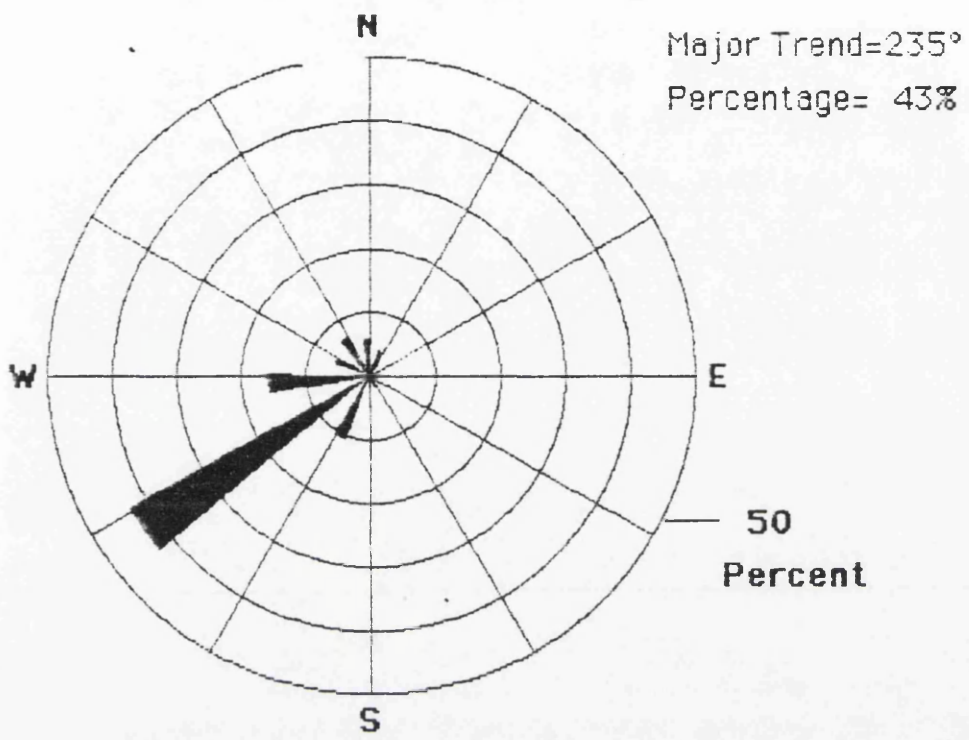


Figure 4.41 Windrose from RAF Kinloss 1990-91

#### 4.2.1.6 Beatrice Alpha

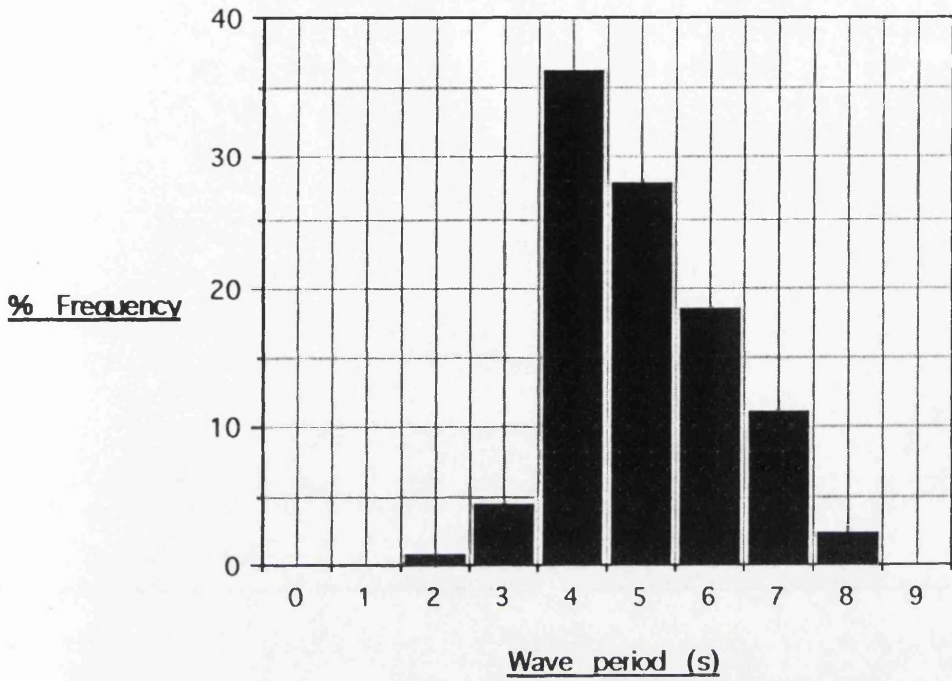
Wave measurement in the Moray Firth has been undertaken by a number of commercial bodies. The most useful of these was recorded on board the Beatrice Alpha oil platform in the outer Moray Firth. Unfortunately this data set is limited by the lack of swell direction. The use of recorded wind data was initially considered as a possible surrogate for swell direction. Plotting windspeed against recorded wave height shows a clear relationship (Figure 3.10), which suggests that the incident angle of winds in this sector are directly related to wave generation. However, this apparent relationship takes no account of the incidence of swell from the North Sea, which from examination of records from Global Wave Statistics accounts for between 15.46% and 24.12% of total waves at Culbin, depending upon the season. Thus the Beatrice data was used to input a realistic range of wave heights and periodicities into the wave refraction exercise.

The data from the Beatrice Alpha records is presented seasonally. The data is presented as frequency histograms of wave height and period (taken from the original data source values of the zero crossing period,  $T_z$ ) from the most recent record available (1990).

Wave period shows a peak frequency of 4 s in spring and summer, increasing slightly to 5 s in autumn and winter (Figure 4.42). The autumn and winter plots also show a greater spread of wave periods, up to a maximum of 9 seconds in both autumn and winter, whereas the maximum recorded value is 8 seconds in spring and only 7 s in summer. A total of 99.2% of waves display periodicity of 4 s or greater in spring, compared with 96.8% in summer, 95.3% in autumn and 94.6% in winter. Thus a slight difference in the modal wave period can be detected between the spring/summer and autumn/winter data sets. Figure 4.43 shows the data presented as the annual total frequency for 1990. The data shows an essentially normal distribution, with the dominant modal class in the 4-5 s range. The difference between the spring/summer and autumn/winter data sets appears to cancel over the period of a year, producing the normal distribution illustrated by Figure 4.43.

Wave heights recorded from Beatrice Alpha are shown in Figure 4.44. The dominant annual modal class is 1 m. Examination of the seasonal plots of wave height reveals that only the winter plot displays a different modal class from the annual average, at 1.5 m. The plots for spring, autumn and winter all display a positive skew to the data, representing a greater frequency of smaller waves.

Wave period - Beatrice 'A' - Spring 1990



Wave period - Beatrice 'A' - Summer 1990

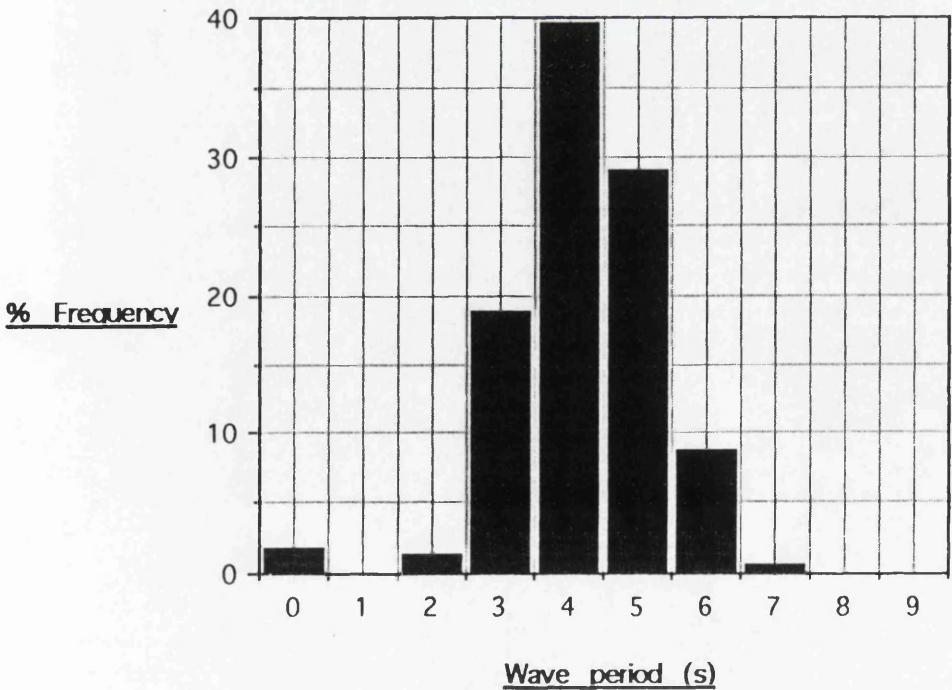
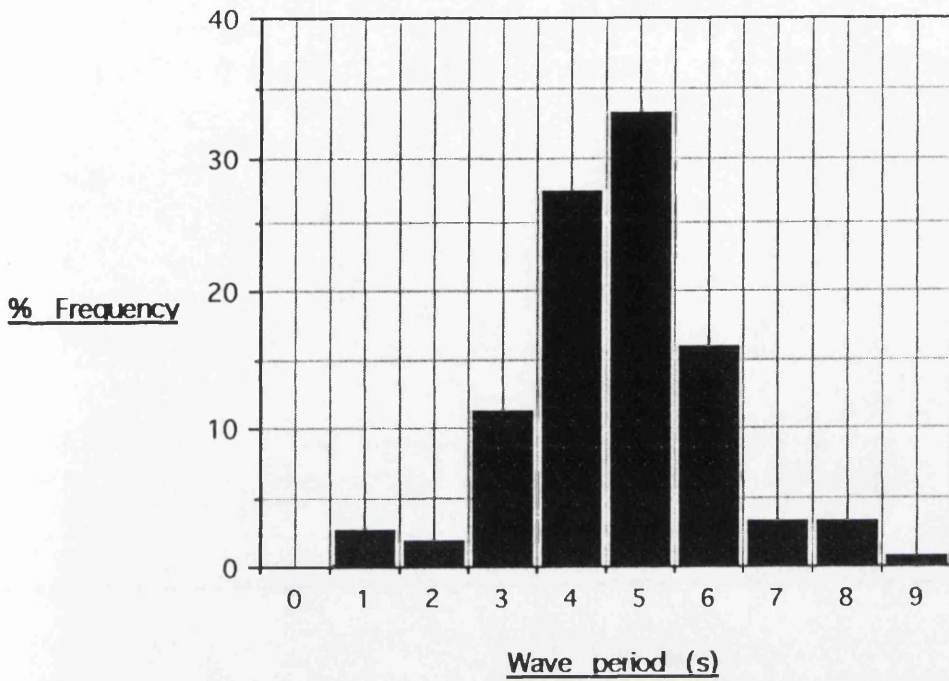
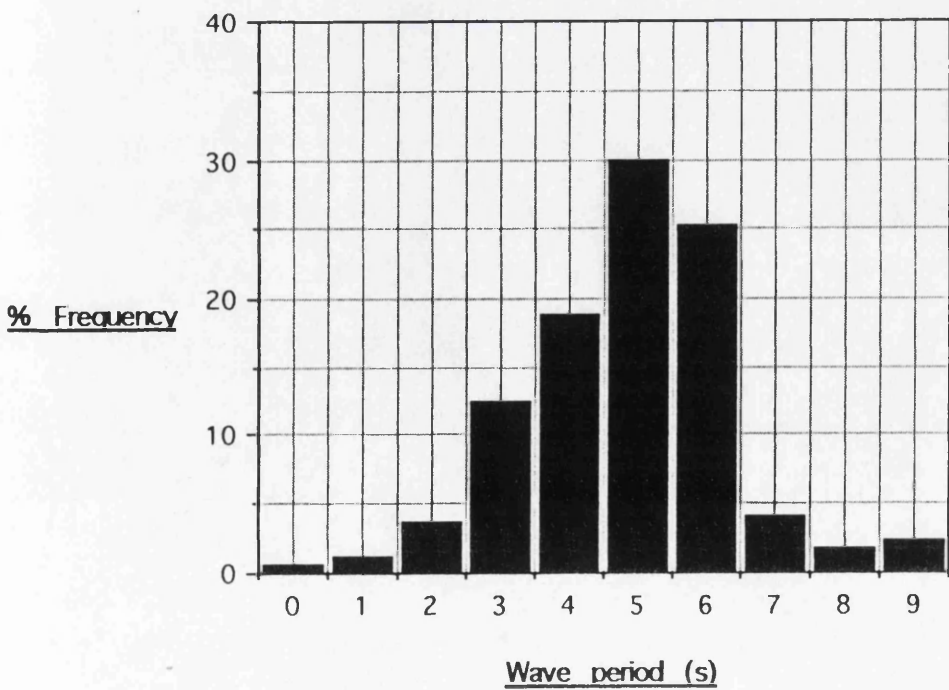


Figure 4.42 Beatrice Alpha: seasonal wave periods

Wave period - Beatrice 'A' - Autumn 1990



Wave period - Beatrice 'A' - Winter 1990



Wave period - Beatrice 'A' - Annual 1990

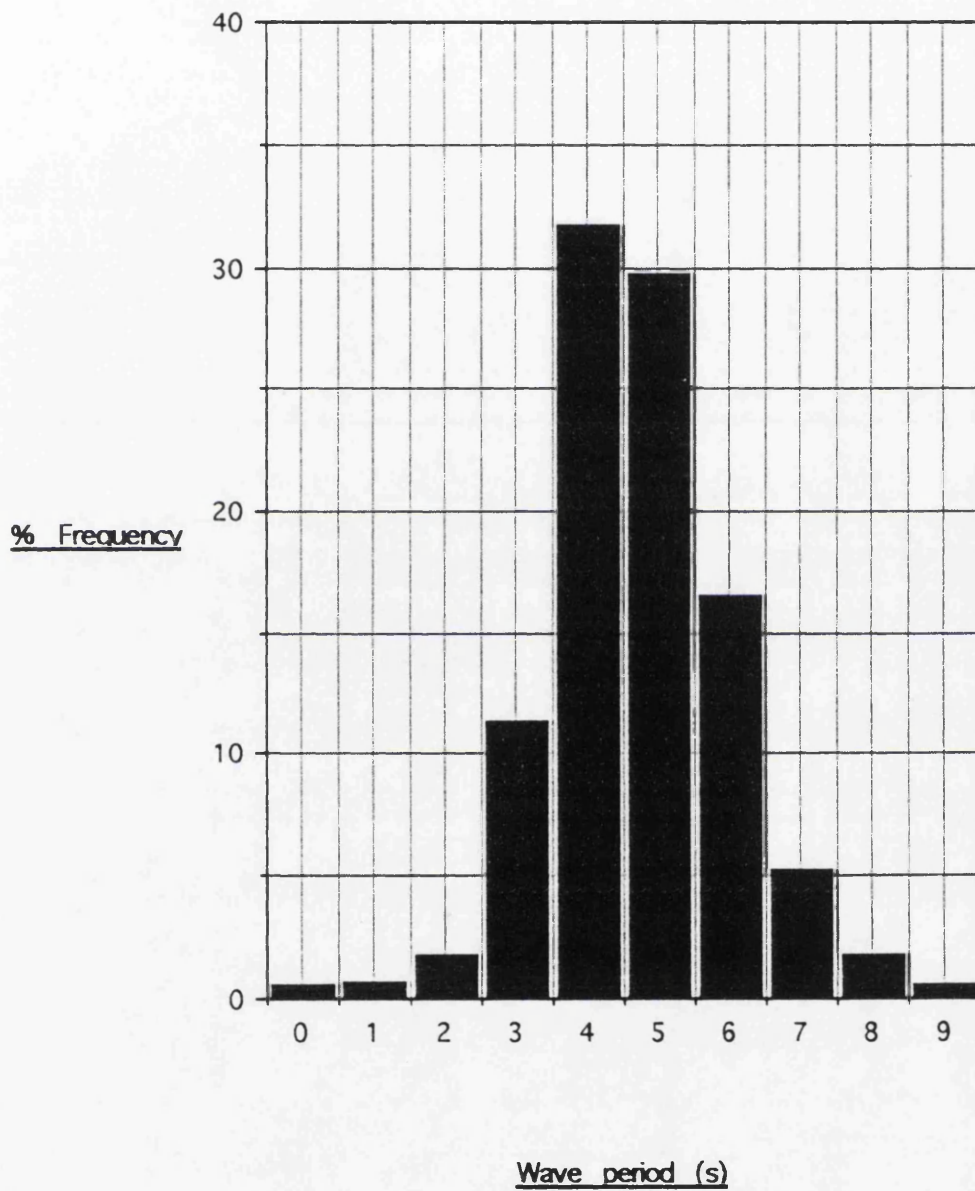
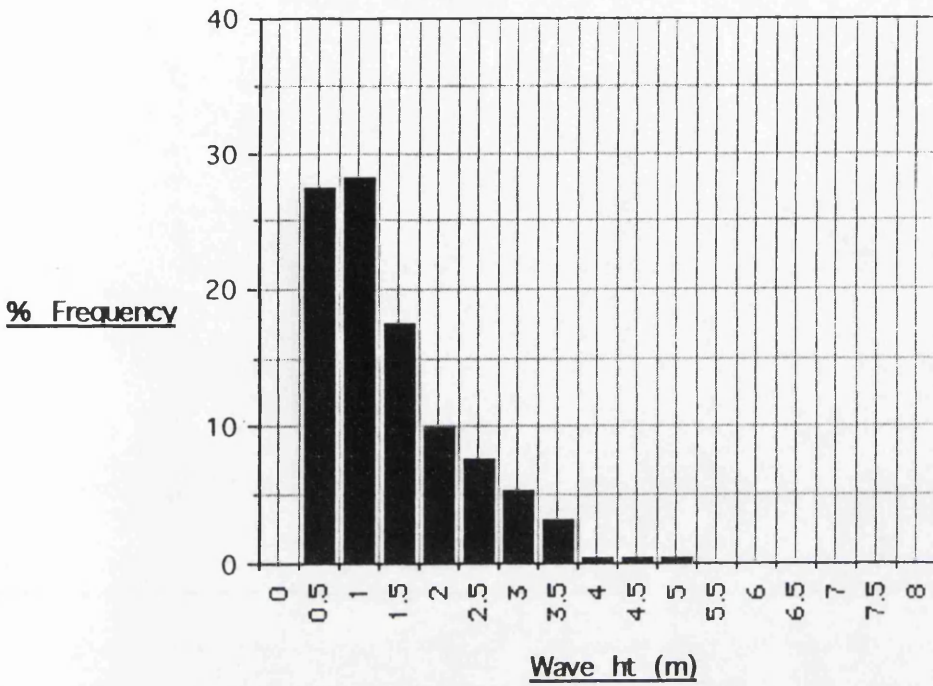


Figure 4.43 Beatrice Alpha: annual wave period

Wave height - Beatrice 'A' - Spring 1990



Wave height - Beatrice 'A' - Summer 1990

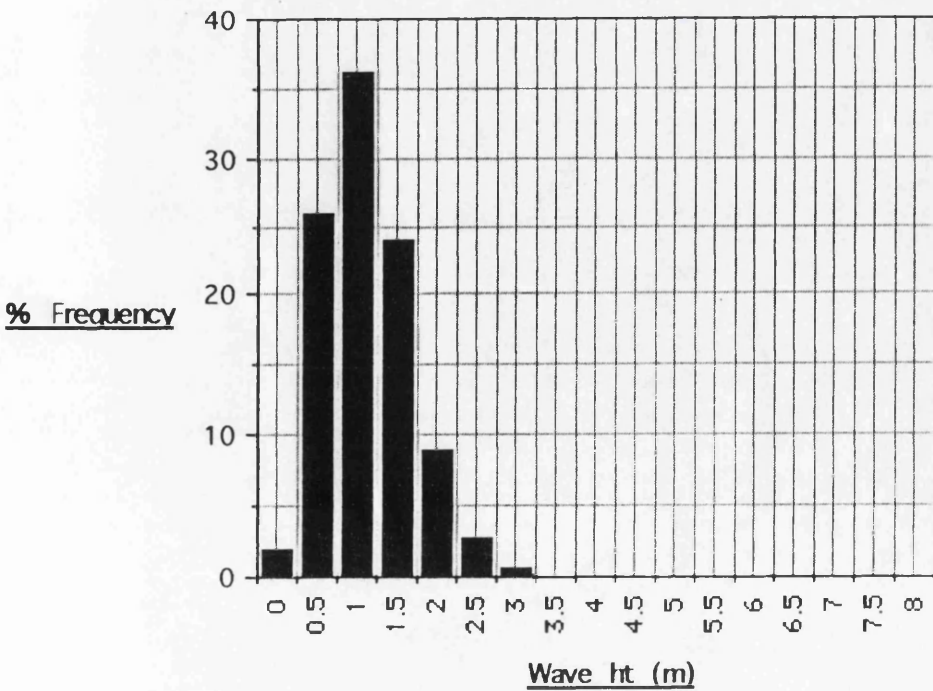
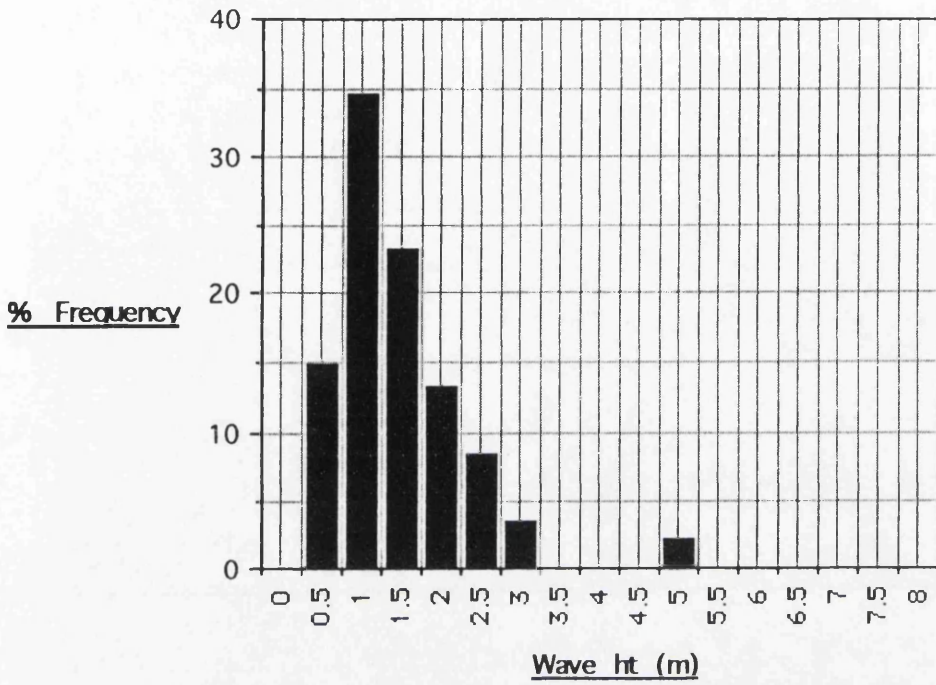


Figure 4.44 Beatrice Alpha: seasonal wave heights

Wave height - Beatrice 'A' - Autumn 1990



Wave height - Beatrice 'A' - Winter 1990

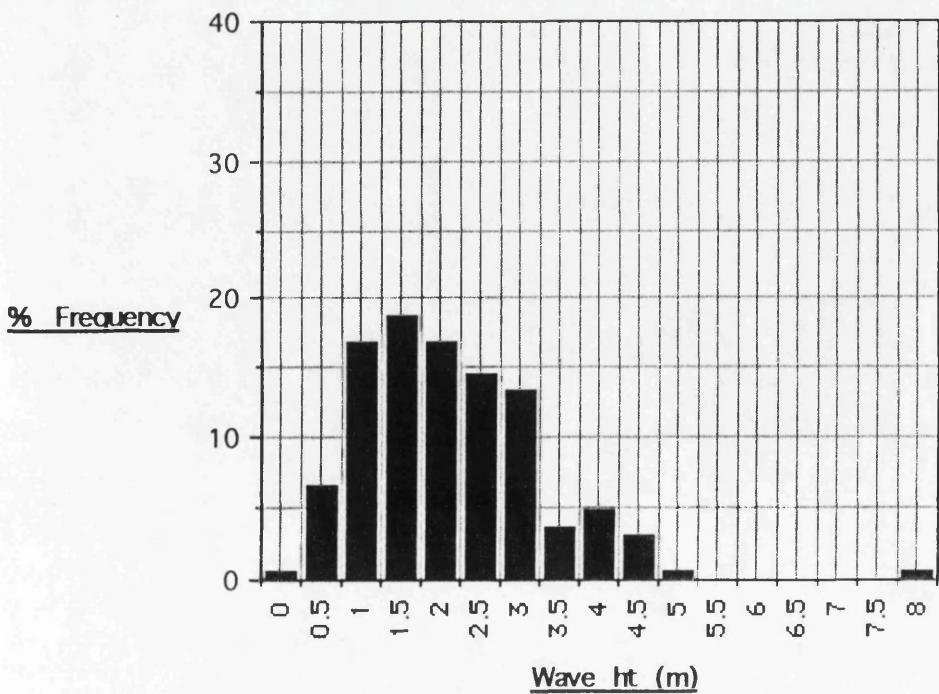


Figure 4.44 (summer) shows an almost normal distribution of wave heights centred around the modal class of 1 m, and displays a narrow spread of data, with the highest wave height recorded being 3 m. Both spring and autumn maximum recorded wave heights are 5 m, whilst the winter maximum is 8 m. Seasonally the frequency of exceedance of the modal class is fairly similar for spring to autumn, with waves of 1 m or greater occurring 72.6% in spring, 72.3% in summer and 85.2% in autumn. Winter data shows a much flatter, wider distribution of wave frequencies, with the annual modal class exceeded for 92.5% of the recording period. Calm conditions are uncommon, occurring for only 2.5% of the total record, and were only recorded during summer and winter. The plot of annual wave height frequencies (Figure 4.45) displays the positive skew and dominant modal class of 1 m noted for the spring-autumn data sets, and illustrates the low frequency of calm conditions experienced in the outer Firth.

From the data collected on board Beatrice Alpha, wave heights of 0.5, 1.0 and 2.0 m appear to represent an acceptable range for wave refraction modelling, covering both the modal conditions and a slightly higher energy (storm) situation. Similarly wave period would be best represented by waves of 4, 6 and 8 s period.

#### **4.2.1.7 Wave recorder deployment: May 1991**

The directional wave recording rig recorded data between 23/05/91-31/05/91. The length of the actual recording period was 19 days, but as noted earlier the rig was not submerged for 10 days. This was due to the nature of the data logger used, which could only trigger its internal memory in multiples of 6 hours. Employed in conjunction with a tidal cycle lasting approximately 25 hours, the problem was unavoidable. However, the high quality of the data produced warranted its inclusion as a check on secondary data sources and to verify the technique for future use.

In order to obtain meaningful results from the record of pressure against time obtained from the data logger, the pressure transducers required calibration prior to field deployment. A realistic operating depth was required in order to ensure that a linear output response to depth occurred. The intended deployment site at station 5 was levelled in to the benchmark survey network, and was located at -0.44 m OD. The frames designed to support the pods were 1 m high, thus the effective altitude of the pods was 0.56 m OD. The height of spring tides during 1991 was no greater than 4.5 m (2.4 m OD) (Admiralty, 1991).

Wave height - Beatrice 'A' - Annual 1990

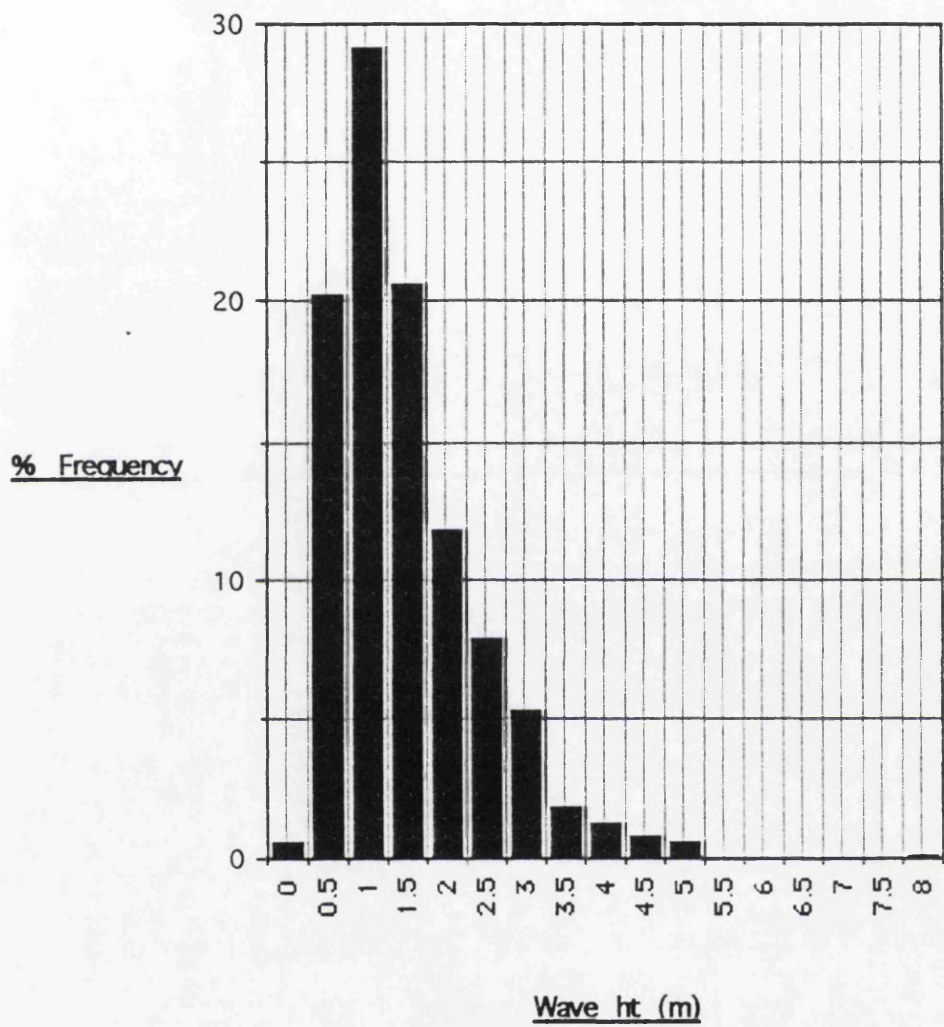


Figure 4.45 Beatrice Alpha: annual wave heights

The highest summer and autumn waves recorded at Beatrice Alpha were no greater than 3 m, and these conditions were only experienced for a maximum of 0.5% and 3.5% of the summer and autumn recording periods respectively. Thus the maximum water depth at the site would be 4.84 m. In order to test the pods to their maximum working capacity a water body of ca. 5 m depth was thus required.

The pods were mounted on a boom and connected to the data logger, which was programmed to display output voltage directly via an internal LCD screen. The boom was then taken to a pond in a local park, a 30 m tape attached and the boom lowered into the water. At 0.5 m increments both pressure and depth were recorded, down to a depth of 5 m. The results of this calibration were plotted, and are presented in Figure 4.46.

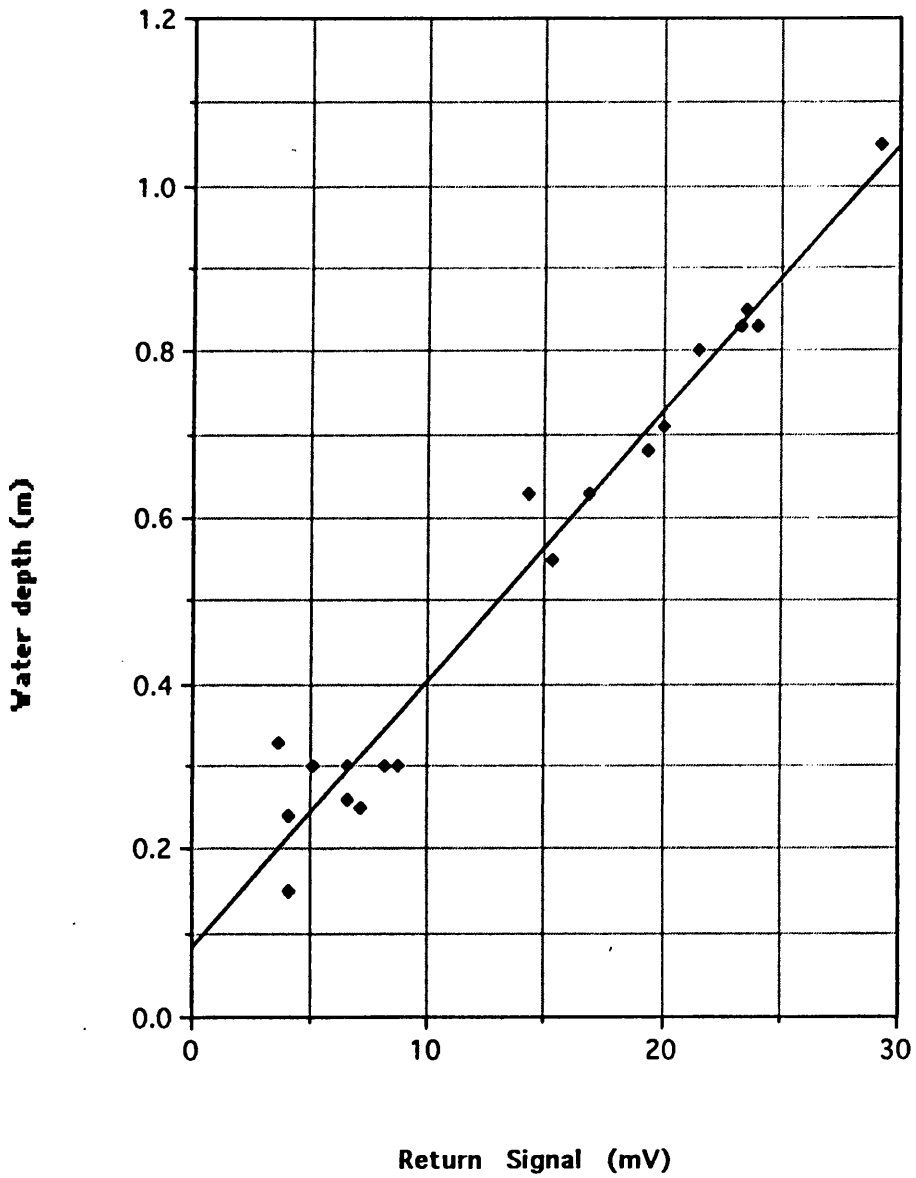
Once calibrated, the pods were deployed during May 1991. The data from the data logger was downloaded onto a BBC microcomputer, and stored in disk form. Output from the data storage file was in printed form, which was transcribed to Macintosh format for subsequent analysis.

Figure 4.47 shows the raw data output from 23/05/91, displayed as return voltage from both transducers simultaneously against time. A series of 5 major wave forms with a periodicity of approximately 11 seconds can be identified at this early stage in the analysis and it is immediately obvious from the peaks of the trace that the return signals are slightly out of phase, suggesting incident wave approach was not exactly shore normal at this time. Additionally, a series of secondary wave forms can be identified from this trace, becoming obscured by the larger waves towards the end of the record as the periods of the two wave trains become increasingly in-phase. The potential information forthcoming from the trace in this raw state revealed that even over such a short timespan full analysis of the plots would be worthwhile.

The final stage in the manipulation of the data was to convert the return signal from voltage to equivalent water depth, and to measure the phase difference between the peaks of the waves. It was found most convenient to measure the phase differences directly from the raw data due to the relatively small amount of data involved. For larger data sets some means of automatically measuring the phase difference would need to be developed.

Wave heights measured over 19 days by the wave recorder are shown in Figure 4.48 as a frequency histogram. The data shows a strong positive skew with a

Pressure transducer calibration curve



$y = 8.2894e-2 + 3.2180e-2x \quad R^2 = 0.964$

Figure 4.46 Calibration curve used for the pressure transducer

Wave Recorder Raw Data 23/05/91

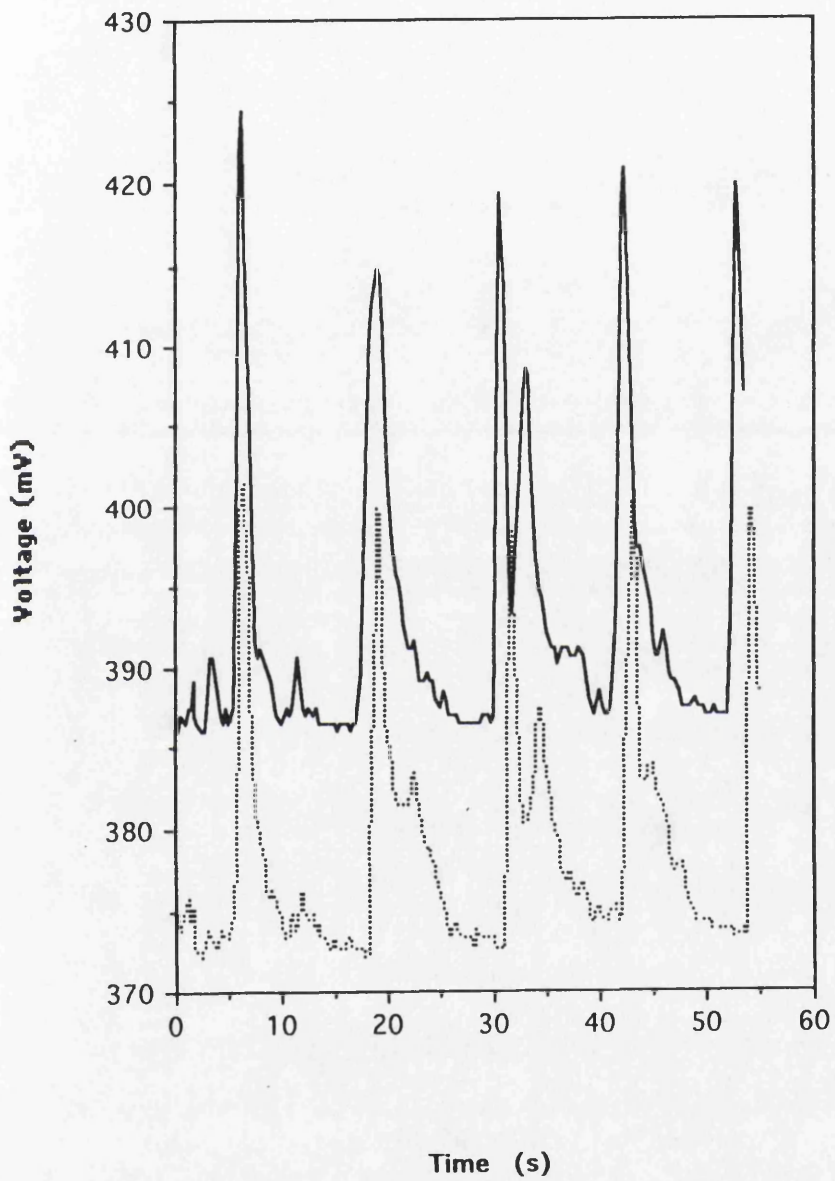


Figure 4.47 Raw data from the wave recorder

Wave recorder-frequency of recorded wave heights

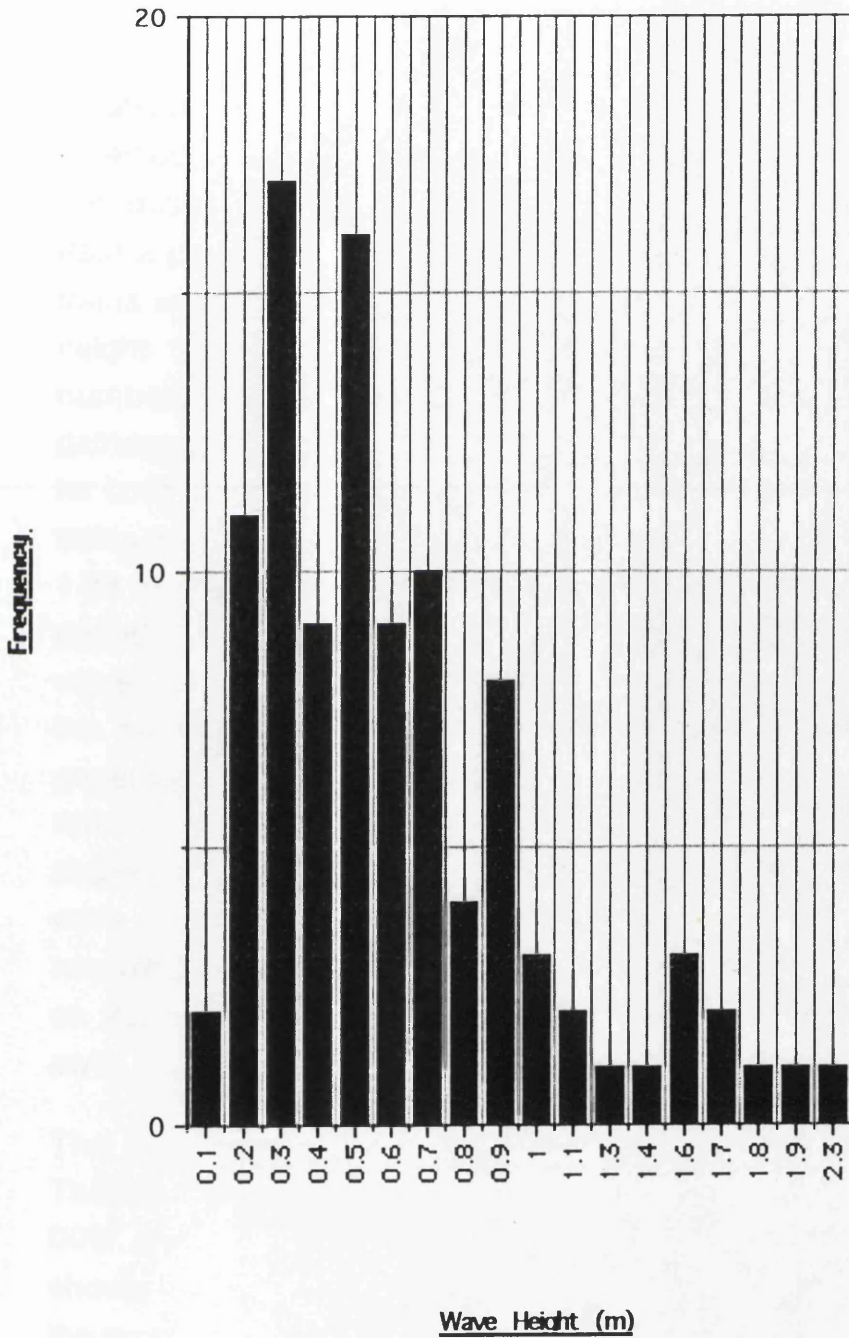


Figure 4.48 Frequency histogram of wave heights: wave recorder

marked bimodal peak height at 0.3 m and 0.5 m. Only 15% of the waves recorded equalled or exceeded the annual modal wave height recorded by Beatrice 'A', and 55% of the waves recorded were 0.5 m or under in height. The maximum individual wave height recorded was 2.3 m on 30/5/91.

As the data set was so small each wave could be measured individually, providing a record of the height, period and angle of approach for the total recorded record. From this it was a simple matter to identify recurring values of height/period/incident angle combinations, and from this to assign each wave to a particular wave train. While the effects of wave interference (both constructive and destructive) complicated this task slightly, it was usually apparent to which train a particular wave belonged. Of the 9 records, 6 showed converging wave trains which were assigned as either 'major' or 'minor' according to mean wave height. Over the recording period 2 simultaneous wave trains was the maximum number noted on any day. Table 4.11 summarizes the wave information gathered over the 9 day record, showing wave height, period and incident angle for both major and minor wave trains on each recording day. The highest wave trains were recorded on 23/05 and 30/05, with mean wave heights of 1.47 m and 1.33 m respectively. However, while the wave train on 23/05 exhibited a long period (10 s) and incident angle of  $003^\circ$ , identifying it as a true ground swell, the waves recorded on 30/05 displayed a much shorter period (3.18 s) and despite the height and incident direction ( $018^\circ$ ) were thought to represent waves generated by onshore winds. This idea was supported by the minor wave train arriving simultaneously, which displayed a similar height (0.9 m) and incident angle, but with a slightly longer periodicity (7.68 s), again suggesting that these were onshore wind-generated waves. Only twice during the recording period did any recognizable trends in westerly waves appear. The ground swell recorded on 23/05 was accompanied by low (0.11 m) waves from  $357^\circ$ , and on 27/05 no swell was visible but the arrival of 0.37 m high waves from  $322^\circ$  was recorded.

The angles between the incident wave crests and the shoreline are plotted in Table 4.11. This shows a dominant trend in waves approaching from the  $000^\circ$ - $005^\circ$  sector, with 24% of all readings in this sector. The remainder of the data shows a predictably narrow spread due to the sheltering effect of the Firth from the north and north-northwest, and the severely fetch limited western sector. This can also be seen by plotting the data as a rose diagram (Figure 4.49).

n = 101

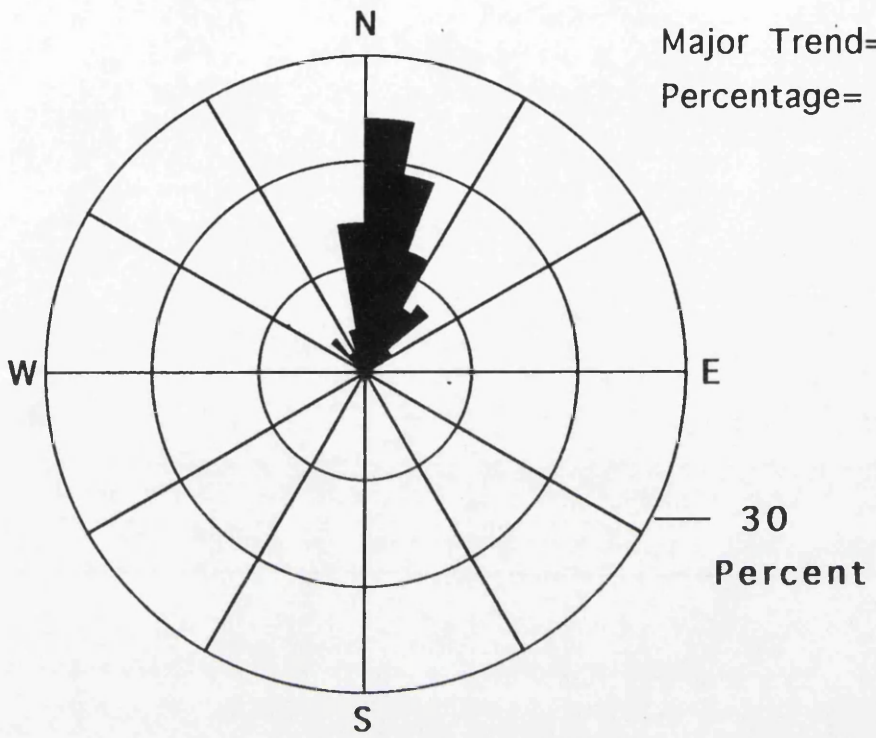


Figure 4.49 Rose diagram of wave directions: wave recorder

It might be expected from both the wave recorder data and the records of waves from sites around the Moray Firth that two sets of waves could typically be identified as arriving at Culbin:

- i) higher, longer period swell waves generated outside the Firth;
- ii) lower, short period waves generated by local winds.

In order to test this hypothesis the wave recorder data was plotted as wave height against incident angle, and is presented in Figure 4.50. Negative incident angles indicate wave approach from the west, positive angles from the east. A total of 75.3% of all waves recorded approached from the 0°-080° sector, and 17.8% approached from the northwestern (310°-000°) sector. The remainder of the waves (6.9%) approached shore-normally. The plot demonstrates a limited spread of incident angles recorded from waves in the 1-2 m height range, with all waves in this range approaching from the 0°-30° sector. Smaller waves (0-1 m high) were found to approach from all available approach angles (310°-080°). This suggested the existence of an "energy window" caused by the alignment of the Firth. Only swell from specific directions is able to enter the Firth from the North Sea, whilst waves generated by onshore winds approach the Culbin foreshore from any onshore sector.

The wave height distribution measured by the transducer array showed a considerably lower modal height (ca. 0.5 m) than the data from the other wave sources referred to so far (1 m). While this was probably due to the short sampling period (9 days), the data clearly shows that *locally generated wind waves* are an important factor to consider within the total energy budget received on the Culbin foreshore.

#### **4.2.1.8 Global Wave Statistics (BMT, 1986)**

The data obtained from Beatrice Alpha was used to obtain values for height and periodicity of swell waves at Culbin. However, as the direction of swell was not recorded, the data could not be confidently resolved into discrete incident sectors. While a strong correlation was noted between windspeed and wave height (Figure 3.10), the generation of swell in the North Sea does not necessarily correlate with wind directions recorded within the Moray Firth. Thus the data on wave direction frequency derived from Global Wave Statistics (BMT, 1986) was used as an alternative source of directional data.

Culbin :- Angle of Wave Approach vs Wave Height May 1991.

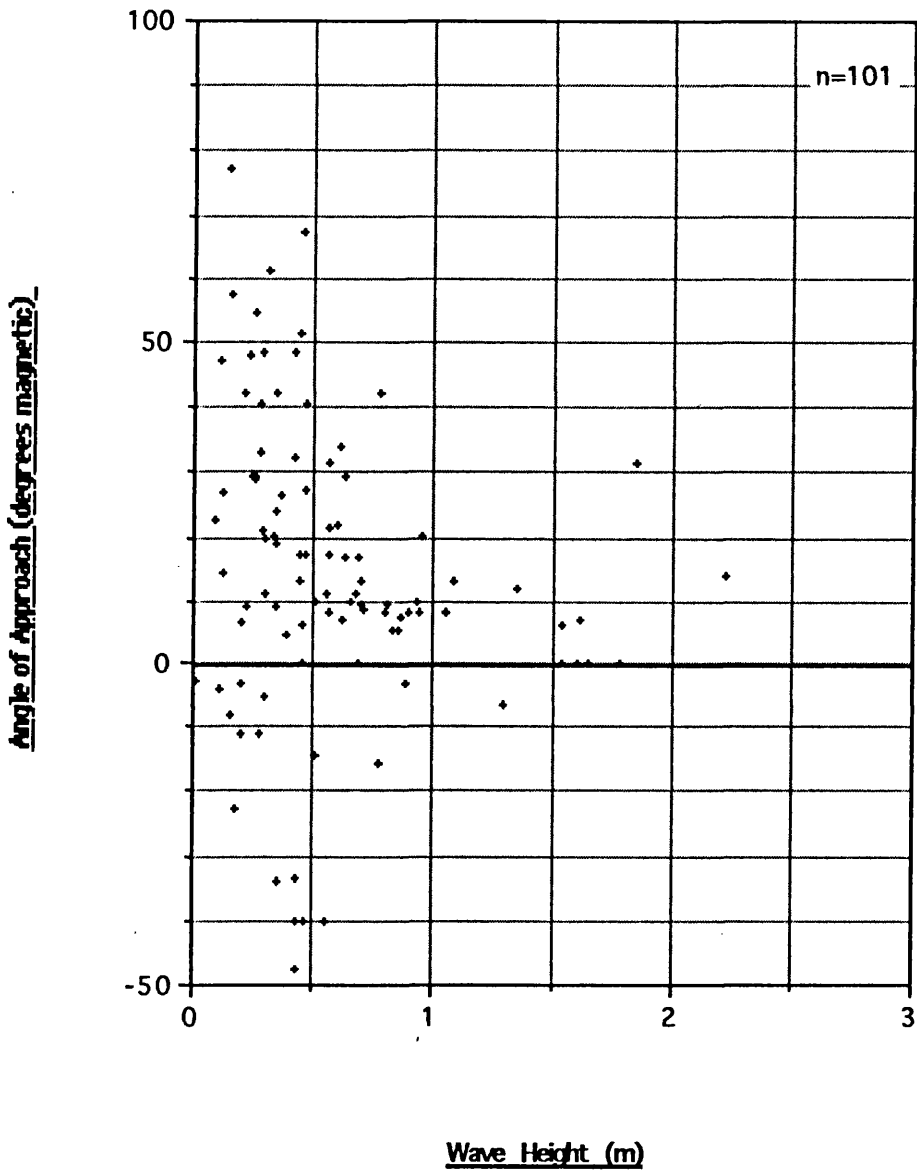


Figure 4.50 Plot of incident ave direction and height: wave recorder

Manipulation of the data from Global Wave Statistics (BMT, 1986) (Chapter 3) produced Table 4.12 below, which shows the proportion of Hs<sub>70</sub> and Hs<sub>30</sub> conditions from each of the approach sectors at Culbin by season, plus the annual breakdown of frequencies.

	N	N	NE	NE	E	E
	Hs <sub>70</sub>	Hs <sub>30</sub>	Hs <sub>70</sub>	Hs <sub>30</sub>	Hs <sub>70</sub>	Hs <sub>30</sub>
SPRING	80.1	19.9	75.7	24.3	69.9	30.1
SUMMER	67.5	32.5	86.4	13.6	84.9	15.1
AUTUMN	72.4	27.6	68.2	31.8	65.3	34.7
WINTER	72.3	27.7	65.3	34.7	74.7	25.3
ANNUAL	79.3	20.7	75.4	24.6	82.4	17.6

Table 4.12 Proportion of waves from each major direction at Culbin, by season.  
(source: BMT, 1986)

Of the total wave field for the North Sea, swell from the N-NE-E sectors accounts for 29% of the total wave year (BMT, 1986), and represents the proportion of the swell wave record which could be incident on the coast at Culbin given the alignment of the Moray Firth. This leaves 71% of the "swell wave year" absent from the coastal wave record at Culbin. However, the incidence of locally generated wind waves is also an important input which must be considered. Winds from the sector 105°-225° (i.e. offshore) were counted as calms for the purposes of this analysis. Winds in this sector accounted for 35.3% of the total wind record derived from RAF Kinloss during 1990, this record providing a typical set of wind speeds and directions for the area. 12.9% of winds blew from the N-NE-E sector, which provided a problem in the calculation of wave generation unless it was assumed that these winds were coincident with swell from the same direction. This would have led to a minor underestimate of wave heights from these sectors, which should be considered when the final sediment budget is calculated.

The remainder of winds, from the sectors 225°-000° were counted as potentially wave-forming, accounting for 51.9% of the total wind year. The proportion of winds from these directions are displayed in Table 4.13.

SECTOR	SPRING %	SUMMER %	AUTUMN %	WINTER %
240	31.1	20.8	24.5	34.7
270	10.3	14.6	11.0	11.5
300	2.6	5.7	11.5	5.9
330	1.4	4.2	6.0	7.5
<b>TOTAL</b>	<b>45.4</b>	<b>45.3</b>	<b>53.0</b>	<b>59.6</b>

Table 4.13 Proportion of wave generating winds by season recorded at RAF Kinloss during 1990

Incident winds from these sectors travels over a limited water body width, and as such generates only low amplitude waves. Table 4.14 shows the direction of incident winds divided into sectors for analysis, along with the maximum fetch length and the maximum wave parameters generated based upon total wind hours recorded monthly at RAF Kinloss.

Direction (deg)	240	270	300	330
Max. Fetch (km)	27.53	21.75	19.50	21.00
Wave period (s)	3.5	3.4	3.3	3.4
Wave height (m)	0.75	0.69	0.63	0.69

Table 4.14 Wave parameters generated from onshore winds at Culbin (excluding those coincident with swell)

Little difference exists between the height or periodicity of wind waves generated from any of the N-NW sectors. The maximum wave height generated by onshore

winds using this method is 0.75 m, which coincided with the longest predicted period of 3.5 s.

Table 4.15 provides a summary of the combined wind and wave frequency data used as input into the wave refraction exercise. The residual between the total swell and wind wave frequencies was assumed to represent calm conditions.

	Wave (%)				Wind (%)					Calm
	N	NE	E	Total	240°	270°	300°	330°	Total	
Spring	6.4	11.7	6.0	<b>24.1</b>	31.1	10.3	2.6	1.4	<b>45.4</b>	30.5
Summer	6.8	8.3	3.6	<b>18.7</b>	20.8	14.6	5.7	4.2	<b>45.3</b>	36.0
Autumn	4.9	7.3	4.1	<b>16.3</b>	24.5	11.0	11.5	6.0	<b>53.0</b>	30.7
Winter	4.3	6.3	4.7	<b>15.3</b>	34.7	11.5	5.9	7.5	<b>59.6</b>	25.1

Table 4.15 Summary wave and wind frequency data at Culbin

Once an appropriate set of wind wave heights had been selected, it was next necessary to calculate the transformation in wave height undergone during the simulated shoaling process using equations shown in Chapter 3. This was undertaken to maximize accuracy in the input of final wave heights to the calculation of longshore sediment transport. This manual calculation was not necessary for incident swell waves being calculated automatically as part of the WAVENRG program. The final wind wave parameters are shown in Table 4.16. These waves could not be differentiated into low or high energy regimes as their generation was fetch limited, and were input into the final calculation as single wave heights for all conditions.

#### 4.2.1.9 Graphical refraction of wind generated waves

As wind generated waves were not run on the program WAVENRG, these waves were generated graphically. The angles between the wave crests and the coast were measured by hand, the breaking wave heights were calculated, and are shown in Table 4.16.

Sector (°)	T(s)	Ho(m)	H <sub>b</sub> (m) Cell B1	H <sub>b</sub> (m) Cell B2
240	3.5	0.75	0.54	0.51
270	3.4	0.69	0.52	0.37
300	3.3	0.63	0.66	0.51
330	3.4	0.69	0.73	0.73

Table 4.16 Wind generated breaking wave heights corrected for refraction. Cells B1 and B2 refer to wave refraction cells on the beach reported below.

Having calculated the wave heights at breaking and the angle between the breaker crest and the coast, a value of  $P_L$  could be calculated (Chapter 3). Table 4.17 shows the results of these calculations.

Sector	$P_L$ B1	$P_L$ B2
240	-151.2	-228.1
270	135	-154.6
300	44.5	-259.4
330	294.7	-155.6

Table 4.17  $P_L$  values derived for wind waves at Culbin: note negative values indicating easterly transport (values in  $J m s^{-1}$ )

These values were used as input to the final sediment budget calculation in conjunction with the values of  $P_L$  derived from the computer simulation exercise.

#### 4.2.1.10 Wave refraction modelling using the computer programme WAVENRG

Section 4.2.1.6 described the swell wave parameters to be used as input data for the wave refraction program WAVENRG. The program produces output in the

form of diagrams of wave orthogonals, and also calculated the longshore component of wave power ( $P_L$ ) for each orthogonal. The calculation of  $P_L$  uses the parameters derived by Komar & Inman (1970), and is consistent with the remainder of calculated  $P_L$  values in the exercise. As wind generated waves from the western sectors were not run on WAVENRG, values of  $P_L$  were obtained by graphical means, and input directly into the final calculation. The method employed is described in Chapter 3.

An example of a wave orthogonal plot is shown in Figure 4.51. The plot allows a visual assessment of the status of wave energy distribution along the coast. Zones of converging orthogonals implies a focussing of wave energy, defining areas of potential erosion, while diverging orthogonals show a spreading of incident wave energy, implying relative stability or even accretion in these areas.

The problem of crossing orthogonals noted in various other uses of the WAVENRG programme (eg. Fico, 1978) were not encountered during any of the runs made for the Culbin foreshore, making the calculation of incident wave energy at the coast considerably easier. Using the data provided from BMT (1986), the representative wave periods for each combination of incident wave direction, season and energy regime were determined. These are presented in Table 4.18.

The selection of only two cells (B1 and B2) for use in the wave refraction modelling exercise was enforced by the scale at which the program operated. The resolution of the program was such that the seven station/cells used in the measurement of beach profiles could not be discerned. As such, cell B1 refers to the western flank of the Culbin foreshore and Buckie Loch spit (profile stations 5-7), while cell B2 refers to the eastern flank (profile stations 1-4), with the divide mid-way between stations 4 and 5 in the vicinity of Shellyhead bothies. The choice of division into cells B1 and B2 was made on morphological grounds and divergent orthogonals.

The derivation of Table 4.18 allowed the choice of the appropriate set of refraction data to be used as representative of the wave conditions incident on each refraction cell under each combination of season, wave approach and wave energy regime. Once these values had been derived it was necessary to convert these values into a single value of  $P_L$  per cell by season. The swell frequency table outlined in Table 4.15 was used for this. At this point the data generated for wind waves generated from the west was included (Table 4.14), the values obtained being subtracted from the values of  $P_L$  as the easterly

WAVE HT :- 1.00 M PERIOD 8.00 SECS.  
DEEP WATER WAVE APPROACH :- 30 DEGREES



Figure 4.51 Sample plot of orthogonal output from WAVENRG

currents thus generated represent a reversal in the net longshore sediment transport trend. Again the formula derived by Mason (1985) was employed. This calculation produced seasonal values of  $P_L$  in units of  $J m^{-1} s^{-1}$ , shown in Table 4.19.

SEASON	B1	B2
SPRING	207.08	263.50
SUMMER	181.91	187.74
AUTUMN	169.36	128.40
WINTER	134.52	90.67

Table 4.19. Resultant longshore power values ( $P_L$ , in  $J m^{-1} s^{-1}$ ) by season using the simulation program WAVENRG

All values in Table 4.19 are positive, representing an E-W trend in sediment movement under all swell conditions modelled.

The final stage in these calculations was the conversion of the data as  $P_L$  to a representative potential longshore sediment transport rate. Komar & Inman (1970) suggested the relationship between  $P_L$  and a longshore sediment transport rate,  $S_L$ , in units of  $m^3 day^{-1}$ , for input into the sediment budget, was:

$$S_L = 0.77 P_L$$

#### 4.2.1.11 Summary

From this section a range of wave heights, periods and frequencies have been determined for both swell and wind waves incident on the Culbin foreshore. Representative swell wave parameters were found to be combinations of 0.5, 1.0 and 2.0 m in height, and 4, 6 and 8 s period. Wind wave generation is fetch limited, producing waves between 0.63 and 0.75 m in height, with periodicity of ca. 3.5 s. Swell wave frequencies were derived from Global Wave Statistics (BMT, 1986), and wind wave frequencies from wind data recorded at RAF Kinloss. These values will be used in the calculation of the longshore component of the sediment budget which follows the results of examining the characteristics of the Culbin landforms.

#### **4.2.2 Contemporary coastal landforms at Culbin: Introduction**

The arcuate Culbin foreland is fronted by a sandy beach extending from the distal end of the spit at Buckie Loch (NH 971638) eastwards into Findhorn Bay, a distance of 5.5 km. The end of the foreshore is taken to be NJ 026648, at the mouth of Findhorn Bay.

The beach is aligned WSW-ENE, with the curve of the beach accentuated westwards along the length of Buckie Loch spit (Plate 6). Westwards beyond the distal end of the Buckie Loch spit is The Bar, a "barrier beach" attached to the mainland by a saltmarsh neck *ca.* 250 m wide at its narrowest point. The feature consists of a shingle barrier, capped by dunes and fronted by a beach of variable sand and shingle composition. The Bar is orientated SW-NE, extending from NH 911591 northeast to NH 972629, a distance of 7.35 km. Both the spit at Buckie Loch and The Bar can be seen from sequential aerial photography to be extending west, a trend noted in other significant drift aligned features around the middle and inner Moray Firth, such as the present "bar" offshore from Findhorn village (NJ 021656), Whiteness Head (NH 803587), Lossiemouth spit (centred on NJ 245203) and the Speymouth bar (NJ 341658).

The Culbin foreshore is variable in width, with mean beach profile lengths between *ca.* 96 and 218 m as measured on spring tides. Figure 3.1 shows the distribution of beach profile stations along the foreland. The widest profiles are found at the east end of the foreland, and narrower profiles at the western end, with an approximate morphological divide centred on Shellyhead bothies (NJ 007648).

Culbin beach is backed by a variety of aeolian dune features. Some are relict, representing cliffed examples of the stabilized inland dune system, while others are true 'coastal' forms. The differentiation of the dunes once more divides the beach into two zones, with the divide placed at Shellyhead bothies. East of the bothies the beach is backed by high dunes (up to 10 m high) experiencing significant frontal erosion and forming dune cliffs (Plate 7). West of the bothies the dunes are lower, (4 m max.), and while some erosion was evident, (eg between profile stations 5 & 6), the majority of the dunes in this zone appeared stable over the two year survey period (Plate 8).

The upper and lower beach along the Culbin foreland is composed mainly of sand. Shingle storm ridges are absent from all profiles east of Shellyhead

Plate 6

Aerial view westwards along Buckie Loch spit and onto The Bar (left).

### Plate 7

Dune cliffing along the eastern Culbin foreshore (cell B2). The height of the dunes (ca. 6 m) means that vegetation at the surface does not bind the toe or face of the dune, allowing undercutting of the upper dune section. The turning moment created as trees exposed to onshore winds begin to fail (upper right) may exacerbate the problem of recession along these dune cliffs.

A derelict zig zag groyne can be seen in foreground, part of the Forestry Commission's aborted 1968 attempt to reduce dune recession and hence timber loss at Culbin.



### Plate 8

Low, yellow dunes at Shellyhead. Dune retreat has exposed the stumps of trees on the foreshore which were formerly growing in the back beach area. These dunes front a sub-horizontal depression which is below HWST, and has been the site of major breaching and marine intrusion into Buckie Loch spit. No recession was recorded along this section during the study, however.



bothies, but a single, continuous shingle storm ridge extends from profile station 6 to a point 700 m west of station 7 along the western flank of the beach.

#### **4.2.2.1 Sediment samples from the Culbin foreshore**

The foreshore at Culbin is composed mainly of sand, in strong contrast to the relict shingle storm beaches located inland. Scattered shingle was found exposed on the foreshore when sediment levels were low, for example after significant storm events, but rarely exceeded a veneer of a single clast thickness. Occasionally sufficient shingle was delivered to the beach to allow the formation of crude beach cusps, particularly at stations 1 and 2. From station 6 extending west to a location *ca.* 700 m west of station 7 a shingle storm ridge was found backing the sand beach. Sizes of clasts ranged up to a maximum 'b' axis length of *ca.* 50 mm. Apart from these examples, there were no other significant shingle accumulations noted on Culbin beach.

Sediment sampling was undertaken in order to assess whether the dominant effect of longshore transport in association with a proximal supply of fluvial sediment would be to produce a net coarsening or fining of sediment with distance downdrift. The available literature reports both downdrift coarsening and fining (summarized in Nordstrom, 1989).

Sediment samples were collected from nine locations on the foreshore and one from the dunes at Shellyhead. Sampling positions are shown in Figure 3.11. After sieving, the samples were weighed at 0.25  $\emptyset$  intervals and the results plotted as cumulative percentage diagrams. From these diagrams the requisite values were read off and input into the equations described by Leeder (1982). Calculation of the values of the mean, median, sorting and skewness of each of the ten beach samples was undertaken. The results are shown in Table 4.20.

SITE	MEDIAN	MEAN	SORTING	SKEWNESS
FHB	1.51	1.54	0.36	0.12
0	1.70	1.78	0.40	0.27
1	1.65	1.77	0.32	0.27
2	1.80	1.88	0.31	0.46
3	1.55	1.56	0.29	0.33
4	1.35	1.43	0.28	0.48
5	1.70	1.72	0.35	0.11
6	2.05	2.03	0.30	-0.08
7	1.95	1.83	0.47	-0.48
Dune	1.60	1.53	0.31	0.55

Table 4.20 Sediment analysis results - Culbin foreshore

Mean grain size value provides a better estimate of the grain size distribution than the median, as it accounts for the extremes of the distribution of grain sizes in a sample, while the median simply divided the sample about the 50 percentile. However, in the case of the data set generated from the Culbin foreshore the results from the calculation of the median and mean grain sizes produced largely the same results. Figure 4.52 provides a summary of the statistical data presented in Table 4.20.

The highest mean grain sizes are found at the western end of the foreshore at stations 6 and 7 (2.03 & 1.83Ø respectively). The lowest mean grain size (1.43Ø) is found at station 4 east of Shellyhead. West of station 4 a generally rising trend in grain size can be identified from Figure 4.52, with only a slight downturn at station 7. From station 2 eastwards along the foreshore and around into Findhorn Bay a reduction in mean grain size occurs, reaching a minimum grain size of 1.54Ø within Findhorn Bay. The trends identified in the mean grain size distributions are mirrored by the median grain size distribution.

Summary plot of median, mean, sorting and skewness-Culbin foreshore

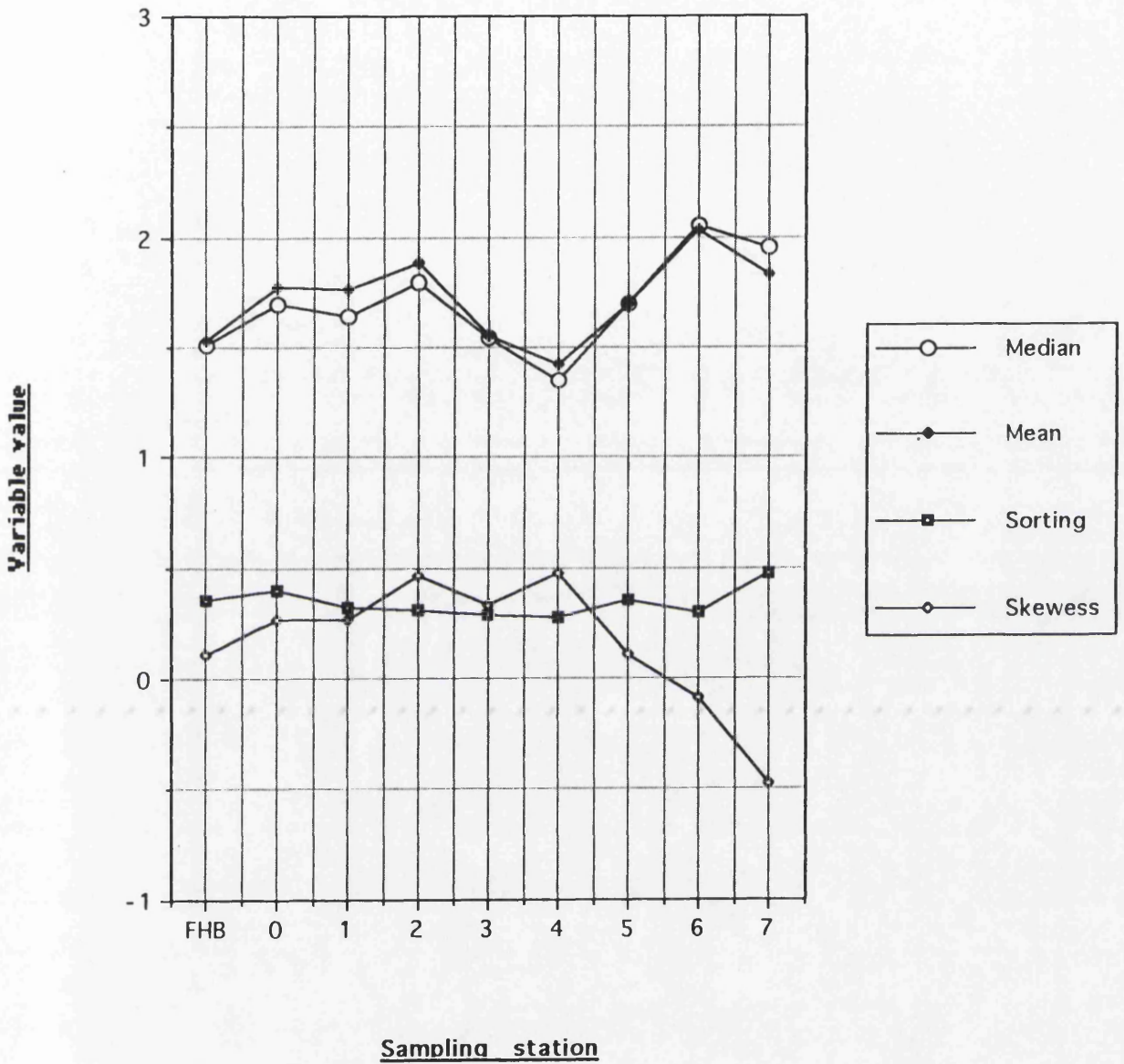


Figure 4.52 Foreshore sediments at Culbin: summary statistics

The values obtained from the calculation of the sorting indices of the samples reveal that all of the sediments collected from the Culbin foreshore fall into the category of well to very well sorted (Leeder, 1982), with all values less than 0.5 $\phi$ . The highest values are found at the eastern and western extremities of the foreshore, in Findhorn Bay, at station 0 and station 7. Even here the greatest value did not exceed 0.47 $\phi$ , representing a well sorted deposit. The remainder of the samples display sorting indices indicating very well sorted deposits (Figure 4.52). The lowest values (highest degree of sorting) occur at the central sampling stations 3 & 4, which display values of 0.28 & 0.29 respectively. A slight decrease in the degree of sorting occurs away from this position both to the east and west, although the values still reflect a very high degree of sorting.

The values obtained from the calculation of skewness indicate that all of the foreshore samples except those from stations 6 & 7 are positively skewed to some degree. While station 6 displays a nearly symmetrical distribution however, station 7 is the only sample which displays a strongly negative skew, suggesting a coarse tail in the sediments at this location. The sharp decline in the nature of the calculated values of skewness west of station 4 is highlighted by Figure 4.52. Stations 5 & 6 display the closest approximations to a normal distribution, station 5 falling into the positive side of the "normal" bracket, and station 6 to the negative side (Table 4.20). Both stations 2 & 4 are strongly positively skewed, suggesting that these deposits contain a large amount of fine material (Table 4.20). Between these stations both station 1 & 3 are also positively skewed, although the degree of skewness is less pronounced at these positions.

To summarize, the distribution of sediment along the Culbin foreshore is characterized by a marked east-west division of sediment characteristics, centred around station 4. West of station 4 the sediments become increasingly skewed towards the coarse fraction, while the degree of sorting decreases. The increasingly negative skew to the data is reflected in the increase in both the median and the mean grain size west of station 4. East of station 4 skewness remains positive, reflecting a higher proportion of finer grained sediment, a feature reflected in the mean and median grain size calculations. However east of station 1 falling mean grain size is accompanied by poorer sorting, with both values reaching a peak at the eastern end of the beach in the mouth of Findhorn Bay.

#### **4.2.2.2 Beach profiles**

Beach profiles were monitored at seven stations over a two year period along the Culbin foreshore. A total of fourteen profiles were measured at each station, with approximately bi-monthly measurements over 1990-91 replaced by monthly measurements made during 1991-2.

Beach profiles were also measured at three locations on The Bar over a summer season in order to gain a first approximation of the characteristics of the foreshore, but were not designed to be used for longer term volumetric calculations, and will be discussed separately.

Profiling positions along the Culbin foreshore and on The Bar are shown in Figures 3.1 and 3.11.

#### **4.2.2.3 Culbin foreshore**

Sweep zone plots for all seven profiling stations are presented in Figure 4.53. Station 1 was the most easterly of the profiling positions used, and is adjacent to the mouth of Findhorn Bay. Profiles measured at station 1 were some of the longest measured on the entire site, reaching 200.05 m.

Figure 4.53 demonstrates a clear division between the upper and lower beach at station 1, with an upper beach length of *ca.* 70 m backing a wide, generally flat lower beach terrace with transitory low amplitude bar features of up to 0.7 m relative relief noted on most profile measurements. A single exception was recorded on 17/03/91, when the lower beach was entirely flat. There was never more than one bar present on the low tide terrace at station 1 during any single profiling period. The maximum vertical displacement range shown on the sweep zone plot on the upper beach is 1.4m, and on the lower terrace 2.1 m.

Station 2 is situated 430 m west of station 1, and displayed the widest beach profiles of all the profiling stations sampled. The single longest profile recorded on the Culbin foreshore throughout the two year monitoring period was on 17/04/91, when a profile length of 401.97 m was exposed at this site. The profile at this station is again sharply divided into an upper and lower beach profile, although the upper profile is slightly shorter than at station 1, with a mean length of *ca.* 60m. The low tide terrace at station 2 is also characterized by low amplitude bar features as at station 1, but the largest bar features noted at this position displayed higher relative relief of up to 1 m. A particular feature of this

profile is a bar feature at the seaward extremity which was not observed to move throughout the duration of the study. The stability of this feature was demonstrated by the presence of a large mussel bed on the bar. Additionally, up to three discrete bar forms were recorded on the terrace as opposed to the single bars at station 1. The sweep zone plot shows a maximum vertical displacement range on the upper profile of 1.4 m, and on the lower terrace 2.2 m (Figure 4.53).

Station 3 is situated 420 m west of station 2, and displays markedly shorter profile lengths than those of stations 1 & 2. The standard profile length calculated at station 3 is only 167.3 m. The beach is again divided into an upper and lower beach profile, with the length of the upper beach at station 3 approximately 55 m in length. The gradient of the upper beach at this point is, however, considerably lower than at stations 1 & 2, and the boundary between the upper and lower beach less distinct. The low tide terrace again displayed ephemeral low bar forms with amplitude up to 1 m, frequently long enough to be traced continuously along the foreshore to station 2, but no further. Mobility of these features was lower than those at stations 1 & 2, with monthly resurveying frequently showing the same bar features virtually unchanged in position, while those on adjacent profiles had altered considerably. The sweep zone plot from station 3 shows a maximum vertical displacement range on the upper profile of 1.3 m, and on the lower profile 2.6 m (Figure 4.53).

Station 4 is situated 500 m west of station 3, and consistently displayed the shortest beach profiles of any of the stations monitored. The standard profile length calculated for this station is only 96.9 m. The beach profiles measured at station 4 display a longer upper beach section than any of those described so far, with a mean of approximately 75 m. There was a narrow low tide terrace present during all of the surveys, but this never exceeded 20 m in width and displayed no bar forms on its surface over the duration of the monitoring period. The effect of this in the field was to produce what appeared to be a short, steep beach profile which on all but the lowest spring tides appeared to descend to LWM without a significant break in slope. The sweep zone plot from this station displays an upper beach vertical displacement range of 1.9 m and a lower beach range of 2.6 m (Figure 4.53).

Station 5 is situated 1400 m west of station 4 and represents a largely constant section of the foreshore fronting the low dune area at Shellyhead. The standard profile length at this point is 121.4 m. The profiles from this station are similar to those at station 4, with a long, steep upper beach section, which owes its form in

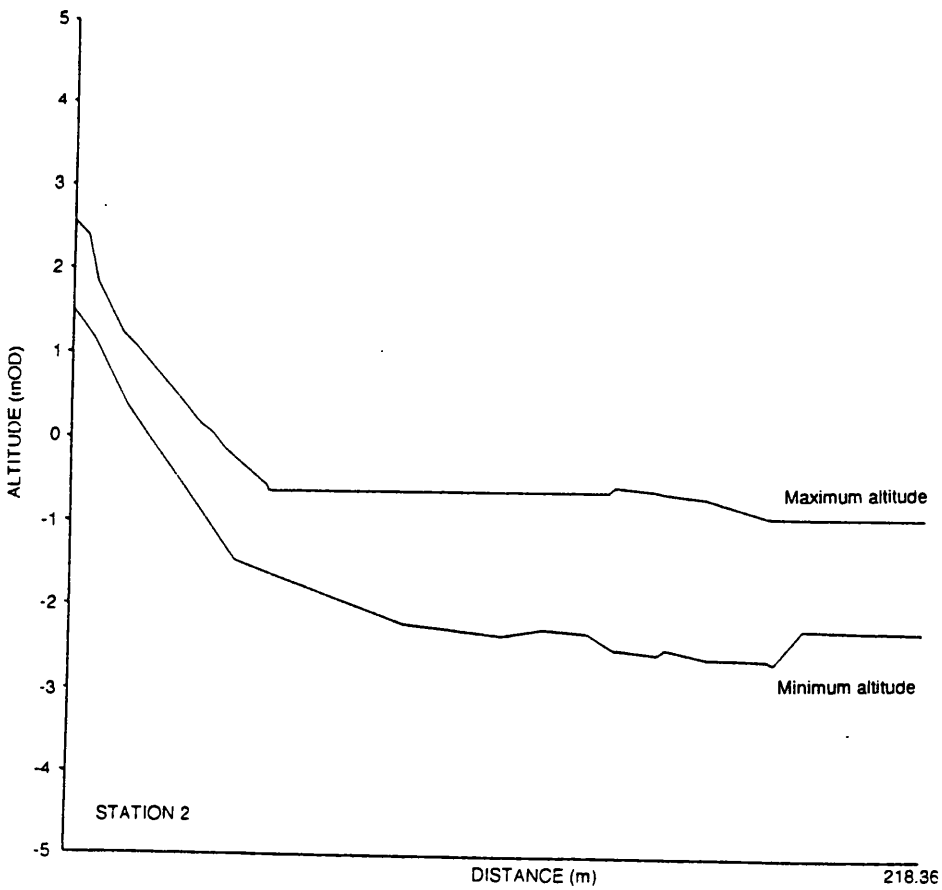
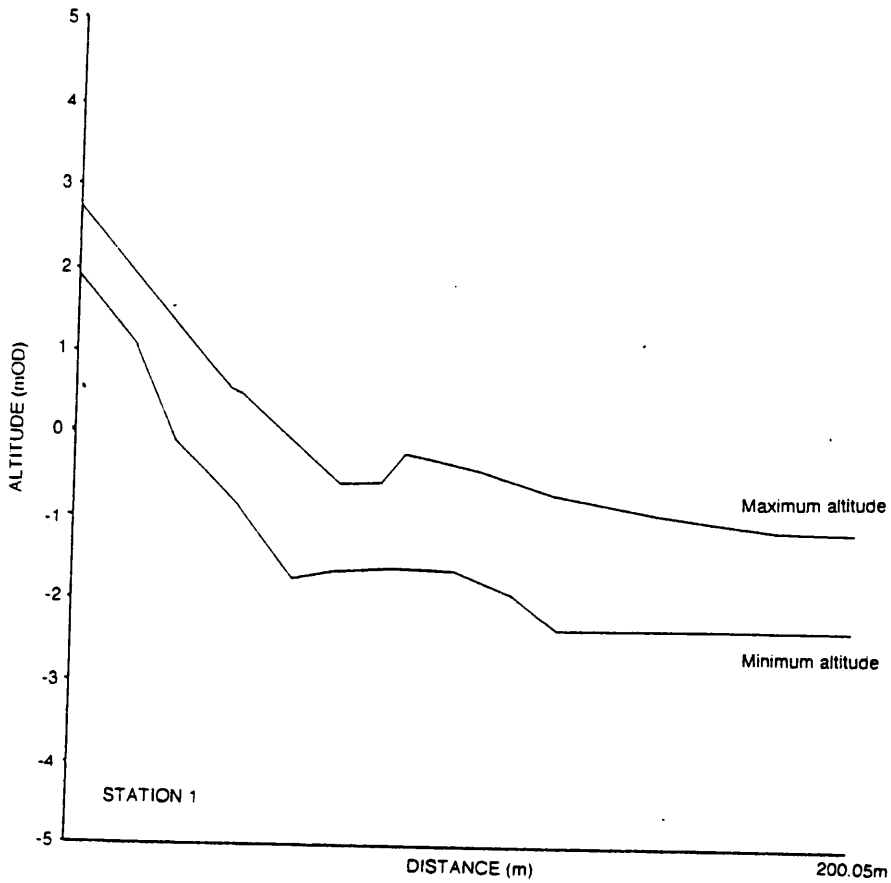
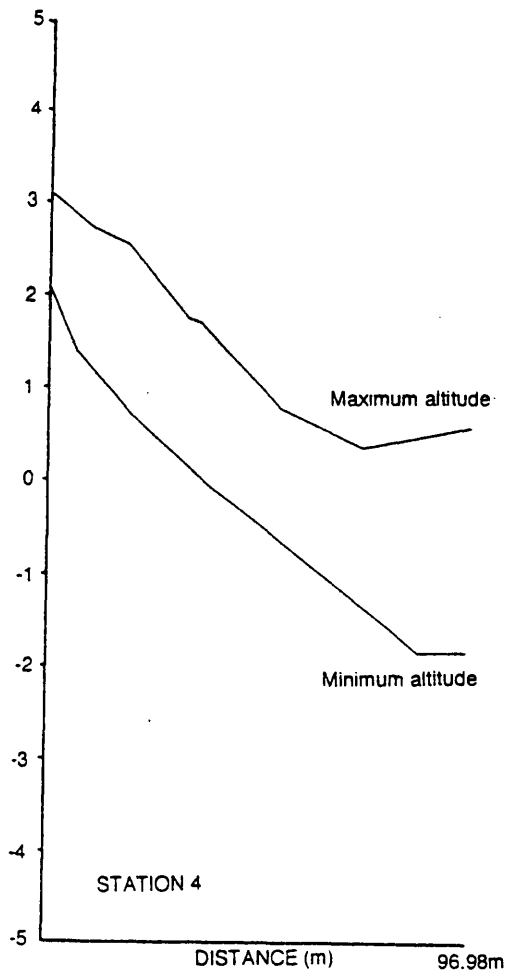
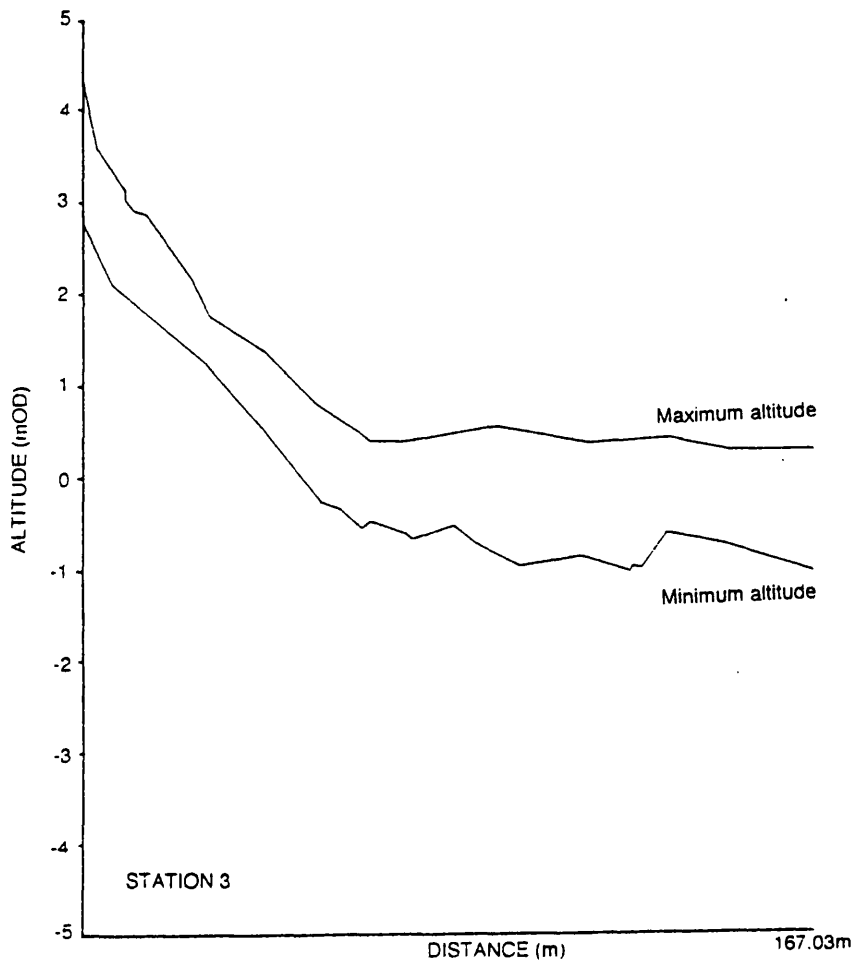
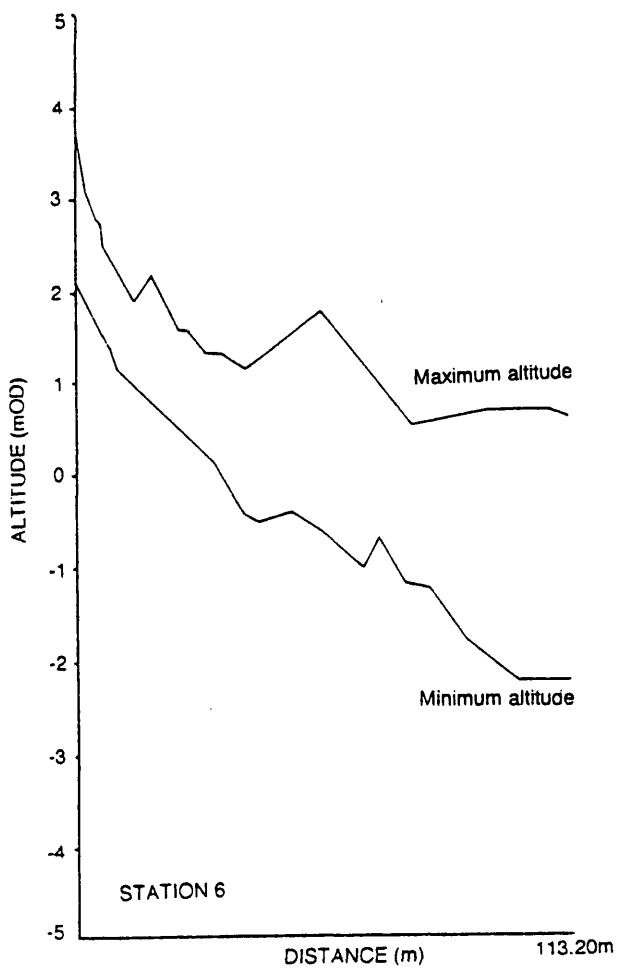
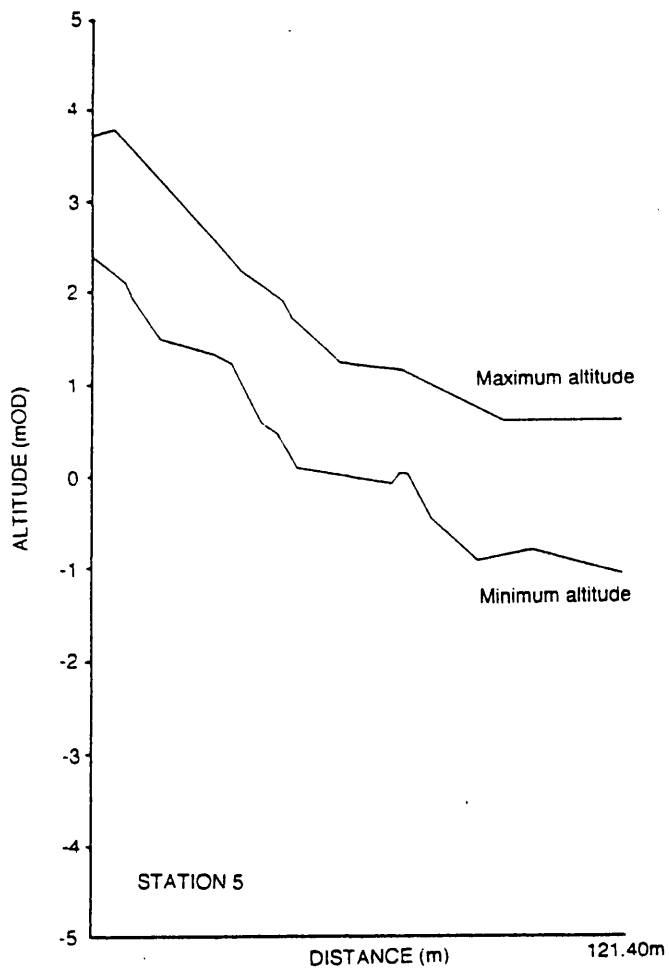
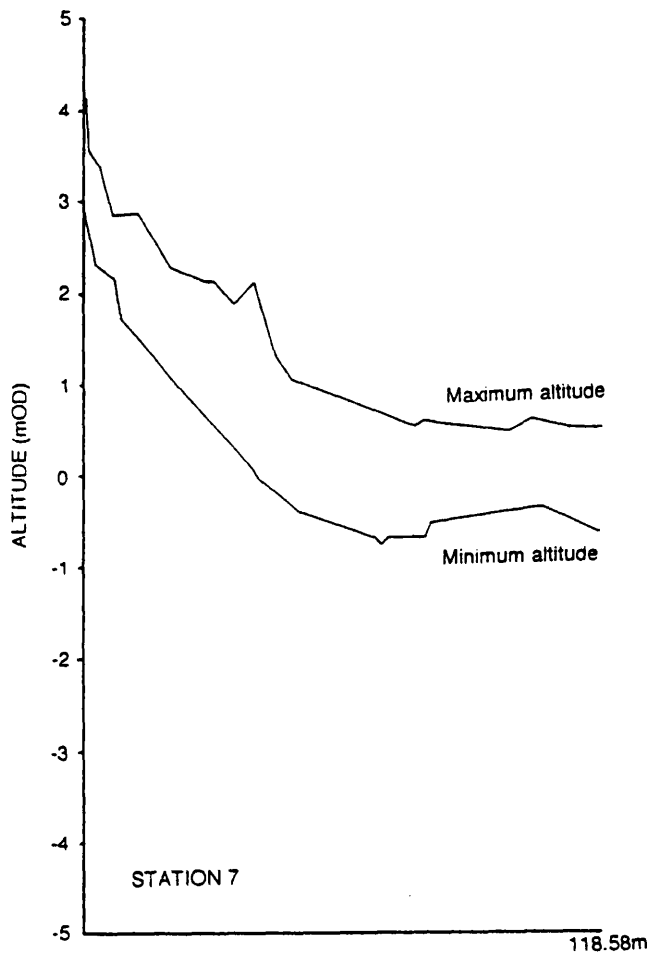


Figure 4.53 Sweep zone plots from the Culbin foreshore







part to a series of backing coastal dunes rather than the dune cliffs of the eastern section of the foreshore. The upper beach at station 5 is approximately 90 m long, fronted seawards by a low tide terrace which intermittently supported bar forms of up to 0.9 m amplitude. These bar forms were noted to migrate across the terrace and on subsequent surveys were observed at positions on the upper beach profile. The degree of bar activity on the low tide terrace at station 5 was relatively low in comparison to the remainder of the profiling stations. Use was made of these measurements when finalizing the site for the wave recorder (Chapter 3). Station 5 was the only position along the Culbin foreshore where this phenomenon was observed. The sweep zone plot from this station displays an upper beach vertical displacement range of 1.8 m and a lower beach range of 3.0 m (Figure 4.53).

Station 6 is located 1000 m west of station 5. Standard profile length at this station is 113.2 m. The profiles recorded from this station are again divided into an upper and lower beach section. The profiles display a marked change from stations 1-5 in that the upper beach is much shorter, with a mean length of 20 m. Additionally, the upper beach is backed by a low shingle storm ridge which appears approximately 40 m east of the profiling station. The remainder of the beach comprises a low tide terrace, characterized by bar forms at a range of scales up to 2 m amplitude, considerably larger than those described at stations 1-5. Up to two discrete bar forms were observed on the profile during any single measurement event. Bars were of such magnitude that frequently tidal water was trapped at the junction of the upper and lower beach creating a long, linear tide pool which could be traced west along the foreshore towards station 7. The largest single bar measured was on 11/10/91, which was 2 m high and 70 m wide at the profiling station. The sweep zone plot from station 6 reveals an upper beach vertical displacement range of 2.0 m and a lower beach range of 3.0 m (Figure 4.53).

Station 7 is situated 1000 m west of station 6, and is the most westerly of the profiling stations. The standard profile length at station 7 is 118.6 m. Reconnaissance prior to the onset of regular beach profile measurement showed that beach profiles beyond this station were essentially the same as those measured at station 7, and so profiles measured at this point were taken as representative of the remainder of profiles further west along the Buckie Loch spit (Chapter 2). The beach profiles measured at station 7 are essentially similar to those from station 6, and the length of the profiles at these stations are virtually identical. A narrow (20 m) upper beach profile is again fronted by a wide low tide

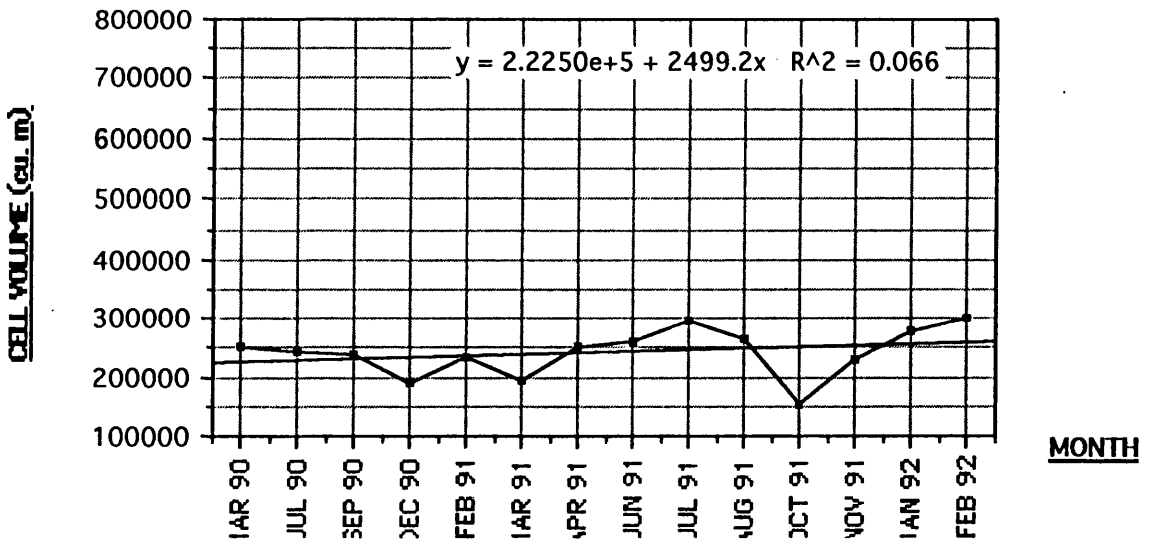
terrace with migratory bar features of up to 1.0 m amplitude. Bars measured at station 6 could frequently be traced along the beach as a continuous feature and would also appear on the profile from station 7. The shingle storm ridge observed at station 6 is more fully developed at station 7, and is approximately 1.2 m high. The height of the ridge varied little over the two year survey period, with a mean altitude of 3.48 m OD. Due to the stability of the shingle ridge backing the profile at this station the upper beach displacement range from the sweep zone plot was limited, and displays a range of only 0.8 m. The lower beach profile was more dynamic however, displaying a vertical displacement range of 2.3 m (Figure 4.53).

The vertical range across which the beach profiles were found in the field was also found to differ between the eastern and western sectors of the Culbin foreland. Stations 1-4 all varied over a maximum range of ca. 5 m, measured between the upper sweep zone foreshore summit and the lower sweep zone terrace foot. At any one time, stations 1-4 varied vertically across ca. 4 m. In contrast, the altitudinal variations at stations 5-7 were higher, ranging between 4-6m across the sweep zone maxima and minima, with the maximum range shown by station 6. However, the total *synoptic* vertical variation was lower, varying across only ca. 3 m.

Having measured beach profiles at seven stations over a two year period, the data was then collated in a computer programme designed specifically to calculate the area beneath the profile for use in volumetric calculations. Once the area of each profile at each recording period had been calculated, the area was multiplied by the length of each cell to provide a volume of sediment in that cell, as outlined in Chapter 3. The cells were assigned numbers 1-7 to coincide with the profile from which the volume was calculated. To re-iterate from Figure 3.11, cells 1-4 coincide with wave refraction cell B2, and cells 5-7 with cell B1. Addition of the volumes from each cell provides a total volume of the Culbin foreshore over the monitoring period.

Figure 4.54 shows the volumes calculated from each cell between 1990-1992, and shows the volumes summed to produce a total beach volume after each measurement was made. Cell 7 displayed the highest volumes, reaching up to  $1.0 \times 10^6 \text{ m}^3$  of sediment contained within the cell. Cell 2, despite having the longest beach profiles, demonstrated the lowest volumes during the study period of  $1.2 \times 10^5 \text{ m}^3$  of sediment. The individual cell volumes are shown in Appendix 9.

### Cell 1 Volumetric Changes 1990-1992



### Cell 2 Volumetric Changes 1990-1992

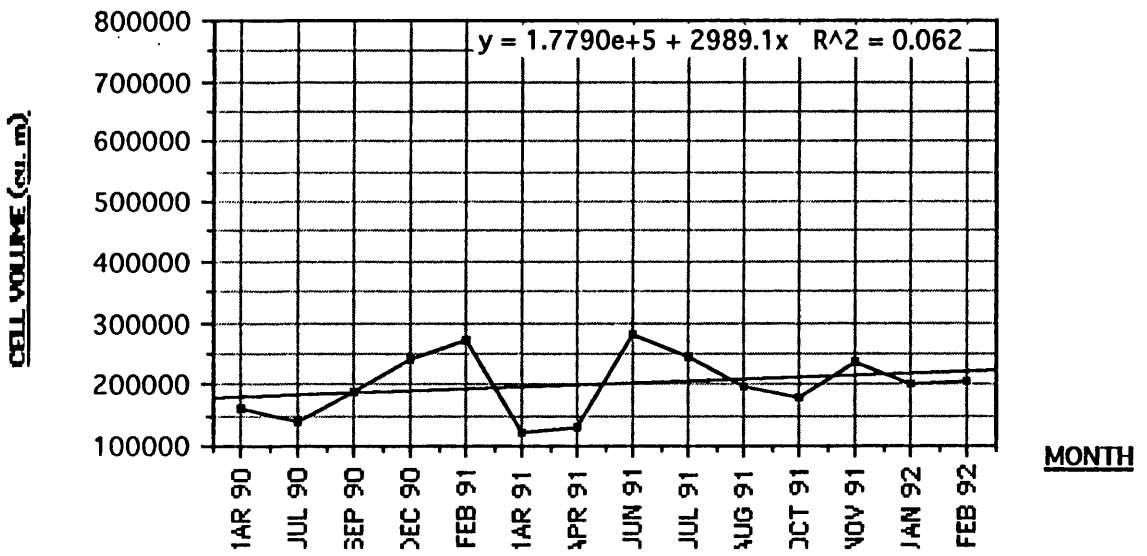
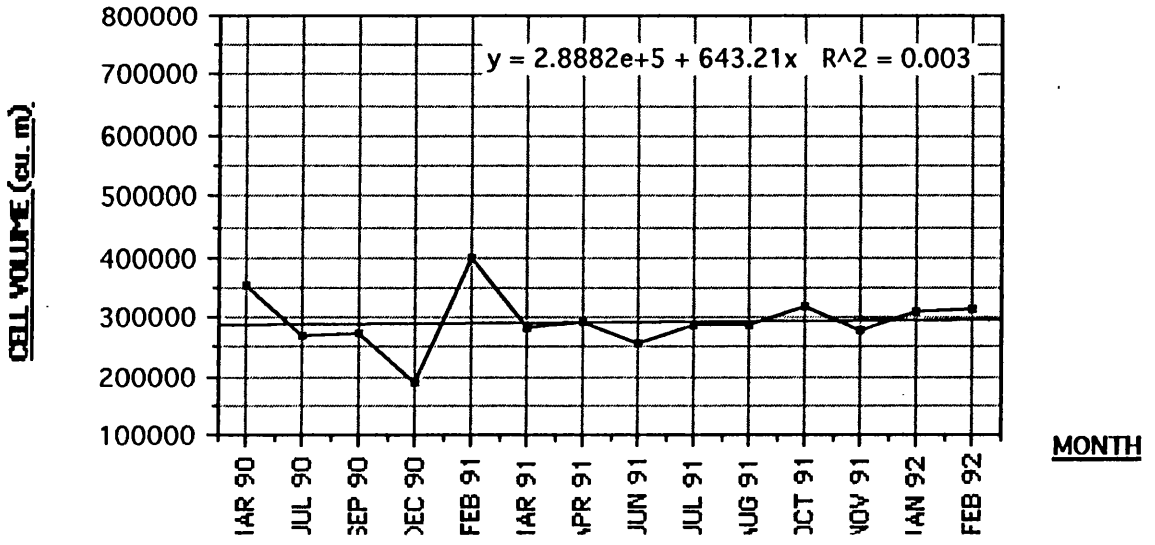
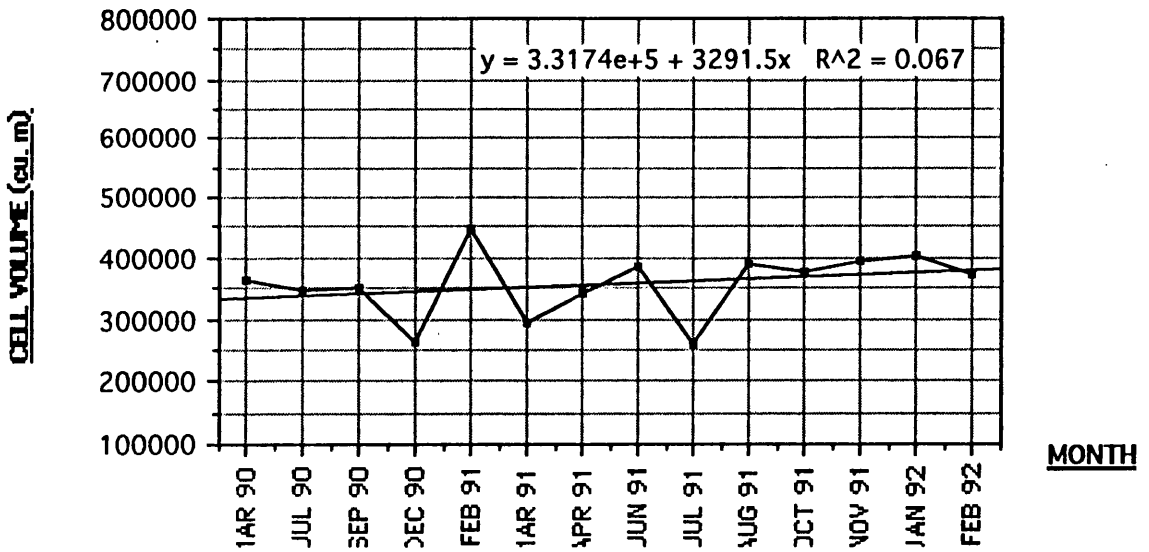


Figure 4.54 Beach volumes recorded at Culbin

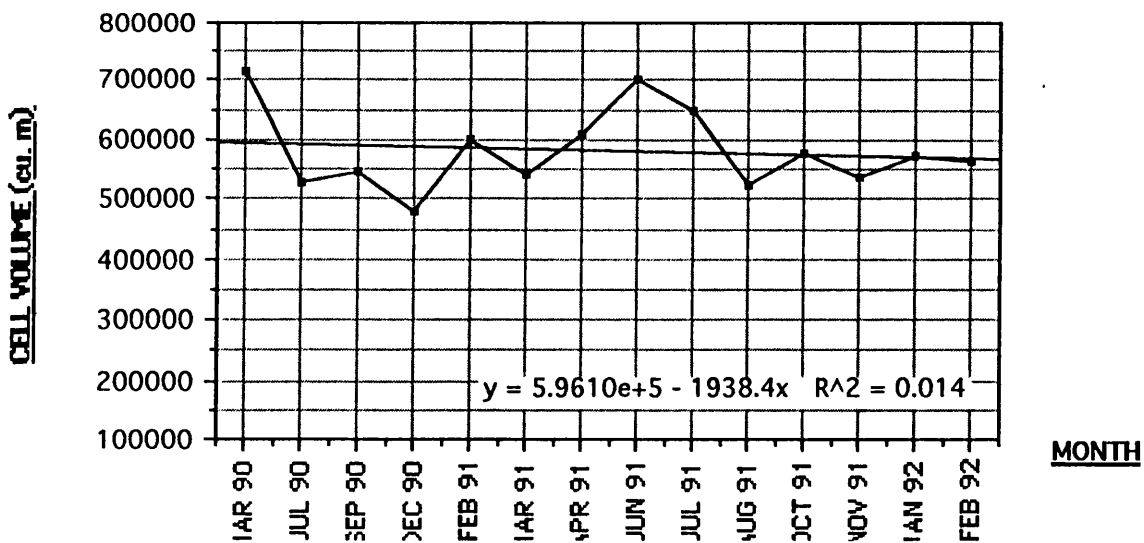
### Cell 3 Volumetric Changes 1990-1992



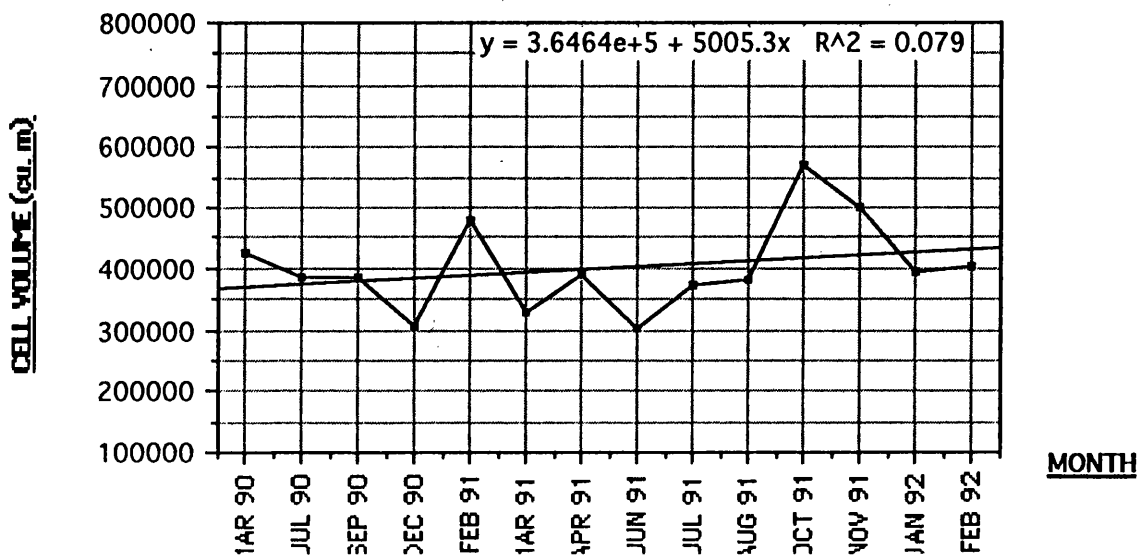
### Cell 4 Volumetric Changes 1990-1992



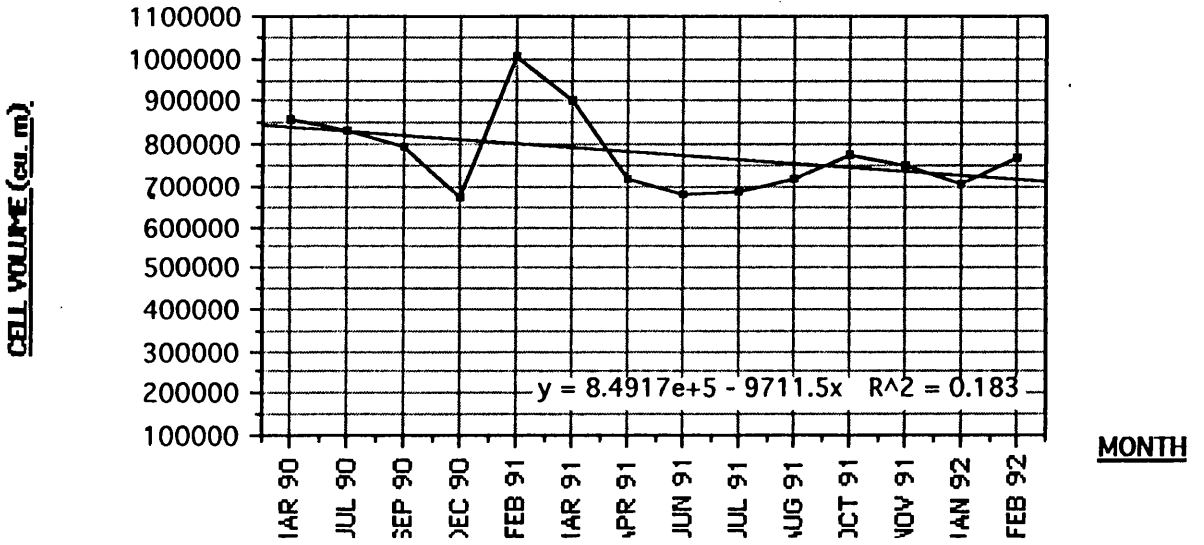
### Cell 5 Volumetric Changes 1990-1992



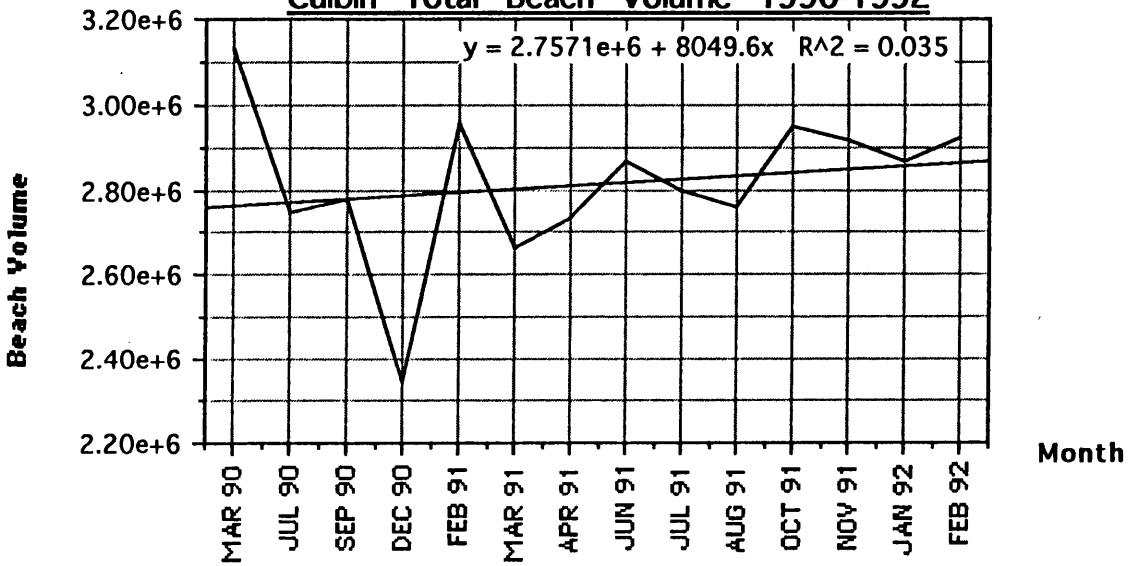
### Cell 6 Volumetric Changes 1990-1992



### Cell 7 Volumetric Changes 1990-1992



### Culbin Total Beach Volume 1990-1992



Fitting a linear regression line to the cell volumes provided an indication of the trend in cell volume over the study period. Only cells 5 and 7 displayed declining trends in cell volume, the remainder displaying a net rise between 1990 and 1992. The lowest beach volume was recorded during 12/90 in most of the cells, but again exceptions to this were cells 1 & 2. Cell 1 did display a reduced volume at this time, although the lowest volume recorded at this cell occurred in 10/91. Cell 2, however, displayed one of the highest volumes recorded in the cell during 12/90, providing a result completely opposed to the remainder of the data, with the lowest volume not recorded until the following March.

The timing of the highest volume recorded in all of the cells differed considerably, and no generalizations could be made regarding this information. Of note was the similarity in the trends in volume displayed by cells 6 & 7, which was to be expected given the morphological similarity of the profiles recorded from these sites. However, the high cell volume recorded in cell 6 during 10/91 effectively reversed the regression fitted to the data, and while cell 7 displayed a falling trend in volume between 1990-1992, cell 6 displayed a rising trend.

Summing the volumes of the seven cells provided an overview of the volumetric state of the entire beach over the period 1990-1992 (Figure 4.54). Fitting a regression line to the data suggests a net gain in sediment volume over the two year period, although this line appears to be heavily influenced by the low beach volume recorded during 12/90 in 6 of the 7 cells. If this anomaly were to be removed the beach volume would be approximately stable over the two year period at ca.  $2.8 \times 10^6 \text{ m}^3$ .

While the individual cells appear to display variation in records of their volumetric changes between 1990-1992, the overall trend in beach volume appears to have remained largely stable. The event which caused the low beach volume during 12/90 clearly had a profound effect on 6 of the 7 cells, stripping them of sediment. While lower magnitude events were recorded in the beach volumetric record at various periods throughout the two years, eg. 06/91, the storms event which caused the low beach levels during 12/90 was by far the most severe in the record. The most severe effects were measured at cell 3, where the volume of the cell was depleted by 35.3% compared to the mean volume recorded over the two years.

#### **4.2.2.4 Echo sounding and offshore beach profile extension**

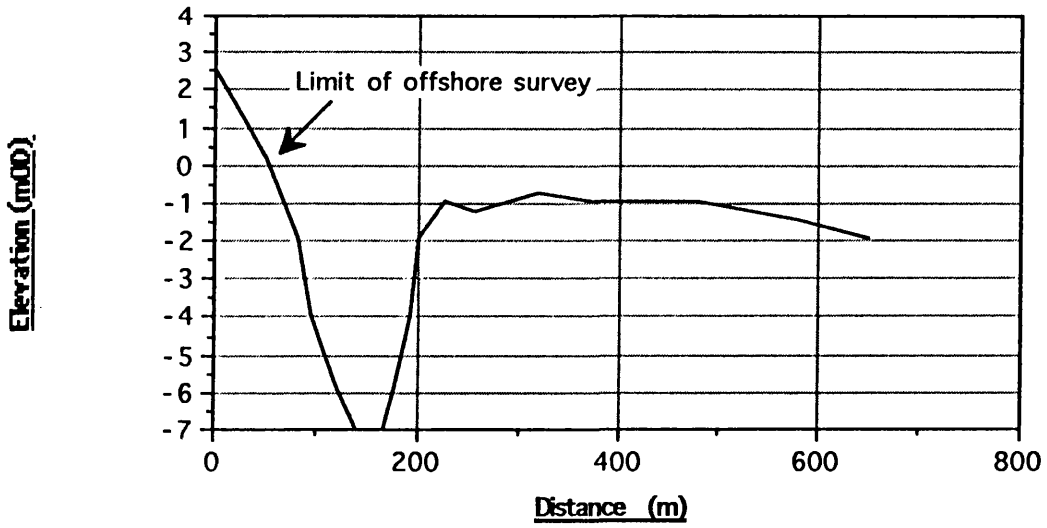
While the beach profiles recorded subaerially were of use in understanding the changes experienced on the beach and in the calculation of a beach sediment budget, it was important to understand the nature of the submarine extension of these profiles. As a synoptic exercise the recording of nearshore submarine profiles at the seven profiling stations along the Culbin foreland was useful, displaying the primary mode of offshore sediment storage in the form of offshore bars. For logistical reasons this was undertaken only once.

Figure 4.55 shows the profiles measured at the mouth of the Findhorn and offshore from each of the profiling stations 1-7. As the runs were made at high water the offshore profiles overlapped with the shore-based surveys, and the limit of the offshore survey is shown. The sub-aerial beach profile is displayed as a mean profile, but due to the length of the offshore survey relative to the beach profile provides little opportunity for detail to be shown on this portion of the plot.

The profile at the mouth of the Findhorn shows a steep drop seawards, crossing the scoured channel at the river exit. The channel depth was at least 6 m deep at this point. Laterally the channel is narrow, *ca.* 110 m across from the Culbin foreshore to the sandbank on the eastern shore. This bank forms part of the bar at Findhorn, and its shallow nature can be clearly seen in Figure 4.55.

Profile 1 displays a flat, shallow offshore zone relative to the other profiles, with a single bar feature 1 m high at 420 m, and a possible second bar at 650 m offshore. The wide, flat nature of the lower sub-aerial profile is continued offshore with little interruption except for two minor bar forms. Profile 2 displayed a more variable offshore topography, with a steep dip seawards from the semi-permanent shingle bar recorded at the seaward extent of the sub-aerial profile. Beyond this three bar forms are displayed on the offshore section at 430 m, 560 m and 710 m offshore at *ca.* -4 m OD, and the profile tends to flatten out with distance offshore. Profile 3 displays a generally flatter, shallower offshore profile than profile 2. Three bar forms are also found on this profile at 300 m, 510 m and 650 m offshore. The outer two features are tentatively linked to the outer bars on profile 2. Profile 4 displays an almost featureless offshore profile, with the end of the sub-aerial profile coinciding with an essentially flat sandy bench extending to 600 m, where a steeper drop in the profile is followed by a minor bar form 0.5 m high at 720 m offshore. Observations made during heavy swell conditions noted waves breaking offshore at stations 1-3 over a bar feature linked to the bar

**Offshore Profile:- River Findhorn Exit Channel and Findhorn Bar**



**Offshore Profile Station 1**

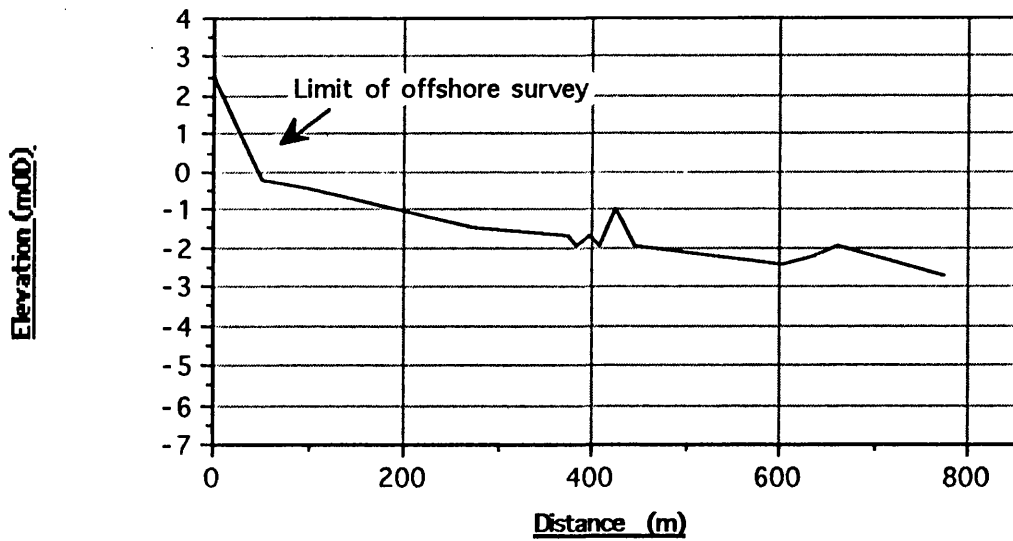
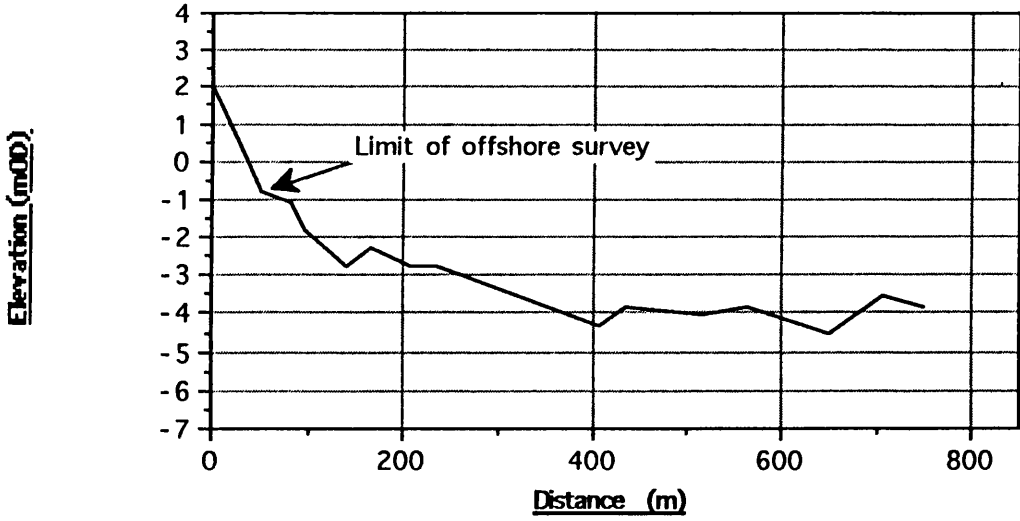
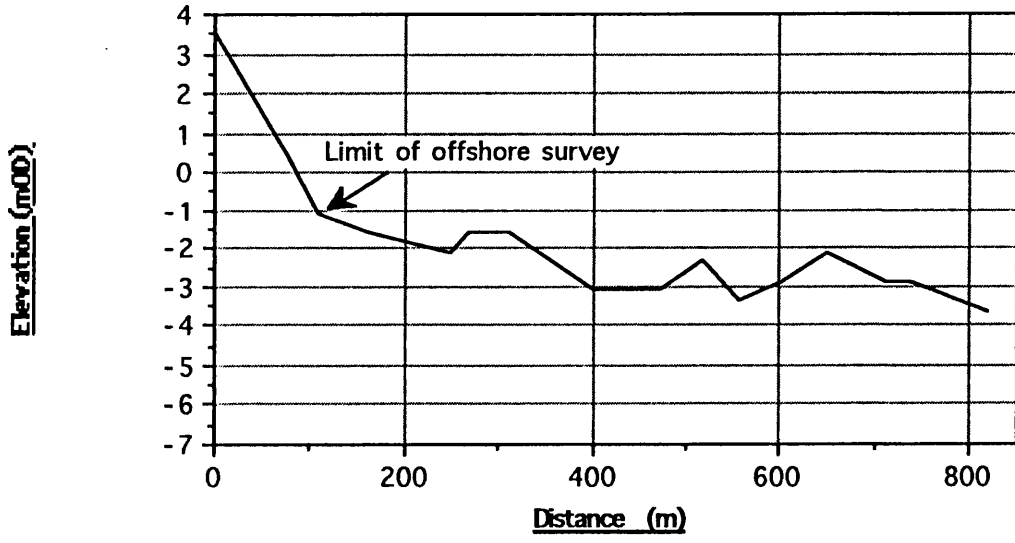


Figure 4.55 Offshore profiles recorded at Culbin

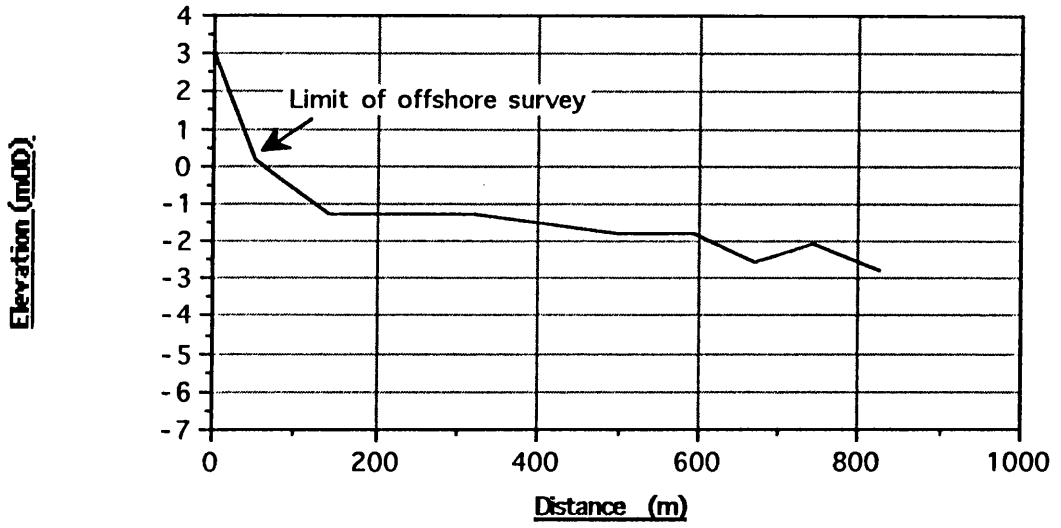
### Offshore Profile Station 2



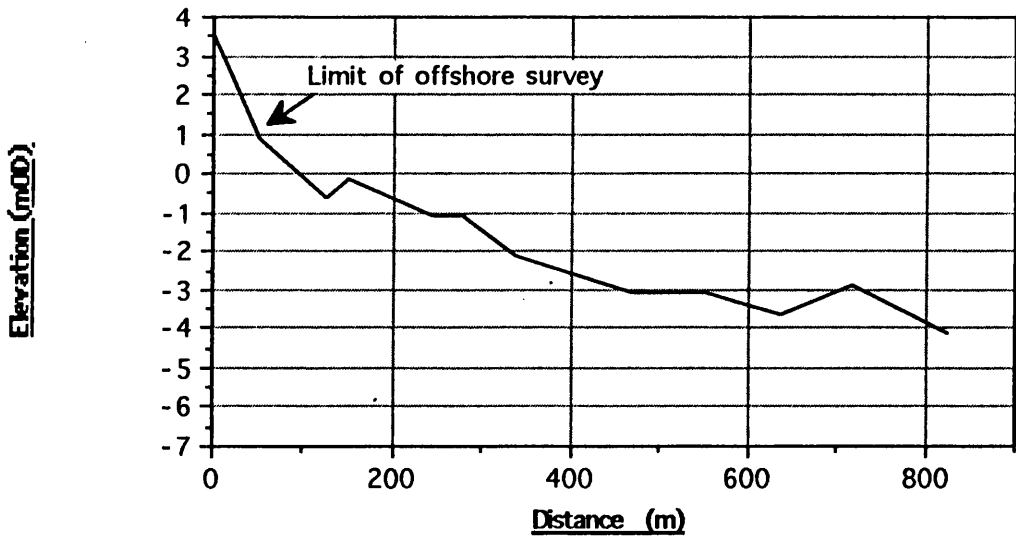
### Offshore Profile Station 3



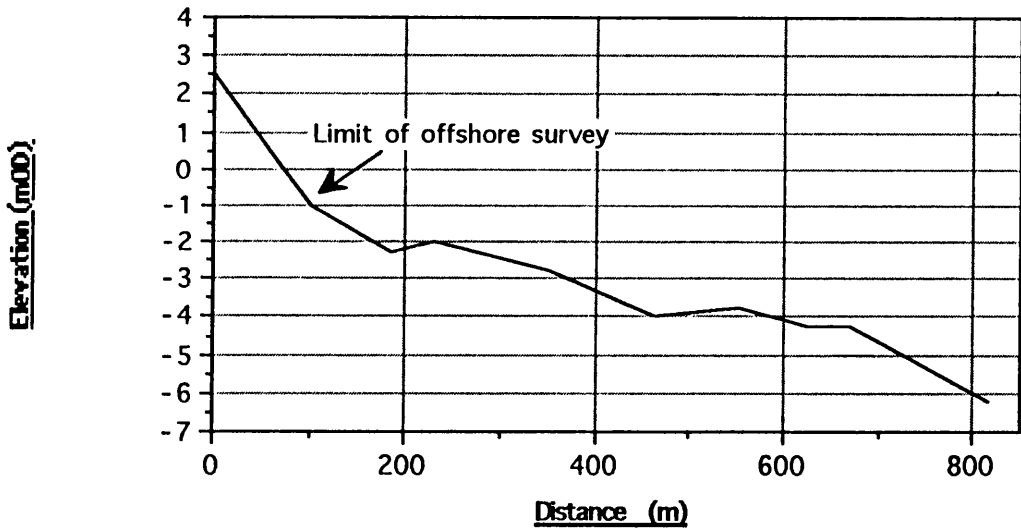
### Offshore Profile Station 4



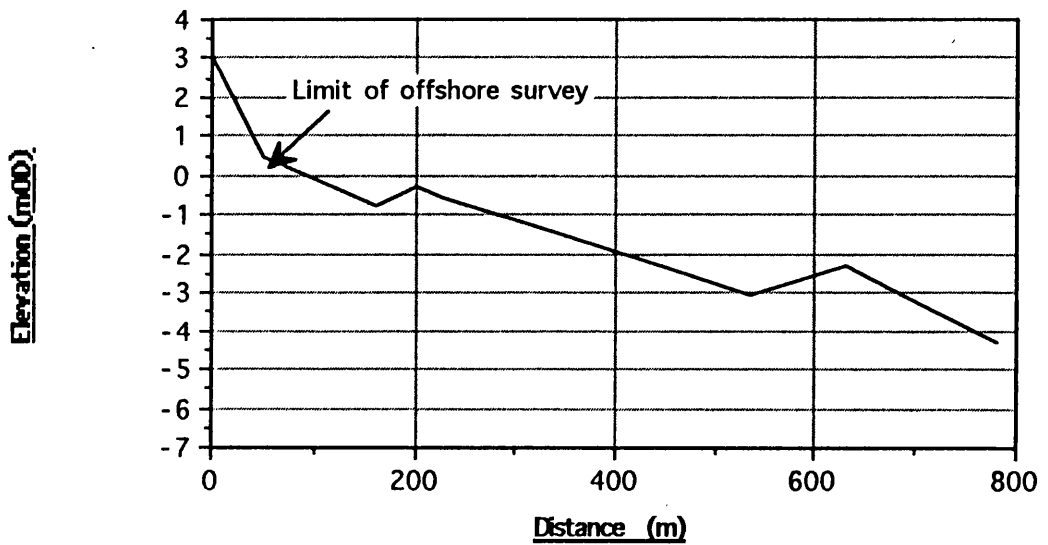
### Offshore Profile Station 5



### Offshore Profile Station 6



### Offshore Profile Station 7



extending across the mouth of the Findhorn. While neither the local Admiralty chart (sheet 233) nor the appropriate O.S. sheet are sufficiently updated enough to mark the extension of the Findhorn bar so far west, it is assumed that the bar features noted on profiles 1-3 at 650 m, 710 m and 650 m respectively represent the westward extension of the Findhorn Bar, and are spatially continuous. This point will be discussed further in Chapter 5.

Profiles 5-7 all display significantly steeper offshore profiles than profiles 1-4, which followed a trend found in the sub-aerial profile. Profile 5 shows a gentle shelf at the seaward edge of the sub-aerial profile, and this continues out to a bar at 170m offshore which is clearly visible from the beach. The profile shelves steeply offshore from this bar, with a second bar form at 720 m offshore. Profile 6 displays two bars, at 230 m and 560 m offshore, and extends to the greatest depth of any of the profiles (minimum elevation ca. -6 m OD). The overall form of this profile is almost flat from the landward point of the sub-aerial profile out to 800 m, a characteristic which is mirrored by profile 7. This profile also exhibits two bar forms, at 200 m and 630 m offshore, and while displaying an essentially straight profile from the top of the sub-aerial profile out to 780 m, is not as steep as profile 6, ending at a minimum altitude of ca. -4.5 m OD. Observation from high dunes at profile station 6 at half tide on 18/03/91 showed the landward bar on profiles 5-7 to be spatially continuous. The seaward (second) bar on each of these profiles appeared at approximately the same distance offshore on each profile, and is tentatively suggested also to be spatially continuous. Limited evidence from oblique aerial photography made during an overflight of the site during September 1992 (Plate 1), coupled with aerial photography from 19/5/89 suggests that continuous offshore bars are a feature of the coast westwards from Shellyhead bothies. This supports the possibility of the seaward offshore bars on profiles 5-7 being linked.

To summarize, profiles 1-4 show a gentle offshore profile gradient, with up to three offshore bar features on the profile. Generally the bars on these profiles are not linked, and represent short features frequently attached to the profile at an oblique angle (Plate 1). Westward extension of the bar at the mouth of the Findhorn exceeds the limits shown on the Admiralty and OS sheets of this area, and is detected on offshore profiles as far west as station 3. Profiles 5-7 show a much steeper gradient than the profiles to the east, with fewer offshore bar features. However the bars on these profiles can be linked alongshore, and are clearly seen to be spatially continuous in Plate 1.

#### 4.2.2.5 The Bar

A somewhat different sedimentary regime exists on The Bar, where the nature of the sediments exerts a powerful influence over geomorphology. Three distinct geomorphic zones can be identified on The Bar:

- i) the NE (proximal) flank (NH 972629-NH 945612);
- ii) the “neck” or central zone (NH 945612-NH 930607);
- iii) the SW (distal) flank (NH 930607-NH 911591).

The NE flank is a narrow (20-70 m wide) stretch of dunes fronted by a wide, (up to 580 m), low gradient sandy foreshore with low amplitude bars. A beach profile surveyed from NH 956622 is shown in Figure 4.56. Examination of deposits on the landward side of the dunes reveals a series of shingle recurves underlying the dunes and recurving strongly from their original southwesterly orientation, often displaying complete 180° reversals (Plate 9). Good examples are found near the bothy at Oldbar (NH 957621), and a series of recurves in this area can be identified from aerial photography (Plate 3, feature 2).

The central zone is characterized by a lack of dunes and generally lower topography. Figure 4.56 shows a beach profile measured in this zone. The beach is considerably narrower than in the NE, and although still composed mainly of sand is backed by a shingle storm ridge with a crest at up to 4.40 m OD. This zone is currently experiencing significant erosion, with outcrops of the back-barrier marsh peat becoming exposed on the rapidly retreating foreshore, itself retreating through overwash processes. During a visit on a spring tide during 08/91, a breach was noted cutting through the east end of the storm ridge at high water in this zone, effectively severing The Bar. This breach was still present during 04/93, suggesting that it had become at least a semi-permanent feature of the neck.

The SW flank differs considerably from either of the zones so far discussed, being composed of a series of shingle storm ridges capped locally by eroding dune fragments. Figure 4.56 shows a beach profile measured in this zone. The lower beach is narrow (*ca.* 50 m max.), and while the lower section is predominantly sand, the majority of the material on the upper beach is shingle. Shingle is also found backing the beach, with the present storm ridge at up to 3.87 m OD backed by a suite of multiple shingle ridges, with 13 sub-parallel ridges backing the bothy at NH 928608. The crests of these ridges are slightly

Plate 9

Shingle recurve on the landward side of The Bar. This ridge displays a complete 180° recurve, with the distal tip now facing east. Note subsequent saltmarsh accretion which has obscured the lower section of the ridge, leaving only the crest exposed above HWST.

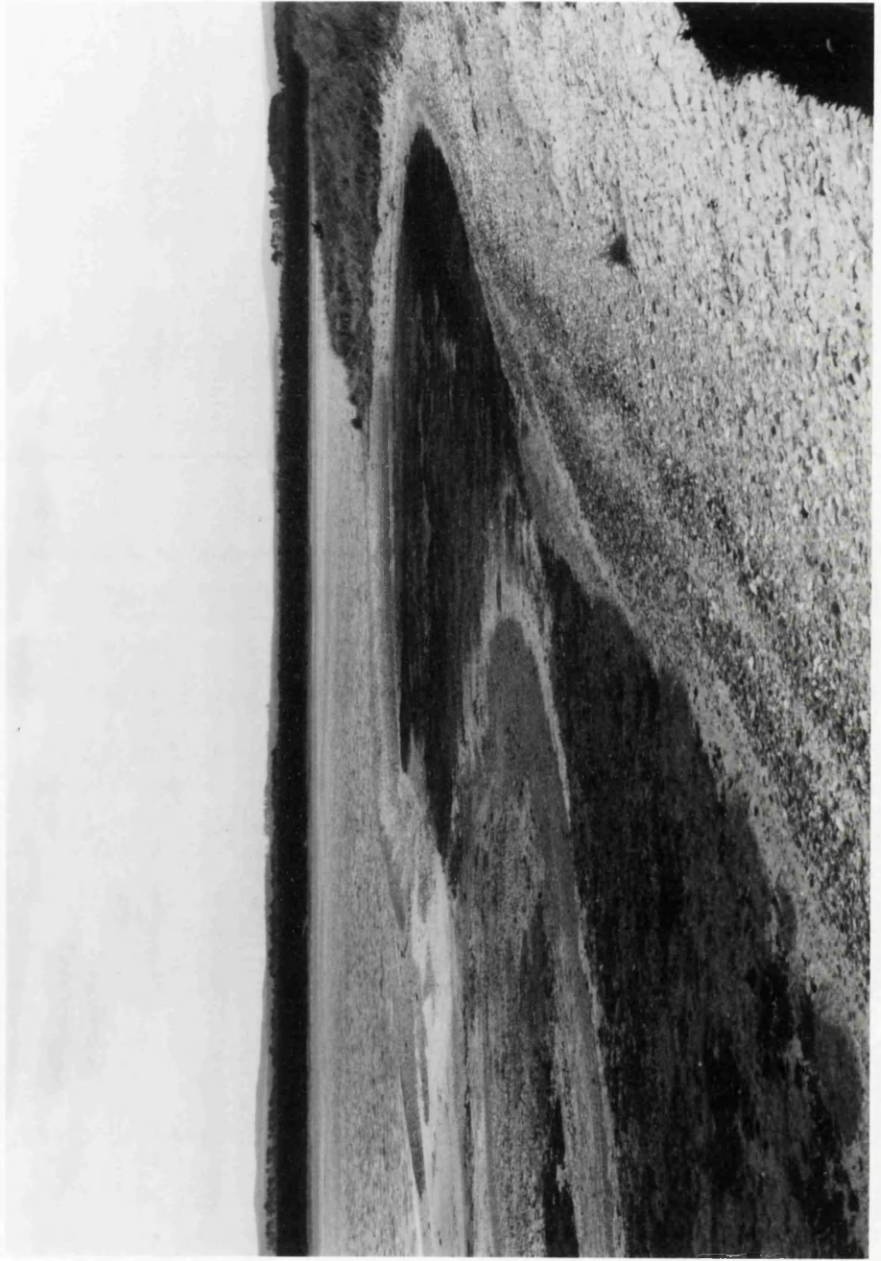
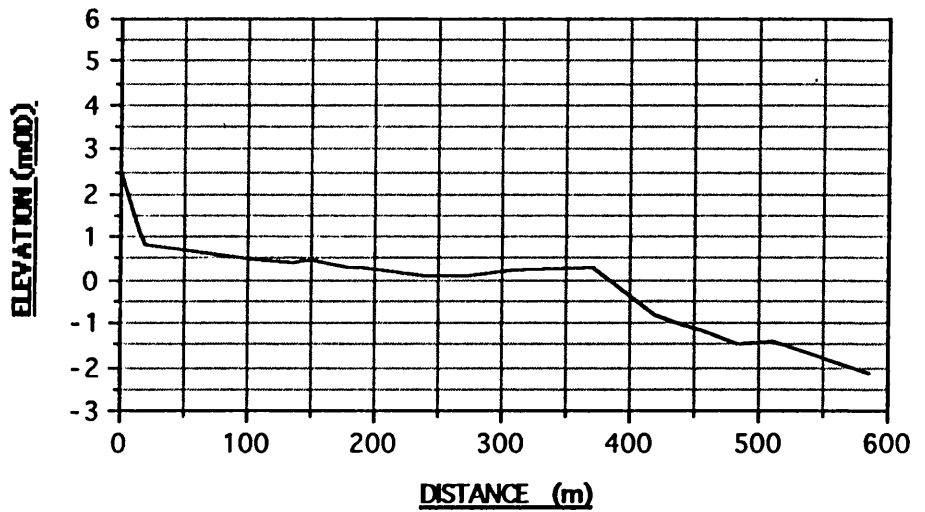
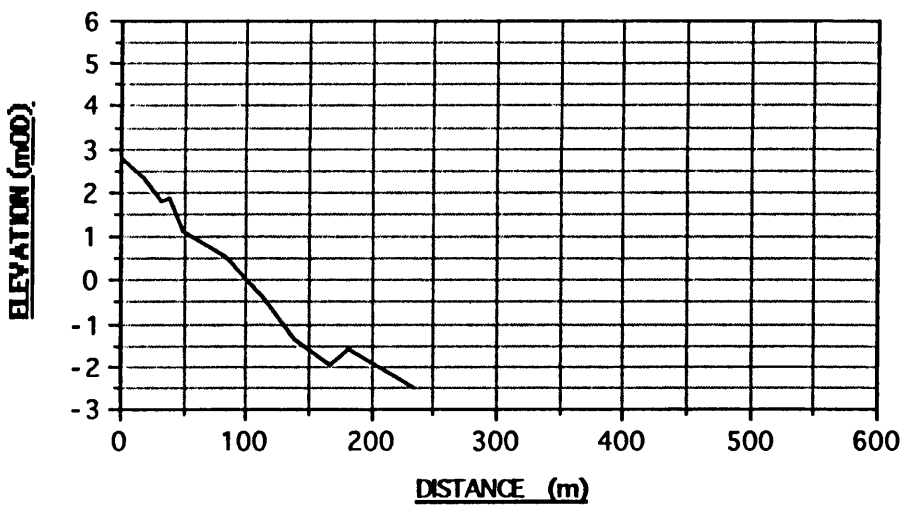


Figure 4.56 Beach profiles recorded on The Bar

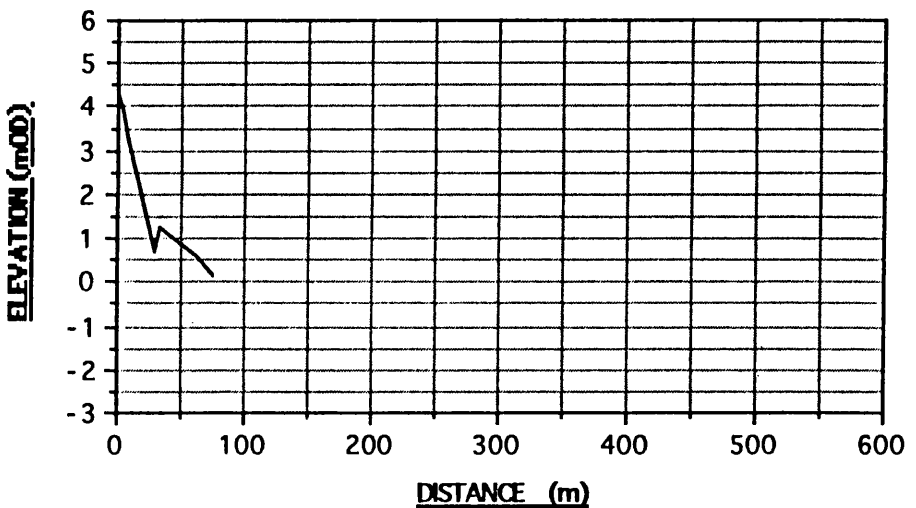
**Profile B1 30/8/91**



**Profile B2 30/8/91**



**Profile B3 30/8/91**



lower than the contemporary storm ridge, appearing more rounded and with occasional dune remnants capping them. These ridges are clearly relict, with lichen growth on the more seaward ridges grading to full vegetation cover on the inner edge of The Bar. The contemporary ridge crest is at 3.87 m OD, whilst the mean altitude of the relict ridges is 3.17 m OD (n=13). This zone is also eroding at its eastern end, with the proximal ends of the inland (relict) shingle ridges truncated by the contemporary storm ridge. The suite of relict shingle storm ridges forms the most distinctive feature of the SW flank of the Bar. The crests of the ridges were very consistent in altitude (standard deviation = 0.37), although the inter-ridge spacing varied between 3.80 m and 13.60 m. This represents the highest recorded standard deviation of any of the shingle ridges (active or relict) on the entire Culbin shingle system. The alignment of the ridges is clearly different to that of the contemporary storm ridge, with the proximal ends of the relict ridges truncated against the modern ridge at an angle of approximately 15°.

#### **4.2.2.6 Spatial distribution of erosion and accretion at Culbin and Burghead Bay**

Erosion of the backing dune system along the Culbin foreshore is thought to provide a significant volume of sediment to the annual beach sediment budget. In order to quantify this volume, the mean dune cliff recession rate was monitored along the length of the foreland over the two year monitoring period. The backing dunes were classified in terms of equal height into 10 zones. These are shown in Figure 4.57, along with the mean dune height in each zone. Within each zone a measurement point was established during summer 1990, and remeasurement of the distance to the cliff edge was made annually for the two following years. Recession values varied between zero and a maximum of 5.90 m (recorded at section 2) over a single year. Sections 4,7,9 & 10 recorded no recession over the two year period. Calculation of the mean recession values over the two year period found the highest recorded recession rate at section 2; mainly on the basis of the exceptional amount of recession recorded in the first year of recording, with only 0.65 m of recession recorded over the second year. Figure 4.58 shows the mean annual recession rates plotted against their location. While it was difficult not to over-generalize at this stage, the data suggests that the eastern section of the foreland experienced higher rates of dune cliff recession between 1990 and 1992 than the western section.

Cliffing of the raised foreshore and dune sediments along the 10 km sweep of Burghead Bay provides a further source of sediment to Culbin . Annual

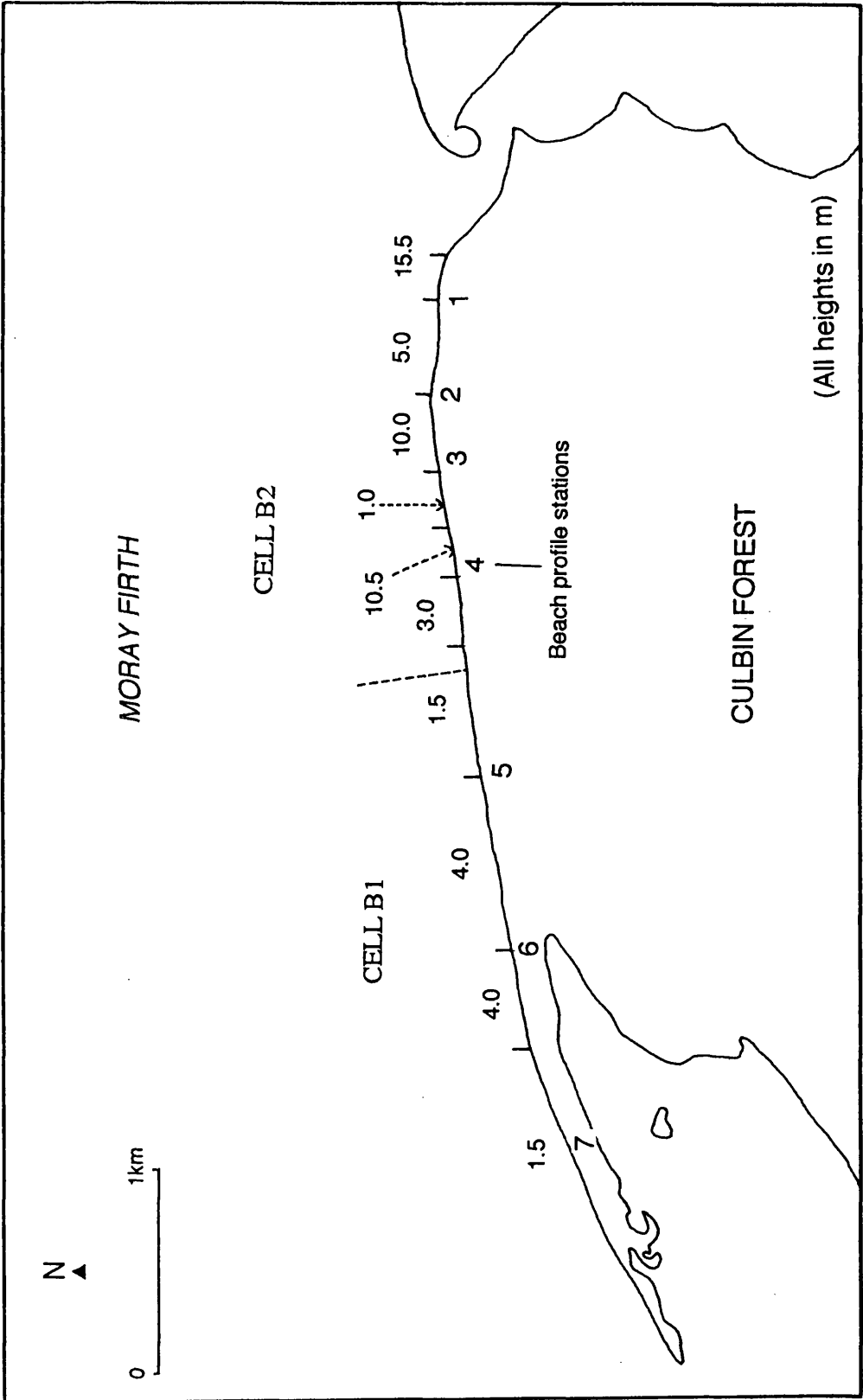


Figure 4.57 Mean dune heights backing the Culbin foreshore

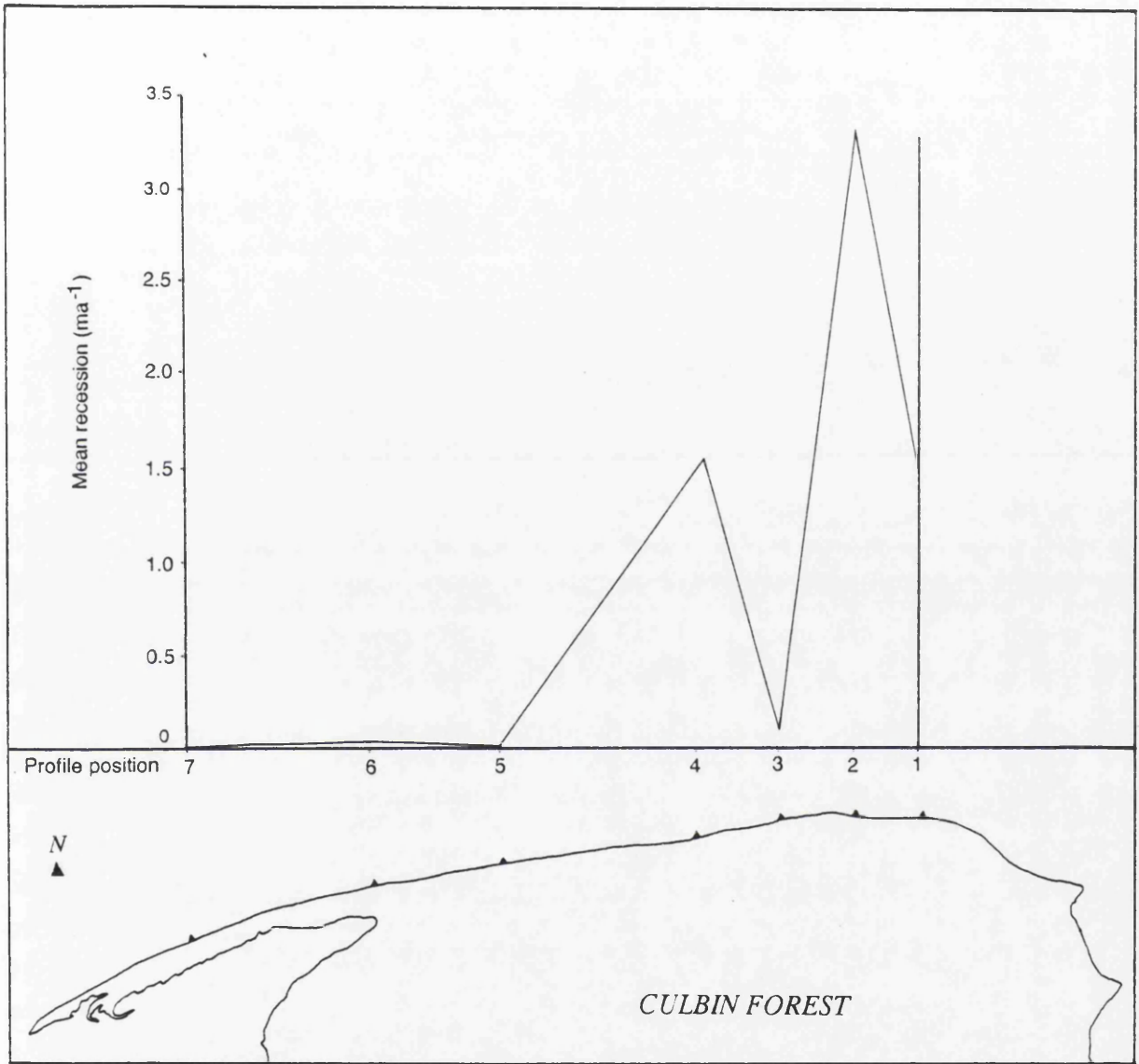


Figure 4.58 Dune cliff recession rates at Culbin 1990-92

recession was not recorded in Burghead Bay for the purposes of this study. However, Ross (1992) recorded a mean annual recession rate of  $1 \text{ m a}^{-1}$  in the vicinity of Findhorn village prior to the emplacement of a rock revetment. A comparison of aerial photographs taken in 1976 and 1989 confirmed this recession rate.

In order to attempt to explain the non-uniform distribution of erosion measured along the Culbin foreshore, qualitative and quantitative exploratory data produced by the WAVENRG program were examined. Output from the program was in two forms. Numerical solutions for various wave parameters at breaking were calculated for each orthogonal, including  $P_L$  and the incident component of wave power (POZ). The program also produced plots of wave orthogonals from each combination of wave height/period and direction. The production of these plots provides a rapid visual assessment of the areas where orthogonals are either converging or diverging, and consequently where wave energy is either focussed or dissipated. Zones of converging orthogonals are likely to coincide with areas of erosion, while diverging orthogonals suggest lower incident wave energy with potentially lower rates of erosion or relative stability.

Plots were produced of orthogonals incident on the Culbin coast from  $010^\circ$ - $060^\circ$ , with wave heights of 0.5 m, 1 m and 2 m. The limited amount of refraction undergone by 0.5 m waves meant that the convergence or divergence displayed on the plots was negligible, and the majority of the orthogonals were parallel.

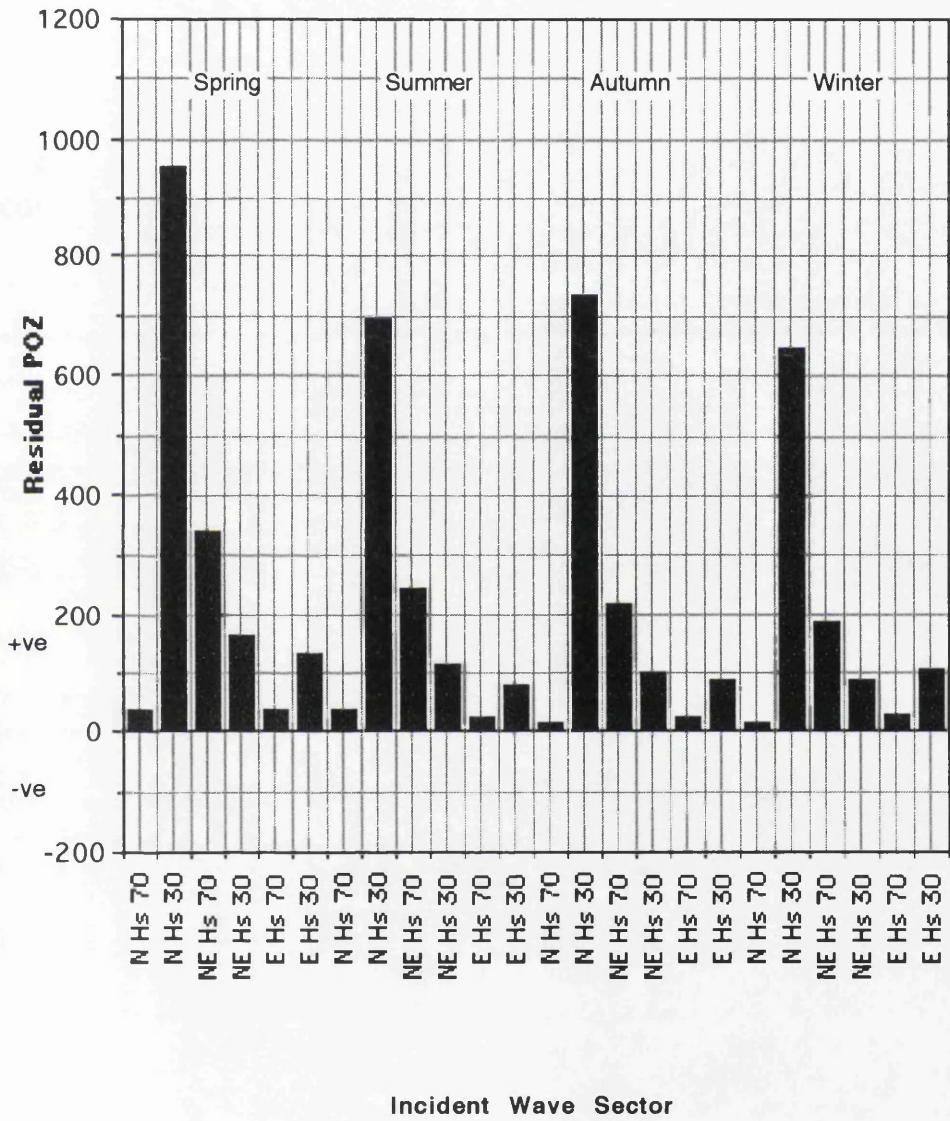
Once again the Culbin foreshore was divided into cells B1 and B2 for the purposes of this exercise. Table 4.21a shows the incident wave parameters and the resultant pattern of the orthogonals in each of the cells on the foreshore. The pattern of the orthogonals was determined qualitatively, but a very clear pattern emerges from Table 4.21b. The orthogonal patterns show a clear pattern of convergence on cell B2, with 61.1% of the record convergent along this stretch of the foreshore. In comparison cell B1 displays only 5.5% orthogonal convergence, with the majority of the wave record suggesting parallel and divergent orthogonals along this cell. Cell B2 displays a higher frequency of convergence under lower wave periodicities (6 & 8 s), while at higher wave periods (10 s), less convergence occurs. Little difference between orthogonal divergence/convergence under any specific incident periodicity was noted at B1.

In addition to this qualitative approach, a quantitative method was also employed to investigate the erosional potential along the Culbin foreshore. This employed the calculated incident component of wave power (POZ, in  $\text{J m}^{-1} \text{ s}^{-1}$ ). The

programme calculated POZ at landfall for each individual orthogonal on each run. All of the values from each of the orthogonals incident on each of the cells B1 & B2 were collated, and a mean value for each set of wave height, period and incident angles calculated for each cell. These were calculated individually as the number of orthogonals incident on the shoreline differed on each run. Once the mean value for each incident condition had been derived, the mean POZ values were broken down into their seasonal frequencies using the percentage wave frequency table (Table 4.15), and the results plotted as incident wave power under high and low wave energy conditions for each season (Figure 4.58a).

Values of POZ appear higher in all seasons and under all wave conditions in cell B2 than in B1. The highest incident wave power values recorded in both cells occurs under high energy events from the northern sector, followed closely by similar events from the NE sector. The highest value of incident wave power is measured from the northern sector with a value of  $2000 \text{ J m}^{-1}\text{s}^{-1}$ . Conversely, the lowest incident wave energy is received at both cells from the eastern sector, with a minimum value of  $5 \text{ J m}^{-1} \text{ s}^{-1}$ . A plot of the residual difference between values of POZ recorded at cells B1 & B2 is shown in Figure 4.58a. In all cases the values were positive, suggesting that under constant incident conditions, cell B2 consistently receives the highest incident wave energy. The greatest differences appear during high energy events from the northern sector during all seasons, with a difference of  $650\text{-}950 \text{ J m}^{-1} \text{ s}^{-1}$ . The smallest differentials appeared in winter from all sectors, and the largest in spring. While the smallest absolute energy differentials between the cells appears under low energy incident waves from the east, these represent the largest relative differential recorded. Cell B1 receives only 46.4% of the incident wave power of B2 from the east during spring, falling to a consistent 23.6% during summer-winter. The total annual record of POZ from all sectors displays a marked difference between the incident wave power received by the two cells, with cell B1 receiving only 52.5% of that received by B1. The minimum energy/maximum differential between the cells occurs under low energy conditions from the east (23.6%) and the maximum energy/minimum differential under northerly high energy conditions (92.2%).

Figure 4.58a Difference in POZ Values:- Cell B2-B1 Culbin Forest



### **4.2.3 Sand sediment budget: Culbin foreshore**

Having examined the contemporary coastal processes operating on the Culbin foreshore, the data obtained can be used for the calculation of a beach sediment budget.

Due to the complexity of the task of quantifying the elements of the beach sediment budget along the Culbin foreland, each element will be detailed individually. The elements of the budget of relevance to Culbin were outlined in Chapter 2, and are described in this section as *inputs to* and *outputs from* the beach. The calculation of longshore sediment transport obviously falls into both categories, as the updrift migration of sediment out of a cell constitutes the longshore input to the next successive cell downdrift. Longshore transport of sediment is referred to as an output simply for the sake of continuity.

## **4.2.4 Inputs**

### **4.2.4.1 Onshore transport**

Direct measurement of onshore transport was not undertaken as part of the beach sediment budget for Culbin due to the disproportionate amount of effort required to obtain results, and due to the constraints imposed on tested methods of measurement under conditions of predominantly longshore transport (Chapter 2). As such, onshore transport was used as a balancing item in the final budget rather than as a direct input into the sediment budget calculation.

### **4.2.4.2 Culbin: dune cliff erosion**

Calculation of the input of sediment to the beach is described in Table 4.22. The length of each dune section was multiplied by its mean height to produce a surface area for each section. This area was then multiplied by the recession rate to provide an annual volume of sediment released to the beach between 1990 and 1992. In order to provide meaningful comparisons with the data produced from wave refraction modelling, the dune sections are shown broken down into a west and an east cell (B1 and B2) developed for the refraction exercise (Figure 4.57). The total mean volumetric release to the Culbin foreshore between 1990 and 1992 was 15 710.8 m<sup>3</sup>.

A clear distinction could be drawn between the eastern and western zones of the foreland in terms of the volumes of sediment released to the beach from dune cliff erosion, with the divide occurring between dune sections 6 and 7, at approximately the position of Shellyhead bothies. Sediment supply from recession along cell B1 represented only 1.2% of the volume released from the dune cliffs of cell B2, reflecting both higher rates of dune cliff recession and greater dune height in the eastern zone in relation to the western zone.

### **4.2.4.3 Burghead Bay: erosion of raised shoreline deposits**

For the purposes of calculating an annual volume of sediment released from the cliffed deposits of Burghead Bay, the mean cliff height was taken to be 3 m at a recession rate of 1m per year over a distance of 10 000m.

Once these values had been obtained, the mean annual rate of sediment release to the nearshore zone was calculated as;

$$10\ 000\ \text{m} \times 3\ \text{m} \times 1\ \text{m}\ \text{a}^{-1} = 30\ 000\ \text{m}^3\ \text{a}^{-1}$$

#### 4.2.4.4 Riverine inputs of sediment to the coast

As noted in Chapter 2, available estimates of sediment to the Culbin foreshore were considered to be overestimates. In order to calculate a more realistic value of sediment input from the River Findhorn, a method of back-calculation was devised. This depended upon the response and local sediment budget of profile cell 1, this representing the closest cell to the mouth of the Findhorn and the first to be affected by sediment arriving at the coast. In considering the possible responses of cell 1, two extreme scenarios were considered;

- i) zero sediment input from the Findhorn (minimum model),
- ii) sediment inputs estimated by Reid & McManus (1987) ( $37840 \text{ t a}^{-1}$ ) (maximum model).

The actual volume of sediment derived from the Findhorn will lie between these two values, and it was clear from field evidence that the river was delivering only limited volumes of sand to the coast. However, the method employed by Reid & McManus (1987) was likely to provide an overestimate of the volume of sediment delivery to the coast due to the use of sediment rating curves derived from flow gauging stations upstream from Findhorn Bay. Calculations regarding bedload transport still remain problematic (Chapter 2). For example the values produced by Reid & McManus (1987), assuming bedload transport to be 10% of the total load, were much higher than the 3-5% values obtained by Al-Ansari & McManus (1979).

In order to provide a sediment volume in comparable units to the remainder of the sediment budget calculations, the total sediment load required conversion into common units ( $\text{m}^3$ ). To do this an estimate of the density of mixed loose, saturated sand was obtained (CERC, 1984), which provided a value of  $1.986 \text{ t m}^{-3}$ . This represented a volume of  $19\,053 \text{ m}^3 \text{ a}^{-1}$  as the maximum input to the system from the Findhorn.

Various assumptions regarding the behaviour of cell 1 had to be made if this method were to be valid:

- i) the beach remained in dynamic equilibrium over a medium term ( $10^2$  years) timescale;
- ii) mean frontal dune recession was constant along the length of the cell;

iii) the balance of sediment was composed solely of inputs from dune cliff recession backing cell 1;

iv) sediment derived from erosion of cliffed deposits in Burghead Bay bypassed cell 1 due to the velocity of fluvially-enhanced currents at the mouth of the river, demonstrated by the construction of the Findhorn bar.

If we consider scenario i) (no sediment arriving via the Findhorn) then the volume of sediment in cell 1 would be controlled entirely by the inputs of sediment from the erosion of backing dune cliffs. The backing dune cliffs along cell 1 were the highest found along the Culbin foreland with a mean height of 10 m. The length of cell 1 was defined in Chapter 2 as 430 m. Mean dune cliff recession in cell 1 over the period 1990-1992 was 1.43 m a<sup>-1</sup>. Converting this to a mean annual volume of sand released to the beach produced a volume of 8793 m<sup>3</sup>a<sup>-1</sup>. From the analysis of beach profiles measured over the two year study period it was found that cell 1 displayed one of the widest beach profiles found along the foreshore, and contains a mean volume of between 2.5x10<sup>5</sup> m<sup>3</sup> and 3.0x10<sup>5</sup> m<sup>3</sup>. Annual dune cliff recession represented only 3.5-2.9% of this value, which if we consider beach sediment flux to be zero would be extremely low. However, data from the wave refraction exercise will demonstrate that the eastern cell (cell B2) is exporting sediment towards the west, with a potential annual sediment export of 32 779 m<sup>3</sup> a<sup>-1</sup>. The total length of this cell is 1950 m, of which cell 1 represents 22.1% by length. If we represent the volume of sediment exported from cell 1 as 22.1% of the total sediment exported from the eastern cell in total, then the volume of sediment exported from cell 1 was only 7244.4 m<sup>3</sup>. This is a lower volume than that entering the beach from the cliffing of the backing dunes alone, and implies that dune erosion could maintain the volumetric status of the fronting foreshore without the need to invoke a fluvial supply of sediment. Thus the supply of sediment from the Findhorn can be excluded from the beach sediment budget for the Culbin foreshore, with the loss of sediment offshore envisaged as the likely fate of this sediment.

## **4.2.5 Outputs**

### **4.2.5.1 Offshore transport**

In a similar fashion to onshore transport, offshore losses were not measured directly in the field (section 4.2.4.4). As such, offshore transport was also used as a balancing item in the calculation of the beach sediment budget for the Culbin foreshore.

#### 4.2.5.2 Volumetric extension of Buckie Loch spit

Measurement of the extension rates of Buckie Loch spit was undertaken in order to quantify both the planimetric and volumetric implications of this process on the sediment budget for the Culbin foreshore. Distal extension of The Bar, however, is facilitated by the addition of shingle, rather than sand as recorded on Buckie Loch spit. This data was used in the calculation of a separate sediment beach budget, concerned specifically with the shingle fraction of the Culbin foreshore sediments. As shingle operates in a hydraulically different manner to sand, it would be expected to produce a different budgetary response.

Aerial extension rates of Buckie Loch spit were measured using maps dating back to 1870, and using aerial photography since the site was first overflowed in 1946, as outlined in Chapter 3. The cross-sectional area of the spit was calculated to be 890.29 m<sup>2</sup>. Multiplication of the annual rate of spit extension by its cross-sectional area produced a value of the annual volumetric extension of the spit over the same periods. The measured rates of aerial and volumetric extension of the spit are presented in Table 4.23

Period	Aerial Extension Rate (m a <sup>-1</sup> )	Volumetric Extension Rate (m <sup>3</sup> a <sup>-1</sup> )
1870-1946	8.5	7594.2
1946-1953	13.0	11591.6
1953-1959	28.8	25658.3
1959-1976	94.6	84195.1
1976-1989	15.5	13817.4

Table 4.23 Aerial and volumetric extension rates measured at Buckie Loch Spit 1870-1989

The rates of extension demonstrated a gradual increase over the measurement period from a minimum extension rate of 8.5 m a<sup>-1</sup> over the period 1870-1946, reaching a maximum extension rate of 94.6 m a<sup>-1</sup> between 1959 and 1976. This was followed by a marked curtailment in the rate of distal extension, with a mean extension rate of only 15.5 m a<sup>-1</sup> measured between 1976 and 1989. A mean

extension rate of 22.3 m a<sup>-1</sup> was thus produced over the entire period 1870-1988, although this could not be taken as a representative value of distal extension experienced at present.

The volumetric calculations follow the trends in planimetric extension as expected when holding cross-sectional area constant. The lowest volumetric extension rate was found during the earliest surveys, with an increase in volume of 7594.2 m<sup>3</sup> a<sup>-1</sup>. The volumetric extension increased gradually, reaching a maximum during the period of most rapid planimetric extension between 1959-1976, with a volumetric extension rate of 84 195.1 m<sup>3</sup> a<sup>-1</sup>. This was followed by a rapid curtailment in the extension rate over the period of the most recent survey, with an extension rate of only 13 817.4 m<sup>3</sup> a<sup>-1</sup> between 1976 and 1989.

#### 4.2.5.3 Longshore sediment transport

The calculation of longshore currents has so far considered the generation of the term  $P_L$  and its conversion to the longshore sediment transport rate  $S_L$ . For input into the final beach sediment budget  $S_L$  had to be converted to m<sup>3</sup> season<sup>-1</sup>. To do this the number of effective wave days in each season was required, represented by the total number of days minus the number of calms per season. Table 4.24 shows the number of effective wave days per season recorded at Culbin, and the multiplication factor involved in the production of a *seasonal* value of  $S_L$ , defined here as the value  $Q_L$ .

SEASON	EFFECTIVE WAVE DAYS	$Q_L$ (m <sup>3</sup> season <sup>-1</sup> )
SPRING	64	164.5 $P_L$
SUMMER	59	151.6 $P_L$
AUTUMN	63	162.2 $P_L$
WINTER	68	174.0 $P_L$

Table 4.24 Effective wave days recorded at Culbin and subsequent conversion factor for  $Q_L$

Calculation of the value of  $P_L$ ,  $S_L$  and  $Q_L$  for each cell again used the method of Mason (1985). The final calculation of a potential seasonal longshore sediment

transport rate was made using the values in Table 4.16, and the final results are presented in Table 4.25.

#### 4.2.5.4 Modelled sand beach sediment budget

Having quantified all of the potential inputs and outputs to the beach system (except on-offshore transport, as described above), the values were tabulated to produce a volumetric budget for the Culbin foreshore (Table 4.26).

Cell	Input	Volume (m <sup>3</sup> )	Output	Volume (m <sup>3</sup> )	Balance (m <sup>3</sup> )
B2	River	0			
	Longshore in	30 000.0	Longshore out	32 779.9	
	Cliffing	16 859.9			
	<b>TOTAL INPUT</b>	<b>46 859.9</b>	<b>TOTAL OUTPUT</b>	<b>32 779.9</b>	<b>+14 080.0</b>
B1	Longshore in	32 779.9	Longshore out	33 710.8	
	Cliffing	200.0			
	<b>TOTAL INPUT</b>	<b>32 979.9</b>	<b>TOTAL OUTPUT</b>	<b>33 710.8</b>	<b>-730.9</b>

Table 4.26 Summary of the inputs and outputs to the modelled sand beach sediment budget: Culbin foreshore

The modelled values show that downdrift cell (B1) has a negative sediment budget, while the updrift cell (B2) has a much stronger positive sediment budget. These results are placed in context with the actual beach sediment budget calculated from beach profile data below.

#### **4.2.5.5 Beach profile data and the calculation of an actual sand sediment budget**

Calculation of the final sand sediment budget was undertaken using two independent sets of data in order to provide a check on the values produced. The modelled beach sediment budget displays *potential* changes using the wave refraction model, incorporating field measurements to verify the inputs to the model. However, the measurement of beach profiles over a two year period provided a measure of the *actual* changes in sediment volume which took place within the beach. Thus while the modelled situation provides information concerning the *potential* sediment interchange, on-site monitoring shows the *actual* state of sediment movement within the beach system.

The calculation of the beach sediment budget using the beach profile data involved the conversion of the beach profile sections to volumetric equivalents (Chapter 2). The difference between the cells was measured between March 1991 and February 1992 in order to provide the most up-to-date estimate of volumetric beach changes possible. The volume of each beach cell after each survey was calculated, and the values are recorded in Appendix 9. From these measurements the mean beach volume over the two year period was calculated, which was considered a sufficiently long period of recording to cover the beach at all volumetric states encountered (i.e. both "swell" and "storm" profiles). Having calculated a mean volume for each cell, the next stage was to compare the means with the actual volumes measured. The difference between the mean and the actual volumes was recorded as a residual beach volume, either positive or negative (Table 4.26). In order to calculate the net change in beach volume over a single year, the difference in volume between each cell was measured, and once again divided into cells B1 and B2. The results of this calculation are shown in Table 4.27, which also shows the results of the modelled beach sediment budget using the information gathered from the wave refraction modelling exercise.

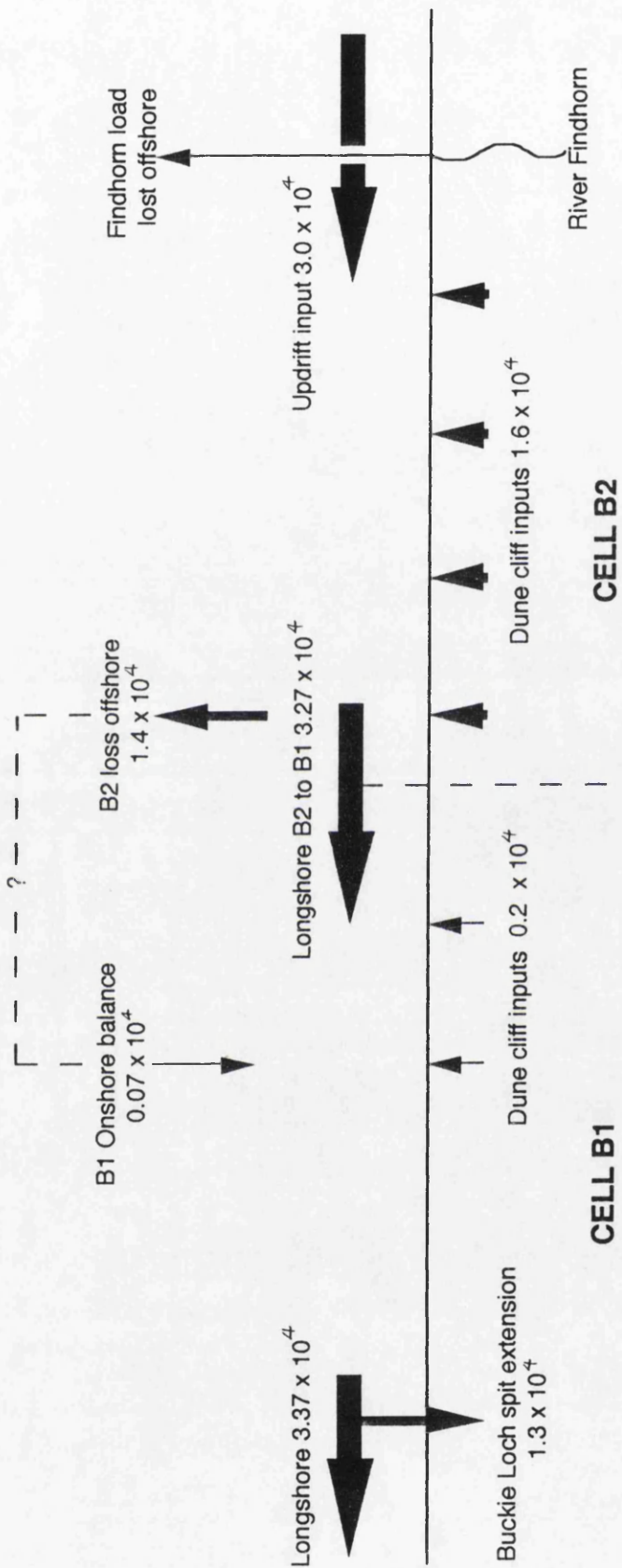


Figure 4.59 Diagrammatic representation of the sand sediment budget  
(all values in m<sup>3</sup>)

	Cell B1	Cell B2
<b>Modelled Volume (m<sup>3</sup>)</b>	-731	+14 080
<b>Observed Volume (m<sup>3</sup>)</b>	+35893.5	-12156.2
<b>Trend</b>	ONSHORE	OFFSHORE
<b>Mean transport/tide (m<sup>3</sup>)</b>	+50.17	-35.94

Table 4.27 Difference between observed and modelled volumetric beach changes: Culbin foreshore

This data is also displayed diagrammatically in Figure 4.59. The difference between the observed and predicted beach sediment volumes indicates the volume of sediment mobile during the survey period. The differences between the modelled and observed changes suggests that a net onshore movement of material took place over the year in cell B1, while in B2 the predominant sediment movement was offshore. The data from the modelled and measured sediment budgets show good agreement. A negative modelled volume in cell B1 implies a greater sediment output than input, which if the beach is to remain in dynamic equilibrium over the short ( $10^0$ ) timescale, requires an onshore movement of sediment. The sediment budget obtained from the field data demonstrates that this must have occurred to produce the positive budget shown in Table 4.26. Conversely, the strongly positive potential budget in cell B2 required an offshore balancing item to remain in dynamic equilibrium due to the potential longshore excess between B2 and B1. Field measurements once more demonstrated that this occurred, with a decline in the actual volume of B2 over the monitoring period. Calculation of the mean sediment transport per tide required to drive the sediment budget demonstrates a greater onshore sediment input per tide in cell B1 than the offshore loss in cell B2, assuming an even distribution of sediment across the surface of the foreshore.

#### 4.2.6 Shingle sediment budget: The Bar

Measurements have been made of the distal extension of The Bar over the period 1878-1989 (Hall, 1989). However, as the western section of The Bar is composed of shingle rather than sand, the results obtained were used both as a

comparison of the extension rates of drift aligned features composed of coarse, clastic material, and also to attempt to quantify the amount of shingle active in the nearshore zone under present conditions. A second beach sediment budget was calculated to quantify this volume.

## **4.2.7 Inputs**

### **4.2.7.1 Onshore**

Once again, measurement of onshore transport was not undertaken as part of the beach sediment budget for Culbin due to the disproportionate amount of effort required to obtain results, and due to the constraints imposed on tested methods of measurement under conditions of predominantly longshore transport (Chapter 2). More importantly in this case, however, is the fact that little or no shingle is reported in the offshore zone in this area (Chesher & Lawson, 1983). The shingle which is present is assumed to have been introduced from the sources described below rather than representing deposits emplaced during the Lateglacial. As such, onshore transport was used as a balancing item in the final budget rather than as a direct input into the sediment budget calculation.

### **4.2.7.2 Erosion of cliffed raised shoreline deposits in Burghead Bay**

The nature of the raised beach deposits exposed in section along Burghead Bay have been described. Much of the exposure consisted of interbedded sand and shingle in varying proportions. The total length of exposed raised sand and shingle deposits in Burghead Bay was 5.25 km, with the remaining 4.75 km composed of sectioned dunes, particularly in the NE of the Bay. Having logged in detail the nature of the interbedded sediments in the cliff, the proportion of shingle exposed in section was estimated to be 20% during 1990/91.

For the purposes of calculating an annual volume of material removed from Burghead Bay, the mean cliff section height in Burghead Bay was taken to be 3 m, and the mean annual recession rate was taken as 1 m a<sup>-1</sup> (Ross, 1992).

Using these values, the annual volumetric rate of sediment release to the nearshore zone was calculated as:

$$5250 \text{ m} \times 3 \text{ m} \times 1 \text{ m a}^{-1} = 15\,750 \text{ m}^3 \text{ a}^{-1}$$

Of this volume, only 20% was actually shingle:-

$$15750 \text{ m}^3 \text{ a}^{-1} \times 20\% = 3150 \text{ m}^3 \text{ a}^{-1}$$

Thus a first approximation of the volume of shingle released from the erosion of the raised beach deposits in Burghead Bay provided a volume of  $3150 \text{ m}^3 \text{ a}^{-1}$ . However, the construction of a series of groynes in 1985 along the western flank of Burghead Bay (Ross, 1992) has trapped shingle moving west towards Culbin, creating a net sediment sink and starving the downdrift area of shingle from this source since construction.

#### **4.2.7.3 Shingle supplied by the River Findhorn**

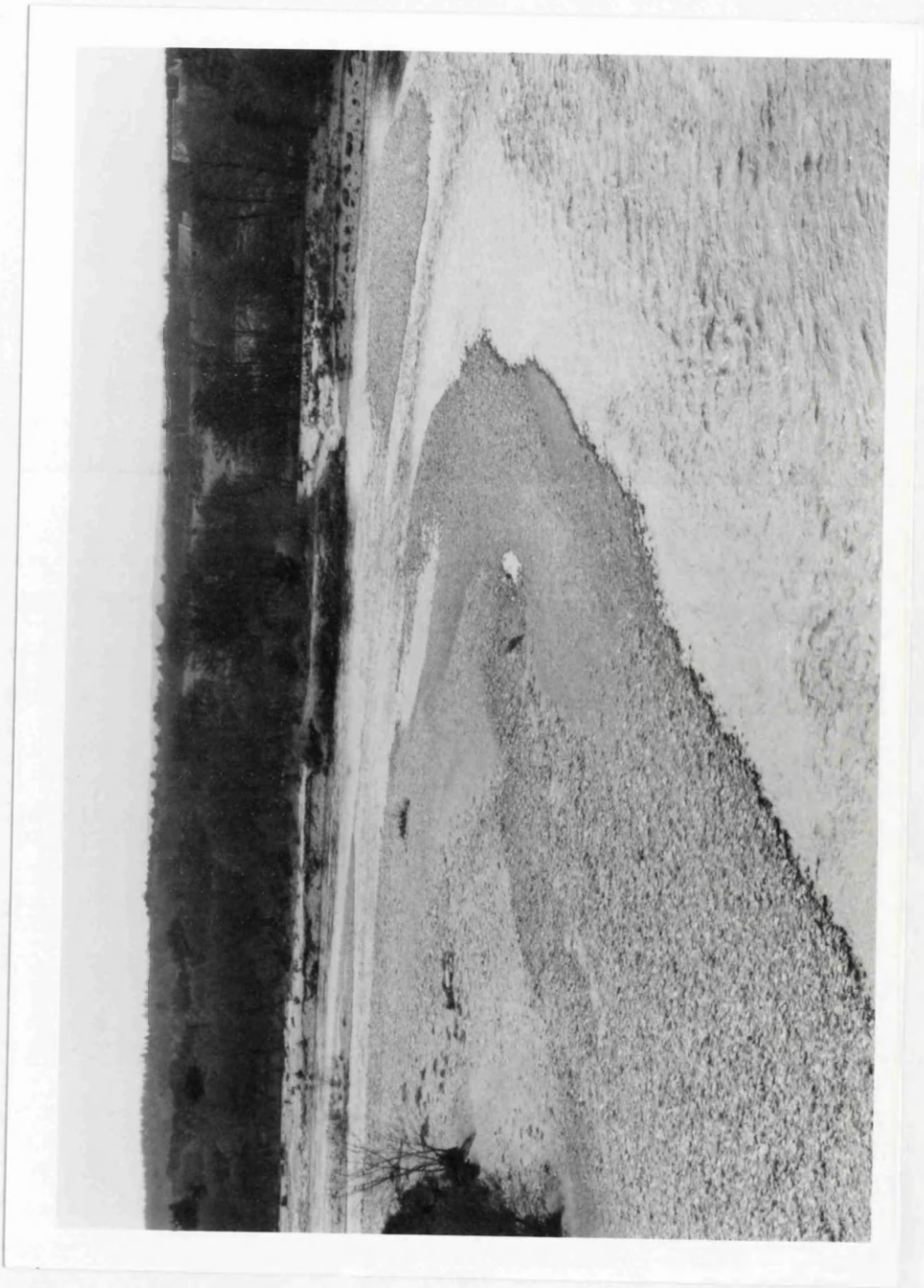
A first estimate of the amount of shingle supplied to the nearshore zone by the River Findhorn was initially considered to have been provided by Reid & McManus (1987). Their estimate of the bedload component of the Findhorn total load was based on Parker *et al.* (1964), who suggested a value of 10% of the suspended load as a maximum bedload fraction. This produced an upper limit of  $1732 \text{ m}^3 \text{ a}^{-1}$  for the bedload of the Findhorn. Studies from the Tay, however, revealed the bedload proportion to be much lower (Al-Ansari & McManus, 1979), and a lower limit based on their calculation of 3-5% of suspended load transported as bedload produced a value of  $520 \text{ m}^3 \text{ a}^{-1}$ .

While stream gradients were not measured, the large quantities of shingle deposited upstream from Findhorn Bay (Plate 10) suggested that a marked drop in gradient coupled with an increase in channel width occurred as the Findhorn emerged from the lateral confines of the terraced section between Struie Gorge and Findhorn Bay. This fall in gradient/increase in channel width resulted in a decrease in transport competence, leading to selective deposition of the coarser fraction of the total river load prior to entering the nearshore zone. Additionally, the marked increase in channel width experienced by the river upon entering Findhorn Bay would enhance the potential for the deposition of coarse material, further reducing the probability of shingle entering the nearshore zone except under high discharge events.

In order to avoid potential overestimates of the volume of shingle presently mobile in the nearshore zone, the lower estimate of shingle load ( $520 \text{ m}^3 \text{ a}^{-1}$ ) was used in the final calculation of shingle supply.

Plate 10

Shingle point bars in the River Findhorn. Viewed upstream from the A 96 Findhorn road bridge, active shingle can clearly be seen along with older, partially stabilized shingle features (right middle). The bed of the river is also composed chiefly of shingle in this area. The flat surface of a high river terrace can be seen in the background behind the treeline.



#### **4.2.7.4 Proximal erosion of shingle ridges in the central section of The Bar**

Trends in the position and orientation of The Bar demonstrated that the central section, or 'neck', was experiencing significant rates of erosion. West of the dune section at NH 935611 this section of the Bar is only prevented from breaching by a narrow shingle ridge, which during the study period was actively retreating landwards through washover, leading to longer term rollover of the entire feature. At the western end of this particular section of The Bar the single shingle storm ridge gradually splays into a series of multiple ridges, the eastern ends of which are truncated by the most seawards ridge at an angle of 5-15°. The clarity and distinctive alignment of the shingle ridges in this section of The Bar allowed the features shown on 1976 aerial coverage to be matched against its 1989 equivalent. From this, the area of surficial shingle removed from the Bar could be determined with accuracy. Over the 13 year period between overflights, a triangular bight 620 m in length was removed from the proximal end of the multiple ridge sequence, with maximum point erosion of 60 m below the 'apex'. This represented the removal of a surficial area of shingle representing 18 600 m<sup>2</sup> over the 13 year period 1976-89. Using the operational depth of shingle calculated from the beach profiles at station B3 (5.27 m), this represents a volumetric removal of 98 022 m<sup>3</sup>. Converting this to an annual volumetric removal rate, this represented 7540.2 m<sup>3</sup> a<sup>-1</sup> of shingle released to the nearshore zone.

### **4.2.8 Outputs**

#### **4.2.8.1 Offshore**

In a similar fashion to onshore transport, offshore losses were not measured directly in the field (section 4.2.4.4). As such, offshore transport was also used as a balancing item in the calculation of the beach sediment budget for the Culbin foreshore.

#### **4.2.8.2 Proximal extension of The Bar**

The method of calculating the volumetric extension rate of The Bar has been described in Chapter 3. The cross-sectional area of the extending section of The Bar is 94.38 m<sup>2</sup>.

Distal extension rates have been measured on The Bar by Hall (1987). These were extended to include air photographs taken on the latest overflight of Culbin

in 1989. These values are shown in Table 4.28, along with the volumetric extension rates of The Bar.

Period	Aerial extension rate (ma <sup>-1</sup> )	Volumetric extension rate (ma <sup>-1</sup> )
1878-1894	11.3	1066.5
1894-1909	18.6	1755.5
1909-1926	4.4	415.3
1926-1947	5.0	471.9
1947-1961/76	45.7	4313.2
1976-1989	14.6	1377.9

Table 4.28 Aerial and volumetric extension rates measured at The Bar 1870-1989

The aerial extension rates measured on The Bar show a similar set of extension trends to those from Buckie Loch spit. The final measurements made from the 1976 and 1989 aerial photographs show a similar extension rate at both Buckie Loch spit and The Bar, with extension rates of 15.5 m a<sup>-1</sup> and 14.6 m a<sup>-1</sup> respectively. However, while this represents 13 817 m<sup>3</sup> of sand on Buckie Loch spit, the equivalent extension on The Bar is only 1377.9 m<sup>3</sup> a<sup>-1</sup> of shingle.

The planimetric extension rates calculated from The Bar suggest that shingle is still being supplied to the distal end at a rate proportional to the volume of sand supplied to Buckie Loch spit. However, the volumes involved in the distal extension of Buckie Loch spit are an order of magnitude greater than those on The Bar.

#### 4.2.8.3 Shingle sediment budget

If the values calculated from all three possible shingle sources to the present nearshore zone are examined, clearly the largest potential source of shingle released to the nearshore zone is that liberated during proximal erosion of the relict shingle ridges on The Bar itself. The next largest supply (3150 m<sup>3</sup> a<sup>-1</sup>) is

that from erosion in Burghead Bay, while the smallest volume was that supplied by the Findhorn, using either the lower ( $520 \text{ m}^3 \text{ a}^{-1}$ ) or upper ( $1732 \text{ m}^3 \text{ a}^{-1}$ ) scenario. The elements of the shingle sediment budget are shown in Table 4.29.

Input	Volume (m <sup>3</sup> )	Output	Volume (m <sup>3</sup> )	Balance
Proximal erosion	7540.2	Distal extension	1377.9	
River Findhorn	520			
Burghead Bay	3150			
<b>TOTAL IN</b>	<b>11 210.2</b>	<b>TOTAL OUT</b>	<b>1377.9</b>	<b>+9832.3</b>

Table 4.29 Summary of the inputs and outputs to the shingle sediment budget:  
The Bar

While the total potential shingle inputs to the nearshore zone amounted to  $11\,210.2 \text{ m}^3 \text{ a}^{-1}$ , the volumetric extension of The Bar was only  $1377.9 \text{ m}^3 \text{ a}^{-1}$ , or 12.3% of this volume. Additionally, it can be seen that the volume of shingle released through proximal erosion of the relict shingle ridges on The Bar alone would more than account for the amount of distal extension measured over the 13 year period. Indeed, as the amount of distal extension accounted for only 18.3% of the volume liberated by proximal erosion, some offshore and alongshore loss from this source is suggested by the data, even assuming that the remainder of the shingle from both Burghead Bay and the Findhorn did not reach The Bar at all. This is a realistic suggestion given the low volumes of shingle supplied by the Findhorn and the interception of shingle from Burghead Bay by the recently constructed groynefield at Findhorn.

The implication of this is that The Bar presently receives no shingle from updrift, and distal extension is fuelled exclusively through proximal reworking of relict shingle. This means that The Bar is effectively reworking itself in a longshore direction.

#### **4.2.9 Contemporary coastal processes and landforms at Culbin: Summary**

- i) Tidal currents in the offshore zone display ebb tide dominance. They are, however, very weak, attaining a maximum of  $28 \text{ cm s}^{-1}$ , and are not efficient at entraining the predominantly fine grained sediments located in the offshore zone. They are thus not included in the sediment budget calculations.
- ii) Waves form the primary mode of energy input to the middle Moray Firth. Waves recorded at the Beatrice Alpha platform display a modal height of 1 m, and a modal periodicity of 4 s. Maximum wave heights recorded were 8 m, with a 9 s period.
- iii) Swell wave directions were obtained from Global Wave Statistics (BMT, 1986). These demonstrate the filtering effect of the Moray Firth, allowing entry by waves from only the N-NE-E sectors. Swell waves from the NE were found to be the most common, occurring for 11.87% of the swell wave year. Wind waves from western sectors were simulated using wind data from RAF Kinloss. These were severely fetch limited, producing maximum wave heights of only 0.75 m.
- iv) Waves drive longshore currents in the middle Firth, with the dominant northeasterlies producing a net westerly transport of sediment and a series of strongly drift aligned landforms. Potential longshore transport is  $32\,779.9 \text{ m}^3 \text{ a}^{-1}$  along the eastern flank, and  $33\,710.8 \text{ m}^3 \text{ a}^{-1}$  on the western flank.
- v). The Culbin foreshore is composed chiefly of sand, displaying downdrift coarsening in sediment size.
- vi) The Bar has a mixed sedimentary system, with a primarily sandy eastern flank giving way to a shingle dominated west flank. This also displays downdrift coarsening in clast size.
- vii). The sandy Buckie Loch spit is currently extending distally at  $15.5 \text{ m a}^{-1}$ . This is similar to the shingle dominated Bar, which is extending at  $14.6 \text{ m a}^{-1}$ .
- viii) Recession of the dunes backing the Culbin foreshore is spatially erratic, with between 0 and  $5.9 \text{ m a}^{-1}$  recorded between 1990-91. Recession is heaviest along the eastern flank, where focussing of wave orthogonals and a higher incident wave energy has been modelled.

ix) Two beach sediment budgets were calculated, one for sand and the other for shingle at Culbin. Both of the sediment budgets were positive. The modelled sand budget on the Culbin foreshore demonstrated a heavily positive budget on the eastern flank of + 14 080.0 m<sup>3</sup> a<sup>-1</sup>, which offset a slightly negative budget (- 730.9 m<sup>3</sup> a<sup>-1</sup>) on the western flank. The shingle budget displayed a positive budget, with a potential excess of + 9832.3 m<sup>3</sup> a<sup>-1</sup> offsetting distal extension of The Bar.

### **4.3 LINKAGES BETWEEN HOLOCENE AND CONTEMPORARY PROCESSES**

The entire Culbin foreland represents a Postglacial shingle based strandplain deposited during a higher RSL than present. Development of the foreland has been dependent on a supply of clastic sediment primarily from updrift. The aim of this section is to attempt to link the delivery of this sediment to the quantity and mode of delivery within Culbin itself.

Having calculated the volume of material present in the Culbin shingle system, this is compared with the total volume of shingle delivered to the coastal zone from the Rivers Spey and Findhorn since the Lateglacial ca. 13 000 BP. As the Culbin foreland is entirely Postglacial in age, then quantification of the delivery of sediment since the Lateglacial would encompass the entire formation period of the foreland. Additionally, as the Lateglacial surface was the only positively identified chronological horizon identified in the area, a more detailed chronological subdivision of the rates of sediment delivery could not be made in spite of the identification of subdivisions within the Culbin shingle ridge system. The calculation will be presented as a sediment budget, quantifying the inputs, outputs and sinks of sediment in the system.

#### **4.3.1 Inputs**

##### **4.3.1.1 River terrace reconstruction**

The source of shingle in this zone of the Moray Firth remains problematic, as seabed surveys presently detect no shingle in the offshore zone which may have accounted for an offshore source (Chesher & Lawson, 1983). Similarly examination of borehole records reveals only the Nairn Basin structure in the immediate offshore zone from Culbin, comprised exclusively of fine grained sediments (Chesher & Lawson, 1983). This implies that either an offshore shingle body formerly existed, but has been forced onshore in its entirety, leaving no lag deposits *in situ*, or that sources of offshore shingle were never significant in this section of the Moray Firth. A second possible solution is that updrift supply of shingle was formerly more significant than is presently experienced at Culbin, and that under a higher RSL the drift system of the Spey was connected to that of Culbin via a marine corridor running north of the Covesea ridge. Both of these options require quantification as potential inputs to the Culbin system.

The method of calculation of the volume of sediment introduced into the coastal zone from both the Spey and the Findhorn differed due to the lack of an accurate map of the Lateglacial terrace surface in the lower Findhorn valley. The results from the calculations based on the map produced by Peacock *et al.* (1968) of the terraces of lower Strathspey will be considered first, followed by the calculations from the lower Findhorn valley.

Calculation of the volume of sediment removed from the lower Strathspey terrace sequence was based upon reconstruction of the terrace fragments identified by Peacock *et al.* (1968) (Figure 4.60). The upper limit of the terrace sequence was taken to be the Lateglacial terrace identified by Peacock *et al.* (1968) & Sutherland (1984) due to its kettled surface, implying proximity to an ice front during formation.

Having remapped these fragments at 1:10 000 scale, the area of each of the terraces was calculated in three zones; north, central and south, due to the shape of the valley in the subject reach. A maximum of five discrete terrace fragments were identified in the central section of the series, with only four in the northern and southern sectors. The terrace fragments were generally not paired across the width of the valley (Figure 4.60). Having calculated the area of each of the fragments, the depth of each of the surfaces was calculated from 1:10 000 scale maps of the area, and the volume of each of the fragments in each of the longitudinal zones calculated. A final calculation of the volume of valley fill removed was made by summing the volume from each zone. The steps in this calculation are presented in Appendix 2. The total volume removed from the lower Strathspey terrace sequence was found to be  $3.35 \times 10^8 \text{ m}^3$  since the formation of the Lateglacial terrace surface.

A problem was encountered in attempting to duplicate these measurements in the lower Findhorn valley, as the terrace sequence had not been mapped in this area. Such a task was beyond the feasibility of this study, and an alternative solution was required.

The method devised considered the volume of sediment removed from the lower river valley to be approximated by a pyramid. The gradient of the sides of the pyramid were defined by the gradient of the river along the target reach, and the width of the base defined by the width of the lower terrace at the point of expansion onto the coastal plain. Figure 3.17 shows a diagrammatic sketch of this method of calculation. The calculations from the lower Findhorn provide a

volume of valley fill removed of  $2.81 \times 10^7 \text{ m}^3$ . This represents only 8.4% of the volume of sediment found in the terrace sequence of lower Strathspey.

In order to test the feasibility of such a model, this volumetric calculation was applied to lower Strathspey, from which a volumetric estimate of the amount of sediment removed had previously been made. The volume recorded from lower Strathspey using this method was  $2.62 \times 10^8 \text{ m}^3$ , which represented 78.2% of the original volume calculated from actual terrace reconstruction, a reasonable estimate of the actual volume removed from lower Strathspey.

These values were considered to provide a first order estimate of the total volume of *sediment* in the lower terrace sequences of the Spey and Findhorn. Of interest to this study was the amount of *shingle* supplied to the littoral zone over the Postglacial period from these sources. The volumes calculated were clearly an overestimate, as the terraces contain both shingle and sand units. In order to calculate the amount of shingle removed from these terraces, an estimate of the proportion of shingle present in the terraces was required.

Borehole data was obtained from a site south of Fochabers on the Spey (Grid NJ 3357). Of 20 boreholes sunk through the lower Spey terraces, only three reached rockhead. Using these three boreholes, the amount of shingle present was calculated as a proportion of the total borehole depth. The results are shown in Table 4.30.

Borehole	% shingle
W2	90.1
6	84.2
10	92.0
Mean	88.8

Table 4.30 Percentage of shingle present in boreholes sunk in lower Strathspey (borehole data courtesy of Grampian RC)

The mean proportion of shingle in the three significant boreholes was found to be 88.8%. Using this value, the volume of sediment removed from the lower river terraces of the Spey and Findhorn was reduced accordingly, assuming an equal proportion of shingle in the Findhorn terraces as that in those of the Spey. This produced adjusted volumes representing the volume of shingle supplied to the littoral zone of  $2.94 \times 10^8 \text{ m}^3$  from the Spey and  $2.47 \times 10^7 \text{ m}^3$  from the Findhorn. The volume from the Spey was thus approximately one order-of-magnitude greater than that from the Spey. These volumes were then used in the calculation of a palaeosediment budget for the stretch of the southern Moray Firth between Speymouth and the western extremity of The Bar at Culbin.

#### 4.3.2 Outputs

A brief comparison between the volumes of sediment present in the Culbin foreland and the volume of sediment which had been removed from the lower Findhorn terrace sequence revealed that there was simply not sufficient sediment transported by the Findhorn alone over the Postglacial period to account for the volume of shingle found in the Culbin system. In order to explain the size of the Culbin foreland a secondary sediment source had to be invoked, either from updrift or from offshore.

While it is clear from the volumetric reconstruction made above that the Spey supplied considerably more shingle to the coast than the Findhorn, a major difference existed between the potential and actual supply of shingle between the rivers, aided by the presence of a large submarine delta located at the mouth of the Spey (Chesher & Lawson, 1983). The apex of the delta is approximately

8.2 km offshore, with a landward base ca. 10.9 km wide, producing a surface area of 44.69 km<sup>2</sup>. A borehole sunk at the seaward extremity of the fan (BGS borehole 71/15, Andrews *et al.*, 1990) revealed two distinct shingle units within the fan at this location. The upper shingle unit was 3 m thick, separated from a lower unit 2 m thick by 16 m of gravelly sand. As no borehole information was available further landwards, it was assumed for the purposes of calculation that these two units maintained their stratigraphic continuity landwards as far as the river mouth. Addition of the two shingle units and multiplication by the surface area of the fan produced a shingle volume in the fan of  $2.24 \times 10^8 \text{ m}^3$ . Using the volumes of the two discrete shingle beds in the fan alone as representative of the amount of shingle present clearly represented an underestimate of the volume of shingle actually present in the fan. Examples of sections through coarse-grained fans from other locations suggest that coarser units tended to thicken up-fan as transport competence tails off rapidly (Davis, 1983); thus the two shingle units in the borehole were probably far thinner at this point than units further landwards. Secondly, no estimate could be made of the amount of shingle present in the loosely labelled "gravelly sand" unit found between the shingle units, again representing a probable underestimate of the volume of shingle present in the fan. However, even if these problems are ignored, the volume of shingle present in the fan is calculated as 76.2% of the amount of shingle removed from the lower Strathspey terrace sequence.

It is proposed that the Spey shingle, once in the littoral zone and not having been lost to the submarine fan continued to drift west, by-passing the Lossiemouth-Burghead ridge to the north, entering a "proto-Burghead Bay" and continuing westwards to the Culbin foreland. However such a simple scenario was complicated by the construction of shingle depositional features *en route*, found in the field as the multiple ridge features at Spey Bay, Lossiemouth and Burghead Bay. In order to quantify the loss of shingle to these areas, the area of surficial shingle at each site was measured. This was multiplied by the operational depth of 6 m used in the calculations of the Culbin shingle volume. The results of the three volumetric calculations are shown in Table 4.31.

Location	Surficial area (m <sup>2</sup> )	Volume (m <sup>3</sup> )
Spey Bay	51 000	306 000
Lossiemouth	19 600	117 600
Burghead Bay	33 200	199 200
	<b>TOTAL</b>	<b>622 800</b>

Table 4.31 Volumetric calculations of shingle exposures at sites between Speymouth and Culbin

The total volume of shingle in the three shingle systems calculated in Table 4.31 is 622 800 m<sup>3</sup>.

#### **4.3.2.1 Volumetric calculations based on the Culbin shingle sequence**

The calculation of the volume of shingle present in the Culbin system was undertaken once the geomorphological map of the area had been completed. To briefly recap, the areas of shingle were measured as locations inner 1-outer 3 at a series of confidence levels (1-3). The details of the methods employed in the determination of these volumes has been described in chapter 2. The results of the volumetric calculations are presented at the three confidence levels in Table 4.32 below.

The volume of shingle recorded at confidence level 3 is considerably higher than in levels 1 and 2, suggesting that the results may be a significant underestimate of the actual volumes of shingle present. However, experience gained in the field suggested that the method of calculation was accurate considering the nature of the deposits. Additionally, while the values presented above are given to the nearest cubic metre, these measurements artificially overestimate the accuracy of the actual calculations. The most accurate value which could be used with confidence on the basis of these calculations would be limited by the scale of the original maps from which the secondary data (confidence levels 2 & 3) was obtained. Potential errors arising from the calculation of the volume of shingle in the Culbin ridge sequence are outlined in Chapter 6.

	Level 1	Level 1 (uncontrolled)	Level 2	Level 3	TOTAL
Inner 1	1364421	205537	68897	1885112	3523967
Inner 2	1055924	832536	15310	6700283	8604053
Outer 1	-	442105	3833380	12514468	16789953
Outer 2	265822	417224	3573101	14263699	18519846
Outer 3	1495894	-	1222930	15167022	17885846
<b>TOTAL</b>	<b>4182061</b>	<b>1897402</b>	<b>8713618</b>	<b>50530584</b>	<b>65323665</b>

Table 4.32 Shingle volumes in the Culbin foreland (all values in m<sup>3</sup>)

#### 4.3.3 Calculation of the palaeosediment budget

Input	Volume (m <sup>3</sup> )	Output	Volume (m <sup>3</sup> )	Balance (m <sup>3</sup> )
Spey	2.94 x 10 <sup>8</sup>	Speymouth delta	2.24 x 10 <sup>8</sup>	
Findhorn	2.47 x 10 <sup>7</sup>	Spey Bay ridges	306 000	
		Lossiemouth ridges	117 600	
		Burghead Bay ridges	199 200	
		Culbin foreland	6.53 x 10 <sup>7</sup>	
<b>TOTAL</b>	<b>3.19 x 10<sup>8</sup></b>	<b>TOTAL</b>	<b>2.90 x 10<sup>8</sup></b>	<b>+2.9 x 10<sup>7</sup></b>

Table 4.33 Summary of the inputs and outputs to the palaeosediment budget

The elements of the palaeosediment budget for this section of the southern Moray Firth are shown in Table 4.33, and the palaeosediment budget is shown diagrammatically in Figure 4.61. Total inputs to the system were taken to be accounted for by the fluvial sediment sources. As the calculation of the fluvial supply of shingle from the reconstruction of the river terraces is based upon dating the Lateglacial terrace surface, then it can be assumed that all shingle from the terraces since the Lateglacial has entered the nearshore zone. As sediment inputs during the wasting of ice during the Lateglacial represent the main sources of sediment supplied to the nearshore zone, then these sources have effectively been counted in the calculation of the *total* supply of shingle to the nearshore zone.

If the volume of shingle from the lower Findhorn terraces ( $2.47 \times 10^7 \text{ m}^3$ ) is added to the volumetric input from the Spey, and the losses en route subtracted, then a potential volume of  $9.40 \times 10^7 \text{ m}^3$  would have been potentially available for construction of the Culbin foreland as found in its present state, including the contemporary shingle structures on The Bar. As the total volume of shingle in the Culbin system was calculated to be  $6.53 \times 10^7 \text{ m}^3$ , then this volume is clearly sufficient to have constructed the Culbin foreland. Additionally, a residual volume of  $2.88 \times 10^7 \text{ m}^3$  would have been lost to the Culbin system, taken to end at the western extremity of The Bar. The likely fate of this shingle was reworking to form the raised shingle expanse of the Carse of Delnies (NH 830565) and the shingle spit forming Whiteness Head (NH 834573-NH 803588). The small River Nairn was unlikely to have supplied sufficient shingle alone to have deposited these relatively large features, and with the Culbin system leaking shingle downdrift, it would appear likely that this represents the eventual fate of the residual shingle.

#### **4.3.3.1 Volumetric development of the lower shingle ridge series at Culbin**

This section aims to tentatively expand the scope of the data in order to demonstrate the potential power of the palaeosediment budget technique in explaining the development of large landforms such as those at Culbin. This is done by examining dated constraints over established volumetric calculations in order to relate these to estimated rates of sediment supply. This section is seen only as a first approximation towards such a methodology, based upon the dating method employed for the shingle ridge series at Culbin, and as such can be relied upon only for order of magnitude estimates of the sediment supply link to shoreline response.

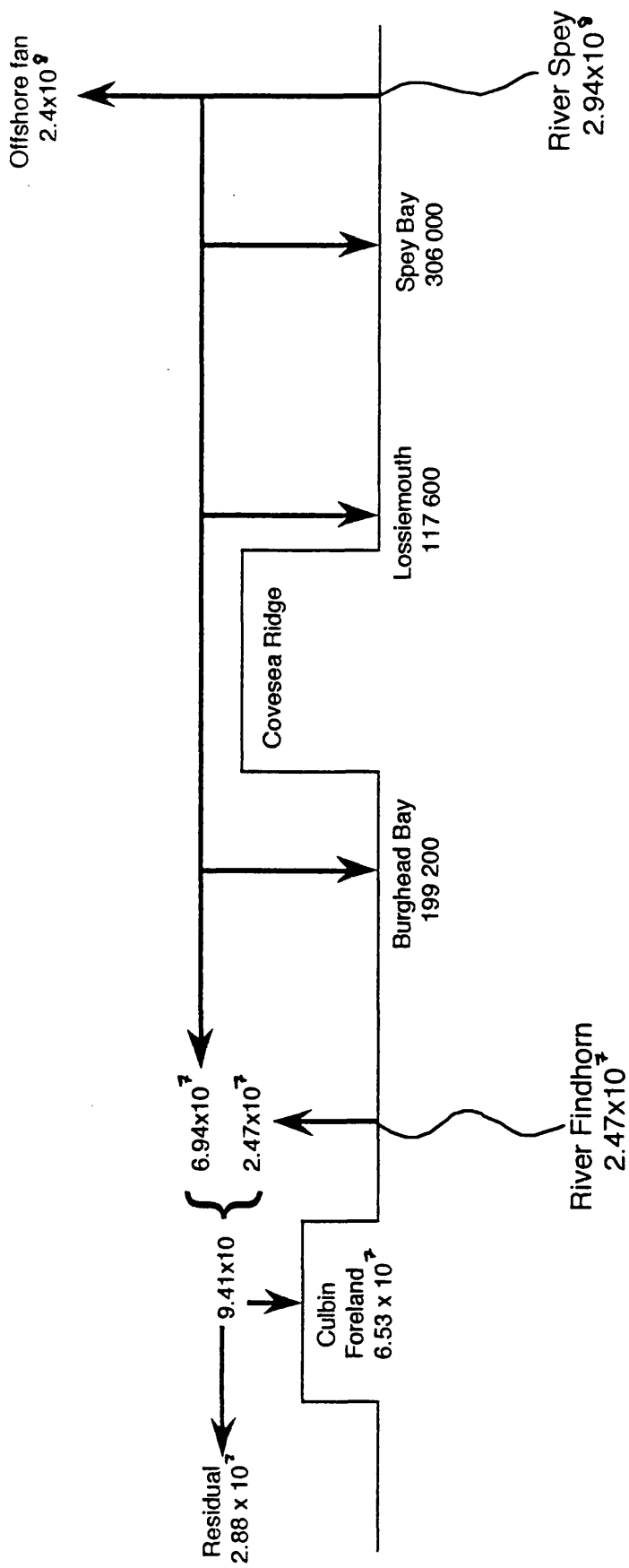


Figure 4.61 Elements of the palaeosediment budget  
(all volumes in  $m^3$ )

Lack of dating control made the subdivision of phases within the Holocene volumetric development of the entire Culbin foreland problematic. However, it was possible to investigate the accumulation of the lower series of shingle ridges (outer 3, Figure 3.14) having established both the relative ages of the shingle ridges bounding the area, and the likely sources of sediment to these ridges at that time.

The ridges in series outer 3 are contained between the base of the abrupt drop in ridge crest altitudes (section 4.1.4.3) and the most seaward shingle ridges (sets X, Y, Z, Figure 4.1). It was proposed in section 4.1.4.4 that the abrupt drop in shingle ridge crest altitude relates to the period when shingle supply from the Spey was curtailed due to water depths in excess of 6 m around the Covesea Ridge. The end of this period can be dated to *ca.* 4300 BP based upon RSL rise taking water depths to below the limiting depth of 6 m. However, this date coincides with only the onset of the altitudinal decline in the shingle ridge altitudes. The end of the decline can be dated to a minimum of 1900 BP based on the most seaward shingle ridge crest. This is located at +5.15 m OD, corrected to a sea level of +1.98 m OD using the ridge correction factor. Inclusion of the maximum altitudinal error term reduces the effective altitude of the ridge crest further, to a minimum altitude of +1.11 m OD. Insertion of this altitude into the sea level trends in Figure 4.31 produces a date of 1900 BP for the latest possible abandonment age of this ridge. Thus, the total difference between the ages of these two ridges suggests that the outer 3 series of ridges developed over a maximum period of *ca.* 2700 years between 4300 and 1900 BP.

It has been established that sediment supply from the Spey was reinstated post-4300 BP when operating depths around the Covesea Ridge fell below 6 m. However, the morphological evidence from the shingle storm ridges at Culbin suggests that shingle supply at this time was failing rapidly, producing the rapid decline in ridge crest altitude across the central section of the ridge "staircase". This point will be addressed in Chapter 5

Similarly, the reinstatement of the supply of shingle from the Spey would have been accompanied by a lag, giving time for the new supplies of shingle to feed through the Burghead Bay shingle system, to find its way to Culbin by *ca.* 3600 BP (Table 4.8). Thus in order to quantify the supply of shingle to the outer 3 zone over the period 4300-1900 BP, both the Findhorn and the Spey have to be invoked as potential shingle supplies.

It has been established earlier that the present shingle accumulation rate at the distal end of The Bar is  $1377.9 \text{ m}^3 \text{ a}^{-1}$ , currently supplied primarily by the reworking of relict proximal shingle ridges. The mean annual volume of shingle delivered to the coastal zone by the two rivers since the Lateglacial is:

$$\text{Spey: } \frac{6.92 \times 10^7}{13\ 000} = 5323 \text{ m}^3 \text{ a}^{-1}$$

$$\text{Findhorn: } \frac{2.47 \times 10^7}{13\ 000} = 1900 \text{ m}^3 \text{ a}^{-1}$$

The value for the Findhorn clearly exceeds that which is currently supplied to the nearshore zone ( $520 \text{ m}^3 \text{ a}^{-1}$ ), supporting the view that, even on the coarse resolution used in this calculation, the supply of shingle to the nearshore from the Findhorn has fallen significantly. It also demonstrates that at the present rate of accumulation, distal extension of The Bar could in the fairly recent past have been fuelled exclusively by shingle from the Findhorn if required.

Using the calculations above, then over a 2700 year span, these two sources could thus supply:

$$\text{Spey: } 2700 \times 5323 \text{ m}^3 \text{ a}^{-1} = 14\ 638\ 250 \text{ m}^3$$

$$\text{Findhorn: } 2700 \times 1900 \text{ m}^3 \text{ a}^{-1} = 5\ 130\ 000 \text{ m}^3$$

$$\text{TOTAL } 19\ 768\ 250 \text{ m}^3$$

Since it has been demonstrated that there is  $17\ 885\ 846 \text{ m}^3$  of shingle in the outer 3 ridge suite (Table 4.32), it can be seen that the Spey and Findhorn supply was capable of delivering 100% of the Culbin "outer 3" shingle as well as allowing 9.5% of the supply to bypass into the Carse of Delnies/Whiteness Head areas.

Considering the scale of measurement and the coarse dating resolution, the values obtained for the volumetric development of the lowest shingle ridge suite at Culbin (outer 3) produced a reasonable estimate of the possible supply of shingle to the foreland, to within 10% of the actual amount of shingle present. It also demonstrates that the mean supply of shingle to the nearshore zone has been significantly higher over the Postglacial period than at present.

#### **4.3.3.2 Linkages between Holocene and contemporary processes: Summary**

- i) The calculation of a palaeosediment budget represents a first order estimate of the inputs and outputs of sediment to Culbin over the Holocene.
- ii) Inputs to the system were quantified using a volumetric reconstruction of the river terraces of the lower Spey and Findhorn, a method not formerly used in British Quaternary studies. This provided a volume of  $2.47 \times 10^7 \text{ m}^3$  from the Findhorn, which was found to be insufficient to account for the accumulation of  $6.53 \times 10^7 \text{ m}^3$  of shingle in the Culbin foreland.
- iii) The additional source of shingle required to supply the extra volume of sediment at Culbin was  $2.94 \times 10^8 \text{ m}^3$ , supplied by the Spey, of which  $2.24 \times 10^8 \text{ m}^3$  was lost to a submarine delta, and  $622\,800 \text{ m}^3$  to shingle landforms constructed between Spey Bay and Culbin. This left  $6.94 \times 10^7 \text{ m}^3$  to augment the Findhorn supply to Culbin.
- iv) Having accounted for the volumetric construction of Culbin, a residual  $2.90 \times 10^7 \text{ m}^3$  of shingle was left to be transported west, adding to the smaller volume introduced by the River Nairn to form the Carse of Delnies and Whiteness Head.
- v) The volumes supplied by both Spey and Findhorn in the period 4300 -1900 BP amounts to ca.  $1.97 \times 10^7 \text{ m}^3$ , a volume which agrees well with the  $1.78 \times 10^7 \text{ m}^3$  of shingle contained within the outer ridges at Culbin.

Thesis  
9795  
copy 1  
vol 2



## CHAPTER 5 DISCUSSION

The aim of this chapter is to examine the results described in Chapter 4 in the light of existing literature in both Late Quaternary and contemporary coastal processes and landforms, and to attempt to link these together to provide an analysis of how the Culbin shoreline has responded to RSL change.

The structure of this chapter will firstly analyze relative sea level trends in the Moray Firth as a framework within which to locate the elements of the sedimentary and landform sequence. An interpretation of the contemporary beach status and sediment budget is next presented, followed by the presentation of the palaeosediment budget and response of Culbin over the early/mid Holocene in comparison with its present situation. Finally a conceptual model of shoreline response to RSL change in the Culbin/Burghead Bay area is presented, followed by comments on the possible future development of Culbin.

### 5.1 THE HOLOCENE DEVELOPMENT OF CULBIN AND BURGHEAD BAY

#### 5.1.1 Relative sea level history of the Culbin area

The establishment of a RSL history for Culbin represents an essential initial step towards understanding its coastal evolution. The position of HWM has varied enormously over the Holocene due both to changes in eustatic sea level and isostatic adjustment to changing ice loads, producing a range of locations across which foreshore sedimentation has occurred. Effectively, RSL forms the locus for coastal deposition in the medium term ( $10^2$  years), and a thorough understanding of sea level movements constitutes an essential element in reconstructing the developmental history of the area.

Collection of dateable material from the coastal deposits of the Culbin/Burghead Bay areas revealed all of the deposits seawards of the abandoned cliffline to be Holocene in age. This supports the view of Firth (1984) that the raised cliffline provides a division between the Holocene deposits to seaward, and Late Devensian features to landward.

A range of dates between *ca.* 9330 & 1300 BP was obtained from the deposits sampled, and while the majority of the samples were not actually obtained from the Culbin foreland, the regional isostatic regime in the Moray Firth allows inferences to be made regarding changes in RSL which are applicable to the

entire stretch of the coast from Burghead Bay at least as far west as Nairn. The sterility of the Culbin shingle ridge system was unexpected, with field investigations over 30 months producing only one piece of buried driftwood, which had been exposed at the surface and as such was likely to have been contaminated. A lack of organic matter found within the ridge sequence meant that material from further afield had to be sought in order to provide dating control on RSL events in this part of the Moray Firth. The following section describes the dated samples in the context of their importance to both the RSL history of Culbin and to the regional RSL history of the inner/middle Moray Firth.

The sea level data collected from the Culbin/Burghead Bay area provides the basis for a chronological development history of a previously unrecorded middle Firth site. The data was seen to fit the established chronology for the Beaully/Dornoch Firths based upon existing literature (Haggart, 1983, 1986, 1987; Firth & Haggart, 1989; Hansom & Leafe, 1990), and although the detailed timing of RSL reversals appear to be slightly earlier than those from inner Firth sites due to their location up-isobase (Figure 5.1), the use of minimum age sea level indicators (peats and shells in death positions) excluded such detailed interpretation. Indeed, the heavy dependence placed on such indicators in the inner Moray Firth studies requires considerably more caution in interpretation than has been used in the past. Consequently wider error margins, particularly around dated reversals in RSL trend, are used here than has been the case in British sea level studies. The accuracy implied by a single line is simply untenable in sea level reconstruction (Kidson, 1982), and such curves should be abandoned in favour of graphed sea level indicator points and an associated error envelope (eg Haggart, 1983).

Despite this cautionary note, the RSL trends provided by the Culbin sea level indicators produce a good fit with the trends published for the Beaully and Dornoch Firths, and as such the chronology is used as a framework against which the sea level indicators can be compared.

Figure 5.2 shows an altitude/age plot of the samples collected in the Culbin area combined with samples from the Beaully Firth (Haggart, 1986), Cromarty Firth (Peacock *et al*, 1980) and Dornoch Firth (Hansom & Leafe, 1990). The five indicators dated between 9610 and 8750 BP combine to produce a convincing falling trend in RSL after the end of the Loch Lomond Stadial (*ca.* 10 300 BP, Lowe & Walker, 1977, 1984). After reaching a low stand at *ca.* -6 m OD (Peacock *et al.*, 1980), RSL rose to the Holocene sea level maximum, which although not

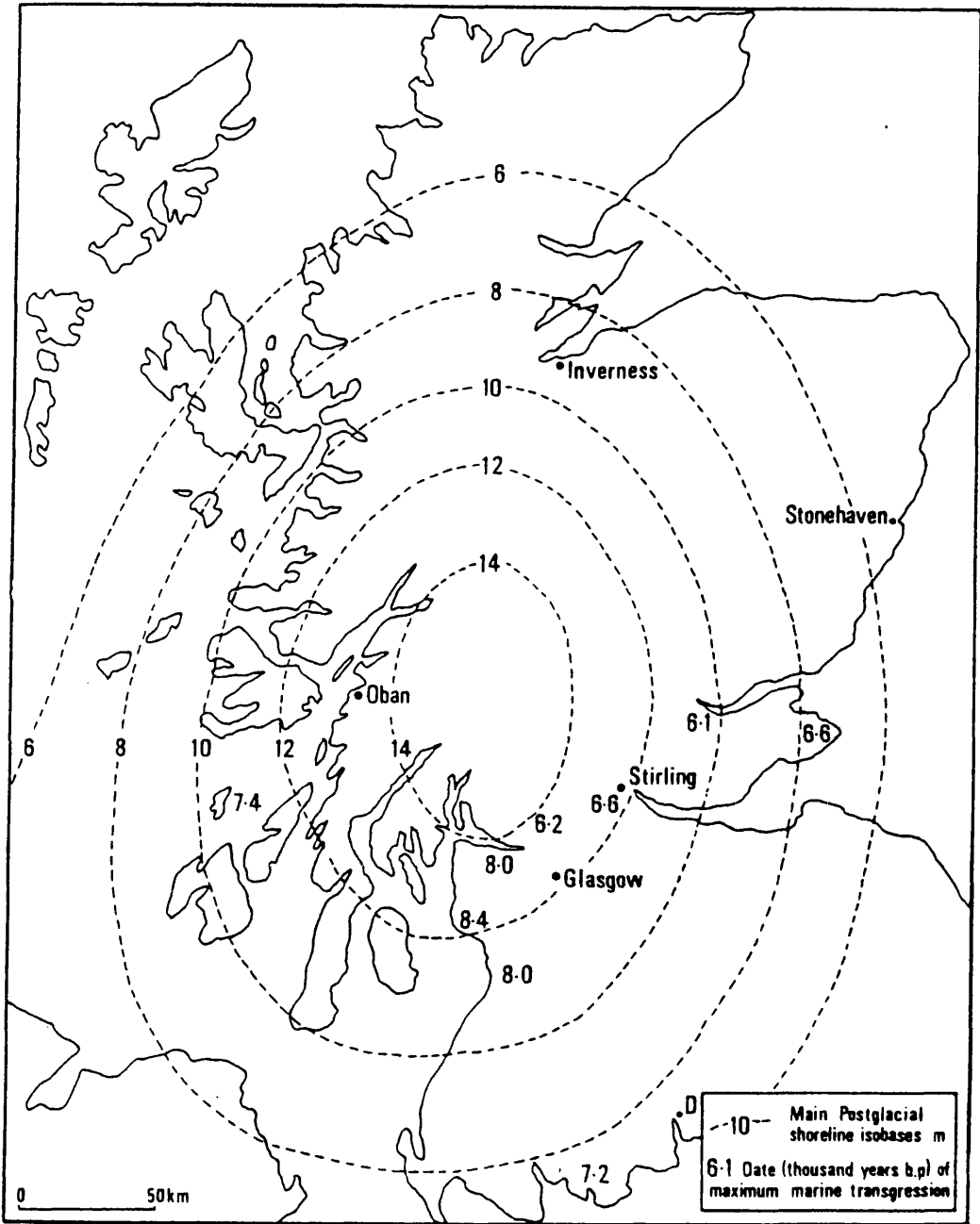


Figure 5.1 Isobase map of the Main Postglacial Shoreline (MPG) in Scotland (source; Price, 1983)

based upon any of the Culbin sea level indicators, reached a peak of ca. 7-7.5 m OD based on data from Haggart (1983). A strongly falling RSL signal after the peak of the Holocene sea level maximum is suggested by Haggart (1983), Hansom & Leafe (1990) and the Culbin data. However, a group of dates/altitudes detected by Haggart (1983) appear to be higher than would be expected for their relatively young ages. A similar series of dates were obtained from Culbin. The provenance of these deposits does not appear to fit the strongly falling trend of the younger deposits below them. The high level deposits from Culbin will be discussed below.

The trends in RSL shown in Figure 5.2 can be subdivided using data from the landforms and sediments described in the field into four chronological units:

1. Glacigenic sedimentation >13 000 BP
2. RSL trends 13 000-8000
3. RSL trends 8000-6500 BP
4. RSL trends 6500 BP-present

#### **5.1.1.1 Evidence for glacigenic sedimentation >13 000 BP**

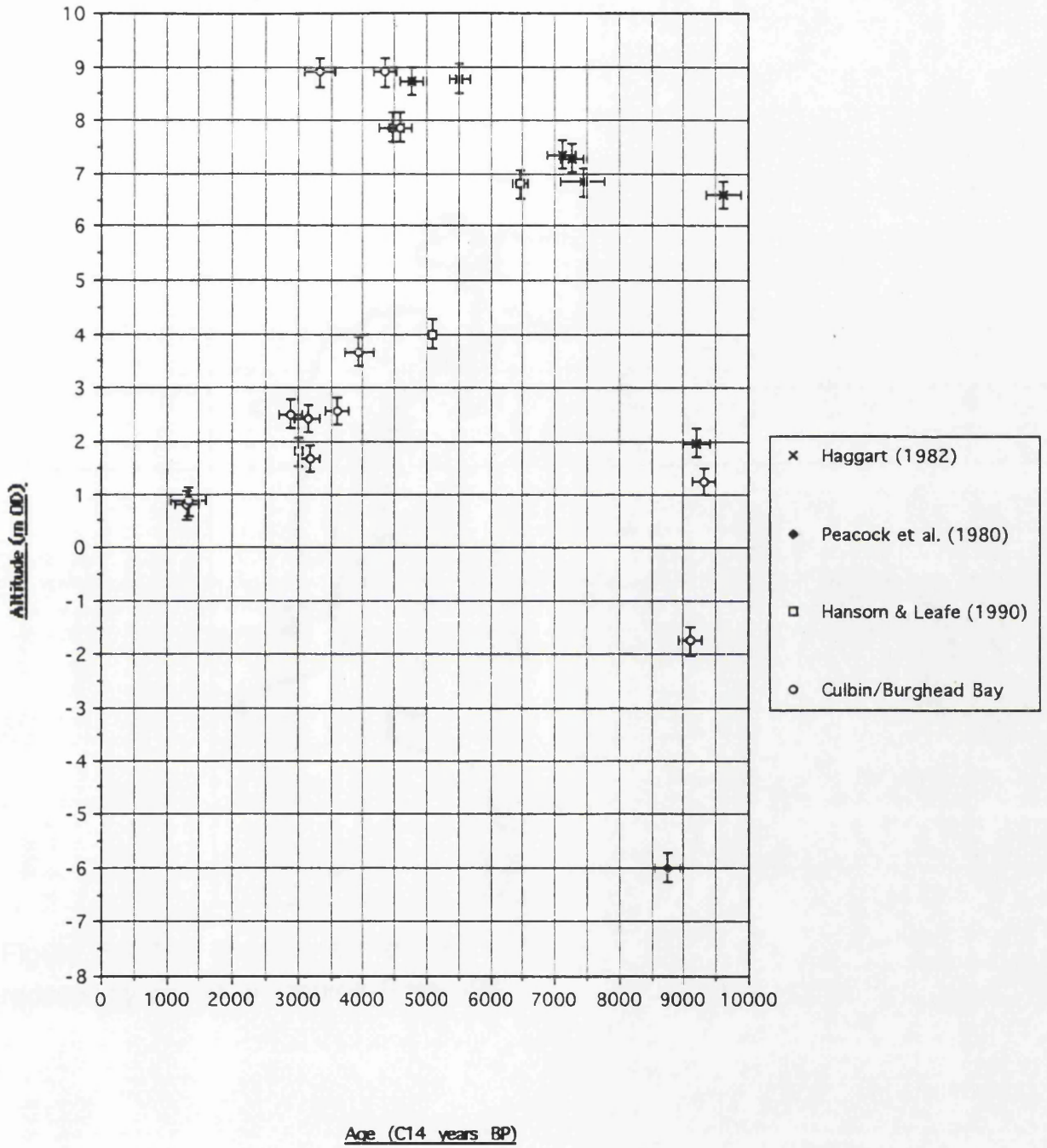
Late Devensian sediments were identified in the Burghead Bay lowlands from the extensive borehole information obtained from RAF Kinloss. At this time, RSL in the Moray Firth was low, reflecting a glacio-eustatic low stand with much of the water from the world's oceans locked up as glacier ice (Firth, 1984). As a result, with eustatic sea level at ca. -121 m (Fairbanks, 1989), the Scottish coast would have appeared as in Figure 5.3, and therefore the Late Devensian sedimentary record in the Culbin area is represented entirely by glacigenic and glaci-fluvial sediments. Rapidly rising eustatic sea level following the ongoing decay of the major ice masses of Canada and Northern Europe (Fairbanks, 1989) would have been accompanied locally by rapid isostatic uplift following deglaciation, producing an initial rapidly rising RSL, followed by falling RSL during the Lateglacial, as the rate of isostatic rebound outpaced the rate of eustatic sea level rise.

#### The sub-peat surface

Evidence from borehole records sunk through the relict foreshore and estuarine sediments which form the present site of RAF Kinloss suggest that rockhead is

Figure 5.2

Composite sea level curve from the Moray Firth



Vertical error bars  $\pm 0.265$  m (Shennan, 1982)

Horizontal error bars  $\pm 2$  standard deviations

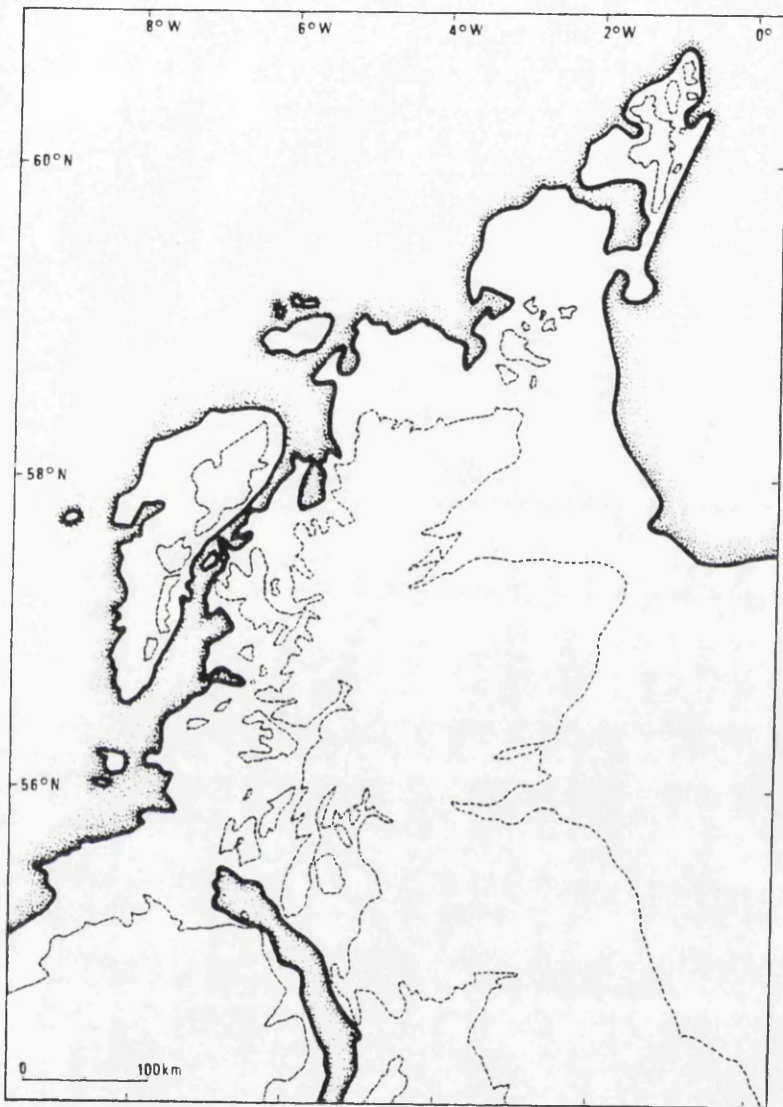


Figure 5.3 The approximate location of the Scottish coastline with sea level reduced by ca. 100 m (source: Price, 1983)

located between -23.7 m OD and at least 34.4 m OD. The undulating nature of this bedrock surface was also noted by Ross (1992). In the NE of the area, BH 1 & 2 display a considerably shallower amount of fill, with bedrock located at ca. 0 m OD. This is in accord with the outcrop of ORS slightly north of BH 1 & 2, suggesting the bedrock surface slopes gently upwards east across the width of Burghead Bay before finally outcropping to the west of Burghead. The boreholes display a diamicton directly above the bedrock surface. This is interpreted as a till, representing the intrusion of the Moray Firth glacier across the Burghead lowlands. Substantial evidence can be found in the area to support this idea (Berridge & Ivimey-Cook, 1967; Peacock *et al.*, 1968). In the vicinity of the airfield the only report of a unit resembling a till is from BH6 at the Findhorn Foundation site. The remainder of the boreholes which reach rockhead (KBH 9, 26, 35) display basal disaggregated units of angular/subangular gravel with coarse interstitial sand. These units are interpreted as glacial outwash material, deposited at the glacier front during the active westward decay of Moray Firth ice (Sutherland, 1984; Firth, 1984). The absence of a basal till unit across the airfield, with the single exception of the presence at BH6 is surprising, particularly given its presence in BH 1 & 2. This may reflect the low frequency of boreholes which reach rockhead, retaining the possibility that the remaining boreholes are simply too shallow to locate a basal till unit. Ross (1992) describes a basal till unit extending across the entire airfield, but data to support this theory is not evident from existing borehole records.

#### **5.1.1.2 Evidence for RSL trends 13 000-8000 BP**

At this stage RSL continued the falling trend exhibited from Stage 1, to reach a low stand at ca. -6 m OD (Peacock *et al.*, 1980). Isostatic rebound continued to outpace eustatic sea level rise in northern Scotland, while over the same period the eustatic signal is also suggested to have declined slightly (Fairbanks, 1989).

Evidence for such trends in RSL in the Culbin area is taken initially from the borehole data from RAF Kinloss. Above the lower gravel unit (section 4.1.3) is an extensive series of fine grained sediments, which correlate well across the central and the west transects (Figure 4.14). These units comprise silts and silty clays, with an upper surface at a relatively constant depth of ca. -7m OD. The depth is more variable, reaching a maximum of -32.25m OD in KBH 25. The fine-grained nature of the deposit, combined with reported laminations in borehole drilling schedules suggests that the unit was water-lain. The eastern transect only partly records this unit, with sands and gravels recorded in BH 10 at the

same altitude further seawards, while the silt/clay unit appears only in the more landward boreholes. This reflects the shallow nature of the more seaward boreholes, but the deeper gravel of BH 10 may represent a remnant of a fronting gravel ridge which retained a lagoonal, possibly estuarine, environment to landward, a low energy environment in which the deposition of the silt/clay unit could occur. The only other borehole in a location seawards of BH 10 was BH 9, which displays a sand unit between -9.45 & -3.45 m OD. Above this sand unit was the extensive peat unit described in Chapter 4. This peat may represent the same unit which outcrops on the foreshore in Burghead Bay (section 4.1.3). The sand unit beneath the peat sampled from the intertidal zone in Burghead Bay displays similar sorting characteristics to modern beach sand. By inference, the sand unit below the peat in BH 9 also represents a beach sand. Given the location of the sand seawards of the shingle unit, this assemblage is interpreted as a shingle storm ridge with a fronting sand terrace, as currently found on The Bar. Backponding of fine-grained estuarine units landwards of a shingle storm ridge and fronting sand beach is considered as an adequate interpretation of this particular sedimentary environment, particularly given the good spatial coverage of boreholes in this locality.

Firth (1989a) describes a series of raised shoreline fragments located between Cothill (NH 952587) and Nairn. These were interpreted as having formed after the period of rapid eustatic sea level rise immediately following ice retreat, outpacing the rate of isostatic readjustment and leading to progressive marine inundation as the Moray Firth glacier backwasted. A suite of up to ten beaches can be identified between Cothill and Inverness along the southern shore of the Moray Firth, with the highest fragments reaching ca. 25 m OD in the vicinity of Loch Loy (NH 935587). Firth (1989a) interprets the upper beaches as contemporaneous with stagnant glacier ice based on the associations between shoreline fragments and glacial landforms, in particular the middle beach sequence ILG 3A-ILG5A, and as such the upper deposit represents the marine limit in this section of the Moray Firth. Figure 5.4 displays the shoreline relationships along the southern Moray Firth, and clearly shows the steepening of the upper sections of the shorelines as they merge into kame features.

The staircase effect displayed by Figure 5.4 demonstrates the continuous fall in RSL during the formation of this series of beaches. Firth (1989a) suggests that all of the beaches predate 11 000 BP due to their truncation by the MLG in the inner Firth (Sissons, 1981; Firth, 1984; Sutherland, 1984). As ice occupied the Cromarty Firth until ca. 13 500 BP (Peacock, 1981), morphological evidence

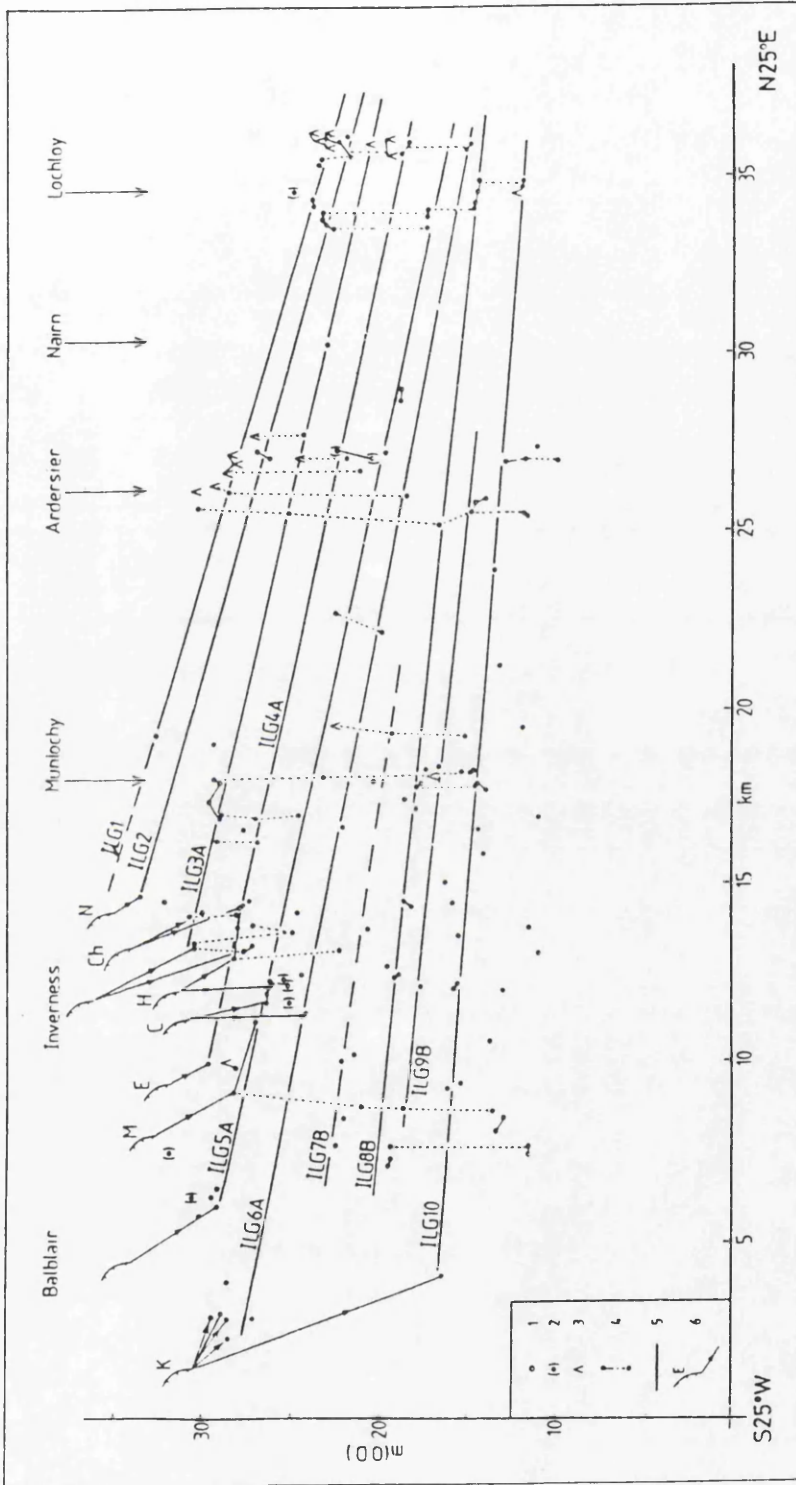


Figure 5.4 Lateglacial shorelines in the Loch Lomond area (source: Firth, 1989a)

demonstrates that beaches ILG 4A-ILG 10 formed after this time, under a falling RSL.

The regressive sequence suggested by Haggart (1983, 1986, 1987) from the two samples dated  $9610 \pm 130$  at 6.59 m OD and  $9200 \pm 100$  BP at 1.94 m OD is interpreted as a falling Postglacial trend in RSL. A similar sequence is identified in Burghead Bay and at the head of the Findhorn estuary, where this peat was found at 1.24 m OD and was dated at  $9335 \pm 45$  BP. The close agreement between this date and that of the foreshore peat bed at  $9010 \pm 45$  BP suggests that the deposits represent the landward and seaward extremities of a continuous peat/clay surface which extended across the head of a proto-Findhorn estuary and Burghead Bay. If this is accepted, then the environment of deposition and the dating of the seawards sloping surface need to be addressed. Haggart (1986) argues that a regressive offlap is represented by a decrease in age and altitude seawards, while a transgressive overlap decreases in age whilst increasing in altitude landwards, assuming that the change in altitude is greater than that attributable to local sedimentation factors and differential compaction. In the case of the Burghead Bay sediments the seawards decline in both altitude and age of the peat surface would, by Haggart's (1986) definition, represent a regressive offlap, and might thus represent a fall in relative sea level. This scenario fits well with the surrogate sea level curve adopted for the southern Moray Firth. Additionally, the gradient of the falling section of the RSL curve for the Culbin area was found to be close to that produced from Haggart's (1983) dated samples from around this period (Figure 2.4). Historical evidence suggests that the intertidal peat bed in Burghead Bay was formerly more extensive than is found at present, and extended into the deeper water of the Bay, with ships riding at anchor in the Bay reported to have dragged up tree stumps (Gordon, 1859, in Ross, 1992). This suggests that the peat exposed on the foreshore extends beyond this depth, and that RSL fell to a lower altitude than -1.75 m OD. Evidence for a low sea stand in the Moray Firth has been provided by Peacock *et al.* (1980), who suggested that a contact at -6 m OD dated  $8748 \pm 100$  BP from the Cromarty Firth represented a possible positive sea level tendency immediately prior to the onset of the Holocene Transgression. Additional information from the Dornoch Firth (Hansom & Leafe, 1990) corroborated this altitude as a possible RSL minimum, with borehole evidence of abrupt reversals in the sedimentary sequence from sands to large cobbles at -6 m OD.

The existence of the intertidal peat at -1.75 m OD on the foreshore in Burghead Bay introduces some interesting questions regarding the spatially extensive nature of this deposit. The peat has been widely recognized from early literature (Wallace, 1896; Ogilvie, 1923; Steers, 1937), although an absolute date from the bed has not previously been obtained. Initial analysis of the pollen assemblage present in the deposit suggested it to be Boreal in age (Haggart, pers. comm.). This age is supported by the radiocarbon date of  $9010 \pm 45$  BP obtained from the base of the intertidal peat as part of this study.

The Burghead Bay peat altitude conforms with the altitude of the extensive peat bed found in borehole records from below Kinloss airfield between -1.4 & -2.65 m OD in the west transect, and 0.3 & -3.25 m OD in the W-E transect. It is proposed that the foreshore peat represents the outcrop of the extensive peat surface indicated below Kinloss airfield at ca. 2-3 m OD, and that the bed is spatially continuous across the area (Figure 5.5).

West of the foreshore exposure of peat in Burghead Bay an extensive exposure of clay has been recorded on the foreshore at ca. -1.5 m OD by Ross (1977, 1992). The clay was described as 0.5 m thick, horizontally laminated, grey-green in colour and containing small shells concentrated in the upper layers (Ross, 1977). Below the clay was a unit of dark grey sandy silt containing whole bivalves, which in turn rested on coarse shingle. Again borehole evidence from below Kinloss airfield suggests that this clay bed may be more extensive. BH6 (NJ 049640) shows a grey-green shelly clay with a base at -5.5 m OD overlying a cobble band, which in turn was overlain by 2 m of grey-green clayey silt containing shell fragments. Additionally borehole KBH 24 records 3.9 m of green-grey organic rich clayey sandy silt containing shell and wood fragments at -6.4 m OD, although this was not found in proximity to a cobble band. However, the similarity of the clay bed in both of these borehole records suggests that the clay might be spatially continuous.

The similarity in altitude between the green-grey clay layer on the western Burghead Bay foreshore to the peat in the east might suggest that the units were contemporaneous. Indeed the information from borehole records on RAF Kinloss suggests that both the peat and the clay units are spatially extensive, and are mutually exclusive in the borehole logs. However, simple altitudinal relationships alone may not be interpreted as inferring a similar age of deposit. Identification of the complete bivalves in the basal silt bed below the clay demonstrated species which are presently found in the Moray Firth, with the exception of *Bittium*

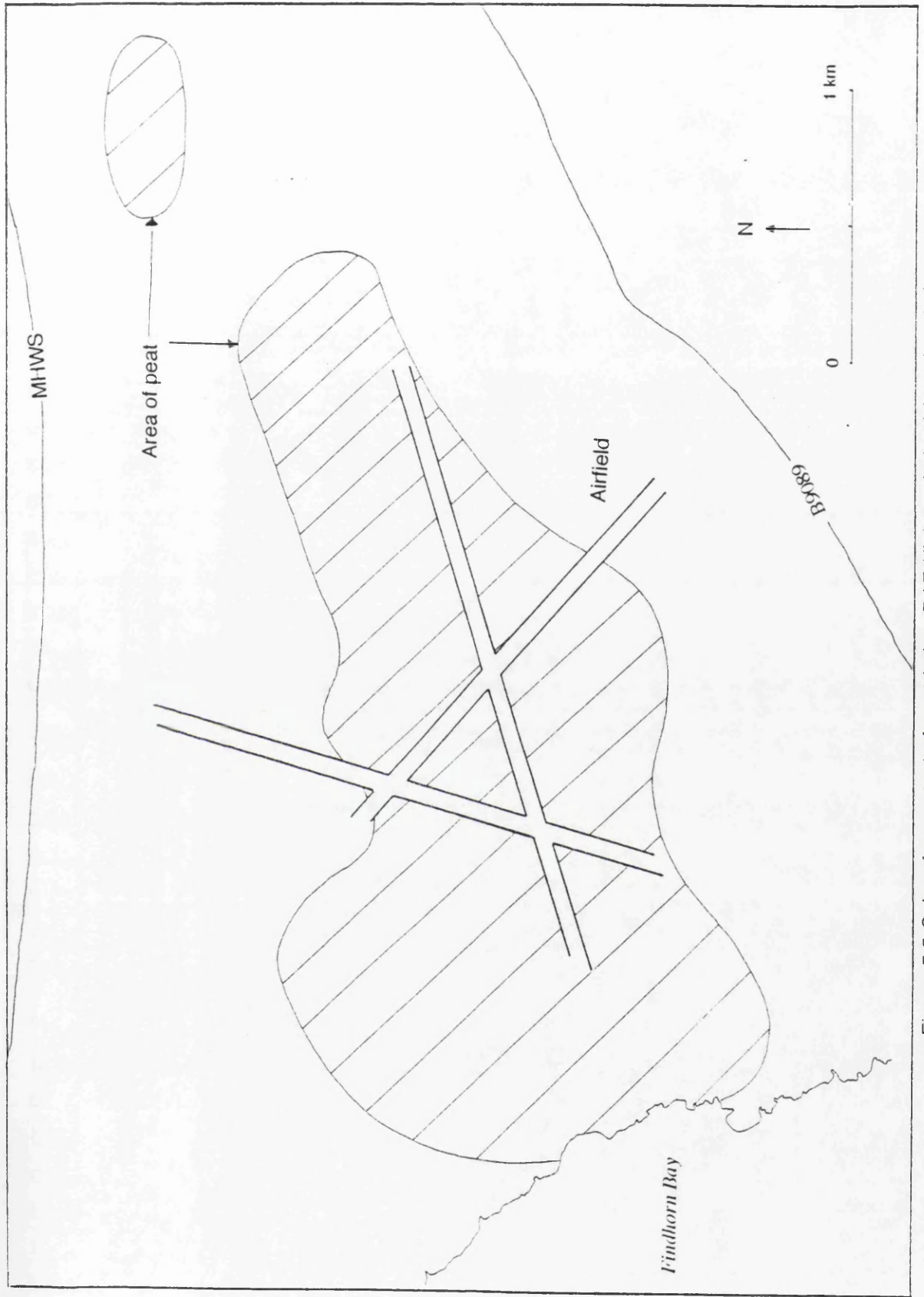


Figure 5.5 Subsurface extent of peat below RAF Kinloss derived from borehole information

*reticulatum*, (identified by Dr D.K. Graham, BGS Edinburgh), which inhabits warmer waters than are presently experienced in the Moray Firth. Price (1983) describes periods of warmer conditions in Scotland at 13 000 & 9500 BP. Ross (1977; 1992) suggests two other warmer periods also occurred, at 5000 & 500 BP, and that the clay might thus relate to one of these four periods. Despite the danger of over-reliance on identification of a single species, the coincidence of the 9500 BP period associated with the clay, coupled with a Boreal pollen assemblage and a radiocarbon date of  $9105 \pm 45$  BP from the peat suggests that the deposits may indeed be contemporaneous.

The incidence of freshwater/brackish peats contemporaneous with, and abutting shell bearing clays as described at these sites suggests a quiescent depositional environment. The close proximity of the peats to the brackish/marine clays suggests that the deposits were laid down at a saltmarsh fringe, where the edge of the marsh clays and the peat would be expected to interdigitate, producing a spatially variable contact within a limited altitudinal range around a former HWST level, as was found in the Burghead Bay deposits. Although an interdigitated vertical sequence of clays and peats was not found, the resolution at which the commercial boreholes were sunk may not have been sufficient to detect such a localized feature (Chapter 6).

The evidence from Burghead Bay provides only part of the inferred trend in RSL at this time, but what is clear from the data is that RSL was falling at the time of peat formation. Fitting this into the trend of RSL between 13 000 and 8000 BP, continued isostatic uplift recorded in Scotland at this time as a response to glacial unloading was occurring at a faster rate than eustatic sea level was rising through the downwasting of glacier ice on a global scale. The definition of this falling trend in the Culbin/Moray Firth area is discussed below.

However, two problems arise from the data. Firstly the acceptance of one standard deviation from the radiocarbon dates provides an artificially high level of confidence in the dates. Kidson (1982) recommends accepting a date of between two and three standard deviations about the mean. If this is done to the dates from the landward and seaward ends of the peat surface, the difference between the dates would only be 55 and 145 radiocarbon years for two and three standard deviations respectively. Over the spatial and temporal range of this study these differences are insignificant, and it is suggested that the difference between the dates in this case may be more apparent than real.

In spite of this, the formation of peat on a surface at -1.75 m OD is sufficiently strong evidence to suggest that relative sea level was at a lower level than at present at the time of formation. Corroboratory evidence from historical records suggested that peat also outcrops on the sea bed in Burghead Bay at a lower altitude than the intertidal peat from Burghead bay. If this is the case, then it supports the evidence that the intertidal peat represents a seawards advancing vegetation surface following a falling RSL, and that RSL fell to an altitude below that of the intertidal peat. If the peat unit at the head of the Findhorn estuary is spatially continuous across the width of the airfield and the intertidal zone in Burghead Bay, then this raises questions regarding the preservation potential for such a lithologically weak deposit across such a wide area. While it might be expected that fragments of a formerly more extensive peat unit could be preserved, the existence of a spatially continuous bed across 5 km, covered by raised beach deposits suggests that the peat was buried extremely rapidly during foreshore sedimentation under rising RSL during the rise to the Holocene sea level maximum.

#### Formation of the abandoned cliffline

The abandoned cliffline in the Culbin area forms a continuous feature of the southern Moray Firth from Buckie to the Beaully Firth. Explanation of its formation has been skirted by workers in the Moray Firth, although clearly parts of it postdate Late Devensian foreshore deposits which it truncates, for example at Cothill (Firth, 1984).

Haggart (1986, 1987) proposed that falling RSL following deglaciation deposited a series of marine silts and clays in the Beaully Firth. Following deposition, the onset of the Loch Lomond Stadial was invoked as a mechanism to induce crustal redepression in the Moray Firth (Sissons, 1981; Firth, 1989b), creating a rise in RSL to ca. 11 m OD, depositing a unit of coarse sand and gravel over the silts and clays, and re-occupying the abandoned cliffline (Haggart, 1986). Both Haggart (1986) and Firth & Haggart (1989) consider the cliffline to have been cut during a stillstand at 2 m OD during the early part of the Stadial, followed by a rapid rise in RSL to re-occupy and retrim the cliff.

Closer examination of both the field evidence and geophysical data suggests, however, that a rise in RSL of the magnitude proposed during the Loch Lomond Stadial (Cullingford *et al.*, 1986; Firth, 1986, 1989b) would have been unlikely.

Sissons' (1981) interpretation of the sand and gravel layer in the Beaully Firth as a Stadial deposit was based on geomorphological evidence alone, and is unsupported by absolute dates. Indeed, the marine provenance of the deposit is questioned on the grounds of the proximity of the Moniack alluvial fan (Figure 5.6). Such a feature would input a large volume of mixed grade sediment to a large area fronting the structure. Further evidence to support this contention is provided by the description of a marked break in slope of the sand and gravel unit from 2 m to ca. 6.6 m OD to landward (Sissons, 1981). This break in gradient was explained by Sissons (1981) as evidence of an increase in the rate of RSL rise during the Loch Lomond Stadial. However, such a change in gradient is unknown in any other marine or foreshore deposit in the Moray Firth, and to produce such a feature would require a high magnitude event occurring over a short period. Alternatively, with the sand and gravel unit deposited at the head of a large delta, then such a change in gradient could be interpreted as the junction between foreset and bottomset units of a simple deltaic sequence. Haggart (1987) stated that a gravel layer had been identified on either side of the fan, which confirmed its limited extent. However, no details were provided as to how the sand and gravel unit was differentiated from the fan deposits on the basis of borehole data alone.

Geophysical data suggests that a small ice sheet similar in size to that formed during the Loch Lomond Stadial would be unlikely to create >10 m of crustal redepression. Quinlan & Beaumont (1981) demonstrated that a 110 x 80 km ice sheet (i.e. similar in size to the 175 x 100 km Stadial ice sheet [Gray & Coxon, 1991]), readvancing for 1000 years, would produce only 4 m of RSL rise. This change is considered too small to actually register on a graph of RSL trends in relation to a potential measurement error band.

Lambeck (1991a, b) produced a model of glacio-isostatic response of a visco-elastic earth to glaciation. Early reconstructions of Scottish ice sheets (Boulton *et al.*, 1977; Denton & Hughes, 1981) were considered to be too large, and consequently Lambeck's model uses as input the minimum ice reconstruction proposed by Boulton *et al.* (1985). The results are reproduced in Figure 5.7, and if the erroneous Wester Ross Readvance is ignored, the glacio-isostatic curve demonstrates a negligible signal at the peak of the Loch Lomond Stadial. Lambeck (1991a) stated that the Stadial ice mass would have to be much greater in extent than presently assumed to produce a significant signal in the sea level record.

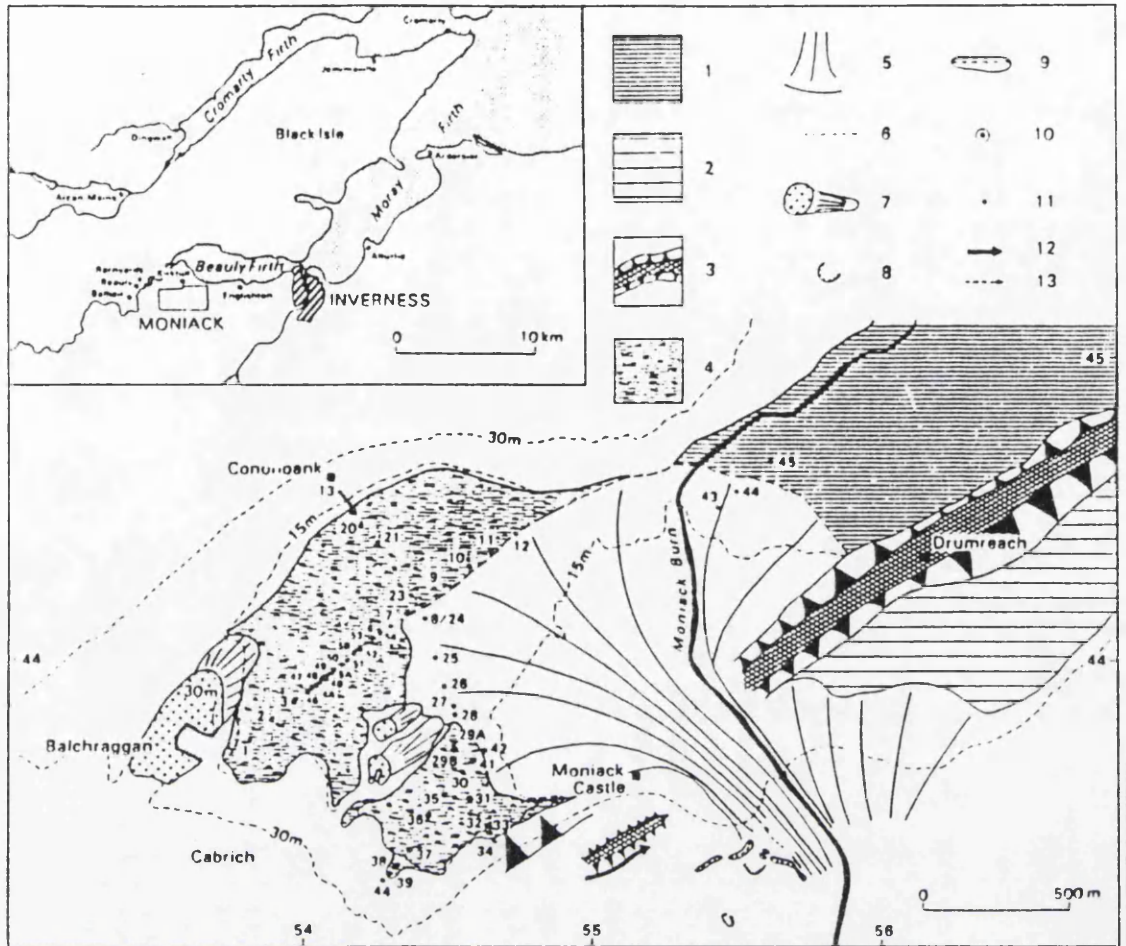


Figure 5.6 The extent of the Moniak alluvial fan (feature 5) in the Beaully Firth (source: Haggart, 1987)

### Key

1. Kirkhill carse.
2. Undifferentiated Late Devensian marine deposits.
3. Ridge forms.
4. Surface peat.
5. Alluvial fan.
6. Boundary of fan uncertain.
7. Crag and tail forms.
8. Dead ice hollows.
9. Eskers.
10. Pollen, diatom and C14 sampling sites.
11. Boreholes.
12. Meltwater channel.
13. Small channel form.

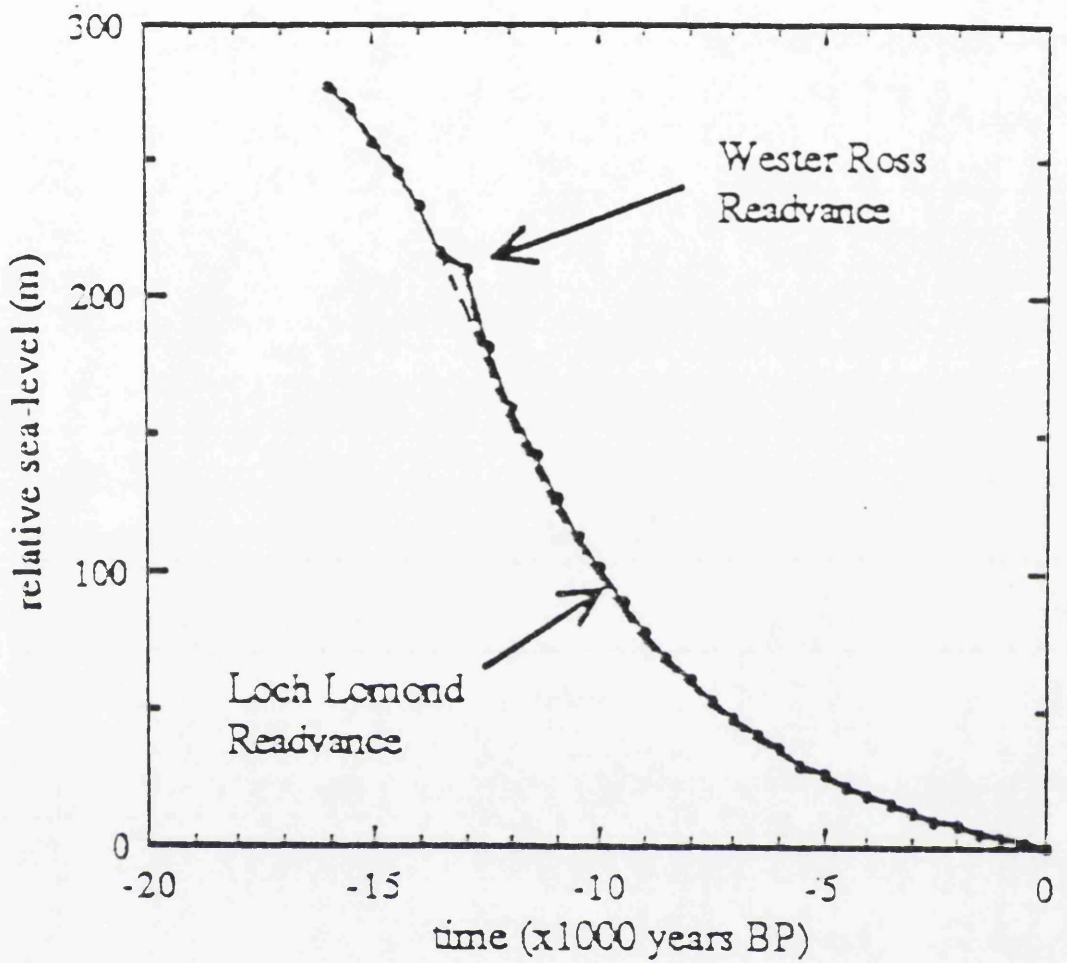


Figure 5.7 Scottish isostatic rebound curve showing the negligible impact of a modelled Loch Lomond Readvance (source: Lambeck, 1991a)

If rising RSL during the Loch Lomond Stadial is accepted, then a similar signal would be expected from sites closer to the former Stadial ice mass. Sea level curves from Gartmore/Arnprior (Upper Forth Valley: Sissons & Brooks, 1971), the Earn-Tay system (Cullingford *et al.*, 1980; Paterson *et al.*, 1981), Grangemouth (Browne *et al.*, 1984), Lochgilphead & Ardyne (Peacock *et al.*, 1978) and Oban (Syngé, 1977) show no similar anomaly.

This short review of both available field data and evidence from geophysical models suggests that evidence in favour of crustal redepression during the Loch Lomond Stadial is weak, and as such the formation of the abandoned cliffline around the Moray Firth is unlikely to have occurred at this time. As such, invoking a period of RSL rise in order to explain the formation of the cliffline may not be realistic. The only period when RSL was low enough to form the cliffline prior to the emplacement of the fronting Holocene deposits was during falling RSL to the Postglacial low stand *ca.* 8750 BP (Peacock *et al.*, 1980). It is thus proposed that the cliffline was cut either during a stillstand in this falling trend, or at the low stand. If the latter is the case, then the buried foot of the cliffline forms the MLG in this area.

#### **5.1.1.3 Evidence for RSL trends 8000-6500 BP**

After *ca.* 8750 BP RSL in the Moray Firth began to rise once more (Haggart, 1983, 1986, 1987; Firth & Haggart, 1989) as the final decay of the Laurentide and Fennoscandian ice masses occurred (Dyke & Prest, 1987; Fairbanks, 1989; Mathewes, 1989; England, 1992). This caused a rise in eustatic sea level which outpaced the rate of isostatic rebound in Scotland, creating a rise in RSL to a Holocene sea level maximum (the "Holocene Transgression").

Unfortunately no dated transgressive contacts representing a reversal in RSL trend at the onset of the rise in RSL to the Holocene sea level maximum were recorded in the Culbin area. Three dates provided by Firth & Haggart (1989), based on Haggart (1986, 1987) demonstrate rising RSL at  $7430\pm 170$ ,  $7270\pm 90$  and  $7100\pm 110$  BP, providing only a minimum age for the onset of the rise in RSL to the Holocene sea level maximum, which clearly predates these samples. The peak of the Holocene transgression was bracketed by the youngest of these dates ( $7100\pm 110$  BP) and a younger regressive contact dated  $5510\pm 80$  BP found at 8.81 m OD. In the Dornoch Firth the Holocene sea level maximum was dated to  $6445\pm 30$  BP on peat overlying beach sands at 6.8 m OD, representing the Main Postglacial Shoreline in this area (Hansom & Leafe, 1990). While this is substantially lower than the upper deposits from the Beaully Firth it brackets the

Holocene sea level maximum more closely. Evidence from Culbin of a high RSL at this time is provided by the highest shingle ridges in the Culbin series, which reach a maximum altitude of 10.995 m OD. Using the ridge correction factor, this value is reduced to an equivalent MSL of  $7.825 \pm 0.87$  m OD, which using the lower error band produces a value of 6.995 m, in agreement with the isobase map of the MPG in this area (Figure 5.1). It is thus proposed that the MPG at Culbin is represented by a shingle storm ridge, demonstrating the sediment rich environment of deposition of Culbin during the peak of the Holocene sea level maximum. Thus this period was characterized by rising RSL at a time when sediment availability was still potentially high (Maizels & Aitken, 1991).

#### **5.1.1.4 Evidence for RSL trends 6500 BP-present**

After the peak of the Holocene sea level maximum and the formation of the Main Postglacial Shoreline, RSL began to fall once more from ca. 7 m OD in the Culbin area at ca. 6500 BP. This falling trend has continued through until the present, and is strongly supported by the altitudinal "staircase" relationship displayed by the extensive shingle storm ridge suite at Culbin (section 4.1.1).

Firth & Haggart (1989) record falling RSL by  $5510 \pm 80$  BP. Evidence from both the Dornoch Firth (Hansom & Leafe, 1990) and Culbin also suggests falling RSL at this time (Figure 4.21). The RSL indicators on the falling limb of the curve from the Dornoch Firth were found to be significantly lower in altitude than those from both the Beaully Firth, while dated samples from this period were absent from the Culbin area. A possible explanation for this lies in the fact that the samples from the Beaully Firth were closer to the isostatic uplift centre and thus are located on a higher isobase than those from the Dornoch Firth (Figure 5.1). Thus while both sets of dates were obtained from lithologically similar units ("carse clays"), relative proximity to the former Scottish ice centre led to a significantly different recovery altitude. Should samples have been recovered from the Culbin area of comparable age and from comparable deposits they might have been expected to have been at similar altitudes to those recovered from the Dornoch Firth due to their similar position on the 7 m Postglacial isobase (Price, 1983).

The recovery from Snab of Moy of peats overlying a shingle storm bank abutting the foot of the abandoned cliffline and overlying sand deposits north of this location produced dates which, in relation to their altitude, do not fit the graph of RSL trends at Culbin (Figure 5.2). A date of  $4335 \pm 45$  BP was obtained from peat overlying the shingle bank, while two dates ( $4450 \pm 45$  &  $4570 \pm 45$  BP) were

obtained from organic material contained within the sand unit fronting the shingle.

The peat dates clearly represent the minimum ages of the associated deposits. The altitude and position of the shingle are located at 8.90 m OD and banked against the foot of the cliffline. Although not a true reflection of its relationship with MSL, application of the ridge correction factor produces a corrected altitude of  $5.73 \pm 0.87$  m OD. It was seen earlier, that shingle beach formation was ongoing since the formation of the MPG, located *ca.* 4 km NNE of Snab of Moy. The formation of the shingle bank predates the formation of the peat, but postdates the formation of the MPG, despite being located landwards of it. In order to explain such a situation, evidence from locations nearby had to be examined.

Evidence from dated material in the pond sediments sampled at Snab of Moy provided information vital to the interpretation of the formation of the shingle bank. The dates obtained from the basal peat units of the ponds are  $3330 \pm 60$  and  $3600 \pm 45$  BP (SRR 4684 & SRR 4685 respectively), with the ponds probably representing areas of back-beach deposition in depressions landwards of the fronting shingle ridge series. The apparent date reversal from the middle peat unit sampled (SRR 4688, dated  $3935 \pm 55$  BP) unfortunately casts doubt on the accuracy of the age of these three samples. The large difference in altitude shown between the two basal peat units (*ca.* 2 m) and their position at the western end of a series of shingle ridges (Figure 3.6) suggests that the higher of the samples (SRR 4684) may have been obtained from a buried shingle ridge crest, while SRR 4685 was removed from a swale. Due to the dating reversal in the sequence a precise date for the formation of the peat, and hence a minimum age for the emplacement of the shingle ridges can not be inferred with accuracy. However, from the range of available dates a minimum age of *ca.* 3000-4000 BP would seem appropriate for the emplacement of these particular shingle ridges.

A shell midden located at NH 993618 yielded a date of  $3209 \pm 75$  BP (Coles & Taylor, 1969). The midden is located on the recurving shingle ridges slightly inland from those at the base of the Snab of Moy ponds, and provides a further control on the minimum age of the ridges.

The emplacement of the distal ends of the shingle ridges thus postdates the formation of the shingle bank at the foot of the cliffline. Furthermore, examination of Figure 3.1 reveals that shingle ridge formation had not extended this far west by *ca.* 3000 BP, leaving an "energy window" to the NW open to allow the

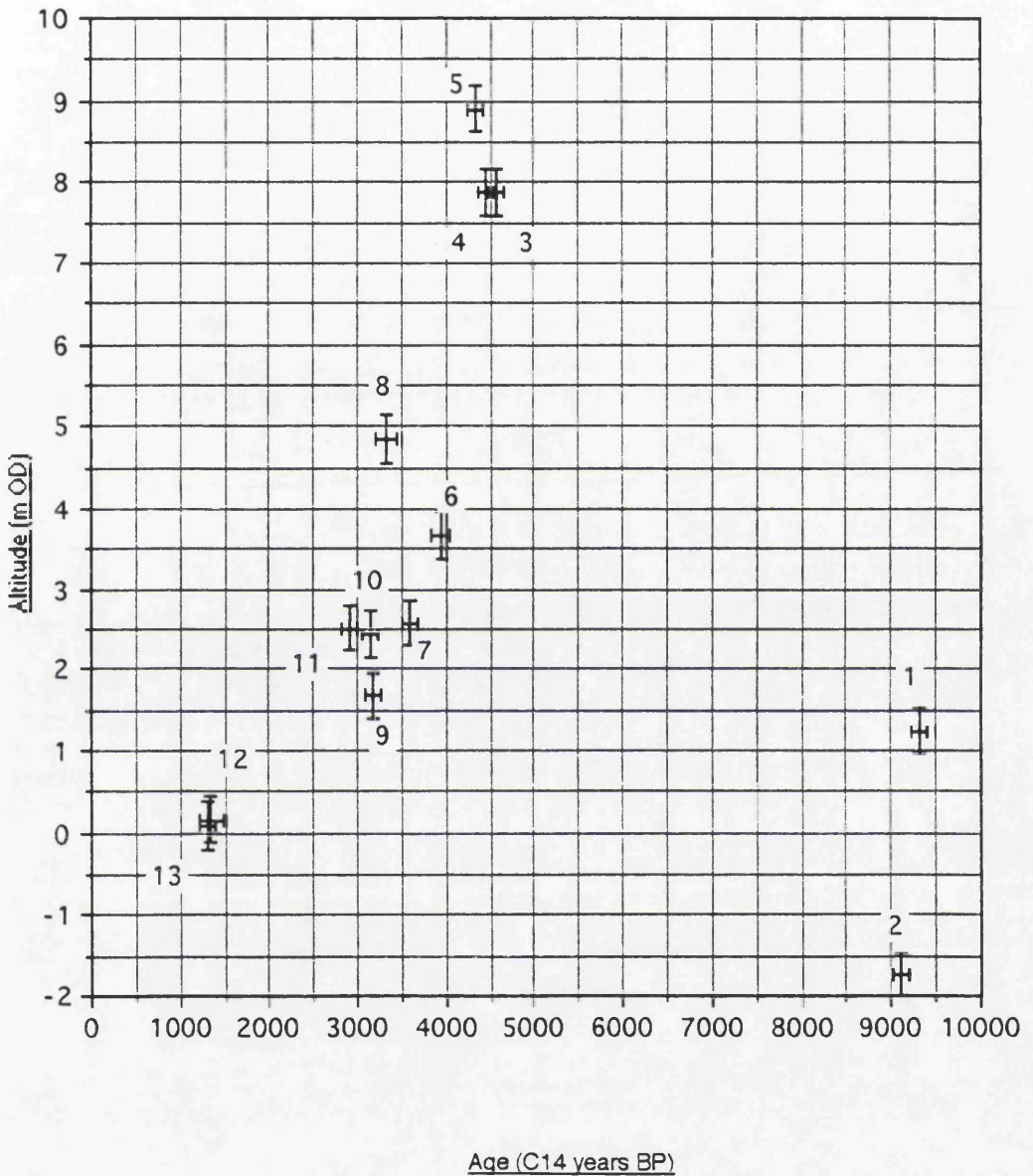
encroachment of waves. Waves from this sector could only be locally generated wind waves, assuming a palaeogeography of the Firth essentially similar to present. Thus the shingle bank is interpreted as a small, secondary shingle structure unrelated to the major series of shingle ridges actively forming seawards of the MPG, and representing a structure formed by lower, wind wave activity depositing residual shingle in a back-barrier environment.

The lower samples SRR 4679 & 4681 were recovered from peats infilling former stream channels in Burghead Bay, graded to a slightly higher RSL than at present, and are dated  $3140\pm45$  &  $2900\pm45$  BP respectively. The altitude/age relationship of these samples correlate well with the lower sample from the Dornoch Firth curve. Sample 6 was recovered from a swale between two shingle ridges in the Bessie Burn section, and as such the fit of the sample with the remainder of the deposits at the lower end of the curve is probably more apparent than real. Swale elevation was noted to be related to crest elevation in the Dungeness shingle ridge sequence (Long & Fox, 1988), but no constant relationship was recorded. Intervening swale depths relate to the relative height of the two enclosing ridges and the angle of repose of the constituent shingle rather than to any particular depositional process. However, the peats provide a minimum age for the abandonment of the surrounding shingle ridges between  $3140\pm45$  and  $2900\pm45$  BP.

Samples SRR 4680 & 4682 were recovered from within shingle ridges at 3.96 and 4.03 m OD respectively. These were revealed in section in Burghead Bay, and were dated  $1300\pm45$  and  $1340\pm65$  BP respectively. Their altitudes were corrected according to the correction factor outlined in section 4.1.3. The corrected age/altitudes are shown in Figure 5.8. The altitudinal trends shown by the samples clearly display an exponential relationship between altitude and age.

The dated sea level indicators described in this section support the evidence from the Beaully and Dornoch Firths of a continuously falling RSL trend from the Holocene sea level maximum at ca. 7 m OD dated 6500 BP through until the present. Both Shennan (1989a) and Dawson (1992) suggest that a slowing isostatic element combined with a relatively stable eustatic sea level would produce such an exponential response. In NE Scotland the reduction in the isostatic signal, trending perpendicular to isobase, runs approximately E-W along the southern Moray Firth coast (Figure 5.1). Shennan (1989a) summarized RSL signals from the inner Moray Firth, and suggested that isostatic rebound has

**Figure 5.8 Sea level indicators from Culbin and Burghhead Bay (corrected altitudes)**



Sample number codes correspond to the following key:

- |                       |                        |
|-----------------------|------------------------|
| 1. 9305±45 (SRR 4689) | 8. 3330±60 (SRR 4684)  |
| 2. 9105±45 (SRR 4677) | 9. 3170±40 (SRR 4678)  |
| 3. 4570±45 (SRR 4687) | 10. 3140±45 (SRR 4679) |
| 4. 4450±45 (SRR 4686) | 11. 2900±45 (SRR 4681) |
| 5. 4335±45 (SRR 4683) | 12. 1340±65 (SRR 4682) |
| 6. 3935±55 (SRR 4688) | 13. 1300±45 (SRR 4680) |
| 7. 3600±45 (SRR 4685) |                        |

occurred at a maximum rate of  $1.6 \text{ mm a}^{-1}$  for the past 4750 years at the head of the Beaully Firth.

#### **5.1.1.5 Summary**

A low sea stand during the Lateglacial period led to glacigenic and glacialfluvial sedimentation in the Culbin area prior to 13 000 BP. Backwasting ice in the Moray Firth was accompanied by marine flooding, forming shoreline features at the marine limit in the Lochloy area (Firth, 1984, 1989a). Isostatic uplift continued after this period, while the rise in eustatic sea level slowed (Fairbanks, 1989), leading to a fall in RSL down to a low stand at *ca.* 8750 BP with the formation of the peat/clay units in Burghead Bay occurring across newly abandoned foreshore surfaces. A rise in RSL between 8750 and 6500 BP occurred as eustatic sea level rose once more, outpacing the rate of isostatic uplift in the Moray Firth and forming the MPG at *ca.* 7 m OD in the Culbin area. While this is recognized as a well formed shoreline feature in lower energy environments in the inner Firth (Firth, 1984), in the Culbin area it is represented by a high set of shingle storm ridges at up to *ca.* 11 m OD. A continuous fall in RSL has occurred since the Holocene sea level maximum through until the present, leading to the emplacement of the extensive Culbin shingle ridge suites and the smaller Burghead Bay series. The use of a correction factor based on a modern analogue from The Bar, coupled with dated altitudes from shingle ridge crests in Burghead Bay, demonstrates that shingle storm ridges in sufficient numbers and with adequate altitudinal control can provide first order information regarding RSL trends at the time of their formation.

#### **5.1.2 The use of shingle storm ridges in the reconstruction of RSL at Culbin**

One of the aims of this study was to investigate whether shingle storm ridges, if represented in sufficient numbers, might be used to indicate the level of RSL at which they were formed, and the sedimentary regime as they were forming. This section discusses the work undertaken, and demonstrates the relative success of the method employed.

##### **5.1.2.1 Shingle ridge correction factors**

The collection of four radiocarbon dates from within shingle ridges in Burghead Bay, coupled with the use of the correction factor from the contemporary set of shingle ridges found on The Bar proved extremely useful in the determination of

the age/altitude relationships between shingle ridge crests and similarly aged deposits obtained from more "traditional" marine indicators. The correction factor was defined as the mean shingle ridge crest altitude (in m OD), which at The Bar is 2.1 m above chart datum, or approximately mean water level (MWL). The mean crest altitude of the shingle ridges on The Bar is 3.17 m OD. This value was subtracted from the inland ridge crest altitudes at Culbin in order to present a series of corrected shingle ridge altitudes relating to MWL.

Former studies of multiple shingle ridges in the context of RSL changes in Britain have been limited to work at Dungeness, the only shingle based landform of a similar size and quality of preservation to Culbin in Britain. Shingle storm ridges have formed more minor elements of RSL studies in Scotland (eg Firth, 1984; Hansom & Leafe, 1990), but have generally been allied with other sea level indicators. Elsewhere, the use of shingle storm ridges has been largely ignored. This has been mainly due to the large error term involved in relating ridge crest altitude to absolute sea level, perceived as problematic when the ridge crest altitude is related mainly to the intensity of the storm which formed it and the rate at which (if any) the ridge is abandoned by seawards accretion of a fronting ridge. Firth & Haggart (1989) used the value proposed by Gray (1983) of 0.80 m to relate the variability of ridge crest altitude to that of its formative RSL. From the investigation of the shingle ridges on The Bar, it was apparent that this value represented a slight underestimate of the variability in altitude of shingle ridge crests, and a revised value of 0.87 m was proposed as a more realistic alternative, based upon the mean difference between the altitude of the contemporary storm ridge crest and the altitude of the formative RSL.

Dating the altitude of the shingle ridge crests using absolute techniques provides a further control over the inferred RSL trends which may be obtained from shingle structures. The collection of dateable material was limited in the Culbin area to only two ridge crests located in Burghead Bay. These two palaeosol units (samples SRR 4680 & 4682) display a particularly convincing fit with the remainder of the marine indicators from both Culbin and the Beaully Firth diagrams (Figure 5.2). Sample SRR 4678, collected from the stream section on the Bessie Burn in Burghead Bay, display an anomalous altitudinal relationship with the remainder of the indicators due to its position on a shingle basement in a swale between two intervening shingle ridge crests. Sample SRR 4683, obtained from the shingle storm ridge at the foot of the raised cliffline at Snab of Moy farm, also displays an anomalous altitude/age relationship, being located at 8.90 m OD but dated  $4335 \pm 45$  BP. However, in this case the age of the peat

provided a minimum age for the abandonment of the feature, whereas the nature of the landform in this case differed from the remainder of the shingle ridges in Culbin, representing a storm bank resting against the foot of the cliff rather than a free standing shingle structure.

Such an interpretation would fit the known tendencies in shingle storm ridge sedimentation under differing conditions of sediment supply. With excess sediment supplied to the ridge at a constant rate, the construction of shingle storm ridges will mirror the incidence of storm events, with the construction of an individual storm ridge rapidly superceded by a new ridge to seaward, creating a regularly spaced series of seawards accreting storm ridges, each exposed to formative storm events for only a limited period. Conversely, under conditions of low or irregular sediment supply, the tendency is for the construction of a single, large storm ridge as the frequency of storms outstrips the rate of sediment supply, reworking the beach face and throwing shingle into an ever higher bank. The implications of these findings will be discussed more fully in the light of the palaeosediment budget in section 5.3.2.

Across the relict shingle series in Culbin Forest there is a general decline in altitude of the ridge crests in a seawards direction, reflecting deposition during a fall in RSL after the Holocene sea level maximum *ca.* 6500 BP (Firth & Haggart, 1989). A marked drop in altitude was recorded across a short lateral traverse on the central and eastern sets of ridges. This was also noted on the western traverse across the shingle fan, but these ridges were later discounted from analysis due to the presence of a declining gradient of between 4.6 and 8.6 m km<sup>-1</sup> along their crests, reflecting refraction and deposition around a distal recurve.

Given the variability demonstrated by the shingle ridge crests, an error factor of 0.87 m was successfully applied to this data to relate them to their formative sea level. Similar techniques have been used elsewhere with some success (Sollid *et al.*, 1973; Møller, 1989). Figure 4.31 demonstrates that the subtraction of the mean altitude of the ridge crests located on The Bar from crest altitudes in Culbin provides a convincing fit ( $R^2 = 0.79$ ) onto the projected exponential trend in RSL following the peak of the Holocene sea level maximum (Shennan, 1989a; Dawson, 1992). The number of dated control points necessitates caution and would require more samples if confidence is to be placed in the method. The convincing fit allows the curve to be used to place approximate dates on individual ridges at specific altitudes.

Corroboratory data supporting the concept of shingle ridges as a valid indicators of RSL changes was obtained from the pond sites at Snab of Moy. The shingle ridge correction factor was applied to the altitude of the inferred ridge crest below sample SRR 4684. If the interpretation of the underlying shingle deposits as shingle storm ridges is correct then it might be expected that the resulting corrected age/altitude would fit the sea level curve for the Culbin area. The base of the sample is located at 6.40 m OD, with a possible error of -0.10 m imposed by the nose section of the Russian corer. This produces a minimum altitude of 6.30 m OD. Subtracting the correction factor of 3.17 m provides a minimum corrected altitude of 3.13 m OD, falling into a maximum age bracket of 3000-4000 BP assuming the dates obtained from the pond samples were broadly correct. Plotting this age/altitude onto the sea level curve, the resultant point shows a convincing fit within the accepted error term, suggesting that the interpretation of the undulating basal surface of the ponds is correct.

#### **5.1.2.2 Impact of enhanced storminess on shingle ridge development during the Holocene.**

Lamb (1982) demonstrated that the global pattern of cyclone and anticyclone tracks tends to change with variations in the circumpolar vortices. This has implications for changes in global climate patterns (Wendland & Bryson, 1974), affecting Britain in particular through the incidence of westerly tracking, storm-inducing anticyclones. Expansion of the northern vortex during full glacial periods forces weather systems further south beyond Britain, while interglacials are characterized by a northerly migration of westerly cyclone tracks across Britain. Within such long term fluctuations, shorter term fluctuations in the frequency of storm conditions occur in Britain due to variations in the strength and magnitude of wave forms within the circumpolar vortex.

While direct evidence for periods of enhanced storminess in Britain cannot be obtained before reliable records began (during the Medieval period), indirect evidence from dated periods of enhanced *sand dune* activity around the British coast provides a surrogate variable for periods of enhanced storminess. Periods of dune instability have been identified at *ca.* 3500 BP in England (Tooley, 1990) and Scotland (Ritchie, 1979), 2000-1000 BC (*ca.* 3900-2900 BP) in the Netherlands (Jelgersma *et al.*, 1970), 600-400 BC (*ca.* 2100-1900 BP) in Britain (Brooks, 1949), AD 500-800 (Lamb, 1991) and AD 1300-1700 (Hickey, 1991).

If the Holocene can be characterized by periods of enhanced storminess which affected dune development, interspersed with less energetic spells, then these

periods might also be major formative periods for shingle ridges. However, such a suggestion contains two major problems;

1/ that shingle ridges are formed under *storm* conditions,

2/ that shingle ridge altitudes are directly related to storm intensity.

While it is true that shingle ridge crest altitude will be influenced by storm intensity during formation, the actual crest altitude will more fully represent the level of MSL at the time of formation, *modified* by the intensity of the formative storm. This will produce a series of shingle storm ridges at a series of altitudes within an error bracket, the variation in which will be centred on a mean crest altitude which can be related to a formative MSL.

Secondly, the mechanism for storm beach formation (Orford, 1977) at HAT under conditions of spilling breakers suggests that storm wave activity at the tidal maximum is not as significant as previously suggested (King, 1972). Thus while an increased frequency of storm events might indeed produce more storm events (and not necessarily more severe storms and higher ridges), this will lead only to the production of more shingle ridges at similar altitudes within the same error bracket. Thus the incidence of periods of enhanced storm frequency during the Holocene does not interfere with the premise that shingle ridge crest altitudes relate (within a given error band) to the MSL at the time of formation.

### **5.1.2.3 Dating the abrupt drop in shingle ridge crest altitude recorded in the Culbin ridge suite**

Having established that the corrected shingle ridge altitudes fit a sea level trend for the Moray Firth, they can be used to bracket the timing of an abrupt fall of 4.00 and 3.31 m between successive ridge crests of the central and eastern transects. Both transects produced an upper date limit of between 4300-4600 BP for the onset of the fall, but the lower ridge crest altitudes on the central transect fell into the asymptotic section of the exponential curve (Figure 4.31), producing a wider error margin. On the eastern transect, however, the higher crest altitude at the base of the drop produced a smaller error, dating the base of the drop to *ca.* 3300 BP, and bracketing the timing of the event to between *ca.* 4650 and 3300 BP. The abrupt nature of the altitudinal drop matched against a smooth and gradually falling RSL trend suggests that the drop was related to interruption in the supply of sediment from updrift, rather than to a specific sea level event. The

implications of this are discussed further below in relation to an overview of the Holocene supply of sediment to Culbin.

### 5.1.3 A model of RSL and sediment supply at Culbin

What emerges so far from the RSL trends at Culbin using both traditional C14 dating techniques augmented by shingle ridge altitudes is that while RSL provides a *general* picture of shoreline genesis, it does not explain the *detailed* elements of coastal evolution at Culbin. The supply of sediment is clearly a key element which has not been fully addressed, and so this section aims to describe the combined effect of RSL and sediment supply on the coastal evolution of Culbin. A three stage model of RSL and sediment supply is presented, followed by a series of four case studies demonstrating the varied response of the shoreline to changes in RSL under different sedimentary scenarios.

Figure 5.2 demonstrates the RSL trends identified from this study and from previous work in the inner Moray (Haggart, 1983, 1986, 1987) and Dornoch Firths (Hansom & Leafe, 1990). What has not been considered, however, has been the impact such changes might have on the status of sediment, and particularly shingle, transport. Shingle becomes immobilized as water depths increase beyond a critical limit. Studies on the mobility of shingle in the nearshore zone suggest that shingle becomes totally immobile at depths of 9 m (Trask, 1955; Steers & Smith, 1956; Neate, 1967; King, 1972; Hansom, 1992). This provides a maximum depth for shingle mobility, but Kidson *et al.*, (1958) demonstrated that shingle is mobile between 5.5 and 7.5 m under waves of 0.91 m height. Thus a depth of 6 m represents a maximum depth to which shingle is *normally* mobile. Additionally, Figures 5.8a & b display the bathymetry of the offshore zone at both Burghead and Lossiemouth. The steep gradient of the nearshore slope (particularly at Lossiemouth) adds weight to the conviction that, even under rising RSL, shingle would tend to simply be drowned *in situ* rather than be forced onshore up such a slope. Thus the Covesea ridge acts as a "valve" to the flow of shingle from Spey Bay to Burghead Bay, opening when absolute water depths fall below 6 m, and closing when water depths exceed 6 m.

Morphological evidence from The Bar found shingle mobile to a minimum depth of 1.4 m, while a further 3.87 m is deposited subaerially as a shingle storm ridge, producing a minimum thickness of the entire shingle landform of *ca.* 6 m. Similarly borehole 8 from Burghead Bay located 6 m of shingle, although as the

Figure 5.8a

**Submarine section offshore from Burghead**

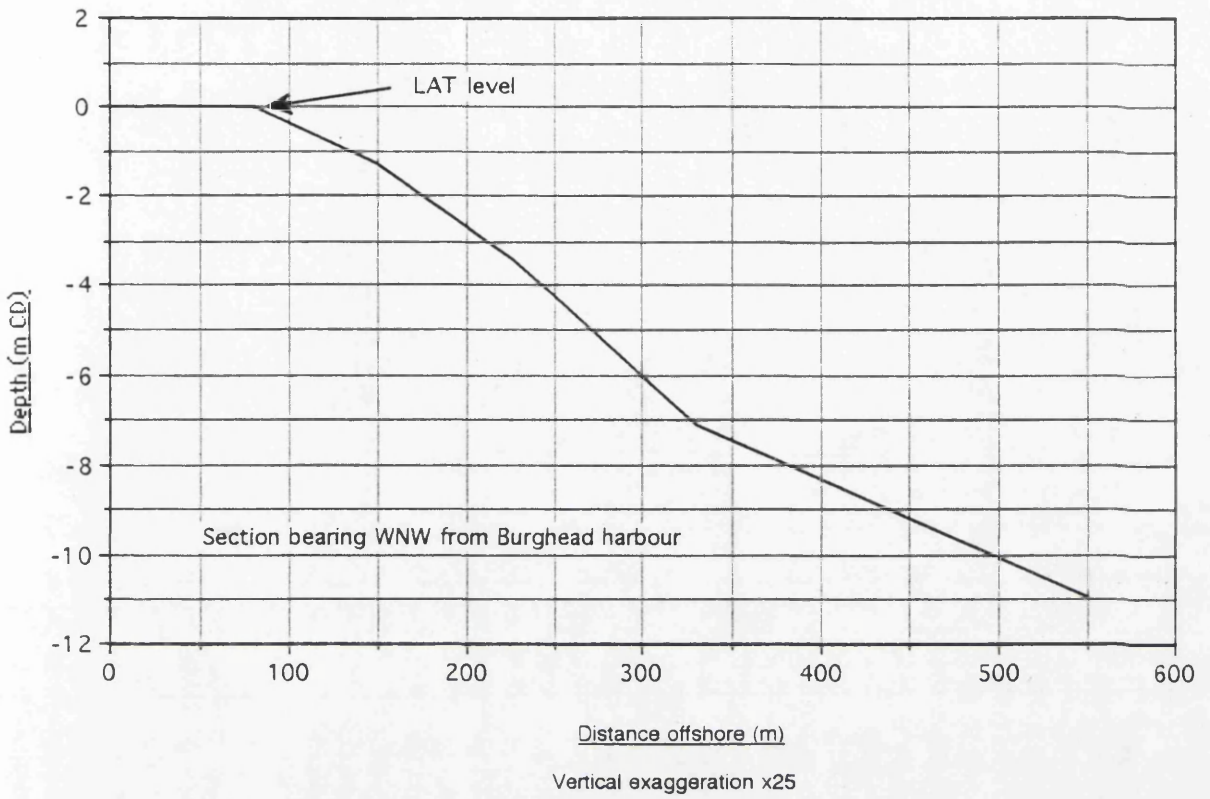
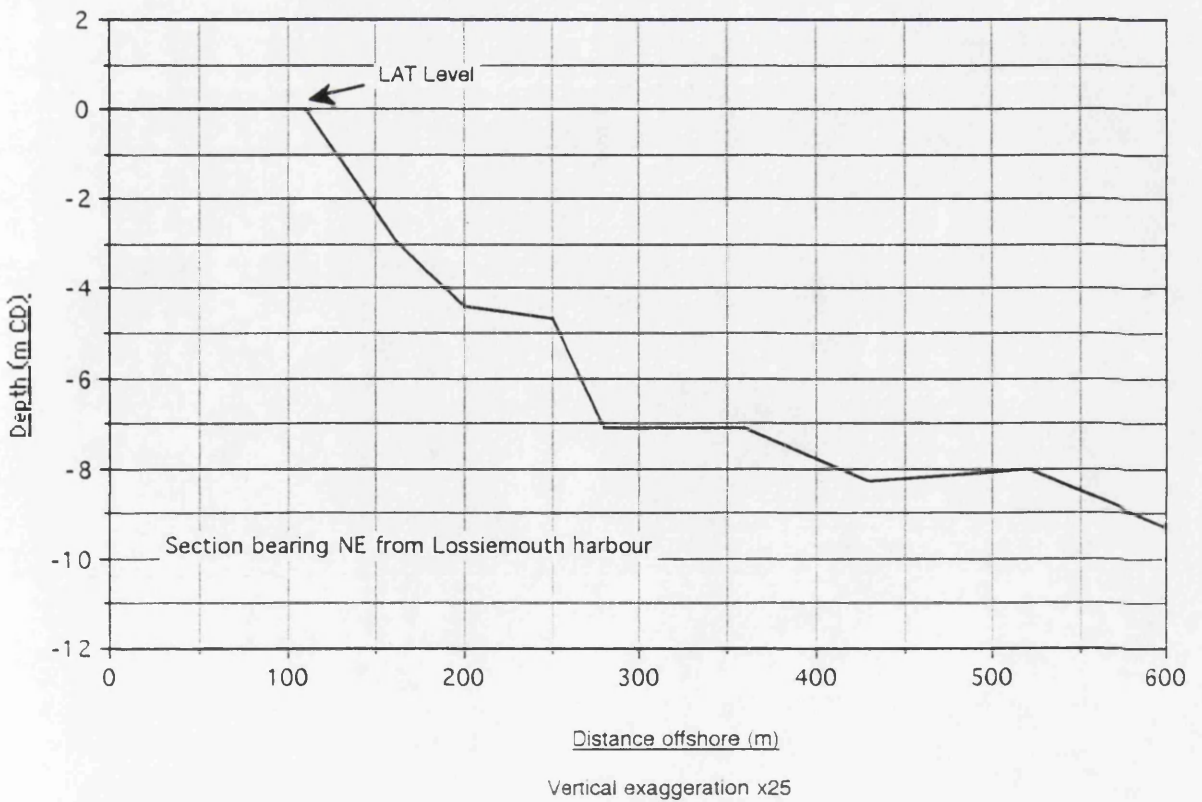


Figure 5.8b

**Submarine section offshore from Lossiemouth**



stratigraphic details of the immediate surroundings are not known, this value can also provide only a minimum shingle thickness. Carter (1988) suggests that the zone of maximum shingle mobility is in the swash zone, while earlier data (Steers & Smith, 1956; Kidson *et al.*, 1958) demonstrate shingle to be mobile to at least depths of 6 m under moderate wave heights. Thus 6 m was selected as the maximum operational depth for shingle in the Culbin area, and at greater water depths it is assumed that shingle is immobile.

In the light of this evidence, Figure 5.9 shows a conceptual model of RSL and sediment supply potential to Culbin over the Holocene. The model is divided into three phases centred around a critical RSL of +3.9 m OD, representing a water depth of 6 m. When water depths are less than 6 m then sediment movement can be achieved around the northern flank of the Covesea ridge, allowing a connection between the Spey and Burghead Bay and providing a passage for Spey shingle onto the beaches at Culbin. Phases 1 & 3 show RSL below 3.9 m OD, allowing the Spey shingle to augment that from the Findhorn. Thus Phases 1 & 3 are seen as periods of high sediment supply to Culbin.

Phase 2 occurs between 7200 and 4300 BP, and represents a period when RSL around the Covesea ridge is in excess of 6 m. At this depth, shingle is immobilized and the supply from the Spey is terminated, leaving the only supplies of shingle to Culbin as those from the Findhorn and from the reworking of shingle ridges in Burghead Bay. Phase 2 is thus seen as a period of potentially lower sediment supply to Culbin.

The case studies of shoreline response to RSL and sediment supply will now be examined in the light of this conceptual model.

#### **5.1.4 Shoreline response to RSL change**

Various pieces of evidence from different stages during the Holocene are used to illustrate the nature of shoreline response to RSL change. These are described in a series of four case studies, demonstrating the variable nature of coastal evolution under different combinations of RSL and sediment supply.

##### **5.1.4.1 Case study 1: Events postdating the Holocene sea level maximum**

Case study 1 describes the development of the Culbin shingle ridge suite, which developed on the declining limb following the Holocene sea level maximum during Phases 2 and 3. Typically if the supply of sediment is high, then multiple

**Conceptual three stage model of sea level and sediment supply at Culbin**

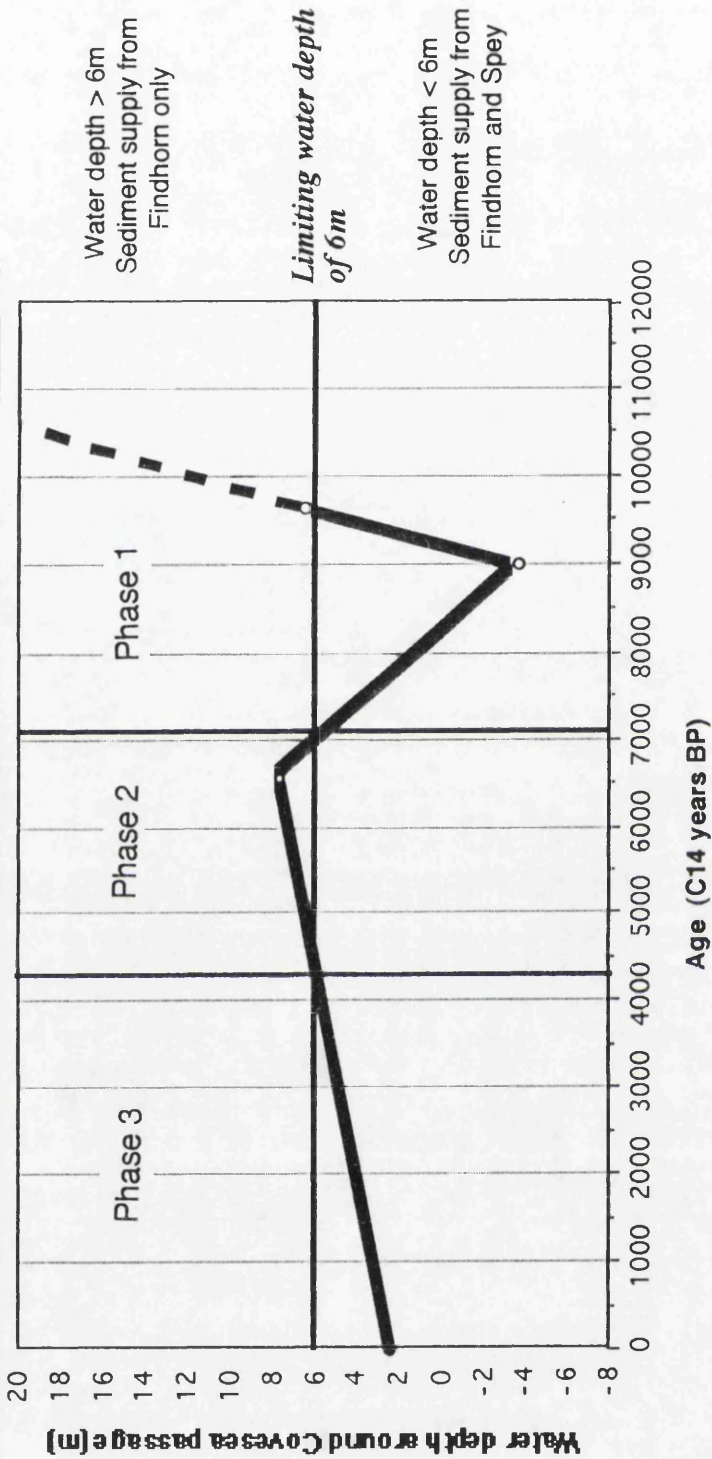


Figure 5.9

storm ridges develop as the supply of sediment at all points along the foreshore exceeds the periodicity of storm events. However, if sediment supply is low, then the tendency is for a single storm ridge to develop, with reworking of shoreface sediments into a single, large structure with a critical crest altitude ultimately determined by the angle of repose of the constituent shingle and the width of the structure (Orford, 1987).

Measurement of the wavelength of the shingle ridge structures was undertaken in order to demonstrate the spacing of the ridge crests, representing a possible surrogate variable for the regularity of sediment supply. Although only a crude measurement of a variable which is affected by a variety of environmental controls (RSL change, storm intensity, shoreline orientation, pre-existing ridge topography), the spacing of shingle storm ridges will be primarily influenced by the volume of shingle available for construction in the nearshore zone. A more even distribution of shingle ridges (i.e. a low standard deviation of crest spacing) would be expected to reflect low supply of sediment, because shingle storm structures, when starved of shingle, tend to build larger individual forms (Carter, 1988), eventually approaching an equilibrium crest altitude related to the angle of internal shear of the constituent clastic material. A more uneven spacing (i.e. a high standard deviation of crest spacing) would reflect a higher rate of sediment supply, resulting in rapid, irregular progradation as storms of varying intensity threw up storm ridges of varying altitude, with little time for further ridge consolidation prior to storms constructing the next ridge seawards.

In order to assess the relationships between the relict shingle ridges located in Culbin Forest and their contemporary analogues on The Bar, the wavelength (crest-crest distance) and altitude were measured on as many ridge sequences as possible. Clearly the lowest altitudes were recorded from the shingle ridges only recently abandoned on the distal flank of The Bar, having been deposited during the recent historical period and relating to a RSL similar to that of the present. Measurement of the wavelength characteristics of the ridges on the Culbin foreland reveals mean crest-crest distances of between 5.32 m (set D, n=19) and 41.22 m (sets X, Y, Z, n=8), a considerable difference. Standard deviations of altitude provides a measure of the regularity of crest altitude, with sets X, Y, Z once more providing the highest standard deviation (2.44), and the DB lower set providing the lowest standard deviation (i.e. most internally similar crest altitudes)(0.14). Perhaps more revealing are the calculations of the standard deviations of ridge wavelength, which act as an index of the regularity of spacing of each ridge set. These also display marked differences, following

the same trends as those of altitude standard deviation, with the highest value recorded from sets X, Y, Z (24.55) and the lowest from set D (1.80).

Plotting mean wavelength against mean altitude (Figure 4.3) provides no clear relationship, suggesting that across the declining foreland surface there was no particular trend in ridge crest spacing. However, the plot of standard deviation of wavelength against standard deviation of altitude (Figure 4.4) displays a positive but weak relationship ( $R^2=0.57$ ), which although heavily dependent on two data points in particular, might suggest that increasing irregularity in the storm ridge spacing may be accompanied by increasing irregularity in ridge crest altitude.

Such a relationship would not be unexpected. Under conditions of high, regular sediment supply the shingle ridges would form as a response to the occurrence of storm events. Orford (1977) suggested that crest overtopping, and hence ridge crest altitude, relates to the occurrence of spilling breakers at the tidal extremity (HAT, not MHWS), rather than the throwing of shingle up to the beach crest by plunging breakers (King, 1972). The upper limit of storm ridge crest activity is thus not completely random, but relates instead to the level of the storm surge under which it formed. The altitudes of the ridge crests on The Bar support this idea, with the crest of the contemporary storm ridge at 3.87 m OD, while the highest spring tides at Nairn reach only 2.2 m OD (Table 4.9). Despite a wide margin of error (0.87 m), ridge crest altitudes will be significantly more even in their vertical distribution than has previously been implied, provided sediment supplies are high, and as such form a potentially useful first order indicator of MSL. Thus the relationship suggested by Figure 4.4 is theoretically supported, although more field data would be required to test it more vigorously.

Ridge wavelength measurements have not been considered in any previous studies on shingle landforms in the UK. Their potential use as a surrogate variable for the regularity of sediment supply, is manifest in the abrupt drop in crest altitude recorded in the Culbin ridge series. Morphologically, a change in the status of sediment supply would feed through in the form of more frequent shingle beach reworking. Shingle beaches naturally migrate onshore due to a lack of a return mechanism to the foreshore for shingle following storm sedimentation (Carter & Orford, 1984). Thus even under falling RSL shingle beaches will tend to attempt to rework themselves under conditions of low sediment supply rather than remaining static. The landward forcing of the ridge crest through washover processes will produce a more irregular ridge crest spacing than under accretionary conditions.

Measurement of the standard deviation of wavelength reveals a marked rise between the ridge crests seawards of the drop in altitude relative to those landwards of it. This suggests that although sediment supply had been low prior to the drop (Phase 2), it had been regular. After the drop, a larger number of storm ridges are found (the "outer 3" zone, Figure 3.14) with a high standard deviation of wavelength. This supports the suggestion that sediment supply from the Spey and the Findhorn was becoming more sporadic and possibly beginning to fail.

Thus the detailed measurement of morphological characteristics of the shingle storm ridges at Culbin demonstrates that under conditions of falling RSL, the shoreline has responded in a different manner depending on the availability of sediment. A low but regular supply of sediment produces a regularly spaced series of shingle ridges with low variability in crest altitude, whereas a higher but possibly failing sediment supply produces a more irregularly spaced series of shingle ridges with a more variable ridge crest altitude.

#### **5.1.4.2 Case study 2: Estuarine sediments**

The presence of fine grained sediments landwards of the shingle ridge sequence in Culbin Forest provided a further example of the variety of shoreline responses to RSL change. Detailed sampling of the estuarine sediments was undertaken at three sites, although test cores were taken from a much wider area, confirming the presence of similar sedimentary sequences in the areas of estuarine sediments identified by Gauld (1981). No foreshore sediments finer than sands are located seawards of the shingle ridge series, as expected in an energetic wave environment.

These estuarine deposits clearly post-date the shingle ridge sequence, which must have been emplaced prior to the creation of a low energy depositional zone in their lee. Sampling concentrated on the basal unit at each of the sites, which appeared in the field to be a similar deposit of fine white sand/silt overlying a shingle unit of indeterminate thickness. Laboratory analysis of the basal unit from each of the three sites suggests that units LAG 2 & 3 are relatively similar in terms of grain size and skewness characteristics, although their sorting parameter differs considerably, LAG2 being very well sorted, and LAG1 only moderately sorted. LAG1 displays a much larger mean grain size than the other sites and much lower skewness and poorer sorting values, suggesting a generally coarser, less well sorted deposit.

The presence of occasional rounded clasts within the basal sand units, plus the sorting indices suggests that these deposits were water laid, although under slightly different energy environments. LAG1 and 2 were deposited in a slightly higher energy environment than LAG3, although all three still appear to represent back barrier units. The overlying units of LAG3 display an upper silt unit overlying a thin organic layer, which in turn overlies a fine sand unit with iron staining. This sand was slightly coarser than the basal sand, which was not sampled for detailed analysis, although in the field it was noted as similar in texture to contemporary dune sand. Considering the dip angle noted on the organic layer, plus the relatively fine sand unit below, this sequence is interpreted as a former dune surface, with the angle of dip representing a lee slope with a low angled, apparent southerly dip.

Taken together, the evidence from these three sites suggests a former low energy environment in which fine grained sands and silts were deposited. Preliminary evidence from the other sites cored also display little evidence of organic layers within the units. However, thin organic units were observed in both LAG1 and 2, although redeposition of sediment over the organic unit was noted in LAG1, suggesting that the site was not heavily vegetated.

This data appears to support the hypothesis that the fine grained sediment assemblage represents a former low energy, possibly estuarine environment as suggested by Gauld (1981) and Ross (1992). The location of the shingle ridge sequence seawards of these sediments on all sides at altitudes of ca. 3.5m above these deposits would have provided the requisite shelter required for their deposition, in an environment similar to that presently experienced at the western end of The Bar. The sandy nature of even these relatively fine sediments is also reflected in the contemporary sedimentology of The Bar, where the high sand content of the salt marsh surface has been recorded (Blionis, 1991).

The enclosing shingle ridges are located at 11.39 m OD, providing a corrected altitude of  $8.22 \pm 0.87$  m ASL, with a further set of ridges at  $8.70 \pm 0.87$  m ASL seawards of them. The Postglacial marine limit at Culbin is located at 8.90 m OD, and so these shingle ridges represent the high energy equivalents of the Postglacial marine limit. As the estuarine sediments were deposited landwards of these shingle ridges, then they may be contemporaneous, but are located at a lower altitude, reflecting deposition under lower energy conditions. Such barrier/backbarrier relationships have been reported from other sites with an altitudinal range difference between environments related to a similar formative

sea level (eg van de Plassche & Roep, 1989). The altitude of the estuarine surface is located at 7.36 m OD, ca. 1.5 m below marine limit. Firth & Haggart (1989) describe the indicative range of saltmarshes (the closest approximation to this environment) in the contemporary intertidal zone of 0.30 m. As the locus of saltmarsh sedimentation is at MHWS, which, assuming no change in tidal range over the Holocene, is +2.2 m above MSL (Table 4.9). With an upper surface at 7.36 m OD, this represents a contemporaneous MSL of 5.16 m OD. If the upper value of the indicative range is added, this suggests formation under a sea level of 5.46 m OD. From the trends in RSL (Figure 5.2) it is clear that this deposit must have formed at ca. 5200 BP, 1300 years after the Holocene sea level maximum under conditions of falling RSL.

Thus at this time two very different sedimentary environments were functioning, with coarse beach shingle being actively deposited on the shoreface, and fine grained sediments being deposited in the lee of the fronting shingle beach. Such conditions have been a feature of coastal sedimentation at Culbin throughout the Holocene, and may still be seen operating on The Bar.

This also addresses the point that fine grained sediments were a feature of the nearshore zone at this time. Stress has so far been placed on the importance of shingle landforms. Fine sands and silts have played a part in sedimentation along the Culbin coast, but their relative proportions would have been lower due to the high volumes of active shingle.

#### **5.1.4.3 Case study 3: Raised beach deposits and upper peat units in Burghead Bay**

Exposure of 5.25 km of inorganic sediments deposited vertically above the peat unit in Burghead Bay provides information regarding their mode of deposition after the Holocene sea level maximum. The bulk of the exposed units consists of interbedded sands and shingle, two conspicuous peat units and a variable thickness of aeolian sand cover.

Underlying the entire cliff section is a unit of interbedded sand and shingle, displaying an altitudinally variable upper contact with the overlying units. The depth of this unit was not ascertained due to the altitude of the contemporary storm ridge which obscured the lower section, abutting against the cliff at a mean altitude of 2.27 m OD.

The majority of the sand and shingle units exposed in the cliff section represent sections sliced obliquely through raised foreshore deposits. In terms of their sedimentology, these units are similar, if not identical to those currently exposed on the contemporary foreshore fronting the cliff. The juxtaposition of sand and shingle on the contemporary foreshore relates to the relative supply of each element, combined with the detailed morphodynamic response of foreshore sediment to the incident wave climate during the particular depositional event. Falling RSL led to the progressive abandonment of these sediments, with sediments of the upper foreshore abandoned first. Falling RSL continued to rework the sediments of the lower foreshore into upper foreshore units. If we consider the present position, then the preferential preservation of upper foreshore sediments would lead to the selective preservation of the coarser sediment fraction. In the sedimentary record, this could produce an artificial over-representation of shingle in the exposed section, a factor which should be considered while discussing deposition in Burghead Bay.

Between logs E and I erosion has revealed a section through three shingle storm ridges. The oblique angle formed between the ridges and the contemporary shoreline meant that the ends of the ridges are exposed in section. The crests of the ridges were located at 5.37 m OD, 8.53 m OD and ca. 8.40 m OD. The thickness of the shingle exposed in the ridges is variable, increasing gradually from the east and merging with lower, individual units to form a clast supported shingle body with little interstitial sand. Within this massive shingle unit crude bedding was observed, but the unit remained composed of shingle for a vertical depth of (3.13 m). The individual beds within the shingle unit were up to 0.90 m thick, and displayed only one minor sand parting. These observations were broadly consistent with those of Hey (1967), who reported crude bedding in exposures in shingle ridges on Dungeness. However, the unimodal distribution of the clast sizes recorded by Hey (1967) were not recorded in Burghead Bay, where clast sizes ranged between 18 & 130 mm 'A' axis length. Within the shingle ridges at Dungeness, angles of dip of the bedding structures were recorded at up to 10° by Hey (1967). On the Burghead Bay ridges a dip of 12° was noted, but the acute angle formed between the ridge crest and the shoreline meant that this was an apparent dip only, and as such the true dip may have been greater. The total thickness of the shingle ridges observed in the Burghead Bay units was considerably lower than those which were penetrated by boreholes further landwards. The shingle in the landward boreholes attained a maximum thickness of 6 m, while that of the exposed units in the cliff section

reached only 3.13 m. This variability was also reflected in sections at Dungeness, where depths of between 3 and 8 m were recorded (Hey, 1967).

The exposure in section of the shingle ridges in Burghead Bay provides a useful insight into the internal structure of these features in the absence of sections at Culbin. The observations were in agreement with the only other known description of the internal structure of shingle ridges at Dungeness (Hey, 1967).

The peat units were of particular interest as they represented former stream or lochan beds exposed in section at an altitude slightly higher than the contemporary beach. The eastern peat unit (log A1) was the thicker and wider than the western peat unit (log M1), with the base of the unit at a slightly higher altitude. Both of the peats displayed a typically concave upwards exposure, with thinning towards the edges, as the thickest section of the peat would have formed in the hollow of the depression. The presence of such units agreed well with map evidence of a string of shallow lochans and mosses between the former Loch Spynie and Burghead Bay shown on the Anderson Map of 1749 (Figure 5.10, from Ross, 1992). Due to the scale of reproduction, only the larger water features were shown on this map, but presumably the existence of a relatively flat stretch of land in this area was conducive to the formation of a series of such features at a variety of scales.

The age of the two peat units from the Burghead Bay cliff section provide a minimum age for the emplacement of the surrounding deposits. The eastern peat produces a date of  $3140 \pm 45$  BP, and the western peat  $2900 \pm 45$  BP (SRR 4679 & 4681). The difference between these dates at two standard deviations was only 55 radiocarbon years, suggesting that the initiation of peat formation at each site was approximately simultaneous. These dates agreed well with the date obtained from the peat located on the Bessie Burn stream section ( $3170 \pm 40$  BP), and together these dates suggested that the emplacement of the series of raised marine features upon which the peats developed was complete by at least ca. 3000 BP.

The evidence presented so far has presented three points vital to the understanding of shingle landform evolution in the Culbin area:

- i) the development of Burghead Bay has been essentially the same as Culbin;

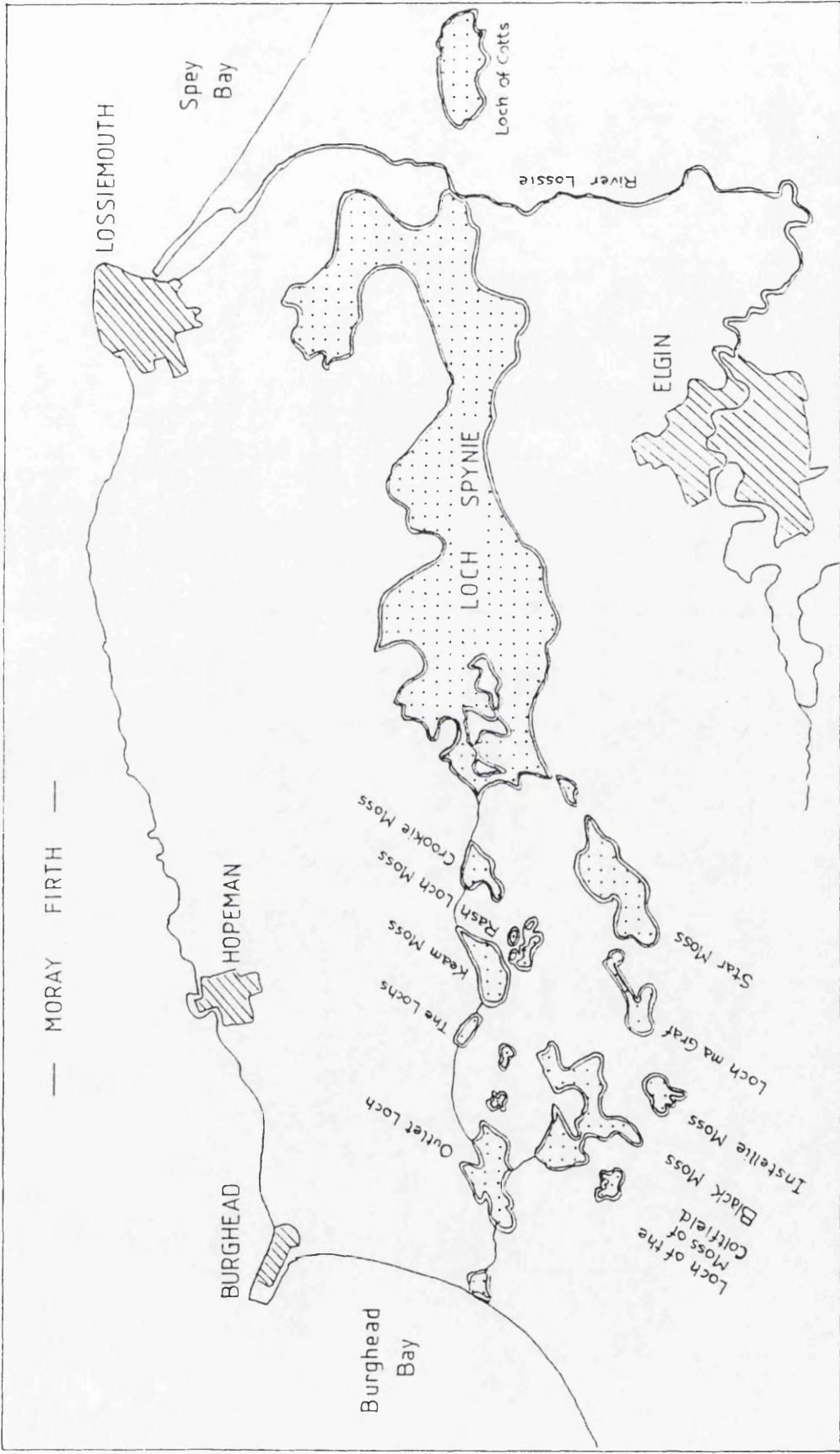


Figure 5.10 Reproduction of the Anderson map of 1749 (source: Ross, 1992)

ii) shingle has been moving west through Burghead bay to fuel the development of Culbin;

iii) supply of shingle has been from updrift.

i) The dates from the peat units provide a minimum age for the surrounding shingle landforms, suggesting that they had been emplaced between  $3170 \pm 40$  BP &  $2900 \pm 45$  BP. This places the deposits in Phase 3 of the RSL/sediment supply model, on a falling RSL after the Holocene RSL maximum. The shoreline at this time was extending west, with both sedimentological evidence from the internal structure of the shingle ridges and the geomorphological evidence of longshore trending shingle bars with well developed recurves at their western extent (Steers, 1937 & Figure 4.11), as found on The Bar today. Evidence from clast fabric analysis at ten locations along the bay suggests that the deposits had been emplaced along a straighter section of foreshore than is presently found in Burghead Bay. This evidence, combined with the geomorphological map of the shingle ridges (Figure 4.11) and the dates from the associated peats demonstrates that the foreshore in Burghead Bay was accreting seawards until at least 2900 BP into a RSL of ca. 2.5 m OD, whilst westerly extension is likely to have continued beyond this date. This date thus provides a minimum age for the onset of frontal erosion in Burghead Bay. Thus the shingle ridges in Burghead Bay have followed a similar mode of evolution to those at Culbin, with both seawards accretion and distal extension occurring, fed by an updrift supply of shingle and fuelled at a later stage by proximal erosion.

Points ii) and iii) may be addressed together. The westward extension of the shingle ridge suite in Burghead Bay, accompanied in its early stages by seawards accretion, provided a mechanism for the transport of shingle alongshore to Culbin. It has been proposed that shingle from Spey Bay could have by-passed the Covesea ridge to enter Burghead Bay given the appropriate water depths. The alignment of the shingle ridges in Burghead Bay support the contention that shingle was unlikely to have entered Burghead Bay via a marine channel through the present Spynie lowlands south of Burghead/Covesea.

The graph of RSL trends (Figure 5.9) shows that, with a limiting depth of 6 m, shingle could not have by-passed the Covesea ridge until 4300 BP. Using this date as a minimum, then together with the peat dates from the shingle ridges sectioned at the foreshore, shingle sedimentation must have taken place in Burghead Bay for at least ca. 1400 years under conditions of falling RSL.

#### **5.1.4.4 Case study 4: Volumetric development of the lower shingle ridge series at Culbin: variable sediment supply and RSL**

From case study 3 it has been demonstrated that the supply of sediment from the Spey was re-introduced after *ca.* 4300 BP, until at least 2900 BP. The shingle ridges at Culbin display a marked drop in altitude between *ca.* 10 and 7 m OD over a short distance, interpreted as the morphological expression of the suspension of Spey shingle during development Phase 2 (section 5.1.3), when the Covesea passage was drowned prior to 4300 BP. Volumetric calculations (section 4.3.3, Chapter 4) show that a sedimentary input from the Spey was required to account for the volume of sediment in the lower shingle ridge series at Culbin. However, the dates of the abrupt drop in altitude at Culbin and the reinstatement of Spey shingle to Burghead Bay poses a problem, in that the dates coincide at 4300 BP. This does, however, provide a further case study of the response of the Culbin shoreline to RSL change, for which an appreciation of the entire Holocene development of the area is required.

Figure 5.9 shows the status of RSL and the provision of shingle from the Spey and Findhorn throughout the Holocene. The Culbin shingle ridges were emplaced on the falling limb of the Holocene sea level maximum (Figure 5.2) in a staircase, from a maximum elevation of *ca.* 11 down to 5.15 m OD, with a drop in altitude encountered between *ca.* 10 and 7 m OD (Table 4.8). Figure 5.9 demonstrates that during Phase 1, both the Spey and the Findhorn were supplying sediment to the Culbin area. Under a rising RSL this shingle would have been progressively reworked as it was forced landwards as a series of shingle bars or barriers (Orford, 1987). With rising RSL, however, water depths around the northern flank of the Covesea ridge would have exceeded the critical depth of 6 m (3.9 m OD), *ca.* 7200 BP (Figure 5.9), isolating the supply of shingle from the Spey. However, a rising RSL would have continued to rework the sediments previously emplaced at Culbin and initiating erosion of the updrift shingle deposits in Burghead Bay. By the peak of the Holocene sea level maximum, the shingle ridges had been reworked to their maximum altitude (*ca.* 11 m OD), and RSL was once again beginning to fall. Continued reworking of the shingle deposits would have continued, together with a limited input of fresh shingle from the Findhorn, plus material from Burghead Bay. With falling RSL, the altitudes of the shingle ridges at Culbin fell, depositing them as a staircase of features down to between 7 and 10 m OD until 4300 BP. Thus the response of the shoreline during the falling limb of Phase 2 (falling RSL post-Holocene sea

level maximum) was seawards accretion under a supply of sediment largely emplaced at an earlier stage of development.

4300 BP marks a critical phase in the Culbin development sequence, heralding the onset of development Phase 3 (Figure 5.9). At this time water depths around the Covesea ridge would have shallowed to 6 m once more, reinstating the shingle supply from the Spey to the eastern section of Burghead Bay. This date coincides with the age of the shingle ridge at the top of the abrupt decline in ridge crest altitude recorded in the Culbin shingle ridge sequence. This decline is interpreted as evidence of a collapse in the supply of sediment to Culbin, producing a hiatus in the depositional record. Thus under conditions of continued falling RSL, the shoreline at Culbin responded to a significantly reduced supply of sediment by depositing very few shingle ridges across a large (ca. 3 m) vertical range, despite the reinstatement of the supply of sediment from Spey Bay into Burghead Bay.

A time lag would be inevitable between the first appearance of Spey shingle in Burghead Bay and its arrival on the beaches of Culbin. A date derived from the altitude of the shingle ridge at the base of the decline on the eastern transect suggests that this shingle finally arrived at Culbin ca. 3600 BP, possibly reflecting activation of sediment from Burghead Bay itself prior to the arrival of the "new" Spey shingle. As soon as the dual sediment supplies were operational again, the shoreline once more began to accrete heavily, producing the lower set of shingle ridges at Culbin. Analysis of the inter-ridge morphology suggests that sediment supply during phase 3 was sporadic, producing more irregularly spaced shingle ridge crests than those of phase 2, deposited when sediment supply was apparently less but more regular. Thus although the Spey was once more supplying shingle to feed through Burghead Bay and onto Culbin, the morphological evidence from shingle ridges at Culbin suggests that supplies of shingle from both the Spey and the Findhorn were beginning to fail. Indeed, the youngest shingle ridges at Culbin (ca. 1900 BP) suggest that after this date, the shoreline once again changed its mode of development dramatically in the face of a declining sediment supply, this time to move from a shingle to a sand dominated system.

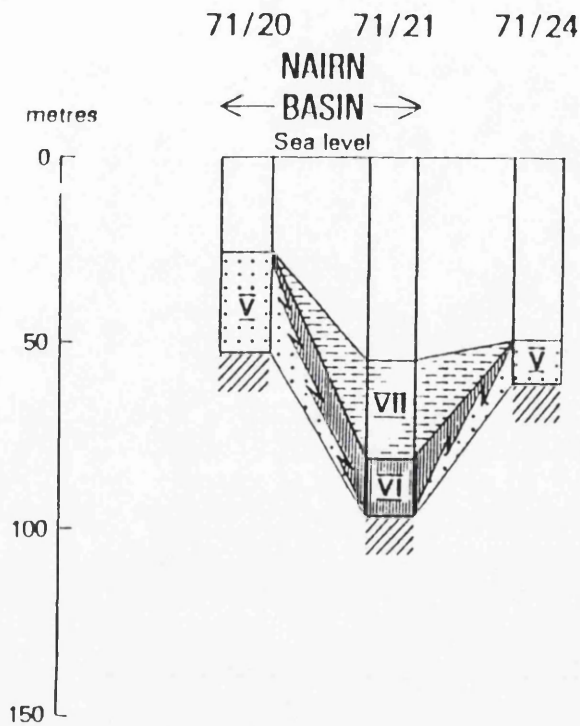
As the sedimentary system matured and sand became the dominant sediment type, the locus of remaining shingle deposition would have migrated downdrift. Once the Holocene sea level maximum had passed, conditions for the onshore forcing of shingle deposited during the immediate Postglacial low sea stand

ended. Examination of the present sea floor sediments offshore from Culbin reveals a lack of shingle (Chesher & Lawson, 1983), and boreholes sunk through the Nairn Basin (Figure 5.11) reveal only fine grained sediments present in the Holocene sequence. This suggests that either there was little shingle deposited this close inshore at Culbin during the Postglacial low sea stand, or more probably that the majority of the shingle which was deposited had already been incorporated into the Culbin system, being swept onshore by a rising RSL towards the Holocene sea level maximum.

With migration of the shingle "head" of the system westwards, the foreshore would have contained increasing volumes of sand. This resulted in a general lowering of the gradient of both the foreshore and the immediate offshore zone, producing a more dissipative environment (albeit still within a predominantly shingle system). This would have resulted in a slight lowering of the incident energy levels on the beach at this time under both swell and storm conditions, producing the lower mean clast sizes observed on these ridges. Simultaneously RSL was falling, depositing the resultant shingle storm ridges at a lower altitude than those landwards.

This trend was curtailed, however, as these inner ridges began to recurve at their western extremity (sets A and B). Subsequently lower energy conditions associated with increasing amounts of wave refraction prevailed with distance along the recurving section, producing a reduction in ridge crest altitudes (section 4.1.4), and a reduced capability for sediment transport.

Thus over the Holocene, the development of Culbin has been strongly, if not entirely, dependent on the response of the shoreline to changing conditions of RSL and sediment supply. Lags in geomorphological systems are not uncommon (Chappell, 1983), and in this case such an effect has been highlighted by the morphology of the Culbin shingle ridge suite, which has been tentatively demonstrated to relate to a lag between the re-establishment of Spey shingle to Burghead Bay and the receipt of this sediment on the foreshore at Culbin.



Generalised stratigraphic succession

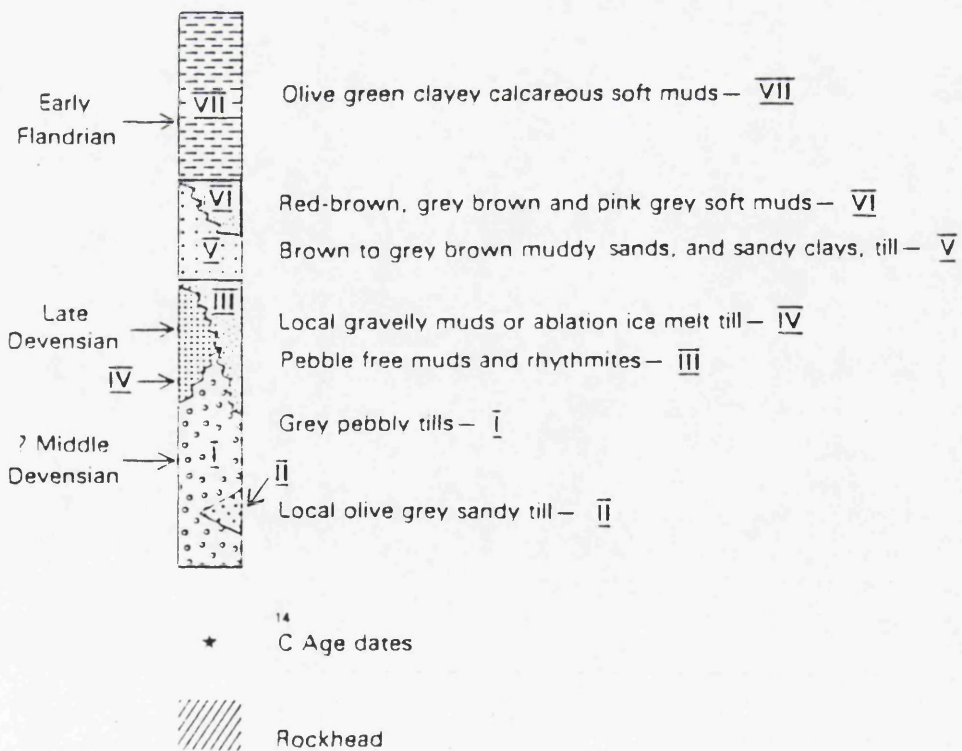


Figure 5.11 Stratigraphy of the Nairn Basin (source: Chesher & Lawson, 1983)

## 5.2 CONTEMPORARY COASTAL PROCESSES AND LANDFORMS AT CULBIN

### 5.2.1 Contemporary coastal processes

In order to satisfactorily explain the evolution of the contemporary coastal *landforms* of the Culbin area of the southern Moray Firth, a full understanding of the nature and magnitude of the *processes* operating along this stretch of coast is required. Chapter 4 described the results of work carried out in order to quantify the processes responsible for driving the sedimentary system in the Culbin area, from which was ultimately obtained a beach sediment budget. The expected aim of this is to examine whether the contemporary processes can be linked with Holocene coastal changes in order to demonstrate how the shoreline has responded to changes in RSL via the sediment budget.

#### 5.2.1.1 Tidal currents

In order to quantify the various elements of sediment transport involved in the beach sediment budget, transport via tidal currents had to be considered. Measurements were made over a neap-spring-neap cycle in order to assess the likely impact of tidal currents on the sediment transport regime in the vicinity of Culbin.

It has generally been accepted that while wave induced transport is the dominant process acting on a foreshore experiencing significant rates of longshore transport (Clayton, 1980), the importance of tidal currents increases with distance offshore (Mason, 1985).

The data collected 1.2 km offshore from the Culbin supports the contention that a tidal divide may be present off the southern Moray Firth coast, as recognized by Craig (1959). The ebb tide flows east, while the flood tide sets towards the west. This is supported by tidal stream data (Admiralty, 1981), and reflects the inflow of tidal waters from the Atlantic, flowing south along the Easter Ross coast before meeting the southern Moray Firth (Lee & Ramster, 1981), and dividing at a location slightly east of Culbin. The situation is shown diagrammatically in Figure 5.12.

The tidal current velocities actually recorded were extremely low (Table 4.10), in agreement with both Lee & Ramster (1981) and Admiralty chart 233 (Admiralty, 1981), which both record current velocities at below  $0.5 \text{ m s}^{-1}$  as dominant in this

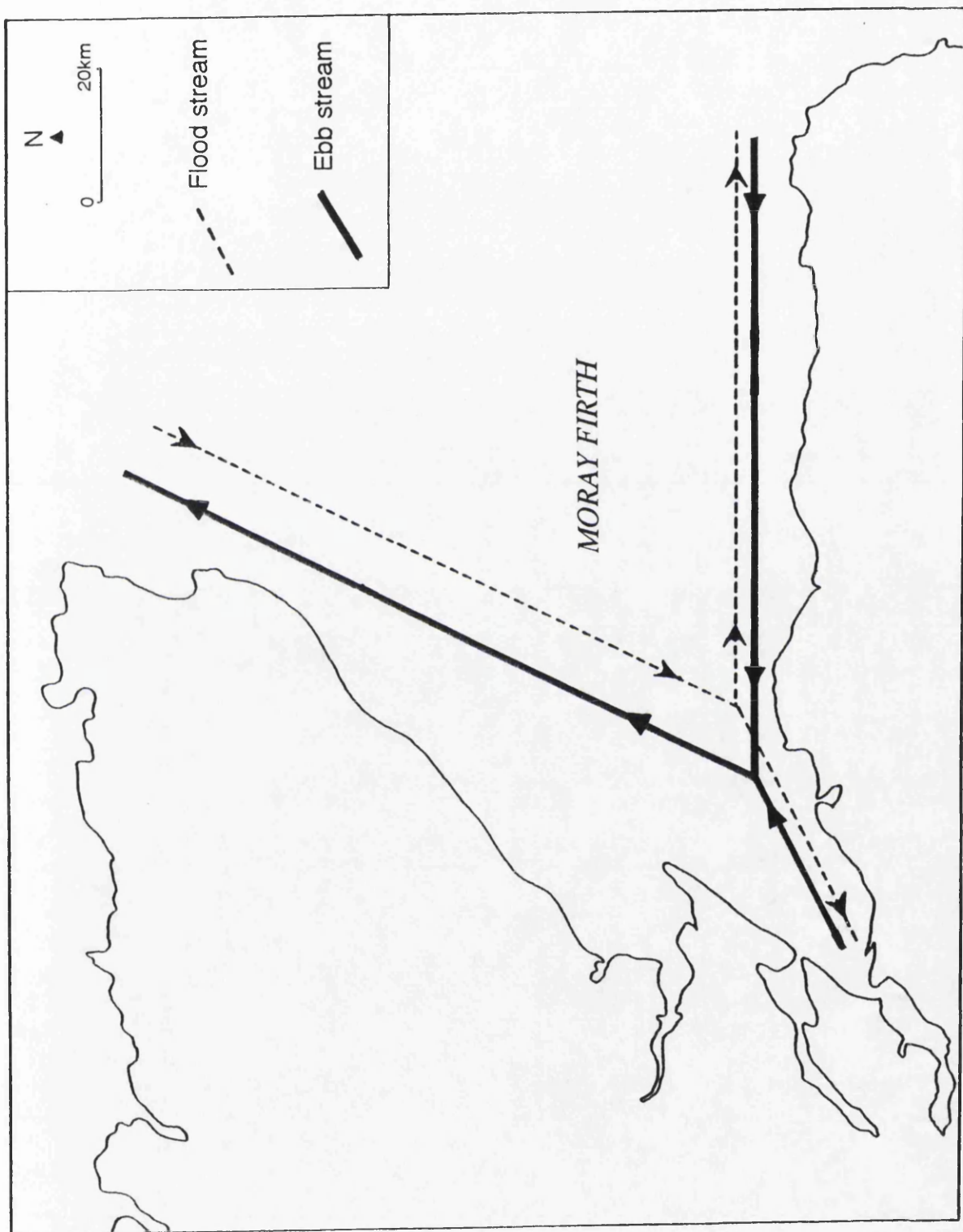


Figure 5.12 Tidal streams in the Moray Firth

section of the Firth. The maximum current speed recorded in the offshore zone at Culbin was  $0.28 \text{ m s}^{-1}$ , on a spring tide, while a maximum of only  $0.19 \text{ m s}^{-1}$  was recorded on neap tides.

Examination of the scatter of data points (Figure 4.37) clearly demonstrates that the ebb tide is dominant in terms of the frequency of recording, appearing as the larger of the two peaks on the typically bimodal distribution Figure 4.37. While this does not fully support the 75% of recorded easterly flow reported by Dooley (1971) further offshore, it does suggest that the ebb tide is dominant in terms of the frequency of observations, with 42.2% of recordings made on the ebb, compared to 20.2% on the flood. This possibly reflects the relative proximity of the current meter to the coast at Culbin and increased wave interference.

A comparison between the peak neap and spring tidal streams demonstrates clear differences between the signals recorded at the tidal maxima. The abrupt reversal in current direction recorded at the spring tidal peak was not recorded at the neap maxima, when a longer period of slack tide was recorded between the setting of each ebb and flood.

Tidal currents were measured in order to assess their potential sediment transport capability. In order to assess their impact, tidal currents had to be resolved into a residual velocity, reflecting the *net* movement of sediment over a single tidal cycle after the passage of both one ebb tide and one flood tide. Plots of tidal speeds demonstrate that on only five occasions was the current speed of sufficient magnitude to entrain sediment, and the maximum grain size diameter which could be entrained was 0.8 mm. All of the entrainment periods occurred on ebb tides (easterly flow), coinciding with the maximum velocity records.

Conversion of the current data into an equivalent sediment entrainment volume during each tidal cycle depended heavily on the definition of an operational area over which tidal currents were assumed to act, and the time periods over which current speeds of sufficient magnitude were operating. Calculation of these factors produced a potential volume of  $5.0 \times 10^8 \text{ m}^3 \text{ a}^{-1}$  of sediment entrained and transported in an easterly direction. Calculation of the residual tidal currents were heavily influenced by the magnitude of the ebb stream relative to the flood, and also suggested a net easterly transport pathway.

These results were unexpected, appearing opposed to the long term sediment transport pathways in the middle and inner Firth (Lee & Ramster, 1981; Reid, 1988; NERC, 1991). If the values for suspended sediment transport were also

included in this calculation, the reported transport volumes would have been greater still. The potential sediment transport volumes for tidal transport greatly exceeded those for longshore transport in the nearshore zone, and strongly suggested that this calculation was in error.

The two most likely sources of error stem from the assumption that the depth of sediment is infinite in order to allow the continuity in the calculation of the suspended sediment transport rate, and that the sediment in the offshore zone is predominantly sandy. Examination of the nature of the sea bed in the offshore zone at Culbin suggests the sediments to be primarily sands (Chesher & Lawson, 1983). However, the offshore zone in this area is dominated by the Nairn Basin, an infilled Late Quaternary trough formed either directly by ice or through drainage of the Beaully/Ness system. Boreholes sunk into the structure (IGS boreholes 71/20 & 71/21 [Chesher & Lawson, 1983]) reveal a prevalence of clay/mud, with no sand evident throughout the profiles (Figure 5.11). This suggests that the sands shown on the surface sediment chart represent a thin veneer overlying predominantly fine grained sediments down to rockhead, although locally at the mouth of the Findhorn the thickness of sand would be expected to increase significantly.

As a result, it is suggested that the assumption of an infinite depth of sand grade sediment on the sea bed in this vicinity is incorrect, and is not supported by field evidence. This means that the derivation of the volume of sediment theoretically entrained by tidal action is far too high. Additionally, with a higher predominance of fine grained sediments (silts and clays), the critical entrainment velocity required to entrain them increases significantly (Allen, 1985), with the maximum current speeds recorded during the investigation ( $28 \text{ cm s}^{-1}$ ) only capable of entraining sediment particles down to 0.04 mm diameter (coarse silt [Wentworth scale, Leeder, 1982]).

This net easterly sediment transport remains diametrically opposed to the net long term sediment transport pathways indicated in the middle/inner Moray Firth (Reid, 1988; NERC, 1991). These both display a net westerly trend in sediment transport towards the inner Firth. While the volumes of sediment calculated from this exercise were clearly erroneous, the trend in residual currents also indicated ebb tide dominance and a net easterly drift of previously suspended sediment would result under such conditions. Again this is at odds with long term net transport predictions, suggesting that an effect opposed to the net trend is operating along the Culbin flank of the Moray Firth at relatively inshore sites. It is

also possible that the current sampling site was unrepresentative of wider conditions. Either way, the issue of tidally induced sediment transport requires further investigation.

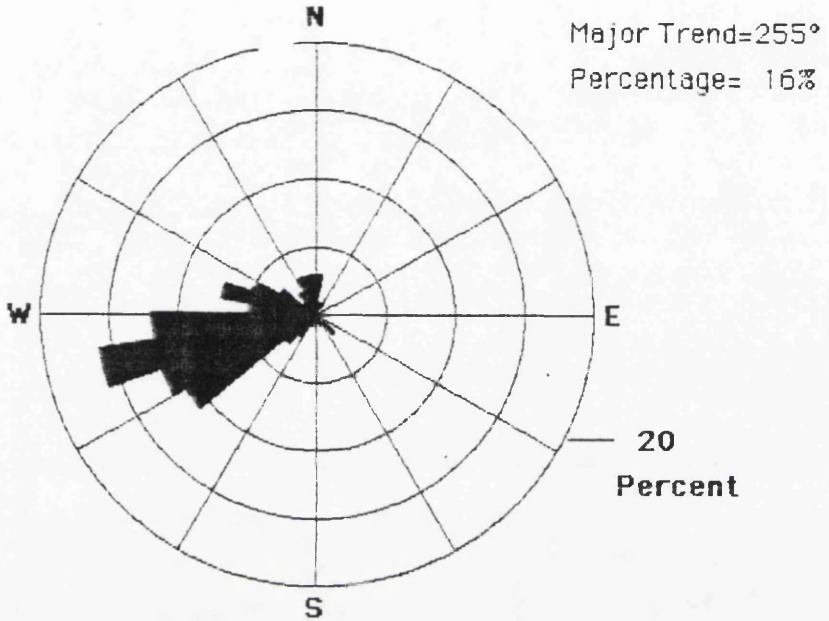
### 5.2.1.2 Winds

The windfield encountered along the coast of the inner and middle Moray Firth at least as far east as Burghead is strongly influenced by the occurrence of southwesterlies, channelled along the Great Glen. Due to the alignment of the coast at Culbin, this produces a predominantly offshore wind along the foreland, and an almost shore-parallel wind along The Bar. Analysis of the wind directions recorded during 1990-91 at RAF Kinloss showed this trend to have continued throughout the monitoring period, with a dominant wind direction recorded from 235°. This agrees with various unquantified accounts of a predominantly westerly-southwesterly windfield at Culbin (Ogilvie, 1923; Steers, 1937; Ovington, 1950, Gauld, 1981). Edlin (1976) reported winds with a westerly component blowing for 46% of a total record at Nairn, compared to 26% from all other directions, and 28% calms. These trends were reflected by those recorded at RAF Kinloss over 1990-91, with 72% of all winds  $>11 \text{ m s}^{-1}$  including a westerly component, and 24% from all other directions.

Ross (1992) presented a ten year record of the direction of winds greater than  $15 \text{ m s}^{-1}$  recorded at RAF Kinloss, which allowed a check to be made on the representativeness of the data from 1990-91 in relation to a longer record from Ross (1992). This was replotted as a wind rose, and is presented in Figure 4.41, together with the wind rose from 1990-91 as Figure 5.13. While the spread of data was greater from the ten year record due to the larger data set, the preferential orientations are very similar. The ten year record displays a preferred orientation of 255° with a range between 230° and 270°, while the dominant trend over 1990-91 was from 235°. This demonstrates that the wind data recorded during the monitoring period were typical of at least the medium term conditions experienced along this section of the southern Moray Firth. In terms of the beach sediment budget, these winds may act to dampen wave activity, blowing offshore and against the dominant wave direction from the North Sea.

If a representative sediment budget is to be calculated, then it was important to ensure that the monitoring period is typical of the average conditions experienced at the study site. Increased storm activity, for example, would lead to more frequent draw-down of the beach surface, increasing the mobility of the

n = 950



n = 625

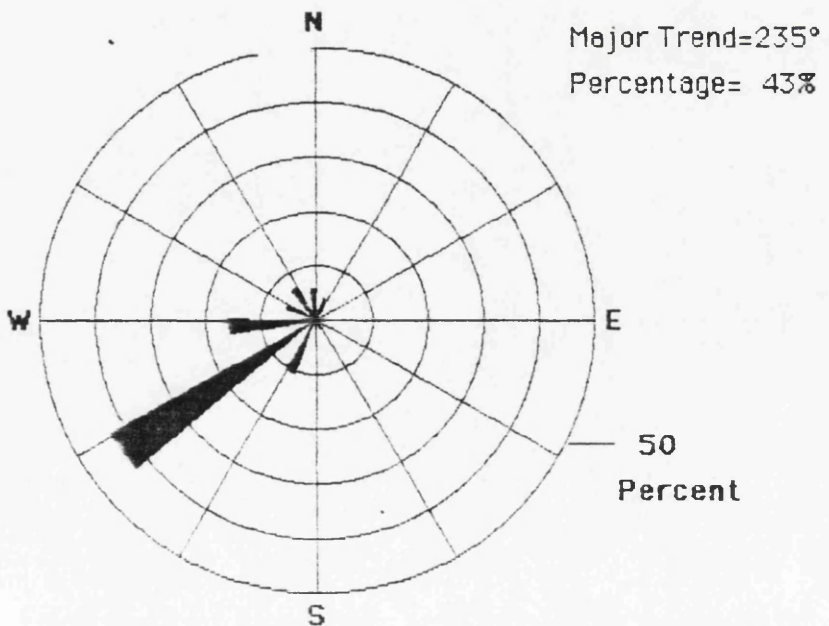


Figure 5.13 Wind data from RAF Kinloss a) 10 years data (modified from Ross, 1992) b) data from 1990-91

sediment in the nearshore zone leading to the calculation of an enhanced sediment budget. Conversely, atypically quiet conditions at the coast would reduce the mobility of sediment in the nearshore zone, leading to a reduced estimate of the sediment budget.

Windspeeds recorded during 1990-91 were plotted against windspeed data obtained by Ritchie *et al.* (1978) from RAF Kinloss (Figure 5.14). The data show similar broad trends, with a modal windspeed of 3.5-5 m s<sup>-1</sup>. The 1990-91 data showed a greater frequency of lower windspeeds than that of Ritchie *et al.* (1978), but a much lower frequency of calms. Thus the environmental conditions during the study period were seen to be of a slightly lower energy than the long term average as recorded by Ritchie *et al.* (1978).

### **5.2.1.3 Waves**

The data collected for the production of a wave climate for the southern Moray Firth depended on data from the Beatrice Alpha platform and from Global Wave Statistics (BMT, 1986), with a detailed but short data set provided by on-site monitoring using a wave recorder. Secondary sources of wave data from around the Moray Firth and the North Sea were used as a check on the representativeness of the primary data sources utilized.

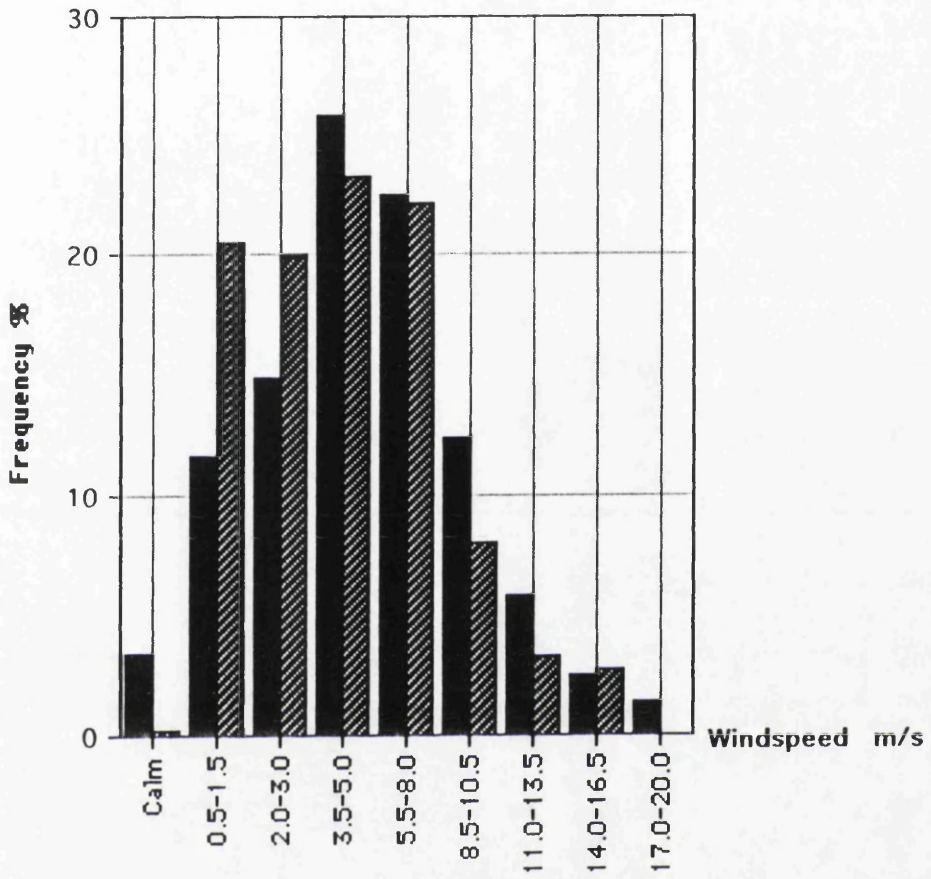
The data from Beatrice Alpha provided the most accurate view of wave conditions during the monitoring period. However, two problems were identified with the use of Beatrice Alpha data;

- i) the raw data did not include swell direction,
- ii) the recording period was considered to be slightly less energetic than longer term records suggested as average.

As a result, it was considered realistic to use the data from Beatrice Alpha for wave height and periodicity input, with data concerning wave direction derived from Global Wave Statistics (BMT, 1986).

### **5.2.1.4 Beatrice Alpha**

The wave parameters recorded at Beatrice Alpha were the most representative of the actual conditions experienced at the coast during the monitoring period. A peak modal periodicity of 4 s was experienced in spring and summer, increasing to 5 s in autumn and winter. Wave heights remain low throughout the year, with



■ Data from Ritchie et al, 1978

▨ RAF Kinloss mean 1990-1

Figure 5.14 Winds at RAF Kinloss

modal classes of 1 m, increasing slightly to 1.5 m in winter. Maximum wave heights of 8 m were recorded in winter, falling to 5 m in spring and autumn, and 3 m in summer. Calms were uncommon during the recording period, reflecting the collection of data from an offshore location. Closer to the shore, an increased frequency of calms might have been expected, reflecting the dampening impact of offshore winds on the nearshore wave climate. Swell waves in the Moray Firth are generally low, reflecting the relatively sheltered environment within the Firth in relation to the open North Sea.

#### **5.2.1.5 Global Wave Statistics**

Since swell direction was not recorded directly on board Beatrice Alpha, swell direction frequency was obtained from data published in Global Wave Statistics (BMT, 1986), and filtered to reflect the limited range of wave directions which can enter the Moray Firth. As a result, only the frequency of waves from the N-NE-E sectors was used. The dominance of northeasterlies is clear from the frequency table (Table 4.12), although this still only accounts for 11.87% of the wave year. Culbin is sheltered from the extreme north by the orientation of the Sutherland coast, while the Burghead promontory provides shelter from easterlies. As a percentage of the swell year, the highest frequency of swell waves are recorded in spring (24.1%), while the lowest are recorded in winter (15.3%). Winter also experiences the lowest incidence of northeasterlies in the Moray Firth (6.3%), which still represents a greater proportion of swell than from the north (4.3%) and east (4.7%). This represents a significant reduction in gross frequency and suggests a more varied wave climate during the winter, as reflected in the records of wave height and periodicity from Beatrice Alpha.

Directional frequencies from Global Wave Statistics (Table 4.15) clearly displays the dominance of northeasterly waves at Culbin during all seasons, primarily due to the shelter from extreme east and north offered by the configuration of the Moray Firth. Easterly waves are the least common except during winter, when they are marginally more frequently recorded than northerlies.

#### **5.2.1.6 Wave recorder**

Despite the short period over which the wave recorder was operational, the exercise was highly successful, and its inclusion was considered as a useful contribution to the field of low cost, simple directional wave recording.

The frequency histogram (Figure 4.45) demonstrates a positively skewed distribution of wave heights recorded between 23/5 and 31/5/91. This trend was in accord with the frequency histogram from Beatrice Alpha (summer-Figure 4.44), but displayed lower wave heights, reflecting the considerably shortened recording period enforced by the nature of the experiment, and the fact that the data includes *all* waves rather than recording only the significant wave height ( $H_s$ ). This was done deliberately, as it emphasizes the high frequency of low (<0.5 m) waves which would have been recorded as calms on board Beatrice Alpha, and as such highlights a potential shortcoming in the use of commercial wave records, which record only  $H_s$ . However, the potential for sediment transport under such conditions would be low.

Recording and plotting all waves demonstrates the sensitivity of the system under test conditions, displaying the fact that the data collected was of sufficient resolution to detect the convergence of wave trains from different directions. Six of the nine recording periods indicates that two or more wave trains were incident on the shoreline simultaneously, as indicated in Table 4.11. Such measurements have implications for the calculation of future sediment budgets. These results imply that if the usual practice of simplifying the incident wave spectrum to a monochromatic series is undertaken in an area where the dominant wind directions differ from the direction of net longshore transport, as occurs at Culbin, then the calculated sediment budget may represent an overestimate of the actual amount of sediment transported in a longshore direction. At Culbin, the dominant wind direction is from the southwest, while the net longshore transport direction is east-west. In combination with the "energy window" effect imposed by the configuration of the Moray Firth, incoming swell from the east would meet locally generated wind waves from the west, as recorded. Due to their greater height and periodicity, the swell would determine the dominant trend in sediment movement, but the volumes transported would be reduced by the effects of wind waves operating in the opposite direction.

The plot of wave approach angle and wave height (Figure 4.50) clearly shows the selective filtering effect of the "energy window" of the Moray Firth. Waves from the easterly sectors attains the greatest recorded frequency (75.3%), with fewer waves (17.8%) recorded from the western sectors, reflecting the mode of wave generation from the west via wind stress at the water surface. Additionally, the highest waves (up to 2.3 m) were consistently recorded from the eastern sectors, reflecting both swell waves entering the Firth from the North Sea, and lower

waves which represented locally generated wind waves from an accompanying direction.

Where these waves are input into a wave refraction model and a sediment budget calculated, this data suggests that the assumption of a monochromatic wave regime is a gross oversimplification of the real situation. The inclusion of accompanying wind generated waves into the sediment budget would account for a proportion of the potential error which might occur should a monochromatic wave regime be assumed (section 4.2.1). However, such an assumption implies that the incidence of swell and wind waves remains discrete. The data presented suggests that this may not be a realistic assumption, and that the incidence of swell and wind generated waves from different directions might be a common occurrence, recorded for 67% of the recording period during this experiment. On the Culbin foreshore such a coincidence would result in the dampening of the net westwards sediment transport.

Alternatively, it might also be considered that the incidence of wind waves from an accompanying direction as that of the incident swell waves might increase their height slightly, enhancing their transport capability in a westerly direction. This factor was considered in the calculation of the sediment budget (section 4.2.6).

The superposition of wave trains meant that the potential for the creation of surf beat had to be considered in this study. Surf beat is a phenomenon resulting from wave trains of different periodicity coinciding at the shoreline, creating constructive and destructive interference between the wave crests (Komar, 1976; Pethick, 1984). Problems in identifying surf beat arise due to the very short logging periods (60 s) used in the experiment, which were considerably shorter than reported surf beat periodicity (Tucker, 1950). In only one of the records (25/5) did any evidence for surf beat appear (Table 4.11). In this case the two incident wave trains arrived from  $345^\circ$  and  $009^\circ$ , with mean wave heights of 0.65 and 0.67 m respectively. The waves from the west had a considerably longer periodicity than those from the east (14.9 s & 8.8 s respectively). The effect of destructive interference between the two wave trains can clearly be seen in Figure 4.47, where the mean wave height was reduced by ca. 0.30 m at 25 s into the logging period. The length of the recording period was sufficient in this case to detect the occurrence of surf beat, but was insufficient to detect any constructive effects, and as such the potential effects on sediment transport could not be quantified.

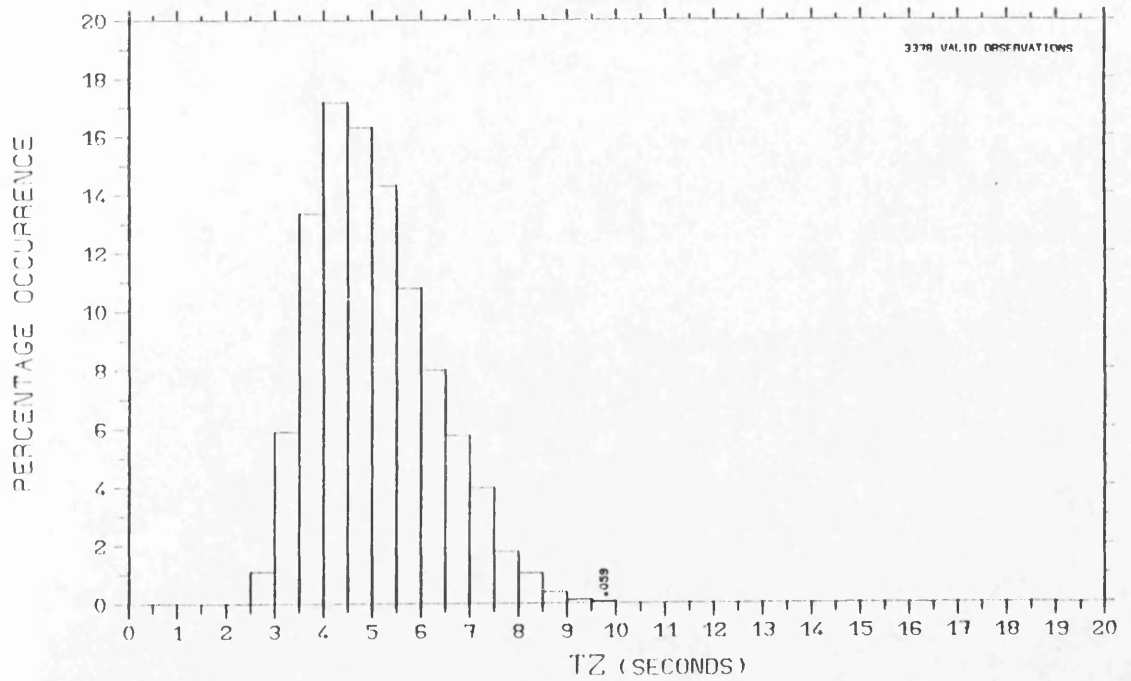
The presence of surf beat would have affected both shore-normal and shore-parallel sediment transport, although over the timespans required for the wave trains to fall in and out of phase (frequently 3-5 minutes), the effects of both constructive and destructive interference were likely to cancel each other out. This would leave a net sediment drift dependent on the wave train with the greatest transport capability, which in the case of Culbin would generally result in a westerly drift of sediment, in agreement with the remainder of the results from this study.

#### **5.2.1.7 Data recorded at Kinnairds Head (outer Moray Firth)**

Figure 5.15 show the records of wave height and period recorded at Kinnairds Head in the outer Firth over the period February 1980-January 1982 (Thorne & Gleason, 1986). This site is considerably more exposed to swell from the open North Sea than Culbin and the inner Firth. It is also less subject to the filtering effect of the mouth of the Firth, and thus incident waves from a greater range of directions than sites on the inner and middle Firth are recorded. Direct comparisons between the data sets must be treated with caution as the Beatrice data spanned only one year, whilst the Kinnairds Head data covered two years. This was unlikely to affect the modal classes of the data sets, but the frequency of extreme wave conditions was likely to be higher at Kinnairds Head and therefore cannot be quantitatively compared. Additionally the definition of the wave year used at Kinnairds Head differed by a month from that of BMT (1986), (noted in Chapter 2), and defined summer as April-September, and winter as October-March, with spring or autumn not defined. Thus for the basis of comparison the data is of little use for seasonal comparison with Beatrice Alpha, and so only the total record data are used.

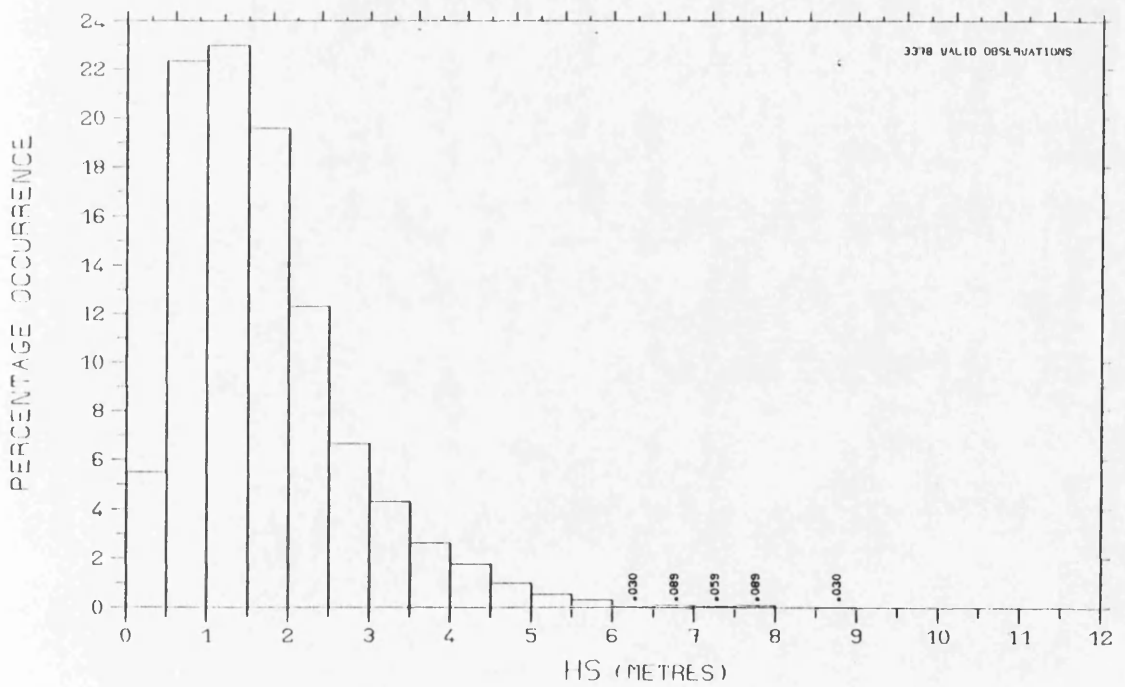
Comparison of total records of wave period for both Beatrice Alpha (Figure 5.16) and Kinnairds Head (Figure 5.15) shows the same modal class at 4 s. Surprisingly the range of values was greater at Beatrice Alpha than Kinnairds Head, with the lower range of the period spectrum absent from the Kinnairds Head data set, although the upper limit was almost identical (9 s at Beatrice Alpha, 10 s at Kinnairds Head). This suggested longer period waves were relatively more common at Kinnairds Head than at Beatrice Alpha, and that no very short period waves (< 2.5 s) were logged at Kinnairds Head at all over the two year recording period.

Wave heights were recorded at Kinnairds Head as  $H_s$ , the significant wave height (height of the highest one-third of all waves recorded), allowing a direct



PERCENTAGE OCCURRENCE HISTOGRAM

KINNAIRDS HEAD FEB 1980 - JAN 1982



PERCENTAGE OCCURRENCE HISTOGRAM

KINNAIRDS HEAD FEB 1980 - JAN 1982

Figure 5.15 Wave parameters recorded at Kinnairds Head (source: Thorne & Gleason, 1986)

Wave height - Beatrice 'A' - Annual 1990

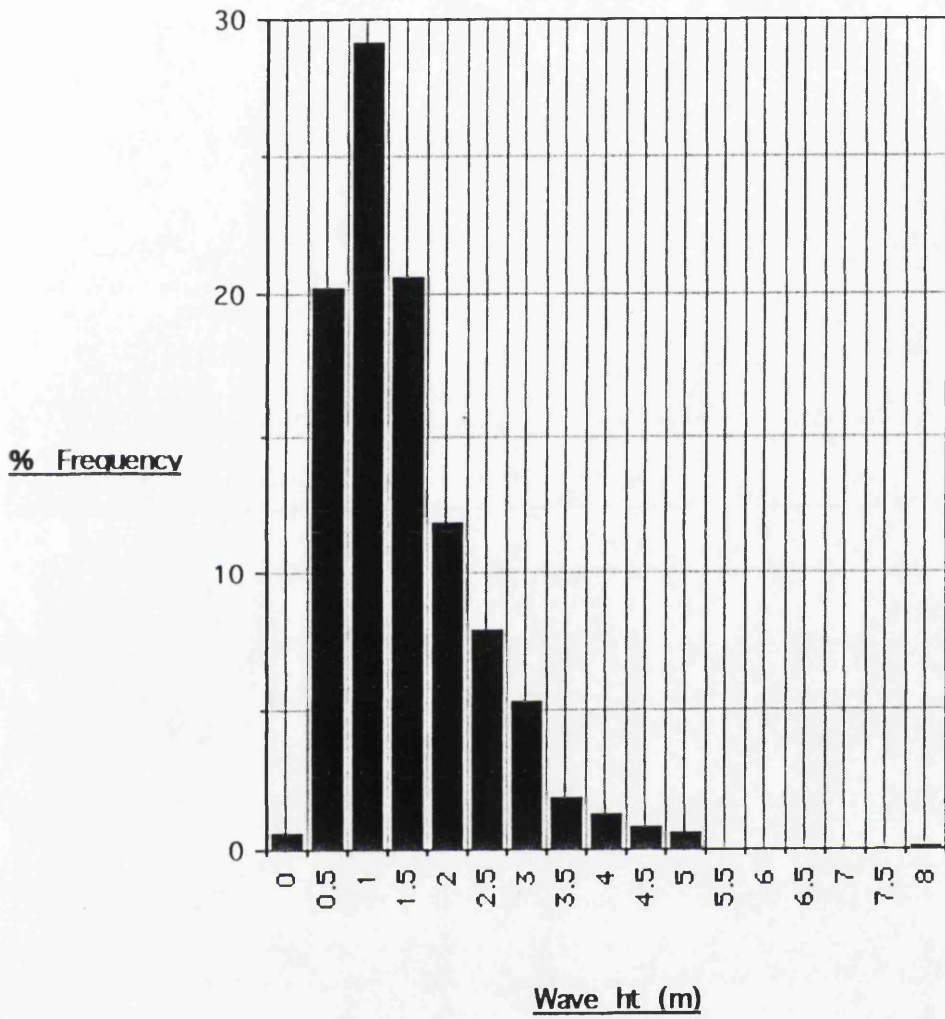


Figure 5.16 Beatrice Alpha: annual wave heights

comparison with the Beatrice Alpha data set in this respect. These are shown in Figure 5.17. The records from each site both show a modal peak at 1 m and a strong positive skew to the data, suggesting greater frequencies of smaller waves, as was demonstrated by the wave recorder experiment. The maximum recorded wave height at Kinnairds Head was in the 8.5-9.0 m class, while the highest wave at Beatrice Alpha was 8 m. At the lower end of the spectrum the frequency of calms could not be compared as the Kinnairds Head data collection standard counted conditions with  $H_s < 1$  m as calm, accounting for 28% of the record, whilst the Beatrice Alpha data set counted calms as conditions with  $H_s < 0.5$  m, accounting for only 1.2% of the record.

The most extreme wave conditions recorded at Kinnairds Head over the recording period were noted during February 1981. Wind conditions at this time were reported as "near gale force south easterly".  $H_s$  reached 8.65 m, with a period of 9.7 s. This situation almost exactly matches the single extreme event noted from Beatrice Alpha, where the maximum wave height of 8 m was recorded with an accompanying wave period of 9 s during the winter season.

#### 5.2.1.8 Conoco Ltd

The data produced for Conoco was intended for specific risk assessment during the deployment of an offshore installation 4.3 km offshore. The data provided thus only serves to outline the magnitude of the 10 year return wave conditions for each month. Table 5.1 shows the significant wave height and period of the 10 year return wave for each month.

Month	$H_s$ (m)	T (s)	Month	$H_s$ (m)	T (s)
January	6.7	11.5	July	3.2	7.5
February	7.8	12.5	August	3.7	8.0
March	6.4	11.0	September	5.5	10.0
April	4.6	9.0	October	6.7	11.5
May	3.7	8.0	November	9.1	13.5
June	2.4	6.5	December	8.3	12.5

Wave period - Beatrice 'A' - Annual 1990

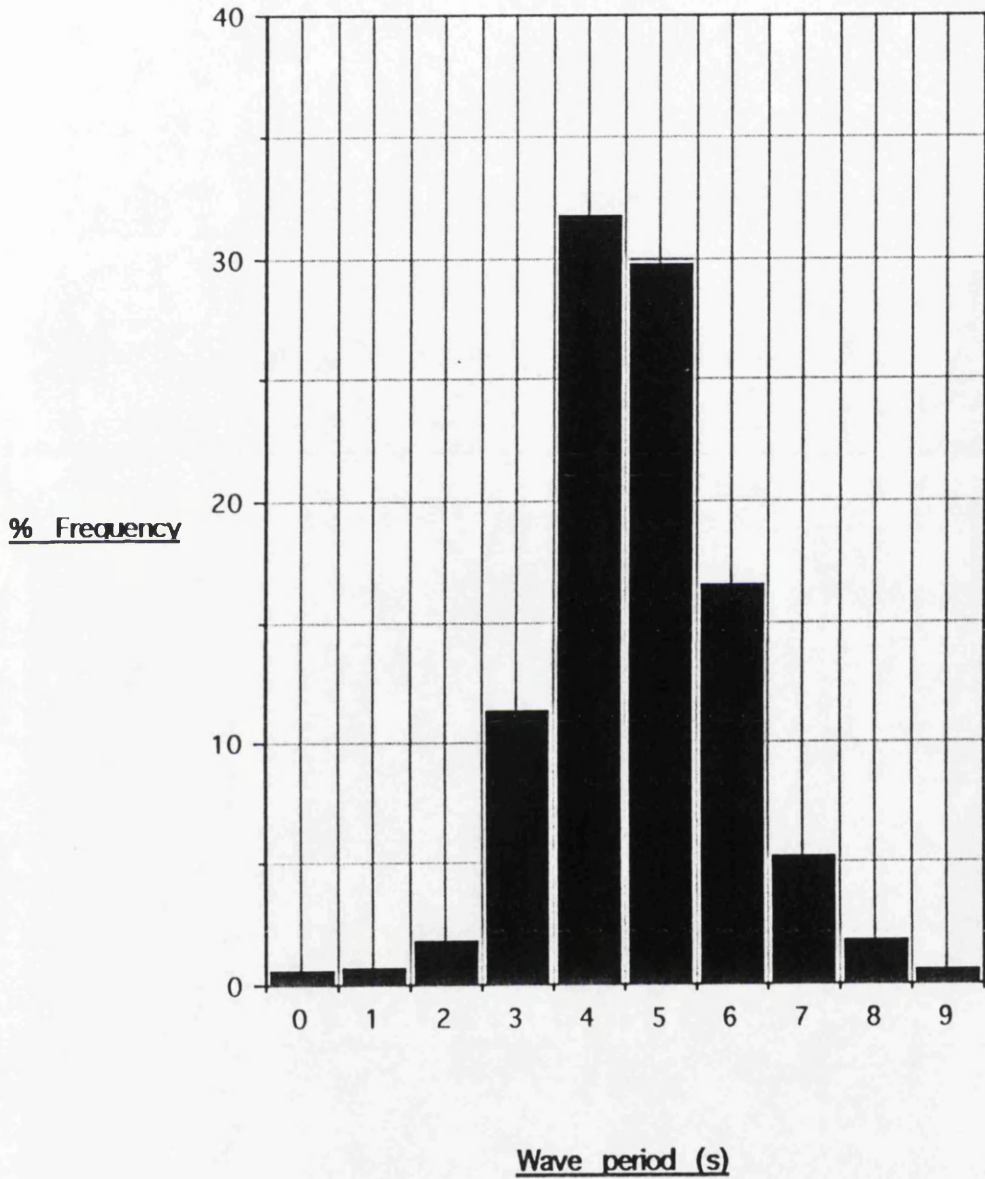


Figure 5.17 Beatrice alpha: annual wave period

Table 5.1 10 year return wave parameters calculated for the middle Moray Firth  
(source: Conoco Ltd.)

The highest wave height is predicted during winter, with a maximum wave height of 9.1 m, and a period of 13.5 s. Summer shows the smallest 10 year return wave heights, with a maximum of 3.2 m and a 7.5 s period. Comparing the extreme waves predicted here with the data from Beatrice Alpha suggests that the 8 m wave recorded during winter 1990 was approaching the height of the 10 year return wave for this sector of the Moray Firth.

#### **5.2.1.9 Miscellaneous North Sea wave reports**

Whilst not directly applicable to the wave conditions experienced in the inner Moray Firth, consideration must be taken of the open sea conditions recorded in the North Sea in order to examine the validity of the wave records used as input to the wave refraction model.

Records made east of the Shetlands (61°20'N., 00°00'E) (MAREX, 1975) over winter 1975 noted 100% exceedance of the modal value noted at Beatrice 'A' over December and January, and 96% exceedance during February, as compared to 92.8% exceedance at Beatrice Alpha over winter 1990. Highest values of  $H_S$  were noted as 8.7 m, 8.1 m and 8.2 m for the three winter months, although the maximum recorded wave heights ( $H_{max}$ ) were 16.2 m, 15.2 m and 15.4 m.

Further south records taken from Dowsing Light Vessel off Spurn Head (Humberside) (Draper, 1976) showed percentage exceedance of annual modal  $H_S$  from Beatrice Alpha as 70% in winter, falling to 58% in spring to a low of 49% in summer before rising to 82% in autumn. Modal wave periods were recorded as 4.5 s in winter and summer, whilst both spring and autumn displayed bimodal periodicities at 4 and 5.5 s, and 4.5 and 6.5 s respectively.

From this limited ancillary data it is suggested that a north-south energy gradient exists in the North Sea. Data from the Shetlands (MAREX, 1975) suggests that wave heights are higher than those experienced in the outer Moray Firth, although data was only available for the winter season. The values recorded for  $H_{max}$  are certainly far in excess of any wave conditions experienced either at Beatrice Alpha or Kinnairds Head over their respective recording periods, and even extreme wave forecasting in these areas fails to produce waves of this magnitude. Data from Dowsing (Draper, 1976) suggest that lower wave heights

were more common in this zone than in the outer Moray Firth, with the percentage exceedance values of the modal peak recorded at Beatrice Alpha much lower than those at either Beatrice Alpha or Kinnairds Head.

### **5.2.1.10 Summary**

Overall the wave parameters used as input to the wave refraction model fall well within both the conditions recorded in the open North Sea, as expected, and within the extreme conditions calculated for the middle firth by Conoco. Data from Beatrice Alpha shows a modal wave height of 1 m, and a modal period of 4 s, reflecting the sheltered environment of the Moray Firth. The lack of directional wave data recorded at Beatrice Alpha was supplemented by information from Global Wave Statistics, filtered to allow only waves from the North Sea generated in the sectors N-NE-E to enter the Firth.

### **5.2.1.11 Wave refraction and longshore current generation**

Wave refraction modelling was undertaken in order to quantify the magnitude of longshore currents generated by the incidence of obliquely approaching waves at the shoreline. While swell waves from the northeastern sectors produce the dominant westerly longshore currents at Culbin, wind waves generated within the firth are also capable of creating longshore currents. These westerly waves drive easterly longshore currents, opposed to the dominant westerly trend. These currents were quantified using the graphical technique of wave refraction modelling, and as such were not input into the wave refraction package WAVENRG.

Having established the nature of the waves used as input to the wave refraction modelling program WAVENRG, the program was then run. A slight modification was made to the range of wave periods used in the final wave refraction exercise, discarding 4 s waves and increasing the periodicity of the input waves to 6, 8 and 10 s. This was done as the resolution of the data produced using a range of 4, 6 and 8 s waves did not account for high energy conditions encountered from the easterly sector, which were considered sufficiently important despite their low frequency to warrant their inclusion. Additionally, test plots using low period waves from the easterly sector produced too few incident waves on the Culbin foreshore from which to make calculations, as refraction was not heavy enough to produce incident waves at the resolution of the model. Thus the use of slightly higher period waves was seen as justified given the limitations of the program.

The plots of wave orthogonals produced by the program were particularly useful in providing a semi-quantitative assessment of the erosion potential along the

Culbin foreshore. Orthogonal patterns display strong convergence on the eastern section of the foreshore, with 61.1% of the total wave record convergent (Table 4.21). This contrasts strongly with the western section of the foreshore, where only 5.5% of the wave record is convergent, the remainder being either parallel or divergent. This division is almost certainly created by the bathymetry of the nearshore zone at Culbin, with concave landwards contours displayed along the eastern section, and virtually straight contours along the western section (Admiralty, 1981). Additionally, the alignment of the eastern section of the foreland (cell B2) is such that incident swell waves approach more shore-normally, resulting in a greater proportion of the incident wave energy being directed shore-normally, enhancing erosion. Along the western section of the foreshore (cell B1) the increasing westerly component of foreshore alignment means that waves approach at progressively lower angles, and so a higher proportion of wave energy is directed shore-parallel. Calculation of values of the incident component of wave power (POZ) confirmed the findings of the qualitative study using wave orthogonals, with positive residual calculations made between cell B2 and B1 demonstrating higher incident wave energy received along cell B2. While seasonal values of POZ were calculated, it was not considered appropriate to divide the recession measurements into smaller units than one year, this falling below the resolution of the measurement of dune cliffing. However, the results are of interest, and are useful in understanding the seasonal distribution of wave energy received by the foreshore. The total calculation demonstrates that cell B2 receives only 52.5% of the energy of B1, with the most equal reception of incident wave energy during the spring, while the remainder is divided more evenly across summer-autumn-winter. During the spring, B2 receives 46.4% of the wave energy of B1, while during summer and winter this falls to 23.6%.

Examination of the spatial distribution of the incident component of wave power also helps to explain the higher potential values of longshore sediment transport calculated for the western cell than the eastern cell. Additionally, given the generally higher dune cliffs backing cell B2, and lower dunes backing B1, then with higher incident wave energy, the enhanced rates of erosion measured in cell B2 will supply a greater volume of sediment to the foreshore, producing the wide beach profiles at stations 1-3 (section 4.2.2). Conversely, the shorter beach profiles recorded at stations 5-7 coincided with lower backing dune heights and a lower incident wave energy regime.

The program also produced output in the form of values of  $P_L$ . Once converted to their seasonal frequencies using the method described by Mason (1985), the values of  $P_L$  show a clear pattern, with the highest values of  $P_L$  recorded during spring, coinciding with the highest incidence of swell waves (24.1%) on the Culbin foreshore (section 4.2.1). The highest values of  $P_L$  are experienced in cell B2 during spring and summer, reaching  $263.50 \text{ J m}^{-1} \text{ s}^{-1}$  in spring, while during autumn and winter B1 displays the highest  $P_L$  values, reaching  $169.36 \text{ J m}^{-1} \text{ s}^{-1}$  in autumn. With a dominant swell wave climate generated from the NE, the longshore currents are all positive, demonstrating a westerly trend which explains the westerly deflection of drift aligned landforms in this section of the Firth recognized from air photographs (Plates 3 & 6). The conversion of these values to a sediment transport rate and its relevance in the calculation of a beach sediment budget is discussed in section 5.2.3.9.

## **5.2.2 Contemporary coastal sediments and landforms**

Waves in the Moray Firth have been identified as the primary source of energy involved in the transport of sediments, with a secondary role played by tidal currents. The predominant sediment transport direction is west towards the inner Firth (NERC, 1991). Having established the primary sources of energy driving the nearshore system in the middle Moray Firth, the nature of the landforms produced by these forces can now be investigated.

### **5.2.2.1 Foreshore sediment analysis at Culbin**

Prior to an analysis of the landforms of the contemporary coastal landforms of the Culbin area, it is important to understand the nature of their constituent sediments. While the description of raised Holocene foreshore sediments located at Culbin have stressed the importance of shingle storm ridge deposition, it is clear that a major sedimentary change has occurred to leave the contemporary Culbin foreshore dominated by sand. Shingle storm ridge deposition is limited on the Culbin foreshore to a small shingle bank extending west of station 6, with the primary locus of shingle deposition now located on the distal (western) end of The Bar. Dating the youngest (most seawards) shingle ridges at Culbin suggests that this change occurred *ca.* 1900 BP at the earliest.

The nine samples selected from sites along the Culbin foreland all display a high degree of sorting, with all values less than  $0.5\phi$ . This reflects the sorting processes active in the surf zone. The strong oscillatory motion of water in the surf zone selectively removes the finest sediment fraction (silts and clays)

offshore, leaving a relatively well-sorted lag deposit on the foreshore (Friedman, 1967). Such conditions are found at all stations at Culbin, where sorting ranges between well sorted at the extreme east and west ends of the foreshore and into Findhorn Bay, through to very well sorted at the sampling stations in the central section of the foreshore (stations 3 & 4). Sedimentary characteristics of the samples obtained from stations 0 and 1 at the eastern end of the foreshore are strongly influenced by the River Findhorn. The degree of sorting of the samples from these stations is particularly noteworthy, displaying poorer sorting indices (0.36 and 0.40 respectively) than all but the most westerly sample (sample 7). Tanner (1959) noted from studies along the Florida panhandle that sediments collected from the mouth of estuaries display the finest grain sizes but the poorest sorting, a feature recorded at Culbin. Self (1977) also reports lower sorting indices of sediments collected from the mouth of the Rio Nautla in the Gulf of Mexico than from adjacent beach sands. McLaren (1981) and Nordstrom (1989) both report higher sorting indices with distance downdrift, and suggest that the degree of sorting was improved when the transport mechanism operated at a constant energy level. Self (1977) suggests that skewness could be used as a relative measure of the degree of fluvial influence along a beach, with positive skewness near the river mouth decreasing with distance. This is also indicated by Mason & Folk (1958), who consider that the tail of the sediment size distribution is most heavily influenced by the incident process regime.

The samples collected from the Culbin foreshore do not support such a model, although comparison of the two most easterly and westerly samples alone might suggest that on a gross scale skewness does decline with distance from the Findhorn. However, the sampling stations located in the central section of the foreshore (stations 2-5) display a much stronger positive skewness than those at the river mouth, suggesting an increase in grain size in this central section of the foreshore. This is opposed to Self's (1977) interpretation, which suggests that the coarsest fraction of the river load would be deposited at the mouth through both declining flow velocity and increased flocculation at the confluence with saline seawater (Freidman, 1967). Additionally, tidal influx will also tend to transport sediment into the mouth of the estuary from the adjacent foreshore, enhancing the positive nature of the skewness at the river mouth (Komar, 1976). Increased grain sizes in the central section of the Culbin foreshore possibly reflect an enhanced energy receipt in this zone (Nordstrom, 1989), resulting in the selective removal of the finer grades of sediment.

Within the foreshore deposits a marked longshore sorting of sediment grades occurs (Figure 4.52). Some disagreement exists in the literature over whether grain sizes increase or decrease downdrift (Clayton, 1980; Nordstrom, 1989). A closer examination of the literature suggests that the coarsening debate stems from a question of accurate definition of a "coarse" as opposed to "fine" sediment. This is a particular feature of Nordstrom's (1989) work, which, whilst the title indicated downdrift coarsening, proceeds to discuss the fact that "...sediments become finer downdrift at the the broad, regional scale." (Nordstrom, 1989). Pioneering work on the longshore sorting of sediments (Evans, 1939) suggests that the finest fraction of foreshore sand deposits will be transported at a slower rate than the coarser fraction, while above a critical grain diameter the rate of transport declines once more. This is due to the tendency for the finest fraction to be transported high up the foreshore on the swash and temporarily abandoned, while the coarser fraction is moved back down the foreshore slope by backwash aided by gravity. As a result, the coarser fraction remains in the potential transport zone for a longer period, and thus if acted upon by waves approaching the shoreline obliquely would be selectively transported further than the finer material. Conversely, the coarsest fraction would be transported seawards beyond the surf zone by gravity-aided backwash, and being of such a mass as to be unable to be transported landwards by the swash would remain outside the zone of maximum transport potential (Evans, 1939). This explanation is accepted as a feasible mechanism to explain the sedimentological characteristics observed on the Culbin foreshore. Literature suggesting that downdrift fining is a feature of foreshore sediments focus on coastlines with tidal inlets present, where sediments are typically coarser. In relation to the sediments updrift, these sediments will display downdrift fining.

Komar (1977) attempted to quantify these effects, and found that a critical grain size of  $-0.25\phi$  was the most rapidly transported, with a reduction in transport rates on either side of this grade. However, the short term nature of the experiment meant that the exact value of the most mobile sediment grade was a function of both wave and current conditions, and over a longer timescale would encompass a wider range of sediment sizes (Komar, 1977). Similar downdrift coarsening has also been recorded by Winkelmoen (1978) along Spurn Head, McCave (1977) along the East Anglian coast and Balsillie (1975) along the Florida panhandle.

The results from the Culbin foreshore suggest a very general increase in grain size along the foreshore (Figure 4.52). The coarsest sediment is located at

station 6, and the finest within Findhorn Bay, broadly supporting the patterns described by Komar (1977). This also supports the contention that coarsening sediments occur in the direction of longshore transport (Clayton, 1980), E-W in the case of Culbin.

#### **5.2.2.2 Culbin beach profiles**

The beach profiles measured at seven locations along the Culbin foreshore provide a record of the morphological changes to the beach cross-section throughout the two year monitoring period. However, the frequency of sampling was increased in the final year (1991-92) to monthly resurveys of the beach profile.

#### **5.2.2.3 Culbin foreshore a) intertidal morphology**

The beach profiles measured along the Culbin foreland display marked differences in morphology and length, with a continuous series of changes recorded over the two year period. These changes are summarized by the sweep zone plots produced in Figure 4.53, which show the maximum vertical range of beach profile variation at each measuring station between March 1990 and February 1992.

Stations 1-3 consistently display the longest profiles of the seven recording stations, with a standardized profile length of up to 218.36 m recorded at station 2, and an actual maximum profile length of ca. 402 m, also recorded at station 2 during April 1991. The lengths of these profiles contrasts sharply with the extremely short profile recorded at station 4, which was generally <100 m long. West of station 4, the profiles were more consistent in length, varying between ca. 110-120 m. The longer profiles measured along the eastern section of the foreland reflect the higher volumetric input of sediment to this section of the beach, primarily from the high dune cliffs backing the foreshore at stations 1-3.

West of station 4 the length of the beach profiles increases slightly once more, with station 5 displaying the longest of the 'western' profiles (121 m). Dune cliff erosion is assumed to provide the sediment for the construction of these profiles. Additionally, longshore movement of sediment from updrift (stations 1-3) begins to influence the sediment flux to these stations, providing an additional sedimentary input.

The beach profiles measured at Culbin appear to be indirectly proportional to incident wave energy on a gross scale, with the eastern profiles (1-4, refraction

cell B2) subject to higher incident wave energy, and the western profiles (5-7, refraction cell B1) to a lower incident wave energy (section 4.2.2.6). The effect of focussing of wave energy demonstrated by the patterns of wave orthogonals leads to a higher receipt of wave energy along cell B2, reflected in the high rates of erosion ( $1.20 \text{ m a}^{-1}$ ) recorded along the dunes backing this section of the Culbin foreshore. This leads to high rates of sediment release to the foreshore along cell B2 which, combined with the supply of sediment from updrift, produces a relatively wide foreshore. Conversely, lower mean rates of dune recession ( $0.03 \text{ m a}^{-1}$ ) arising from the lower incident wave energy received along cell B1 produces a narrower foreshore.

The morphology of the beach profiles supports Short's (1979) assertion that the size and scale of beach morphology was inversely proportional to beach gradient. Typically a wide profile accompanies a low gradient foreshore at Culbin.

The morphology of the beach profiles which were recorded provided useful information regarding the nature of the foreshore development in this section of the southern Moray Firth. The form of the beach profiles recorded along the Culbin foreland match the range of beach profiles developed in meso-macro tidal environments, grouped by Short (1991) into three characteristic groups:-

GROUP 1. High sea/swell wave environment. Relatively steep concave upwards profile. Dissipative lower foreshore.

GROUP 2. Multibarred (ridge & runnel) system. Lower intertidal gradients and episodic sea wave attack. Limited swell wave attack.

GROUP 3. Transitional beach/tidal flat. Low wave energy system.

From this classification, the beach profiles measured at Culbin clearly fall into group 1, although the relative energy receipt of the Culbin beaches was somewhat lower than that implied by the Short classification. Wright & Short (1982) devised a measure of the reflectivity of the foreshore face, which they termed the surf scaling factor ( $\epsilon$ ), defined by the term:

$$\epsilon = \frac{a_b \cdot 2\pi}{gT \tan^2 \beta} \quad (20)$$

where  $a_b$  = wave amplitude (height) at breaking (m)

$$g = 9.81 \text{ m s}^{-1}$$

T = wave period (s)

$\beta$  = foreshore slope ( $^\circ$ )

Threshold values were defined as  $\epsilon > 33$  (dissipative foreshore) and  $\epsilon < 2.5$  (reflective foreshore), with  $33 > \epsilon > 2.5$  defined as a transitional form.

The mean foreshore gradients along the Culbin foreland of *ca.*  $1^\circ$  produces a value of 350, exceeding the critical value of 33 to firmly classify them as dissipative forms. The shingle storm ridge recorded in a fully formed state at station 7 attained a maximum angle over the study period of  $11^\circ 20'$  (11/91), producing a surf scaling factor of 2.65, falling into the intermediate/reflective classification as might be expected from a coarse, clastic storm beach deposit.

The variation in profile morphology around Shellyhead bothies is demonstrated when considering the maximum vertical elevations attained by the beach profiles. The eastern profiles (stations 1-4) vary across a lower, but stable extreme range of *ca.* 5 m (measured between the upper beach on the upper sweep zone and the lower beach on the lower sweep zone). This contrasts with the more varied and higher extreme range of 4-6 m displayed by the western profiles (stations 5-7). While this variation is higher in the western profiles, the at-a-point variation in foreshore topography is actually lower, reaching only 3 m, while in the eastern section the vertical range of any profile is *ca.* 4 m. This once more highlights the apparent divide in beach profile morphology occurring at Shellyhead bothies between stations 4 and 5.

#### **5.2.2.4 Culbin foreshore b) subtidal morphology**

As recorded in Chapter 3, measurement of the submarine beach profiles in the nearshore zone at Culbin was undertaken as a synoptic exercise in order to demonstrate the nature of the nearshore bedforms rather than to provide input into the beach sediment budget.

The submarine profiles display a marked change in both morphology and number, centred once more between profiles 4 and 5 (at Shellyhead), as was recorded on the subaerial profile measurements (section 4.2.2). Generally the profiles east of Shellyhead display a much flatter section, with up to three

offshore bar features on the profile. West of Shellyhead the profiles are steeper, with fewer bar features, but those which were recorded are spatially more continuous than the fragmented bar forms of the east beach. This supports observations by Komar (1976) which demonstrate that the number of offshore bars is inversely proportional to the gradient of the sea bed.

The morphology of the profiles along the east beach are thought to reflect the higher rates of sediment delivery to this section of the foreshore. Profiles 1-3 (Figure 4.55) display a more undulating morphology, and contain up to three bar forms along the profile. Despite their relative amplitude, these bar forms are short in an alongshore direction, possibly reflecting a slightly more energetic environment of deposition. This would be particularly true in the vicinity of station 1 at the river mouth, where the interaction between tidal, fluvial and wave activity would provide a highly energetic sea bed environment in which the formation of continuous longshore bar features would be hindered.

In contrast, the submarine profiles measured along the western section of the Culbin foreshore (Profiles 5-7) display a more regular series of offshore bars ca. 200 m offshore (Figure 4.55). Evidence from the field suggested that the bar feature shown on each profile is a continuous feature extending for at least 2.8 km alongshore. This differs from the short, discrete bar forms located on the eastern profiles, possibly reflecting the response of the foreshore to a previous storm event, i.e. flattening of the beach profile coupled with offshore storage of sediment in linear, shore-parallel/sub-parallel bar forms (Zenkovitch, 1967). Under lower wave energy conditions these features typically begin to migrate onshore, "welding" onto the foreshore face (Sonu, 1973). These often form a characteristic runnel feature in the foreshore surface which, with the progression of a tidal cycle, eventually closes as the bar form incorporates itself onto the foreshore. Such an effect was recorded through daily observations made at station 6 during September 1991.

Once more it can be demonstrated that a divide between the characteristic morphologies of the submarine profiles occurs between profiles 3 and 5, in the vicinity of Shellyhead bothies. The transition is marked by profile 4, which although displaying the lower angle profile characteristic of profiles 1-3, also displays a relatively flat profile, with only a minor bar form at the seaward limit of the survey at ca. 750 m offshore (Figure 4.55), and no such features closer to the low water line.

From this exercise it is apparent that a division in the characteristics of the nearshore profile characteristics occurs in the vicinity of profile 4/Shellyhead bothies, a feature also noted during the analysis of the subaerial profile data.

#### **5.2.2.5 Culbin foreshore: changes in beach forms and processes**

Having examined the nature of the morphological responses of the Culbin foreshore, their volumetric changes over the period 1990-92 will be examined. Due to the detailed measurements made in the field, these changes will be categorized as cells 1-7 once more. Cells 1-4 (east beach) represent wave refraction cell B2, while cells 5-7 (west beach) represent wave refraction cell B1.

Multiplying the cross-sectional area of each profile by the length of the process cell it was selected to represent, the volumetric changes to the Culbin foreshore were calculated. These are shown in Figure 4.54. The volumes represented by these graphs is largely dependent upon the length of the cell areas which the profile represents. This means that although *station 2* displays the largest cross-sectional area, *cell 2* actually contains the lowest volume, and cell 7 displaying the highest volume (Figure 4.54). Additionally, cell 7 is also subject to an annual increase in volume due to the distal extension of the Buckie Loch spit at the western extremity of cell 7, at a rate of  $13\ 817.4\ \text{m}^3\ \text{a}^{-1}$ .

Of interest when analyzing the volumes displayed in each cell was the non-uniform response of individual cells to events which led to significant draw-down of beach levels in some cells, but not in others. The majority of the cells displayed a low beach volume during December 1990, which coincided with one of the highest volumes recorded in cell 2. The lowest volume in cell 2 did coincide with a fall, albeit of a minor nature, in the remainder of the cells during March 1991. The highest cell volumes were recorded during February 1991 in cells 3, 4 and 7, with more minor peaks in volume also recorded in all other cells, suggesting rapid readjustment to the low volumes of two months previous.

Spatial relationships between the timing of the extremes of beach volumes were weak, and in some cases were diametrically opposed. For example, the high volume recorded in cells 3-7 during October 1991 coincided with very low volumes in cells 1 & 2. The only volumetric "event" which was recorded at all stations was a peak in volume recorded during February 1991. Even this event, which represented the highest volume recorded in cells 3, 4 & 7, registered only as a minor peak in cells 1 & 5. Similarly the lowest beach volumes were recorded during December 1990 in cells 3-7, but were not represented in cells 1

& 2. The patterns of volumetric change are similar in cells 3 & 4, and 6 & 7, suggesting that their profiles respond in a similar fashion to erosional and accretional events. Additionally, a change in response in cells 6 & 7 once more appears to represent a divide in the process regime between the "east" beach (refraction cell B2, containing cells 3 & 4) and the "west" beach (refraction cell B1, containing cells 6 & 7). This again corresponds with the approximate location of Shellyhead bothies, adding weight to the proposal that this location represents a process boundary on the present Culbin foreshore.

The data discussed so far illustrates the point that the classification of beach profiles into seasonal 'types' is not realistic. The classic work on this aspect of beach morphology (Shepard, 1950) suggested that during summer, low energy wave conditions prevailed, leading to constructional effects on the foreshore and a build-up of the beach profile and associated volume. Under the higher wave energy conditions experienced during winter, the beach would be 'combed down', producing a flatter profile containing a lower volume of sediment.

As demonstrated by the Culbin profiles, while some of the lowest individual cell volumes occurred during winter 1990 (eg cells 3-7), winter 1991 actually produced the highest total beach volume. This illustrates the view of Wright *et al.* (1979) and Short (1980) that profile morphology at this scale is controlled more by breaker type than seasonality. This is a particular feature of British beaches, where the variable wave climate experienced around the majority of the coast means that seasonal divides in wave energy on a medium timescale are artificial. Carr *et al.* (1982), in a study of beach profiles from Swansea Bay, Start Bay and the Suffolk coast, found no marked seasonal element in beach profile change. Clarke & Eliot (1988) similarly found no distinctly seasonal beach profile response in their study on Warilla Beach, NSW. Dubois (1988) did recognize a seasonal disparity between summer and winter profiles from studies on the Delaware coast, but correctly attributed the differences to changing wave climate which, in this case, happened to coincide with the seasonal divide in Atlantic wave energy.

Sonu & Young (1971) recognized that beach profile changes are essentially stochastic in nature, although they must possess an element of Markovian memory (Mason & Hansom, 1986). While beach profile changes are controlled to a certain extent by external variables, the study of the process-response relationship between the beach profile and incident conditions remains a "grey-box" system. Problems still remain when attempting to relate changes in the

beach profile to specific energy inputs, particularly when lag periods are observed between causative event and beach profile response, as was observed by Carter (1975) in his study of the Magilligan foreland, Ireland. Additionally, beach profiles have been noted to produce "atypical" responses to certain events which might otherwise have been expected to produce different results. At Culbin, for example, a peak in cell volume was recorded across the entire recording network during October 1991; in the case of cell 6 this represented the highest recorded cell volume over the study period. Such results might formerly have been suggested to represent 'constructional' conditions. However, October 1991 saw cell 1 reach the lowest volume recorded over the same two year period. One cannot imply that either erosional or constructional processes were operating on the foreshore at this time, as the profile-scale morphological response of the foreshore indicates that both might have occurred, with the response simply exacerbated by the distribution of the sampling framework. This is clearly not the case, and it appears that the element of Markovian memory in the beach profile (Mason & Hansom, 1986), coupled with the local availability of sediment at this time combined to produce the profile response recorded.

Such atypical results have been observed elsewhere. Dubois (1988) reported that both storm and swell conditions produced accretion on the Delaware coast, with storm events accounting for 20% of the accretion recorded on the beach face. Attempting to equate storm conditions with periods of low beach volume is clearly problematic, although on the gross scale such relationships can still be demonstrated (eg. Aubrey, 1979). The total beach volume recorded in October 1991 at Culbin, for example, still displayed a volumetric peak, suggesting that the entire beach underwent net accretion at this time.

In addition to these changes, Clarke & Eliot (1988) described a series of beach changes measured over a 10 year period from Warilla Beach, NSW, which suggested that beach profiles may have undergone low magnitude responses to cyclic processes. Eigenfunction analysis revealed that sediment movements were taking place with regular periodicities of 3.0, 2.0, 1.7 and 1.0 years. The possible processes controlling these events were considered to be variations in incident wave regime and variations in MSL, although these were not analyzed in detail. While it would be possible to quantify such events over the timescale used by the authors, in terms of relatively short studies such as at Culbin, the implications are potentially large, although the actual volumetric changes were found to be minimal.

Schumm & Lichty (1965) recognized that time is not a geomorphological process. In the light of the data produced from this study, and the available literature, it remains that the concept of *seasonal* beach profile forms and changes should be abandoned, and replaced by process-based distinctions where possible. In the case of British beaches this is frequently not possible, as the temporal variability in wave climate around the coast means that few uniform trends can be detected in beach profile elevations or volumes (Carr *et al.*, 1982). If the anticipated changes in wave climate under a "Greenhouse" scenario occur (section 2.4.7), then increasing storminess might become a feature of the British coast, and the predictability of beach profile morphology might be further reduced.

Fitting linear regressions to the volumetric data calculated for each cell demonstrates that 5 out of the 7 cells displayed a rising trend in volume over the two year study period. Only cells 5 and 7 displayed a falling trend. Summing these data produces a plot of total foreshore volume (Figure 4.54) which also displays a net increase in volume: i.e. the foreshore underwent net accretion. However, the low gradient of the line demonstrates that this accretion represents only a minor volumetric increase, amounting to a *net* change of *ca.*  $0.10 \times 10^6$  m<sup>3</sup> over the study period.

While this result might appear to indicate that the Culbin foreshore was in a sedimentologically healthy state between 1990-92, it would clearly be unwise to extrapolate the possible effects of this result. As indicated by the volumetric calculations for cells 6 and 7, trends across a 2 year period can easily be altered by one low frequency, high magnitude event. The similar trend between these cells was altered by the large build-up in beach volume at cell 6 during October 1991, which was mirrored but not matched by cell 7. This led to a reversal in the linear volumetric trends displayed in these cells, despite their adjacent locations. This example serves to illustrate the point that non-uniform, spatio-temporal responses of the beach profile might produce apparently significant results in the short term, but which over a longer timespan are not representative of the actual situation.

#### **5.2.2.6 Coastal erosion at Culbin and Burghead Bay**

Erosion along the Culbin foreshore has been described as severe by Ritchie *et al.* (1978), who estimated the rates of dune cliff recession along the Culbin foreland to be *ca.*  $0.60 \text{ m a}^{-1}$ . The emplacement of a series of wooden groynes during the late 1960s by the former Forestry Commission (Forestry Commission,

1988) may have initially reduced erosion rates slightly (Ritchie *et al* , 1978), but continued erosion has led to decoupling of the landward ties of the groynes, leaving them some distance down the foreshore and in a poor state of repair.

The validity of measuring coastal recession over the short period of a study raises questions of representativeness of both sampling and wave climate during the study relative to longer term baseline conditions. Erosion of unconsolidated cliff materials has produced typically erratic values when monitored at fixed positions (Mason, 1985; Bye, 1988). Dune cliff erosion is also both spatially and temporally sporadic, with single storm events frequently the cause of an entire year's "average" erosion at a single site, whilst positions nearby may experience no erosion at all.

The series of erosion measurements made along the crests of the dune cliffs of the Culbin foreland displayed marked differences in magnitude, with a maximum of 5.90m recorded at section 2 on the eastern section of the foreshore in 1990-91: during the following year, erosion at the same position was only 0.65 m. The generally higher mean recession values from the 1990-1991 season produced a mean dune recession value of 1.26 m, while the values from 1991-1992 produced a much lower value of 0.30 m. Ross (1983) recorded 8 m of dune recession along the section west of Shellyhead during a single storm surge event which occurred on 01/02/83, while 200 m east of Shellyhead the same event produced no recession.

Section 4.2.2.6 describes the patterns of orthogonal convergence and divergence and their quantification through the incident component of wave power (POZ). The strongly convergent orthogonal patterns (61.1%) along the eastern foreshore (cell B2) explains the higher rates of dune cliff recession recorded there in relation to the western foreshore (cell B1), where only 5.5% of the othogonals are convergent. Conversely, along cell B2 only 19.4% of orthogonals are divergent, while 38.8% diverge along cell B1. Table 4.21 displays the fully quantified implications of wave orthogonals at Culbin, where it is clear from a calculation of residual POZ that all recorded values are greater in cell B2 than in cell B1, by up to  $950 \text{ J m}^{-1} \text{ s}^{-1}$ . thus a strong difference exists between the eastern and western flanks of the Culbin foreshore in terms of relative wave energy receipt, despite an morphologically similar appearance. Slight differences in the orientation of the foreshore to incoming swell, coupled with a convex-seawards series of submarine contours along cell B2 (east foreshore) serve to magnify the effects of incident wave energy, with

repercussions for the rates of dune cliff recession and detailed profile morphology.

Carter & Stone (1989) described the mechanism of dune cliff erosion as an initial saturation/liquefaction as water reaches the foot of the cliff, leading to localized failure and the "sloughing" of saturated sand onto the beach. Removal of the toe in this fashion leaves the upper cliff unsupported, eventually exceeding its own factor of safety and ultimately leading to the failure of a section of the cliff face. Such processes could clearly be seen along the Culbin foreland throughout the duration of the study, particularly along the high dunes between Findhorn Bay and Shellyhead bothies.

At Culbin, the failure of the dune cliff is enhanced by the presence of mature pines cresting the dune cliff along the eastern flank of the foreland (Plate 7). While the root systems bind the surficial sand, the loss of lateral stability creates a turning moment leading to enhanced cliff top erosion. Minor tabular and rotational failures were also noted, created by the presence of understory vegetation binding "rafts" of sand together. Carter & Stone (1989) recognized a continuum of coastal slope failure forms based upon shear strength and time relative to tidal mode. The localized increase in shear strength resulting from the vegetation understory at Culbin classifies the cliff failures as those requiring the maximum immersion of the cliff toe for failure to occur in the Carter & Stone continuum model. However, the height of the dune cliffs at Culbin means that lower, unvegetated surfaces tend to act as an essentially unconsolidated deposit, failing *en masse* beneath the vegetation bound units above and becoming obscured by the rafting of root-bound blocks down the cliff face. The arrival of these units at the foot of the cliff temporarily protects the cliff above from direct wave attack and swash liquefaction. However, their limited size protects only a short stretch of the cliff toe, while adjacent areas continue to erode, thus enhancing localized differences in the mean erosion rate recorded along the Culbin dune cliffs.

West of Shellyhead bothies, the nature of the dunes changes from high, cliffed tabular dunes to lower, true coastal forms having developed in association with the distal extension of Buckie Loch spit. This can be seen in Plate 1 (frontispiece). Cliffling of these dunes was only observed between recording stations 5 & 6, where localized high dune development (Figure 4.57) shows evidence of cliffling, although erosion rates along this stretch remained low between 1990-1992. Along the remainder of the foreshore (between Shellyhead

and station 5, and west of station 6) the dunes are of the low, rounded forms typical of foredunes or early yellow dunes (Hansom, 1988), with little evidence of blowout activity. Between Shellyhead bothies and station 5, the dunes are completely vegetated with marram (*Ammophila arenaria*) and sea lime grass (*Elymus arenaria*). Erosion along this section occurs via the complete removal of the dune face through slumping. West of station 6 the presence of a shingle storm ridge at the foot of the dunes protects them from direct encroachment of swash and waves, and no erosion was recorded during the study period along this stretch of coast.

The importance of nearshore bars in the potential modification of the nearshore wave energy environment is discussed by Carter & Balsillie (1983). They reported that between 78 and 99% of wave energy may be lost through waves breaking over nearshore bars. However, the reformation of high frequency, low amplitude waves between the bar and the shoreline was considered to account for up to 20% of the wave energy transmitted to the shoreline. Thus the location and morphology of nearshore bars may have an important secondary effect on the transmission of wave energy to the shoreline, particularly at low water. The impact of such modification on detailed foreshore morphology was described by Holman & Bowen (1982), who considered the impact of nearshore bars on the generation of rhythmic foreshore sedimentation. The low amplitude bars reported from the Culbin submarine profiles 1-4 were generally located in water depths greater than that required to create breaking conditions (approximately equal to wave height). However, those on profiles 5-7 were observed to be both exposed at low water on half tides, and thus are potentially important factors in reducing the incidence of wave energy along this stretch of the coast. The poorly formed series of welded bars visible in Plate 1 lend limited support to the presence of a heavily longshore-modified system of rhythmic foreshore topography, in a similar scenario to that described by Holman & Bowen (1982).

While measurements of coastal recession along the Culbin foreland made for the purposes of this study were clearly limited by the time available, measurements of recession along the Culbin foreshore and Burghead Bay have been produced regularly since 1974 by Ross. The mean recession rate recorded between 1981-1989 was 1.94 m a<sup>-1</sup>, which was higher than that recorded over the monitoring period. However, between 1987-89 conditions were described as "quiet", with minimal erosion along the high dunes of cell B2 (Ross, 1987, 1988, 1989). Circumstantial evidence of the approximate rates of erosion in the central section of the foreland at Shellyhead comes from the emplacement of groynes

during 1968 by the Forestry Commission, which by 1979 were found 26 m down the beach (Ross, 1979), implying a mean recession rate of  $2.36 \text{ m a}^{-1}$ .

Recession has been exceptionally heavy on the Culbin side of the Findhorn estuary, especially on the promontory opposite Findhorn village (NJ 033647). Ross (1979) suggested a mean rate of recession at this point of  $4.00 \text{ m a}^{-1}$ , although a maximum loss of 11.80 m was recorded in 1983 (Ross, 1983). The westwards extension of the spit north of Findhorn village on the outer coast has forced the channel of the Findhorn across to the west where it directly impinges on the Culbin side of the estuary at high water. The high rates of recession at this point are aided by the lack of supporting shingle underlying this section of the foreland. The net westerly transport of aeolian sand across the Culbin foreland eventually extended beyond the shingle basement and out into a formerly larger Findhorn Bay. Continued eastwards accumulation of sand out into the Bay proceeded, creating a large area of dune sand along the eastern flank of the Culbin foreland. As the shingle spit on the eastern side of the Bay developed, it forced the river channel west across the mouth of the estuary against these relatively weak dune sands, resulting in high rates of recession in this vicinity.

The mean value of cliff top recession recorded was based on 10 sampling locations along the foreland produced a mean value of  $1.94 \text{ m a}^{-1}$ . Due to the inherently variable rates of dune cliff recession, the derivation of a meaningful rate of erosion along the Culbin foreland remains problematic, reflecting the representativeness of the sampling strategy as much as the actual at-a-point rate of recession. A comparison between the 1976 and 1989 air photographs for this section of the coast suggests a mean rate of recession of  $1.50 \text{ m a}^{-1}$  along the eastern flank and as far west as station 5, beyond which the rate of recession declines markedly. This suggests that the medium term rate of recession falls somewhere between the rates recorded by the author, and those recorded by Ross (1992).

#### **5.2.2.7 The Bar**

Geomorphological boundaries are extremely well defined on The Bar, delimiting process boundaries and also reflecting the relative energy receipt, as reported by Short (1991). The NE flank displays a low energy, dissipative energy regime, with a wide, flat sandy beach backed by dunes formed over a shingle basement. The SE flank by contrast represents a high energy, reflective foreshore system, with a narrow upper beach composed of coarse clastic material fronted to seaward by a narrow sandy terrace. The central zone falls between these two

extremes, representing a transitional beach type with a narrower sandy beach than found on the NW flank but backed by a shingle storm ridge. This transitional zone is also experiencing the highest rates of erosion, and from the evidence provided by the outcrop of back-barrier marsh sediments on the foreshore and the breaching of the storm ridge appears to be the most unstable zone on The Bar. Examination of historical map evidence over the past century shows heavy erosion of the central zone. This zone represents the proximal end of the shingle ridge system, with erosion removing sediment from this zone and redepositing it at the distal end of the Bar. Thus the feature migrates further SW towards Nairn.

The morphological similarity of The Bar to many barrier islands suggests that the processes which formed it and which are currently maintaining it might also be similar. Stiegler (1976) defines a barrier island as:

"An elongated accumulation of sand, shingle or in-situ rock lying roughly parallel to the coast but separated from it by a channel, lagoon or other water area."

Under this definition, The Bar is quite clearly a barrier island in terms of its geomorphology. However, in terms of its developmental history, The Bar differs greatly from the majority of the world's major barrier islands. Early work on barriers stressed the importance of a rapid rise in RSL forcing large quantities of offshore sediment into the nearshore zone, followed by a slower rate of RSL rise to allow the barrier to develop (Hoyt, 1967, Leontynev, 1969). Subsequent development occurs through rollover/washover mechanisms (Dillon, 1970) and tidal inlet processes (Pierce, 1970, Lauternauer *et al.*, 1979) forcing the barrier onshore. Whether this is a continuous process (Leatherman, 1983a, b) or a more intermittent one (Rampino & Sanders, 1983) remains contentious, although as Swift (1975) noted, initial development is insignificant in relation to the processes currently maintaining the barrier.

Sediment interactions in the tidal races at the proximal, and especially the distal channels, are vital to the maintenance of the landform's integrity, with washover/rollover processes characteristic of low relief barriers (Leatherman, 1979; 1983b; Carter & Orford, 1984; Orford *et al.*, 1991; Forbes *et al.*, 1991) only important in the central section of The Bar where updrift supply of shingle is failing. On the eastern flank, stability is maintained by the protection afforded by high dune development capping the underlying shingle, as proposed by King (1972). On the western flank, the altitude of The Bar is maintained by the deposition of shingle storm ridges which, having developed into a wide shingle strandplain, now prevent overwash in all but the most proximal zone.

The development of The Bar has not followed the "typical" sequence of events and processes which maintain a barrier island, i.e. onshore forcing of sediment under rapidly rising RSL followed by a period of consolidation under slowly rising or stable RSL. However, the processes operating on The Bar remain similar to those reported from other barriers, and remain as important in the development and maintenance of "true" barriers as in detached spit forms represented at Culbin (Hoyt & Henry, 1967; King, 1972). The genesis of the Bar is discussed further below.

#### **5.2.2.8 Recent historical coastal evolution of The Bar**

Elucidation of the development of The Bar and its possible predecessors has been possible through the use of historic maps, charts and air photographs. The first relatively accurate map of the Culbin area was produced by Timothy Pont in 1590 (Figure 5.18). This shows two bar features in the Culbin area, a shorter one fronting the western flank of the present Culbin foreland, and a longer one extending west from a point north of Findhorn. The bar at Culbin is notable as on it appears to be located the village of "Nevestown", or Maviston, north of Loch Loy. Given the current location of Maviston Farm south east of Loch Loy, this early map probably represents an earlier incarnation of the fishing village of Maviston, now destroyed. However, the alongshore location of this bar coincides approximately with the present location of the western flank of the modern Bar. The second bar is seen extending from Findhorn along the entire frontage of the present Culbin foreland which, although the map has no scale, in relation to the size of Findhorn Bay, would produce a feature approximately 6 km long.

The first accurate map of the Culbin area to be produced was the May map of 1758 (Figure 5.19). This was surveyed and drawn to aid the settlement of a dispute over fishing rights at the mouth of the Findhorn, and as such the accuracy of the map remains impressive for its age. Remeasurement of ten of the key distances marked on the May map made between existing farms reveals errors in survey of between +32% and -15.1% maximum, as shown in Table 5.2. In spite of these errors some very clear features emerge in the coastal configuration.

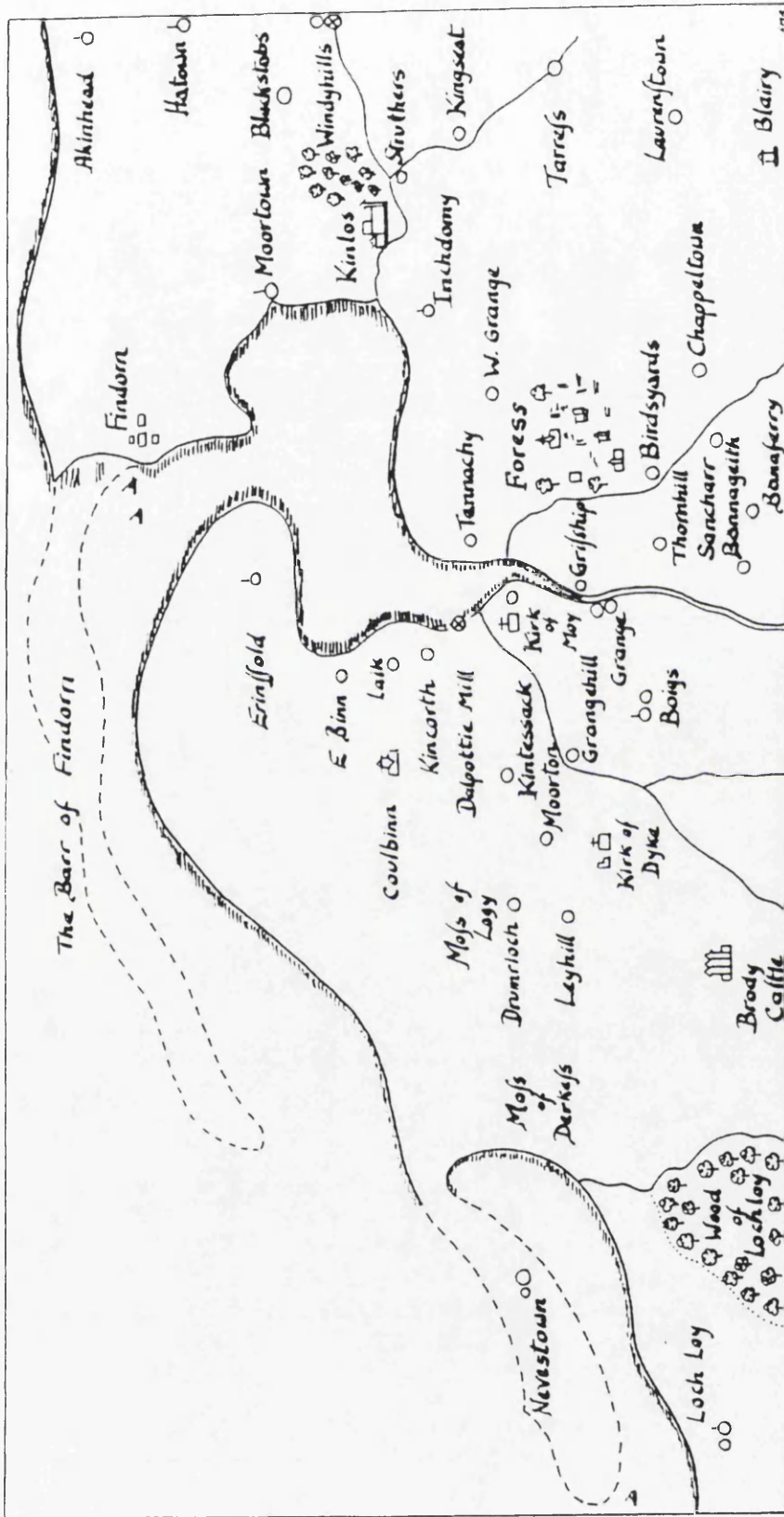


Figure 5.18 The Pont map of 1590

Measurement stations	May 1758 (m)	O.S.1977 (m)	Error (%)
Kincorth-Earnhill	891	1000	-10.9
Earnhill-Balnageith	3333	3150	+5.8
Balnageith-Mill of Grange	3399	3375	+0.71
Mill of Grange-West Grange	792	600	+32.0
West Grange-Binsness	3069	3025	+1.4
Binsness-Kincorth	2409	2225	+8.2
Balnageith-Mundole	1188	1400	-15.1
Kincorth-Moy House	1749	1725	+1.3
Earnhill-Moy House	990	775	+27.7
Balnageith-Kincorth	4158	4125	+0.8

Table 5.2 Distances and errors measured from the May map of 1758

Reference to Figure 5.19 shows a very clear bar feature extending west from a point apparently north of the central Culbin foreland, labelled as "The Old Barr of Findhorn", this coinciding with the bar feature on the Pont map seen extending west from Findhorn. The village of Findhorn is clearly marked on the May map, and a second bar extends towards the NE in a similar fashion to that seen today at low water, although the scale of the feature on the May map is much larger. Whether this simply represents artistic licence at the margins of the disputed area is unknown. The westerly of the two bars is of particular relevance to this study. Projection of the two ends of the bar onto the 1977 map of Culbin was undertaken using simple triangulation from the more accurately surveyed farms on the May map (Balnageith and Kincorth). The eastern end of the feature would have been located at NH 997646, west of profile station 5, while the western end would have been located at NH 956623, at approximately the position of Oldbar Bothy on The Bar (Figure 4.31 and Plate 3, feature 2). Examination of the sequence of historical map surveys carried out since this time has been



summarized by Ross (1992). These clearly demonstrate that there has been a large, westwards extending bar feature in existence along this stretch of the Culbin coast throughout the period 1758 to the present, with the suggestion of an even earlier stage of development from a position in the vicinity of The Island dated 1685 (Figure 5.20). This evidence strongly supports the idea that The Bar is a direct descendant of the bar shown on the May map from 1758, with a bar continuously in evidence at some position along the Culbin foreland since at least 1685.

Field evidence supports the theory of massive westerly extension of The Bar. Landwards of the bothy at Oldbar (NH 956623) are located a series of strongly recurving shingle ridges, extending from beneath a thick cover of dune sand south, becoming exposed above the level of the surrounding saltmarsh. These can be clearly located in Plate 3 (feature 2). In the field these ridges appear as low, linear, bare shingle structures surrounded by upper saltmarsh vegetation, extending for up to 60 m. These recurves clearly developed from the east and display reversals in direction of up to 180° (Plate 9). Given the location of the western end of the bar shown on the May map, then these recurves probably represent the western end of the Bar as it existed in 1758.

It is clear that The Bar represents a stage in a process of proximal erosion and distal extension which has been occurring continuously on the Culbin coast since at least 1685. Figure 5.20 shows the location of the distal ends of features identified as the forerunners of the present Bar measured by Ross (1992).

The Bar represents a feature which, while presently highly dynamic at its western (distal) extremity, is clearly relict at the eastern (proximal) end. Distal extension rates of up to 45.7 m a<sup>-1</sup> were recorded between 1947 and 1961, although this has slowed considerably to 14.6 m a<sup>-1</sup> between 1976 and 1989. At the eastern end, erosion of the high dunes has been occurring continuously, although the relatively stable shingle basement upon which the dunes sit has meant erosion rates do not appear to have attained the magnitude of those along the exclusively sandy Culbin foreshore.

#### **5.2.2.9 Distal extension rates**

The rates of distal extension measured both at Buckie Loch spit and The Bar produced similar rates over the time periods selected for the study. Under the sedimentary regimes of a sand system at Buckie Loch and a shingle system at The Bar, the high degree of similarity was not expected. Volumetrically, however,



the addition of sand and shingle to these respective landforms is very different, due primarily to the width of the features. Buckie Loch spit being much wider than The Bar at the distal point of extension.

The thickness of shingle on The Bar is based on morphological evidence, with the shingle storm ridge being 3.87 m thick. Below this, however, shingle is clearly mobile across the shoreface (Carter, 1988), and field observations recorded shingle at LWST covered by a veneer of sand. This suggests that The Bar is a shingle structure attaining a minimum thickness of 5.27 m, with a veneer of sand on the lower foreshore obscuring details below LWST. As this thickness represents a minimum, volumetric extension rates were thus once again based on a thickness of 6 m.

The linear extension rate of Buckie Loch spit was found to be  $15.5 \text{ m a}^{-1}$ , while The Bar was extending at a similar rate of  $14.6 \text{ m a}^{-1}$ . However, while this represents  $13\,817.4 \text{ m}^3 \text{ a}^{-1}$  of sand added annually to the spit, on The Bar the volumetric equivalent is only  $1377.9 \text{ m}^3 \text{ a}^{-1}$ . The difference in the mode of deposition between Buckie Loch spit and The Bar is explained by the availability of sediment and the relative mobility of shingle to sand. In the depositional environment of the mid-Holocene, shingle was clearly more abundant than at present, giving rise to the relict, shingle dominated beach systems of Culbin Forest and Burghead Bay. Under these conditions the rapid input of shingle from updrift allowed distal extension via longshore transport and aggradation of mainly shingle-based structures. Due to the higher mobility of shingle in the traction carpet, the concept of the shingle 'head' and sand 'tail' must once more be envisaged. With excess shingle available for transport, the shingle 'head' of the system was able to progress rapidly westwards, depositing into relatively deep water (up to 6 m at least) ahead of the sand 'tail'. Subsequent storm ridge construction would then be constructed on this shingle basement, creating a deeper shingle cover at the head (distal) of the Bar, while sand would be left downdrift to form Buckie Loch spit. However, under conditions of failing shingle supply as experienced presently, a greater proportion of shingle relative to sand would be immobilized in storm ridge sedimentation. On a net scale this would create an artificially sand-enriched foreshore environment on The Bar, within which the relative mobility of the sand would be apparently increased. This has resulted in sand bypassing the shingle and extending preferentially, creating the sand "flyer" west of the shingle dominated zone on The Bar.

### **5.2.3 Sand sediment budget: Culbin foreshore**

The beach sediment budget calculated for the Culbin foreshore was designed to highlight both the *actual* changes measured at the beach surface via the series of beach profiles established over a two year survey period, plus the *predicted* rates of sediment transport calculated from wave refraction modelling. The values produced from this analysis were calibrated using the volumetric distal extension rates measured on Buckie Loch spit. Having calculated a sediment budget for the predominantly sandy Culbin foreshore, a second budget was calculated using the distal extension rates measured on The Bar, representing a shingle sediment budget. The aim of this was to provide a modern analogue with which to compare the rates of accretion of the predominantly shingle beaches abandoned in Culbin. Thus by calculating budgets for both sand and shingle, the development of the Culbin foreshore during both stages of its development i.e. under a sand and shingle dominated shoreface, could be understood.

#### **5.2.3.1 Dune cliff inputs from Culbin and Burghead Bay**

Erosion of the dunes backing the Culbin foreshore forms an important sediment input source to the foreshore. Direct monitoring in the field allowed an accurate assessment to be made of the linear rate of dune recession along the Culbin dune frontage, which was subsequently converted into a volumetric equivalent. However, since the cliffs do not retreat in a linear fashion (Carter & Stone, 1989), problems are potentially created in the calculation of a mean rate of recession. In terms of the calculation of the sediment budget, the compartmentalization of the dune cliffs into ten discrete units allowed more accurate volumes of sediment released to the foreshore to be calculated over the time period. Additionally, the boundary between the two major foreshore cells B1 & B2 used in the wave refraction analysis also coincided with a dune compartment boundary, allowing a true separation between the sedimentary input from dune erosion into each cell to be made.

Dune recession was noted as spatially erratic, with four compartments recording no recession over the two year monitoring period, while a maximum value of 5.90 m of recession was recorded in compartment 2 during 1990-91. However, Figure 4.58 highlights the general difference in the nature of dune cliff recession recorded along the Culbin frontage between 1990-92, with much higher rates of recession recorded along the eastern section of the beach (coinciding with cell B2) than along the western section (cell B1). Indeed, along the western section

of the beach, the maximum recession recorded over any year at any location was only 0.10 m, while during 1990-91 there was no recession recorded at all.

Recession was also temporally erratic, highlighted by the fact that the exceptional amount of recession in compartment 2 was followed by only 0.65 m of recession over the following year. Despite these problems, a mean rate of dune recession along the Culbin frontage was calculated to be  $1.12 \text{ m a}^{-1}$  over the study period. This agreed well with the published value of  $1.0 \text{ m a}^{-1}$  by Ross (1992), but was higher than the  $0.65 \text{ m a}^{-1}$  reported by Ritchie *et al.* (1978). Whether the mean rate of erosion along the dune cliffs has increased in the intervening period, or whether the measurements had been made at a single location was not clear, but with the highly variable nature of recession along the Culbin dunes demonstrated clearly by these results, it remains that mean values of coastal recession in such environments should be viewed with caution, as localized pockets of recession may greatly exceed the mean rate.

The volumetric implications of these calculations are significant in the release of sand to the foreshore. The volumes released from the backing dunes along the eastern flank of the Culbin foreshore amounted to a mean annual release rate of  $15\,554.8 \text{ m}^3$ , representing 99% of the volume released from all dune recession to the entire Culbin foreshore.

Cliffing of raised foreshore deposits in Burghead Bay also contributed a significant volume of sediment to the nearshore zone, which is subsequently transported west to form another supply of sediment to the Culbin foreshore. The volume supplied to Culbin by cliffing in Burghead Bay was calculated to be  $30\,000 \text{ m}^3 \text{ a}^{-1}$ .

The calculation of this value depended on the accuracy of an estimated rate of recession around the Bay provided by Ross (1992). However, measurements from air photographs demonstrated that the value of  $1.0 \text{ m a}^{-1}$  represented the mean rate of recession around the Bay over the period 1976-1989, and was seen as adequate for the purposes of this study.

### **5.2.3.2 Fluvial inputs**

The method used to calculate the fluvial input of sediment to the Culbin foreshore depended on a knowledge of the volumetric status of the cell immediately adjacent to the river mouth, the inputs to this cell from erosion of the backing dune cliffs along the cell and the modelled longshore sediment transport

volume along this section of the foreshore. This effectively constituted a sediment budget in itself, serving to demonstrate that the sediment input from erosion of the backing dune cliffs alone is sufficient to supply the volumetric input necessary to maintain the volume of cell 1, without the need to invoke a further sedimentary source from the River Findhorn. A volumetric input of  $8793 \text{ m}^3 \text{ a}^{-1}$  was calculated from dune cliff erosion, and a potential export of  $7244 \text{ m}^3 \text{ a}^{-1}$  from longshore transport calculated using the longshore rates of sediment transport from the wave refraction exercise. Thus inputs to cell 1 exceed outputs without the need to invoke extra sedimentary input from the Findhorn.

Morphological evidence such as the infilling of Findhorn Bay and the substantial submarine sand deposit offshore from the mouth of the estuary (Figure 5.21) clearly shows that the river is continuing to transport sediment, predominantly sand, to the coast. However, the calculations demonstrate that in order to maintain the volumetric integrity of cell 1 required less sediment than was potentially available. As the primary input of sand to this cell is from the erosion of the backing dune cliffs, it is most likely that the load from the river is lost to the nearshore zone, transported beyond the surf zone at the mouth of the river.

### **5.2.3.3 Longshore sediment transport**

The calculation of longshore sediment transport used the computer simulated wave refraction program WAVENRG (May, 1974) to simulate swell waves, and a graphical method to simulate wind waves generated within the firth. Having determined a series of waves which could be used to represent the wave climate of the Moray Firth, these were used as input to the model. Wave heights of 0.5, 1.0 and 2.0 m were used, with periodicities of 6, 8 and 10 s. Incident wave approach was broken down into  $10^\circ$  sectors, and each combination of height, period and incident direction run on the program between the sectors  $010\text{-}070^\circ$ . Due to the failure of some orthogonals from the east to actually reach Culbin, Table 4.18 outlines the actual wave combinations used in the final analysis. Due to the resolution of the program, the Culbin foreshore was divided into two cells, an east cell (B2) and a west cell (B1).

The program calculated values of  $P_L$  at landfall for each orthogonal, which were converted to values of  $S_L$ , the longshore sediment transport rate, using equation 2 (Komar & Inman, 1970). The refraction of the graphically generated wind waves were also converted to equivalent values of  $P_L$  using equations 8-12. These were finally converted into values of  $Q_L$ , a seasonal value of  $S_L$ , in order to calculate the annual potential longshore sediment transport rate, with the

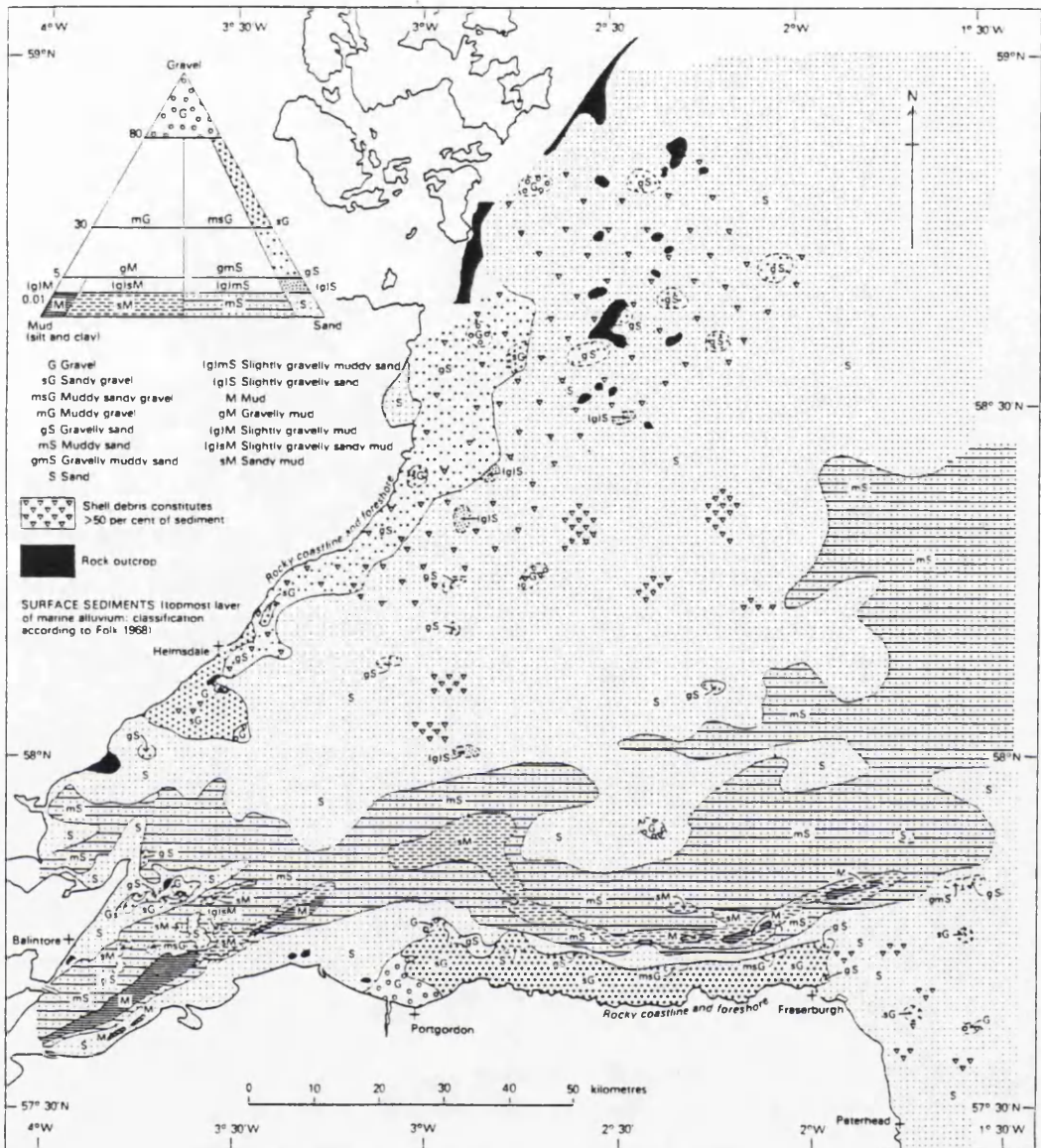


Figure 5.21 Offshore sediments in the Moray Firth (source: Chesher & Lawson, 1983)

easterly values of PL derived from the wind waves subtracted from the final calculation. The total potential longshore sediment transport rate in cell B1 (west) was 33 710.8 m<sup>3</sup> a<sup>-1</sup>, with a slightly lower rate in cell B2 (east) of 32 779.9 m<sup>3</sup> a<sup>-1</sup>.

#### **5.2.3.4 Onshore-offshore transport**

The quantification of a volume of sediment representing the shore-normal movement of sediment was beyond the scope of this study. Methods have been proposed for measuring this factor (Hardisty, 1984; Hardisty *et al.*, 1984), but break down if the predominant mode of sediment transport is alongshore. Thus this element of the beach sediment budget was used as a "balancing item", with an excess of sediment in the budget disposed of via offshore transport, and a shortfall made up by invoking onshore transport. As noted in the calculation of the sediment budget, under the predominant westerly sediment transport regime of Culbin, the volume of sediment required to be moved onshore to maintain the foreshore levels in cell B1 could have been derived from the offshore loss used to balance the sediment budget in cell B2. As B2 lies updrift of B1, then such an explanation is compatible with both the total sediment budget for the Culbin foreshore, and the geomorphological evidence from the beach profiles.

#### **5.2.3.5 Sediment budget**

The elements of the beach sediment budget for the Culbin foreshore are shown in Table 4.26 (repeated as Table 5.3 below).

The changes in beach volume used in the calculation of the observed beach sediment budget were calculated between March 1991 and February 1992. This period represented the most continuous run of data collected from the foreshore, with data collected at monthly intervals throughout the year of study. The two cells comprising the Culbin foreshore displayed different volumetric response characteristics over this period, although the total beach volume was seen to have increased over the study period (Figure 4.54). Cell B2 displays a negative sediment budget, with a general decrease in the volume of sediment in each of the sub-cells represented by the beach profiling stations 1-4 (east beach) during 1991-92. Cell B1 displays a positive sediment budget, with volumes of sediment in all sub-cells displaying rising volumes of sediment over 1991-92. However, the modelled sediment budgets displayed different trends. Cell B2 displays a positive modelled sediment budget, while B1 is negative. In cell B2, the modelled sediment budget (positive) exceeds the observed (negative) budget by

26 236 m<sup>3</sup>, while in cell B1 the observed budget exceeds the modelled budget by 35 162 m<sup>3</sup>. This implies that more sediment is moving onshore in cell B1, reflected in the values of the mean sediment transport volume per tide in order to balance the sediment budget over the 12 month period (Table 5.3).

	Cell B1	Cell B2
<b>Modelled Volume (m<sup>3</sup>)</b>	-731	+14 080
<b>Observed Volume (m<sup>3</sup>)</b>	+35893.5	-12156.2
<b>Trend</b>	ONSHORE	OFFSHORE
<b>Mean transport/tide (m<sup>3</sup>)</b>	+50.17	-35.94

Table 5.3 Difference between observed and modelled volumetric beach changes: Culbin foreshore

The extreme difference between the observed beach volumes in each of the cells was offset by the difference in the modelled volumes. Examination of the qualitative data produced during the generation of wave orthogonals suggested that focussing of wave energy occurs at the eastern end of the Culbin foreshore (cell B2), while at cell B1 minimal convergence was observed, with orthogonals mainly divergent or parallel. In terms of the sediment budget, this means that the erosion potential at cell B2 is much greater than cell B1, and coupled with the potential influx of sediment from updrift, offshore transport would need to be initiated to retain the foreshore in a quasi-stable form. This interpretation was in accord with field measurements of erosion rates along the Culbin foreshore, where erosion rates of up to 1.26 m were recorded along B2, while a mean erosion rate of only 0.30 m was recorded along cell B1.

The differences between the observed and predicted beach volumes are clearly reflected in the calculations of the mean transport rates per tide and the change in beach elevation per tide. Cell B1 shows a potential onshore mean sediment transport rate per tide of +50.17 m<sup>3</sup>, while B2 shows a potential offshore movement of sediment of -35.94 m<sup>3</sup> per tide. These calculations were in no way designed to be an accurate reflection of the state of the foreshore at any one time. While more traditional coastal studies have attempted to classify beach states into 'storm/swell' or 'summer/winter' profiles, the capriciousness of the

wave climate experienced on the British coast clouds such simplifications. Periods of cut and fill can be experienced on British beaches during almost any season, exemplified by the severe storm conditions which produced some of the lowest beach volumes recorded at Culbin during July 1991. This further supports the contention that the seasonal divide in beach profile should be replaced by a process based differentiation (Komar, 1976). Additionally, the detailed response of the beach face is generally not one of net accretion across the entire profile width. Rather, the flattening of the profile during storm conditions is reversed by the onshore migration of longshore bar features (Zenkovitch, 1967; Sonu, 1973), which produce accretionary conditions at the seaward edge of the beach profile, and subsequently migrate up-profile, altering the at-a-point response to net 'accretionary' conditions. Thus the values of mean elevation per tide are included simply to demonstrate the order-of-magnitude at which the beach could react under ideal conditions.

Calculation of the volumetric extension of Buckie Loch spit was important both to provide a calibration of the longshore rates of sediment transport, and as an important element in the sediment budget of cell B1. The volumetric extension of Buckie Loch spit at  $13\ 817.4\ \text{m}^3\ \text{a}^{-1}$  accounts for 41% of the potential longshore sediment transported in cell B1, and as an order-of-magnitude control on the potential longshore sediment transport rate was seen as adequate. As the potential sediment transport in this cell exceeded the actual input from updrift and from cliff erosion by  $731\ \text{m}^3$ , then to provide a continuous supply of sediment to fuel distal extension of the spit, onshore sediment transport equal to this volume into cell B1 had to be invoked.

#### **5.2.3.6 Comparisons with published sediment budgets**

The calculation of a sand sediment budget for the Culbin foreshore was undertaken using two data sources: potential sediment transport using wave refraction modelling, and an actual sediment budget measured between 03/91 & 02/92.

The modelled sediment budget demonstrates a positive budget for cell B2, attaining  $+14\ 080.0\ \text{m}^3\ \text{a}^{-1}$ . Field measurements suggested the opposite, with a strongly negative sediment budget ( $-12\ 156.2\ \text{m}^3\ \text{a}^{-1}$ ) calculated. The opposite situation was recorded in cell B1, where a modelled negative sediment budget of  $-730.9\ \text{m}^3\ \text{a}^{-1}$  and a measured positive sediment budget of  $+35\ 893.5\ \text{m}^3\ \text{a}^{-1}$  were found. A further check on the beach sediment budgets was provided using the calculated extension rates of The Bar and Buckie Loch spit.

Modelled beach sediment budgets give an impression of the overall status of the beach, based on average conditions derived from summarized wave records. These show that, along the Culbin foreshore, for a sediment budget to balance, the rate of potential longshore transport in cell B2 is less than that in B1, requiring an onshore component in B1 to account for the difference given the low sediment inputs from dune cliffing along this cell. In cell B2, however, the higher rates and volumes input from dune cliffing, coupled with supply from updrift, means that the modelled sediment budget in this cell is positive, requiring offshore losses to balance the sediment budget in this case.

Over the period 03/91-02/92, however, field measurements demonstrated that cell B2 displayed a positive sediment budget, with net accretion occurring, while cell B1 displayed a negative budget. This data, while demonstrating that the modelled sediment budget was of the correct order-of-magnitude, represents a measurement period selected on the intensity of sampling alone. Section 4.2.2 demonstrated the variability inherent in the status of British beach profiles due to the predominant storm wave environment of the North Sea (Davies, 1980). Thus while over this particular measurement period the actual sediment budgets were positive in cell B1 and negative in cell B2, the reverse could occur in the medium-long term. Indeed, in this respect the modelled sediment budget possibly provides a better indication of the likely development of the beach at Culbin, with the results based on average environmental conditions rather than relying on the possibility of low frequency, high magnitude events interfering with the start and end points of the measured budget. As reported by Everts (1973), the gross rate of sediment transport on the foreshore may be much greater than the net transport rate. Thus beach profile data gives an impression of the absolute range of the sediment budget, while a potential beach sediment budget will provide a more realistic impression of the medium term changes in the foreshore sedimentary environment.

The positive beach sediment budget in cell B2 is driven by heavy erosion of the backing dune cliffs and inputs from erosion in Burghead Bay, but with a lower potential longshore transport output capacity than B1. The negative beach sediment budget in cell B1 is driven by low inputs from dune cliffing, plus a large (41%) volumetric requirement to fuel the distal extension of Buckie Loch spit. Heavy erosion at B2 is caused by predominantly convergent wave orthogonals, increasing the incident wave energy (POZ) along this stretch of the coast. B1 experiences mainly parallel or divergent wave orthogonals (Table 4.21), with lower POZ values and consequently lower rates of dune cliff erosion. Lower

dunes along B1, coupled with a high sedimentary requirement to fuel distal extension of Buckie Loch spit and a higher potential longshore transport rate thus produces the negative sediment budget experienced along this stretch of coast.

Comparison of the values obtained from the Culbin foreshore with other published sediment budgets demonstrates that the values obtained are of a similar order-of-magnitude, despite differences in process environments. Davidson-Arnott & Amin (1983) calculated an annual sediment budget on the shoreline of Lake Ontario (Canada) of  $2.5 \times 10^4 \text{ m}^3 \text{ a}^{-1}$ , a lower value than that recorded at Culbin. This was however a function of the lower relative wave heights experienced on the lake shoreline coupled with ice cover for part of the year, reducing the actual time available for wave activity to affect the shoreline. Davidson-Arnott & Pollard (1980) retained the separate elements of an earlier sediment budget for the southern shore of Lake Ontario, mainly due to the fragmentation of their sample coastline in Nottasawaga Bay (Canadian Great Lakes) into a series of smaller bays. Thus despite a similar methodology, results were retained in  $\text{J m s}^{-1}$  and not converted to potential sediment transport rates. Allen (1981) recorded  $4.6 \times 10^5 \text{ m}^3 \text{ a}^{-1}$  transported from a sample section at Sandy Hook Spit in New Jersey, USA, although of this total he attributed enhanced wave heights due to wave refraction as accounting for up to  $1.0 \times 10^5 \text{ m}^3 \text{ a}^{-1}$  of this total. The summary values provided by Clayton (1980) from sediment transport studies at a range of sites demonstrated that potential longshore transport could attain values of up to  $750 \times 10^3 \text{ m}^3 \text{ a}^{-1}$ , a considerably higher value than was achieved at Culbin. The only British example cited by Clayton (1980) was from East Anglia, where values of  $400 \times 10^3 \text{ m}^3 \text{ a}^{-1}$  were reported. However, values as low as  $12 \times 10^3 \text{ m}^3 \text{ a}^{-1}$  were reported from Galveston Island, Texas (Clayton, 1980). Vincent (1979) reported between  $0.41$  &  $3.65 \times 10^5 \text{ m}^3 \text{ a}^{-1}$  of sediment transport for different cells around the East Anglian coast, based on a 13 year mean annual transport rates using refracted waves hindcast from wind data. Mason (1985) reported potential transport rates along the Holderness coast (Humberside) of  $0.33 \times 10^5 \text{ m}^3 \text{ a}^{-1}$ . From these latter studies, both conducted on North Sea coasts, it is suggested that the values calculated from Culbin are of the correct order-of-magnitude.

### 5.2.3.7 Shingle sediment budget: The Bar

Zenkovitch (1967) and Kirk (1980) both recognized that the transport rates of sand and shingle in the nearshore zone will differ significantly. It was thus necessary to calculate a separate shingle sediment budget in order to quantify the volume of shingle mobile in the nearshore zone in the Culbin area, and also to provide a modern analogue against which the supply and accumulation of shingle throughout the Holocene could be compared at an experimental level.

Quantification of the amount of *shingle* deposited in the current Culbin shingle system depends on the identification of the spatial limits of the shingle in the field. Identification of the longshore limit of the Culbin shingle was undertaken using the existing modern analogue of the present Culbin beach and The Bar. Investigation of the geomorphology of this landform revealed a possible mode of formation of the Culbin shingle sequence. While the shingle element of the landform is that which is of concern to this study, the contemporary beach at Culbin is composed mainly of sand, with only a minor proportion of shingle found as a low storm ridge on the Buckie Loch spit. However downdrift at the distal end of The Bar a significant proportion of shingle can be found, again with a large quantity of sand found updrift in the central and eastern sections of The Bar. The shingle "head" of the system, while naturally highly mobile under most wave conditions, is severely limited in its actual rate of migration. On account of its topographic position as a storm ridge deposit, it is only active under a combination of high tides and/or storm wave activity. The sand "tail", while naturally less mobile, is however active under the majority of wave conditions, and hence does not become completely divorced from the shingle body.

### 5.2.3.8 Inputs

Proximal erosion of relict shingle ridges presently forms the largest supply of shingle to the distal section of The Bar. Erosion currently centred at the eastern end of the shingle strandplain produced a volume of  $7540 \text{ m}^3 \text{ a}^{-1}$  between 1976 and 1989 based upon volumetric measurements converted from linear extension rates using aerial photographs taken in 1976 and 1989.

The volume of shingle derived from Burghead Bay depended heavily on the measured rate of recession around Burghead Bay. The erosion rate of  $1 \text{ m a}^{-1}$  was derived from Ross (1992), and is supported by measurements from aerial

photographs between 1976 and 1989. This produced a total shingle release rate of 3150 m<sup>3</sup> a<sup>-1</sup>.

The review of available literature demonstrated the difficulties involved in the calculation of bed load transport. The calculations used in this study used two values as a possible upper and lower limit on the amount of total sediment transported as bedload, 5% as proposed by Al-Ansari & McManus (1979), and 10% from Reid & McManus (1987). As the larger of these two values represents an extreme upper limit, the lower value (5%) was used in the calculation of a volume of shingle in order to avoid overestimation of the volume of shingle transported to the nearshore zone by the Findhorn, particularly given the morphological evidence suggesting that the majority of the shingle load is deposited prior to the river entering Findhorn Bay (Plate 10). This produced a potential input of shingle of 520 m<sup>3</sup> a<sup>-1</sup>.

### 5.2.3.9 Outputs

The primary outputs from the shingle system are from loss to the distal section of The Bar, and to the offshore zone. Clearly, as quantification of only distal extension can be made, the balance in the shingle budget is provided by on-offshore transport. In this case, distal extension amounts to 1377.9 m<sup>3</sup> a<sup>-1</sup>, only 12.3% of the total input value.

### 5.2.3.10 Shingle sediment budget

Input	Volume (m <sup>3</sup> )	Output	Volume (m <sup>3</sup> )	Balance
Proximal erosion	7540.2	Distal extension	1377.9	
River Findhorn	520			
Burghead Bay	3150			
<b>TOTAL IN</b>	<b>11 210.2</b>	<b>TOTAL OUT</b>	<b>1377.9</b>	<b>+9832.3</b>

Table 5.4 Summary of the inputs and outputs to the shingle sediment budget:  
The Bar

Table 5.4 shows the inputs and outputs to the shingle sediment budget. The budget is strongly positive, primarily due to the magnitude of the input from proximal erosion. This element alone could account for the measured volumetric extension of The Bar. Given the depleted state of the single shingle ridge east of the main erosional bight on The Bar, it appears that shingle from Burghead Bay and the small amount from the Findhorn are not reaching The Bar, and as such the primary source of shingle is supplied by erosion of the proximal shingle ridges. This suggests that The Bar is reworking itself, "self-cannibalizing" from the proximal ridges to fuel distal extension. The release of shingle exceeds the volume required to maintain distal extension, and thus offshore loss is suggested to account for the majority of the shingle removed from this section, being transported west onto Whiteness Head.

#### **5.2.3.11 Summary of contemporary processes**

Tidal currents in the middle Moray Firth were found to be very weak, and in combination with generally fine sediments flooring the Firth, are capable of entraining little sediment. Waves form the primary energy source to the middle Firth, entering via a limited "energy window" from the N-NE-E sectors due to the confining nature of the Moray Firth. Modal wave heights are 1 m, with 4 s periodicity. However, the one in ten year wave in the middle Firth may attain *ca.* 9 m height (Conoco, pers. comm). The incidence of swell waves from the NE sector drives longshore currents along the beaches of the middle Firth, creating a net westerly drift of sediment towards the inner Firth. This has led to the development of strongly drift aligned landforms in the vicinity of Culbin, such as the Bar and Buckie Loch spit.

Foreshore sediments in the middle Firth are primarily sandy, although locally shingle is important, for example on the distal flank of The Bar. Differential transport of sand and shingle makes the calculation of a single beach sediment budget unrealistic, and thus two budgets are required to quantify the amounts of sediment mobile in the nearshore zone. Calculation of a sand budget from the Culbin foreshore demonstrates a *modelled* positive potential sediment budget of +13 349.1 m<sup>3</sup> a<sup>-1</sup>, and an *actual* positive beach sediment budget of +23 737.3 m<sup>3</sup> a<sup>-1</sup>. A shingle sediment budget calculated on The Bar also suggests a positive sediment budget of +9832 m<sup>3</sup> a<sup>-1</sup>, fuelled primarily through proximal erosion and reworking of existing relict shingle.

### 5.3 LINKAGES BETWEEN HOLOCENE AND CONTEMPORARY PROCESSES

Erosion now forms one of the most striking features of the Culbin foreland, particularly along the high dunes of the eastern foreshore. Measured rates of erosion have produced a mean value of  $1.24 \text{ m a}^{-1}$  over the period 1990-1992, contrasting with the mean value of  $0.6 \text{ m a}^{-1}$  reported by Ritchie *et al.* (1978) and the derived value of  $1.94 \text{ m a}^{-1}$  from recording by Ross (1992). Examination of the wind and wave records over the study period suggested that conditions were only slightly less energetic than a 10 year average of conditions.

The Holocene development of the Culbin foreland has been characterized by accretion of shingle storm beaches since at least the Holocene sea level maximum, and possibly earlier (section 2.6.5). Under a falling RSL since ca. 6500 BP this has led to the abandonment of these ridges at elevations up to 11 m OD, up to 3 km inland, and their subsequent inundation by a large dune complex. Since the construction of the the May map of 1758, considered to be the earliest reliable map of the area, it has been clear that the Culbin foreland has been experiencing change, firstly through the westerly migration of The Bar, and subsequently through direct frontal erosion of the dune cliffs along the eastern flank.

It also appears that over the Holocene the Culbin foreshore has changed the nature of its sedimentary and morphological state, from one of a coarse, clastic dominated foreshore displaying a high reflectivity index and net accretion under a strongly positive sediment budget, to a sand dominated foreshore displaying a dissipative regime, backed by sand dune cliffs, migrating landwards under a balanced or slightly negative sediment budget.

Two sediment budgets were constructed to represent the sedimentary conditions experienced along both the Culbin foreshore and The Bar presently. A sand budget revealed potential longshore transport volumes of the order of  $3.0 \times 10^4 \text{ m}^3 \text{ a}^{-1}$ , while a shingle budget derived from the distal extension rates at The Bar revealed volumetric extension of  $1377.9 \text{ m}^3 \text{ a}^{-1}$ .

The continued evolution of drift-aligned landforms such as Buckie Loch Spit and The Bar suggests that processes which have been active over the recent historical period are continuing presently. Similarly the evidence from the raised shingle ridge sequence in Culbin Forest suggests that such processes have

been a feature of the evolution of the foreland since at least the Holocene sea level maximum, while the palaeosediment budget calculations suggest that westerly drift of sediment has been occurring since at least the end of the Loch Lomond Stadial. As such, the change in the nature of foreshore sedimentation along the Culbin foreland may reflect a change in the sedimentary regime rather than in the process regime in spite of changes in RSL over the Holocene.

The primary source of sediment to the Culbin foreshore is currently derived from erosion of the backing dune system, with the River Findhorn and the cliffs in Burghead Bay providing only a secondary source of material. It is clear from field investigation that the majority of coarse sediment in transit along the Findhorn is no longer reaching the coast. Instead, the rapid decline in gradient experienced at the head of the Findhorn estuary encourages upstream deposition in the lower reaches of the river, rather than delivering the sediment to the coast (Plate 10). This produces a largely sand dominated sediment load to reach the coast, with shingle only appearing in quantity after high river discharge events. Limited evidence from the immediate offshore zone suggests that shingle is present at the mouth of the Findhorn, but the presence of seaweed and algal growth over the individual clasts demonstrates that movement is infrequent. The delivery of shingle from erosion of the cliffs in Burghead Bay was calculated to be  $3150 \text{ m}^3 \text{ a}^{-1}$ . The delivery of shingle from the dune cliffs backing the Culbin foreland was clearly zero.

Thus the sedimentary regime along the Culbin foreland has changed in character from a former environment where the supplies of shingle were from both the Findhorn, and from shingle in Burghead Bay ultimately derived from Spey Bay, to one where sand has replaced shingle as the primary sediment source, and supplies from the Findhorn have been superseded in importance by supplies from the erosion of the backing dune cliffs. Sediment is also derived from erosion in Burghead Bay, of which *ca.* 20% is shingle. On The Bar, the sediment budget demonstrates that the feature is currently reworking itself. While a low volume ( $3670 \text{ m}^3 \text{ a}^{-1}$ ) is still being potentially delivered from updrift, the volumetric rate of distal extension can be accounted for by the erosion of the proximal shingle ridges alone.

### **5.3.1 Synthesis of Holocene and contemporary coastal studies: the application of the coastal sediment budget at Culbin**

The coastal sediment budget has been used widely in the field of contemporary coastal study as a tool in understanding the nature of beach changes, but it has

not generally been applied in a quantitative manner to the study of Holocene coastal development. This section aims to demonstrate the links between the sediment budget and coastal development over both the Holocene and the present period.

The calculation of a palaeosediment budget for the sector of the southern Moray Firth between Culbin and Spey Bay was designed to provide a synoptic view of the delivery of sediment to the coastal zone, explaining the sources, transport pathways and sinks *en route* to better understand the evolution of the Culbin foreland. An integral part of the sediment budget for Culbin has been, and indeed remains, the longshore supply of sediment. During the Holocene, periods of low RSL have facilitated the passage of sediment from neighbouring Spey Bay, while under high sea stands this passage has been severed. Volumetric calculations made at Culbin clearly demonstrate that the volume of sediment from the Findhorn alone would have been insufficient to supply the shingle necessary for its formation, and thus an updrift source of sediment had to be invoked.

Thus the Holocene development of Culbin has been dependent on the supply of sediment, which in turn has been demonstrated to be at least partly controlled by the status of RSL. The description of these two elements and their impacts on the palaeosediment budget will form the remainder of this chapter.

#### **5.3.1.1 Sediment supply**

The two main rivers supplying sediment to this sector of the southern Moray Firth over the Holocene have been the Spey and the Findhorn. The smaller River Nairn has contributed a relatively small amount of sediment to the coastal zone in relation to these two much larger sources. The dominant westerly drift of sediment along this stretch of the Firth combined with the proximity of the Culbin foreland to the mouth of the Findhorn strongly suggests that the original source of clastic sediment forming the foreland was derived from the Findhorn. However, the presence of shingle ridges in Burghead Bay demonstrates that shingle grade material was being introduced from a source updrift of the Findhorn, and as such might not have represented the exclusive source of material to Culbin during the Holocene.

During the immediate Postglacial period, westwards retreating ice left a marine limit in the Findhorn Bay area at ca. 27 m (Sutherland, 1984). Under such a scenario the palaeogeography of the present Culbin area would have been

significantly different, with the site of the present Culbin foreland submerged, possibly existing as a shallow bay into which the Findhorn was then flowing (Steers, 1937). Rapidly falling RSL following deglaciation would have exposed the inner continental shelf to subaerial depositional processes, with large volumes of sediment delivered from the Spey and Findhorn under higher discharges than experienced at present (Young, 1978; Maizels, 1987). Sediment delivery to this exposed shelf would have been enhanced by the presence of large tracts of un- or partially vegetated surfaces in the upper catchments of the local rivers (Milliman, 1991). With the onset of the rise in RSL towards the Holocene sea level maximum, large quantities of clastic sediment were forced from the exposed inner continental shelf onshore. Additionally the Spey and Findhorn would have continued to deliver sediment to the littoral zone over this period, providing a sediment rich environment in which the accretion of the Culbin foreland could have occurred.

#### **5.3.1.2 Inputs from the Spey and Findhorn**

Identification of the sources of sediment, and the estimation of the amount of sediment introduced to the coastal zone over the Holocene period was required before matching this volume against that contained in the Culbin shingle ridge suite. While it was clear that the Findhorn had formerly played an important role in supplying shingle to Culbin, updrift sources of shingle were also considered to have been important elements in the palaeosediment budget, in particular the sedimentary input from the Spey. A method was thus required to quantify the fluvial input of sediment to the coastal zone.

The method employed has not apparently been employed in British Quaternary studies, but has been used in studies in the US (Renwick, pers. comm.). This involved the reconstruction of the lower terrace sequences of the Spey and the Findhorn, and calculation of the volume reworked from these and input into the coastal zone. Testing the method was undertaken on the Spey, where the extent of the terraces had been mapped by Peacock *et al.*, (1968), before applying it to the Findhorn. The volume calculated from the Findhorn alone was found to be  $2.47 \times 10^7 \text{m}^3$ . Comparing this with the volume of sediment calculated to be present in the Culbin shingle series ( $6.53 \times 10^7 \text{m}^3$ ), it was clear that the volume of sediment introduced from the Findhorn alone could not account for the volume of sediment in the Culbin system, with a shortfall of  $4.06 \times 10^7 \text{m}^3$  of shingle. It was thus clear that an additional source of sediment must have been feeding the Culbin shingle ridge system, with the Spey as the most likely source.

From the reconstruction of the lower Strathspey terrace sequence, the volume of sediment introduced to the coastal zone in Spey Bay was calculated to be  $2.94 \times 10^8 \text{ m}^3$ . However,  $2.24 \times 10^8 \text{ m}^3$ , or 76% of this was calculated to have been lost to the large submarine delta located at the mouth of the Spey (Chesher & Lawson, 1983). A lack of detailed borehole information meant that the estimate of the volume of shingle lost from the longshore system to the delta may have represented an underestimate. The representation of the two distinct shingle units in the delta as identified in BGS borehole 71/15 (Chesher & Lawson, 1983) was made at 8.2 km offshore, and in spite of a thickening sequence noted with distance landwards in other deltaic environments (Davis, 1983), the simple double unit sequence as identified in the borehole was retained for simplicity in the ensuing calculations.

Once the loss to the coastal zone from deposition in the submarine delta had been accounted for, the remaining volume of sediment was free to be transported westwards within Spey Bay. Continuous deposition of shingle storm ridges west of Kingston (NJ 338656) would have depleted the volume of shingle travelling west, as would the creation of the storm ridge sequence presently located between Caysbriggs (NJ 249670) and Lossiemouth (NJ 235701). Using the estimates of surficial area covered by these ridge systems from maps by Steers (1937) and the operational shingle depth of 6 m, their combined volume was calculated to be  $622\,800 \text{ m}^3$ . Thus the volume of shingle from Spey Bay was calculated to be  $6.95 \times 10^7 \text{ m}^3$ . Continued westwards drift was required to account for the passage of shingle from Spey Bay into Burghead Bay, for eventual inclusion in the Culbin sequence. In total, the volume potentially delivered to Culbin, after losses are removed, via both the Findhorn and the Spey amounts to  $9.41 \times 10^7 \text{ m}^3$ .

### **5.3.1.3 The importance of RSL**

At this juncture it is crucial to consider the status of RSL fluctuations during the Holocene. During the immediate Postglacial, RSL was falling, reaching a low of -6 m OD at ca. 8750 BP (Figure 5.2). Delivery of sediment from both the Spey and the Findhorn during this period would have been via alluvial fans and outwash plains to the exposed inner continental shelf, although the dominant westerly trend in shingle transport would have continued. Due to the relatively steeply shelving inner shelf in the vicinity of both Spey and Burghead Bay, this would have produced a zone of net deposition at a maximum of only ca. 1.5 km offshore from the contemporary shoreline. Effective shallowing of the nearshore

zone north of the Covesea Ridge would have been a consequence which would allow the free passage of shingle from Spey Bay through into Burghead Bay. Direct evidence of the longshore passage of shingle along this corridor is demonstrated by the presence along the northern fringe of the Covesea Ridge of raised shingle ridges with no apparent source (eg between Lossiemouth and Covesea Skerries Lighthouse, east of Covesea and at Hopeman [Peacock *et al.*, 1968]) suggesting that shingle was formerly mobile and more extensive in this area than at present.

However, this low sea stand was relatively short lived, and the onset of the Holocene transgression would have created increasing water depths along this section of the coast. The transgression would also have caused net onshore forcing of sediment as wave base was located increasingly further landwards. Examination of the bathymetry of the Covesea Ridge nearshore zone shows a steeply shelving nearshore profile down to a depth of ca. -4 m CD (-6 m OD) (Admiralty, 1986). Shingle is mobile down to depths of 6 m (except when high tidal current speeds are operating), but is immobilized at depths of 9 m and a rise in RSL to +3.9 m OD would create water depths in this vicinity which would not allow the free passage of shingle. Examination of the sea level trends (Figure 5.2) shows that a RSL at this altitude would have been attained ca. 7200 BP. Further examination of the sea level curve shows that RSL remained above this critical altitude until ca. 4300 BP, representing a potential hiatus in sediment delivery from Spey Bay to Burghead Bay of ca. 2900 radiocarbon years. Once RSL fell below the critical altitude of +3.9 m OD, then shingle delivery to Burghead Bay was able to recommence. Geomorphological evidence from the shingle ridges in Burghead Bay suggests that the series of ridges currently located at the eroding seawards edge of the Bay represent the most northerly set of ridges deposited in Burghead Bay. Figure 4.11 demonstrates that these ridges are spatially continuous, with no eroded fragments of ridges located seawards of them. The sea level indicators collected from Burghead Bay were collected from this set of shingle ridges. The dates obtained from these samples all post-date ca. 3170 BP (Table 4.7), which if combined with the geomorphological evidence, suggests that these ridges formed *after* the re-establishment of the link between Spey Bay and Burghead Bay after ca. 4300 BP.

However, the timing of the re-establishment of a potential link between Spey Bay and Burghead Bay poses a problem in the interpretation of the geomorphology of the dated drop in altitude recorded across the shingle ridges of the Culbin foreland (section 4.1.4.3). Dating of this event, using storm ridges as sea level

indicators, suggests that storm ridge sedimentation at Culbin underwent a marked change at this time, with the drop in altitude followed by a greater variation in the spacing and altitude of the ridge crests deposited seawards of the drop. This is interpreted, in the absence of fluctuations in the rate of RSL fall, as evidence of a hiatus or decline in the supply of sediment to Culbin, yet the timing of the re-establishment of potential hydraulic linkage between Spey Bay and Burghead Bay is dated at ca. 4300 BP, representing a minimum lag of 750 years.

Assuming both dates are correct, then to account for this pattern of accretion in Burghead Bay and sediment starvation at Culbin, the supply of sediment from updrift to Culbin must have at this time been reduced through the preferential expansion of the shingle structures in Burghead Bay. Geomorphological evidence and C14 dating suggests that these ridges were accreting at this time, possibly absorbing any sediment passing through from Spey Bay rather than leaking shingle downdrift to supplement the volume arriving at the coast from the Findhorn. As such, with a diminished supply of shingle, accretion on the Culbin foreland became increasingly erratic, with storm ridges R, S, X, Y, Z tending to build higher and in a more irregular manner under lower sediment input, rather than the more regular storm ridge accumulations which are seen landwards of the drop in altitude (sets A, B, C, D, DB).

As RSL continued to fall, the throughput of shingle was once more curtailed as the Covesea Ridge formed a headland, against which shingle simply began to pile rather than by-pass, an effect recognized elsewhere by Carter *et al.* (1987). Once the supply of shingle from the Spey had stopped ca. 7200 BP, and with the offshore zone unlikely to supply sediment to Burghead Bay under a falling RSL, a sediment deficit would have been created in the Bay. The onset of erosion in Burghead Bay then began to resupply sediment to Culbin.

The passage of shingle around the northern side of the Covesea Ridge was thus curtailed by the high RSL experienced during the Holocene sea level maximum. However, rising RSL also led to marine inundation of the low-lying area to the south of the Covesea Ridge, in the vicinity of the former Loch Spynie. The deposits of this area were mapped by Ogilvie (1923), who considered that at the Holocene sea level maximum, the Covesea Ridge itself would have become fragmented, appearing as a series of three islands fronting an "island-studded" marine channel (Figure 5.22) submerged to his 50' level. The highest marine feature in this area was identified by Ogilvie at 85' (28.3 m), which represents the

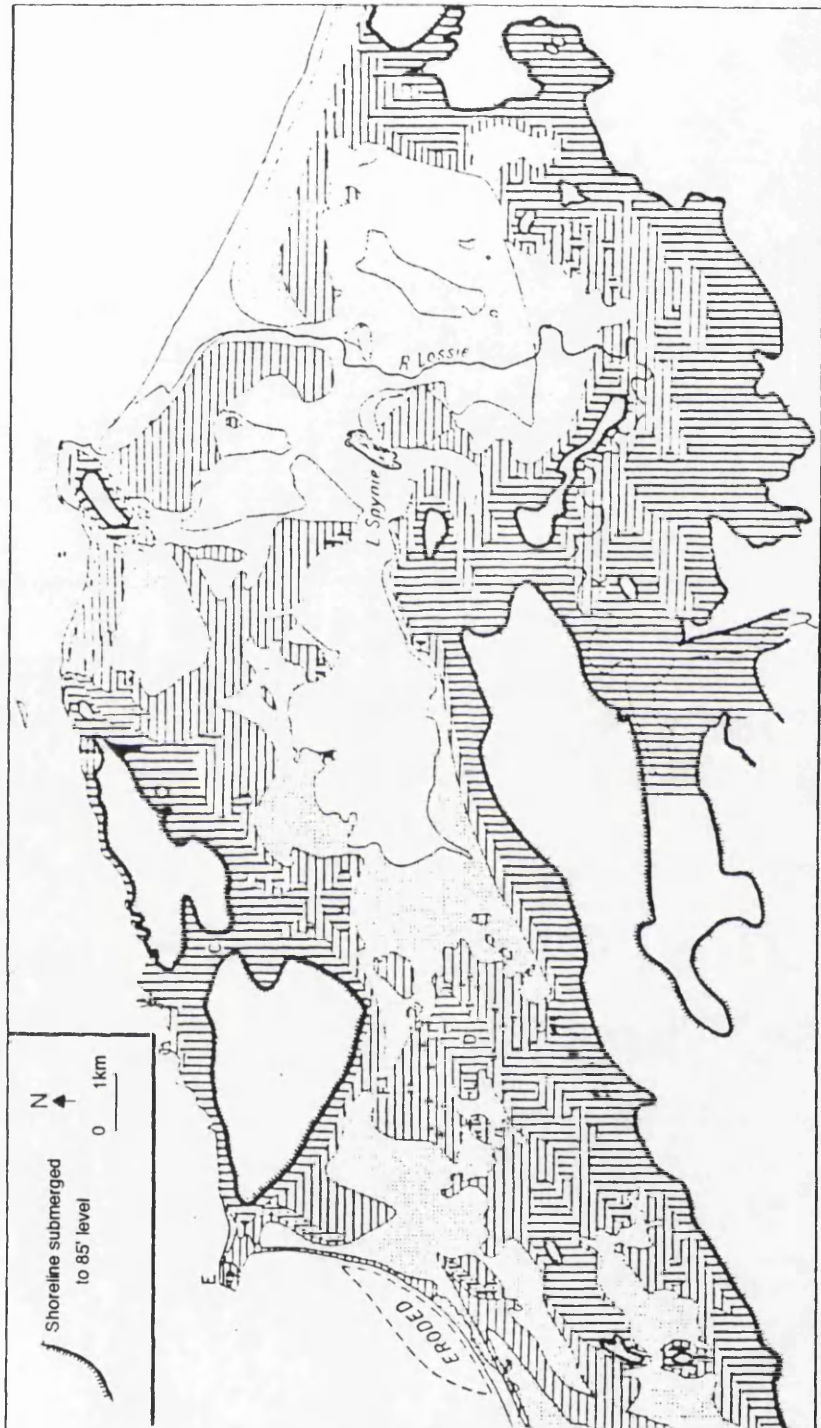


Figure 5.22 The Covesea Ridge and the flooded Spynie channel (source: Ogilvie, 1923)

Late Devensian marine limit in this section of the Moray Firth (Sutherland, 1984), and as such is unrelated to the "submergence chronology" established for the development of the marine channel during the Holocene. Additionally, the features related to Ogilvie's 50' sea level were also likely to be Late Devensian in age, and as such the wide bay shown in Figure 5.22 would have been considerably more restricted during the Holocene sea level maximum.

Of importance to this study is the possibility that the Spynie Channel was of sufficient depth to allow the passage of shingle into Burghead Bay south of the Covesea Ridge. From the alignment of the large shingle barrier between Caysbriggs and Lossiemouth coupled with the volumes of sediment drifting west in Spey Bay, it would appear that such a narrow channel entrance would quickly become choked with shingle, and bypassing to the north would be more likely. Geomorphological evidence from the Spynie Channel area (Ogilvie, 1923; Ross, 1992) suggests that there are no large shingle structures located south of the Covesea Ridge, with exposures limited to the Caysbriggs-Lossiemouth series in the east, and the southerly trending shingle ridge located south of Burghead town to the west of the channel.

Geomorphological evidence thus suggests that there was no passage of shingle from Spey Bay to Burghead Bay via the Spynie Channel. The maintenance of the high land forming Covesea Ridge would have sheltered the channel from incident wave attack, creating low energy conditions under which the deposition of shingle storm ridges and the throughput of shingle to Burghead Bay would be extremely unlikely to occur. Shingle deposition would most likely have occurred in the higher energy environment at the exits to the channel. Shelter provided by the Covesea Ridge would have led to reduced wave activity, creating a low energy, shallow bay into which the Lossie flowed, in a similar situation to that currently found in Findhorn Bay.

Having established that the passage of shingle was likely to be limited to the north of the Covesea Ridge, and was thus temporally discontinuous, the remainder of the palaeosediment budget may now be considered.

#### **5.3.1.4 Volume of sediment present in the Culbin system**

Calculation of the volume of sediment present in the Culbin shingle ridge sequence was undertaken as the first step in the calculation of a palaeosediment budget. The subdivision of the shingle units into three levels of confidence was based upon the available sources of information. The best possible volumetric

calculation was thus made using primary and secondary data sources. While the optimal situation would have involved the measurement of the altitude, crest-crest spacing (wavelength) and length of all of the individual ridge elements, the deep cover of dune sand which accumulated both on ridge crests and in intervening swales after the emplacement of the shingle suite meant that this was operationally impossible. The method employed aimed to provide the most accurate calculation of the volume of shingle present, while stressing the potential errors in the estimate. A further potential error was introduced into the calculation by the detected presence of shingle landwards of the "inner" shingle units. Shingle was frequently detected at depth during coring in the estuarine sediment series (section 4.1.2.1). A volumetric estimate of the amount of shingle represented by simple presence could not be made with accuracy, and thus the calculation probably represents an underestimate of the actual amount present.

The technique used to calculate the volume of shingle present in the Culbin ridge suites was based on a three stage confidence system, reflecting the accuracy of the survey on which the location of the shingle ridges was based. Calculation of the volume included within the highest confidence bracket used a simplified morphological model of the shingle ridges based on field measurements to calculate the volume of shingle in these areas. The lower confidence levels depended on the calculation of a block of shingle to represent the morphology of the ridges, given a lack of ground control through derivation from maps and aerial photographs. The depth of shingle in these calculations was derived from borehole data from below RAF Kinloss, and was assumed to be 6 m. Using this technique, the volume of shingle calculated to be present in the Culbin shingle sequence is  $6.53 \times 10^7 \text{m}^3$ .

#### **5.3.1.5 Palaeosediment budget**

From these calculations it is clear that while the amount of shingle available from the Findhorn alone is only  $2.47 \times 10^7 \text{m}^3$ , an insufficient volume to account for the volume of shingle in the Culbin ridge sequence ( $6.53 \times 10^7 \text{m}^3$ ), if combined with the residual volume available from the Spey ( $6.94 \times 10^7 \text{m}^3$ ) then the formation of the Culbin foreland could easily be explained in a volumetric sense (Figure 5.23). The potential volume of sediment available for construction of the Culbin foreland was  $9.41 \times 10^7 \text{m}^3$ , while the amount of shingle actually deposited in the ridge sequences was only  $6.53 \times 10^7 \text{m}^3$ , leaving a shortfall of  $2.90 \times 10^7 \text{m}^3$ .

This shortfall would have been lost to the Culbin system, taken for the purposes of calculation to be the western end of The Bar. The likely fate of the majority of

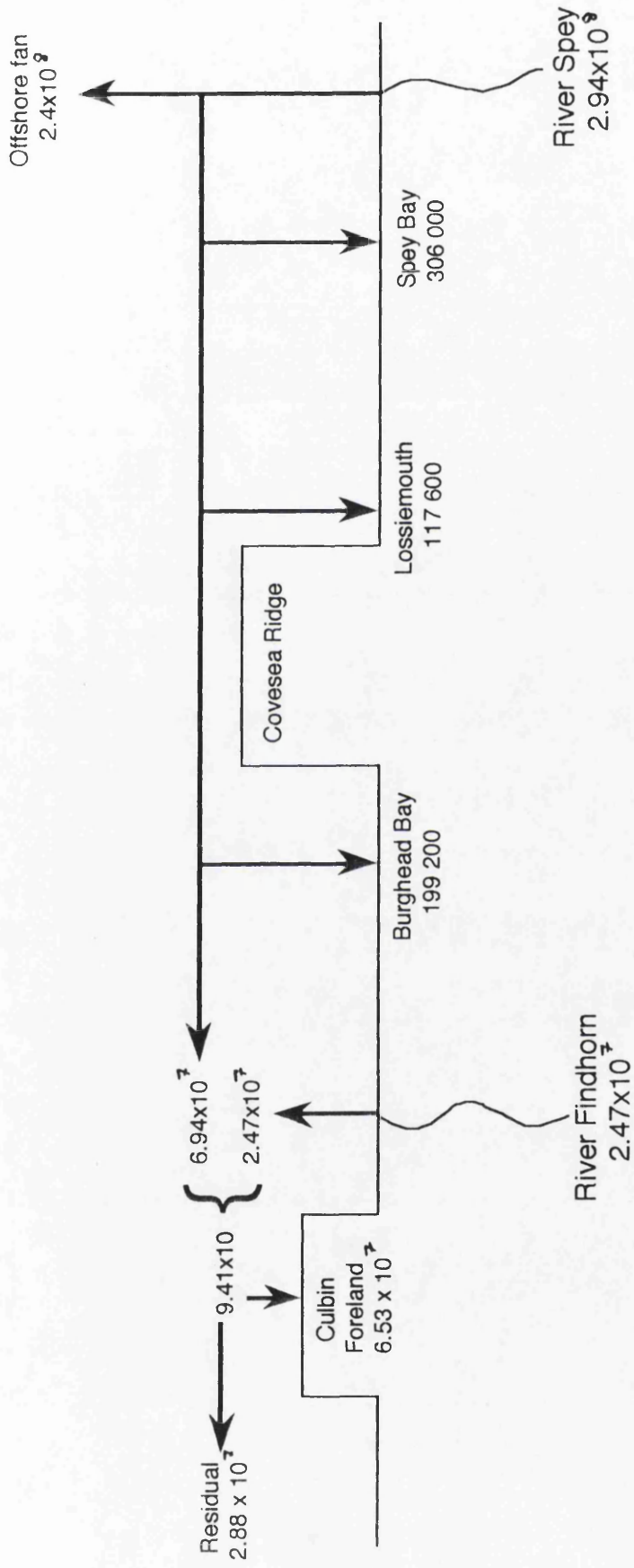


Figure 5.23 Elements of the palaeosediment budget  
(all volumes in m<sup>3</sup>)

this shingle lies in the raised shingle expanse of the Carse of Delnies (NH 830565) and the shingle spit forming Whiteness Head (NH 834573-NH 803588), with deposition also possible in the western zone of Culbin, landwards of The Bar. The small River Nairn was unlikely to have supplied sufficient shingle unaided to have created the relatively large landforms at Carse of Delnies and Whiteness Head, and with a westwards leaking shingle system of the magnitude of Culbin updrift, it would appear that these landforms represented the eventual fate of the majority of the residual shingle from the Findhorn and the Spey.

It is clear that without an understanding of the nature of RSL fluctuations in this area, reconstruction of the sedimentary history of the site would remain problematic. The volumetric calculations clearly display that without invoking an additional supply of shingle from neighbouring Spey Bay, the Culbin foreland could not have evolved to its present extent. Having established the RSL history of the site, and knowing the hydraulic limitations imposed on shingle movement through contemporary studies, the sedimentary history of the Culbin foreland can be more fully interpreted.

Differences exist between the contemporary and palaeosediment budgets produced during this study, although the underlying concept remains the same; the quantification of the specific inputs, storage and outputs of sediment to a coastal unit. The main differences between the two calculations were derived from the scale of the operation, both spatially and temporally, leading to a difference in the stress placed upon each aspect of the calculation. The contemporary sediment budget attempts to quantify the inputs and outputs to a spatially limited section of the coast of the southern Moray Firth, while accepting that the base upon which these changes were calculated (the current beach) would be likely to remain essentially unchanged throughout the duration of the study. In contrast, the palaeosediment budget tended to stress the importance of the magnitude of the inputs and outputs in terms of their potential impact on the base landform (the beach), in order to gauge whether the residual between them was of sufficient magnitude to create the larger scale landform.

Additionally, the timescale over which the calculations were concerned differed by two orders-of-magnitude, between the single year calculation made for the contemporary sediment budget and the effective 10 000 year calculation made for the palaeosediment budget calculation.

However, the calculation of a palaeosediment budget for this section of the southern Moray Firth has been particularly successful, and illustrates the nature

of sediment supply to the Culbin foreland over the Holocene under different stages of RSL. It also demonstrates that the application of a concept from mainstream contemporary coastal studies can be applied to aid reconstruction of the developmental history of the site over a longer time period.

Quantification of the sedimentary inputs to the coastal zone over such a long time period is a field which has not been approached in the general literature, mainly due to the potential order-of-magnitude errors which attend such calculations. The rate of sediment supply to the coastal zone has the potential to vary enormously, both spatially and temporally, and considering the scale over which the calculations are made, the results can be viewed as no more than first order estimates. The success of this exercise demonstrates that without accurate determination and quantification of the potential sediment sources and an appreciation of the RSL history of the area, misinterpretation of the developmental history of landforms can be made. In the case of the Culbin foreland, sited at the mouth of the River Findhorn, it would have been a simple matter to interpret the accretionary sequence which led to the emplacement of the shingle storm ridge assemblage as a function of the supply of sediment from the river and from updrift erosion in Burghead Bay. The production of a sediment budget for this scenario demonstrates that sediment supply from the Findhorn ( $2.47 \times 10^7 \text{m}^3$ ) is insufficient to produce a composite shingle landform the size of Culbin ( $6.53 \times 10^7 \text{m}^3$ ), and hence an additional sediment supply had to be invoked. The largest potential sediment supply in the southern Moray Firth was from lower Strathspey ( $2.94 \times 10^8 \text{m}^3$ ), in comparison to which the lower Findhorn terraces composed only 8.4% by volume. Applying the concept of the sediment budget to this sedimentary scenario, then by subtracting the volume of sediment removed from the nearshore circulatory system through accretion, the remainder would be theoretically available for accretion further downdrift. Once this additional supply of sediment was invoked, the development of the Culbin foreland from this dual sediment supply could proceed.

A criticism of this technique might be that the onshore component of sediment supply has been largely discounted, with the additional supply of sediment required for the construction of the Culbin foreland invoked from an updrift source. However, the timescale over which the calculation was made, initially perceived as problematic in terms of temporal resolution, was actually advantageous in this situation, in that the loss of sediment from the lower terrace series of the two major rivers of the area was dated relative to the adjacent Lateglacial surface. Thus while it was accepted that sediment supply would have

been significant during the glacial maximum, the majority of the sediment supplied to the inner continental shelf would have been emplaced during and immediately preceding the downwasting of Moray Firth ice, while freshly deglaciated surfaces remained unvegetated. This time period was therefore incorporated within the timescale of the terrace reconstruction, and thus the potential offshore sources were already counted within the calculation.

Evidence supporting the supply of shingle from the Spey to the Culbin foreland is provided by Ross (1992 & pers. comm.), who identified igneous clasts derived from the Ardclach and Kinstearry granitic intrusions in Strathspey in both the contemporary foreshore deposits in Burghead Bay, and in the relict shingle ridge sequences on the Culbin foreland. Glacier flow directions from Strathspey are thought to be unlikely to have transported erratics into the Culbin area (Ross, 1992). Thus while the calculation of a sediment budget invokes the Spey as a requisite sediment source for the construction of the Culbin foreland, limited geological evidence also exists to support this theory.

A similar methodology was adopted by Jennings & Smyth (1990), who attempted to match the volume of shingle present in the Crumbles and Dungeness composite landforms with the release of flint clasts from the chalk cliffs of East Sussex in southern England. Their calculations, based on a flint content of 5% in the chalk cliffs, demonstrated that the volume of shingle released to the nearshore zone from cliff erosion at  $0.5 \text{ m a}^{-1}$  exactly matched estimates of the amount of shingle currently in transit along Eastbourne beach. However, in order to have produced the volumes of shingle required to account for the magnitude of both Dungeness and The Crumbles, either a previously higher rate of erosion or an offshore sediment source had to be invoked. The proximity of a branch of the drowned channel system of the English Channel excluded the idea of a formerly higher rate of cliff erosion, leaving an offshore supply as the only possible sediment source for these landforms.

### **5.3.2 Shoreline response to RSL change at Culbin and Burghead Bay**

The discussion so far has established the nature of RSL changes and their impact on the supply of sediment in the middle Moray Firth during the Holocene, and has placed the data into a chronology corroborated by studies from the inner Moray and Dornoch Firths. Interpretations based on the landforms and sediments, together with their relative positions and ages has introduced the concept of a variable response of the shoreline to changes in RSL depending on

the availability of sediment. From this basis, a conceptual model can be developed, describing the development of Culbin over the Holocene period under conditions of variable RSL and rates of sediment supply (Figure 5.9), which can be calibrated using field data (Huggett, 1985).

Ross (1992) describes a possible mode of formation of the shingle sequences of the Culbin foreland and Burghead Bay based on morphological evidence, but with little dating or sedimentological control. Despite this, the basic development sequence outlined by Ross (1992) appears to be broadly in agreement with the data presented here. The sequence has been described through a series of maps, some of which are reproduced in Figure 5.24. These will be used as a template with which the data collected during the course of this investigation will be compared.

### **5.3.2.1 Glacigenic sedimentation >13 000 BP**

Figure 5.3 shows the approximate position of the coastline during the Late Devensian glacial maximum, ca. 18 000 BP (Price, 1983), when eustatic sea level was 100-120 m below present (Fairbanks, 1989; Dawson, 1992). At this stage coastal development would have been completely absent from Culbin, with the area dominated by glacial and glacifluvial deposition (Peacock *et al.*, 1968; Firth, 1984; Sutherland, 1984).

### **5.3.2.2 RSL trends 13 000-8000 BP**

With the decay of Late Devensian ice from the Moray Firth, isostatic rebound, once past the phase of restrained rebound, would have been rapid (Dawson, 1992). The decay of Moray Firth ice was initially accompanied by marine inundation of the freshly deglaciated surfaces (Firth, 1984; 1989a). Continued isostatic uplift at this time outpaced the rate of eustatic sea level rise, producing a fall in RSL following deglaciation. Evidence from the Cromarty Firth showed that this area was ice free ca. 13 500 BP (Peacock *et al.*, 1980). Falling RSL during the immediate Postglacial period is supported by a staircase series of raised foreshore deposits, found intermittently along the southern coast of the Moray Firth between Cothill and the Beaully Firth, and located between 12 and 25 m in the Culbin area (Firth, 1984; 1989). The upper feature represents the Lateglacial marine limit in this section of the southern Moray Firth (Price, 1983; Sutherland, 1984). It is tentatively suggested that the abandoned cliffline, located below these features but above Holocene deposits to seaward was cut during a period of slower falling RSL or even a minor stillstand event at this time.

RSL continued to fall, reaching a low stand of ca. -6 m OD at 8748 BP (section 2.6.5). C14 dates from the peat surface in Burghead Bay tentatively support a falling RSL at this time.

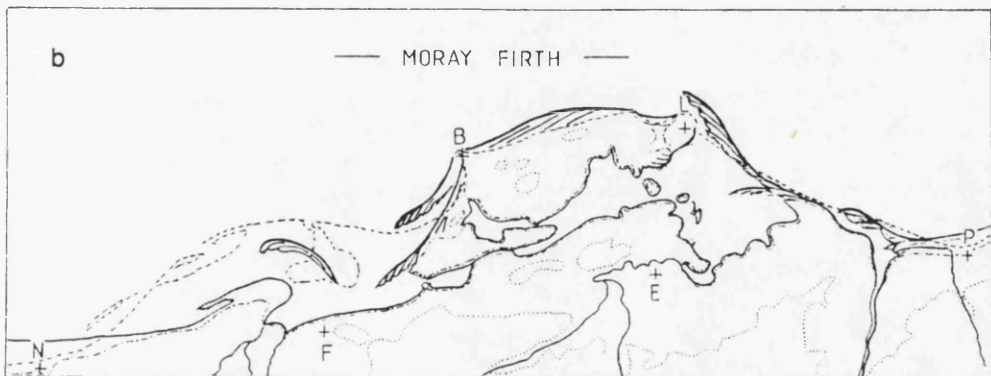
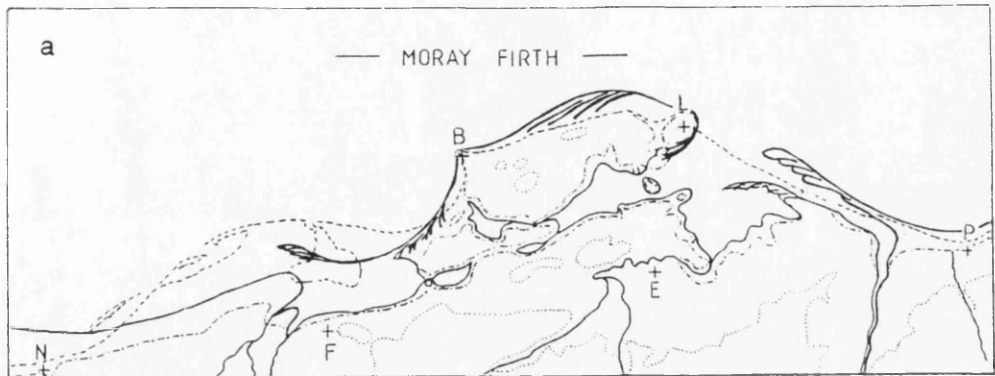
Ross (1992) sees this as the period when the intertidal peat developed in Burghead Bay. His interpretation does not allow for the peat unit to extend below LWST, and as such the interpretation depends on the minimum altitude of the peat to be at -1.75m OD. The radiocarbon date obtained from the intertidal peat in Burghead Bay of 9105±45 BP (SRR 4677) demonstrates that the peat is substantially older than the date assigned by Ross (1992), whose interpretation, with reference to the sea level diagram (Figure 5.2), would date the peat to ca. 7000 BP. Additionally, the relationship between the dated intertidal peat and the surrounding deposits and the relationships between this and other dated sea level indicators from around the Moray Firth discussed earlier suggest that the peat developed during conditions of falling RSL rather than under rising RSL towards the Holocene sea level maximum, as envisaged by Ross (1992).

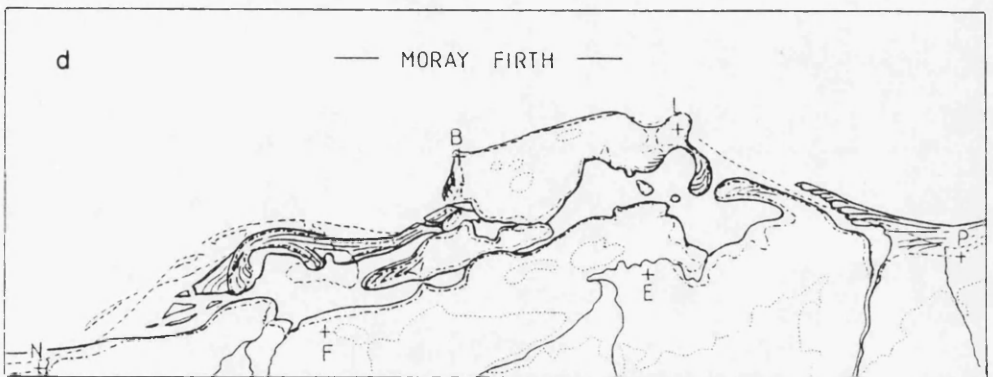
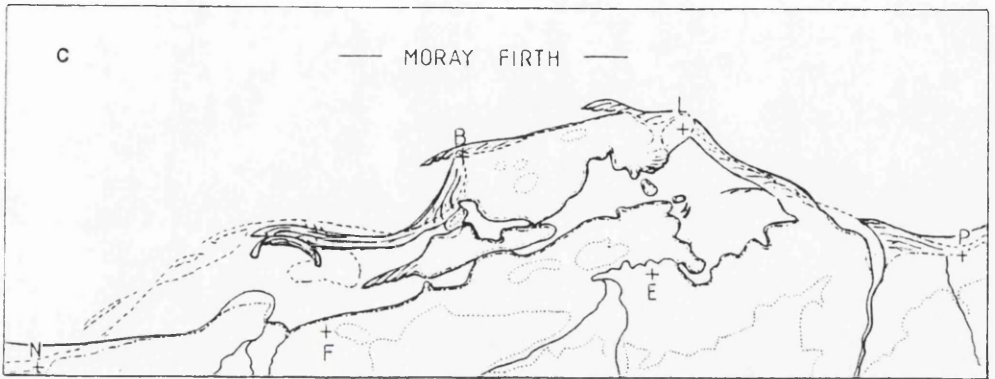
At this stage in the development sequence (Figure 5.9, Phase 1), water depths along the northern flank of the Covesea Ridge would be sufficiently shallow to allow the passage of shingle (section 3.3.3). The conditions would therefore be ideal for the initiation of shingle barriers at Lossiemouth and in Burghead Bay, with an abundant sediment supply from the westwards drifting shingle from the Spey. However, the exact magnitude of the barrier system in Burghead Bay at this time remains unknown. The westward extension of the bar from Burghead across the present location of Culbin may have been invoked to provide a westwards draining estuarine environment at the former mouth of the Findhorn. While borehole evidence supported the existence of fine grained materials in the vicinity of RAF Kinloss on the east side of Findhorn Bay, no evidence was forthcoming to suggest that the bar system extended this far west at this time to provide sheltered conditions under which low energy sedimentation could take place at the present location of Culbin.

### **5.3.2.3 RSL trends 8000-6500 BP**

Figure 5.24a shows the situation with RSL rising during the early part of the rise to the Holocene sea level maximum. The early part of this stage still coincides with Phase 1 of the RSL/sediment model, with water depths still sufficiently shallow around the northern margin of the Covesea Ridge to allow shingle from the Spey to enter Burghead Bay. However, once RSL exceeds +3.9 m OD, the sequence enters Phase 2 (Figure 5.9), with sediment supply curtailed by the

Figure 5.24 Stages in the development of Culbin and Burghead Bay (source: Ross, 1992)





exceedance of the operational depth around the Covesea ridge. Ross (1992) placed RSL at this time at +2 m OD, and Figure 5.2 demonstrates that this period occurred *ca.* 7500 BP. At this stage Ross (1992) allows the first of the Culbin shingle to become emplaced, represented in this scheme by the set of ridges on the western side of Findhorn Bay. However, three important lines of evidence need to be considered here:

- i) the altitude of the shingle ridges;
- ii) the onshore forcing of shingle deposited by the Findhorn under a lower RSL;
- iii) the continuing delivery of shingle to the coastal zone by the Findhorn throughout the period of development.

The first point is addressed by the morphological evidence from the field, which suggests that the emplacement of the particular shingle ridges on the western flank of the present Findhorn Bay at this stage may be too early. These ridges (set T) are located at *ca.* 10 m OD. Applying the shingle ridge altitude correction factor, the timing of their emplacement coincides with a MSL of 6.8 m OD, dated to either 7000 or 6000 BP, either side of the Holocene sea level maximum. At this stage of the transgression it is unclear whether the shingle ridges were deposited before or after the peak of the Holocene sea level maximum. Shingle would have been forced onshore and reworked under rising RSL, and preservation of the landforms from the peak of the sea level maximum would be dependent on their altitude and the frequency of storms at this time to rework them. Whichever is the case, these ridges are not those found today as set T. This point is discussed further below.

The second point is problematic in the development history of Culbin. It is presumed that during the fall in RSL, the area fronting the raised cliffline would have been a wide, shallow bay. With the delivery of shingle from the Findhorn possibly at its highest level during the immediate Postglacial, coarse sediment would have been deposited along the advancing seaward edge as RSL previously fell to the Postglacial low level of *ca.* -6 m OD *ca.* 8750 BP (Peacock *et al.*, 1980). Again, under a rising RSL the shoreface deposits in this bay would have been reworked, creating potentially large shingle units located to the north of the cliffline. However, the mode of deposition would have played a crucial role in determining whether the deposits were emplaced as offshore barrier units or as sequential shingle beaches attached to the mainland. If the former were the

case, then it might be expected that the sedimentary units landward of these and underlying the majority of the Culbin shingle sequences would be fine grained, estuarine units. If, however, the shingle beaches were attached to the mainland, then the units would be more likely to be shingle. Whichever is true, the deposits will now be buried, and investigation awaits detailed subsurface investigation at Culbin.

The final point is that with the high rates of shingle delivery to the coastal zone envisaged during this period, the emplacement of shingle units at depth in the vicinity of the present Culbin foreland would be more extensive than those which appear in Figures 5.24a & b. Again, until definitive borehole studies are made in this area, this point will remain academic.

Figure 5.24b shows the situation as RSL was rising towards the Holocene sea level maximum. A southerly developing series of shingle ridges in Burghead Bay appears to fit with the geomorphological evidence from this area. Whether the southern set of ridges was actually linked to the unusual shingle remnant formation on the western side of Findhorn Bay as shown by Ross (1992) is questionable. The features will be located at different heights to those at Culbin due to their completely different orientation, affecting the degree of exposure to storm waves, and as such may bear little altitudinal relationship in the field. Under the envisaged scenario it would be extremely unlikely that the shingle remnant on the western side of Findhorn Bay would survive as the landform illustrated, if indeed such a feature could exist at all. If the scenario at the peak of the Holocene sea level maximum is extended to include Figure 5.24c, at the Holocene sea level maximum, then the situation becomes considerably clearer. At this point, Ross envisages extension of the Burghead Bay ridge series across the location of the present mouth of the Findhorn, with sediment from the river forced westwards between the raised cliffline and the shingle ridge sequence to seaward. The westward extending series of ridges from Burghead Bay is seen as the precursor to the main area of shingle ridges on the Culbin foreland, joining the existing shingle remnant on the western side of Findhorn Bay to create the majority of the shingle ridges as found on the Culbin foreland currently.

Figure 5.24c shows the envisaged status of the Culbin coast as RSL was at the Holocene sea level maximum ca. 6500 BP (Phase 2, Figure 5.9). A major flaw in this section of the development sequence is apparent if the status of shingle movement from the northern passage around the Covesea Ridge is examined.

At the Holocene sea level maximum, RSL in the Culbin area is considered to have re-occupied the raised cliffline, depositing a sand beach and shingle bank at its base. Minimum age dating of these deposits from peat growth on the former surfaces provides dates of ca. 4500 BP on surfaces at altitudes of up to 8.90 m OD at the base of the cliffline, demonstrating that the underlying deposits pre-date this age. Data from the shingle ridge sequences in the central section of Culbin found the maximum altitude of the ridges at ca. 11.0 m OD. The altitudinal correction factor applied to shingle ridges of this altitude provided a convincing overlap, suggesting that the Holocene sea level maximum attained an altitude of ca. 8.5 m OD. At the Holocene sea level maximum, RSL would have exceeded the maximum operational depth for shingle in the nearshore zone around the northern flank of the Covesea Ridge, preventing the passage of shingle from Spey Bay to Burghead Bay (Figure 5.24c). In this respect, the diagram is inaccurate, with a supply of shingle from the north of the Covesea ridge envisaged throughout this period by Ross (1992), which from geomorphological evidence (Steers & Smith, 1956; Kidson *et al.*, 1958; King, 1972) is unlikely to occur without accompanying high tidal current speeds.

Under the conditions experienced during the Holocene sea level maximum, it is more likely that the supply of shingle to Culbin was predominantly supplied by the Findhorn and reworking of deposits in Burghead Bay. From the calculation of the palaeosediment budget, the supply of sediment from the Findhorn at this time was  $2245 \text{ m}^3 \text{ a}^{-1}$ , while a maximum supply of  $3150 \text{ m}^3$  of shingle from erosion in Burghead Bay is also envisaged. Mapping of the shingle ridges in Burghead Bay by Steers (1937) demonstrates no evidence of substantial reworking of shingle ridges (e.g. directional truncations) except in the extreme eastern section of the bay. Little evidence of frontal erosion is apparent along the majority of the length of the fronting shingle ridges. This evidence, coupled with the young (ca. 3000 BP) dates from the eroding ridges fronting the bay presently (Figure 4.11) suggests that erosion in Burghead Bay was then localized, and input only small amounts of shingle into the nearshore zone at this time. From this situation, the question arises as to the efficiency of the fronting shingle ridges in diverting the Findhorn towards the west. Ross (1992) supports the view that the periodic extension of the shingle ridges in Burghead Bay crossed the current position of the mouth of the Findhorn, with the subsequent diversion of the river to the south of the main body of ridges forming the Culbin shingle ridge series. Evidence from the field concerning the linkage of shingle ridges across the current mouth of the Findhorn is weak. The shingle ridges along the eastern side of Findhorn Bay display strongly recurved western ends (Figure 4.11), morphologically similar to

the recurve currently located at the mouth of the river on the contemporary foreshore above LWST. This is suggestive of a body of water existing between the western end of the ridges in Burghead Bay and those of the Culbin series, although it could be argued that the body of water was emplaced after the ridges had been breached, reworking the distal ends of the existing ridge sequence. The ridge series located north of the present airfield display very clear recurves along their length (Figure 4.11). The ridges located further north in the area presently occupied by the back beach car park at Findhorn village also display recurves along their lengths, although these have been truncated by frontal erosion. Additionally, the orientation of the ridges in Burghead Bay in no way match those proposed by Ross (1992), and attempting to link the ridges across Findhorn Bay would produce features with some extremely unlikely angular relationships in their central sections. A final piece of evidence to support the concept that the two shingle ridge populations have evolved separately is provided by the morphology of the shingle ridges of sets R, S & T on the eastern side of Culbin, to which Ross (1992) proposes that the Burghead Bay ridges were linked. The morphology of these ridges is unrelated to any of the other ridge populations in Culbin, with an extremely erratic distribution of wavelengths and altitudes. It is suggested that these ridges developed under conditions of high sedimentary inputs from the Findhorn flowing along their NE flanks, coupled with potential shelter provided by the ridge population located on the eastern side of a proto-Findhorn Bay.

At the Holocene sea level maximum the main shingle ridge series of Culbin would have existed as a barrier bar environment in a similar fashion to that located on The Bar at present. Landwards of the shingle barrier, fine grained deposits were free to be deposited in a wide, shallow estuarine environment dominated by intertidal landforms. These were located in the field as the series of estuarine deposits located landwards of the shingle sequences (sites LAG 1-3). The altitude of these deposits is between 6.56 and 7.40 m OD, suggesting that they were emplaced either immediately before or after the Holocene sea level maximum. However, if the deposits had been emplaced prior to the sea level maximum, they would have been buried by a higher series of deposits, assuming that the eastern flank of the Culbin shingle series remained open to inundation from the Findhorn in the east. The altitudinal relationship between these units and RSL is discussed fully in section 5.1.4.3, with formation occurring *ca.* 5300 BP. The implication of this is that estuarine conditions existed landwards of the north Culbin shingle series after the Holocene sea level maximum, with an effective extension to Findhorn Bay stretching westwards

behind a fronting shingle barrier system, in a situation similar to that currently seen at The Bar. This suggests that the present location of the River Findhorn has been at least semi-permanent, with only minor deflections from its channel west of the current location of Findhorn village.

#### **5.3.2.4 RSL trends 6500-present**

After the Holocene sea level maximum, RSL began a continuous fall through until the present (section 5.1.1). This period overlaps between Phases 2 and 3 of the RSL/sediment supply model, with the early phase prior to *ca.* 4300 BP experiencing lower rates of sediment input than during the onset of Phase 3.

Figure 5.24 d shows the position under falling RSL. No indication was made by Ross (1992) of the height of sea level during this stage. Extension of the now well established Culbin shingle ridge series towards the west and SW was strengthened by the continued passage of shingle from the Burghead Bay ridges west onto the Culbin foreland, while an estuarine environment was maintained south of the Culbin shingle ridges. Under conditions of falling RSL, the re-establishment of the sedimentary link between the Spey and Burghead Bay would have occurred, supporting the theory of a period of substantial westerly extension of the ridges during this period.

#### **5.3.2.5 The former mouth of the River Findhorn**

Once again the problem of ridge linkage across Findhorn Bay is raised at this stage. However, if it is once more assumed that linkages did not exist, then this produces a more acceptable explanation for the situation shown at the distal section of the Culbin shingle ridges (Figure 5.24d). Ross considered that with the closure of the mouth of the Findhorn, westerly diversion would have forced the river mouth to exit south of the distally extending Culbin shingle ridges. Evidence for such a substantial deflection both during and after the Holocene sea level maximum lies in a series of peat-filled depressions at Claymoss (near Kintessack), the former Logie Moss (Snab of Moy), Cloddymoss, Moss of Dyke and close to Cran Loch. Located below a surface elevation of between 5 and 9 m OD, the peat can still be widely located in the field, although it is frequently obscured by subsequent dune development.

The low-lying area underlain by the peat displays a distinct seaward margin defined by the recurved edges of the shingle ridges. This is particularly apparent on the 1947 aerial photographs of the area, although these are now obscured by

forestry and blown sand cover, so that the shingle no longer outcrops along the margin. The shingle landforms to the north may have deflected the Findhorn along the base of the cliffline at this time. As the peat dates from Snab of Moy represent minimum ages, then if the Findhorn did occupy this area, it must have done so prior to the development of the peat. However, the re-instatement of shingle from Spey Bay ca. 4300 BP enhanced volumes of shingle moving west may have blocked the river mouth, creating a diversion along the base of the abandoned cliffline around this time. As the shingle continued to extend west, erosion of the proximal end eventually led to breaching in the vicinity of the present exit. With the channel abandoned and the shingle from the Spey/Burghead Bay now feeding onto the Culbin beaches, rapid westward extension would have led to the formation of the outer shingle ridges of the shingle fan, the ends of which were emplaced across the former exit of the Findhorn near Snab of Moy. The now-falling RSL led to progressive infill of the old course and eventual peat development. Radiocarbon dating of the basal peat from ponds at Snab of Moy suggests that the peat development over the basal shingle ridges began ca. 3900 BP, indicating a minimum date of abandonment after this time.

Alternatively, the low, flat estuarine-like channel could be interpreted as an estuarine sandflat to the rear of a spit or bar, as occurs today landwards of The Bar. In the field, the location of shingle at depths between 4.85 & 6.30 m OD below the pond units at Snab of Moy farm suggests that the shingle ridge series extends to within approximately 100 m of the base of the raised cliffline, while discovery of shingle in a drain immediately north of the raised cliffline suggests that the shingle ridges extend even closer to the cliffline at this point. The sediments from within the pond sediments sampled at Snab of Moy possibly indicate a marginal shallow marine/estuarine environment, which may have partially supported the exit channel theory of Ross (1992). However, the location of these units vertically above the basal shingle means that they are younger, and could be interpreted as back-barrier sediments deposited in the lee of the fronting shingle ridge series. If the pond units represent intertidal units bordering an exit channel in this location, then the presence of the shingle ridges at close proximity to the raised cliffline would not have been expected. A narrow exit channel such as that proposed in this area by Ross (1992) would have scoured a deep channel similar to that presently located at the mouth of the Findhorn, which is currently at least 6 m deep (section 4.2.2.4). The presence of such a channel would lead to abrupt truncation of the shingle ridges in the surrounding vicinity. The evidence from the field does not support such a hypothesis, and this

alternative theory suggests that the mouth of the Findhorn did not substantially alter its position until the recent historical period. Verification of the fluvial or estuarine genesis of this area awaits detailed deep coring and stratigraphic analysis.

With continuing fall in RSL, the development of the lower series of shingle ridges on the Culbin foreland would have occurred as the supply of shingle from the Findhorn was supplemented by shingle from the Spey, heralding the onset of the RSL/sediment model Phase 3 (Figure 5.9), and forming ridge units D, Y, Z, R. Development of these ridges occurred through until the recent historical period, when the rapid accumulation of sand along the northern shoreline of Culbin, coupled with a failing shingle supply due to the impact of the development of a widening Findhorn Bay as RSL fell, altered the sedimentary dynamics of the Culbin foreshore from a predominantly shingle environment to one dominated by sand. Under conditions of falling RSL, the supply of shingle from the offshore zone would theoretically have been enhanced if supplies were still available on the inner continental shelf after the rising RSL towards the Holocene sea level maximum. Examination of the map of offshore sediments at Culbin (Figure 5.21) demonstrates that the supplies of shingle deposited on the inner shelf by the Findhorn are exhausted, and presently only a relatively small shingle rich zone can be located immediately west of the river mouth in *ca.* 2 m of water. This suggests that with the only available supplies of shingle available from the Findhorn and the initiation of erosion in Burghead Bay, sand would have been the most abundant source of sediment to become mobilized in sufficiently large quantities to be responsible for the construction of a fronting barrier across the western section of Culbin.

The major elements of this stage of the model are acceptable, although the breach at the mouth of the Findhorn was thought to have occurred prior to this stage of development. The main problem with such a scenario is the development of the saltmarsh environment west of the Culbin shingle ridges in the absence of sheltering structures: an unlikely scenario for this section of the Moray Firth. As the development of these units pre-dates the development of The Bar (first recognized at a location east of its current position), then an earlier "proto-Bar" is required to provide shelter for these deposits to develop.

Historical maps and records demonstrate the scale of changes which have been experienced along the Culbin foreshore since the sixteenth century. The deposition of the estuarine sediment series in the west of Culbin would have

required the presence of a fronting barrier unit, as argued above. Under conditions of continuing westerly sediment drift, the formation of drift aligned landforms along the Culbin foreshore would have been common. Early references to the development of the Culbin shoreline include the presence of bar forms in the area. The Pont map of 1590 suggests the enclosure of a "lagoon" north of the current position of Loch Loy by a bar-like feature. Although the accuracy of maps of this age must be questioned, the bar appears as a well-marked feature (Figure 5.18). Additionally, the Pont map also shows a large bar feature at the mouth of the Findhorn, upon which is constructed one of the predecessors of the current Findhorn village, of which there have apparently been two. Of particular interest from the Pont map is the lack of any distinguishable landforms landwards of the bar at Loch Loy. Allowing for poor map quality, this still suggests that accretion in the western section of the Culbin foreland may have been ongoing since this time, and that the low lying areas landwards of the Bar saltmarshes may be relatively young.

#### **5.3.2.6 Future development of Culbin**

Having examined the evidence for past changes at Culbin under different scenarios of RSL and sediment supply, it is possible to begin to attempt to assess the likely future evolution of Culbin. In the light of Figure 5.9, it is suggested that Culbin has now entered a phase of development which has previously been unrecorded at the site, viz. stable or rising RSL combined with a failing supply of sediment. Such a scenario would effectively represent a "Phase 4" in Figure 5.9, and as such has implications for the future survival of Culbin.

#### **5.3.2.7 The future of The Bar**

The integrity of The Bar as a single landform is currently threatened by the very processes which have been responsible for its massive distal extension. With a failing supply of sediment from updrift as the spit at Buckie Loch continues to extend, then distal extension of The Bar has been fuelled via the erosion of the proximal shingle ridges deposited over the last two centuries. The large erosional bight in the central section of The Bar (Plate 3) has deepened since surveys in the 19th century, which showed The Bar as an essentially straight feature. The volume removed over the period 1976-1989 has been demonstrated to be of sufficient magnitude alone to account for distal extension recorded over this period (section 4.2.8.3). However, continued removal of the shingle from this section of The Bar has left only a single shingle storm ridge between the narrow foreshore and the saltmarsh. Landward retreat in this

section is occurring via washover processes, with prominent fans at the rear of the storm ridge extending across the saltmarsh surface between NH 944613 and NH 935611. In the wake of this incursion, marsh peats are becoming exposed on the foreshore as the Bar rolls over them and continues to migrate landwards. Breaching of this section of The Bar was observed on spring tides during August 1991. This has continued, and a site visit during April 1993 revealed a scoured breach in the ridge at the same location. The probability of this breach becoming a permanent feature appears high, with little shingle input from the east to replenish the ridge. Should breaching occur, then the survival of The Bar in its present form appears in doubt. Erosion of the central section would lead to the destruction of the central section of saltmarsh to landward. Deepening of this section would create refraction of swell waves through the newly-formed breach rather than maintaining the net westerly drift along The Bar, reducing the capacity for erosion west of the breach. If this occurred, then the supply of shingle to fuel distal extension on the Bar would be reduced, enhancing the self-cannibalizing nature of the western flank of The Bar. The rate of self-cannibalization will begin to accelerate downdrift, leading to the eventual reworking of the entire western flank. Should the western flank survive intact, the present trend in extension would eventually lead to its encroachment on the coast in the vicinity of Nairn. For landfall to occur, the tidal channel at the western end of The Bar would have to close. Widening and deepening of the breach in the central section of The Bar could possibly form an alternative channel for tidal evacuation of the saltmarsh, facilitating the closure of the western channel and allowing the distal end of The Bar to reach the coast. However, Carter *et al.* (1984) suggested that due to the high permeability of shingle storm ridges, it is not common for these features to lose coherence through crest breaching. Thus it remains to be seen whether a continued decline in sediment supply will enhance the breach by reducing the size of the adjacent shingle storm ridge, reducing its permeability and leading to a larger, permanent breach, or whether the permeability of the ridge will enhance its survival.

However, it does appear that the breach will enlarge as sediment supply to the proximal end continues to fall. This will be accompanied by the continued westwards extension of Buckie Loch spit, which will begin to encroach on the tidal channel at the eastern end of The Bar. Measurements of the depth and speed of the tidal race in this channel were not made, but field observations showed that, contrary to the Admiralty chart of the area (Admiralty, 1981), the channel does not dry at LWST, and that tidal currents in the channel are rapid. Continued westwards extension of Buckie Loch spit has produced a submarine

bar which now fronts the eastern flank of The Bar, diverting the tidal channel west. Continued westwards extension of the spit will create conditions whereby the tidal channel will eventually breach the spit. Once this occurs, the Culbin coast will effectively see a new bar spawned from the westerly extension of Buckie Loch spit, in the same manner in which May's "Old Barr" of 1758 apparently formed through the breaching of the Findhorn spit recorded on the Pont map of 1590.

Thus a cycle of coastal evolution on the Culbin coast is envisaged, with the westerly extension of drift aligned landforms under an easterly swell dominated wave environment leading to eventual updrift breaching. This is followed by a period of gradual decay as the supply of sediment from updrift becomes increasingly divorced from the original landform, becoming incorporated into a new feature and beginning the cycle once more. However, in the past this cycle has been driven by conditions of a more abundant supply of sediment under a falling or stable RSL. Future developments will take place under conditions of failing sediment supply in the face of stable or rising RSL, with the primary sources of sediment provided by the erosion of landforms located updrift.

#### **5.3.2.8 The future of the Culbin foreland**

The future of the Culbin foreland poses a different scenario. Continued erosion of the fronting sand dune cliffs appears set to continue, with failing sediment supplies and the possibility of a stable or rising RSL in this area over the next century. However, the dune cliffs are emplaced over shingle storm ridges, the most seawards of which are presently only *ca.* 300 m from MHWS. At a continued rate of recession of between 1.2 & 1.9 m a<sup>-1</sup>, this could lead to the exposure of the shingle basement formed by ridges R, X and Y in 158-250 years time. Should this occur, then the effects on the future development of this stretch of coastline would be profound. Reactivation of the raised shingle ridges would lead to a change in the state of the foreshore. Initial shingle release would be sporadic, leading to the strengthening of the existing shingle storm ridge on the western flank of the foreland along the Buckie Loch spit, although with the present failure of shingle supply and continued downdrift migration (Ross, 1983), the location and status of this feature is now unclear. With increasing exposure, the upper foreshore would become increasingly reflective, increasing the offshore component of wave energy and leading to the scour of sand from along the foreshore. Foreshore steepening would thus occur, coupled with a general

buildup in the height of the reworked fronting shingle ridge as sediment supply from updrift remained low (Carter *et al.*, 1987).

With a refreshed supply of sediment to the foreshore, this material will become incorporated into Buckie Loch spit. The cycling theory of drift aligned landforms in the Culbin area suggests that a new bar will be created by Buckie Loch spit. If this occurs, then with a reactivated shingle supply reaching the foreshore, conditions would exist for the creation of a new Buckie Loch spit, this time formed primarily from shingle.

Such a development scenario will be modified, or at least speeded up, if a rise in eustatic sea level exceeds the rate of isostatic uplift in the middle Moray Firth. Chapter 2 presented the nature of the evidence used in the calculation of eustatic sea level trends, highlighting the point that despite potential errors in measurement (Carter, 1987; Barnett, 1990; NRC, 1990), an *average of mean global sea level trends* suggests eustatic sea level is rising by 1-1.5 mm a<sup>-1</sup> (Pirrazoli, 1990). Pugh (1990) presented values of anticipated RSL rise at Aberdeen, down-isobase from Culbin and the closest port to the Moray Firth with a sufficiently long tide gauge record for meaningful trends to be derived. Tide gauge data from Aberdeen between 1919 & 1982 suggests that RSL has been falling at a rate of 1.29±0.22 mm a<sup>-1</sup> (Woodworth, 1987), but Pugh (1990) suggests that a rise of 0.90 m by 2027 may increase to 0.51 m by 2087.

Analysis of regional trends in data from the inner Moray Firth by Shennan (1989a) provides a linear solution for RSL trends over the last 4750 years, suggesting a fall in RSL of 1.6 mm a<sup>-1</sup> over this period. However, fitting a linear function to a series of data which Shennan (1989a) states as showing an exponential decline is misleading. Fitting a true exponential function to this data would provide a much lower rate of uplift than 1.6 mm a<sup>-1</sup> at the present time.

If eustatic sea level is rising at 1-1.5 mm a<sup>-1</sup>, using Shennan's (1989a) uplift rate of 1.6 mm a<sup>-1</sup> as an upper limit of isostatic uplift would suggest that RSL is approximately stable in the inner Moray Firth at present. Given the location of Culbin down-isobase from the inner Moray Firth, then the evidence strongly suggests that RSL at Culbin must be at least stable, if not beginning to rise. Unfortunately records from the 'A' class tide gauges in the Moray Firth (Buckie & Portgordon, Woodworth, 1987) are not of sufficient length for statistically significant trends to be discerned.

If RSL rises once more, then a possible extension to the three phase model (section 5.1.3) is proposed, with a fourth phase characterized by rising RSL but a low sediment supply. Such a scenario would have implications for the coast of the southern Moray Firth. The widescale erosion of unconsolidated deposits recognized presently would clearly accelerate as wave base is transferred landwards. Such conditions would not significantly alter the development sequence of Culbin outlined earlier, but would accelerate their rate of onset and operation. Similarly the implications for the future of the extensive saltmarshes located landwards of The Bar depend more heavily on both a continued supply of sediment and the existence of The Bar for shelter rather than a rise in RSL in the medium term.

With rising wave base, the potential for offshore losses of sediment will increase, producing a further sink for sediment released from the foreshore. However, given the present scenario of a declining sediment supply and the onset of widescale erosion of unconsolidated deposits in the Culbin area, any rise in RSL can only accelerate the dynamic reworking of the coastline.

## CHAPTER 6 ESTIMATION OF ERRORS

The results presented in Chapter 4 represent the most accurate measurements considered possible using the available data within the limitations of time and field support available. However, measurements are inevitably subject to errors, associated with either measurement inaccuracy/tolerance, or with assumptions associated with the calculation of terms. This chapter presents the results of the calculation of known and assumed error terms associated with each results section, in order to demonstrate the potential magnitude of such terms, and to briefly comment on their likely impact on the results presented.

### 6.1 SURVEYING ERRORS

The measurement of the altitude of various Holocene raised shoreline features around Culbin and Burghead Bay was made from an initial circular traverse made from Findhorn Village to Shellyhead along the foreshore, establishing a TBM at Shellyhead bothies, and returning via a series of raised marine features in Culbin Forest. Closure error on this 7 km transect was 0.227 m over 43 stations, producing a mean error term of  $\pm 0.05$  m per station. Closed traverses from this surveyed network produced errors no greater than  $\pm 0.01$  m per station.

### 6.2 ERRORS IN THE MAGNITUDE OF STRATIGRAPHIC BOUNDARIES

Shennan (1982) identified a series of potential errors which might occur when measuring the altitude of stratigraphic boundaries during his study on the English Fens. These are outlined in Table 6.1, but with a correction made for a lower levelling estimate in this study through the use of a 6" theodolite and EDM rather than the optical level and staff of Shennan (1982).

<b>Factor</b>	<b>Error (m)</b>
Identification of boundary	±0.01
Measurement depth-hand coring	±0.01
Measurement depth-commercial boring	±0.25
Angle of borehole	up to ±0.04
Accuracy benchmark to OD Newlyn	±0.20 (Scotland)
Levelling error	±0.05
<b>Total error (hand samples)</b>	<b>±0.265</b>
<b>Total error (commercial boreholes)</b>	<b>±0.515</b>

Table 6.1 Possible error factors in the measurement of stratigraphic boundaries  
(source: Shennan, 1982)

Since pits were used infrequently in this investigation, the estimated error term for the density of boreholes relative to the sampling area were not calculated and are not presented.

Clearly the records obtained from secondary sources are more likely to contain inaccuracies than those obtained specifically for this study, and as such the stratigraphic boundaries from these sources should be interpreted with care.

### 6.3 SEDIMENT BUDGET CALCULATION

#### 6.3.1 Surveyed sediment budget

With an error factor of 0.005 m included within the surveying stations, then across each surveyed profile the potential cross-sectional error at each station is shown in Table 6.2 using the standardized profile lengths from the volumetric calculations.

Station	SPL (m)	Section length (m)	Error ( $\pm$ )	Volumetric Error (m <sup>3</sup> )
1	200.05	490	0.005	980.2
2	218.36	425	0.005	928.0
3	167.03	460	0.005	768.4
4	96.98	950	0.005	921.3
5	121.40	1200	0.005	1456.8
6	113.20	1000	0.005	1132.0
7	118.58	1675	0.005	1986.2
<b>Total</b>				<b><math>\pm 8172.9</math></b>

Table 6.2 Potential errors resulting from the surveyed sediment budget

The total potential error per survey was thus 8172.9 m<sup>3</sup>. This represents 0.26% of the total calculated maximum beach volume (recorded 03/90), and 0.35% of the minimum beach volume (recorded 12/90).

Such small error terms will not greatly affect the final result of the beach sediment budget calculations, representing a net error over the total beach area of only  $\pm 0.01$  m. This is less than the potential error arising from the assumption inherent in all studies involving beach profiles that the beach surface is smooth between profiling stations. Such irregularities might only be addressed by increasing the density of sampling, but without resorting to micro-scale measurements, this problem remains inherent in the technique.

### 6.3.2 Inputs to the modelled beach sediment budget

#### 6.3.2.1 Dune cliff recession

The assumption of a linear rate of dune cliff recession at Culbin could clearly not be made in the face of highly variable rates of local recession measured at ten stations along the foreshore. The subdivision into these ten units increased the

accuracy of sediment inputs to the beach sediment budget. However, these measurement stations were a mean distance of 616 m apart, and the rates of recession between even these had to be assumed to be linear, which was unlikely to represent the actual situation (Carter & Stone, 1989). While the maximum rate of recession measured from cell B2 was unlikely to occur along the longest dune section (located in cell B1), if such an event did occur it would represent the maximum potential error based upon the field measurements. This would produce a volume of

$$1550 \text{ m} \times 1.5 \times 5.9 \text{ m} = 13\,717.5 \text{ m}^3$$

which would represent 87% of the mean annual volumetric release rate to the Culbin foreshore. Given the morphodynamic regime of cell B1, then such an event is unlikely to occur, but the calculation highlights the potential error involved in using a mean value to quantify the recession of unconsolidated deposits.

#### **6.3.2.2 Inputs from the Findhorn**

The calculation of the potential sediment input to the Culbin foreshore from the Findhorn provided another potential error in the calculation of the modelled sand beach sediment budget. The calculation assumes that the mean recession rate of the backing dune cliffs is representative of the medium term conditions experienced at profile station 1, with a recession rate of  $1.43 \text{ m a}^{-1}$ . If the lower of the measurements (0.35 m) had been used in the calculation, then this would have produced an input into the foreshore of only  $2152 \text{ m}^3$ , which is significantly less than the volume required to maintain the cell in dynamic equilibrium. This meant that the Findhorn would have had to be invoked as a sedimentary input to the sand sediment budget, supplying  $5092.2 \text{ m}^3 \text{ a}^{-1}$  of sand to the foreshore.

In terms of the final beach sediment budget this point remains academic, as the method itself ultimately defines the source of sediment, and the volumetric outcome will remain the same. However, in terms of the sources of sediment to the budget, it does raise the possibility of the Findhorn supplying sediment to the foreshore, rather than discounting it as an offshore loss.

### 6.3.2.3 The choice of a longshore sediment transport term

A second major source of potential error in the calculation of a longshore sediment transport rate stemmed from the conversion factor used when calculating the longshore sediment transport term  $S_L$  from the original calculation of  $P_L$ . The constant used in this study produced the relationship

$$S_L = 0.77 P_L$$

based on Komar & Inman (1970). Alternative values for this constant have been proposed by Allen (1981), who used  $k = 1.77$ , and Vincent (1979) who used  $k = 3.37$ . The choice of  $k = 0.77$  was based on the derivation of the value from field studies on sand beaches with a similar morphology to that at Culbin

## 6.4 PALAEOSEDIMENT BUDGET CALCULATIONS

This section of the study provided volumetrically the largest potential errors. However, such errors are inherent in gross-scale calculations such as these, and as such the potential for large errors must be accepted. Despite this cautionary note, the final results produced volumes which were of similar orders-of-magnitude, and were thus considered successful.

The accuracy of the final result was strongly dependent on two areas;

depth of shingle movement,

areal mapping accuracy.

### 6.4.1 Depth of shingle movement

The operational depth of shingle movement was taken to be 6 m. Field evidence suggests that *contemporary* shingle structures may not be as thick as this, and their depth is based on field observations in the surf zone, a less than ideal situation. Thus one might assume that shingle depths might be lower than 6 m, as was the case on The Bar, where an actual shingle depth of 3.87 m could be measured.

Conversely, empirical studies have demonstrated the movement of shingle in water depths of up to 9 m under the influence of wave orbital motion (Steers & Smith, 1956). In this case the argument might be made for more substantial

shingle depths if the transport of shingle landwards across the entire operational depth were considered.

The compromise between these two extremes was reached and an operational depth of 6 m was used in the volumetric calculations, based on borehole evidence from Burghead Bay. If a depth of only 3.87 m had been used throughout, the final volume of shingle in the Culbin foreland would have amounted to  $3.4 \times 10^7 \text{ m}^3$ , whereas if 9 m had been used, the final volume would have been  $9.7 \times 10^7 \text{ m}^3$ , representing 52% and 149% of the final calculated volume respectively.

In terms of the final interpretation of the developmental history of the Culbin foreland, it makes little difference which of the terms was used. Even using the lowest estimate of the volume of shingle in the foreland, the volume still exceeds that calculated to have been removed from the lower Findhorn terrace series, requiring the invocation of additional sediment supplies from updrift to account for the accumulation of the foreland.

#### **6.4.2 Areal mapping accuracy**

The final calculation of a volume of shingle present in the Culbin foreland was also dependent on the accuracy of the mapping of the areas of shingle. Field measurements were accurate to at least 0.1 m, which far exceeds the tolerance of mapping accuracy imposed from the determination of the extent of shingle from map evidence alone. Using a map at a base scale of 1:17 000, the areas of shingle at confidence levels two and three were measured. Assuming a maximum measurement error of 1 mm (line standard), the maximum ground error at 1:17 000 would be 17 m. The measured area of shingle at confidence levels two and three was  $9\,874\,035 \text{ m}^2$ , which with a 17 m potential error factor produced a maximum areal error of  $190\,254 \text{ m}^2$ . Multiplying by the operational depth of shingle (6 m), this produced a potential volumetric error of  $1\,141\,528 \text{ m}^3$ , or 1.74% of the calculated volume of shingle present in the Culbin foreland.

#### **6.4.3 River terrace reconstruction**

The calculation of a wedge of sediment which represents the volume of sediment removed from the lower river terrace sequence was also a potential source of error in the calculation of a palaeosediment budget. Using the reconstruction of the Spey terraces as a control, the wedge method produced a volume which represented 78.2% of the original volume of sediment in the terraces. Calculation of the equivalent volume from the Findhorn produced a volume of  $1.92 \times 10^7 \text{ m}^3$ ,

which required multiplication up by 100/78, or 128%, to produce an original volume of  $2.47 \times 10^7 \text{ m}^3$  based on the error term produced from the reconstruction of the more accurate Spey terrace sequence. The errors implicit in such a calculation remain unquantified, the technique adopted representing the best method from which to calculate out the potential underestimate involved in the use of the wedge method.

## **6.5 General Critique**

The areas causing most problems over the duration of this thesis were undoubtedly caused by the construction of the palaeosediment budget. The introduction of a new technique into the reconstruction of the Holocene coastal evolution of the Culbin sector of the southern Moray Firth was aimed specifically at the production of an order-of-magnitude calculation of the volumes of sediment available for the construction of the Culbin foreland. Coupled with this calculation was the construction of a three-stage development model of longshore sediment supply to Burghead Bay and Culbin, based upon a critical water depth of 6 m to create a "valve" between Spey Bay and Burghead Bay. This valve opens when local water depths are less than this, and closing at depths greater than this. Justification for the use of this value has been described in Chapter 5, primarily due to its basis in field measurements. While it is accepted that this is a major assumption, upon which the calculations of the sediment volume contained in the Culbin shingle ridge sequence depends, as noted in section 6.4.1, the entire series of input and volumetric calculations are thus relative. This means that even if the value of 6 m is incorrect, the calculations still require the invocation of an additional source of sediment from Spey Bay to account for the coastal genesis of the Culbin foreland.

Thus while the calculations are presented as the best possible given the sources of data available, their resolution allows them to be accepted only at an order-of-magnitude scale. As this work has been largely experimental in its execution, it is important that the results of the palaeosediment budget are treated as first order measurements.

## CHAPTER 7 CONCLUSIONS

### 7.1 GENERAL CONCLUSIONS

The aims of this research were to:

- i) establish a sea level history and developmental history of a previously unrecorded site in NE Scotland;
- ii) examine and assess contemporary coastal processes and landforms, and calculate a sediment budget for the field site;
- iii) attempt to link aims i) and ii) through the medium of a palaeosediment budget, in order to assess former responses of the shoreline to changes in RSL and sediment supply.

By its nature, the work has been experimental. While the individual elements of i) and ii) have their own established sets of literature and methodologies, scant attention has been paid to the potential cross-fertilization of ideas which may, and for the progression of the subject should, arise from attempting to marry elements of both fields. Frequently Quaternary geomorphologists are accused of making sweeping statements without considering detailed evidence, for example from sedimentological and micropalaeontological studies. Conversely, micropalaeontologists are equally guilty of considering site-specific details without due consideration toward the geomorphological representativeness of their findings. Similarly, few Quaternary sea level researchers take full advantage of modern analogues offered by studies of contemporary coastal environments, a problem currently being redressed by their hard rock counterparts (eg Hart & Plint, 1989; Muto & Blum, 1989).

### 7.2 SUMMARY OF FINDINGS

#### 7.2.1 Holocene sea level studies

The reconstruction of a Holocene RSL history for the Culbin area was successful. Thirteen dated sea level indicators were used in the construction of a sea level curve, the trends in which fit with trends identified in the literature from the inner Moray and Dornoch Firths. Additionally, the altitudes of the extensive suite of raised shingle storm ridges in Culbin were also corrected to yield a successful equivalent MSL by the use of modern equivalent ridges on The Bar. Preliminary

evidence from dated indurations within shingle ridges in Burghead Bay demonstrates that the altitude/age relationships suggested by the corrected ridge crest altitudes are broadly correct. Studies on the detailed morphology of the shingle ridges demonstrates a weak but positive link between the standard deviation of wavelength (crest-crest distance) and the standard deviation of altitude. Using standard deviation of wavelength as a surrogate variable for the regularity of sediment supply, it is tentatively suggested that this supports the contention that the supply of sediment to Culbin has varied through time. A model of sediment supply to Culbin under different stages of RSL successfully uses the critical water depth around the Covesea Ridge to control the supply of sediment from the the large Spey system to supply Culbin and to drive its morphological development.

The data collected from Culbin/Burghead Bay was used in combination with published data from the inner Moray and Dornoch Firths to produce a RSL history for the area. Falling RSL during the Late- and early Postglacial periods reached a low stand *ca.* 8750 BP, forming the Main Lateglacial Shoreline (MLS) at *ca.* -6 m OD prior to rapid rise to the Holocene sea level maximum, and forming the Main Postglacial Shoreline (MPG). At Culbin this feature is represented by the highest shingle ridge, located at 10.995 m OD, correlating with MSL at an altitude of *ca.* 7 m OD *ca.* 6500 BP. RSL has fallen from this high stand through until the present. Estimates of present eustatic sea level rise, combined with an exponentially declining rate of isostatic uplift suggests that RSL in the Culbin area is either approaching stability, or beginning to rise once more, with implications for the future of Culbin.

Secondary data collected during the course of the investigation into RSL trends in the Moray Firth suggests that the evidence used to support the concept of a rise in RSL due to crustal redepression during the Loch Lomond Readvance may be in error. Evidence both from field based studies and geophysical modelling suggests that the size of the ice sheet during the Loch Lomond Stadial was insufficient to cause crustal redepression, while field evidence from the Beaully Firth for such an event appears open to alternative explanation.

Dated sea level indicators also aid in the interpretation of the formation of the abandoned cliffline. This is thought to represent a Lateglacial feature which was re-occupied at selected locations by the Holocene sea level maximum. C14 dating of pond and estuarine deposits between the cliff and the landward shingle ridges indicate abandonment by 5200 BP, at a sea level of *ca.* 5 m OD. It is possible that

these deposits and the overlying peats represent the former course of the Findhorn, as suggested by Ross (1992). However, it is equally as likely that the ponds and peats represent a stabilized back-barrier environment not occupied by the river. Further research in this particular locality would be required to solve this problem.

### **7.2.2 Contemporary coastal studies**

A detailed study of the geomorphology of the present Culbin coast was undertaken to explain the location and status of the contemporary landform assemblage. This provides both a series of modern analogues from which inferences can be made regarding the Holocene development of the site, and a setting to attempt to explain the future development of the site.

The foreshore at Culbin is composed primarily of sand, with only a limited amount of shingle found as a storm ridge backing the foreshore along Buckie Loch spit. The Bar displays a different sedimentary regime, with the eastern (proximal) foreshore composed of sand, which grades into shingle on the western (distal) flank. Sediment sorting within the sands along the Culbin foreshore was found to be marked, with a downdrift coarsening evident. Similarly, downdrift coarsening was identified within the shingle on the western flank of The Bar. A similar trend occurred within the relict shingle ridges in Culbin Forest, suggesting that the processes of longshore shingle transport acting along the present Bar have been operating for at least 6500 years since the emplacement of the Culbin ridge suite.

The Culbin foreshore exhibits two distinct shore-parallel geomorphological zones with a divide centred on Shellyhead bothies, coinciding with the wave refraction cells B1 and B2. Along the eastern flank (cell B2), long (up to *ca.* 200 m) beach profiles are backed by high, tabular dunes which originally developed inland but are currently being sectioned by erosion. This cell is experiencing high rates of erosion, in combination with predominantly convergent wave orthogonals and a high incident component of wave power. Conversely, the western flank (cell B1) exhibits shorter beach profiles (*ca.* 120 m) backed by lower dunes, primarily formed by deflation from the foreshore. Erosion rates along this cell are low or negligible, coincident with parallel or divergent wave orthogonals and consequently a lower incident component of wave power. The division between these two zones is marked by a slight change in the orientation of the coast, and a straightening of the bathymetric contours with distance west. It is proposed that the eastern cell (B2) receives the brunt of incident swell wave energy owing to its orientation, with the effect exacerbated by convex-seawards submarine contours,

which focus wave energy along this section of the coast. The western flank (B1) presents a lower angle of attack to incoming swell, diverting a greater proportion of the incident wave energy alongshore. Shore-parallel submarine contours encourage incident orthogonals to remain parallel, or even to diverge, further reducing the wave energy incident along this flank.

Investigation of the processes operating along the Culbin foreshore contributed towards the calculation of a sand beach sediment budget, while a simpler, separate sediment budget was calculated for shingle on The Bar. Wave refraction modelling demonstrated that the primary mode of sediment transport is alongshore, with up to  $3.3 \times 10^4 \text{ m}^3 \text{ a}^{-1}$  of sand potentially transported. This value is supported by measurements of the volumetric extension rates on Buckie Loch spit, where  $1.3 \times 10^4 \text{ m}^3 \text{ a}^{-1}$  of sediment are annually added to the spit through distal extension. On-offshore sediment transport is the balancing item of the budgets. On the Culbin foreshore, the east cell (B2) displays a positive sediment budget, with net offshore transport invoked to maintain dynamic equilibrium. In the west cell (B1) the sediment budget is slightly negative, where an onshore supply of sediment is envisaged, possibly fuelled by the strongly positive budget in cell B2. Tidal current speeds 1.2 km offshore from Culbin are very low, and are incapable of entraining much sediment. The fine nature of the sediments on the sea bed offshore from Culbin would require much higher current speeds to entrain them in quantity than were measured. However, calculation of residual currents in the offshore zone at Culbin suggests that these may operate in the opposite direction to the long term sediment transport direction.

The shingle sediment budget on The Bar is also positive. The primary input of shingle is from erosion of relict proximal storm ridges, while Burghead Bay and, to a lesser extent the Findhorn form possible secondary sources. The volume released from proximal erosion alone is  $7540.2 \text{ m}^3 \text{ a}^{-1}$ , which exceeds the rate of distal extension measured presently ( $1377.9 \text{ m}^3 \text{ a}^{-1}$ ), suggesting that The Bar is effectively reworking itself as it continues to migrate downdrift.

### **7.2.3 Linkages between Holocene and contemporary processes**

Attempting to link the fields of Holocene and contemporary coastal studies was undertaken using a palaeosediment budget. Having reconstructed the RSL history of this section of the Moray Firth, it was clear that supplies of shingle could have been introduced into Burghead Bay from updrift sources in Spey Bay during periods of low RSL, when operating depths were sufficiently shallow for shingle to bypass the deep water around the northern flank of the Covesea Ridge.

Quantification of the input of shingle to the system used the technique of large scale river terrace reconstruction from below a dated horizon, in this case the Lateglacial terrace of the lower Spey. In the absence of a detailed map of similar features in the lower Findhorn, a gross-scale method was devised to calculate the volume of sediment removed, and calibrated using the more accurate data from the Spey. This volume was then recalibrated to account only for the proportion of shingle delivered to the coast.

The volume of shingle potentially delivered by the Spey was  $2.94 \times 10^8 \text{ m}^3$ , an order-of-magnitude greater delivery than that from the Findhorn ( $2.47 \times 10^7 \text{ m}^3$ ). As the volume of shingle at Culbin was calculated to be  $6.53 \times 10^7 \text{ m}^3$ , it was clear that the supply of shingle from the Findhorn alone could not account for the development of the Culbin shingle ridges. Invoking the Spey as a supply of shingle allows the Culbin palaeosediment budget to appear more balanced. Losses to the Spey shingle occurred prior to reaching Culbin, primarily to the large submarine delta at the mouth of the river, which accounted for  $2.4 \times 10^7 \text{ m}^3$ , and to the shingle structures at Spey Bay, Lossiemouth and Burghead Bay, which together accounted for a further  $6.2 \times 10^4 \text{ m}^3$ , leaving a residual  $6.94 \times 10^7 \text{ m}^3$  to arrive at Culbin. Added to the input from the Findhorn ( $2.47 \times 10^7 \text{ m}^3$ ), this accounts for the volumetric development of Culbin and leaves a residual volume of  $2.88 \times 10^7 \text{ m}^3$  to be transported west, adding to the smaller input from the River Nairn to form the shingle landforms of the Carse of Delnies and Whiteness Head.

The supply of shingle to Culbin from Spey Bay was controlled by RSL. The high stand at the Holocene sea level maximum was represented morphologically at Culbin by an abrupt drop in shingle ridge altitude from *ca.* 10 m OD to *ca.* 6 m OD. Applying the corrected shingle ridge dates to this event, it was found to relate to the period 7200-4300 BP. From contemporary coastal studies it is found that shingle is largely immobilized in water depths of *ca.* 6 m, and it is proposed that when water depths shallower than this occurred around the north of the Covesea Ridge, then shingle was transported between Spey and Burghead Bay and onto the beaches at Culbin. When water depths at Covesea exceeded 6 m, the supply from the Spey was cut off. A conceptual three stage model was constructed to demonstrate the effect of a limiting water depth on the supply of shingle from the Spey. Using this model, a developmental model of Culbin is presented, based around a division of the primary RSL events in the Moray Firth, and a series of case studies presented which demonstrate the varied response of the shoreline to a change in RSL under varying conditions of sediment supply.

The first phase of the model suggests that between *ca.* 9500 and 7200 BP RSL was falling and then rising, but sediment supplies were abundant. Phase 2 sees rising RSL to the peak of the Holocene sea level maximum, with sediment supply from the Spey curtailed. Phase 3, between *ca.* 4300 and the present envisages a falling RSL and a falling supply of sediment. Extension of this model into the present suggests that in the current scenario of stable/rising RSL and falling sediment supplies, a completely different scenario will be experienced to any of those described so far.

## **7.3 CRITIQUE**

### **7.3.1 Holocene sea level studies**

#### **7.3.1.1 Dating control**

The work undertaken in relation to RSL changes in the Culbin area provided information which, in conjunction with data from the inner Moray and Dornoch Firths produces a picture of RSL fluctuations during the Holocene period. However, the data was of limited use in a stand alone situation as:

- i) the dates were all minimum ages, based upon the onset of peat formation;
- ii) the dates were all obtained from regressive contact positions.

This meant that essential sea level control information regarding, for example, the onset of transgressive RSL trends could not be dated using the Culbin samples alone, and thus relied on allied studies from adjacent areas. However, this study has established that with a relatively well established chronology of RSL events produced for the inner Moray and Dornoch Firths, the data could then be calibrated using Culbin data in order to allow the use of the sea level trends in the calculation of a palaeosediment budget.

#### **7.3.1.2 Shingle ridge studies**

The use of shingle ridge altitudes as RSL indicators was considered as a useful step in the construction of a sea level history for Culbin, particularly given the lack of alternative dateable material. The quantification of a ridge correction factor based upon shingle ridges on The Bar supported the altitude/age inferences made on the basis of the composite sea level curve from the Moray Firth. The location of a peat and a palaeosol within the shingle ridges sectioned by erosion in Burghead

Bay provided an initial control over the altitudinal relationships suggested by the Culbin ridges. Being limited to only two samples meant that the altitudinal relationship between shingle ridge crest altitude and age could not be fully tested, and thus the link remains tentative. However, in the absence of further dateable material, and in the light of the convincing fit with the remainder of the dated samples on the declining limb of the sea level curve between 6500 BP and the present, these preliminary results support the contention that shingle ridges in sufficient numbers and if sufficiently controlled by modern analogues provide a reasonable first order measure of sea level at the time of formation.

### **7.3.1.3 Stratigraphic control**

Since there is no recorded commercial borehole activity at Culbin, subsurface investigations were limited to the areas of estuarine sedimentation landwards of the shingle sequences. Thus, the environmental conditions in the Culbin area prior to the emplacement of the shingle cannot be specified. Additionally, this lack of data meant that for the purposes of the palaeosediment budget, the thickness of shingle at Culbin had to be inferred from geomorphological evidence from The Bar, and from borehole and section data in Burghead Bay. Given the nature of shingle sedimentation during the Holocene under a limiting water depth of ca. 6 m, then the good agreements between the contemporary measurements from The Bar and the borehole data from Burghead Bay would appear to support a shingle depth at Culbin of 6 m. Verification would require powered coring equipment to penetrate the shingle cover.

## **7.3.2 Contemporary coastal studies**

### **7.3.2.1 Wave data**

Wave measurements used as input to the wave refraction model were intended to be obtained from the wave recorder built specifically for this project to provide an on-site record of all waves, together with their angles of incidence on the foreshore. Failure of the data logger meant that only 19 days of data were recorded, and thus an alternative source of wave data was required. The use of offshore wave records from the Beatrice Alpha platform was used to generate a series of input wave heights for use in the wave refraction exercise, but directional data still proved problematic. The use of a second data source (Global Wave Statistics; BMT, 1986) was thus required to provide the essential directional data required to produce realistic wave parameters for input to the model.

Thus while the original technique failed to produce a data run of sufficient length to be used as input to the computer generated refraction model, alternative sources of data were available. The data obtained from the wave recorder was also of sufficient quality to justify its inclusion, demonstrating that high quality data can be obtained from low cost equipment, even in such a challenging environment.

### **7.3.2.2 Sediment budgets**

The calculation of two sediment budgets, separately quantifying the transfer of sand and shingle in the Culbin area was successful. However, quantification of the on-offshore element of the budget was not undertaken directly, which provided a potential for error in the calculation. Quantification of the on-offshore transfer of sediment has been investigated by Hardisty (1988, 1990), and a series of equations produced which depend upon the quantification of the swash and backwash elements of wave run-up. The amount of effort required to quantify this value, in relation to the actual amount of information it would yield was considered excessive for the purposes of this study. From inspection of aerial photographs it is clear that the majority of sediment transport at Culbin occurs in a longshore direction. Hardisty (1988) reported that the equations developed for on-offshore transport break down under conditions of strong longshore transport, and thus to attempt to quantify the element of shore normal sediment transport via this method would be flawed.

### **7.3.3 Linkages between Holocene and contemporary processes**

#### **7.3.3.1 Dating control**

The use of the river terrace reconstruction technique represents a relatively new concept in the calculation of the volume of sediment delivered to the coastal zone over the Holocene. However, the technique depends heavily on the identification of dated surfaces for chronological control over the volumes introduced to the coastal zone. In this example, the only surface which could be dated with confidence was the Lateglacial surface in lower Strathspey, identified by Peacock *et al.* (1969). Geomorphological evidence was similarly used to identify the Lateglacial surface in the lower Findhorn valley. This produced only a single dated surface from which to infer the delivery of sediment over *ca.* 13 000 years. Ideally a series of dated surfaces would be required, constraining a narrower time band within each, and from which lower volumes with a tighter chronological control could be obtained. This should form the focus for a separate research project.

#### **7.3.3.2 Three stage conceptual model**

The definition of a conceptual model of RSL and sediment supply to Culbin provides a useful tool with which to define periods of sediment influx from either the Findhorn alone or the Findhorn and Spey together. However, the dating of the exceedance of a critical water depth upon which the model hinges was based upon morphological evidence in the form of the abrupt decline in shingle ridge crest altitude, combined with a critical water depth inferred from field studies applied to a sea level curve to produce a date. The coincidence of these dates suggested that the method was reasonably accurate, but for increased confidence in the technique, the shingle ridges at the top and bottom of the drop should be dated using absolute techniques, followed by testing against the critical water depth theory. In the absence of this dating control, however, the fit of the model with field data appears good, and as an experimental investigation into this field provides a useful predictor of sediment supply under different stages of RSL in the Moray Firth.

## **7.4 SCOPE FOR FUTURE RESEARCH**

### **7.4.1 Sea level studies**

For the production of a more complete RSL history for the Culbin area, the sheltered environment produced by the present Burghead-Lossiemouth high ground in the vicinity of the former Loch Spynie is a likely site for profitable investigation. Geomorphological evidence supports the contention that this area was formerly a marine channel (Ogilvie, 1923, Peacock *et al.*, 1969), and limited coring in the area during the initial stages of this project located marine shell fragments in clays north of Elgin at Lochside (NJ 204658). Eyles & Anderson (1947) similarly noted large thicknesses of clays in this area, while Berridge & Ivimey-Cook (1967) located shell fragments within silt units in a borehole sunk at Lossiemouth airport further north.

Within a relatively sheltered environment such as that in the lee of the Burghead-Lossiemouth ridge the preservation potential for RSL indicators which perhaps bear a closer relationship to the sea level at which they formed is higher. Similarly in a low energy environment the potential for the preservation of transgressive contacts is higher, providing a tighter control on RSL events during the Late Quaternary rather than only the regressive indicators preserved in the higher energy environment along the open Culbin coast.

### **7.4.2 Shingle ridge studies**

The detailed study of shingle ridge morphology, altitude and relationship to formative sea level has been limited in Britain, primarily due to a lack of large, well-preserved shingle landforms. Dungeness forms the only other structure upon which such studies have been made (Lewis & Balchin, 1940; Green & McGregor, 1986; Long & Fox, 1988). Extension of the present study would be difficult in Britain due to this lack of large shingle structures together with modern analogues in close proximity from which control measurements can be made. However, extending the study abroad would be profitable, particularly to areas where high rates of isostatic uplift are occurring in conjunction with a continued high rate of coarse sediment supply, for example in the coastal zones of Greenland, Iceland, Norway or northern Canada.

### **7.4.3.Sediment budget**

The sediment budget and the allied data required for its calculation provides one of the most useful measures of the relative stability of a coastal area. Such data has important implications, both from a geomorphological and a legislative viewpoint. Interruption of the updrift supply of sediment will have implications for cells located downdrift. Such an effect was recognized at Findhorn, where the response to erosion was the construction of a groynefield and revetment in 1985 (Ross, 1992). The groynefield is clearly successful, increasing the residence time of shingle and raising the level of the backbeach area, providing protection for this stretch of the coast. However, this sediment was formerly transported downdrift to find its way onto the foreshore at Culbin and possibly The Bar. Erosion along the Culbin foreshore will clearly have been influenced by the interruption in the supply of sediment from updrift, and while in this case the effect is not a major contributor to the problem due to the deflecting influence of the Findhorn Bar, clearly in other cases the effects of updrift feeder sterilization may be profound.

The calculation of an annual sediment budget at Culbin would be a useful monitoring exercise, providing a running check on the sediment status of the foreshore, and targetting areas which might require remedial action in advance of problems becoming physically manifest in the sediment system.

### **7.4.4 Wave recorder**

The construction of directional wave recorder was undertaken in order to provide a record of waves incident on the Culbin foreshore, which could be used as input to the wave refraction model WAVENRG. Despite logger failure after 19 days, the data produced by the rig was of sufficient quality to include the methodology employed in its construction and deployment.

Future deployments of a similar system would see the rig permanently submerged to provide a total record of waves at specified sampling intervals (10 minutes every three hours [Hardisty, 1988]), and the use of a data logger with a high speed recording capacity and a significantly larger memory than that employed in this study. With the advent of such a capability, a means of sorting and classifying the large amounts of data produced would also require development.

#### 7.4.5 Palaeosediment budget

The construction of a palaeosediment budget here has demonstrated the successful application of combined concepts from both contemporary and Quaternary coastal studies. Calculation of the volumetric removal of sediment from the lower river terraces of the Spey and the Findhorn, and matching them against the volumes in the Culbin ridge suite is a methodology not used before in the UK, and one which proved remarkably successful given the potential volumetric errors. Application of the volumes obtained from these sources proved vital to the palaeosediment budget, demonstrating that the accepted concept of the Findhorn supplying the shingle necessary for the construction of the Culbin foreland was clearly not the case, and that an additional supply of sediment had to be invoked from neighbouring Spey Bay was more likely. Further research from the field of contemporary coastal studies identified the point at which water depths became limiting to the transport of sediment from Spey Bay to Findhorn Bay via the northern flank of the Covesea Ridge. This allowed the construction of a three stage model to quantify the potential amounts of sediment released to the coastal zone from either the Findhorn alone, or the Findhorn in combination with the Spey. From this, the volumetric construction of Culbin could be accounted for, while producing a volumetric residual which supplemented the potential sediment supply from the River Nairn, helping to explain the shingle structures of the Carse of Delnies and Whiteness Head.

The success of this exercise suggested that the method could be used elsewhere. The prime requisite for repeating such a series of calculations were considered to be;

- i) knowledge of the input sediment volumes to a site. In this case the use of the lower river terrace sequences was aided by the presence of the relative age-dated Lateglacial surface of lower Strathspey (Peacock *et al*, 1968) in the absence of an equivalent surface dated by absolute techniques (C14, TL, tephra etc.).
- ii) knowledge of the depth of shingle contained within the individual storm ridge landform assemblages. A lack of an absolute defined value for the Culbin shingle series meant that a surrogate depth was adopted from borehole records in neighbouring Burghead Bay.

Once these criteria have been met, it would be a straight forward task to perform a similar series of calculations to those reported in this study in order to ascertain the magnitude of the sedimentary inputs relative to an accretionary landform, and from this to determine the likely sources of sediment from which it was derived.

## 7.5 Conclusion

The strength of this research has been in the breadth of its coverage. An investigation into the Holocene RSL history of Culbin helps to elucidate the genesis of the raised landforms and sediments forming the present coast. By examining the nature of the modern landforms and their allied processes, then the present erosional status of Culbin and Burghead Bay can be fully understood. Inferences can then be made concerning the mode of development of this section of the coast during the Holocene, using both techniques from the field of Late Quaternary sea level studies (to produce a sea level trend), and contemporary coastal studies (in the application of the sediment budget). Finally, with an appreciation of how the coast *has reacted* to changes in RSL and sediment supply, and similarly how it is *currently reacting* to such changes, the shape of possible *future changes* at Culbin becomes clearer.

In terms of addressing the aims stated at the outset of the thesis, the work has been successful. The use of multiple working hypotheses allowed the freedom to explore the concepts of relative sea level change, rates of sediment supply and the implications for landform development during the Holocene. Of particular interest was the development of a method for calculating the former supply of sediment to the coastal zone throughout the Holocene. This was found to depend heavily on certain input variables, but at the provisional and exploratory level for which it was intended proved to be successful, and provides a potentially fruitful avenue for further research. Using such a tool combined with a study of the contemporary coastal sediment budget, the potential for the identification of both present and former littoral cells becomes more tenable, allowing sediment sources to be identified more positively.

## REFERENCES

- ADMIRALTY, 1981. Sheet 233: Dunrobin Point to Buckie. (Hydrographer of the Navy, Taunton).
- ADMIRALTY, 1992. Tide Tables Volume 1. European Waters including the Mediterranean. (Hydrographer of the Navy, Taunton).
- AL-ANSARI, N.A. & McMANUS, J. 1979. Fluvial sediments entering the Tay estuary: sediment discharge from the River Earn. Scott. J. Geol. 15, pp 203-216.
- ALLEN, J.R.L., 1981. Beach erosion as a function of variation in the beach sediment budget, Sandy Hook, New Jersey, USA. Earth Surface Processes and Landforms 6, pp 139-150.
- ALLEN, J.R.L., 1985. Principles of Physical Sedimentology (Allen & Unwin).
- ANDREWS, I.J., LONG, D., RICHARDS, P.C., THOMSON, A.R., BROWN, S., CHESHER, J.A. & McCORMAC, M. 1990. The geology of the Moray Firth. B.G.S. U.K. Regional Offshore Report. (H.M.S.O.).
- ANDREWS, J.T. 1970. A geomorphological study of post-glacial uplift with particular reference to Arctic Canada. I.B.G. Special Publ. 2.
- ANDREWS, J.T. 1987. Glaciation and level: a case study. In Devoy, R.J.N. (ed) Sea Surface Studies: A Global View. pp 95-126.
- ASHLEY, G.M & RENWICK, W.H. 1983. Channel morphology and processes at the riverine-estuarine transition, the Raritan River, New Jersey. Sp. Publ. Inst. Ass. Sedimentology. 6, pp 207-218.
- AUBREY, D.G. 1979. Seasonal patterns of onshore/offshore sediment movement. J. Geophys. Res. 84, pp 6347-6354.
- AUTON, C.W. 1990. The middle Findhorn valley. In Auton, C.W. *et al.*, (eds.) Beaulieu to Nairn: Field Guide. pp 74-81. (QRA, Cambridge).
- BALSILLIE, J.H. & CARTER, R.W.G. 1984. The visual estimation of shore breaking wave heights. Coastal Engineering 8, pp 367-385.
- BARNETT, T. 1990. Recent changes in sea level: a summary. Ch. 1 in Sea Level Changes. Nat. Res. Council 1990. (Nat. Academic Press, Washington. D.C.).
- BARR, D. 1985. 3-D palinspastic restoration of normal faults in the Moray Firth: implications for extensional basin development. Earth & Planetary Science Letters 75, pp 191-203.
- BELDERSON, R.H., JOHNSON, M.A. & STRIDE, A.H. 1978. Bedload partings and convergences at the entrance to the White Sea, USSR and between cape Cod and Georges Bank, USA. Marine Geology 28, pp 65-75.
- BERRIDGE, N.G. & IVIMEY-COOK, H.C. 1967. The geology of a borehole at Lossiemouth, Morayshire. Bul. Geol. Survey GB. 27, pp 155-169.

- BIRD, E.C.F. 1985. Coastline Changes: A Global Review (Wiley).
- BLIONIS, G. 1991. An ecological study of vegetation changes due to vehicles passing through the saltmarshes of Culbin Sands SSSI, Moray Firth, Scotland. Unpublished MSc thesis, University of Aberdeen. 61pp.
- BLUCK, B.J., 1969. Particle rounding in beach gravels. Geol.Mag. 106, pp1-14.
- BMT CEEMAID LTD, 1990. Wirral-Dee Study Report no. 46287 to Wirral Metropolitan Borough Council.
- BOULTON, G.S., JONES, A.S., CLAYTON, K.M., & KENNING, M.J., 1977. A British ice sheet model and patterns of glacial erosion and deposition in Britain. Ch 17 in Shotton, F.W. (ed.) British Quaternary Studies: Recent Advances. (Clarendon, Oxford).
- BOULTON, G.S., SMITH, G.D., JONES, A.S. & NEWSOME, J. 1985. Glacial geology and glaciology of the last mid-latitude ice sheets. J. Geol. Soc. London 142, pp 447-474.
- BOWEN, D.Q. 1978. Quaternary Geology: A Stratigraphic Framework for Multidisciplinary Work. (Pergamon, Oxford). 221 pp.
- BOWMAN, D., 1981. Efficiency of eigenfunctions for discriminant analysis of subaerial non-tidal beach profiles. Mar. Geol. 39. pp 243-258.
- BRADLEY, R.S. 1985. Quaternary Palaeoclimatology 472pp. (Unwin Hyman).
- BRAZIER, V., WHITTINGTON, G., & BALLANTINE, C.K., 1988. Holocene debris cone evolution in Glen Etive, W. Grampian Highlands, Scotland. Earth Surface Processes & Landforms 13. pp 525-531.
- BRIGGS, D.J., 1977. Palaeohydrological analysis of braided river terrace deposits. In Briggs, D.J., & Waters, R.S.(eds.). Studies in Quaternary Geomorphology. Proceedings 6th British & Polish Seminar, Sheffield, 1977. (Geobooks, Norwich).
- BRIGGS, D.J & SMITHSON, P.A. 1985. Fundamentals of Physical Geography. (Hutchison, London). 558 pp.
- BRITISH MARITIME TECHNOLOGY (BMT), 1986. Global Wave Statistics 1986. Area 11 - North Sea. 661 pp. (Unwin)
- BROOKS, C.L., 1972. Pollen analysis and the Main Buried Beach in the western part of the Forth Valley. Trans. Inst. Brit. Geog. 55. pp 161-170.
- BROWNE, M.A.E., GRAHAM, D.K. & GREGORY, D.M. 1984. Quaternary estuarine deposits in the Grangemouth area, Scotland. BGS Rep 16/3.
- BRUUN, P., 1984. Cost-effective coastal protection with reference to Florida and the Carolinas, U.S.A. J. Coastal Research 1, pp 47-55.

- BRYANT, E.A. 1974. A comparison of air photograph and computer simulated wave refraction patterns in the nearshore area, Richibucto, Canada and Jarvis Bay, Australia. Maritime Sediments 10, pp 85-95.
- BUCHAN, G. & RITCHIE, W. 1979. Aberdeen beach and Donmouth spit: an example of short term coastal dynamics. Scott. Geog. Mag. pp 27-43.
- BULLER, A.T. & McMANUS, J. 1973. Sediment sampling and analysis. In Dyer, K.R. (ed) Estuarine Processes and Sedimentation. pp 87-129.
- BYE, C.J. 1988. Factors leading to spatial variations in types of mass movement in cliffs of Pleistocene deposits between West Runton and Overstrand, N. Norfolk coast. Unpubl. undergraduate dissertation, University of Sheffield.
- CAMERON, T.D.J., STOKER, M.S. & LONG, D. 1987. The history of Quaternary sedimentation in the UK sector of the North Sea basin. J. Geol. Soc. London 144, pp 43-58.
- CARR, A.P. 1965. Shingle spit and river mouth: short term dynamics. Trans. I.B.G. 36, pp 117-129.
- CARR, A.P. 1969. Size grading along a pebble beach: Chesil Beach, England. J. Sed. Petrology 39, pp 297-311.
- CARR, A.P. 1971. Experiments on longshore transport and sorting of pebbles: Chesil Beach, England. J. Sed. Petrology 41, pp 1084-1104.
- CARR, A.P. & BLACKLEY, M.W.L. 1972. Investigations bearing on the age and development of Chesil Beach, Dorset, and the associated area. Trans. I.B.G. 58, pp 99-112.
- CARR, A.P. & BLACKLEY, M.W.L. 1974. Ideas on the origin and development of Chesil Beach, Dorset. Proc. Dorset Nat. Hist & Arch. Soc. 95, pp 9-17.
- CARR, A.P., BLACKLEY, M.L.W. & KING, H.L., 1982. Spatial and seasonal aspects of beach stability. Earth Surface Processes & Landforms 7, pp 267-282.
- CARTER, R.W.G. 1975. Recent changes in the coastal geomorphology of the Magilligan foreland, Co. Londonderry. Proc. Royal Irish Academy 75, pp 469-497.
- CARTER, R.W.G. 1983. Raised coastal landforms as products of modern process variations and their relevance in eustatic sea level studies: examples from eastern Ireland. Boreas 12, pp 167-182.
- CARTER, R.W.G. 1988. Coastal Environments. (Academic).
- CARTER, R.W.G. & BALSILLIE, J.H. 1983. A note on the amount of wave energy transmitted over nearshore sand bars. Earth Surface Processes & Landforms 8, pp 213-222.

- CARTER, R.W.G., JOHNSTON, T.W. & ORFORD, J.D. 1984. Stream outlets through mixed sand and gravel coastal barriers: examples from southeast Ireland. Zeit. für Geomorph. 28, pp 427-442.
- CARTER, R.W.G. & ORFORD, J.D. 1984. Coarse clastic barrier beaches: a discussion of the distinctive dynamic and morphosedimentary characteristics. Marine Geology 60, pp 377-389.
- CARTER, R.W.G., JOHNSTON, T.W., McKENNA, J. & ORFORD, J.D., 1987. Sea level, sediment supply and coastal changes: examples from the coast of Ireland. Prog. Oceanography 18. pp 79-90.
- CARTER, R.W.G. & ORFORD, J.D. 1988. Conceptual model of coarse clastic barrier formation from multiple sediment sources. Geogr. Review 78, pp 221-239.
- CARTER, R.W.G. & STONE, G.W. 1989. Mechanisms associated with the erosion of sand dune cliffs, Magilligan, Northern Ireland. Earth Surface Processes and Landforms 14, pp 1-10.
- CERC (COASTAL ENGINEERING RESEARCH CENTER) 1984. Shore Protection Manual. Volume 1.(USACE, Vicksburg).
- CHAPPELL, J., 1983. Thresholds and lags in geomorphic changes. Austr. Geogr. 15. pp 357-366.
- CHESHER, J.A. & LAWSON, D., 1983. The geology of the Moray Firth. Rep. Inst. Geol. Sci. 83/5.
- CHURCH, M., WOLCOTT, J. & MAIZELS, J., 1990. Palaeovelocity: a parsimonious proposal. Earth Surface Processes and Landforms 15. pp 475-490.
- CLAPPERTON, C.M. & SUGDEN, D.E. 1975. The glaciation of Buchan:- A re-appraisal. In Gemmel, A.M.D. (ed.) Quaternary Studies in NE Scotland. pp 19-22. (Aberdeen University Press, Aberdeen).
- CLARK, D.J. & ELIOT, I.G. 1988. Low frequency changes of sediment volume on the beachface at Warilla Beach, NSW, 1975-85. Mar. Geol. 79, pp 189-211.
- CLARK, J.A., 1985. Forward and inverse models in sea level studies. Ch\*\*In Woldenberg, M.J. (ed.) Models in Geomorphology. (Allen & Unwin).
- CLARK, J.A., FARRELL, W.E. & PELTIER, W.R. 1978. Global changes in Postglacial sea level: a numerical calculation. Quaternary Research 9, pp 265-287.
- CLAYTON, K.M. 1980. Beach sediment budgets and coastal modification. Prog. Phys. Geog. 4, pp 471-486.
- COLES, J.M. & TAYLOR, J.J. 1969. The excavation of a midden in the Culbin Sands, Morayshire. Proc. Soc. Ant. Scot. 102, pp 87-98.

- COMBER, D.P.M. & HANSOM, J.D. 1993. Culbin Sands, Culbin Forest and Findhorn Bay SSSI: Documentation and Management Prescription. Report to Scottish Natural Heritage. 74 pp.
- COODE, J. 1853. Description of the Chesil Bank, with remarks upon its origin, the causes which have contributed to its formation and upon the movement of the shingle generally. Minutes Proc. Inst. Civ. Engns. 12, pp 520-557.
- CURRAY, J.R. 1964. Transgressions and regressions. In Miller, R.L. (ed) Papers in Marine Geology: Shepard Commemorative Volume. (Macmillan, New York) pp 175-203.
- CRAIG, R.E., 1959. Hydrography of Scottish Waters. Marine Research 2, Scottish Home Dept. (H.M.S.O.).
- CULLINGFORD, R.A., 1977. Lateglacial raised shorelines and deglaciation in the Earn-Tay area. In Gray, J.M. & Lowe, J.J. (eds) Studies in the Scottish Lateglacial Environment. (Pergamon).
- CULLINGFORD, R.A., CASELDINE, C.J. & GOTTS, P.E., 1980. Early Flandrian land and sea level changes in lower Strathearn. Nature 284. pp 159-161.
- CULLINGFORD, R.A., FIRTH, C.R. & SMITH, D.E., 1986. Relative sea level changes in eastern Scotland from the Loch Lomond Stadial to the present: a summary of present knowledge. IGCP 200 Montrose field meeting 23-25 May 1986. Review paper.
- CUNLIFFE, B.W., 1980. The evolution of Romney Marsh: a preliminary statement. In Thompson, F.H. (ed.) Archaeology And Coastal Change. Society of Antiquities Occ. Paper (New Series) No.1.
- DAVIDSON-ARNOTT, R.G.D, & AMIN, S.M.N. 1974 Application of computer modelling and sediment budget techniques to shore erosion problems, S.W. Lake Ontario. Canadian Coastal Conference 1983, Nat. Res. Co., Ottawa, Canada.
- DAVIDSON-ARNOTT, R.G.D. & POLLARD, W.H. 1980. Wave climate and potential longshore sediment transport patterns, Nottawasaga Bay, Ontario. J. Great Lakes Res. 6, pp 54-67.
- DAVIES, J.L. 1978. Geographical Variation in Coastal Development. 2nd edition. (Longman, London).
- DAVIS, R.A. Jr. 1983. Depositional Systems: A Genetic Approach to Sedimentary Geology. (Prentice-Hall). 669 pp.
- DAVISON, C., 1902. The Inverness earthquake of September 18th and its accessory shocks. Q. J. Geol. Soc. 58. pp 378-398.
- DAWSON, A.G. 1992. Ice Age Earth: Late Quaternary Geology and Climate. (Routledge, London). 293 pp.

- DAWSON, A.G., LONG, D. & SMITH, D.E. 1988. The Storegga Slides: evidence from eastern Scotland for a possible tsunami. Mar. Geol. 82, pp 271-276.
- DAWSON, A.G., SMITH, D.E. & LONG, D., 1990. Evidence for a tsunami from a Mesolithic site in Inverness, Scotland. J.Arch. Sci.17. pp 509-512.
- DEAN, R.G. & MAUMEYER, E.M., 1983. Models for beach profile response. Ch\*\*in Komar, P.D.(ed.) Handbook of Coastal Process and Erosion. (C.R.C. Press, Boca Rotan, Fla.).
- DENTON, G.H. & HUGHES, T.J. 1981. The Last Great Ice Sheets. (Wiley, New York) 484 pp.
- DEVOY, R.J.N., 1987. First principles and the scope of sea surface studies. In Devoy, R.J.N. (ed) Sea Surface Studies: A Global View. (Croon Helm, London) 649 pp.
- DILLON, W.P. 1970. Submergence effects on a Rhode Island barrier and lagoon and inference on barrier migration. J.Geol. 78. pp 94-106.
- DOBKINS, J.E. & FOLK, R.L. 1970. Shape development on Tahiti-Nui. J. Sed. Petrology. 40, pp 1167-1203.
- DOE (DEPARTMENT OF THE ENVIRONMENT) 1991. The Potential Impacts of Climate Change in the United Kingdom. Report by the UK Climatic Impacts Review Group. (HMSO, London). 123 pp.
- DOOLEY, H. 1971. Currents off the north east of Scotland. Scottish Fisheries Bulletin 39, pp 48-52.
- DONNER, J.J. 1969 [1974]. A profile across Fennoscandia of Late Weichselian and Flandrian shorelines. In Andrews, J.T. (ed.) "Glacial Isostasy". (Dowden, Hutchison & Ross, Pennsylvania). 491 pp.
- DRAPER, L. 1976. Waves at Dowsing Light Vessel, North Sea. Inst. Oceanographic Sci.Report no. 31 (NERC./IOS, Godalming).
- DUBOIS, R.N., 1988. Seasonal changes in beach topography and beach volume in Delaware. Mar. Geol. 81, pp 79-96.
- DURY, G.H., 1976. Discharge prediction, present and former, from channel dimensions. J. Hydrology. 30. pp 219-245.
- DYKE, A.S. & PREST, V.K. 1987. Late Wisconsinan and Holocene Retreat of the Laurentide Ice Sheet. Geol. Surv. Canada Map 1702A. (1:5 000 000).
- DYKE, A.S., MORRIS, T.F. & GREEN, D.E.C. 1991. Postglacial tectonic and sea level history of the central Canadian Arctic. Geol. Surv. Canada Bul. 397. (Dept. of Energy, Mines & Resources).
- EDDISON, J., 1983. The evolution of the barrier beaches between Fairlight and Hythe. Geogr. J. 149, pp 39-53.

- EDLIN, H.L. 1976. The Culbin Sands. In Lenihan, J. & Fletcher, W.W. (eds.) Reclamation. pp 1-13. (Blackie).
- EDWARDS, K.J. & ROWNTREE, K.M. 1980. Radiocarbon and palaeoenvironmental evidence for changing rates of erosion at a Flandrian stage site in Scotland. Ch. 15 in Cullingford, R.A., Davidson, D.A. & Lewin, J. Timescales in Geomorphology. pp 207-223. (Wiley).
- ELIOT, I.G. & CLARKE, D.J. 1988. Semi-diurnal variation in beachface aggradation and degradation. Mar. Geol. 79, pp 1-22.
- EMERY, K.O. & AUBREY, D.G. 1985. Glacial rebound and relative sea levels in Europe from tide gauge records. Tectonophysics 120, pp 239-255.
- ENGLAND, J. 1983. Isostatic adjustments in a full glacial sea. Can. J. Earth Sci. 20, pp 895-917.
- ENGLAND, J. 1992. Postglacial emergence in the Canadian High Arctic: integrating glacioisostasy, eustasy and late deglaciation. Can. J. Earth Sci. (in press).
- ESA (EUROPEAN SPACE AGENCY) 1990. Space techniques support the monitoring of sea level. Earth Observation Quarterly 29, pp 1-7.
- EVANS, D.J.A. 1989. An early Holocene narwhal tusk from the Canadian high Arctic. Boreas 18, pp 43-50.
- EVANS, D.J.A. 1990. The last glaciation and relative sea level history of Northwest Ellesmere Island, Canadian high Arctic. J. Quat. Science 5, pp 67-82.
- EVANS, O.F. 1939. Sorting and transportation of material in swash and backwash. J. Sed. Petrol. 9, pp 28-31.
- EVERTS, C.H. 1973. Beach profile changes on western Long Island. Ch.13 in Coates, D.R. (ed.) Coastal geomorphology. (Allen & Unwin)
- FAIRBAIRN, W.A., 1967. Erosion in the River Findhorn Valley. Scott. Geog. Mag. 83(1), pp 46-52.
- FAIRBANKS, R.G. 1989. A 17 000 year glacio-eustatic sea level record: influence of glacial melting rates on the Younger Dryas event and deep oceanic circulation. Nature 342, pp 637-642.
- FAIRBRIDGE, R.W. 1961. Eustatic changes in sea level. Physics and Chemistry of the Earth 4, pp 99-185.
- FAIRBRIDGE, R.W. & JELGERSMA, S. 1990. Sea level. In Paepe, R *et al* (eds.) Greenhouse Effect, Sea Level and Drought. pp 117-143. (Kluwer).
- FARREL, W.E. & CLARK, J.A. 1976. On Postglacial sea level. Geophys. J. R. Astr. Soc. 46, pp 647-667.
- FERGUSON, R.I. 1987. Accuracy and precision of methods for estimating river loads. Earth Surface Processes & Landforms 12, pp 95-104.

- FICO, C. 1978. Influence of wave refraction on coastal geomorphology- Bull Island to Isle of Palms, South Carolina. Tech. Report No. 17-CRD. Coastal Research Division, Dept. of Geology, University of South Carolina.
- FIRTH, C.R. 1984. Raised Shorelines and Ice Limits in the Inner Moray Firth and Loch Ness areas, Scotland. Unpubl. PhD thesis, Coventry Polytechnic.
- FIRTH, C.R. 1986. Isostatic depression during the Loch Lomond stadial: preliminary evidence from the Great Glen, N. Scotland. Quat. Newsletter 48, pp 1-9.
- FIRTH, C.R. 1989a. Late Devensian raised shorelines and ice limits in the inner Moray Firth, N. Scotland. Boreas 18, pp 5-21.
- FIRTH, C.R. 1989b. Isostatic depression during the Loch Lomond Stadial (Younger Dryas): evidence from the Moray Firth, Scotland. Geoliska Föreningens i Stockholm Förhänlinger 111, pp 296-299.
- FIRTH, C.R. & HAGGART, B.A. 1989. Loch Lomond stadial and Flandrian shorelines in the inner Moray Firth, Scotland. J. Quat. Science 4, pp 1-14.
- FORBES, D.L., TAYLOR, R.B., ORFORD, J.D., CARTER, R.W.G. & SHAW, J. 1991. Gravel barrier migration and overstepping. Mar. Geol. 97, pp 305-313.
- FORESTRY COMMISSION, 1988. Culbin Conservation Management Plan. Forestry Commission Moray Forest District internal document. 18pp.
- FORMAN, S.L., MANN, D.H. & MILLER, G.H. 1987. Late Weischelian and Holocene relative sea level history of Bröggerhalvöya, Spitsbergen. Quat. Res. 27, pp 41-50.
- FRANCIS, E.H., FORSYTH, I.H., READ, W.A. & ARMSTRONG, M. 1970. The Geology of the Stirling District. Mem. Geol. Surv. GB. Sheet 39.
- FRIEDMAN, G.M. 1967. Dynamic processes and statistical parameters compared for size frequency distribution of beach and river sands. J. Sed. Petrol. 37, pp 327-354.
- GAULD, J.H. 1981. The soils of Culbin Forest, Morayshire: their evolution and morphology, with reference to their forestry potential. Applied Geography 1, pp 199-212.
- GODWIN, H. 1943. Coastal peat beds of the British Isles and North Sea. J. Ecology 31, pp 199-247.
- GODWIN, H. & CLIFFORD, M.H. 1938. Studies of the Post-glacial history of British vegetation. Phil. Trans. R. Soc. London 562, pp 323-406.
- GOLDSMITH, V. 1976. Wave climate models for the continental shelf : critical links between shelf hydraulics and shoreline processes. In Davis, R.A. Jr. & Ethington, R.L. (eds) Beach and Nearshore Sedimentation. Society of Economic Palaeontologists and Mineralogists sp. publ. 24, pp 24-47.

- GOMEZ, B. & CHURCH, M. 1989. An assessment of bedload sediment transport formulae for gravel bed rivers. Water Resources research 25(6), pp 1161-1186.
- GORNITZ, V., LEBEDEFF, S. & HANSEN, J., 1982. Global sea level trend in the past century. Science 215, pp 1611-1614.
- GORNITZ, V. & LEBEDEFF, S. 1987. Global sea level changes during the past century. In Nummedal, D., Pilkey, O.H. & Howard, J.D. (eds.) Sea Level Fluctuation and Coastal Evolution. Society of Economic Palaeontologists and Mineralogists Sp. Publ. No 41.
- GOUDIE, A.S. 1990. Geomorphological Techniques. (Unwin Hyman).
- GRAY, J.M. 1983. The measurement of shoreline altitudes in areas affected by glacio-isostasy with particular reference to Scotland. In Smith, D.E. & Dawson, A.G. (eds.) Shorelines and Isostasy. pp 97-128. (Academic).
- GRAY, J.M. & COXON, P. 1991. The Loch Lomond glaciation in Britain and Ireland. In Ehlers, J., Gibbard, P.L. & Rose, J. (eds) Glacial Deposits in Britain and Ireland. pp 89-105. (Balkema).
- GREEN, C.P. & MCGREGOR, D.F.M. 1986. Dungeness: A Geomorphological Assessment. Report to N.C.C. by Royal Holloway & New Bedford College. 68pp.
- GREEN, R.D. 1968. Soils of Romney Marsh. Soil Survey G.B. Bul. No.4.
- GUZA, R. & INMAN, D.L. 1975. Edge waves and beach cusps. J. Geophys. Res. 80, pp 2997-3012.
- HAGGART, B.A. 1983. Summary of Flandrian sea level changes in the inner Moray Firth. In Ritchie, W (ed.) North East Scotland Field Guide and Geographical Essays. (University of Aberdeen).
- HAGGART, B.A. 1986. Relative sea level change in the Beaulie Firth, Scotland. Boreas 15, pp 191-207.
- HAGGART, B.A. 1987. Relative sea level changes in the Moray Firth area, Scotland. In Tooley, M.J. & Shennan, I. (eds.) Sea Level Changes. pp 67-108. (Blackwell).
- HALL, A. 1987. Migration and Development of The Bar, Nairn, Scotland. Unpublished undergraduate dissertation, University of Sheffield.
- HALL, A.M. & WHITTINGTON, G. 1989. Late Devensian glaciation of southern Caithness. Scott. J. Geology 25, pp 307-324.
- HANSOM, J.D. 1988. Coasts. (CUP, Cambridge) 96 pp.
- HANSOM, J.D. 1992. Dredging in the Bristol Channel. Assessment of a report by Hydraulics Research Ltd. Unpubl. report to English Nature, 8/5/92.
- HANSOM, J.D. & LEAFE, R.L. 1990. The Geomorphology of Morrich More: Development of a Scientific Database and Management Prescription. Report to the Nature Conservancy Council, Peterborough. 174 pp.

- HARDISTY, J. 1984. A dynamic approach to the inter-tidal profile. In Clark, M.W. (ed.) Coastal Research: UK Perspectives pp 17-37.
- HARDISTY, J. 1988. Measurement of shallow water wave direction for longshore sediment transport. Geo-Marine Letters 8, pp 35-39.
- HARDISTY, J. 1990. An introduction to wave recording: with special reference to pressure transducers and geomorphological applications. B.G.R.G. Tech. Publ. 76pp.
- HARDISTY, J., COLLIER, J & HAMILTON, D. 1984. A calibration of the Bagnold Beach Equation. Mar. Geol. 61, pp 95-101.
- HARDY, J.R. 1964. The movement of beach material and wave action near Blakeney Point, Norfolk. Trans. I.B.G. 34, pp 53-69.
- HARRIS, A.L. & PEACOCK, J.D. 1969. Sand and Gravel Resources of the Moray Firth. Inst. Geol. Sci. Report 69/9. (N.E.R.C.)
- HART, B.S. & PLINT, A.G. 1989. Gravelly shoreface deposits: a comparison of modern and ancient facies sequences. Sedimentology 36, p 551-557.
- HASTINGS, A. 1991. A Qualitative Examination and a Quantitative Investigation into the Changing Configuration of The Bar, Culbin Sands, NE Scotland. Unpubl. undergraduate dissertation, University of Sheffield.
- HEIJNIS, H. 1990. Dating the Odhar peat at the Allt Odhar site by the uranium series disequilibrium dating method. In Auton, C.W., Firth, C.R. & Merritt, J.W. (eds.) Beaulieu to Nairn: Field Guide. pp 72-74. (QRA, Cambridge). 149 pp.
- HEMSLEY, J.M., McGEHEE, D.D. & KUCHARSKI, W.M. 1991. Nearshore oceanographic measurements: hints on how to make them. J. Coastal Research 7, pp 301-315.
- HEY, R.W. 1967. Sections in the beach plain deposits of Dungeness, Kent. Geol. Mag. 104(4), pp 361-370.
- HICKEY, K.R. 1991. Sand dune movements and sand deflation: an example from the Culbin Sands, NE Scotland. In Firth, C.R. & Haggart, B.A. (eds) Late Quaternary Coastal Evolution in the inner Moray Firth: Field Guide pp 29-31. (West London Press, London).
- HOFFMAN, J.S., WELLS, J.B. & TITUS, J.G. 1986. Future global warming and sea level rise. In Proceedings of the Iceland Coastal and River Symposium. pp 245-266 Reykyavik, National Energy Authority.
- HOLMAN, R.A. & BOWEN, A.J. 1982. Bars, bumps and holes: models for the generation of complex beach topography. J. Geophys. Res. 87. pp 457-468.
- HOYT, J.H. 1967. Barrier island formation. Geol. Soc. America Bul. 78, pp 1125-1136.

- HOYT, J.H. & HENRY, V.J. 1967. Influence of island migration on barrier island sedimentation. Geol. Soc. America Bul. 78, pp 77-86.
- HUGGETT, R.J. 1985. Earth Surface Systems. (Springer-Verlag). 270 pp.
- JARDINE, W.G. 1975. Chronology of Holocene marine transgression and regression in south west Scotland. Boreas 4, pp 173-196.
- JARDINE, W.G. 1982. Sea level changes in Scotland during the last 18 000 years. Proc. Geol. Ass. 93, pp 25-41.
- JELGERSMA, S. 1966. Sea level changes during the last 10 000 years. In Sawyer, J.S. (ed) World Climate 8000 - 0 BC. International Symposium on World Climates, 18-19th April 1966. (R. Met. Soc., London).
- JELGERSMA, S. 1980. Late Cenozoic sea level changes in the Netherlands and the adjacent North Sea basin. In Morner, N.A. (ed.) Earth Rheology, Isostasy and Eustasy. pp 435-447. (Wiley).
- JELGERSMA, S. *et al.*, 1970. The coastal dunes of the western Netherlands: geology, vegetational history and archaeology. Meddedelingen Geol. Sticht (Nieuwe Series) 21.
- JENNINGS, S. & SMYTH, C. 1990. Holocene evolution of the gravel coastline of East Sussex. Proc. Geol. Ass. 101, pp 213-224.
- JOHNSON, J.W., O'BRIEN, M.P. & ISAACS, J.D. 1948. Graphical Construction of Wave Refraction Diagrams. U.S. Navy Hydrographic Office Publ. No. 605. (U.S. Navy Hydrographic Office).
- KEMPEMA, E.W., REIMITZ, E. & BARNES, P.W. 1989. Sea ice sediment entrainment and rafting in the Arctic. J. Sed. Petrology 59, pp 308-317.
- KIDSON, C. 1963. The growth of shingle spits across estuaries. Z. für Geomorph. N.F. Bd. 7, pp 1-22.
- KIDSON, C. 1977. The coasts of South West England. In Kidson, C. & Tooley, M.J. (eds) The Quaternary History of the Irish Sea. Geol. J. Sp. Issue 7, pp 257-298.
- KIDSON, C. 1982. Sea level changes in the Holocene. Quat. Sci. Rev. 1, pp 121-151.
- KIDSON, C., CARR, A.P. & SMITH, D.B. 1958. Further experiments using radioactive methods to detect the movement of shingle over the sea bed and alongshore. Geog. J. 124, pp 210-218.
- KIDSON, C. & HEYWORTH, A. 1976. The Flandrian sea level rise in the Bristol Channel. Proc. Usher Soc. 2(6), pp 565-584.
- KIDSON, C. & HEYWORTH, A. 1978. Holocene eustatic sea level change. Nature 273, pp 748-750.
- KING, C.A.M. 1972. Beaches and Coasts. (Edward Arnold). 570 pp.

- KIRK, R.M. 1980. Mixed sand and gravel beaches: morphology, processes and sediments. Prog. Phys. Geog. 4, pp 189-210.
- KNIGHTON, A.D. 1984. Fluvial Forms and Processes. (Arnold, London)
- KOMAR, P.D. 1976. Beach Processes and Sedimentation. (Prentice Hall).
- KOMAR, P.D. 1977. Selective longshore transport rates of different grain size fractions within a beach. J. Sed. Petrology 47(7), pp 1444-1453.
- KOMAR, P.D. & INMAN, D.L. 1970. Longshore sand transport on beaches. J. Geophys. Res. 75, pp 5914-5927.
- KÖSTER, R. 1971. Postglacial sea level changes on the German North Sea and Baltic shorelines. Quaternaria 14, pp 97-100.
- KRUMBEIN, W.C. 1941. Measurement and geological significance of shape and roundness of sedimentary particles. J. Sed. Petrology 11(2), pp 64-72.
- LAKE, R.D. & SHEPARD-THORN, E.R. 1987. Geology of the country around Hastings and Dungeness. B.G.S. memoir for 1:50 000 sheets 320 & 321 (England & Wales). (H.M.S.O.)
- LAMB, H.H. 1982. Climate, History and the Modern World. (Methuen, London).
- LAMB, H.H. 1991. Historic Storms of the North Sea, British Isles and Northwestern Europe. (Cambridge University Press, Cambridge).
- LAMBECK, K. 1991a. Glacial rebound and sea level change in the British Isles. Terra Nova 3, pp 379-389.
- LAMBECK, K. 1991b. A model for Devensian and Flandrian glacial rebound and sea level change in Scotland. In Sabadini, R., Lambeck, K. & Boschi, E. (eds.) Glacial Isostasy, Sea Level and Mantle Rheology. pp 33-62.
- LAUTERNAUER, J.L., CLAGUE, J.J., CONWAY, K.W., BARRIE, J.V., BLAISE, B. & LEATHERMAN, S.P. 1979. Migration of Assateague Island, Maryland, by inlet and overwash process. Geology 7, pp 104-107.
- LEATHERMAN, S.P. 1983a. Barrier island evolution in response to sea level rise: a discussion. J. Sed. Petrology 53, pp 1026-1031.
- LEATHERMAN, S.P. 1983b. Barrier dynamics and landward migration with Holocene sea level rise. Nature 301, pp 415-417.
- LEATHERMAN, S.P. 1989. Response of sandy beaches to sea level rise. In Scott, D.B. et al (eds.) Late Quaternary Sea Level Correlation and Applications. pp 57-69. NATO ASI Series. (Kluwer Academic).
- LEATHERMAN, S.P. 1991. Modelling shoreline response to sea level rise on sedimentary coasts. Prog. Phys. Geog. \*\*\*\*, pp 447-464.
- LEE, A.J. & RAMSTER, J.W. 1981. Atlas of the Seas around the British Isles. Fish Res Tech Rep., MAFF Direct. Fish Res., Lowestoft. 2pp+75 sheets.
- LEEDER, M.R. 1982. Sedimentology. (Allen & Unwin).

- LEONTYEV, O.K. 1969. Flandrian transgression and the genesis of barrier bars. In Schwartz, M.L. (ed.) Barrier Bars \*\*\*\*
- LEWIS, W.V. 1932. The formation of Dungeness foreland. Geogr. J. 80, pp 309-324.
- LEWIS, W.V. 1938. The evolution of shoreline curves. Proc. Geol. Ass. 49, pp 107-127.
- LEWIS, W.V. & BALCHIN, W.G.V. 1940. Past sea levels at Dungeness. Geogr. J. 96, pp 258-285.
- LONG, A. & FOX, S. 1988. The Geomorphology of Denge Beach. Report to NCC by the University of Durham, 1988.
- LOWE, J.J. & WALKER, M.J.C. 1977. The reconstruction of the Lateglacial environment in the southern and eastern Grampian Highlands. In Gray, J.M. & Lowe, J.J. (eds.) Studies in the Scottish Lateglacial Environment. pp 101-118. (Pergamon, Oxford).
- LOWE, J.J. & WALKER, M.J.C. 1984. Reconstructing Quaternary Environments. (Longman). 389 pp.
- MAIZELS, J. 1987. Geology and geomorphology of the Spey valley. In Jenkins, D. (ed) Land Use in the River Spey Catchment. Aberdeen centre for Land Use (ACLU) Symposium no 1, Grantown-on-Spey, 6-8th November 1987. pp 29-35.
- MAIZELS, J. & AITKEN, J. 1991. Palaeohydrological change during deglaciation in upland Britain: a case study from northeast Scotland. In Starkel, L., Gregory, K.J. & Thornes, J.B. (eds) Temperate Palaeohydrology: Fluvial Processes in the Temperate Zone during the last 15 000 years. (Wiley, Chichester), pp 105-146.
- MARCUS, W.A. & KEARNEY, M.S. 1991. Upland and coastal sediment sources in a Chesapeake Bay estuary. Ann. Ass. American Geogr. 81(3), pp 408-424.
- MAREX, 1975. Environmental Conditions East of the Shetlands. Stevenson Station Winter 1974/75. Marine Exploration Ltd. Report No. 170.
- MASON, C.C. & FOLK, R.L. 1958. Differentiation of beach, dune and aeolian flat environments by size analysis, Mustang Island, Texas. J. Sed. Petrol. 28, pp 211-226.
- MASON, S.J. 1985. Beach Development, Sediment Budget and Coastal Erosion at Holderness. Unpublished PhD thesis, University of Sheffield. (318 pp ).
- MASON, S.J. & HANSOM, J.D. 1986. Cliff erosion and its contribution to a sediment budget for part of the Holderness coast, England. Shore and Beach 56, pp 30-38.
- MASON, S.J. & HANSOM, J.D. 1988. A Markov model for beach changes on the Holderness coast of England. Earth Surface Processes and Landforms 14, pp 731-743.

- MATHEWES, R.W. 1989. Late Pleistocene terrestrial deposits on the continental shelf of western Canada: evidence for rapid sea level change at the end of the last glaciation. Geology 17, pp 357-360.
- MAY, J.P. 1974. WAVENRG: a computer program to determine the distribution of energy dissipation in shoaling water waves, with examples from coastal Florida. Symposium Proceedings 22-26. Dept. of Geology, Florida State University, Tallahassee, Florida.
- MAY, J.P. & TANNER, W.F. 1975. Estimates of net wave work along coasts. Z.für Geomorph. Supp.Bd. 22, pp 1-7.
- McCAVE, I.N. 1977. Sediments of the East Anglian Coast. E. Anglian Coastal Research Programme Report no. 6.
- McCLAREN, P. 1981. An interpretation of trends in grain size measures. J. Sed. Petrol. 51, pp 611-624.
- McCLEAN, R.F. & KIRK, R.M. 1969. Relationship between grain size, size sorting and foreshore slope on mixed sand-shingle beaches. New Zealand J. Geol. & Geophys. 12, p 138-155.
- McEWAN, L.J. & WERRITY, A. 1993. Findhorn Terraces. In Gordon, J.E. & Sutherland, D.J. (eds.) Quaternary of Scotland pp 187-189. (Joint Nature Conservation Committee GCR document). (Chapman & Hall, London). 695 pp.
- McMANUS, J. 1986. Land derived sediment and solute transport to the Forth and Tay estuaries, Scotland. J. Geol. Soc. London 143, pp 927-934.
- MERCER, J.H. 1978. West Antarctic ice sheet and CO<sub>2</sub> greenhouse effect: a threat of disaster. Nature 271, pp 321-325.
- MERRITT, J.W. 1990a. Evidence for events predating the maximum development of the last ice sheet. In Auton, C.W., Firth, C.R. & Merritt, J.W. (eds.) Beaulieu to Nairn: Field Guide. pp 1-2. (QRA, Cambridge). 149 pp.
- MERRITT, J.W. 1990b. New evidence for ?glaciomarine deltaic deposits at Alturlie gravel pit. In Auton, C.W., Firth, C.R. & Merritt, J.W. (eds.) Beaulieu to Nairn: Field Guide. pp 102-115. (QRA, Cambridge). 149 pp.
- MERRITT, J.W. & AUTON, C.W. 1990. The Dalcharn interglacial site near Cawdor, Nairnshire: lithostratigraphy. In Auton, C.W., Firth, C.R. & Merritt, J.W. (eds.) Beaulieu to Nairn: Field Guide. pp 41-54. (QRA, Cambridge). 149 pp.
- MILLIMAN, J.D. 1991. Flux and fate of fluvial sediment and water in coastal seas. In Mantoura, R.F.C, Martin, J.M. & Wollast, R. (eds.) Ocean Margin Processes and Global Change. pp 69-89. (Wiley).
- MØLLER, J.J. 1989. Geometric simulation and mapping of Holocene relative sea level changes in northern Norway. J. Coastal Research 5, pp 403-417.

- MÖRNER, N.A. 1971. Eustatic changes during the last 20 000 years and a method of separating the isostatic and eustatic factors in an uplifted area. Palaeogeography, Palaeolimnology, Palaeoecology. 9, pp 153-181.
- MÖRNER, N.A. 1976. Eustasy and geoid changes. J. Geology 84, pp 123-151.
- MÖRNER, N.A. 1987. Models of global sea level changes. In Tooley, M.J. & Shennan, I. (eds.) Sea Level Changes. pp 332-355. (Blackwell, Oxford). 397 pp.
- MORRISON, J., SMITH, D.E., CULLINGFORD, R.A. & JONES, R.L. 1981. The culmination of the Main postglacial transgression in the Firth of Tay area, Scotland. Proc. Geol. Ass. 92, pp 197-207.
- MUNK, W.H. & TRAYLOR, M.A. 1947. Refraction of ocean waves: a process linking underwater topography to beach erosion. J. Geol. 55, pp 1-26.
- MUTO, T. & BLUM, P. 1989. An illustration of a sea level control model from a subsiding coastal fan system: Pleistocene Ogasayama formation, C. Japan. J. Geology 97, pp 451-463.
- NAKATO, T. 1990. Tests of selected sediment transport formulas. J. Hydraulic Engineering 116(3), pp 362-379.
- NATURAL RESOURCES COUNCIL 1990. Sea Level Changes. (National Academic Press, Washington D.C.).
- NEATE, D.J.M. 1967. Underwater pebble grading of Chesil Beach. Proc. Geol. Ass. 78, pp 419-426.
- NERC. 1991. United Kingdom Digital Marine Atlas. Version 1.0, NERC/BODC, Birkenhead.
- NEWSON, M.D. & LEEKS, G.J. 1985. Mountain bedload yields in the United Kingdom: further information from undisturbed fluvial environments. Earth Surface Processes and Landforms 10, pp 413-416.
- NORDSTROM, K.F. 1989. Downdrift coarsening of beach foreshore sediments at tidal inlets: an example from the coast of New Jersey. Earth Surface Processes and Landforms 14, pp 691-701.
- OGILVIE, A.G. 1923. The physiography of the Moray Firth coast. Trans. R. Soc. Edinburgh LIII, pp 377-404.
- ORFORD, J.D. 1975. Discrimination of particle zonation on a pebble beach. Sedimentology 22, pp 441-463.
- ORFORD, J.D. 1977. A proposed mechanism for storm beach sedimentation. Earth Surface Processes and Landforms. 2, pp 381-400.
- ORFORD, J.D. 1987. Coastal processes: the coastal reponse to sea level variation. Ch. 13 in Devoy, R.J.N. (ed.), Sea Surface Studies. (Croon Helm).

- ORFORD, J.D., CARTER, R.W.G. & FORBES, D.L. 1991. Gravel barrier migration and sea level rise: some observations from Story Head Barrier, Nova Scotia, Canada. J. Coastal Res. 7, pp 477-488.
- O'SULLIVAN, P.E. 1976. Pollen analysis and radiocarbon dating of a core from Loch Pityoulish, Eastern Highlands of Scotland. J. Biogeography 3, pp 293-302.
- OVINGTON, J.D. 1950. The afforestation of the Culbin Sands. J. Ecology 38, pp 303-319.
- PARKER, G.G., HELY, A.G., KEIGHTON, W.B. & OLMSTED, F.H. 1964. Water resource of the Delaware river basin. Prof. Paper USGS 381, pp 1-200.
- PATERSON, I.B., 1974. The supposed Perth Re-advance in the Perth district. Scott. J. Geol. 10 (1), pp 53-66.
- PATERSON, I.B., ARMSTRONG, M., & BROWNE, M.A.E., 1981. Quaternary estuarine deposits in the Tay-Earn area, Scotland. Rep. Inst. Geol. Sci. 81/7.
- PAYNE, R., 1963. Bottom currents in the Moray Firth. Scottish Fisheries Bulletin 20, pp 26-27.
- PEACOCK, J.D., 1974. Borehole evidence for late- and post-glacial events in the Cromarty Firth, Scotland. Bul. Geol. Surv. G.B. 48, pp 55-67.
- PEACOCK, J.D., 1981. Scottish lateglacial marine deposits and their environmental significance. In Neale, J., & Flenley, J. (eds.) The Quaternary in Britain. pp 222-236. (Pergamon).
- PEACOCK, J.D., BERRIDGE, N.G., HARRIS, A.L. & MAY, F. 1968. The Geology of the Elgin District. Mem. Geol. Surv. G.B. Sheet 95.
- PEACOCK, J.D., GRAHAM, D.K. & WILKINSON, I.P. Lateglacial and postglacial marine environments at Ardyne, Scotland, and their significance in the interpretation of the history of the Clyde sea area. IGS report 787/17, Edinburgh. 25 pp.
- PEACOCK, J.D., GRAHAM, D.K., & GREGORY, D.M., 1980. Late- and postglacial marine environments in part of the Cromarty Firth, Scotland. Rep. Inst. Geol. Sci. 80/7.
- PELTIER, W.R. & ANDREWS, J.T. 1976. Glacio-isostatic adjustment I. The forward problem. Geophys. J. R. Astr. Soc. 46, pp 605-646.
- PETHICK, J., 1984. An Introduction to Coastal Geomorphology. (Arnold).
- PIERCE, J.W., 1970. Tidal inlets and washover fans. J. Geology 78, pp 230-234.
- PILKEY, O.H. & DAVIS, T.W., 1987. An analysis of coastal recession models: North Carolina coast. In Nummedal, D, Pilkey, O.H. & Howard, J.D. (eds.) Sea Level Fluctuations and Coastal Evolution. Society of Economic Palaeontologists & Mineralogists Special Publication 41, pp 59-68.

- PIRAZZOLI, P.A. 1990. Present and near-future sea level changes: an assessment. In Paepe, R. *et al* (eds.) Greenhouse Effect, Sea Level and Drought. pp 153-163. (Kluwer).
- PRESTWICH, J. 1875. On the origin of the Chesil Bank, and on the relation of the existing beaches to past geological changes independent of the present coast action. Minutes Proc. Inst. Civ. Engns. 40, pp 61-114.
- PRICE, R.J., 1983. Scotland's Environment During the Last 30 000 Years. (Scottish Academic Press). 224 pp.
- PUGH, D.T., 1990. Sea level rise. Ch. 4 in Doornkamp, J.C. (ed.) The Greenhouse Effect and Rising Sea Levels in the U.K. (M1 Press).
- QUINLAN, G. & BEAUMONT, C., 1981. A comparison of observed and theoretical postglacial relative sea level in Atlantic Canada. Canadian J. Earth Sciences 18, pp 1146-1163.
- RAMPINO, M.R. & SANDERS, J.R., 1983. Barrier island evolution in response to sea level change: reply. J. Sed. Petrology. 53, pp1031-1033.
- REID, G.S., 1988. Sediment distribution in the Moray Firth, N.E. Scotland: transport pathways, sources & sinks. Unpubl. PhD thesis, University of Dundee.
- REID, G.S. & McMANUS, J., 1987. Sediment exchanges along the coastal margin of the Moray Firth, eastern Scotland. J. Geol. Soc. London 144, pp 179-185.
- REID, I., FROSTICK, L.E. & LAYMAN, J.T., 1985. The incidence and nature of bedload transport during flood flows in coarse grained alluvial channels. Earth Surface Processes and Landforms 10, pp 33-45.
- RENWICK, W.H. & ASHLEY, G.M. 1984. Sources, storages and sinks of fine grained sediments in a fluvial-estuarine system. Geol. Soc. Am. Bul. 95, pp 1343-1348.
- RICHARDS, K & McCAIG, M., 1985. A medium term estimate of bedload yield in Allt a' Mhullin, Ben Nevis, Scotland. Earth Surface Processes and Landforms 10, pp 407-411.
- RITCHIE, W. 1979. Machair development and chronology of the Uists and adjacent isles. Proc. R. Soc. Edinburgh 78, pp 179-200.
- RITCHIE, W., SMITH, J.S. & ROSE, N. 1978. The Beaches of North East Scotland. Report to the Countryside Commission for Scotland. 278 pp.
- RITCHIE, W., WOOD, M., WRIGHT, R. & TAIT, D. 1988. Surveying and Mapping for Field Scientists. (Longman).
- ROBERTSON-RINTOUL, M.S.E., 1986. A quantitative soil-stratigraphic approach to the correlation and dating of post-glacial river terraces in Glen Feshie, western Cairngorms. Earth Surface Processes & Landforms 11, pp 605-617.

- ROSS, S.M. 1977. A marine clay from Burghead Bay. Moravian Field Club Bul. 5, pp19-20.
- ROSS, S.M. 1979. Erosion at the Culbin Sands 1979. Moravian Field Club Bul. 7, pp 18-19.
- ROSS, S.M. 1983. Erosion at Culbin Sands and Burghead Bay. Moravian Field Club Bul. 11, pp 21-23.
- ROSS, S.M. 1987. Erosion at Culbin Sands and Burghead Bay. Moravian Field Club Bul. 15, pp 17-18.
- ROSS, S.M. 1988. Erosion at Culbin Sands and Burghead Bay. Moravian Field Club Bul. 16, pp 31-33.
- ROSS, S.M. 1989. Erosion at Culbin Sands and Burghead Bay. Moravian Field Club Bul. 17, pp 27-29.
- ROSS, S.M. 1992. The Culbin Sands-Fact and Fiction. (Centre for Scottish Studies, University of Aberdeen).
- RUSSELL, R.J. 1968. Where most grains of very coarse sand and fine gravel are deposited. Sedimentology. 11, pp 31-38.
- SAMES, C.W. 1966. Morphometric data of some recent pebble associations and their application to ancient deposits. J. Sed. Petrology 36, pp 126-142.
- SCHUMM, S.A. & LICHTY, R.W. 1965. Time, space and causality in geomorphology. Am. J. Science 263, pp 110-119.
- SELF, R.P. 1977. Longshore variations in beach sands, Natula area, Veracruz, Mexico. J. Sed. Petrology. 47, pp 1437-1443.
- SHACKLETON, N.J. & OPDYKE, N.D. 1973. Oxygen isotope and palaeomagnetic stratigraphy of Equatorial Pacific core V28-238: oxygen isotope temperatures and ice volumes on a  $10^5$  and  $10^6$  year scale. Quat. Res. 3, pp 39-55.
- SHAW, J. & FORBES, D.L. 1990. Relative sea level change and coastal response, northeast Newfoundland. J. Coastal. Res. 6 (3), pp 641-660.
- SHENNAN, I. 1982. Interpretation of Flandrian sea level data from the Fenland, England. Proc. Geol. Ass. 93, pp 53-63,
- SHENNAN, I. 1983. A problem of definition in sea level research. Quat. Research 39, pp 17-19.
- SHENNAN, I. 1989. Holocene crustal movements and sea level changes in Great Britain. J. Quat. Sci. 4, pp 77-89.
- SHEPARD, F.P. 1950. Beach cycles in S. California. USACE Beach Erosion Board Memo. 20. 26 pp.
- SHEPARD, F.P. 1963. Submarine Geology. (Harper & Row, New York).

- SHORT, A.D. 1979. Three-dimensional beach stage model. J. Geol. 87, pp 553-571.
- SHORT, A.D. 1980. Beach response to variations in breaker height. Proc. 17th Coastal Engineering Conference, Sydney, NSW. ASCE 1980, pp 1016-1035.
- SHORT, A.D. 1991. Macro-meso tidal beach morphodynamics - an overview. J. Coastal Res. 7, pp 417-436.
- SISSONS, 1962 (1973). A re-interpretation of the literature on lateglacial shorelines with particular reference to the Forth area. Ch. 14 in Andrews, J.T. (ed.) Glacial Isostasy. pp 249-257. (Dowden, Hutchinson & Ross.).
- SISSONS, J.B. 1969. Drift stratigraphy and buried morphological features in the Grangemouth-Falkirk-Airth area, C. Scotland. Trans. Inst. Brit. Geog. 48, pp 19-50.
- SISSONS, J.B. 1981a. A former ice-dammed lake and associated glacier limits in the Achnasheen area, central Scotland. Trans. I.B.G. NS7, pp 98-116.
- SISSONS, J.B. 1981b. Lateglacial marine erosion and a jokulhlaup deposit in the Beaully Firth. Scott. J. Geol. 17 (1), pp 7-19.
- SISSONS, J.B. & BROOKS, 1971. Dating of early postglacial land and sea level changes in the western Forth valley. Nature 234, pp 124-127.
- SISSONS, J.B., SMITH, D.E. & CULLINGFORD, R.A. 1966 (1973). Lateglacial and postglacial shorelines in S.E. Scotland. Ch.15 in Andrews, J.T. (ed.) Glacial Isostasy. pp 259-273. (Dowden, Hutchinson & Ross).
- SMITH, D.E., SISSONS, J.B. & CULLINGFORD, R.A. 1969. Isobases for the Main Perth raised shoreline in S.E.Scotland as determined by trend surface analysis. Trans. I.B.G. 46, pp 45-52.
- SMITH, D.E., MORRISON, J., JONES, R.L. & CULLINGFORD, R.A. 1980. Dating the Main Postglacial Shoreline in the Montrose area, Scotland. In Cullingford, R.A., Davidson, D.A. & Lewin, J. (eds.) Timescales in Geomorphology. pp 225-245. (Wiley).
- SMITH, D.E., CULLINGFORD, R.A. & SEYMOUR, W.P. 1982. Flandrian relative sea level changes in the Philorth valley, N.E. Scotland. Trans.I.B.G. 7, pp 321-336.
- SMITH, D.E., CULLINGFORD, R.A. & BROOKS, C.L, 1983. Flandrian relative sea level changes in the Ythan valley, N.E. Scotland. Earth Surface Processes & Landforms 8, pp 423-438.
- SMITH, D.E., DAWSON, A.G., CULLINGFORD, R.A. & HARKNESS, D.D. 1985. The stratigraphy of Flandrian relative sea level changes at a site in Tayside, Scotland. Earth Surface Processes & Landforms 10, pp 17-25.

- SMITH, J.S. 1966. Morainic limits and their relationship to raised shorelines in the eastern Scottish Highlands. Trans. I.B.G., 39, pp 61-64.
- SMITH, J.S. 1968. Shoreline Evolution in the Moray Firth. Unpubl. PhD thesis, University of Aberdeen.
- SMITH, J.S. 1977. The last glacial epoch around the Moray Firth. Inverness Field Club Sp. Vol. pp 72-82.
- SMITH, J.S. 1986. The coastal topography of the Moray Firth. Proc. R. Soc. Edinburgh. 91B, pp1-2.
- SNEED, E.D. & FOLK, R.F. 1958. Pebbles in the Lower Colorado River, Texas. A study in particle morphogenesis. J. Geol. 66, pp 114-150.
- SOLLID, J.L., ANDERSON, S., HAMRE, N., KJELDSEN, O., SALVIGSEN, O., STURØD, S., TVEITA, T & WILHELMSON, A. 1973. Deglaciation of Finnmark, North Norway. Norsk Geografisk Tidsskrift 27, pp 233-325.
- SONU, C.J. 1973. Three dimensional beach changes. J. Geol. 81, pp 42-64.
- SONU, C.J. & YOUNG, M.H. 1971. Stochastic analysis of beach profile data. Proc. 12th Coastal Engineering Conference, Washington D.C. ASCE 1970.
- SONU, C.J. & VAN BEEK, J.L. 1971. Systematic beach changes on the Outer Banks, North Carolina. J. Geol. 79, pp 416-425.
- STEERS, J.A. 1926. Orford Ness: A study in coastal physiography. Proc. Geol. Ass. 37, pp 306-325.
- STEERS, J.A. 1937. The Culbin Sands and Burghead Bay. Geogr. J. 90, pp 498-528.
- STEERS, J.A. & SMITH, D.B. 1956. Detection of movement of pebbles on the sea floor by radioactive methods. Geog. J. 122, pp 343-345.
- STEPHENS, N. & McCABE, A.M. 1977. Late Pleistocene ice movements and patterns of Late- and Postglacial shorelines on the coast of Ulster. In Kidson, C. & Tooley, M.J. (eds.) The Quaternary History of the Irish Sea Geol. J.. Sp. Issue 7, pp 179-198.
- STIEGELER, S.E. 1976. A Dictionary of Earth Sciences. (Macmillan, London). 301 pp.
- STUIVER, M., BRAZIUNAS, T., BECKER, B. & KROMER, B. 1991. Climatic, solar, oceanic and geomagnetic influences on Late-glacial and Holocene Atmospheric  $^{14}\text{C}/^{12}\text{C}$  change. Quat. Research 35, pp 1-24.
- SUTHERLAND, D.G. 1984. The Quaternary deposits and landforms of Scotland and the neighbouring shelves: a review. Quat. Sci. Reviews 3. pp157-254.
- SWAIN, A. 1989. Beach profile development. Ch.7 in Lakhan, V.C. & Trenhaile, A.S. (eds.) Applications in Coastal Modelling. (Elsevier).

- SWIFT, D.J.P. 1975. Barrier island genesis: evidence from the central Atlantic shelf, E. U.S.A. Sed. Geol. 14, pp 1-43.
- SYNGE, F.M. 1956. The glaciation of north east Scotland. Scott. Geog. Mag. 72, pp 129-143.
- SYNGE, F.M. 1977. Land and sea level changes during the waning of the last regional ice sheet in the vicinity of Inverness. in Gill, G. (ed) The Moray Firth Area Geological Studies. Inverness Field Club Sp. Vol., pp 88-102.
- SYNGE, F.M. & SMITH, J.S. 1980. Inverness: Field Guide. Quaternary Research Association, Cambridge.
- TANNER, W.F. 1959. Near-shore studies in sedimentology and morphology along the Florida Panhandle coast. J. Sed. Petrol. 29, pp 564-574.
- THORNE, K.L. & GLEASON, R. 1986. Waves recorded off Kinnairds Head. IOS Report no. 226.
- TITUS, J.G. 1987. The greenhouse effect, rising sea level and society's response. In Devoy. R.J.N. (ed). Sea Surface Studies: A Global View. (Croon Helm, London) 649 pp.
- TOOLEY, M.J. 1974. Sea level changes during the last 9000 years in N.W.England. Geogr. J. 140, pp 18-42.
- TOOLEY, M.J. 1978. Sea level changes in NW England during the Flandrian Stage. (Clarendon, Oxford).
- TOOLEY, M.J. 1980. Theories of coastal change in N.W. England. In Thompson, F.H. (ed.) Archaeology and Coastal Change. pp 74-86.
- TOOLEY, M.J. 1982. Sea level changes in northern England. Proc. Geol. Association. 93, pp 43-51.
- TOOLEY, M.J. 1985a. Sea level changes and coastal geomorphology in N.W. England. In Johnson, R.H. (ed.) The Geomorphology of N.W. England. pp 94-121. (Manchester University Press, Manchester).
- TOOLEY, 1985b. Climate, sea level and coastal changes. In Tooley, M.J. & Sheail, G.M. (eds.) The Climatic Scene pp 206-234. (Allen & Unwin, London).
- TRASK, P.D. 1955. Movement Around S. Californian Promontories. BEB Tech. Memo. no. 76.
- TOOLEY, 1990. The chronology of coastal dune development in the United Kingdom. In Bakker, Th. W., Jungerius, P.D. & Klijn, J.A. (eds) Dunes of the European Coasts. Geomorphology-Hydrology-Soils. Catena Supplement. 18, pp 81-88.
- TUCKER, M.J. 1950. Surf beats: sea waves of 1 to 15 minute period. Proc. R. Soc. London Series A 202, pp 565-573.

- TUSHINGHAM, A.M. & PELTIER, W.R. 1993. Implications of the radiocarbon timescale for ice sheet chronology and sea-level change. Quat. Research 39, pp 125-129.
- UNITED NATIONS, 1982. Technologies for Coastal Erosion Control. Dept. of International Economic & Social Affairs, Ocean Economics and Technology Branch Report ST/ESA/116. 132pp. New York, 1982.
- VAN DE PLASSCHE, O. & ROEP, T.B. 1989. Sea level changes in the Netherlands during the last 6500 years: basal peat vs. coastal barrier data. In Scott, D.B., Pirazzoli, P.A. & Honig, C.A. (eds.) Late Quaternary Sea Level Corelation and Applications. pp 41-56. N.A.T.O. ASI Series. (Kluwer Academic).
- VILES, H. 1989. The greenhouse effect, sea level rise and coastal geomorphology. Prog. Phys. Geog. \*\*\*\*, pp 452-461.
- VINCENT, C.E. 1979. Longshore sand transport rates - a simple model for the East Anglian coastline. Coastal Engineering 3, pp 113-136.
- WALCOTT, R.I. 1975. Recent and late Quaternary changes in water level. Trans. Am. Geophys. Union. 56, pp 62-72.
- WALKER, M.J.C. 1975. Lateglacial and early Postglacial environmental history of the central Grampian Highlands, Scotland. J. Biogeog. 2, pp 265-284.
- WALLACE, T.D. 1896. Recent geological changes and the Culbin Sands. Trans. Inverness Sc., Soc. and Field Club 5, pp105-109.
- WALTON, T.L. 1977. Beach Nourishments in Florida and on the Lower Atlantic and Gulf Coasts. Florida Sea Grant Tech. Paper No. 2.(University of Florida).
- WALTON, T.L. & PORPURA, J.A. 1977. Beach nourishment along the southeast Atlantic and Gulf coasts. Shore and Beach 45, pp 10-18.
- WARD, G. 1931. Saxon Lydd. Archaeologica Cantiana 43, pp 29-37.
- WARRICK, R.A. & BARROW, E.M. 1991. Climate change scenarios for the U.K. Trans. I.B.G. N.S. 16, pp 387-399.
- WENDLAND, W.M. & BRYSON, R.A. 1974. Dating climatic episodes of the Holocene. Quat. Research 4, pp 9-24.
- WINKELMOLEN, A.M. 1978. Size, shape and density sorting of beach material along the Holderness coast, Yorkshire. Proc. Yorks. Geol. Soc. 42, pp 109-141.
- WOODWORTH, P.L. 1987. Trends in U.K. mean sea level. Marine Geodesy 11, pp 57-87.
- WRIGHT, L.D., CHAPPELL, J, THOM, B.G. BRADSHAW, M & COWELL, P. 1979. morphodynamics of reflective and dissipative beach and inshore systems, S. Australia. Mar. Geol. 32, pp 105-140.
- WRIGHT, L.D & SHORT, A.D. 1982. Dynamics of a high energy dissipative surf-zone. Mar. Geol. 45, pp 41-62.

WYATT, L.R. 1990. Progress in the interpretation of HF sea echo: HF radar as a remote sensing tool. I.E.E. Proc. 137 pt F no. 2. April 1990.

YOUNG, J.A.T. 1978. The landforms of upper Strathspey. Scott. Geog. Mag. 94, pp 76-94.

ZENKOVITCH, V.P. 1967. Processes of Coastal Development. (ed Steers, J.A.) (Oliver & Boyd, Edinburgh).

## GLOSSARY

**BP** Before present.

**DEVENSIAN** The period between 124 000 and 10 000 BP .The Devensian spans the time period between the last (Ipswichian) interglacial (oxygen isotope stage 5e, Heijnis, 1990) and the end of the Lateglacial Stadial (Younger Dryas) (Price, 1983).

**GEOID** The equipotential surface of the global ocean. Because this is related to terrestrial gravity (Fairbridge, 1983), this surface will not be perfectly spherical.

**HOLOCENE or FLANDRIAN** The period between 10 000 BP and the present (Price, 1984; Lowe & Walker, 1984; Firth, 1984).

**ISOBASE** "A line joining points of equal post-glacial emergence...where these elevations are the result of...emergence operating over the same period of time." (Andrews, 1970).

**LATE DEVENSIAN** This period has been poorly defined. Some see the end of this period coinciding with the end of the last major Scottish ice sheet ca 13 000 BP (Shackleton & Opdyke, 1973), while others consider the end to coincide with the end of the Younger Dryas ca. 10 000 BP (Firth, 1984).

**LATEGLACIAL (WINDERMERE) INTERSTADIAL** Period of climatic amelioration ca. 13 000 - 11 000 BP, after the decay of Devensian ice and prior to the onset of the Loch Lomond Stadial.

**LOCH LOMOND STADIAL** Period of limited glacial re-advance experienced in Scotland, the English Lake District and upland Wales. The limits of this period are generally accepted as between 11 000 and 10 000 BP (Price, 1983; Lowe & Walker, 1984). This period correlates with the Younger Dryas period of NW Europe.

**ORDNANCE DATUM (OD)** Altitudinal control marker defined from readings of mean sea level at Newlyn (Cornwall) between 1915-21.(Ritchie *et al.*, 1977). All altitudes referred to in this thesis are relative to OD for comparative analysis as part of IGCP project 274.

**POSTGLACIAL** A second poorly defined time period. The definition for the purposes of this work will follow that of Firth (1984), who correlated it with the Flandrian.

**QUATERNARY** The last subdivision (Period) of geological time, which includes the present day (Bowen, 1978). The Quaternary spans the last 1.6-1.8 million years of geological time (Lowe & Walker, 1984), and includes the Pleistocene (2 million - 10 000 years ago) and the Holocene (10 000 - present) epochs.

**RAISED BEACH** It is proposed that the term raised beach referred to extensively in early literature be dropped from general useage. The term "beach" in the contemporary environment is defined loosely:-

"...an accumulation of loose materials around the limit of wave action." (King, 1959).

"...the seaward zone over which sediments may be moved by waves." (Pethick, 1984).

"...an accumulation of loose sediment...sometimes confined to the backshore but often extending across the foreshore as well." (Bird, 1984).

Komar (1976a) used the term "littoral zone" to include the submarine portion of the beach out to ca 10-20 m depth as a fully inclusive geomorphological definition of the "beach" rather than simply the subaerial zone. If this definition were accepted then the "beach" could exist in a vertical plane between -20 & +13.1 m (Carr, 1971) of mean sea level, causing considerable problems in altitudinal control of raised "beach" features. The term "raised shoreline" has been more recently accepted in marine studies. Bird (1984) defined the shorelline as

"...strictly the water's edge, migrating to and fro with the tide."

whilst Firth (1984) defined the shoreline as

"...a synchronous marine or lacustrine water level and as such is not represented by a morphological feature."

This view was mirrored by Smith (1968), who noted that the term "shoreline" implied a morphological feature which in reality did not exist:- it is simply not possible to pinpoint a fossil shoreline on a raised coastal feature. In the light of this it is proposed to use the term "raised shoreline", but to follow the criterion set

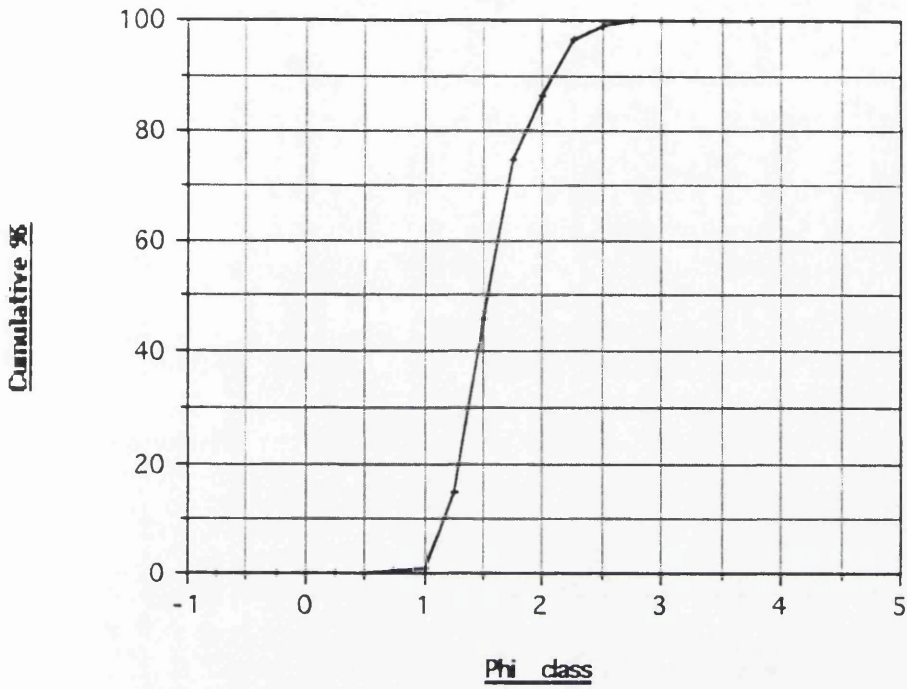
by Smith (1968) by referring to the shoreline as *the highest line washed by the sea* .

**RELATIVE SEA LEVEL (RSL)** The apparent level of the sea at a fixed time in relation to the vertical trend in either isostatic and/or eustatic elements.

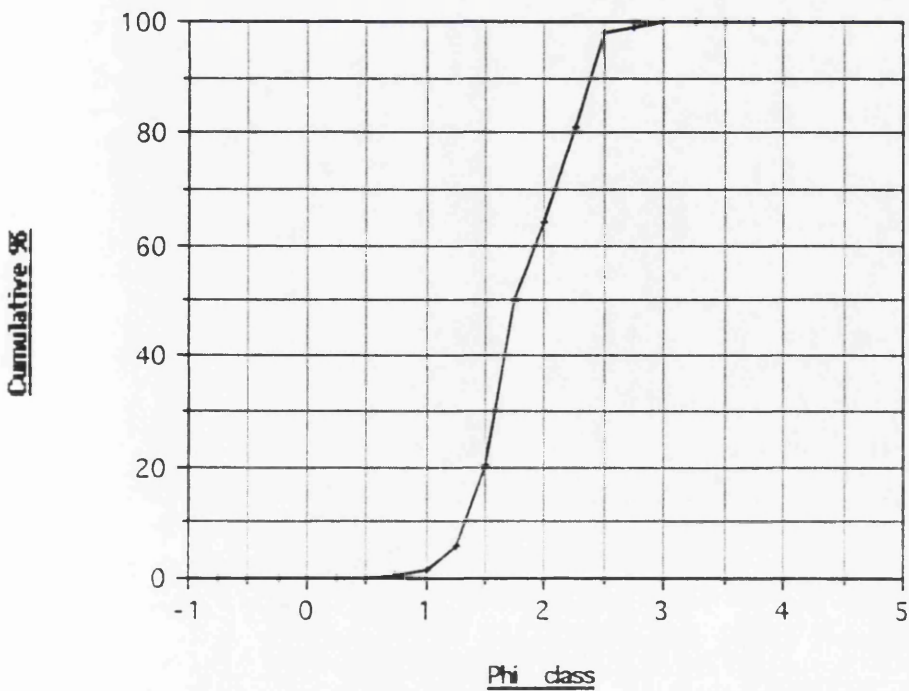
## **APPENDICES**

Appendix 1 Cumulative percentage curves: Culbin foreshore sediment samples

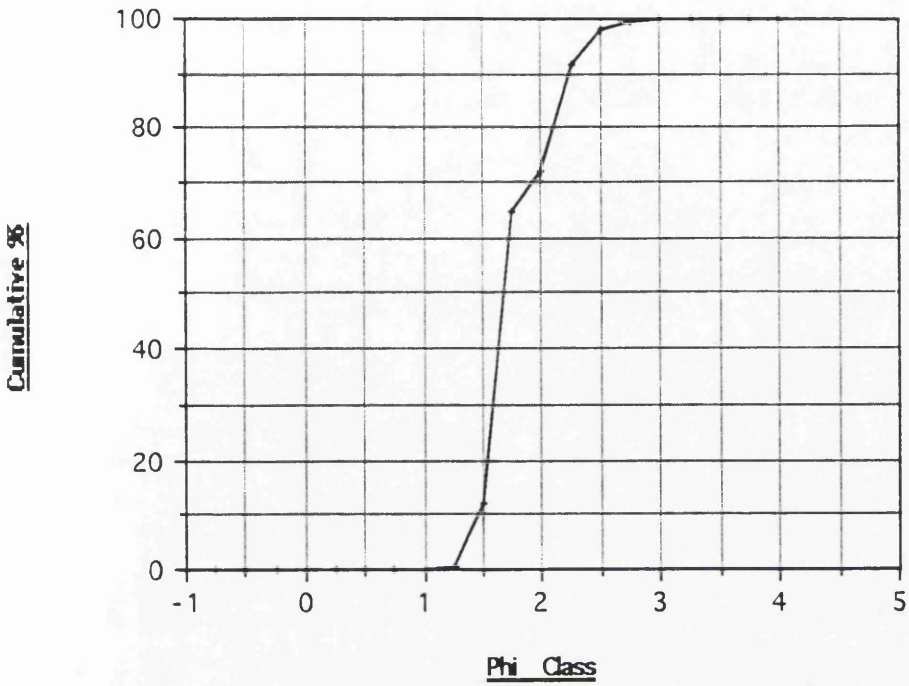
Findhorn Bay Station



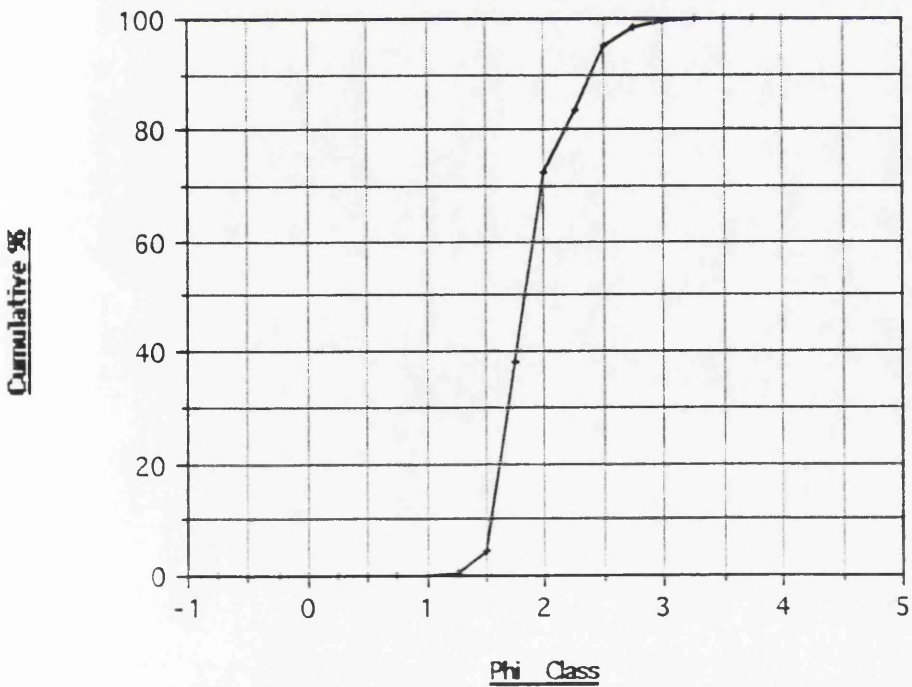
Findhorn Mouth Station



Station 1



Station 2



### Station 3

Cumulative %



Phi class

### Station 4

Cumulative %

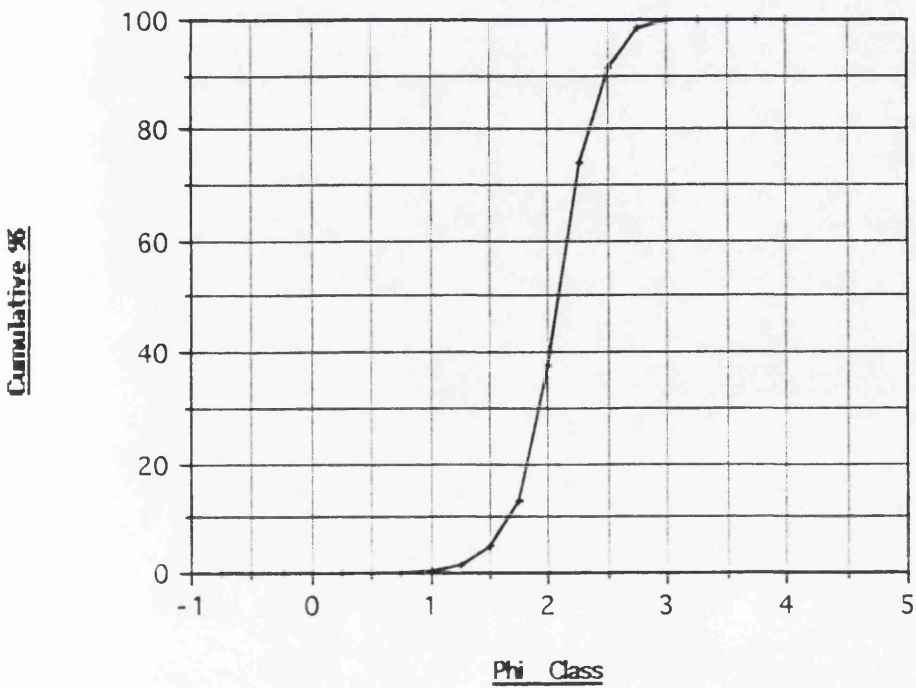


Phi Class

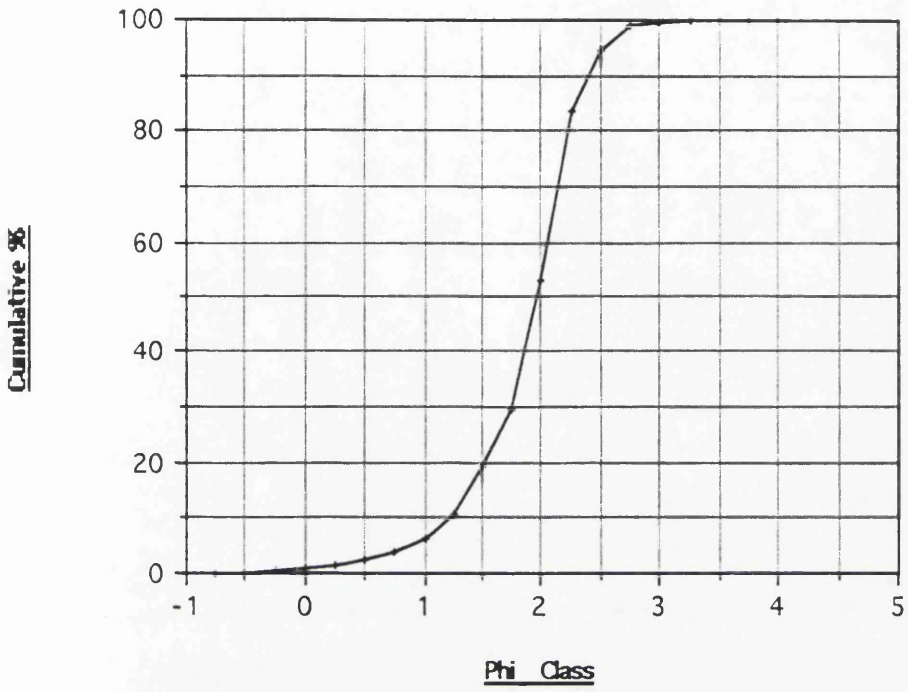
Station 5



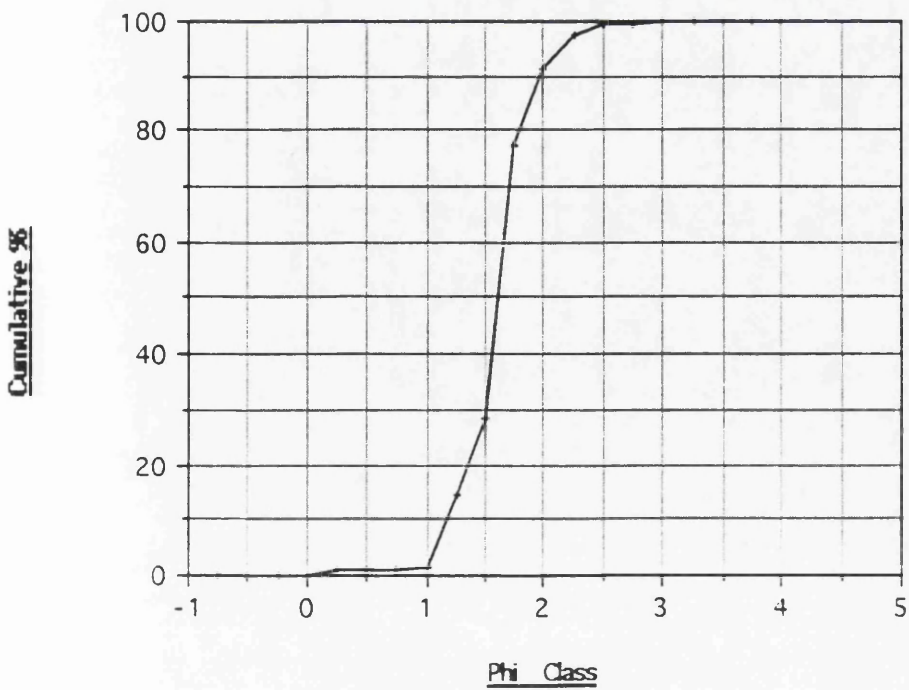
Station 6



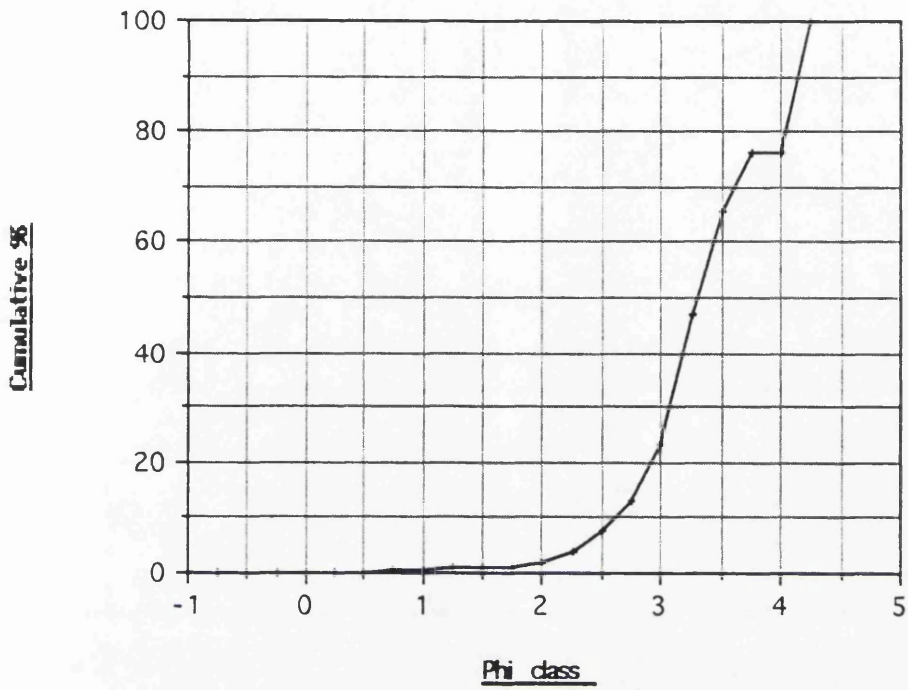
Station 7



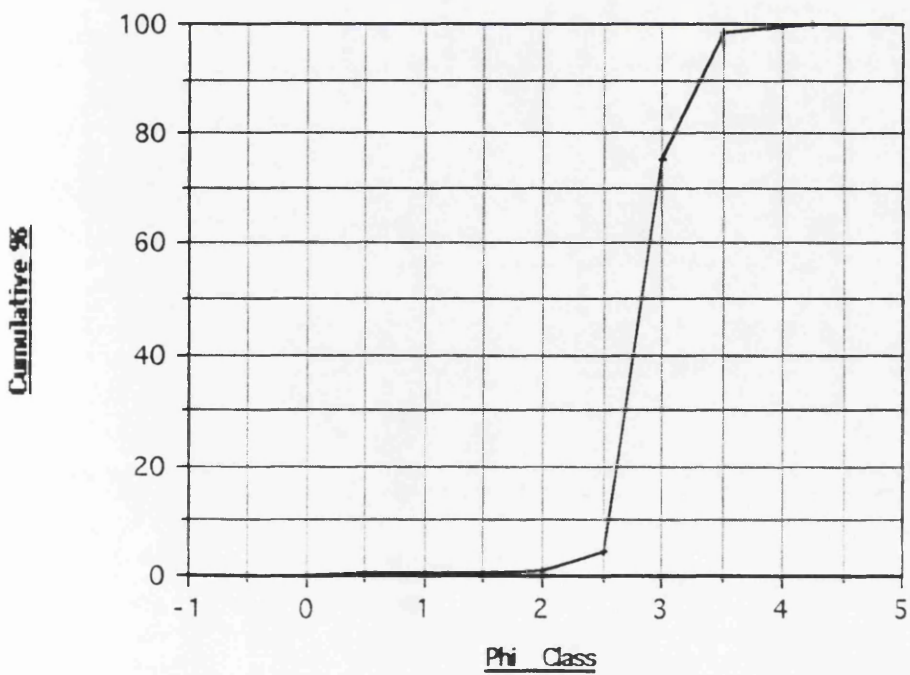
Contemporary Dune Sand (Station 5)



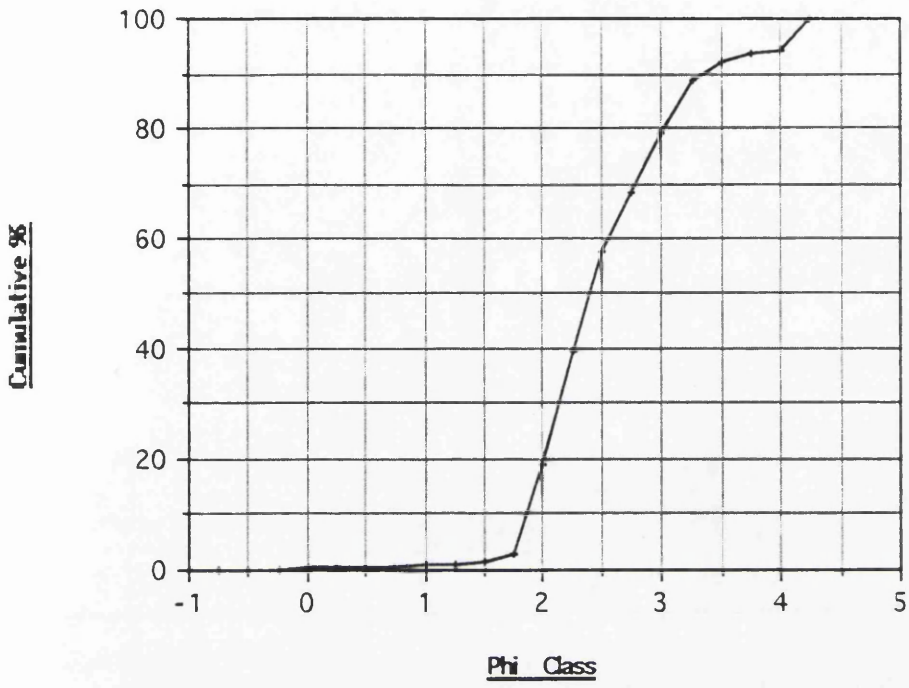
Site LAG 1



Site LAG 2



Site LAG 3



## Appendix 2 Volumetric reconstruction of the Spey Terrace sequence

The reconstruction of the Spey river terraces depended on dividing the area mapped by Peacock *et al.* (1969) into three zones; north, central and south. This made the calculation of the volume of sediment formerly contained within each terrace fragment much more accurate. North refers to terrace fragments seawards of terrace I (NJ 340610), while the southern terraces extend from Burnside of Dipple (NJ 330570) to the point of valley constriction between Haugh of Orton (NJ 314539) and Collie Farm (NJ 312516). The central zone lies between these two points.

### SOUTH

$$\text{ABE} = 2.28 \text{ km}^2 = 2\,280\,000 \text{ m}^2$$

$$\text{Depth} = 5 \text{ m}$$

$$\text{Volume} = 11\,400\,000 \text{ m}^3$$

$$= 11\,400\,000 \text{ m}^3$$

$$\text{II} = 1.33 \text{ km}^2 = 1\,330\,000 \text{ m}^2$$

$$\text{Effective depth} = 7.5 \text{ m}$$

$$\text{Volume} = 9\,975\,000 \text{ m}^3$$

$$+ (2\,280\,000 \text{ m}^3) \times 15 \text{ m}$$

$$= 44\,175\,000 \text{ m}^3$$

$$\text{IV} = 1.13 \text{ km}^2 = 1\,130\,000 \text{ m}^2$$

$$\text{Effective depth} = 5 \text{ m}$$

$$\text{Volume} = 5\,650\,000 \text{ m}^3$$

$$+ (2\,280\,000 \text{ m}^3 + 1\,330\,000) \text{ m}^3 \times 10 \text{ m}$$

$$= 41\,750\,000 \text{ m}^3$$

$$\text{TOTAL SOUTH} = 97\,325\,000 \text{ m}^3$$

### CENTRAL

$$\text{ABE} = 1.68 \text{ km}^2 = 1\,680\,000 \text{ m}^2$$

$$\text{Depth} = 11 \text{ m}$$

$$\text{Volume} = 18\,480\,000 \text{ m}^3$$

$$= 18\,480\,000 \text{ m}^3$$

$$\text{C} = 0.69 \text{ km}^2 = 690\,000 \text{ m}^2$$

$$\text{Effective depth} = 5 \text{ m}$$

$$\text{Volume} = 3\,450\,000 \text{ m}^3$$

$$+ (1\,680\,000 \text{ m}^3) \times 10 \text{ m}$$

$$= 20\,250\,000 \text{ m}^3$$

$$II = 2.08 \text{ km}^2 = 2\,080\,000 \text{ m}^2$$

$$\text{Effective depth} = 5 \text{ m}$$

$$\text{Volume} = 10\,400\,000 \text{ m}^3$$

$$+(1\,680\,000 \text{ m}^3 + 690\,000 \text{ m}^3) \times 10 \text{ m}$$

$$= 34\,100\,000 \text{ m}^3$$

$$\text{TOTAL CENTRAL} = 72\,830\,000 \text{ m}^3$$

## **NORTH**

$$ABE = 5.65 \text{ km}^2 = 5\,650\,000 \text{ m}^2$$

$$\text{Depth} = 10 \text{ m}$$

$$\text{Volume} = 56\,500\,000 \text{ m}^3$$

$$= 56\,500\,000 \text{ m}^3$$

$$I = 1.95 \text{ km}^2 = 1\,950\,000 \text{ m}^2$$

$$\text{Effective depth} = 2 \text{ m}$$

$$\text{Volume} = 3\,900\,000 \text{ m}^3$$

$$+(5\,650\,000 \text{ m}^3) \times 4 \text{ m}$$

$$= 26\,500\,000 \text{ m}^3$$

$$II = 3.04 \text{ km}^2 = 3\,040\,000 \text{ m}^2$$

$$\text{Effective depth} = 4.5 \text{ m}$$

$$\text{Volume} = 13\,680\,000 \text{ m}^3$$

$$+(5\,650\,000 \text{ m}^3 + 1\,950\,000 \text{ m}^3) \times 9 \text{ m}$$

$$= 82\,080\,000 \text{ m}^3$$

$$\text{TOTAL NORTH} = 165\,080\,000 \text{ m}^3$$

$$\text{Total spey terraces} = 97\,325\,000$$

$$72\,830\,000$$

$$\underline{165\,080\,000}$$

$$335\,230\,000 \text{ m}^3$$

### Appendix 3 Mann-Whitney U Test: Shingle Ridge Sets B & C

$H_0$ : No significant difference exists between the altitudes of the two ridge sets.

$H_1$ : A significant difference exists between the altitude of the two ridge sets.

Testing U using 2-tailed test at  $\alpha_2 = 5\%$ .

Test Statistic:

$$RB - [0.5MB(MB+1)] = 59 = U'$$

$$RC - [0.5MC(MC+1)] = 29 = U$$

Test value (U) must be  $\leq$  tabulated value. Using  $n_1=8$ ,  $n_2=11$ , tabulated value = 19 (Neave, 1981). Test statistic = 20.

$\therefore$  At the stated rejection level we cannot reject the null hypothesis, & hence no statistically significant difference exists between the altitude of shingle ridge sets B and C.

#### Appendix 4 Mann-Whitney U test: upper & lower shingle ridges in set D

$H_0$ : No significant difference exists between the altitudes of the upper and lower shingle ridges in set D.

$H_1$ : A significant difference exists between the altitudes of the upper and lower shingle ridges in set D.

Testing using 2-tailed test at  $\alpha = 5\%$ .

Test statistic:

$$R_A - [0.5M_A(M_A + 1)] = 20 = U$$

$$R_B - [0.5M_B(M_B + 1)] = 80 = U'$$

Test value must be  $\leq$  tabulated value. Using  $n_1 = 10$ ,  $n_2 = 10$ , tabulated value = 23 (Neave, 1981). Test statistic = 20.

$\therefore$  At the stated rejection level, we can reject the null hypothesis, & hence a statistically significant difference exists between the altitudes of the upper and lower shingle ridges in set D.

## Appendix 5 Mann-Whitney U test: Culbin Forest shingle ridge clast analysis, sites 2 & 6

$H_0$ : No significant difference exists between the mean 'b' axis lengths of the two sample populations.

$H_1$ : The mean clast 'b' axis length of clasts at site 6 was greater than those at site 2.

Testing using directional (1-tailed) test at  $\alpha_1 = 5\%$

Test statistic:

$$R_A - [0.5M_A(M_A + 1)] = 825 = U$$

$$R_B - [0.5M_B(M_B + 1)] = 1576 = U''$$

Test value must be  $\leq$  tabulated value. Using  $n_1 = 50$ ,  $n_2 = 50$ , tabulated value = 1010 (Neave, 1981). Test statistic = 825.

At the stated rejection level, we can reject the null hypothesis.

$\therefore$  The clast sizes recorded at site 6 are statistically larger than those recorded at site 2.

This supported the visual inspection of the data, which also suggested an east-west increase in mean clast size across the relict shingle ridges in Culbin Forest.

## Appendix 6 Mann-Whitney U test: The Bar clast analysis, sites 1 & 5

$H_0$ : No significant difference exists between the mean 'b' axis lengths of the two sample populations.

$H_1$ : The mean clast 'b' axis length of clasts at site 5 was greater than those at site 1.

Testing using directional (1-tailed) test at  $\alpha_1 = 5\%$

Test statistic:

$$R_A - [0.5M_A(M_A + 1)] = 940.5 = U$$

$$R_B - [0.5M_B(M_B + 1)] = 1302 = U''$$

Test value must be  $\leq$  tabulated value. Using  $n_1 = 50$ ,  $n_2 = 50$ , tabulated value = 1010 (Neave, 1981). Test statistic = 940.5.

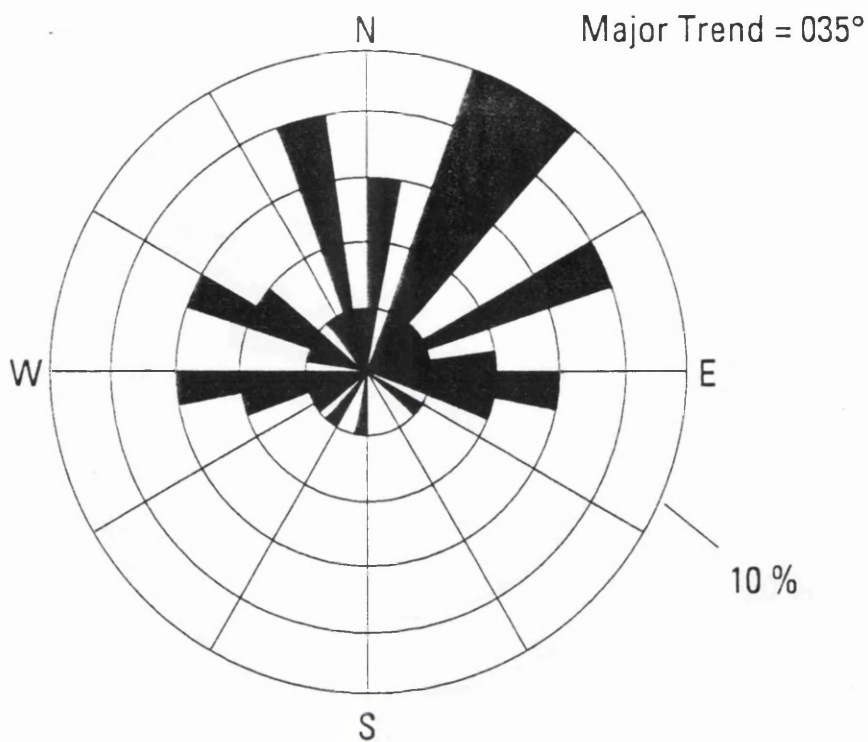
At the stated rejection level, we can reject the null hypothesis.

$\therefore$  The clast sizes recorded at site 5 are statistically larger than those recorded at site 1.

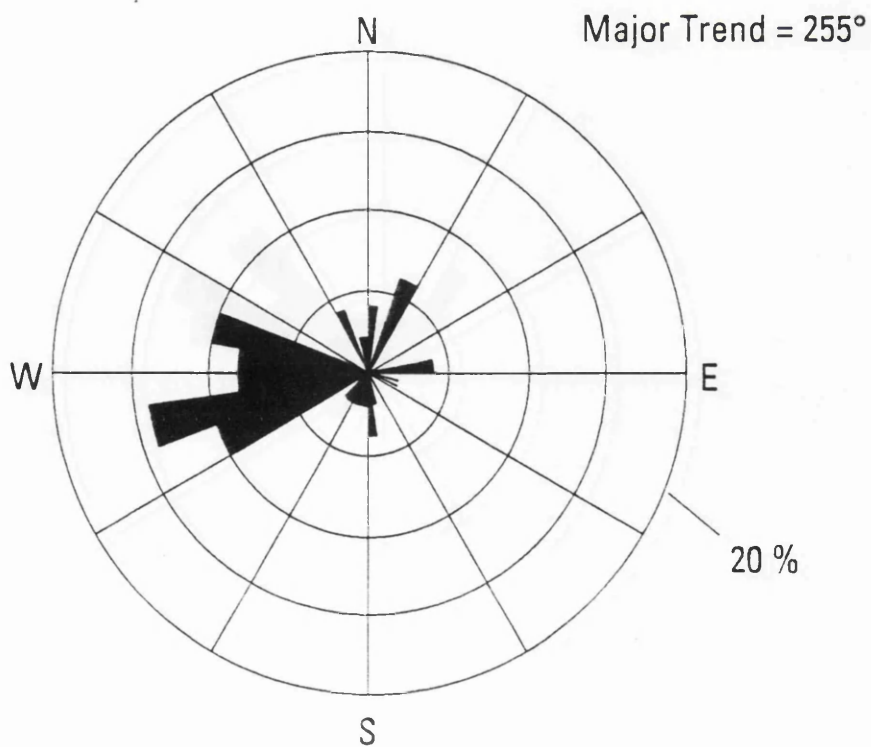
This supports the visual inspection of the data, which also suggested that down-drift coarsening was recorded along the western flank of The Bar.

Appendix 7 Clast fabric diagrams from Burghead Bay cliff section

SITE 1



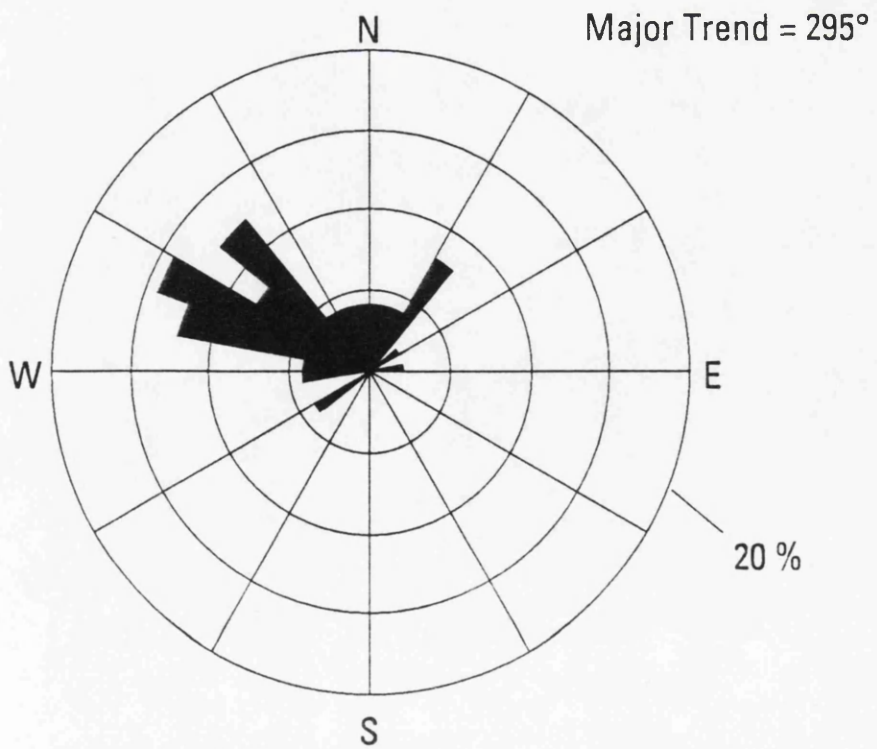
SITE 2



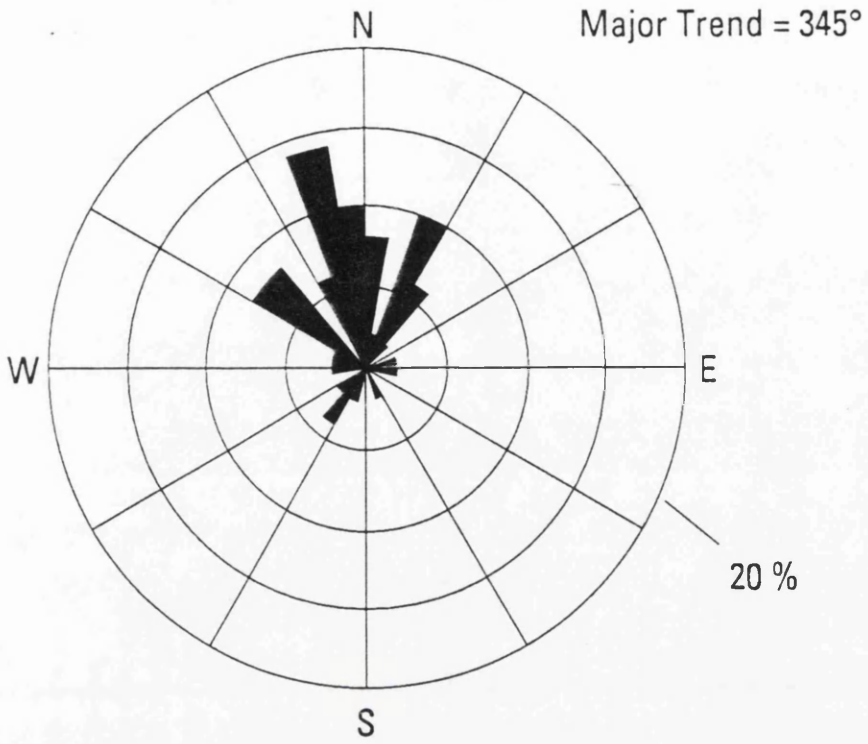
### SITE 3



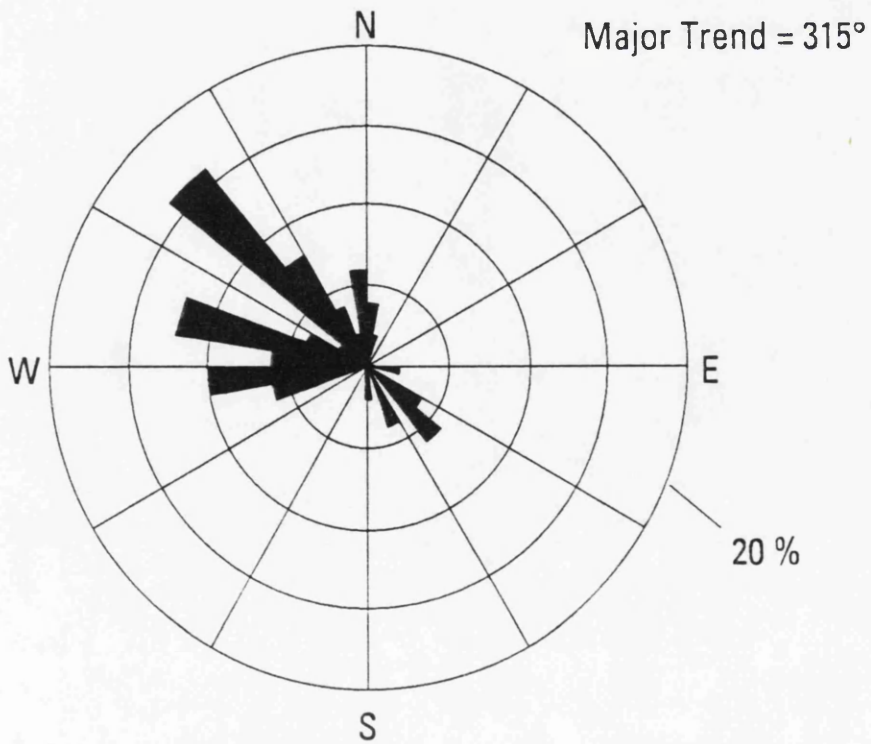
### SITE 4



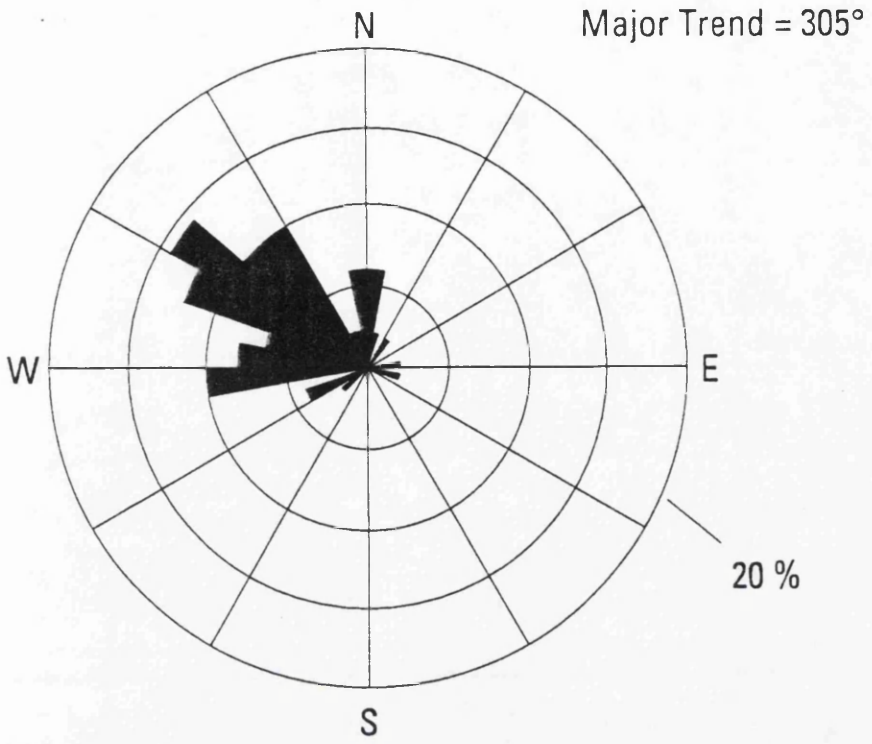
### SITE 5



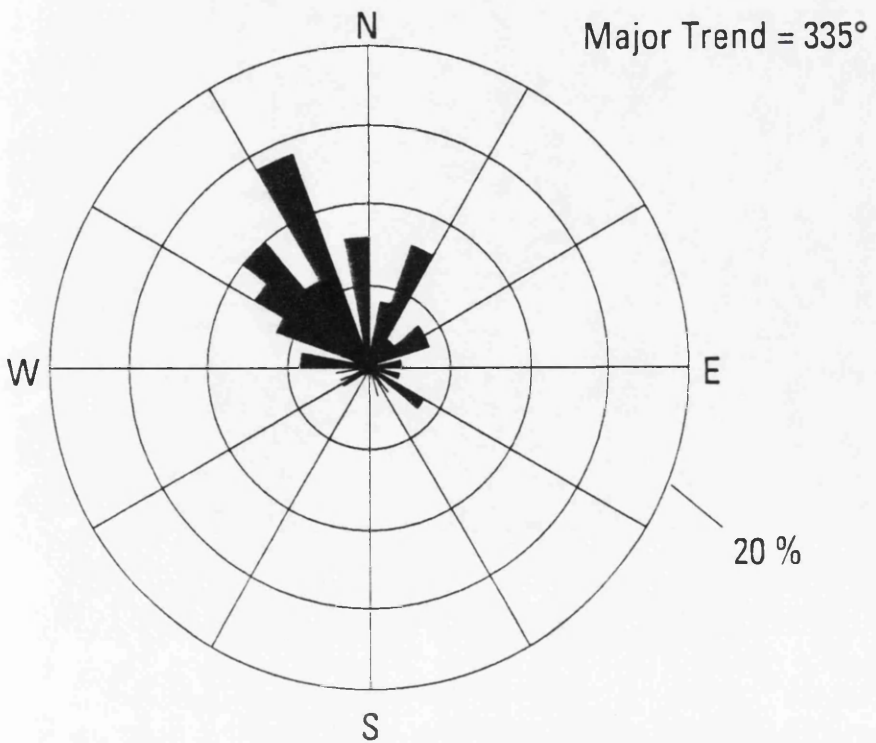
### SITE 6



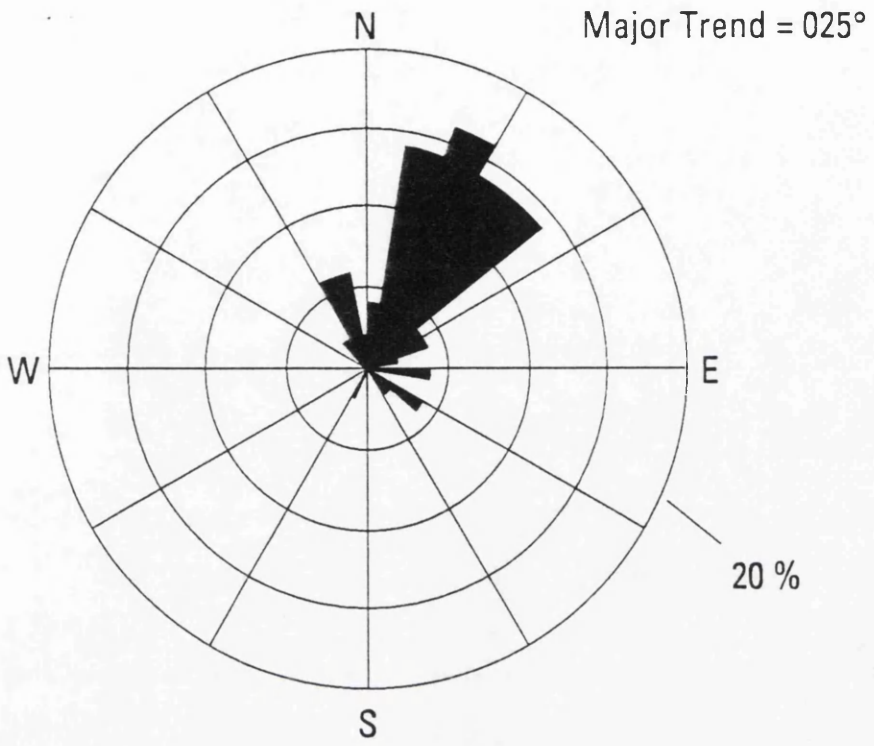
SITE 7



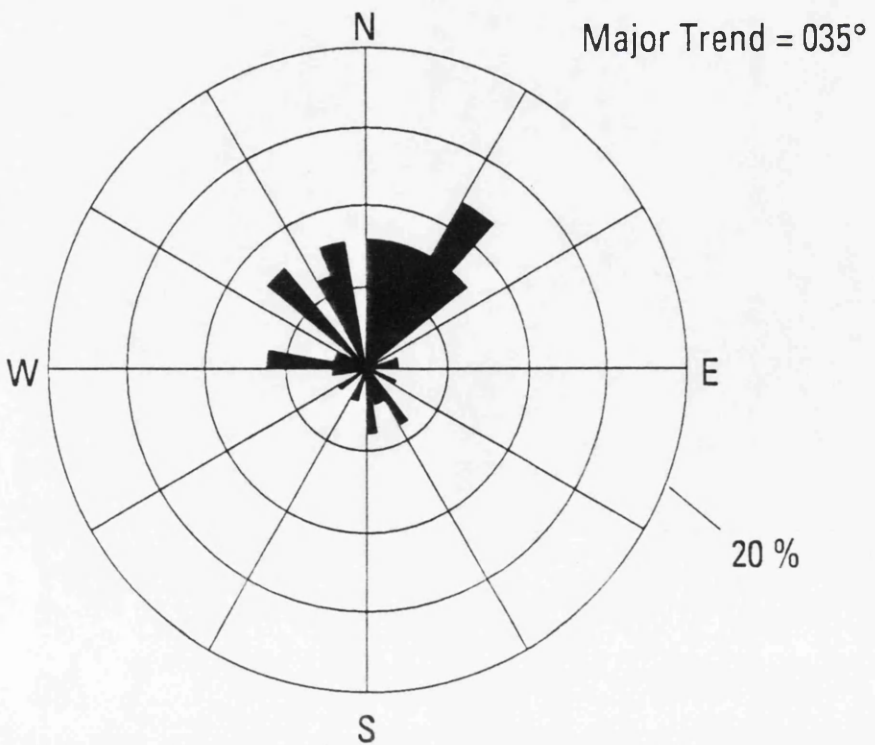
SITE 8



### SITE 9



### SITE 10



## Appendix 8. Calculation of vector magnitude in coarse clastic deposits

The calculation of vector magnitude is a technique designed to aid in the preliminary interpretation of the depositional environment of a sedimentary unit. The calculation proceeds in three stages.

### 1/ Azimuth of the resultant vector (vector mean) ( $\sigma$ )

$$\tan \sigma = \frac{\sum n \sin \sigma}{\sum n \cos \sigma}$$

where  $\sigma$  = azimuth of each observation ( $0^{\circ}$ - $360^{\circ}$ )

$n$  = observation magnitude (1)

$\sum n \sin \sigma$  = E-W component

$\sum n \cos \sigma$  = N-S component

### 2/ Magnitude of the resultant vector (magnitude of the mean A-axis alignment, and comparable to the standard deviation) ( $r$ )

$$r = \sqrt{(\sum n \sin \sigma)^2 + (\sum n \cos \sigma)^2}$$

### 3/ Conversion to a percentage value ( $L$ )

$$L = \frac{r}{\sum n} \times 100$$

03/90	250 583	153 526	353 379	354 458	716 837	425 922	658 555
07/90	242 540	140 399	267 352	346 395	527 747	385 523	635 476
09/90	289 264	189 976	276 922	352 677	729 649	317 657	791 457
12/90	191 051	240 762	190 041	254 235	775 079	675 658	675 658
02/91	232 503	239 503	368 579	369 611	738 114	1 036 726	1 036 726
03/91	192 354	122 954	293 525	355 307	548 661	501 953	801 953
04/91	250 507	190 392	361 506	437 716	898 722	7 645	7 645
06/91	262 043	280 460	354 000	437 979	1 114 482	636 367	1 260 367
07/91	394 731	247 139	267 701	394 411	959 736	630 830	630 830
08/91	263 719	197 047	298 376	369 014	1 367 516	729 012	2 768 012
10/91	154 071	180 051	318 036	375 495	753 531	573 765	2 948 765
11/81	227 865	294 507	577 992	632 811	1 210 803	501 415	749 549
01/82	377 412	202 663	306 610	404 590	980 875	384 557	704 453
02/82	230 656	203 050	313 690	376 974	924 370	401 996	766 970

Appendix 9 Total beach volumes recorded at Culbin 1990-1992 (all volumes in m<sup>3</sup>)

Date	STATION							TOTAL
	1	2	3	4	5	6	7	
03/90	250 683	163 528	353 379	364 496	715 362	425 922	858 355	3 131 725
07/90	242 840	140 539	267 352	346 390	527 757	385 523	835 476	2 745 877
09/90	288 264	189 916	275 922	352 675	547 669	384 933	791 457	2 830 836
12/90	191 081	240 762	190 041	264 204	479 754	304 808	675 686	2 346 336
02/91	232 508	269 528	398 579	449 618	601 284	479 521	1 003 196	3 452 234
03/91	192 354	122 954	283 525	295 306	540 454	328 763	901 925	2 665 281
04/91	250 507	130 337	291 506	340 646	608 736	390 449	719 350	2 730 731
06/91	262 043	280 460	254 920	384 379	701 367	303 527	680 324	2 867 023
07/91	394 731	247 138	287 701	259 411	648 796	373 663	688 900	2 855 340
08/91	263 719	197 047	288 376	389 014	521 967	382 163	720 012	2 762 298
10/91	154 071	180 061	318 086	375 485	575 842	573 169	772 943	2 949 657
11/91	227 368	234 507	277 980	392 811	535 046	501 415	749 649	2 918 776
01/92	277 412	202 683	309 810	404 590	574 138	394 667	704 453	2 867 753
02/92	299 856	205 050	313 830	370 974	563 650	401 998	766 970	2 922 328

**Appendix 10 Radiocarbon samples: details and stratigraphic locations**

Sample	Material	Location	Grid Ref.	Age (BP)	$\delta^{13}\text{C}$ (‰)
SRR-4677	Peat	Burghead Bay	NJ 106664	9105±45	-27.6
SRR-4678	Peat	Burghead Bay	NJ 097653	3170±40	-27.3
SRR-4679	Peat	Burghead Bay	NJ 092650	3140±45	-28.4
SRR-4680	Peat	Burghead Bay	NJ 091649	1300±45	-28.4
SRR-4681	Peat	Burghead Bay	NJ 089648	2900±45	-28.5
SRR-4682	Palaeosol	Burghead Bay	NJ 091649	1340±65	-27.5
SRR-4683	Peat	Culbin	NH 989603	4335±45	-28.7
SRR-4684	Peat	Culbin	NH 988607	3330±60	-27.7
SRR-4685	Peat	Culbin	NH 987607	3600±45	-28.1
SRR-4686	Peat	Culbin	NH 989603	4450±45	-29.4
SRR-4687	Wood	Culbin	NH 989603	4570±45	-25.0
SRR-4688	Peat	Culbin	NH 987607	3935±55	-29.8
SRR-4689	Peat	Findhorn Bay	NJ 050609	9305±45	-29.9
AA-(AMS/ )	Shell	Burghead Bay	NJ 066646	Awaiting result	

**DETAILS OF SAMPLING LOCATIONS**

**BURGHEAD BAY SAMPLES (57°40'N, 3°32'W)**

**SRR-4677.** 9105±45. Location NJ 106664. Intertidal zone 0.25 km SW of Forestry Commission Roseisle car park beach access point. Basal 5 cm layer of compacted peat with wood (*Betula*) fragments overlying sand with contact at -1.75 m OD.

**SRR-4685.** 3600±45. Location NH 987607, in a freshwater pond ca. 150 m north of main farm buildings immediately within the Forestry Commission boundary fence. Brown fibrous peat with wood fragments with contact at 2.60 m OD, forming a basal layer underlying 2.15 m of deposits at the base of the pond.

**SRR-4678.** 3170±40. Location NJ 097653. Exposed in a stream section 71 m inland along the Bessie Burn. Basal 5 cm of ca. 90 cm thick layer of clayey peat with contact at 1.67 m OD overlying pebbly sand, buried by 2.11 m of aeolian sand.

**SRR-4679.** 3140±45. Location NJ 092650. Exposed in sectioned raised foreshore deposits 1.06 km west of the Bessie Burn exit. Basal 5 cm of ca. 43 cm thick layer of stiff fibrous peat resting on coarse sand with contact at 2.43 m OD, buried by 2.33 m of aeolian sand.

**SRR-4680.** 1300±45. Location NJ 091649. Exposed in sectioned raised foreshore deposits 1.29 km west of the Bessie Burn exit. Dense, black clayey peat ca. 10 cm thick resting on and indurating a raised shingle storm ridge at 5.49 m OD, and buried in turn by 4.14 m of aeolian sand.

**SRR-4681.** 2900±45. Location NJ 089648. Exposed in sectioned raised foreshore deposits 1.53 km west of the Bessie Burn exit. Basal 5 cm of ca. 40 cm thick peat layer resting on fine white sand with contact at 4.60 m OD, and buried by 2.80 m of aeolian sand.

**SRR-4682.** 1340±65. Location NJ 091649. Exposed in sectioned raised foreshore deposits 1.26 km west of the Bessie Burn exit. Thin organic induration (possibly a poorly formed palaeosol) formed over/within a raised shingle storm ridge at 5.80 m OD, and buried by a further 0.70 m of aeolian sand.

#### SNAB OF MOY FARM SAMPLES (57°37'N, 3°42'W)

**SRR-4683.** 4335±45. Location NH 989603. Exposed at base of prominent abandoned cliffline 80 m east of main farm buildings. Basal 5 cm of ca. 60 cm thick layer of compacted peat resting on a raised shingle storm ridge. Peat base/ridge crest located at 8.90 m OD.

**SRR-4684.** 3330±60. Location NH 988607, in a freshwater pond ca. 150 m north of main farm buildings immediately within the Forestry Commission boundary fence. Brown fibrous peat with wood fragments with contact at 4.85 m OD, forming a basal layer underlying 2.5 m of deposits at the base of the pond.

**SRR-4685.** 3600±45. Location NH 987607, in a freshwater pond ca. 150 m north of main farm buildings immediately within the Forestry Commission boundary fence. Brown fibrous peat with wood fragments with contact at 2.60 m OD, forming a basal layer underlying 2.15 m of deposits at the base of the pond.

**SRR-4686.** 4450±45. Location NH 989603. Exposed at the surface of a field fronting a prominent abandoned cliffline ca. 200 m east of main farm buildings. Basal 5 cm of brown compacted peat with base at 7.88 m OD overlying unstructured sand/peat containing macrofossil remains. Peat layer currently 0.55 m thick, but upper surface is vegetated and eroded.

**SRR-4687.** 4570±45. Location NH 989603, within the sand/peat unit underlying SRR-4686. Macrofossil remains of *Betula* branch, removed from ca. 7.80 m OD.

**SRR-4688.** 3935±55. Location NH 987607, in a freshwater pond ca. 150 m north of main farm buildings immediately within the Forestry Commission boundary fence. Black, fibrous peat ca. 10 cm thick with contact at 3.67 m OD, resting on medium/fine grey micaceous sand and overlain by medium grey sand with organic rich layers.

MILTON OF GRANGE FARM (57°37'N, 3°35'W)

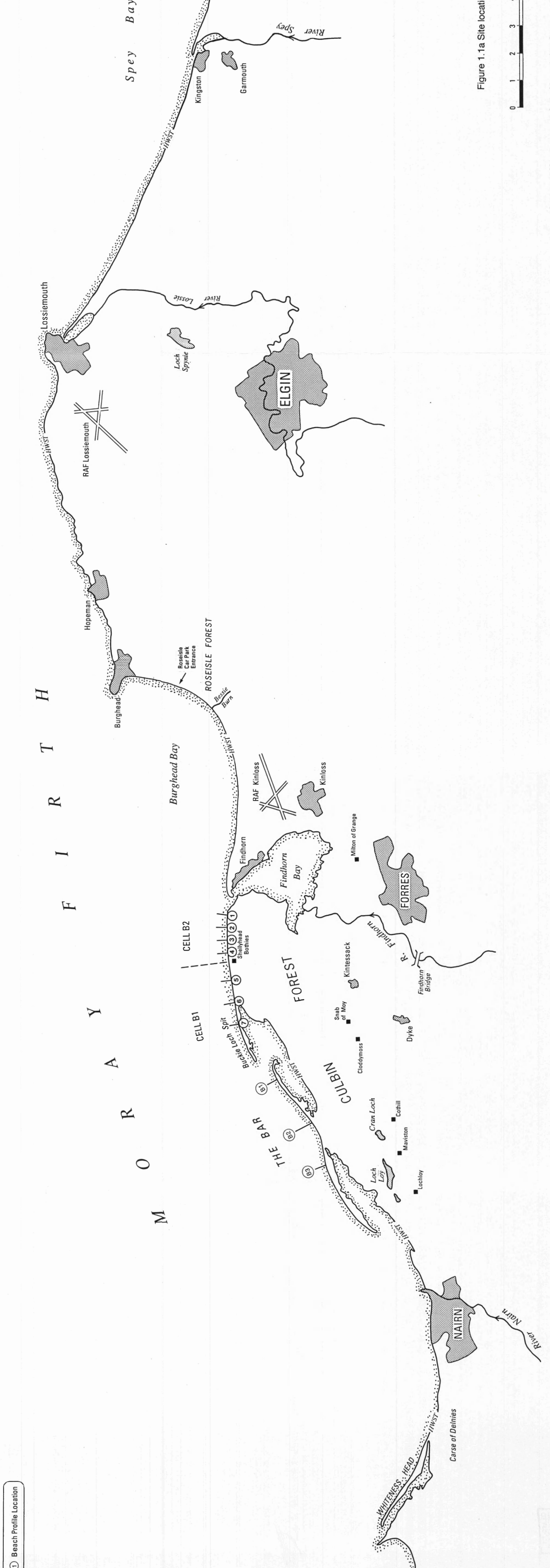
**SRR-4689.** 9305±45. Location NJ 050609. Exposed in a drainage ditch ca. 700 m NE of main farm buildings. Basal 5 cm of ca. 80 cm thick stiff brown peat with contact at 1.24 m OD. Peat rests on organic rich silty sand with pebbles, and is overlain by 0.60 m of aeolian sand.

**Radiocarbon samples: laboratory procedure (extract from NERC East Kilbride laboratory report on radiocarbon allocation 485/1291).**

Prior to  $^{14}\text{C}$  assay all peat and wood samples were digested in 2M hydrochloric acid (at 80° C for 24 hours) then washed to neutral pH and oven dried to constant weight. Throughout the digestion and washing individual samples were examined and any suspect rootlet and/or phragmites debris was removed and discarded.

The shell sample was reacted with sufficient 0.5 M hydrochloric acid to discard the outermost 25% by weight of the carbonate. The remainder was washed in distilled water and the constituent carbon recovered by acid hydrolysis. Due to restricted size this sample was dated by accelerator mass spectrometry (AMS).





① Beach Profile Location

Figure 1.1a Site location map



Based on the Ordnance Survey 1:50,000 map sheets 27 & 28 with permission of the Controller H.M.S.O.